

UNIVERSAL
LIBRARY

OU_160143

UNIVERSAL
LIBRARY

OSMANIA UNIVERSITY LIBRARY

Call No. *551.5/H61M* Accession No. *34820*

Author *Hewson & Longley.*

Title *Meteorology ; theoretical and applied.*
1951.

This book should be returned on or before the date
last marked below.

METEOROLOGY THEORETICAL AND APPLIED

By

E. WENDELL HEWSON, Ph.D.,

DIRECTOR, DIFFUSION PROJECT
THE MASSACHUSETTS INSTITUTE OF TECHNOLOGY

and

RICHMOND W. LONGLEY, M.A.

METEOROLOGIST IN THE METEOROLOGICAL
SERVICE OF CANADA

NEW YORK
JOHN WILEY & SONS, INC.
CHAPMAN & HALL, LTD.
LONDON

COPYRIGHT, 1944
BY
EDGAR WENDELL HEWSON
AND
RICHMOND WILBERFORCE LONGLEY

All Rights Reserved

*This book or any part thereof must not
be reproduced in any form without
written permission of the publisher.*

SECOND PRINTING, AUGUST, 1951

PRINTED IN THE UNITED STATES OF AMERICA

PREFACE

Two main considerations have prompted us to write a text on meteorology. Recent books on the subject are either too elementary or too advanced for effective use in our own and similar classes for beginners; the need for an introductory treatment of basic meteorological theory is particularly great. In the second place, a closer integration of forecasting technique with the theory on which it is founded is desirable. The present work endeavors to meet both these needs.

The development of the subject is an outgrowth of experience gained by one of us (Hewson) in 1938 and for several years thereafter in teaching students of meteorology in the University of Toronto, and more recently by both of us in instructing technical personnel entering the Meteorological Service of Canada. The book is designed to appeal to two types of readers: (1) persons studying meteorology for the first time, either in a university, in one of the official weather services, or in a private meteorological organization; (2) practising forecasters who may wish to brush up on the latest developments in their field. An elaborate knowledge of mathematics and physics is not presumed; the development should be followed without difficulty by anyone with an understanding of basic physical principles who has had a first course in calculus. Even the knowledge of calculus is not essential for most of the second part of the book.

The two parts, the first on basic theory and the second on applications, may be studied at the same time or consecutively. Each is to a certain extent a self-contained unit, although cohesion is maintained by numerous cross references. Thus those interested primarily in the theory will concentrate on the first part, dipping into the applications only here and there, whereas the student of forecasting will spend most of his time on the second part, going back to the theory only when he wishes to learn the assumptions on which a given result depends. Mathematical formulas used in the applied meteorology are derived rigorously in the theoretical portion so that the student may judge for himself the scope and degree of validity of any given equation.

The aim of the book is to give a well-rounded view of the essentials of the science of meteorology at the present time, as shown by the inclusion of chapters on instruments and observations, climatology, map analysis

and forecasting procedure, the applications of meteorology to other specialized fields, and the statistical analysis of meteorological data. So far as the authors know the last-named subject is treated here for the first time in any textbook. The problems and exercises provide a means for the student to clarify his ideas on the topics discussed.

We are indebted to the following persons and organizations for permission to reproduce a number of illustrations: Mr. W. H. Bigg, Professor J. Bjerknes, Professor S. Chapman, Dr. W. Elsasser, Mr. J. J. George and Eastern Airlines, Professor B. Haurwitz and McGraw-Hill Book Co., Mr. R. K. Linsley, Jr., and the U.S. Weather Bureau, Macmillan and Co., London, Mr. W. E. K. Middleton, Mr. C. M. Penner, Dr. S. Petterssen, the Royal Society of London, Sir Napier Shaw, Sir George Simpson and the Royal Meteorological Society, Dr. G. I. Taylor, and Professor G. T. Trewartha and McGraw-Hill Book Co. We wish to thank Mr. H. T. Gisborne, the U.S. Forest Service, and the U.S. Weather Bureau for the originals of various figures. We are also indebted to Dr. N. K. Johnson, Professor H. Landsberg, Mr. C. M. Penner, and to the Toronto Transportation Commission.

We regret that it has been impossible under present conditions to obtain permission for the use of certain diagrams. Full acknowledgment, however, has in all cases been made at the point of insertion.

A number of other persons have provided greatly appreciated assistance. Among these are Mr. J. M. Leaver who made a number of valuable suggestions of material which could advantageously be included and Mr. W. E. K. Middleton who suggested several revisions. We are also greatly indebted to Dr. D. Brunt, Professor of Meteorology in the University of London, under whom one of us (Hewson) studied for several years. We have drawn freely on the material covered in Professor Brunt's lectures.

The careful typing of the manuscript by Mr. D. W. Robertson and the accurate drafting of the figures by Mr. Frank Rayfield are much appreciated.

E. WENDELL HEWSON
RICHMOND W. LONGLEY

Toronto
November, 1943

CONTENTS

CHAPTER	PAGE
1. OBSERVATIONAL FACTS OF THE ATMOSPHERE	
1. Surface Temperature Distribution	1
2. Upper Air Temperature Distribution	4
3. The General Pressure Distribution over the Earth	8
4. Wind Distribution	10
5. Composition of the Atmosphere	11
<i>PART I. THEORETICAL METEOROLOGY</i>	
2. STATICS OF THE ATMOSPHERE	
6. Pressure and Temperature Units	14
7. The Equation of State for Dry Air	15
8. Geopotential	16
9. The Variation of Pressure with Altitude	18
10. Units of Atmospheric Water Vapor Content	20
11. Virtual Temperature and Height Computations	23
3. THERMODYNAMICS OF DRY AIR	
12. The First Law of Thermodynamics	28
13. Adiabatic Relationships for Dry Air. Potential Temperature	30
14. The Dry Adiabatic Lapse Rate. The Stability of Dry Air	31
15. The Adiabatic Lapse Rate for Moist, Unsaturated Air	34
16. The Effect of Ascent and Descent on Lapse Rate and Sta- bility	36
17. The Carnot Cycle. Heat Engine Efficiency	40
18. Entropy	43
4. THERMODYNAMICS OF MOIST AIR	
19. The Clausius-Clapeyron Equation	47
20. The Saturated Adiabatic Lapse Rate. The Stability of Saturated Air	50
21. Condensation Level. Dew-Point Changes in Adiabatic Motion	52
22. Thermodynamic Diagrams	54
23. The Psychrometer Equation	59
24. Wet-Bulb Temperature. Wet-Bulb Potential Temperature	60
25. Equivalent Temperature. Equivalent Potential Tempera- ture. Rossby Diagram	63

CHAPTER	PAGE
5. RADIATION IN THE ATMOSPHERE	
26. The Laws of Black-Body Radiation	67
27. The Law of Absorption	70
28. Solar Radiation	72
29. Terrestrial and Nocturnal Radiation	76
30. Radiation with Cloudy Skies	80
31. The Heat Balance in the Atmosphere	82
32. Radiative Equilibrium in the Stratosphere	85
6. ATMOSPHERIC MOTIONS UNDER BALANCED FORCES	
33. The Pressure Gradient Force	88
34. The Deflecting Force of the Earth's Rotation (Coriolis Force)	90
35. The Geostrophic Wind Equation	96
36. The Thermal Wind Component	98
37. The Gradient Wind Equations	101
7. FRONTAL SURFACES	
38. The Slope of Frontal Surfaces	105
39. The Pressure Trough at Fronts	108
40. Pressure Tendencies below a Frontal Surface	110
41. Frontogenesis and Frontolysis. Temperature Gradient Changes in a Wind Field	112
8. GENERAL KINEMATICS AND DYNAMICS OF AIR MOTIONS	
42. The Movement of Significant Curves in the Pressure Field	115
43. The Movement of Troughs, Wedges, and Fronts	118
44. Streamlines and Trajectories	123
45. The Equation of Continuity. Divergence and Convergence	125
46. The Isallobaric Wind	128
47. The Origin of Pressure Changes	131
48. The Movement of Upper Troughs and Wedges	132
49. Circulation and Vorticity	135
50. Rate of Change of Circulation	136
9. TURBULENCE	
51. Streamline and Turbulent Motion	144
52. Turbulent Transfer of Momentum. The Wind Variation with Height in the Frictional Layer	145
53. Turbulent Transfer of Heat	150
54. Turbulent Transfer of Matter	154
55. Evaluation of the Coefficient of Eddy Diffusivity	157
10. STATISTICAL ANALYSIS OF METEOROLOGICAL DATA	
56. The Purpose of Statistics	161
57. Measures of Central Tendency. Computation of the Mean	161

CHAPTER	PAGE
58. Measures of Variability. Standard Deviation.....	166
59. The Theory of Errors.....	169
60. Method of Least Squares.....	174
61. Correlation.....	177
62. Harmonic Analysis.....	179

PART II. APPLIED METEOROLOGY

11. METEOROLOGICAL INSTRUMENTS AND OBSERVATIONS

63. Pressure.....	186
64. Temperature.....	190
65. Humidity.....	192
66. Wind.....	193
67. Clouds.....	197
68. Precipitation.....	204
69. Sunshine and Radiation.....	206
70. Visibility.....	207

12. THE GENERAL CIRCULATION OVER THE EARTH

71. Circulation on a Non-Rotating Globe.....	209
72. The Effect of the Earth's Rotation.....	211
73. The Influence of the Land Masses.....	213
74. Air Masses and Their Source Regions.....	214

13. TEMPERATURE AND HUMIDITY IN THE ATMOSPHERE

75. The Temperature of the Air at the Earth's Surface.....	217
76. Temperature in the Free Air.....	218
77. Conservative and Representative Properties.....	221
78. Lapse Rate and Stability.....	222
79. Diurnal Temperature Variations.....	222
80. Potential Temperature.....	224
81. Water Vapor Content.....	224
82. Dew Point.....	226
83. Wet-Bulb Temperature.....	227
84. Wet-Bulb Potential Temperature.....	232
85. Equivalent and Equivalent Potential Temperatures.....	232
86. Summary of Degree of Conservatism of Properties.....	235

14. STABILITY AND INSTABILITY

87. General Considerations.....	236
88. Conditions Required for Stability.....	236
89. The Stability of Moist, Unsaturated Air.....	237
90. Conditional Instability.....	237
91. Stable Type of Conditional Instability.....	239

CHAPTER	PAGE
92. Latent Instability	240
93. Potential Instability	242
94. The Relationship between Latent and Potential Instability	244
95. The Development of Potential and Latent Instability	244
96. Summary of Stability and Instability of Moist, Unsaturated Air	246
15. CHARACTERISTIC PROPERTIES OF DIFFERENT AIR MASSES	
97. Systems of Classification	248
98. Polar Continental (P_C) Air Masses in Winter	249
99. Polar Maritime (P_M) Air Masses in Winter	251
100. Tropical Maritime (T_M) Air Masses in Winter	254
101. Tropical Continental (T_C) Air Masses in Winter	256
102. Polar Continental (P_C) Air Masses in Summer	257
103. Polar Maritime (P_M) Air Masses in Summer	258
104. Tropical Maritime (T_M) Air Masses in Summer	259
105. Tropical Continental (T_C) Air Masses in Summer	260
106. The Rossby Diagram as an Aid to Classification of Air Masses	260
107. Comparison of Air Masses	262
16. CYCLONES AND ANTICYCLONES	
108. General Characteristics of a Front	264
109. Frontogenesis and Frontolysis in Deformation Fields	265
110. Frontal Zones. Frontogenesis between Air Mass Source Regions	271
111. Air Masses and Cyclones	272
112. Life History of a Frontal Depression	272
113. Upper Air Conditions above Frontal Depressions	281
114. Other Types of Depressions	282
115. Tropical Hurricanes. Tornadoes	283
116. Comparison of Upper Air Conditions above Cyclones and Anticyclones	285
117. The Cold Anticyclone	287
118. The Warm Anticyclone	288
119. Convergence and Divergence in Cyclones and Anticyclones	289
17. WINDS	
120. Geostrophic and Gradient Winds	295
121. Thermal Winds. Isallobaric Winds	298
122. Monsoon Winds	302
123. The Effects of Friction. Diurnal Variations	302
124. Slope and Valley Winds	306
125. Land and Sea Breezes	310

CHAPTER	PAGE
18. CONDENSATION AND PRECIPITATION	
126. Saturation	312
127. Condensation on Nuclei	313
128. The Formation of Rain Droplets	314
129. The Types of Rainfall	315
130. Other Types of Precipitation	319
19. FORMATION AND DISSIPATION OF FOG	
131. The Effect of Evaporation	322
132. Turbulent Mixing	325
133. Adiabatic Cooling	326
134. Non-adiabatic Cooling	326
135. The Dissipation of Fog over a Snow Surface	334
136. The Forecasting of Fog	338
20. CLOUDS	
137. Frontal Clouds	343
138. Convection Clouds	345
139. Turbulence Clouds	350
140. Orographic, Billow, and Artificial Clouds	355
141. Convergence Clouds	356
21. ICING ON AIRCRAFT	
142. Types of Ice Deposit	361
143. Process of Deposition	362
144. Variation of Ice Deposits with Temperature and Season	363
145. Icing, Cloud Forms, and Stability	365
146. Ice Formation by Supercooled Raindrops	367
147. Means of Avoiding Deposition of Ice	367
148. Forecasting the Deposition of Ice	368
22. THUNDERSTORMS	
149. The Potential Gradient. Electrical Charges in the Atmosphere	370
150. The Origin of Thunderstorm Electricity	371
151. Variations in Time and Place of Occurrence of Thunderstorms	373
152. Thunderstorm Forecasting	377
23. CLIMATOLOGY	
153. Importance of Climatology to the Meteorologist	380
154. The Factors Governing Climate	381
155. Köppen's Classification of Climate	385
156. The Tropical Rainy Regions	387
157. The Arid Regions	388

CHAPTER	PAGE
158. The Warm Temperate Rainy Regions	390
159. The Cold Snowy Forest Regions	393
160. The Polar Regions	394
24. MAP ANALYSIS AND FORECASTING PROCEDURE	
161. Material Available for the Forecaster	396
162. The Plotting of Data on the Surface Chart	397
163. Construction of Isobars	398
164. The Identification of Air Masses and the Location of Fronts	401
165. The Use of Upper Air Data	403
166. Isentropic Analysis	405
167. Forecasting Positions of Pressure Fields and Fronts	408
168. Forecasting Condensation Phenomena	414
169. An Example of Map Analysis	415
170. Long-Range Forecasting	427
25. METEOROLOGY APPLIED TO VARIOUS HUMAN ACTIVITIES	
171. Transportation	431
172. Agriculture	433
173. Forestry	436
174. Heavy Industry	438
175. Hydrology	442
176. Public Utilities	445
177. Sports	446
178. Retail Merchandise	451
APPENDIX	453
ANSWERS TO PROBLEMS AND EXERCISES	458
INDEX	459

SYMBOLS

Symbols used in the text but not in this list are defined in that portion of the text in which they are used.

a	Absolute humidity; absorptive power; Wien's constant.
A	Reciprocal of the mechanical equivalent of heat; Austausch coefficient.
$^{\circ}\text{A}$	Degrees Absolute.
c	Velocity of pressure system; deviation of assumed mean from mean.
c_p	Specific heat of dry air at constant pressure.
c'_p, c_{pm}	Specific heat of aqueous vapor and of moist unsaturated air at constant pressure, respectively.
c_v	Specific heat of dry air at constant volume.
C	Circulation.
$^{\circ}\text{C}$	Degrees Centigrade.
$\frac{d}{dt}$	Differentiation with respect to time on an individual particle.
$\frac{\partial}{\partial t}$	Local or partial differentiation with respect to time.
e	Partial pressure of aqueous vapor; emissive power.
e_s	Saturation pressure of aqueous vapor.
E	Radius of the earth; black-body radiation.
f	Relative humidity.
$^{\circ}\text{F}$	Degrees Fahrenheit.
g	Acceleration of gravity.
I	Intensity of radiation.
J	Mechanical equivalent of heat.
k	Absorption coefficient.
K	Coefficient of eddy diffusivity.
l	$2\omega \sin \phi$; generalized absorption coefficient.
L	Latent heat of vaporization.
m	Molecular weight of air; mass of absorbing medium.
m'	Molecular weight of aqueous vapor.
M	Arithmetic mean.
M'	Assumed arithmetic mean.
n	Distance along a normal.
p	Pressure.
Q	Heat.
r	Coefficient of correlation; radius.
R	Gas constant for dry air.

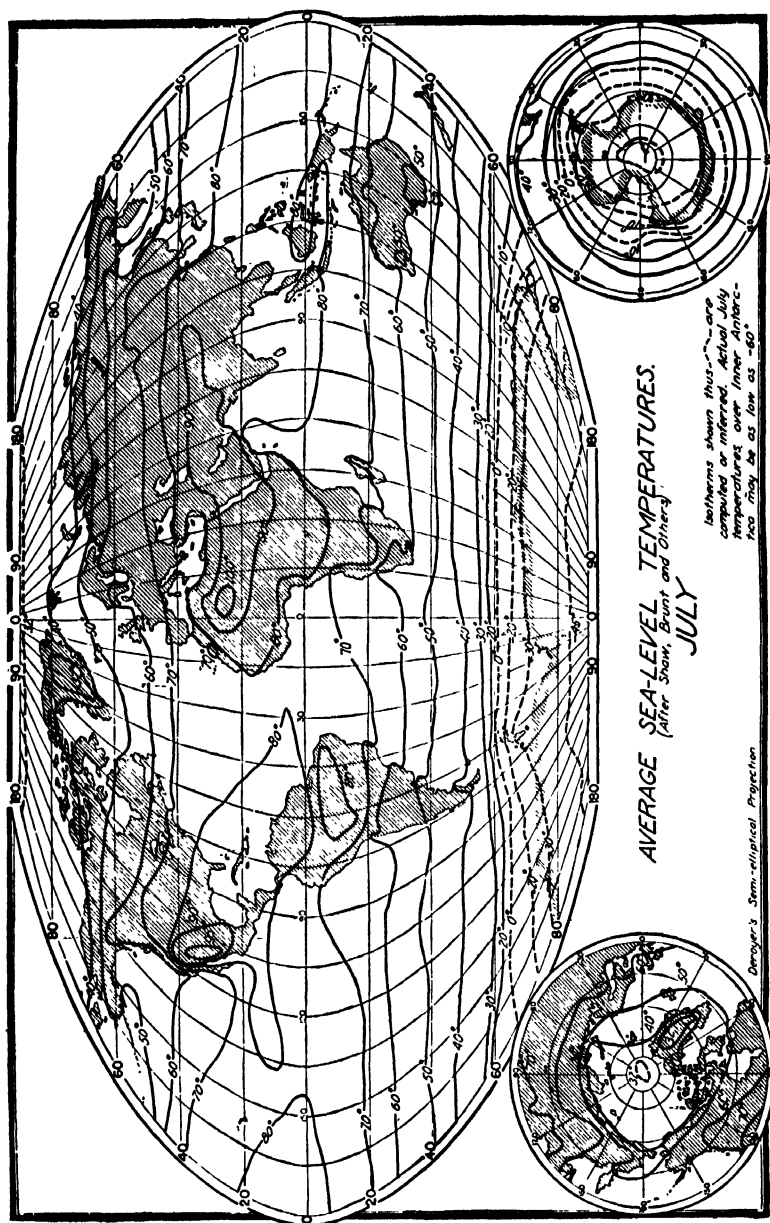


FIG. 1. Surface temperatures over the earth — July. (From Trewartha, *An Introduction to Weather and Climate*, McGraw-Hill Book Co.)

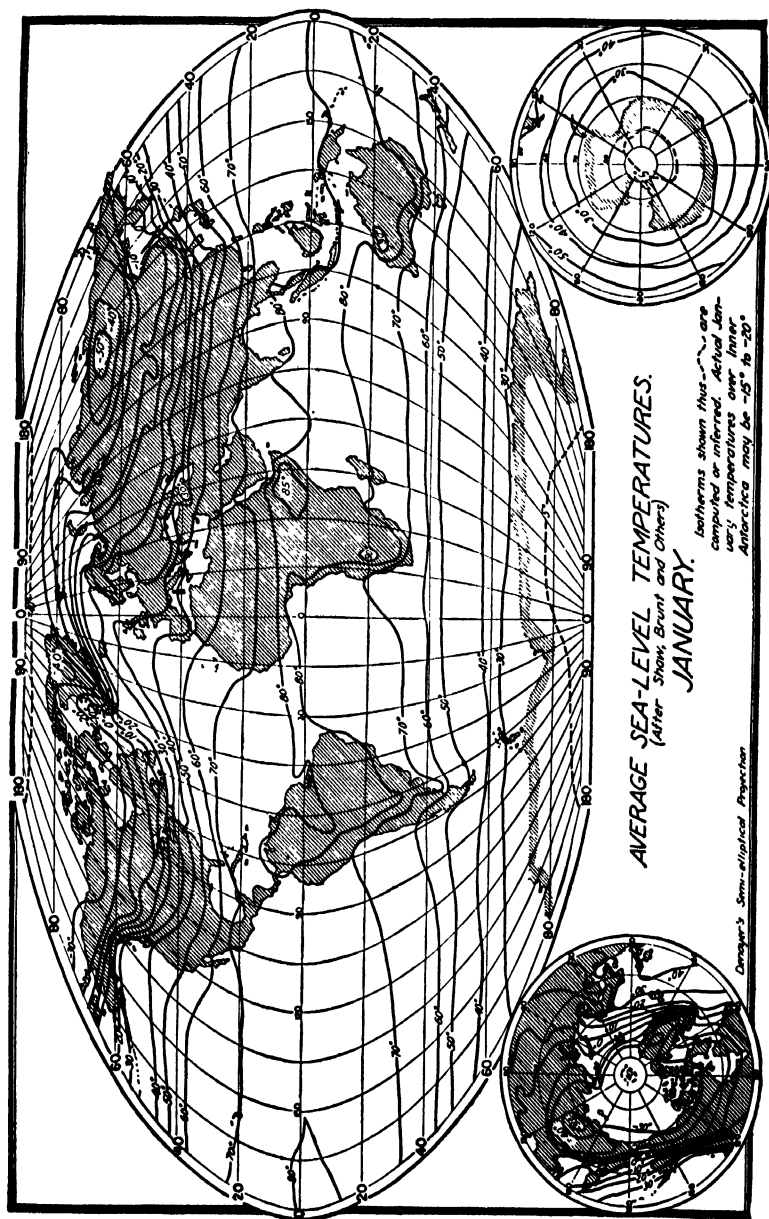


FIG. 2. Surface temperatures over the earth — January. (From Trewartha, *An Introduction to Weather and Climate*, McGraw-Hill Book Co.)

The warmest regions of the earth are found on the land masses, and move north or south with the sun. In July the warmest regions, at about 30° N latitude, are in the southwestern United States, in the Sahara Desert, and in Arabia. During January the Australian Desert is the warmest spot on the earth's surface.

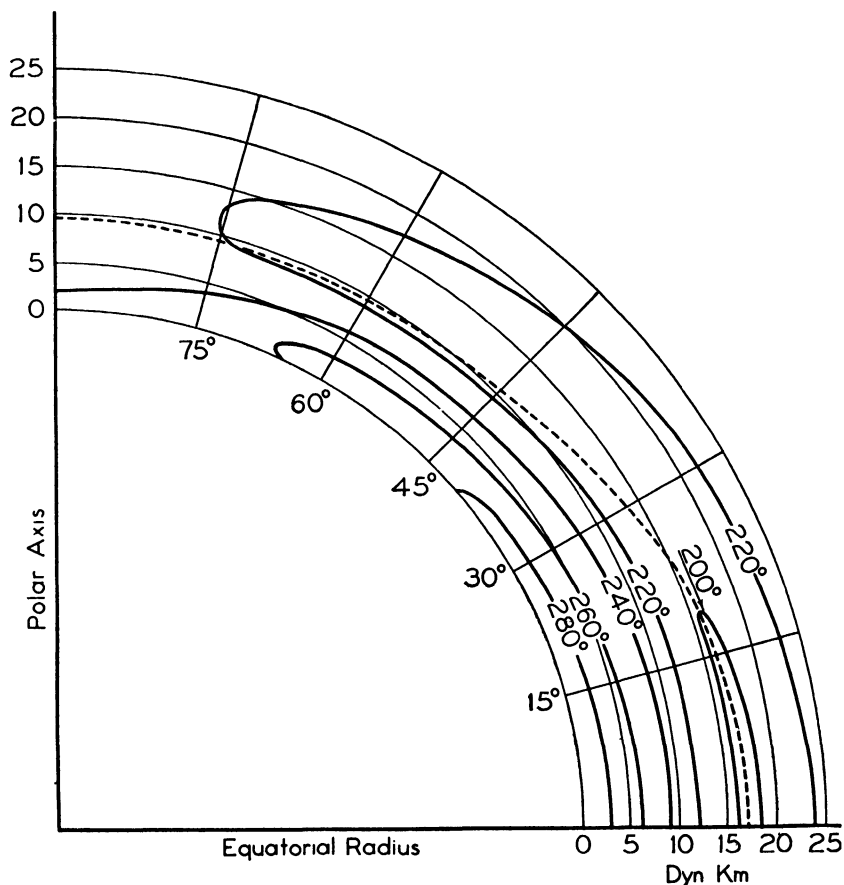


FIG. 3. The variation of free air temperature with latitude.

2. Upper Air Temperature Distribution. The temperature in the free atmosphere decreases with height on the average at the rate of about 6° C per km, or 3° F per 1000 ft. This is an average rate, but decreases as great as 10° C per km are not infrequent, and at times an increase of $5\text{--}10^{\circ}$ C per km occurs.

Under average conditions, the decrease in temperature with height continues until the temperature reaches about -45° C in the polar

regions and about -75°C in the equatorial regions. This takes place at a height of about 9 km at the poles and about 18 km at the equator. At these levels the fall in temperature ceases. The temperature above this height remains constant in the polar regions, whereas above the equatorial regions the temperature begins to rise again. Fig. 3 illustrates the variation of temperature with height up to 25 km at various latitudes of the northern hemisphere in winter. In summer, the temperatures are generally 5 to 10°C higher in the temperate and polar regions.

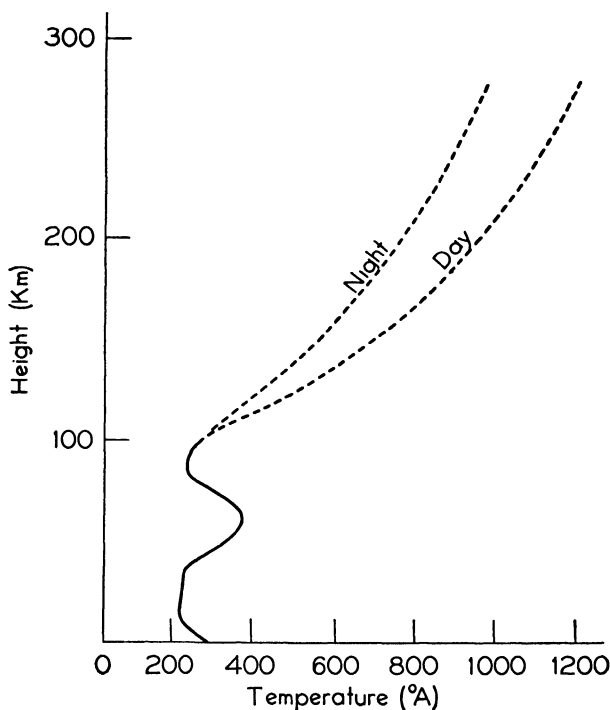


FIG. 4. The variation of air temperature with height. (After Martyn and Pulley.)

In order to distinguish between the two layers of the atmosphere, the lower layer where there is usually a regular drop of temperature with height is called the *troposphere* and the layer above is called the *stratosphere*. The surface separating the two layers is the *tropopause*. Its position is shown by the broken line in Fig. 3.

The average temperature distribution as found for the northern hemisphere is in general duplicated, as far as can be determined from the limited number of observations available, in the southern hemi-

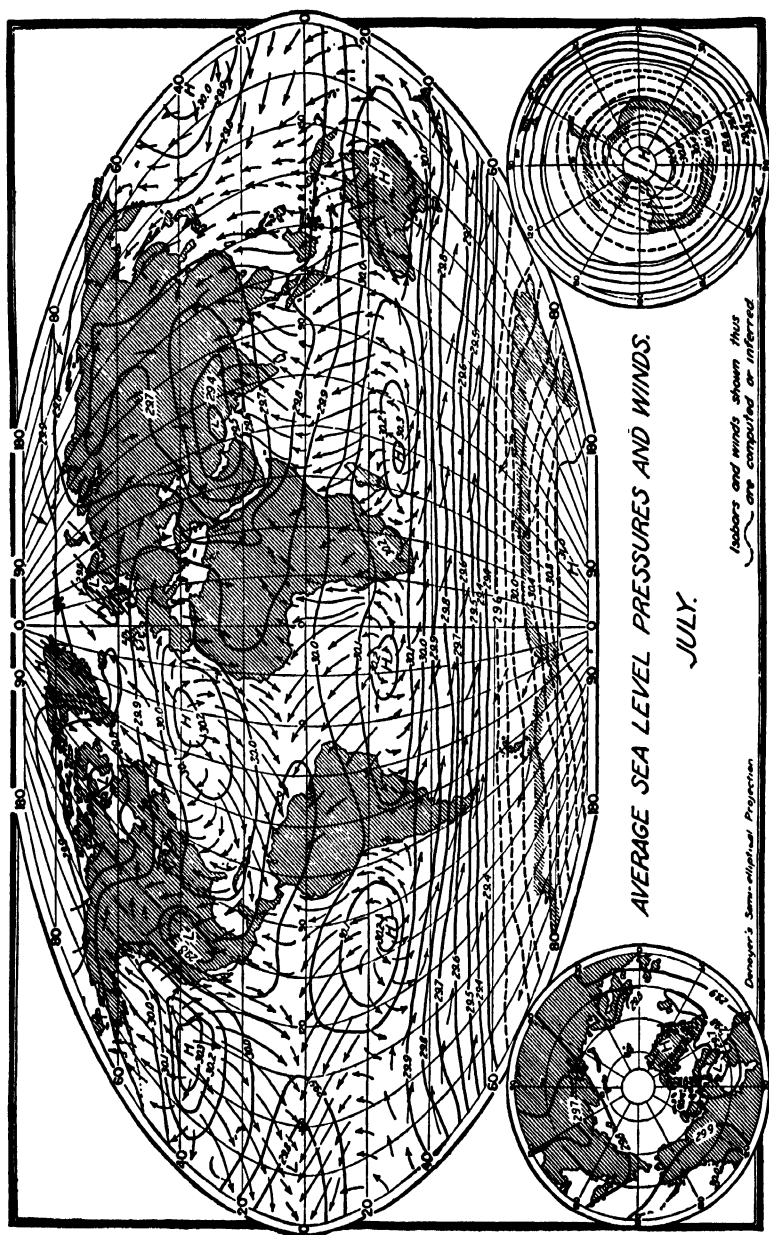


Fig. 5. Pressure and wind distribution at the earth's surface — July. (From Trewartha, *An Introduction to Weather and Climate*, McGraw-Hill Book Co.)

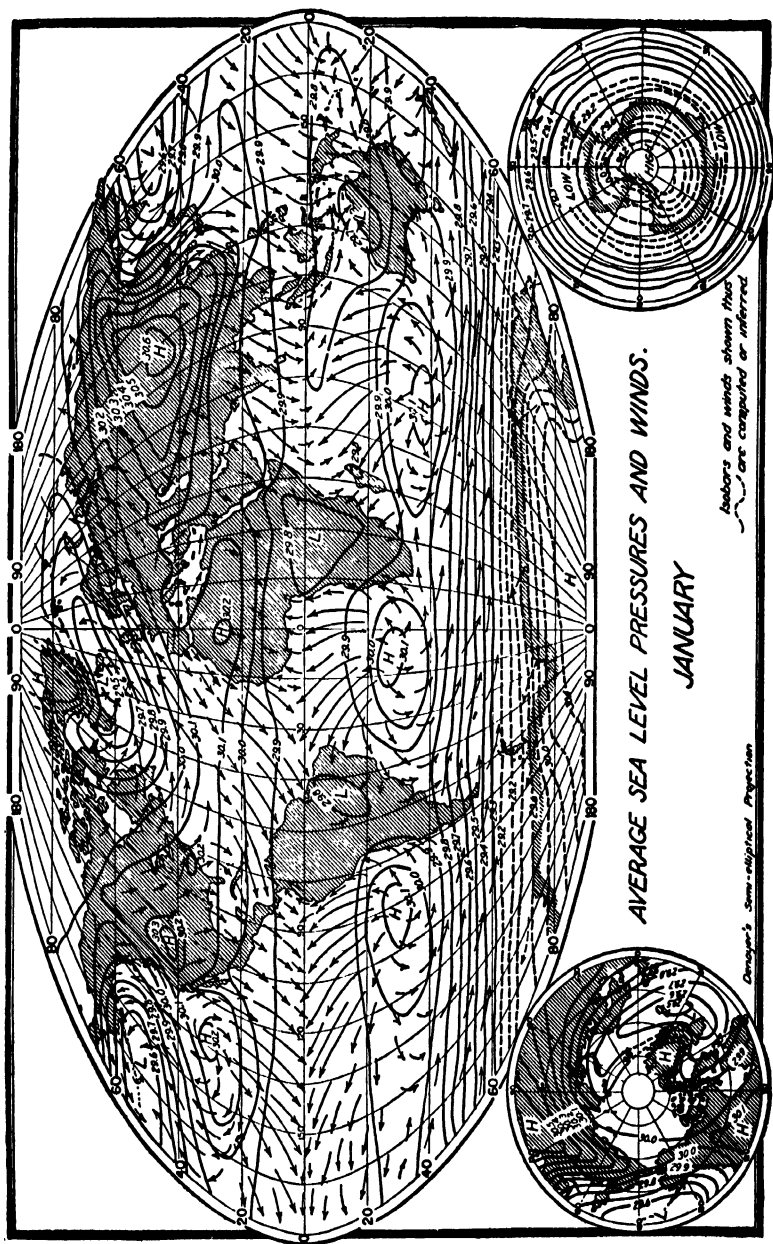


FIG. 6. Pressure and wind distribution at the earth's surface — January. (From Trewartha, *An Introduction to Weather and Climate*, McGraw-Hill Book Co.)

sphere. An anomaly exists, however, during the Antarctic winter. Observations taken by expeditions to the Antarctic continent show that the decrease of temperature with height found in the lowest layers persisted up to a height of 12 km, the upper limit of observations, where the temperature was -80°C . Thus the tropopause found in the Antarctic during the summer and in the Arctic both winter and summer disappears during the Antarctic winter.

Because of the rarity of the atmosphere above 30 km, investigations by direct means cannot be carried out. Through various observations on meteors, abnormal sound wave propagation, noctilucent clouds, aurorae, radio beams, etc., probable values of the temperature at heights ranging from 30 to 300 km have been obtained. The probable variation of temperature with height in the upper atmosphere, based on the results of these indirect investigations, is given in Fig. 4. Above the isothermal layer noted by direct observation there appears to be an increase in temperature to about 60 km, another decrease thereafter until a height of 80 km is attained, and then an increase to about $1000^{\circ}\text{Absolute}$ at 300 km.

3. The General Pressure Distribution over the Earth. The pressure of the atmosphere at a point on the earth's surface is a measure of the weight of a column of air above that point. This pressure varies from day to day, and from one part of the earth to another. There are two causes for this pressure variation at a given point. As a result of the wind distribution, there may be an accumulation of air above a given point on the surface, producing a rise in pressure. A depletion of air would cause a fall in pressure. A second cause which may be in operation is the horizontal transport of air of greater or lesser density, producing a rise or fall of pressure.

The spatial variations in pressure may be indicated by means of isobars. These are curves which join points of equal pressure in the same manner that lines on a contour map join points at the same height above sea level. The isobars are usually much more regular in their shape than contour lines, but they too indicate "highs," "lows," "ridges," and "troughs."

Figs. 5 and 6 give the average pressure distribution over the earth for the months of July and January. The southern hemisphere, with its uniform surface, shows a regular pattern. The most significant features in this hemisphere are a trough of low pressure near the equator, several centers of high pressure at about 25° latitude with connecting ridges, and a high-pressure system over the south pole. There is some displacement of these features north and south with the sun.

In the north, the areas of land and ocean interfere with the regularity

of these main features. In winter the sub-tropical high-pressure belt is connected to high-pressure areas over the continents, while the low-pressure belt in the sub-polar regions is concentrated in two deep lows in the northern Atlantic and northern Pacific. In summer the sub-polar low-pressure belt has extended over the continents, and the high-pressure belt of the sub-tropics is limited to two high-pressure systems over the oceans.

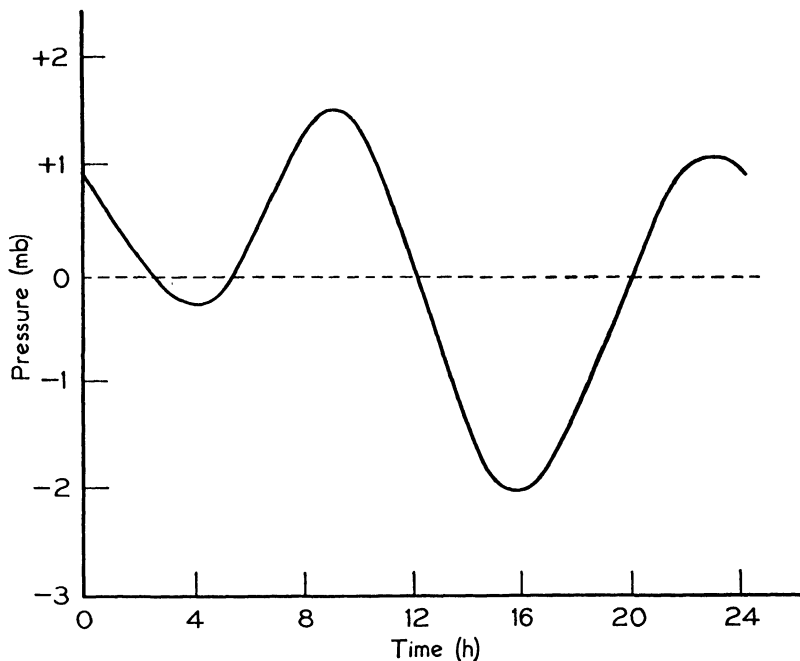


FIG. 7. The diurnal variation of pressure, Batavia. Java.

In the vertical, the pressure decreases rapidly with height as a result of the decreasing amounts of air above. At a height of 5 km or about 18,000 ft, one-half of the atmosphere is below the observer. Only one-tenth of the total atmosphere is spread over the region above 16 km, and observations of the height of the aurora prove that matter is present at heights of 1000 km above the surface.

The pressure at any point varies irregularly, and from many causes. These variations supply one of the major studies for the meteorologist, for they are closely linked with the weather changes. There is, though, a pressure variation that follows a regular cycle. This cycle has a daily period, with two maxima and two minima. It is most in evidence

in the equatorial regions where the lack of other pressure variations permits it to be seen in the daily curve. In the temperate latitudes, the passage of pressure centers causes such wide variations in the pressure that the diurnal wave is apparent only during spells of little barometric activity. By averaging over a long period for each hour of the day, the variations which are due to the passage of cyclones and anti-cyclones are eliminated, and the daily cycle becomes apparent. The daily cycle for Batavia, Java, is given in Fig. 7. The minimum occurs at about 16 h, local time, with a second minimum at about 04 h. The maximum occurs at about 08 h, with the secondary maximum at 22 h. Between 08 h and 16 h the pressure drops approximately 3.5 millibars, then rises by almost the same amount by 22 h. The cycle at higher latitudes has its times of maxima and minima at the same time of day, but the amplitude of the pressure waves is less.

4. Wind Distribution. It will be shown in Chapter 6 that there is a close relationship between the pressure gradient and wind direction and speed. It follows that the average wind directions are related to the average atmospheric pressure distribution. Because of this close relationship, the average wind distributions are given by means of arrows on the appropriate pressure maps, Figs. 5 and 6.

The winds at the earth's surface most nearly approaching constancy are those blowing from the sub-tropical high-pressure systems toward the trough of low at the equator. These are the northeast trades of the northern hemisphere and the southeast trades of the southern hemisphere. The temperate zone lying between the sub-tropical high and the sub-polar low is often called the region of westerlies, since the prevailing direction of the wind is west. The westerlies are more variable in their direction than the trades, as indicated above. About the poles the winds are variable, but tend to be easterly in direction.

The seasonal variation in pressure over the land masses produces a corresponding seasonal variation in the wind distribution. This variation is most marked over Asia. In winter the high-pressure area gives rise to the dry, cold, winter monsoon winds blowing from the center of the continent over China and India. In summer the winds under the influence of the low pressure over the continent blow in the opposite direction, giving warm, moist, southeast to southwest winds over southeastern Asia. A corresponding change in winds occurs over North America, but it is less pronounced, with variations from the general flow occurring more frequently.

The winds found in the free atmosphere will be discussed in connection with the general circulation in Chapter 12.

5. Composition of the Atmosphere. The atmosphere near the earth's surface is a mixture of gases, with very little variation in the relative proportions of its constituents. A sample of pure dry air is made up of 78.09 per cent nitrogen and 20.95 per cent oxygen by volume. The remainder, a little under 1 per cent, is largely argon and carbon dioxide with smaller amounts of hydrogen and the rare gases.

Near human habitations there are variations in the amounts of some of the constituents. But, except for one region, samples of unpolluted air from the troposphere show variations in the amounts which are within the limits of error of the analysis. The exceptional region is the Antarctic continent, where the samples analyzed showed a deficiency in oxygen, with the proportion by volume being 20.54 per cent.

The relative amounts of the different gases were constant in all samples taken in the atmosphere up to a height of 20 km. Above that level there have been a few samples obtained by means of three manned balloons and some free balloons. These have shown that the constancy of composition characteristic of the lower atmosphere no longer prevails. The proportion of helium increases above 20 km, and the proportion of oxygen decreases, although these changes are only small. The maximum height from which samples were obtained was 31 km.

According to Dalton's law, in a mixture of gases the total pressure exerted is the sum of the pressures of the constituents. Therefore the decrease in amount with height will depend on the molecular weight of the gas, the heavier gases being concentrated near the earth's surface. In the lowest layers, turbulent eddy motion is sufficient to produce complete mixing. Above this layer, turbulent mixing is less active, and so the gases tend to follow Dalton's law more closely.

Assuming that the gases are distributed according to Dalton's law, then the amount of oxygen — one of the heavier gases — decreases rapidly with height. Helium and hydrogen, if present in appreciable quantities, would, because of their small molecular weights, extend to great heights, forming a large proportion of the upper atmosphere. An examination of the spectrum of the aurora, which occurs at heights varying from 70 to 1000 km, shows the presence of nitrogen and oxygen bands and lines, but none of hydrogen and helium.

From this fact either of two inferences is possible. One possibility is that hydrogen and helium are not present in appreciable quantities at great heights. The alternative inference is that helium is present in the upper atmosphere, but that the excitation potential is not great enough to produce the emission of helium lines. Helium is being produced constantly as a result of the erosion of igneous rocks which contain radioactive elements. In this manner, 1.2 alpha-particles are

being produced per gram per second. An alpha-particle is a helium atom charged with two units of positive electricity. During geological time, most of these helium atoms have escaped from the upper atmosphere to outer space, but estimates based on geological data suggest that, in the outermost regions, helium still forms a considerable if not

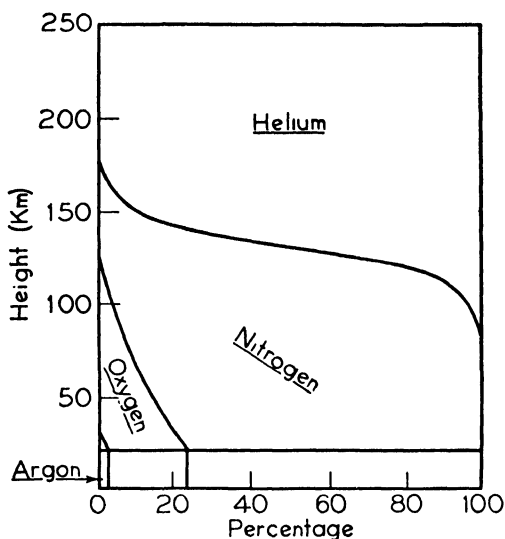


FIG. 8. Proportions (by mass) of the constituents of the atmosphere.
(After Chapman and Milne.)*

preponderant part of the gases present. Fig. 8 shows the composition, by mass, of the atmosphere, under the assumptions that the separation of gases according to Dalton's law starts at 20 km, and that helium, but not hydrogen, is a permanent constituent of the atmosphere at great heights. In this figure, if a horizontal line is drawn at any given height, the lengths of the intercepts made on it by the curves give the proportion of the different constituents. As indicated above, it is not yet clear whether helium predominates at great heights, as indicated in Fig. 8, or if the upper atmosphere is comprised almost exclusively of oxygen and nitrogen.

Measurements have shown that ozone occurs in appreciable amounts in the height interval from 20 to 40 km. The amount of ozone at these levels is correlated with the surface pressure distribution, being a

* In a private communication, Professor Chapman has indicated that the diagram does not accurately portray his present conception of the composition of the atmosphere.

maximum just to the west of a center of low pressure, and a minimum to the west of a center of high pressure. The full significance of this relationship is not yet apparent.

Until now the discussion has been concerned with dry air. But there is one other constituent, water vapor, which is very important in weather processes. Water vapor varies in amount in the atmosphere from almost zero up to a maximum of nearly 3 per cent by mass. Because there is an upper limit to the amount of water vapor which can occupy a given space, and this upper limit decreases with decreasing temperature, very little water vapor is found except in the lowest layers of the troposphere. The variation in the amount of water vapor in the atmosphere is significant to the meteorologist since its condensation produces clouds and rain. A knowledge of the causes and effects of its variations is therefore essential for an understanding of weather processes.

BIBLIOGRAPHY*

- Admiralty Weather Manual*, London, H. M. Stationery Office, 1938. Chapter 8.
Brunt, D., *Physical and Dynamical Meteorology*, London, Cambridge University Press, 1939. Chapter 1.
Shaw, Sir N., *Manual of Meteorology*, London, Cambridge University Press. Vol. 2 (1936).
5. Haurwitz, B., "The Physical State of the Upper Atmosphere," *J. Roy. Astr. Soc. Can.*, 1937, 1938.
5. "The Upper Atmosphere," *Q. J. Roy. Met. Soc.*, **65**, 303 (1939).

* The numbers which appear at the beginning of references are section numbers and indicate that the references are applicable only to the sections referred to. Other references apply to the chapter as a whole.

PART I. THEORETICAL METEOROLOGY

CHAPTER 2

STATICS OF THE ATMOSPHERE

6. Pressure and Temperature Units. The unit of force in the centimeter-gram-second (cgs) system is the dyne. This represents the force which, applied to a mass of 1 gm, produces an acceleration of 1 cm per sec per sec. The unit of pressure in the cgs system is, then, the dyne per square centimeter. A much larger unit, the bar, is equal to 10^6 dynes per sq cm. In meteorology, the pressure unit which is generally used is the millibar, which is one-thousandth of a bar.

$$1 \text{ millibar (mb)} = 10^3 \text{ dynes cm}^{-2}$$

A pressure of 1 bar is the same as a pressure of 1000 mb. The standard pressure of 760 mm of mercury used in physics and chemistry is 1013.2 mb. A pressure of 1 bar is nearly as great as the average sea level pressure over the earth's surface.

The barometer, described in section 63, measures atmospheric pressure in terms of the height of a column of mercury, the weight of which is just sufficient to balance the atmospheric pressure. The relationship between the millibar and the equivalent height of mercury is as follows.

$$1000 \text{ mb} = 750 \text{ mm of mercury} = 29.53 \text{ in. of mercury}$$

The three temperature scales in common usage in meteorology are the Fahrenheit, Centigrade, and Absolute scales. The fixed points in each of the three scales are given in the following table.

SCALE	FREEZING POINT	BOILING POINT	DIFFERENCE
Fahrenheit (F)	32°	212°	180°
Centigrade (C)	0°	100°	100°
Absolute (A)	273°	373°	100°

To convert from one scale to the other, the following equations may

be used.

$$T^{\circ} \text{ F} = \frac{9}{5} T^{\circ} \text{ C} + 32 = \frac{9}{5} T^{\circ} \text{ A} - 459.4$$

$$T^{\circ} \text{ C} = \frac{5}{9} (T^{\circ} \text{ F} - 32) = T^{\circ} \text{ A} - 273$$

$$T^{\circ} \text{ A} = T^{\circ} \text{ C} + 273 = \frac{5}{9} T^{\circ} \text{ F} + 255.22$$

In the English-speaking countries, the Fahrenheit scale is used on the surface weather map to express the air temperature and dew point. It is also used in some of these countries in measuring and plotting upper air data. In others, the Centigrade or Absolute scale is used for this purpose. In other countries practice varies, but the Centigrade scale is used widely. The Absolute scale must be used when carrying out computations in the cgs system. In this book, it will be assumed that the letter T refers to temperature in degrees Absolute unless otherwise indicated.

7. The Equation of State for Dry Air. Two basic relationships of thermodynamics are the laws of Boyle and Charles. Boyle's law states: The pressure of a given mass of a gas at constant temperature varies inversely as the volume. Charles' law is: The temperature in degrees Absolute of a given mass of gas at constant pressure varies directly as the volume. These two laws may be combined in the following manner. First, assume that a unit mass of gas has a pressure p_1 , a volume v_1 , and a temperature T_1 . Let p_1 and v_1 vary at constant temperature T_1 , until a pressure p_2 and a volume v are obtained. From Boyle's law it follows that

$$p_1 v_1 = p_2 v \quad \text{and} \quad v = \frac{p_1 v_1}{p_2} \quad (7.1)$$

Now let the temperature T_1 change to T_2 , the pressure remaining constant at p_2 . From Charles' law, then

$$\frac{v}{v_2} = \frac{T_1}{T_2} \quad \text{and} \quad v = \frac{v_2 T_1}{T_2} \quad (7.2)$$

where v_2 is the resulting volume.

Combining (7.1) and (7.2) gives

$$\frac{p_1 v_1}{p_2 v_2} = \frac{T_1}{T_2} \quad (7.3)$$

The result would have been the same had the conditions varied simul-

taneously. Equation 7.3 indicates that when a unit mass of a perfect gas is undergoing variations in pressure, volume, and temperature,

$$pv \propto T \quad (7.4)$$

Introducing the appropriate constant, (7.4) becomes

$$pv = \frac{R^*}{m} T \quad (7.5)$$

where R^* is called the universal gas constant, and has the value 83.14×10^6 ergs per degree, and m is the molecular weight of the gas. This equation may be used for any perfect gas, when its molecular weight is inserted. It may also be used for a mixture of gases, provided that a value is substituted for m appropriate for the mixture. Of the gases comprising the atmosphere (see section 5), only water vapor condenses at the temperatures and pressures encountered in the atmosphere, so that absolutely dry air may be considered as a perfect gas. Although the constitution of the atmosphere is subject to variations, these are small, and 28.97 may be taken with sufficient accuracy as the molecular weight of dry air. The value of the gas constant for dry air, R , is given by

$$R = \frac{R^*}{m} = \frac{83.14 \times 10^6}{28.97} = 2.87 \times 10^6 \text{ ergs deg}^{-1}$$

or, in basic cgs units

$$R = 2.87 \times 10^6 \text{ cm}^2 \text{ sec}^{-2} \text{ deg}^{-1}$$

The specific volume v of a gas is defined as the volume occupied by unit mass of that gas, so that

$$v = \frac{1}{\rho}$$

where ρ represents the density of the air.

The equation of state for dry air may be given therefore in either of the two following forms.

$$pv = RT \quad (7.6)$$

or

$$p = R\rho T \quad (7.7)$$

8. Geopotential. The earth is not quite a perfect sphere since its equatorial radius is 6378 km, whereas its polar radius is 6357 km. In practically all meteorological problems this divergence from a true

spherical shape is of no significance, and a value of 6370 km may be assumed.

The angular velocity ω of the earth is 7.29×10^{-5} radians per second.

The standard value of the acceleration of gravity g_0 , 980.62 cm per sec per sec, is that at mean sea level at latitude 45° . The acceleration of gravity varies both with latitude ϕ and with height above mean sea level z . The variation is given by the following expression.

$$g = 980.62(1 - 0.00259 \cos 2\phi)(1 - 3.14 \times 10^{-7}z) \text{ cm sec}^{-2}$$

where z is in meters. Accuracy of this order is necessary only in certain phases of meteorological work, and in most instances the variation of g with latitude and height may be neglected, and the value 981 cm per sec per sec assumed.

The concept of geopotential has been introduced into meteorology in order to make allowance for the variation of g with height when that is necessary. The geopotential Φ at a height z is defined as the potential energy of unit mass at that height. The potential energy at a point is, by definition, the work required to raise unit mass from some standard level, usually mean sea level, to that point.

From the inverse square law for gravitational attraction, it follows that at a height z above mean sea level, the acceleration of gravity g is given by

$$\frac{g}{g_0} = \frac{E^2}{(E + z)^2}$$

where E is the radius of the earth. Then, approximately

$$g = g_0 \left(1 - \frac{2z}{E}\right) \quad (8.1)$$

The geopotential is, therefore,

$$\Phi = \int_0^z g \, dz = \int_0^z g_0 \left(1 - \frac{2z}{E}\right) dz = g_0 z \left(1 - \frac{z}{E}\right) \quad (8.2)$$

In cgs units, the unit of geopotential is

$$1 \text{ gm}' \times 1 \text{ cm} \times 1 \text{ cm} \times 1 \text{ sec}^{-2}$$

A more convenient unit for meteorological computations is 10^5 times as great as the cgs unit, and is known as the *dynamic meter*, which, expressed in meter-gram-second units, is

$$10^5 \times 1 \text{ gm} \times \frac{1 \text{ m}}{10^2} \times \frac{1 \text{ m}}{10^2} \times 1 \text{ sec}^{-2} = 10 \text{ mgs units}$$

The geopotential in dynamic meters is, therefore, from (8.2)

$$\Phi = 10^{-1} g_0 z \left(1 - \frac{z}{E} \right) \quad (8.3)$$

where g_0 is given in meters per second per second and z and E are given in meters. The geopotential in dynamic meters is therefore only about 2 per cent smaller than the geometric height in meters. In practice, tables are used to convert from meters to dynamic meters. Table I in the Appendix gives the corresponding values of z and Φ for various latitudes.

From the foregoing, it can be seen that the dynamic meter is not a unit of length, but a unit of energy. This fact must be kept in mind if confusion in its use is to be avoided. The use of the dynamic meter in evaluating the geometric height corresponding to significant points of an aerological ascent is outlined in section 11.

9. The Variation of Pressure with Altitude. The pressure at any height in the atmosphere is, by definition, the weight of the vertical column of air of unit cross section which extends from that height to the top of the atmosphere. It follows directly then that pressure decreases with increasing height in the atmosphere. The difference in pressure between height z and height $z + dz$ may be found in the following manner. Since unit cross section is being considered, the volume of the element of air is dz , and its mass is ρdz , where ρ denotes the average density in the height interval dz . Since weight is given by the product of the mass and the acceleration of gravity, and since p decreases with increasing z , then

$$dp = -g\rho dz \quad (9.1)$$

Substituting for ρ from (7.7), an alternative form is obtained

$$dp = -\frac{gp dz}{RT} \quad (9.2)$$

This is the basic statical relationship of meteorology, and it is used frequently in subsequent sections.

The variables are readily separated, and if T can be expressed as a function of z , the differential equation may be integrated. Two cases are of fundamental importance.

The first of these is the situation in which T is constant with height, i.e., the portion of the atmosphere under consideration is an isothermal layer. Equation 9.2 may be expressed as

$$\frac{dp}{p} = -\frac{g}{RT} dz \quad (9.3)$$

Integration of (9.3) leads to

$$\log \frac{p}{p_0} = -\frac{g}{RT} (z - z_0) \quad (9.4)$$

or

$$p = p_0 e^{-\frac{g}{RT}(z-z_0)} \quad (9.5)$$

where p_0 is the pressure at height z_0 .

The second case is that in which T decreases at a constant rate with increasing z . Then the temperature T at any height is given by

$$T = T_0 - \alpha z \quad (9.6)$$

T_0 is the temperature at z_0 , and α is known as the *lapse rate* of temperature.

Differentiating and rearranging (9.6) lead to

$$dz = -\frac{dT}{\alpha} \quad (9.7)$$

Substituting (9.7) in (9.2) gives

$$\frac{dp}{p} = \frac{g}{R\alpha} \frac{dT}{T} \quad (9.8)$$

Integration of (9.8) then gives

$$p = p_0 \left(\frac{T_0 - \alpha z}{T_0} \right)^{\frac{g}{R\alpha}} \quad (9.9)$$

If, as a first approximation, it is assumed that the troposphere (see section 2) is composed of dry air having a constant lapse rate of temperature, then (9.9) gives the variation of pressure in the troposphere under those conditions. If, in addition, T is assumed to be constant with height in the stratosphere (section 2), the pressure in the stratosphere may be obtained by combining (9.5) and (9.9). Thus the pressure p at any given height z in the stratosphere is given by

$$p = p_0 \left(\frac{T_0 - \alpha z_t}{T_0} \right)^{\frac{g}{R\alpha}} e^{-\frac{g(z-z_t)}{R(T_0-\alpha z_t)}} \quad (9.10)$$

where p_0 and T_0 are the pressure and temperature at z_0 (frequently p_0 and T_0 are taken at the earth's surface, so that $z_0 = 0$), z_t is the height of the tropopause, and $(T_0 - \alpha z_t)$ is the temperature of the stratosphere. Fig. 9 depicts on a temperature-height diagram the situation postulated above.

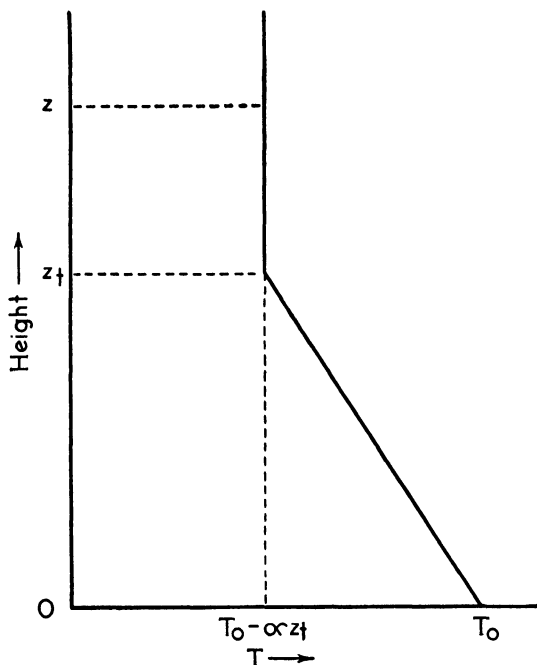


FIG. 9. Temperature changes with height.

10. Units of Atmospheric Water Vapor Content. Up to this section, the atmosphere has been assumed to be perfectly dry, and no allowance has been made for the water vapor present in it. However, water vapor plays a fundamental role in atmospheric processes and must be considered in detail. Not only does water in the gaseous state vary greatly in amount throughout the atmosphere, but also it appears in the liquid and solid states. The effect on weather processes of water in its three states and of changes from one state to another forms the subject matter of a large proportion of meteorological investigations.

As long as water remains in the gaseous state, it acts as a perfect gas, and its variations are subject to the relationship given in (7.5). The molecular weight of water vapor is 18.016, and its gas constant is, according to section 7,

$$R' = \frac{R^*}{m'} = \frac{83.14 \times 10^6}{18.016} = 4.62 \times 10^6 \text{ cm}^2 \text{ sec}^{-2} \text{ deg}^{-1}$$

NOTE. In this and following sections, when water vapor is referred to specifically, the property under consideration is indicated by a prime symbol; thus the density of water vapor is designated ρ' . An

exception to this rule is made in the pressure of water vapor, where e is used instead of p' in order to conform to general practice.

The density of water vapor is, according to (7.5), since $v' = 1/\rho'$

$$\rho' = \frac{e}{R'T'} \quad (10.1)$$

The density of moist air is the sum of the density of water vapor and of dry air. From Dalton's law it follows that if p is the total pressure of the moist air, then $p - e$ is the partial pressure of dry air, and the density of the moist air is

$$\rho = \frac{e}{R'T'} + \frac{p - e}{RT} \quad (10.2)$$

Now $R^* = m'R' = mR$, so that

$$R' = \frac{mR}{m'} \quad (10.3)$$

and (10.1) becomes

$$\rho' = \frac{m'}{m} \frac{e}{RT'} = \epsilon \frac{e}{RT} \quad (10.4)$$

where

$$\epsilon = \frac{m'}{m} = \frac{18.016}{28.97} = 0.622$$

In a mixture of dry air and water vapor, the latter is at the same temperature as the former, so that $T' = T$, and with (10.4), (10.2) becomes

$$\rho = \epsilon \frac{e}{RT} + \frac{p - e}{RT}$$

or

$$\rho = \frac{p}{RT} \left[1 - (1 - \epsilon) \frac{e}{p} \right] \quad (10.5)$$

The above equation shows that a given volume of moist air is lighter than an equal volume of dry air at the same pressure and temperature. This fact should be obvious, since water vapor is lighter than dry air, and mixing them will reduce the density of the mixture.

If a closed vessel contains initially dry air and some liquid water, the whole being at a constant temperature, the space is said to be saturated with water vapor when steady conditions in the space above the liquid water have been attained. Even if the dry air were not

present, the amount of water vapor present at saturation would be the same. When space is saturated in this manner, no more liquid water evaporates, and there is an upper limit to the amount of water vapor which may occupy the given space. The pressure exerted by water vapor under saturation conditions will be denoted by e_s . The foregoing shows that it is not strictly correct to speak of saturated air since space, not air, is saturated. However, that term is commonly used and has the advantage of brevity, if not of literal accuracy. The saturation vapor pressure e_s is a function of temperature. The relationship between e_s and T derived in section 21 is given in tabular form in Table II in the Appendix and is shown graphically in Fig. 133, section 132. The various aspects of saturation are discussed in greater detail in section 126.

The amount of water vapor in the atmosphere may be expressed in any one of four ways. The first of these is in terms of the *absolute humidity*, denoted a , which is the number of grams of water vapor in unit volume, or the density of water vapor. The absolute humidity is then given by (10.4). Thus,

$$a = \epsilon \frac{e}{RT} \quad (10.6)$$

The second measure of water vapor content is the *relative humidity* f , which is defined as the ratio of the actual vapor pressure to the saturation vapor pressure at the temperature of the air in question. The relative humidity is, then

$$f = \frac{e}{e_s} \quad (10.7)$$

If the relative humidity is to be given as a percentage, as is customary in practice, the right-hand side of (10.7) must be multiplied by 100.

The third unit is the *humidity mixing ratio* x , defined as the ratio of the density of water vapor to that of dry air. Using (7.7), with $p - e$ substituted for p , and (10.4), it is seen that

$$x = \frac{\epsilon e}{p - e} \quad (10.8)$$

If the air is saturated, the saturation mixing ratio x_s has the value

$$x_s = \frac{\epsilon e_s}{p - e_s} \quad (10.9)$$

The last measure is the *specific humidity* s , which is the ratio of the density of water vapor to that of moist air. Hence, from (10.4) and

(10.5), it follows that

$$s = \frac{\epsilon e}{p - (1 - \epsilon)e} \quad (10.10)$$

Since p is of the order of one hundred times as great as e , for most practical purposes the latter may be neglected in comparison with the former, and (10.8) and (10.10) become

$$x = s = \frac{\epsilon e}{p} \quad (10.11)$$

or for saturated air

$$x_s = s_s = \frac{\epsilon e_s}{p} \quad (10.12)$$

The absolute humidity is rarely used in meteorology, whereas the relative humidity is used widely. The humidity mixing ratio is often more convenient than the specific humidity for theoretical work, and it will be found frequently in the following sections.

The properties of these units of moisture content and their significance in practical meteorology are discussed in detail in section 81. Their values are in practice usually determined from measurements made with the hygrometer, an instrument described in section 65.

11. Virtual Temperature and Height Computations. For most purposes, the equation of state for dry air may also be used without modification for moist, unsaturated air. On some occasions, however, a more accurate relationship is necessary. The appropriate gas constant R_m for moist, unsaturated air may then be used instead of the gas constant for dry air R . R_m is not constant for all amounts of water vapor in the air, but varies with the vapor pressure e and the total pressure p . The appropriate expression for R_m may be derived in the following manner. The density of moist, unsaturated air is given by (10.5), so that the equation of state for moist, unsaturated air is given by

$$\frac{p}{RT} \left[1 - (1 - \epsilon) \frac{e}{p} \right] = \frac{p}{R_m T} \quad (11.1)$$

and

$$R_m = \frac{R}{1 - (1 - \epsilon) \frac{e}{p}} \quad (11.2)$$

Substituting in (11.2) for e/p from (10.11) leads to an alternate form

$$R_m = \frac{\epsilon R}{\epsilon - x(1 - \epsilon)} \quad (11.3)$$

This equation shows that R_m is a function of the humidity mixing ratio alone.

It is often more convenient to use a different value of the temperature, known as the virtual temperature T_v , rather than a different value for the gas constant. The equation of state for moist, unsaturated air then becomes, using the same procedure as in (11.1)

$$\frac{p}{RT} \left[1 - (1 - \epsilon) \frac{e}{p} \right] = \frac{p}{RT_v} \quad (11.4)$$

and so

$$T_v = \frac{T}{1 - (1 - \epsilon) \frac{e}{p}} \quad (11.5)$$

or with (10.11)

$$T_v = \frac{\epsilon T}{\epsilon - x(1 - \epsilon)} \quad (11.6)$$

Thus the *virtual temperature* of moist, unsaturated air may be defined as the temperature at which dry air of the same pressure would have the same density as the moist air.

Virtual temperature is used to determine the height in the atmosphere corresponding to various pressures as found from aerological ascents. A number of methods of determining heights have been developed, but that of V. Bjerknes and Sandstrom is used widely, and will be given in its broad outlines here.

The statical equation in the form given in (9.2), with T_v substituted for T , since moist air is being considered, may be combined with (8.2) in the differential form to give

$$d\Phi = -RT_v \frac{dp}{p} \quad (11.7)$$

or

$$d\Phi = -RT_v d(\log p) \quad (11.8)$$

On integration, (11.8) becomes

$$\Phi_2 - \Phi_1 = R \int_{\log p_2}^{\log p_1} T_v d(\log p) \quad (11.9)$$

Now on a chart having pressure on a logarithmic scale as ordinate and temperature on a linear scale as abscissa, plot the virtual temperature at each significant point of the aerological ascent against the corresponding pressure. The resulting curve may then appear as depicted in Fig. 10, where the required curve is LM . Consider first

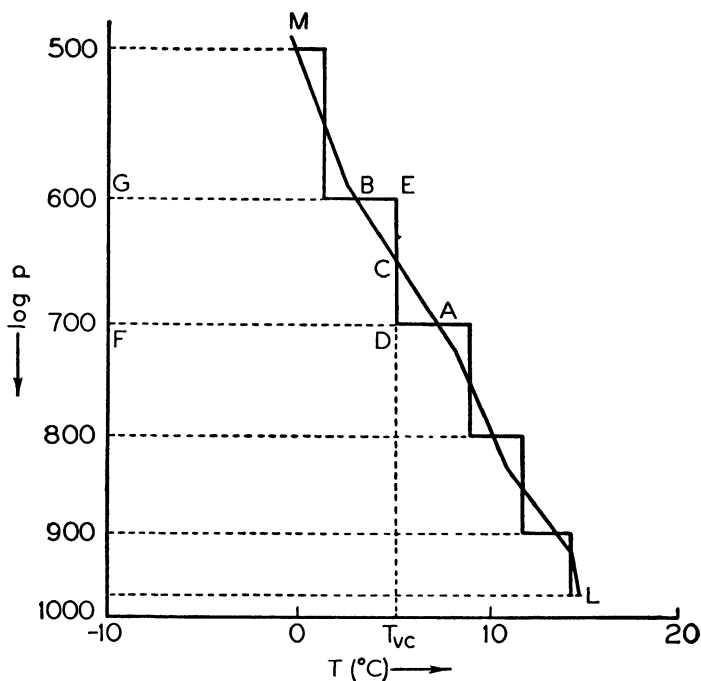


FIG. 10. The computation of heights in the atmosphere.

the portion AB of the curve between 700 and 600 mb, so that $p_1 = 700$ mb and $p_2 = 600$ mb. Draw an isotherm DCE from 700 to 600 mb in such a manner that the area CEB is exactly equal to the area CDA . The virtual temperature at C , T_{vc} , is with sufficient accuracy 5°C .

According to (11.9), the difference in geopotential between 600 and 700 mb is proportional to the area $ABGF$, and since area $CEB = \text{area } CDA$, the difference in geopotential is also proportional to the area $DEGF$. Equation 11.9 may then be written

$$\Phi_2 - \Phi_1 = RT_{vc} \log \frac{p_1}{p_2} \quad (11.10)$$

or in this case

$$\Phi_{600} - \Phi_{700} = R \times 278 \log \frac{700}{600}$$

The difference in geopotential, or in geodynamic height, between any two levels may be computed by means of (11.10). If a similar procedure is followed for other layers, the geodynamic height for the whole column is obtained by a process of summation.

In actual practice, the temperature pressure curve is plotted. Suitable graduations on each standard isobar on the chart permit the rapid determination of the corresponding virtual temperature when the relative humidity is known, without the necessity of having recourse to (11.5) or (11.6). The virtual temperature curve is then plotted beside the other curve. In the above discussion, the cgs system was used, but in practice, the dynamic meter is taken as the unit, so that the difference in geodynamic height between two pressures is obtained. Tables, in which the unit is 0.98 of the dynamic meter, and hence approximately the geometric meter, give the difference in height between the standard isobars, which are 100 mb apart, for various values of the virtual temperature. For the bottom and top portions of the curve which do not extend from one standard isobar to the next a slightly modified procedure is followed. To evaluate the whole ascent, the height differences between the top and bottom of each layer must be added. If now $\log p$ is plotted against height, the resulting curve should be approximately a straight line, and the heights corresponding to the pressures at significant points of the ascent curve can be obtained by interpolation.

PROBLEMS AND EXERCISES

1. (a) Derive the following expression for the vertical distribution of the density when the lapse rate of temperature is constant

$$\rho = \rho_0 \left(\frac{T_0 - \alpha z}{T_0} \right)^{\frac{g}{R\alpha} - 1}$$

Assume that the air is dry and that g is constant.

(b) For what value of the temperature lapse rate is the density constant with height?

2. Assume that the lapse rate of temperature in the troposphere is 6°C per km, whereas the temperature at all heights in the stratosphere is equal to that at the tropopause. Compute the change in surface pressure when the height of the tropopause increases from 10 to 11 km, if initially the surface pressure is 1000 mb, and the surface temperature has a constant value 0°C . Assume that the pressure at a height of 50 km is constant.

Why is the value for the pressure change obtained so much greater than that actually ever observed?

3. Calculate at what height in a dry atmosphere the pressure is one-half of that at the surface when the surface temperature is 10°C , and the lapse rate is (a) 6°C per km, (b) zero. Assume that g is constant.

BIBLIOGRAPHY

- Brunt, D., *Physical and Dynamical Meteorology*, London, Cambridge University Press, 1939. Chapter 2.
- Haurwitz, B., *Dynamic Meteorology*, New York, McGraw-Hill Book Co., 1941. Chapters 1, 2.
- Koschmieder, H., *Dynamische Meteorologie*, Leipzig, Akad. Verlag., 1933. Chapters 1, 2.
- Shaw, Sir N., *Manual of Meteorology*, London, Cambridge University Press. Vol. 3 (1930), Chapter 6.

CHAPTER 3

THERMODYNAMICS OF DRY AIR

12. The First Law of Thermodynamics. In Chapter 2 it was implied that air has a certain heat content, but no attempt was made to consider this heat content in detail. But heat is a form of energy which may be converted into other forms of energy. The study of the dynamical aspect of heat is known as thermodynamics, and it has a wide application to the problems of theoretical meteorology.

The first law of thermodynamics is a statement of the principle of the conservation of energy, expressed in such a manner as to include the energy of heat. Any body in a specified state has an internal energy associated with the configuration and motion of its molecules. It is known that thermal energy may be changed into mechanical energy, i.e., that heat may be converted into work. The first law of thermodynamics states: The heat taken in by a substance is equal to the increase in its internal energy plus the work done by the substance.

The unit of heat in the cgs system is the *calorie*, which is defined as the amount of heat necessary to raise the temperature of one gram of water one degree Centigrade. The cgs unit of work is the *erg*, defined as a force of one dyne acting through a distance of one centimeter. These units are connected by the relationship that 4.18×10^7 ergs are equal to 1 calorie. The mechanical equivalent of heat

$$J = 4.18 \times 10^7 \text{ erg cal}^{-1}$$

In meteorology it is frequently more convenient to use the reciprocal of the mechanical equivalent of heat, denoted by A . It has the value

$$A = 2.39 \times 10^{-8} \text{ cal erg}^{-1}$$

The specific heat c of a substance may be defined as the amount of heat dQ necessary to increase the temperature of one gram of the substance by the amount dT divided by dT . It follows that

$$c = \frac{dQ}{dT}$$

For gases, there are two specific heats to be considered, depending on whether the volume or the pressure is kept constant. The specific

heat at constant volume is denoted as c_v ; the specific heat at constant pressure is denoted as c_p . For air

$$c_v = 0.170 \text{ cal gm}^{-1} \text{ deg}^{-1}$$

$$c_p = 0.239 \text{ cal gm}^{-1} \text{ deg}^{-1}$$

The work done by a gas as it expands may be obtained in the following manner. Let S_1 and S_2 denote the surface of a gas before and after a small expansion against an external pressure p which is constant over the surface (Fig. 11). The pressure of the gas under consideration is assumed to be slightly greater than the external pressure. Consider the element dS of the surface and denote its displacement along the normal as dn . The work done by the gas as it expands is then

$$\Sigma(p dS) dn = p \Sigma dS dn = p dV$$

Therefore, the work dW done by unit mass of the gas is

$$dW = p dv \quad (12.1)$$

Expressed in heat units, (12.1) becomes

$$dW = A p dv \quad (12.2)$$

Consider first the case in which an amount of heat dQ_1 is supplied to unit mass of the gas, volume remaining constant. Then

$$dQ_1 = c_v dT \quad (12.3)$$

This expression gives the increase in internal energy of the gas. If now the volume is permitted to increase by an amount dv , the work done is given by (12.2). When heat dQ is supplied, then, and temperature and volume vary simultaneously, it follows that

$$dQ = dQ_1 + dW = c_v dT + A p dv \quad (12.4)$$

This expression states the first law of thermodynamics in mathematical form.

The relationship between c_p and c_v may be readily obtained with the aid of (12.4). Differentiation of (7.6) leads to

$$p dv = -v dp + R dT$$

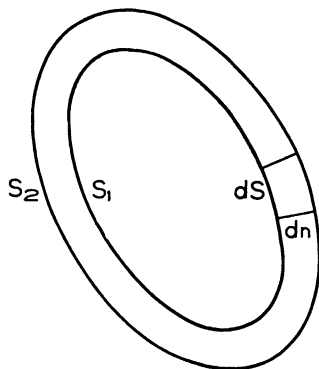


FIG. 11. The work done through the expansion of a gas.

Substitute this expression in (12.4) to obtain

$$dQ = (c_v + AR) dT - A v dp \quad (12.5)$$

If the pressure is constant, $dp = 0$, and from (12.5) it follows that the specific heat at constant pressure

$$c_p = \left(\frac{\partial Q}{\partial T} \right)_p = c_v + AR \quad (12.6)$$

This relationship holds for a perfect gas, and it is therefore applicable to air as long as it remains unsaturated.

13. Adiabatic Relationships for Dry Air. Potential Temperature.

If a mass of a substance such as air undergoes variations in state in such a manner that there is no exchange of heat between the substance and its environment, the process by which this occurs is said to be *adiabatic*. When this condition is fulfilled, (12.5) becomes

$$c_p dT = A v dp$$

or, with (7.6)

$$\frac{dT}{T} = \frac{AR}{c_p} \frac{dp}{p} \quad (13.1)$$

Integration of (13.1) leads to

$$\frac{T}{T_0} = \left(\frac{p}{p_0} \right)^\kappa \quad (13.2)$$

where T_0 is the temperature at pressure p_0 and

$$\kappa = \frac{AR}{c_p} = 0.288$$

Substituting (7.6) in (13.2) gives a second form

$$\frac{v_0}{v} = \left(\frac{p}{p_0} \right)^{1-\kappa} \quad (13.3)$$

and substituting (7.7) in (13.2) leads to a third form for the adiabatic relationship

$$\frac{\rho}{\rho_0} = \left(\frac{p}{p_0} \right)^{1-\kappa} \quad (13.4)$$

It is frequently desirable to have some property of dry air which is invariant during adiabatic processes. Such a property is the *potential temperature* θ , defined as the temperature which the air would attain if brought adiabatically to a standard pressure, usually 1000 mb.

From (13.2) it can be seen that

$$\theta = T \left(\frac{1000}{p} \right)^{0.288} \quad (13.5)$$

The fact that θ is invariant for adiabatic processes may be readily demonstrated. Assume that initially the air at pressure p_0 has a temperature T_0 . According to (13.5), its potential temperature θ_0 is given by

$$\theta_0 = T_0 \left(\frac{1000}{p_0} \right)^{\kappa} \quad (13.6)$$

If, as a result of an adiabatic process, its pressure becomes p_1 , then, according to (13.2), its temperature

$$T_1 = T_0 \left(\frac{p_1}{p_0} \right)^{\kappa} \quad (13.7)$$

The potential temperature of the air is now, from (13.5),

$$\theta_1 = T_1 \left(\frac{1000}{p_1} \right)^{\kappa} \quad (13.8)$$

By substituting for T_1 from (13.7) in (13.8), it follows that

$$\theta_1 = T_0 \frac{p_1^{\kappa}}{p_0^{\kappa}} \times \frac{1000^{\kappa}}{p_1^{\kappa}} = T_0 \left(\frac{1000}{p_0} \right)^{\kappa} \quad (13.9)$$

By comparing (13.6) and (13.9), it is seen that $\theta_0 = \theta_1$. Thus, no matter how many adiabatic processes occur, the potential temperature of the air in question does not change.

In the atmosphere, no processes are completely adiabatic, since there is some mixing between a given mass of air and the surrounding air, and there may be loss or gain of heat by radiation. However, these are secondary effects, and they may usually be neglected. A discussion of the practical aspects of the use of potential temperature is given in section 80 and after.

14. The Dry Adiabatic Lapse Rate. The Stability of Dry Air. The rate of change of temperature with pressure of air ascending or descending adiabatically is given in (13.1). In order to find the rate of change of temperature with height, (9.3) may be utilized in the form

$$\frac{dp}{p} = - \frac{g}{R\bar{T}} dz$$

where \bar{T} indicates the temperature of the surrounding air, not that of the air undergoing adiabatic vertical motion, which is denoted T .

Combining (13-1) and (9-3) in the form given above, it follows that

$$-\frac{dT}{dz} = \frac{Ag}{c_p} \frac{T}{\bar{T}} \quad (14-1)$$

T is very nearly equal to \bar{T} , the difference between the two temperatures being of the order of 1 or 2 per cent of their value. Their ratio may then be taken as unity with sufficient accuracy for most purposes. This rate of decrease of temperature with height of adiabatically ascending dry air is known as the *dry adiabatic lapse rate* Γ , and is given by

$$\Gamma = \frac{Ag}{c_p} = 9.8^\circ \text{ C km}^{-1} \quad (14-2)$$

In most practical work the value of Γ is taken to be $10^\circ \text{ C per km}$.

It follows from (14-2) that, on a chart having height as ordinate and temperature as abscissa, the curve representing the variation of temperature with height of dry air moving adiabatically is a straight line. Such a line, which represents graphically the dry adiabatic lapse rate, is known as a *dry adiabat*. For many purposes, however, it is more convenient to use a chart on which temperature and pressure, rather than temperature and height, may be plotted. A chart of this type, having pressure on a logarithmic scale as ordinate and temperature on a linear scale as abscissa, has already been mentioned in section 11. With the aid of (13-2) it is possible to construct dry adiabats on this diagram, as shown in Fig. 12. The dry adiabats on this chart, descending from left to right, are not straight lines, but their curvature is very small. Since it is possible to determine readily the variation of temperature with pressure during adiabatic processes by means of this chart, it is known as an *adiabatic chart*. The potential temperature of a mass of air may also be found directly from this chart. It is obtained by proceeding from the point in the diagram representing the condition of the air along the dry adiabat through that point until standard pressure (1000 mb) is reached. The temperature at standard pressure is then the potential temperature.

This chart may be used in the discussion of the stability of dry air. Let the curve $ABCDE$ in Fig. 12 represent the variation of temperature with pressure as found by means of an aerological ascent. Consider first a mass of air in the layer AB which has temperature T_1 and pressure p_1 . Now give this air an upward displacement. As it ascends, its temperature decreases at the dry adiabatic lapse rate, so that by the time it reaches pressure p_2 , its temperature is T_2 . Assuming that the surrounding air has not been disturbed by this displacement, the

temperature of the surrounding air at p_2 is \bar{T}_2 . But since $T_2 > \bar{T}_2$, the displaced air is lighter than its environment, and if the displacing force ceases to act, it continues to rise until it comes into equilibrium with the surrounding air. Similarly, if the air has been displaced downward, it will continue to subside after the force acting upon it is released. The air (p_1, T_1) is then said to be in unstable equilibrium. The same considerations apply to any mass of air in the layer AB , so that from

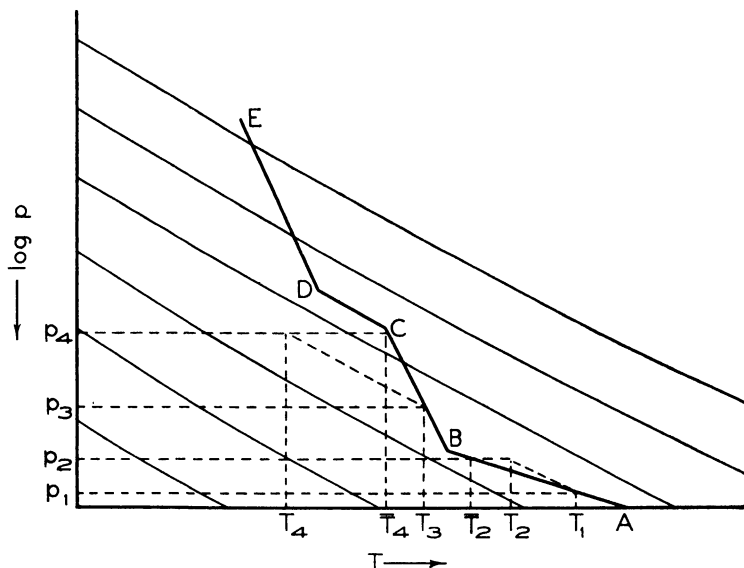


FIG. 12. The relation between lapse rate and stability.

A to B the lapse rate is of the unstable type. The condition for instability is that the lapse rate of the environment shall be greater than the dry adiabatic lapse rate. Next consider a mass of air (p_3, T_3) in the layer BC . Let this air be displaced dry adiabatically from p_3 to p_4 . At p_4 , the temperature of the displaced air is T_4 , and that of the environment is \bar{T}_4 . In this case $T_4 < \bar{T}_4$, the displaced air is heavier than the surrounding air, and if the displacing force is removed, the air sinks back to its initial position. Similarly, air displaced downward tends to return to its initial position. This air is said to be in stable equilibrium. From B to C the lapse rate is of the stable type. The criterion for stability is that the lapse rate of the environment shall be less than the dry adiabatic lapse rate. Similar considerations show that a mass of air in the layer CD , if given an upward displacement, will neither continue to ascend nor descend to its initial position when the

displacing force is removed, but it will remain at the pressure attained as a result of the displacement. The air is then in neutral equilibrium, and the lapse rate is of the neutral type. The criterion for neutral equilibrium is that the lapse rate of the environment shall be equal to the dry adiabatic lapse rate. If the lapse rate of the environment is denoted by α , then the criteria may be stated in the following form.

$$\begin{array}{ll} \text{Unstable} & \alpha > \Gamma \\ \text{Stable} & \alpha < \Gamma \\ \text{Neutral} & \alpha = \Gamma \end{array}$$

15. The Adiabatic Lapse Rate for Moist, Unsaturated Air. The humidity mixing ratio of a mass of air is given by the mass of the water vapor per unit mass of dry air. This follows directly from the definition given in section 10. From this method of expressing the mixing ratio, it follows that it is invariant during ascent or descent, as long as condensation and evaporation processes do not occur and if mixing with the surrounding atmosphere is so small as to be negligible. It will now be shown that the lapse rate for moist, unsaturated air is a function of the mixing ratio, but that this lapse rate is, for all practical purposes, the same as the dry adiabatic lapse rate.

The specific heat at constant pressure of 1 gm of moist, unsaturated air is given by

$$c_{pm} = \frac{c_p + xc'_p}{1 + x} \quad (15.1)$$

where c'_p is the specific heat for water vapor at constant pressure. By using this value for the specific heat and the gas constant R_m for moist, unsaturated air given in (11.3), (13.1) becomes

$$\frac{dT}{T} = \frac{AR_m}{c_{pm}} \frac{dp}{p} \quad (15.2)$$

where p is now the total pressure. Substituting for c_{pm} and R_m , (15.2) becomes

$$\begin{aligned} \frac{dT}{T} &= \frac{A(1+x)\epsilon R}{(c_p + xc'_p)[\epsilon - (1-\epsilon)x]} \frac{dp}{p} \\ &= \frac{A(1+x)\epsilon R}{c_p \left(1 + x \frac{c'_p}{c_p}\right)[\epsilon - (1-\epsilon)x]} \frac{dp}{p} = \frac{AR}{bc_p} \frac{dp}{p} \end{aligned} \quad (15.3)$$

where

$$b = \frac{\left(1 + x \frac{c'_p}{c_p}\right)[\epsilon - (1-\epsilon)x]}{\epsilon(1+x)} \quad (15.4)$$

Now

$$c_p' = 0.465 \text{ cal gm}^{-1} \text{ deg}^{-1}$$

$$c_p = 0.239 \text{ cal gm}^{-1} \text{ deg}^{-1}$$

and

$$\epsilon = 0.622$$

By substituting these values in (15.4) and neglecting x^2 in comparison with x , the equation becomes

$$b = \frac{1 + 1.95x}{1 + 1.61x} = 1 + 0.34x \quad (15.5)$$

Integrating (15.3) gives, then,

$$\frac{T}{T_0} = \left(\frac{p}{p_0} \right)^{\kappa_m} \quad (15.6)$$

where

$$\kappa_m = \frac{AR}{(1 + 0.34x)c_p}$$

Since x is of the order of 10^{-2} , $\kappa_m \approx \kappa$, and (13.2) and (15.6) may be considered as identical. If the moisture content of the environment is taken into account, (9.3) becomes

$$\frac{dp}{p} = - \frac{g}{R\bar{T}_v} dz \quad (15.7)$$

where \bar{T}_v is the virtual temperature of the environment at the pressure under consideration. Combining (15.3) and (15.7) gives

$$- \frac{dT}{dz} = \frac{Ag}{c_p(1 + 0.34x)} \frac{T}{\bar{T}_v} \quad (15.8)$$

Since \bar{T}_v is very little different in value from T , their ratio may be taken as unity, as was done with T and \bar{T} in section 14, and (15.8) becomes

$$- \frac{dT}{dz} = \frac{Ag}{c_p(1 + 0.34x)} \quad (15.9)$$

The error involved in expressing (15.8) as (15.9), or (14.1) as (14.2), will, in practically all cases, be greater than that involved in neglecting $0.34x$ in comparison with 1. It is therefore permissible to state that the adiabatic lapse rate for moist, unsaturated air Γ_m is given by

$$\Gamma_m = \frac{Ag}{c_p} = 9.8^\circ \text{ C km}^{-1} \quad (15.10)$$

Equations 14.2 and 15.10 are identical, and the same equation may be used for the adiabatic lapse rate, whether the air is completely dry or not. The only restriction imposed is that the air shall not be saturated.

16. The Effect of Ascent and Descent on Lapse Rate and Stability.

The ascent and descent of air masses of broad horizontal extent is a frequent occurrence in the atmosphere. When such vertical motions occur, the lapse rate of the air in question usually changes. The

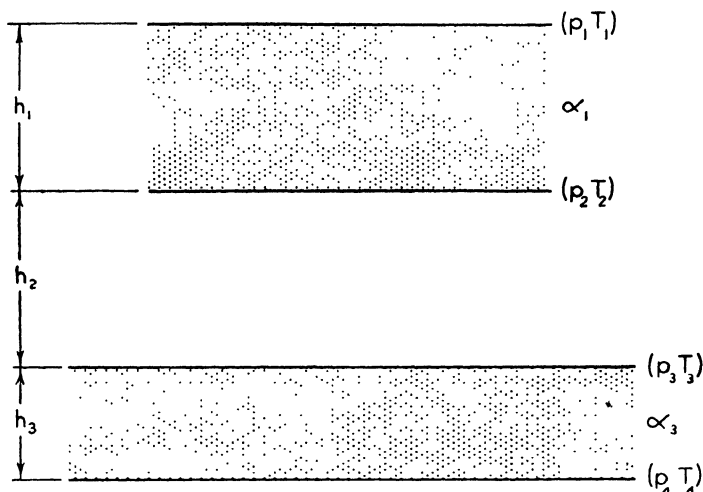


FIG. 13. Variation of lapse rate with subsidence of a layer of the atmosphere.

variation of lapse rate with height, or with pressure, may be determined in the following manner. In Fig. 13, a layer of air is shown before and after subsidence has taken place. At the top of the layer, initially the pressure is p_1 , and the temperature is T_1 , whereas at the bottom of the layer, the pressure is p_2 , and the temperature is T_2 . The lapse rate in the layer is α_1 , and the vertical thickness of the layer is h_1 . After subsidence has occurred, the conditions at the top of the layer are denoted (p_3, T_3) , and those at the bottom are denoted (p_4, T_4) . The top of the layer has subsided through a vertical distance $h_1 + h_2$, and the bottom through a distance $h_2 + h_3$. The new lapse rate resulting from the subsidence is α_3 . To find the value of α_3 , it will first be evaluated in terms of α_1 and h_1 and h_3 , and then in terms of α_1 , p_1 , p_2 , p_3 , and p_4 .

Initially

$$T_2 - T_1 = \alpha_1 h_1 \quad (16.1)$$

and finally,

$$T_4 - T_3 = \alpha_3 h_3 \quad (16.2)$$

In addition, T_1 and T_3 , T_2 and T_4 are related in the following manner.

$$T_3 - T_1 = \Gamma(h_1 + h_2) \quad (16.3)$$

$$T_4 - T_2 = \Gamma(h_2 + h_3) \quad (16.4)$$

By subtracting (16.3) from (16.4), it follows that

$$(T_4 - T_3) - (T_2 - T_1) = \Gamma(h_3 - h_1) \quad (16.5)$$

Substituting (16.1) and (16.2) in (16.5) and rearranging lead to

$$\alpha_3 = \alpha_1 \frac{h_1}{h_3} - \Gamma \left(\frac{h_1}{h_3} - 1 \right) \quad (16.6)$$

To the right-hand side of (16.6) add α_1 and subtract $\alpha_1 \frac{h_3}{h_3}$, and after rearranging further, (16.6) becomes

$$\alpha_3 = \alpha_1 - (\Gamma - \alpha_1) \left(\frac{h_1 - h_3}{h_3} \right) \quad (16.7)$$

Consider now three cases when the initial lapse rate of the layer is less than, equal to, or greater than the dry adiabatic lapse rate.

(a) $\alpha_1 < \Gamma$. If contraction in the vertical accompanies the vertical motion of the layer, $h_1 > h_3$, and it is seen that $\alpha_3 < \alpha_1$. This decrease in lapse rate means that a corresponding increase in stability takes place. If, on the other hand, vertical expansion of the layer occurs, $h_1 < h_3$, and it follows that $\alpha_3 > \alpha_1$. A decrease in stability results from this increase in lapse rate.

(b) $\alpha_1 = \Gamma$. When the actual lapse rate in the layer is the same as the dry adiabatic lapse rate, vertical motion of the layer does not produce any change in lapse rate, irrespective of any expansion or contraction that may occur.

(c) $\alpha_1 > \Gamma$. A similar application of (16.7) shows that, in this case, vertical contraction leads to an increase in lapse rate and, consequently, a further increase in the degree of instability of the air in the layer. Conversely, vertical expansion decreases the lapse rate, and thus decreases the instability.

If it is desired to evaluate the variation in lapse rate in terms of changes in pressure, rather than in terms of changes in height, the following modification is introduced. The relationship between the pressure at the bottom and top of a layer having lapse rate α_1 , accord-

ing to (9.9), may be expressed as

$$\left(\frac{p_1}{p_2}\right)^{\frac{R\alpha_1}{\theta}} = 1 - \frac{\alpha_1 h_1}{T_2}$$

or

$$h_1 = \frac{T_2}{\alpha_1} \left[1 - \left(\frac{p_1}{p_2}\right)^{\frac{R\alpha_1}{\theta}} \right] \quad (16.8)$$

Expanding $(p_1/p_2)^{\frac{R\alpha_1}{\theta}}$ in series results in

$$\left(\frac{p_1}{p_2}\right)^{\frac{R\alpha_1}{\theta}} = 1 + \frac{R\alpha_1}{g} \log \frac{p_1}{p_2} + \frac{R^2 \alpha_1^2}{2g^2} \left(\log \frac{p_1}{p_2} \right)^2 + \text{higher terms} \quad (16.9)$$

Under average lapse rate conditions, i.e., $\alpha_1 \approx 6^\circ \text{C km}^{-1}$, $R\alpha_1/g$ is of the order of 0.2. If conditions in the lower troposphere only, where $p_1 > 500$ mb, are considered, and only layers such that $p_2 - p_1 < 200$ mb are taken, then

$$\frac{R\alpha_1}{g} \gg \frac{R^2 \alpha_1^2}{2g^2} \quad \text{and} \quad \left| \log \frac{p_1}{p_2} \right| > \left(\log \frac{p_1}{p_2} \right)^2$$

and to a first approximation, (16.9) becomes

$$\left(\frac{p_1}{p_2}\right)^{\frac{R\alpha_1}{\theta}} = 1 + \frac{R\alpha_1}{g} \log \frac{p_1}{p_2} \quad (16.10)$$

By substituting (16.10) in (16.8), the latter becomes

$$h_1 = - \frac{T_2 R}{g} \log \frac{p_1}{p_2} \quad (16.11)$$

Similarly,

$$h_3 = - \frac{T_4 R}{g} \log \frac{p_3}{p_4} \quad (16.12)$$

Substituting (16.11) and (16.12) in (16.7) then gives

$$\alpha_3 = \alpha_1 - (\Gamma - \alpha_1) \left(\frac{T_2 \log \frac{p_1}{p_2}}{T_4 \log \frac{p_3}{p_4}} - 1 \right) \quad (16.13)$$

According to (13.2)

$$\frac{T_2}{T_4} = \left(\frac{p_2}{p_4} \right)^\kappa$$

Substituting in (16.13) then gives

$$\alpha_3 = \alpha_1 - (\Gamma - \alpha_1) \left(\frac{p_2^\kappa \log \frac{p_1}{p_2}}{p_4^\kappa \log \frac{p_3}{p_4}} - 1 \right) \quad (16.14)$$

where $\kappa = 0.288$. A further simplification may be introduced in (16.14) by expanding the logarithmic terms in series. Thus

$$\log \frac{p_1}{p_2} = \left(\frac{p_1}{p_2} - 1 \right) - \frac{1}{2} \left(\frac{p_1}{p_2} - 1 \right)^2 + \text{higher terms} \quad (16.15)$$

The logarithmic term in the denominator of (16.14) may be similarly expanded. If only thin layers are considered, such that $p_2 - p_1$ and $p_4 - p_3 < 100$ mb, then only the first term need be retained, and (16.14) becomes

$$\alpha_3 = \alpha_1 - (\Gamma - \alpha_1) \left[\frac{p_2^{\kappa-1} (p_1 - p_2)}{p_4^{\kappa-1} (p_3 - p_4)} - 1 \right] \quad (16.16)$$

It must be emphasized that (16.14) and (16.16) are valid only for the lower troposphere, and for comparatively thin layers. The greater the pressures and the thinner the layers, the greater the accuracy of these expressions becomes. In practice these limitations are not serious, as a knowledge of the variation of lapse rate with ascent or descent is usually required only in the lower atmosphere, and for relatively thin layers. The accuracy of (16.7) is greater than that of either (16.14) or (16.16), but even the use of (16.7) involves a slight error, since the value of Γ , $9.8^\circ \text{ C per km}$, is only approximate, as shown by (14.1).

If an adiabatic chart, or one of the thermodynamic charts discussed in section 22, is available, the variation of lapse rate may be determined directly. It is only necessary to plot the pressure and temperature at the top and bottom of the layer in its initial position, and then move along the appropriate dry adiabats until the pressures at top and bottom of the layer in its final position are reached. The change in lapse rate may then be determined in a qualitative manner by inspection.

The variation of lapse rate which results from vertical displacement is of considerable significance in meteorology. This effect is especially noticeable in anticyclones, where the subsidence of the air often produces a marked decrease in lapse rate and a corresponding increase in

stability. The significance of the foregoing results will be brought out in greater detail in Chapter 15.

17. The Carnot Cycle. Heat Engine Efficiency. In section 12 it was shown that when a gas expands it does work on the environment. The work done by a unit mass of gas as it changes from its initial state

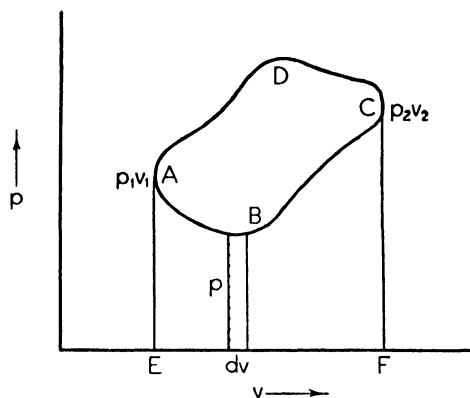


FIG. 14. Work on an indicator diagram.

denoted p_1, v_1 to its final state p_2, v_2 may be evaluated graphically by means of the indicator diagram. In this diagram, the ordinate is pressure and the abscissa specific volume, both on linear scales. Consider, for example, the indicator diagram shown in Fig. 14. According to (12.1), the work done, dW , when the unit mass of gas increases in volume by the amount dv is $p dv$, which is the stippled element of area shown in the diagram. The total work done by the gas as its state changes from p_1, v_1 to p_2, v_2 along the path ABC is then the summation of such elements of area under the curve, which is the area $ABCFEA$. If now the gas at p_2, v_2 returns to its initial state along the same path work must be done on the gas by the environment, since in this case the gas must be compressed as it returns. The amount of work done on the gas in this second stage is exactly the same as that done by the gas in the first stage, so the net amount of work done in the process is zero. If, however, the gas returns, not by the path CBA , but by the path CDA , the resulting amount of work is not zero. The work done on the gas by the environment in this instance is given by the area $ADCFEA$. There is then a net amount of work done on the gas equal to the area $ABCD A$. This fact may be stated in another manner by saying that the work done by the gas as it completes a cycle on the indicator diagram in a counterclockwise manner is negative. If the state changes from p_1, v_1 to p_2, v_2 along the path ADC and returns to p_1, v_1 along the path CBA , i.e., the cycle is carried out in a clockwise manner, the work done by the gas is positive and equal in amount to the area $ABCD A$.

The equations for adiabatic and isothermal changes of dry air in terms of potential temperature on the indicator diagram will now be derived.

Equation 13.3 for adiabatic motion may be expressed as

$$pv^{\frac{1}{1-\kappa}} = p_0 v_0^{\frac{1}{1-\kappa}} \quad (17.1)$$

If the ratio c_p/c_v be denoted γ , then, since

$$\kappa = \frac{c_p - c_v}{c_p} = \frac{AR}{c_p}$$

(17.1) becomes

$$pv^\gamma = p_0 v_0^\gamma \quad (17.2)$$

The temperature of air having pressure p_0 and specific volume v_0 is by definition θ , the potential temperature, so that from (7.6) it follows that

$$p_0 v_0 = R\theta \quad (17.3)$$

Equation 17.3 may be rearranged so as to take the form

$$p_0 v_0^\gamma = j\theta^\gamma \quad (17.4)$$

where the constant

$$j = p_0^{1-\gamma} R^\gamma$$

Combining (17.2) and (17.4) then gives the desired form of the adiabatic equation on the indicator diagram.

$$pv^\gamma = j\theta^\gamma \quad (17.5)$$

Each adiabat on the indicator diagram may thus be designated by a value of the potential temperature.

The amount of heat Q which must be supplied to the air to permit it to move isothermally from adiabat θ_1 to adiabat θ_2 on the indicator diagram will next be obtained. Since T is constant, with the use of (7.6) (12.5) becomes

$$dQ = -Av dp = -ART \frac{dp}{p}$$

By integrating,

$$Q = -ART \int_{p_1}^{p_2} \frac{dp}{p} = ART \log \frac{p_1}{p_2} \quad (17.6)$$

From (13.5) it follows that

$$\left(\frac{p_1}{p_2}\right)^\kappa = \frac{\theta_2}{\theta_1}$$

or

$$\log \frac{p_1}{p_2} = \frac{c_p}{AR} \log \frac{\theta_2}{\theta_1} \quad (17.7)$$

Substituting (17.7) in (17.6) leads to the required equation for isothermal motion,

$$Q = c_p T \log \frac{\theta_2}{\theta_1} \quad (17.8)$$

This equation shows that the quantity of heat which must be supplied to the air to permit it to go isothermally from one adiabat to another adiabat is proportional to the Absolute temperature T of the isothermal.

Since T is constant, the equation for the isothermals on the indicator diagram is, from (7.6),

$$pv = RT = \text{Constant} \quad (17.9)$$

It is now possible with the aid of (17.5) and (17.9) to draw adiabats and isothermals on the indicator diagram. Two adiabats, denoted θ_1 and θ_2 , and two isothermals,

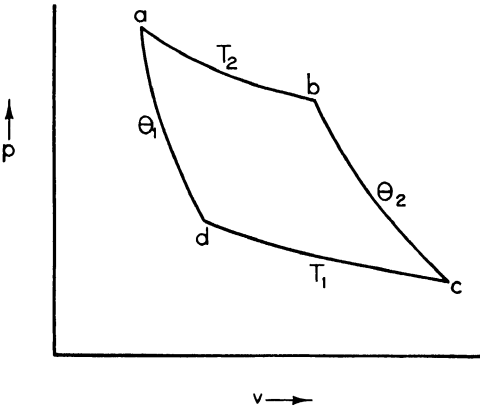


FIG. 15. Carnot cycle.

denoted T_1 and T_2 , on such a chart are shown in Fig. 15. Consider a cycle of changes around the curve $abcda$. The amount of heat which must be supplied to the air to carry it from a to b isothermally at temperature T_2 is, according to (17.8),

$$Q_2 = c_p T_2 \log \frac{\theta_2}{\theta_1} \quad (17.10)$$

The change from b to c is adiabatic, so no heat is supplied. From c to d , heat must be removed of amount

$$Q_1 = c_p T_1 \log \frac{\theta_2}{\theta_1} \quad (17.11)$$

The final stage from d to a is adiabatic, and no heat is supplied or removed.

A cycle of this type, comprising two isothermal and two adiabatic

stages is known as a *Carnot cycle*. It is a cycle of the reversible type. If the process is carried out in the reverse order, counterclockwise around *adcba*, all the operations will be repeated in the inverse order and in the opposite sense. As was shown by means of Fig. 14, the unit mass of air does work on the environment in the original cycle described. When the cycle is carried out in the reverse order, the environment does work on the air.

The Carnot cycle may also be thought of in terms of a reversible heat engine. Such an engine takes in heat Q_2 at temperature T_2 and rejects heat Q_1 at temperature T_1 , the changes in temperature from T_2 to T_1 and from T_1 to T_2 taking place adiabatically. The mechanical work W done in the cycle is equal to the area *abcd*. Since Q_2 is the heat taken in at T_2 along *ab*, and Q_1 is the heat given out at T_1 along *cd*, and as there is no heat transfer along *bc* or *da*, the mechanical work done must also be equal to $Q_2 - Q_1$, expressed in work units. The *efficiency of a heat engine* is defined as the ratio,

$$\text{Efficiency} = \frac{\text{Work output}}{\text{Heat input}}$$

The efficiency of a reversible heat engine is, then,

$$\frac{Q_2 - Q_1}{Q_2} = 1 - \frac{Q_1}{Q_2}$$

If (17·10) and (17·11) are substituted in the above equation, it follows that

$$\text{Efficiency of a reversible engine} = 1 - \frac{T_1}{T_2} \quad (17\cdot12)$$

Carnot's principle and the second law of thermodynamics are implicit in the above treatment. Carnot's principle states that a reversible engine can produce the maximum amount of mechanical work derivable from a given quantity of heat lowered through a given range of temperature. The axiom known as the second law of thermodynamics was stated by Clausius as follows: It is impossible for a self-acting machine, unaided by any external agency, to convey heat from one body to another at a higher temperature.

18. Entropy. By referring again to Fig. 15, it can be seen that the amount of heat which must be supplied to unit mass of air at *a* to take it to *c* along the path *abc* is, according to (17·10),

$$Q_2 = c_p T_2 \log \frac{\theta_2}{\theta_1} \quad (18\cdot1)$$

Similarly, if it goes from a to c along the path adc , the heat supplied is, from (17.11),

$$Q_1 = c_p T_1 \log \frac{\theta_2}{\theta_1} \quad (18.2)$$

It can be seen from this example that the amount of heat which must be supplied to unit mass of air to change its state from p_1, v_1 to p_2, v_2 is not a function of the initial and final states alone, but also depends on the path by which the transformation occurs.

If (18.1) is divided by T_2 and (18.2) by T_1 , the equations become

$$\frac{Q_2}{T_2} = c_p \log \frac{\theta_2}{\theta_1} \quad (18.3)$$

$$\frac{Q_1}{T_1} = c_p \log \frac{\theta_2}{\theta_1} \quad (18.4)$$

If the heat supplied depends on the path, (18.3) and (18.4) show that the heat divided by the temperature at which it is supplied is independent of the path. The quantity Q/T , or the more general expression $\int \frac{dQ}{T}$, is known as the *entropy* ϕ and occupies a fundamental position in thermodynamical theory. It is defined by the equation

$$d\phi = \frac{dQ}{T} \quad (18.5)$$

In the preceding discussion, the transformation from one state to another state was accomplished by one isothermal process and one adiabatic process. Any type of transformation, however, may be treated in a similar fashion by assuming the path to be made up of a series of infinitesimal isothermals and adiabats, and the result is the same.

From (18.3) or (18.4) it may be seen that the increase in entropy from a to c is given by

$$\phi_c - \phi_a = c_p \log \frac{\theta_c}{\theta_a} \quad (18.6)$$

Equation 18.6 may also be derived by substituting dQ from (12.5) in (18.5), using the differential form of (13.5), and then integrating. Since only changes of entropy, not its absolute magnitude, are of significance, (18.6) may be expressed

$$\phi = c_p \log \theta \quad (18.7)$$

Since the change of entropy during a reversible process is a function

of the initial and final states only, it follows that during a reversible cycle, with the air returning to its initial state, there is no change in entropy. If, during the process, heat is lost by some irreversible process such as conduction, the cycle is no longer reversible, and there is a net increase in the entropy of the system. It is therefore necessary to be certain that no irreversible processes occur before assuming the constancy of the entropy during a cycle.

An expression for the entropy of dry air may be derived by substituting dQ from (12.5) in (18.5). With (7.6), it follows that

$$d\phi = c_p \frac{dT}{T} - AR \frac{dp}{p} \quad (18.8)$$

In meteorology, it is frequently assumed for the purposes of computation that air at a pressure of 1000 mb and with a temperature of 100°A has zero entropy. Integrating (18.8) on this assumption gives for the entropy of 1 gm of dry air

$$\phi = c_p \log \frac{T}{100} - AR \log \frac{p}{1000} \quad (18.9)$$

The entropy with respect to some unspecified level of entropy may then be stated as

$$\phi = c_p \log T - AR \log p \quad (18.10)$$

The entropy ϕ' of 1 gm of saturated water vapor at temperature T is equal to the entropy of 1 gm of liquid water at the same temperature plus the entropy necessary to convert it into vapor. Thus

$$\phi' = \int c \frac{dT}{T} + \frac{L}{T} \quad (18.11)$$

where c is the specific heat of liquid water in contact with its saturated vapor, and L is the latent heat of vaporization at temperature T . The assumption that c is constant involves little error, and (18.11) may be written

$$\phi' = c \log T + \frac{L}{T} \quad (18.12)$$

By combining (18.10) and (18.12) and modifying slightly, it is seen that the entropy ϕ_s of 1 gm of saturated air is given by

$$\begin{aligned} \phi_s = \frac{\phi + x_s \phi'}{1 + x_s} &= \frac{c_p + x_s c}{1 + x_s} \log T - \frac{AR}{1 + x_s} \log (p - e_s) \\ &+ \frac{Lx_s}{(1 + x_s)T} \end{aligned} \quad (18.13)$$

$p - e_s$ represents the partial pressure of the dry air and therefore must be used instead of p .

Equation 18-13 cannot be used without modification for the entropy of unsaturated air, since the latent heat of vaporization L is defined as the quantity of heat which is necessary to evaporate 1 gm of liquid water in contact with its saturated vapor. If the entropy of 1 gm of unsaturated water vapor at temperature T is required, the process of evaporation must be considered as taking place at the dew-point temperature T_d , and then the additional entropy required to raise the temperature from T_d to T must be computed.

PROBLEMS AND EXERCISES

1. A layer of dry air extending from 700 to 650 mb has a lapse rate of 1°C per km. If this layer subsides in such a manner that the pressure difference between the bottom and top of the layer does not change during the descent, through what pressure interval must the layer subside if it is to become isothermal?

2. A unit mass of dry air undergoes a reversible cycle of changes. If this cycle is represented by a closed curve on a diagram having entropy as ordinate and temperature as abscissa, show that the work done during the cycle is equal to the area enclosed by the curve. In addition, show that if the cycle is performed in the clockwise direction, work is done on the environment by the air and, conversely, that if the cycle is performed in the counterclockwise direction, work is done on the air by the environment.

BIBLIOGRAPHY

- Brunt, D., *Physical and Dynamical Meteorology*, London, Cambridge University Press, 1939. Chapters 2, 3, 4.
- Haurwitz, B., *Dynamic Meteorology*, New York, McGraw-Hill Book Co., 1941. Chapters 2, 3, 4.
- Koschmieder, H., *Dynamische Meteorologie*, Leipzig, Akad. Verlag., 1933. Chapter 3.
- Shaw, Sir N., *Manual of Meteorology*, London, Cambridge University Press. Vol. 3 (1930), Chapter 6.

CHAPTER 4

THERMODYNAMICS OF MOIST AIR

19. The Clausius-Clapeyron Equation. One of the most interesting applications of thermodynamic theory to problems associated with meteorology is the use of the classical Clausius-Clapeyron equation to determine the rate of change of saturation vapor pressure with temperature. This equation may be derived through the consideration of a specific Carnot cycle.

Consider first a liquid enclosed in a cylinder with a piston at one end. The space between the surface of the liquid and the piston is occupied by saturated vapor at pressure p , which is a function of the temperature only. Keeping the temperature constant, increase the volume by raising the piston. Some of the liquid will then evaporate to maintain the vapor pressure constant. Thus while some liquid remains, increasing volume leaves the pressure unchanged. It follows, then, that the isothermal of a liquid and its vapor in equilibrium is a line of constant pressure. In the p - v diagram shown in Fig. 16, this process is represented by the horizontal lines AB or $A'B'$. When the volume has been increased until all the liquid has evaporated, as at B , a further increase in volume will lead to a decrease in pressure, as in a gas. If, on the other hand, the piston is depressed so that the volume decreases, condensation of the vapor will occur. When all the vapor has condensed, as at A , a further compression leads to a very great increase in pressure, as shown in the figure, because liquids have a very low compressibility.

Fig. 16 shows that the length of the horizontal portion AB or $A'B'$ of the isothermal decreases with increasing temperature until, for the isothermal indicated by a broken line, it reduces to an infinitesimal length. This latter isothermal is known as the critical isothermal, and its temperature T_c is known as the critical temperature. The corresponding volume is v_c , and the corresponding pressure is p_c . The state specified by p_c , v_c , and T_c is known as the critical state. For very high temperatures the isothermals become equilateral hyperbolas, as the properties of the substance approach those of a perfect gas. The dotted line and the broken line in the figure divide the area into four sections. In one section the substance acts as a liquid, in another as

a gas, in a third as vapor, and in the fourth as a mixture of liquid and vapor.

Now focus attention on the portion of Fig. 16 under the dotted line, where liquid and vapor co-exist in equilibrium, and assume that the liquid is water and the vapor is water vapor. The lower curve represents an isothermal for water and its vapor for temperature T , and the upper curve a similar isothermal for temperature $T + dT$. Points A and A' represent the condition of 1 gm of liquid water, and points B

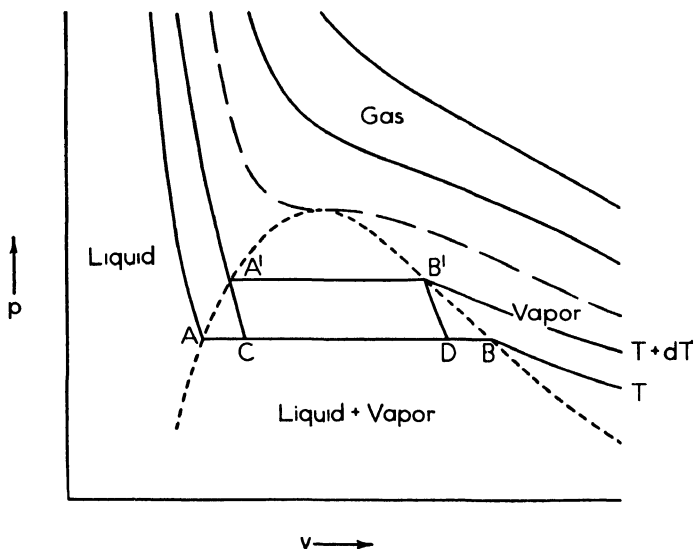


FIG. 16. Pressure-volume changes in the liquid, vapor, and gaseous states of a substance.

and B' that of 1 gm of saturated water vapor at the temperatures T and $T + dT$ respectively. $A'C$ and $B'D$ are adiabats. Take 1 gm of water around the Carnot cycle $A'B'DC$, starting at A' . The heat taken in along $A'B'$ which is necessary to convert the initial 1 gm of liquid water at A' to 1 gm of saturated water vapor at B' is the latent heat of vaporization $L + dL$ at temperature $T + dT$. Now consider the water and its vapor as the working substance in a heat engine which takes in heat $L + dL$ at $T + dT$ and rejects heat L at T . Since the process is a reversible one, the efficiency is, according to (17-12),

$$1 - \frac{T}{T + dT}$$

The work done in the cycle is, then, given by

$$dW = \frac{(L + dL)}{A} \left(1 - \frac{T}{T + dT} \right)$$

in work units and, therefore, to the first order,

$$dW = \frac{L}{A} \frac{dT}{T} \quad (19.1)$$

The work done is also equal to the area enclosed by the cycle $A'B'DC$ and so, with sufficient accuracy,

$$dW = (AB)dp$$

If v_1 and v_2 represent the specific volumes of liquid water and water vapor respectively at T , then

$$dW = (v_2 - v_1)dp \quad (19.2)$$

Equating (19.1) and (19.2) gives the Clausius-Clapeyron equation,

$$\frac{L}{A} \frac{dT}{T} = (v_2 - v_1)dp$$

or

$$\frac{dp}{dT} = \frac{L}{AT(v_2 - v_1)} \quad (19.3)$$

Since the pressure is that of saturated water vapor, replace p by e_s to conform with previous usage. Now $v_2 \gg v_1$, so to a first approximation

$$\frac{de_s}{dT} = \frac{L}{ATv_2}$$

Substituting from the gas equation,

$$e_s v_2 = R'T$$

it follows that

$$\frac{de_s}{dT} = \frac{Le_s}{AR'T^2} \quad (19.4)$$

This equation demonstrates the scope of the second law of thermodynamics, in that its use permits the development, from theoretical considerations, of a formula having significance in certain aspects of meteorology. The special form of the Clausius-Clapeyron equation developed above will be used in the following two sections.

20. The Saturated Adiabatic Lapse Rate. The Stability of Saturated Air. The rate of change of temperature with height in dry air ascending adiabatically was derived in section 14 and expressed by equation 14.2. It is also possible to derive a similar equation for saturated air ascending adiabatically, giving the *saturated adiabatic lapse rate*. The latter is smaller than the dry adiabatic lapse rate since condensation occurs as ascent to lower pressures proceeds, and latent heat of condensation is released and is taken up by the air.

According to (12.5), with (12.6) and (7.6),

$$dQ = c_p dT - AR T \frac{dp}{p}$$

This equation applies when 1 gm of dry air is considered. If saturated air is taken, then 1 gm of dry air is associated with x_s grams of water vapor, where x_s is the saturation humidity mixing ratio. The heat added to the air owing to condensation as it ascends through a pressure interval dp is $-L dx_s$, the minus sign showing that Q increases as x_s decreases. Neglect the effect of the specific heat of liquid water and water vapor, which is very small in comparison with that of the latent heat, and it follows that (12.5) above becomes

$$-L dx_s = c_p dT - AR T \frac{dp}{p} \quad (20.1)$$

Differentiating the approximate equation 10.12 for the saturation humidity mixing ratio gives

$$dx_s = \epsilon \left(\frac{de_s}{p} - \frac{e_s}{p^2} dp \right)$$

or

$$dx_s = \epsilon \left(\frac{1}{p} \frac{de_s}{dT} dT - \frac{e_s}{p^2} dp \right) \quad (20.2)$$

Now, combining (19.4) and (10.3) gives

$$\frac{de_s}{dT} = \epsilon \frac{Le_s}{ART^2} \quad (20.3)$$

Substituting (20.3) in (20.2) gives

$$dx_s = \epsilon \left(\frac{\epsilon Le_s}{pART^2} dT - \frac{e_s}{p^2} dp \right) \quad (20.4)$$

Substitute (20.4) in (20.1) and rearrange to give

$$\left(1 + \frac{\epsilon L}{c_p T} \frac{N}{p}\right) c_p dT = \left(1 + \frac{N}{p}\right) AR T \frac{dp}{p} \quad (20.5)$$

where

$$N = \frac{\epsilon}{AR} \frac{Le_s}{T}$$

The variation of temperature with height, not with pressure, is required. So replace dp by dz with the aid of (9.3). It follows that, if the small difference in temperature between rising and environment air is neglected,

$$-\frac{dT}{dz} = \frac{gA}{c_p} \frac{p + N}{p + \frac{\epsilon L}{c_p T} N}$$

Finally, by making use of (14.2), the following expression is obtained for the saturated adiabatic lapse rate

$$\Gamma' = -\frac{dT}{dz} = \Gamma \times \frac{p + N}{p + \frac{\epsilon L}{c_p T} N} \quad (20.6)$$

Since in the atmosphere $\epsilon L > c_p T$, it is clear that $\Gamma' < \Gamma$ as mentioned above. If the water vapor condenses into liquid water, even at sub-freezing temperatures, the latent heat is given by

$$L = 734 - 0.51T \text{ cal gm}^{-1} \quad (20.7)$$

where T is in degrees Absolute, and the saturation vapor pressure e_s is that with respect to a water surface. Values for the latter may be obtained from Table II in the Appendix, or from (21.4). If the process is one of sublimation from the vapor to the solid (ice) state, then the latent heat of sublimation

$$L = 677 \text{ cal gm}^{-1} \quad (20.8)$$

should be used, along with values of e_s appropriate over ice, as found from Table II in the Appendix.

Some values of the saturated adiabatic lapse rate in $^{\circ}\text{C}$ per kilometer are given in the following table, for which the values are computed with the aid of equation 20.6. Three assumptions were made in the derivation. First, the thermal capacities of the liquid water and water vapor in the air in question were assumed to be negligible. Second, the approximate equation 10.12 for the humidity mixing ratio was

considered to be sufficiently accurate for use in the derivation. Finally, the difference in temperature between rising and environment air was neglected. Computations using more accurate equations, however, show that the error involved is slight, and that the values given in the table are sufficiently accurate for most purposes.

SATURATED ADIABATIC LAPSE RATE				
(°C per kilometer)				
	Condensation		Sublimation	
T (°C) \ p (mb)	1000	600	1000	600
20	4.4	3.6
0	6.5	5.5	5.9	4.9
-20	8.7	8.0	8.6	7.9

The criteria for the stability or instability of saturated air are similar to those for dry air, except that the saturated adiabatic replaces the dry adiabatic lapse rate. To be absolutely rigorous, the water vapor content of the air surrounding the particle under consideration should be taken into account since the density of air is a function of its moisture content. This effect is small, however, and is usually neglected. The following, then, are the criteria for determining the type of equilibrium of a given particle of air.

$$\begin{aligned}
 \text{Stable equilibrium} & \quad \alpha < \Gamma' \\
 \text{Neutral equilibrium} & \quad \alpha = \Gamma' \\
 \text{Unstable equilibrium} & \quad \alpha > \Gamma'
 \end{aligned}$$

If confusion is to be avoided, the stability of saturated air should be considered with respect to upward motion. If no liquid water is present in the air, its temperature will increase at the dry adiabatic lapse rate if given a downward displacement since it is no longer saturated. Only if water droplets are present to maintain saturation constantly by their evaporation will air descend at the saturated adiabatic lapse rate.

21. Condensation Level. Dew-Point Changes in Adiabatic Motion.

It was shown in section 15 that when moist, unsaturated air ascends adiabatically, its temperature decreases at a rate which is very nearly the dry adiabatic lapse rate. As ascent proceeds, the air will reach a temperature at which the water vapor present is just sufficient to saturate the air. The height in the atmosphere at which this occurs is known as the *condensation level*. At this point the dry-bulb temperature and the dew point coincide.

In sections 14, 15, and 20, expressions were found for the rate of change of temperature with height in adiabatically ascending dry air, unsaturated moist air, and saturated air. It is now desirable to determine an expression for the rate of change of dew point with height in adiabatically ascending, moist, unsaturated air. To do this, an expression for the saturation vapor pressure is necessary. Such an expression may be obtained by integrating the special form of the Clausius-Clapeyron equation given by (19.4), assuming L to be constant. Separating the variables gives

$$L \frac{dT}{T^2} = AR' \frac{de_s}{e_s} \quad (21.1)$$

and performing the integration leads to

$$-L \left(\frac{1}{T} - \frac{1}{T_0} \right) = AR' \log \frac{e_s}{e_{s0}} \quad (21.2)$$

When $T_0 = 273^\circ \text{ A}$, $e_{s0} = 6.11 \text{ mb}$, and so (21.2) becomes

$$-L \left(\frac{1}{T} - \frac{1}{273} \right) = AR' \log \frac{e_s}{6.11} \quad (21.3)$$

The gas constant R' for water vapor is, according to section 10, given by

$$R' = 4.62 \times 10^6 \text{ cm}^2 \text{ sec}^{-2} \text{ deg}^{-1}$$

and the constant value of L is taken as 595 cal per gm, that for temperature 273° A . Substituting for L , A , and R' in (21.3) and rearranging give the saturation vapor pressure

$$e_s = 6.11 \times 10^{8.573 - \frac{2340}{T}} \text{ mb} \quad (21.4)$$

By substituting, following Haurwitz, the actual vapor pressure e for e_s and the dew point T_d for T in (21.1), it follows that

$$\frac{de}{e} = 5.38 \times 10^3 \frac{dT_d}{T_d^2} \quad (21.5)$$

Now differentiate the expression for the humidity mixing ratio (10.8), giving

$$dx = \frac{\epsilon(p \, de - e \, dp)}{(p - e)^2} \quad (21.6)$$

But the humidity mixing ratio of ascending unsaturated, moist air is constant, provided there is no mixing between the rising air and its

environment, and so $dx = 0$. It follows, then, that

$$\frac{de}{e} = \frac{dp}{p} \quad (21.7)$$

In addition, equation 9.3 states that for the environment

$$\frac{dp}{p} = - \frac{g}{R\bar{T}} dz$$

Combining (9.3), (21.7), and (21.5) leads to the following expression for the rate of change of dew point with height in adiabatically ascending unsaturated, moist air.

$$- \frac{dT_d}{dz} = 6.35 \times 10^{-8} \frac{T_d^2}{\bar{T}} \quad (21.8)$$

The above equation is used in section 139 to determine an approximate formula for the condensation level which has proved very useful in forecasting the heights of the bases of several types of clouds.

22. Thermodynamic Diagrams. It was indicated in section 14 that dry adiabats may be drawn on a diagram in which atmospheric pressure on a logarithmic scale is ordinate, and temperature on a linear scale is abscissa. It is also possible to allow for the moisture content of the atmosphere on such a chart by introducing lines of constant saturation humidity mixing ratio x_s from (10.9), and saturated adiabats from (20.6), or from a more accurate equation. In practice, true saturated adiabats are not used, but rather pseudo adiabats. Pseudo adiabatic ascent is similar to true saturated adiabatic ascent in all respects, except that liquid water is assumed to be precipitated as soon as it has condensed. Considering the behavior of condensation phenomena such as cloud and precipitation, it can be seen that in the atmosphere the actual process is neither true nor pseudo adiabatic, but somewhere intermediate between the two. Pseudo adiabats can be computed a little more readily than saturated adiabats, since the specific heat of liquid water does not enter the calculations, but the difference between the two is so small that it is of no consequence. Since pseudo adiabats are shown on the chart, it is generally known as the *pseudo adiabatic chart*. On it, both dry and pseudo (or saturated) adiabatic motions may be determined with ease.

Another thermodynamic diagram which is widely used is the *tephigram* (T - ϕ -gram). This diagram has the entropy of dry air as ordinate and temperature as abscissa, both on a linear scale. From (18.7), it follows that potential temperature on a logarithmic scale is equivalent to entropy on a linear scale. In practice, it is usual to think

of the ordinate as $\log \theta$, rather than as ϕ . The tephigram is shown in Fig. 17, with pressure lines sloping upward to the right, pseudo adiabats sloping upward to the left, and saturation humidity mixing ratio lines

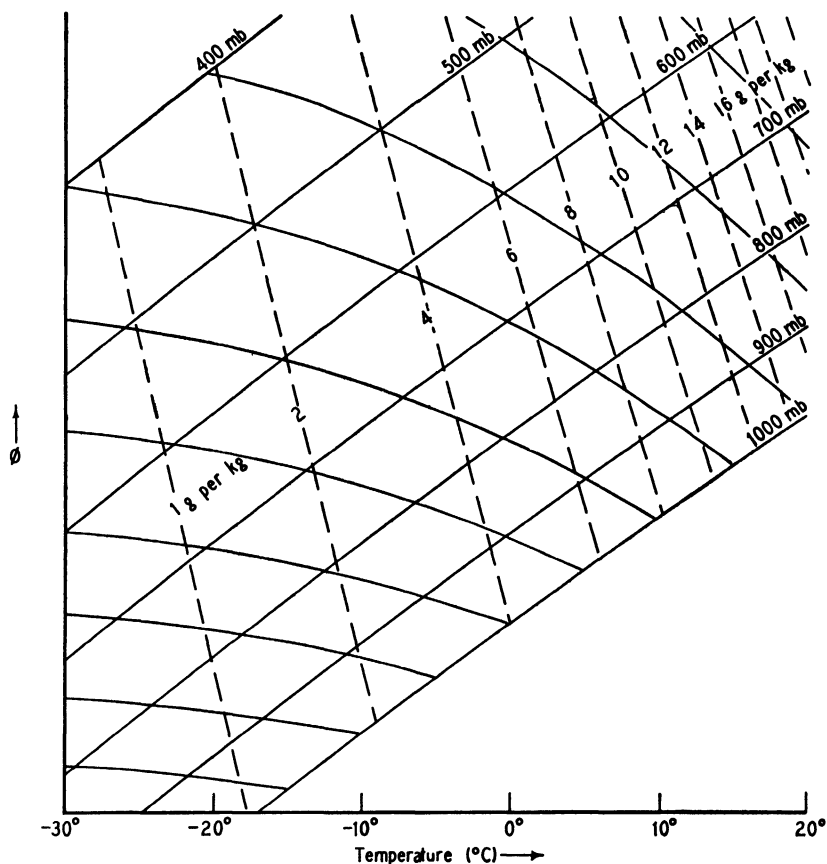


FIG. 17. The tephigram.

not quite vertical, but sloping slightly upward to the left. Dry adiabats are horizontal, and isotherms are vertical. A full-size tephigram is provided with this book in a pocket at the back. Dry adiabats and isotherms are shown on this chart with full green lines. Pressure lines and pseudo adiabats are shown in full orange lines, and saturation humidity mixing ratio lines in broken orange lines.

Other types of thermodynamic charts have been developed from time to time, but the pseudo adiabatic chart and the tephigram are two of the most widely used diagrams.

It was proved in section 17 that the work done by a mass of air in going through a cyclic process is proportional to the area enclosed by the curve representing the various stages of the process on a p - v diagram. It can be shown that on thermodynamic charts of the types given above, areas are also proportional or equal to work done, or energy released. In other words, the pseudo adiabatic diagram and the tephigram are proportional or equal area transformations of a p - v diagram.

Consider a unit mass of air moving vertically, having density ρ , temperature T , and pressure p . The surrounding air at the same level has density $\bar{\rho}$, temperature \bar{T} , and pressure p . The pressure of the moving air is always the same as that of the environment. It follows from Archimedes' principle that the force acting on the rising air is, since $\rho = \frac{1}{v}$,

$$F = a = \rho v a = \bar{\rho} v g - \rho v g$$

and so

$$a = g \left(\frac{\bar{\rho}}{\rho} - 1 \right) \quad (22.1)$$

But

$$p = R \rho T = R \bar{\rho} \bar{T}$$

and therefore

$$\frac{\bar{\rho}}{\rho} = \frac{T}{\bar{T}}$$

It follows then that

$$a = g \left(\frac{T}{\bar{T}} - 1 \right) = g \frac{T - \bar{T}}{\bar{T}} \quad (22.2)$$

Air moving a distance dz does work dW and therefore

$$dW = F dz = g \frac{T - \bar{T}}{\bar{T}} dz = g \bar{\rho} dz \frac{T - \bar{T}}{\bar{\rho} \bar{T}}$$

Using (9.1) and (7.7) and multiplying by A to convert to thermal units give

$$dW = -AR(T - \bar{T}) \frac{dp}{p} \quad (22.3)$$

or

$$dW = -AR(T - \bar{T}) d(\log p) \quad (22.4)$$

Fig. 18 shows the variations of pressure and temperature of an ascending mass of air, plotted on a pseudo adiabatic chart. ABC represents the state of the environment, while DEF indicates the variations of p and T experienced by a mass of air as it rises from position D to position F . The moving air at G is surrounded by air whose con-

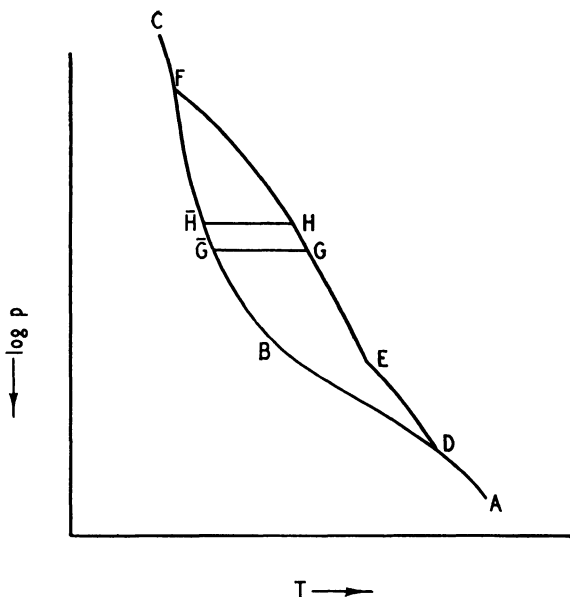


FIG. 18. Energy released by rising air on a T - $\log p$ diagram.

dition is given by the point \bar{G} at the same pressure. $H\bar{H}$ is a later position of $G\bar{G}$, separated by a small interval $d(\log p)$. To a high degree of approximation, $G\bar{G}H\bar{H}$ may be considered as a rectangle of area $(T - \bar{T}) d(\log p)$. From (22.4), since $d(\log p)$ is negative, it follows that

$$dW = AR \times \text{Area } G\bar{G}H\bar{H}$$

Therefore, as the mass of air in question ascends from D to F , the total amount of energy liberated is proportional to the area $DBFED$.

In a similar manner, it is possible to determine from the tephigram the amount of energy released by an ascending mass of air. In Fig. 19, ABC represents the environment curve, while DEF gives the successive values of ϕ and T as the air ascends. The ascending air, when at G , is surrounded by air whose state is represented by \bar{G} at the same pressure. $H\bar{H}$ is the position of $G\bar{G}$ a short time later; the lines

$\bar{G}K$ and $MLGJ$ are ordinates in the diagram. Equation 18.8 states that

$$d\phi = c_p \frac{dT}{T} - AR \frac{dp}{p}$$

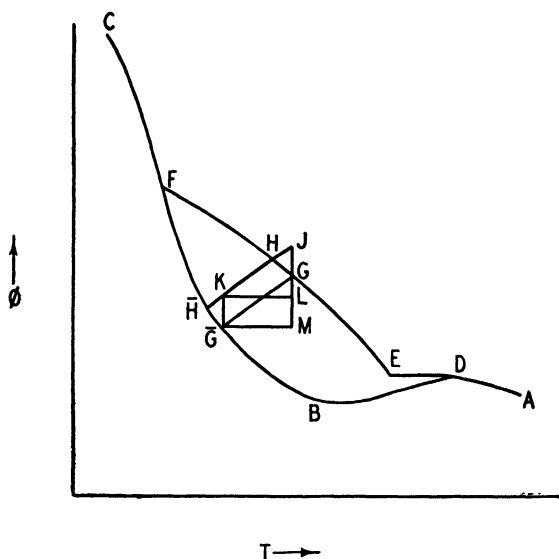


FIG. 19. Energy released by rising air on a tephigram.

Now $\bar{G}K$ is the change in entropy when the pressure changes by dp while T remains constant. It follows that

$$\bar{G}K = -AR \frac{dp}{p}$$

Therefore

$$\begin{aligned} -AR(T - \bar{T}) \frac{dp}{p} &= \text{Area } M\bar{G}KL \\ &= \text{Area } G\bar{G}KJ \\ &= \text{Area } G\bar{G}\bar{H}H \end{aligned}$$

since the ends of the strip, the two triangles $\bar{G}K\bar{H}$ and GJH , can be considered equal, the difference being a small quantity of the second order. Now (22.3) states that

$$dW = -AR(T - \bar{T}) \frac{dp}{p}$$

so that

$$dW = \text{Area } G\bar{G}\bar{H}H$$

By integration, it follows that the energy released during the ascent from D to F is equal to the area $DBFED$, if expressed in heat units.

23. The Psychrometer Equation. The psychrometer, or hygrometer as it is sometimes called, is described in section 65. For present purposes, however, it is sufficient to state that the psychrometer is an instrument for measuring the moisture content of the atmosphere. It consists of two ordinary thermometers, the bulb of one of which is kept moist by one of several suitable processes. If the air is saturated, there is no evaporation from the wet bulb, and both thermometers show the same temperature. If the air is unsaturated, however, there will be evaporation from the wet bulb, cooling it, and the wet-bulb thermometer then gives a lower reading than the dry-bulb one. The theory of this cooling process is given below.

Assume that unsaturated air is moving past the wet-bulb thermometer. The air, as it approaches the wet bulb, has x grams of water vapor associated with 1 gm of dry air at temperature T . Evaporation of water from the wet bulb saturates the air, so that the air leaving the wet bulb comprises x_{sw} grams of water vapor with 1 gm of dry air, now at the temperature of the wet bulb T_w . During this process, $x_{sw} - x$ grams of liquid water have evaporated from the wet bulb, the evaporation occurring at the temperature of the wet bulb, presumably. It is not obvious that evaporation occurs at T_w , but it is an assumption the validity of which must be assessed in the light of the results obtained. The thermodynamical process may be stated mathematically in the following form.

$$(c_p + xc'_p)(T - T_w) = L_w(x_{sw} - x) \quad (23.1)$$

c'_p is about twice as great as c_p , but since x is of the order of magnitude of 0.01, it is permissible to neglect xc'_p in comparison with c_p , as a first approximation. Equation 23.1 then becomes

$$c_p(T - T_w) = L_w(x_{sw} - x) \quad (23.2)$$

Substituting (10.11) and (10.12) in (23.2) leads to

$$e_{sw} - e = \frac{c_p p(T - T_w)}{\epsilon L_w} \quad (23.3)$$

where e_{sw} is the saturation vapor pressure at T_w . With this equation, therefore, it is possible to compute the actual vapor pressure when the values of T and T_w are measured. This equation is commonly referred to as the psychrometer equation. The consistency of the results obtained in using this formula for measuring humidity is the justification for the assumption that the evaporation takes place at the temperature T_w .

24. Wet-Bulb Temperature. Wet-Bulb Potential Temperature. A definition of wet-bulb temperature follows from what has been given in the previous section. Consider $1 + x$ grams of unsaturated air. The mixing ratio of air saturated at the wet-bulb temperature is x_{sw} . Evaporate an amount of liquid water $x_{sw} - x$ grams into the air, which is sufficient to reduce the dry-bulb temperature to the initial value of the wet-bulb temperature. The air is then saturated, and no further evaporation can take place, even if more liquid water is introduced. It follows then that the *wet-bulb temperature* may be defined as the lowest temperature to which air may be cooled by evaporating water into it. It is not necessary that the lowering of the temperature be carried out in one step. Evaporate $x_1 - x$ grams of water into the air, which brings the dry-bulb temperature down to a value intermediate between the initial dry- and wet-bulb temperatures. At this point, it is still possible to cool the air to T_w by evaporating $x_{sw} - x_1$ grams of water into it, making a total evaporation of $x_{sw} - x$ grams in the two stages. Since the limit of cooling has not changed during the process visualized, it follows that the wet-bulb temperature T_w has remained constant. This result, that the wet-bulb temperature of air is unaltered by evaporating water into it, is of considerable significance and finds many applications in both theoretical and practical aspects of meteorology.

Normand deduced the two following propositions from the basic assumption stated in section 23.

Proposition I. The heat content of the air is equal to the heat content of the same air, saturated at the wet-bulb temperature, minus the heat content of the additional liquid water required to saturate it.

Proposition II. The entropy of the air is equal to the entropy of the same air, saturated at the wet-bulb temperature, minus the entropy of the additional liquid water required to saturate it.

Proposition I is obvious, and is indeed just a restatement of the fundamental assumption; the second proposition is not so obvious. The process is not reversible, and there is a gain in entropy, since heat is lost by the air in cooling from T to T_w , and the same amount of heat is taken up by water at the temperature T_w .

It is, however, possible to evaluate the gain in entropy, and so determine the order of magnitude of the increase. With (23.1), the gain in entropy by the water is given by

$$\Delta\phi_1 = (c_p + c'_p x) \frac{(T - T_w)}{T_w}$$

The loss of entropy of the original moist air is

$$\Delta\phi_2 = \int_{T_w}^T (c_p + c'_p x) \frac{dT}{T} = (c_p + c'_p x) \log \frac{T}{T_w}$$

The net gain in entropy of the system is

$$\Delta\phi_1 - \Delta\phi_2 = \Delta\phi = (c_p + c'_p x) \left(\frac{T - T_w}{T_w} - \log \frac{T}{T_w} \right)$$

But

$$\log \frac{T}{T_w} = \log \left(1 + \frac{T - T_w}{T_w} \right) = \frac{T - T_w}{T_w} - \frac{1}{2} \left(\frac{T - T_w}{T_w} \right)^2 + \text{higher terms}$$

It follows then that

$$\Delta\phi = (c_p + c'_p x) \left\{ \frac{1}{2} \left(\frac{T - T_w}{T_w} \right)^2 + \text{higher powers} \right\} \quad (24.1)$$

Equation 24.1 shows that the net gain of entropy of the system is approximately equal to $\frac{1}{2} \left(\frac{T - T_w}{T_w} \right)$ times the gain of entropy of the water. This is a small fraction and may be neglected, and the process visualized may be considered as isentropic. Proposition II may then be assumed to be verified to a high degree of approximation.

This second proposition may be used to prove a third proposition, also due to Normand.

Proposition III. The dry adiabat through the dry-bulb temperature, the saturated adiabat through the wet-bulb temperature, and the humidity mixing ratio line through the dew point intersect at a point.

First consider a mass of $1 + x_s$ grams of air, saturated at B (Fig. 20), which goes through the following process. This air ascends, its temperature decreasing at the saturated adiabatic lapse rate until it reaches D , where its mixing ratio is x . All water which has condensed during the ascent, i.e., $x_s - x$ grams, is shed at D . If descent next takes place, warming will proceed at the dry adiabatic lapse rate, and upon reaching the original pressure, the temperature of the air will be that denoted by A in Fig. 20. It follows that

$$\begin{aligned} \text{Entropy of } 1 + x_s \text{ grams of air, saturated at } B &= \text{Entropy of } 1 + x \\ &\quad \text{grams of moist air at } A + \text{Entropy of } x_s - x \text{ grams of liquid water} \\ &\quad \text{shed at } D \end{aligned} \quad (24.2)$$

Next let A' denote the dry-bulb temperature of $1 + x$ grams of air whose wet-bulb temperature is B , and whose mixing ratio is x . Proposition II states that

Entropy of $1 + x_s$ grams of air, saturated at B = Entropy of $1 + x$ grams of moist air at A' + Entropy of $x_s - x$ grams of liquid water removed at B (24.3)

A comparison of (24.2) and (24.3) shows that

Entropy at A = Entropy at A'

and therefore A and A' must coincide.

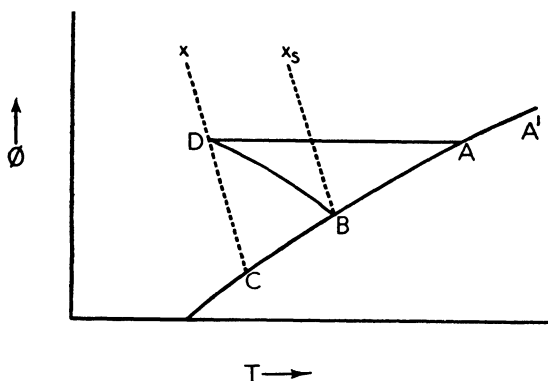


FIG. 20. Dry-bulb, wet-bulb, and dew-point temperature changes in adiabatically ascending air.

The line CD represents the humidity mixing ratio line through D . Since the dew point moves along the actual mixing ratio line during dry adiabatic processes, as indicated in section 21, the point C where CD intersects the isobar through A is the dew point of the air at A .

The above proof is not exact, since in (24.2) the liquid water was removed at D , the temperature of the condensation level, whereas in (24.3) the water was removed at the wet-bulb temperature. However, the errors due to this are only slight, and Proposition III may be taken as verified to a satisfactory degree of accuracy.

The above results show that when air undergoes adiabatic changes in the saturated or unsaturated state, the wet-bulb temperature follows a single saturated adiabat. It is possible, then, to define a *wet-bulb potential temperature* θ_w as the wet-bulb temperature which the air assumes when brought adiabatically to the standard pressure of 1000 mb. The value of θ_w can be determined readily from a pseudo adiabatic chart, a tephigram, or any other thermodynamic chart. Simply follow

the saturated adiabat through the wet-bulb temperature until the 1000-mb line is reached. The temperature at that point is θ_w . The pseudo adiabats on the tephigram in the pocket at the back of this book are labeled with their appropriate values of θ_w . The wet-bulb potential temperature does not change during evaporation or condensation processes in the free air, nor during adiabatic ascent and descent. The properties of wet-bulb and wet-bulb potential temperature are discussed in greater detail in sections 83 and 84. The use of the wet-bulb temperature in forecasting procedures is brought out in Chapters 14, 19, and 20. Normand's third proposition has many applications in practical meteorology, as will be seen in later sections.

25. Equivalent Temperature. Equivalent Potential Temperature. Rossby Diagram. The wet-bulb temperature is invariant for evaporation processes in the free air. There is another quantity, the equivalent temperature T_e , which has similar properties. The *equivalent temperature* may be defined as the temperature attained by a mass of air, originally saturated or unsaturated, when it ascends until all its water vapor is condensed and precipitated, and it is then brought back adiabatically to its initial pressure. Since one dry adiabat, and one only, is asymptotic to the saturated adiabat which the wet-bulb temperature of the rising air follows, the equivalent temperature is a single-valued function of the wet-bulb temperature. In certain circumstances, the two may be used interchangeably, but the wet-bulb temperature has certain advantages in practice which give it a much wider usefulness.

The equivalent temperature may also be defined in a slightly different manner. Consider (23.1)

$$(c_p + x c'_p)(T - T_w) = L_w(x_{sw} - x)$$

If T_e is the temperature of absolutely dry air which has a wet-bulb temperature T_w , then the above equation must be valid when $T = T_e$ and $x = 0$, and it becomes

$$c_p(T_e - T_w) = L_w x_{sw} \quad (25.1)$$

or

$$T_e = T_w + \frac{L_w x_{sw}}{c_p} \quad (25.2)$$

The two definitions are not identical, and give values for the equivalent temperature which are slightly different. The difference is small, however, and for most purposes may be neglected.

The *equivalent potential temperature* θ_e of a mass of air may be defined as the temperature attained when the air ascends until all water vapor

is condensed and precipitated, and it then descends dry adiabatically to the standard pressure 1000 mb. It may also be defined by substituting θ_e and θ_w for T_e and T_w in (25.2) to give

$$\theta_e = \theta_w + \frac{L_w x_{sw}}{c_p} \quad (25.3)$$

where L_w and x_{sw} now have values appropriate for θ_w .

The equivalent and equivalent potential temperatures of a mass of air may be deduced from the pseudo adiabatic diagram or the tephigram without difficulty. Proceed along the saturated or pseudo adiabat through the wet-bulb temperature until the saturated adiabat becomes approximately parallel to the dry adiabats, indicating that the vapor content of the air is so small that it can be neglected. Thereafter, proceed dry adiabatically to the initial pressure for T_e or to 1000 mb for θ_e .

It can be seen from both definitions of θ_e that it is a single-valued function of θ_w . Practical considerations, however, usually favor the use of the wet-bulb potential temperature.

Rossby has constructed a chart in which the ordinate is potential temperature* on a logarithmic scale, and the abscissa is humidity mixing ratio on a linear scale. It follows from the first definition of θ_e given above (due to Rossby) that the value of θ_e of a mass of air is determined by its potential temperature and its mixing ratio. Lines of constant θ_e may then be drawn on a chart with these coordinates. The chart with these coordinates, and with lines of constant equivalent potential temperature on it, is known as the *Rossby diagram*, or the *equivalent potential temperature diagram*.

Since θ and x do not vary during dry adiabatic processes, a curve on the diagram representing atmospheric conditions in the vertical will not change its position as a result of dry adiabatic motion. Evaporation or condensation processes will vary its position, however, since both θ and x are changed thereby. Stability and instability, with respect to both dry and saturated adiabatic displacements, may be determined. No pressure or temperature lines appear on the chart, and the lack of these may be inconvenient at times. It is not an equal or proportional area transformation of a p - v diagram, and therefore it cannot be used to study energy relationships. The Rossby diagram was intended primarily as a tool to assist in air mass analysis, and it is most useful when employed for that purpose. It is better in distinguishing between air masses than other diagrams in general use, since curves

* More accurately, partial potential temperature, the temperature attained by air descending dry adiabatically from the partial pressure of dry air, $p - e$, to standard pressure, 1000 mb.

representing dry cold air appear to the far left of the diagram, while those representing warm moist air are found to the right. Differences between intermediate air masses are brought out clearly. The use of the Rossby diagram in classifying air masses is indicated in section 106.

PROBLEMS AND EXERCISES

1. Integrate the Clausius-Clapeyron equation when the latent heat of vaporization

$$L = 734 - 0.51T \text{ cal gm}^{-1}$$

where T is in degrees Absolute. Use the equation derived to compute the saturation vapor pressure e_s at 293° A . Also compute e_s for the same temperature using (21.4), and compare each value obtained with the observed value as given in Table II in the Appendix.

2. Determine the equivalent temperature of a mass of air with pressure 900 mb, temperature 273° A , and relative humidity 80 per cent by each of the two methods outlined in section 25. When using (25.2), first assume a process of condensation, and then repeat the computation assuming a sublimation process. Compare the three answers, remembering that the pseudo adiabats on the tephigram are constructed on the assumption that water vapor condenses into liquid water, even at sub-freezing temperatures.

3. Show that in Refsdal's "aerogram" (ordinate $T \log p$; abscissa $\log T$), the energy liberated by a mass of air ascending through its environment, which is denser than the rising air at each level, is proportional to the area between the environment curve and the ascent curve.

4. Determine, using the full-scale tephigram at the back of the book, the relative humidity of air with dry-bulb temperature 12° C , at a pressure of 880 mb, when the wet-bulb temperature varies from 11° C to 1° C . The relative humidity should be determined for every other degree Centigrade, as $11^\circ, 9^\circ, 7^\circ, \dots 1^\circ \text{ C}$.

Then determine the relative humidities for the same values, using the following derivative of Regnault's empirical equation. Regnault's formula is the basis of most hygrometric tables.

$$e = e_{sw} - 0.0006p(T - T_w) \left(1 + \frac{T_w}{610} \right)$$

where e = the actual vapor pressure.

e_{sw} = the saturation vapor pressure at the wet-bulb temperature.

p = pressure.

T = dry-bulb temperature in $^\circ \text{C}$.

T_w = wet-bulb temperature in $^\circ \text{C}$.

Saturation vapor pressures are given in Table II in the Appendix.

Plot relative humidity against wet-bulb temperature for each of these two determinations, and show at what relative humidity the maximum difference between the two curves occurs.

5. (a) By using the Clausius-Clapeyron equation and expressing the latent heat of vaporization L in the form

$$L = L_0 + (c'_p - c)(T - T_0)$$

show that the entropy of vaporization of 1 gm of liquid water

$$\frac{L}{T} = (c'_p - c) \log T - \frac{AR}{\epsilon} \log e_s + C$$

(b) Use the above equation and assume that the constant $C = 0$ to show that the expression for the entropy of 1 gm of saturated air given by (18.13) may be modified to the form

$$\phi_s = \frac{c_p + x_s c'_p}{1 + x_s} \log T - \frac{AR}{1 + x_s} \log (p - e_s) - \frac{x_s AR}{\epsilon(1 + x_s)} \log e_s$$

This expression also gives the entropy of unsaturated moist air if the actual value of the vapor pressure e is used instead of the saturated vapor pressure e_s , and if x is used instead of x_s .

BIBLIOGRAPHY

- Brunt, D., *Physical and Dynamical Meteorology*, London, Cambridge University Press, 1939. Chapter 4.
- Haurwitz, B., *Dynamic Meteorology*, New York, McGraw-Hill Book Co., 1941. Chapters 3, 4.
- Koschmieder, H., *Dynamische Meteorologie*, Leipzig, Akad. Verlag., 1933. Chapter 3.
19. Cork, J. M., *Heat*, New York, John Wiley and Sons, 1933. p. 230.
20. Fieldstad, J. E., "Graphische Methoden zur Ermittlung adiabatischer Zustandsänderungen feuchter Luft," *Geofys. Publ.*, 3, No. 13, 1925.
22. Werenskiöld, W., "On Equal Area Transformations of the Indicator Diagram and a New Aerological Chart," *Geofys. Publ.*, 12, No. 6, 1938.
22. Shaw, Sir N., *Manual of Meteorology*, Vol. 3 (1930), p. 269.
24. Normand, C. W. B., *Wet-Bulb Temperatures and the Thermodynamics of the Air*, Mem. Indian Met. Dept., 23, 1, 1921.
25. Rossby, C.-G., *Thermodynamics Applied to Air Mass Analysis*, Mass. Inst. Tech. Met. Papers, 1, No. 3, 1932.

CHAPTER 5

RADIATION IN THE ATMOSPHERE

The general term radiation embraces the energy transmitted by the whole range of electromagnetic waves from cosmic rays, having very short wave lengths of the order of 10^{-12} cm, to long radio waves having wave lengths of the order of 10^6 cm. The meteorologist usually, however, is concerned only with radiation in a relatively small band of wave lengths, from 2×10^{-5} cm to 5×10^{-3} cm. The unit of wave length which is commonly used in meteorology is not the centimeter, but the micron, μ , which is equal to 10^{-4} cm. The range under present consideration is therefore from 0.2 to 50 μ . This range may be divided into two generic groups. The first includes the radiation of the sun, which at its surface has a temperature of about 6000°A . This *solar radiation*, or *short-wave radiation*, as it is often called, occurs in the wave length interval from 0.2 to 4 μ , of which only the radiation from 0.4 to 0.7 μ can be detected by the human eye. The second group of wave lengths is that emitted by the earth and its atmosphere, at temperatures ranging from 200 to 300°A . This radiation, known as *terrestrial* or *long-wave radiation*, extends from 4 to 50 μ .

26. The Laws of Black-Body Radiation. Before discussing the radiative processes in the atmosphere, it is desirable to review the several laws which of necessity form the background of any treatment of radiation.

(a) *Kirchhoff's Law.* If radiation of a specified wave length μ is incident at the surface of any body, then the *absorptive power* a_μ of the body for that wave length is defined by Kirchhoff as the ratio of the radiant energy absorbed to the total incident radiant energy. In addition, Kirchhoff defined a perfectly *black body* as a body which absorbs all the radiation which falls on it, irrespective of whether the radiation is in the visible spectrum or not. It follows therefore that the absorptive power a_μ of such a body is unity. For all actual substances, however, the absorptive power is a proper fraction, the value of which depends on the nature of the substance, on its temperature, and on the wave length of the incident radiation.

If $e_\mu d\mu$ is the radiation emitted per second between the wave lengths μ and $\mu + d\mu$ from unit area of a body, e_μ is known as the *emissive power*

of the body for the wave length μ . Kirchhoff's law states that the ratio of the emissive and absorptive powers for a given temperature and a given wave length is the same for all bodies, and is equal to the emissive power of a perfectly black body. This law may also be stated as

$$\frac{e_{\mu}}{a_{\mu}} = E_{\mu}$$

where E_{μ} represents the black-body radiation at wave length μ , and for any specified temperature. When e_{μ} is a fixed fraction of E_{μ} for all wave lengths, the body is referred to as a *gray body*, and the radiation as gray radiation.

This law is of great importance in discussing atmospheric radiative processes, for it indicates that if a layer of the atmosphere absorbs radiation of a certain wave length, that layer will itself also radiate energy of that same wave length. Conversely, if a layer is transparent to radiation of another wave length, it will not emit radiation of that wave length.

(b) *Planck's Law.* The variation of black-body radiation at known temperatures with wave length was investigated experimentally by Lummer and Pringsheim, and later theoretically, using quantum principles, by Planck. The expression obtained by the latter gave values in good agreement with the experimental values. Planck's formula states that

$$E_{\mu} = c_1 \mu^{-5} (e^{\frac{c_2}{\mu T}} - 1)^{-1}$$

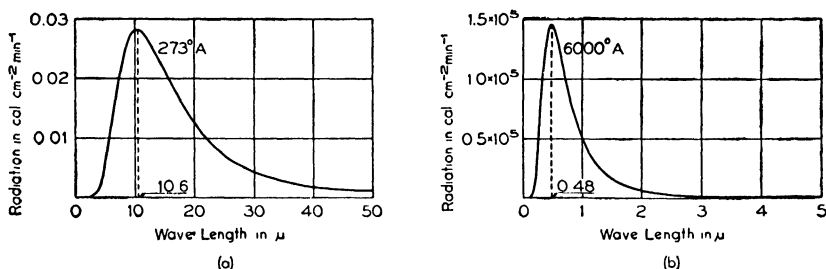


FIG. 21. Energy radiated by a black body at (a) 273° A and at (b) 6000° A.

where c_1 and c_2 are constants. The distribution of energy in the spectrum of a black body at a temperature of 273° A is shown in Fig. 21a, and that at a temperature of 6000° A is shown in Fig. 21b. It may be assumed without serious error that the earth radiates as a black body at a temperature of about 273° A, and that the sun radiates similarly at 6000° A. These two curves show, then, the energy radiated by the

earth and the sun at their respective temperatures. The great difference between the amount of energy radiated by the sun and that radiated by the earth may be seen from a comparison of the vertical scales of the two figures. The maximum energy emitted per unit wave length, area, and time by the sun is very nearly 5×10^6 times as great as that emitted by the earth. The radiation is emitted in the two wave length intervals mentioned in the introductory section of this chapter.

(c) *Wien's Law.* Before Planck derived his expression for the energy distribution of black-body radiation, Wien had developed an equation of the form

$$E_{\mu} = c_1 \mu^{-5} e^{-\frac{c_2}{\mu T}}$$

where the constants are the same as in Planck's equation. This expression is less accurate than that of Planck, but the difference between the two is small, except for large values of μ or T . To determine the value of μ for which E_{μ} is a maximum, differentiate Wien's equation partially with respect to μ , and set the result equal to zero, as indicated below.

$$\frac{\partial E_{\mu}}{\partial \mu} = c_1 \mu^{-6} e^{-\frac{c_2}{\mu T}} (c_2 \mu^{-1} T^{-1} - 5) = 0$$

The wave length μ_m for which E_{μ} is a maximum is then

$$\mu_m = \frac{c_2}{5T} = \frac{a}{T}$$

The constant c_2 has been evaluated as 14,385 micron degrees, so that

$$\frac{c_2}{5} = a = 2877 \text{ micron degrees}$$

This figure agrees well with the average of recent experimental results, 2897 micron degrees.

Wien's law thus states that the wave length for maximum black-body radiation is inversely proportional to the temperature. Using the experimental value of a , μ_m has for 273°A the value 10.6μ , and for 6000°A the value of 0.48μ , in excellent agreement with the positions of the maxima shown in Fig. 21.

(d) *Stefan's Law.* The total emissive power of a black body may be obtained by integrating Planck's expression for all wave lengths from 0 to ∞ . The method of integration is given in advanced textbooks on heat, and will not be reproduced here. When the integration has been performed, the result is

$$E = \int_0^{\infty} E_{\mu} d\mu = \sigma T^4$$

This is Stefan's law, which states that the total black-body radiation is directly proportional to the fourth power of the temperature. Stefan's constant

$$\sigma = 8.14 \times 10^{-11} \text{ cal cm}^{-2} \text{ min}^{-1} \text{ deg}^{-4}$$

It follows that the areas under curves of the type shown in Fig. 21 are proportional to the fourth powers of the respective temperatures.

Of the four laws for black-body radiation given above, Kirchhoff's law and Stefan's law are most widely used in meteorology, as will be noted in the following sections of this chapter.

27. The Law of Absorption. Consider a beam of parallel radiation of intensity I which falls perpendicularly on a layer of some absorbing medium of density ρ and thickness dz . The mass dm of the medium traversed by the radiation is then ρdz . The amount of radiation absorbed dI is proportional to the intensity of the beam and the mass of the absorbing medium traversed. Thus

$$dI \propto -I dm$$

The negative sign indicates that dI represents a decrease in intensity of the beam, rather than an increase, as it traverses the layer. Introducing a constant k , the equation becomes

$$dI = -kI dm \quad (27.1)$$

The constant k is known as the *absorption coefficient* of the absorbing substance. Integration of (27.1) gives

$$\log \frac{I}{I_0} = -km \quad (27.2)$$

or

$$I = I_0 e^{-km} \quad (27.3)$$

where I_0 is the intensity of the radiation when $m = 0$, and I is the intensity after traversing a layer containing mass m . The use of this equation is sometimes facilitated if it is stated as

$$I = I_0 10^{-0.4343km} \quad (27.4)$$

Equations 27.2, 27.3, and 27.4 are mathematical statements of the fundamental law of absorption, known as *Beer's law*.

The transmission by a layer is defined as the ratio of the intensity of the radiation emerging from the layer to that incident on the layer. The *transmission coefficient* τ is defined as

$$\tau = \frac{I}{I_0} \quad (27.5)$$

The coefficient τ is a function of k and m . If the radiation occurs in an interval of wave lengths in which k does not vary, from (27.3) τ may be expressed as

$$\tau = e^{-km} \quad (27.6)$$

If k varies in the wave length interval, some value of k , representing the absorption in that interval, must be adopted.

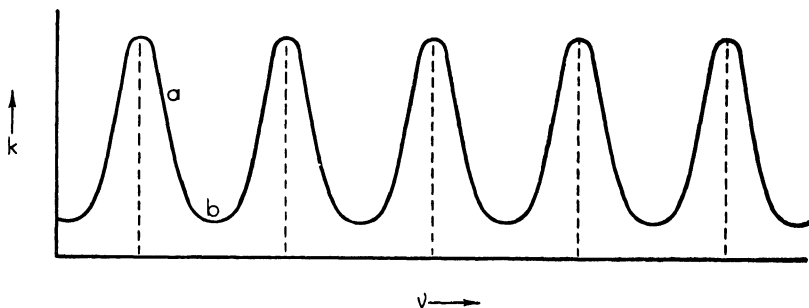


FIG. 22. Variation of absorption with frequency in a line spectrum. (After Elsasser.)

An equation such as (27.6) or a slightly modified form, is adequate if the absorption is continuous throughout the spectrum. However, if the absorption spectrum is not continuous, but is made up of a series of discrete lines, it is much more difficult to set up an adequate transmission formula. Elsasser assumed that the variation of the absorption coefficient k with frequency ν (the reciprocal of the wave length) for a series of lines in a portion of a band spectrum may be represented in the manner shown in Fig. 22. He obtained a transmission function

$$\tau_I = 1 - \phi\left(\sqrt{\frac{lm}{2}}\right) \quad (27.7)$$

where ϕ is the probability integral (see section 59)

$$\phi(x) = \frac{2}{\sqrt{\pi}} \int_0^x e^{-x^2} dx \quad (27.8)$$

and l is the *generalized absorption coefficient*. Elsasser's transmission function may be compared with the simple form given in (27.6) for small values of m , i.e., for thin layers. The probability integral may be expanded in the power series

$$\phi(x) = \frac{2}{\sqrt{\pi}} \left(x - \frac{x^3}{3} + \dots \right)$$

By neglecting terms of higher order, (27.7) becomes

$$\tau_I = 1 - \sqrt{\frac{2lm}{\pi}} \quad (27.9)$$

The expansion of e^{-km} in series gives the relation

$$e^{-km} = 1 - km + \frac{k^2 m^2}{2!} - \dots$$

By neglecting terms of higher order, (27.6) becomes

$$\tau = 1 - km \quad (27.10)$$

A comparison of (27.9) and (27.10) shows that for thin layers the absorption in a band spectrum is proportional to the square root of the absorbing mass, whereas for a continuous spectrum, it is proportional to the mass. The physical basis of this result may be seen from Fig. 22. For thin layers, the absorption occurs in the sloping portions of the curves, as at *a*, giving a non-linear relationship between absorption and mass. As the thickness of the layer increases, the values given by Elsasser's transmission function approach those given by (27.6). For thick layers, the regions between the lines, as at *b*, become effective in absorption, and the absorption then increases directly with mass.

For most purposes, when considering band spectra, the transmission is obtained with sufficient accuracy by substituting *l* for *k* in (27.6).

The above results are of considerable significance in the study of radiation in the atmosphere, since both water vapor and carbon dioxide, which absorb terrestrial radiation strongly, have line or band spectra.

28. Solar Radiation. In discussing the solar radiation which reaches the earth and its atmosphere, it is first necessary to know the intensity of the radiation incident at the outer limits of the atmosphere. The intensity varies with the latitude and the time of year. For instance, the maximum amount of radiant energy falling on a horizontal unit surface just outside the atmosphere during any day of the year is about 1100 calories. This intensity, nearly 0.8 cal per cm² per min, occurs at the poles during the summer solstices. At this time, the energy input varies little with latitude, only decreasing to about 0.6 cal per cm² per min at the equator. The variation with latitude is much more marked at the equinoxes, the values ranging from zero at the poles to about 0.6 at the equator.

A measure of the intensity of the radiation at the outer limits of the atmosphere is the *solar constant*. This is defined as the amount of energy falling perpendicularly on unit area in unit time when the distance between earth and sun is at its mean value. The solar constant has the

value 1.94 cal per cm^2 per min. The determinations of the solar constant are made at solar observatories located on mountains, where the air is clear, and the diminution of the beam in traversing the atmosphere is a minimum. The values obtained show a range of 2 or 3 per cent of its mean value as given above. It is not yet clear whether these variations are real, or if they result from inaccuracies in correcting for the absorption and scattering of the solar beam before it reaches the instruments. The question is an important one, however, for if significant variations in the output of solar energy do occur, such variations may be related to terrestrial weather conditions, and a study of the relationship between the two might lead to improvements in long-range forecasting techniques.

When solar radiation enters the earth's atmosphere, it is attenuated by three distinct processes. The first of these is through scattering by small particles, such as the molecules of the air, and by impurities such as dust particles. This scattering was investigated by Rayleigh, who developed an expression of the type

$$I = I_0 e^{-\beta x}$$

where I_0 is the intensity of the incident beam, I is the intensity of the beam after it has traversed a distance x , and β is the coefficient of scattering. Rayleigh showed that β is inversely proportional to the fourth power of the wave length. Thus in the visible portion of the solar spectrum, blue light is scattered more than red light, since the former has a shorter wave length than the latter. This fact accounts for the blue color of the sky, since blue light is scattered more than red, and there is therefore a preponderance of blue light in the diffuse radiation in the sky. This also accounts for the red color of the sun at sunrise and sunset. The solar rays then traverse a long path through the atmosphere, during which time the blue is scattered from the beam, leaving a preponderance of red in the direct rays which reach the eye.

The second process which depletes the solar beam is absorption. This absorption is almost entirely due to water vapor in the atmosphere. The variation of energy absorption with water vapor content of the atmosphere is shown in Fig. 23. The abscissa in this diagram represents the number of grams of water vapor in the column of atmosphere of cross section 1 sq cm traversed by the solar radiation. By comparing the absorption values shown with the solar constant, it is seen that from 6 to 13 per cent of the solar beam may be absorbed by water vapor in passing through the earth's atmosphere. Ozone at high levels also absorbs a small fraction of the solar radiation, as indicated in section 32.

Finally, the radiation from the sun may be reflected and absorbed by

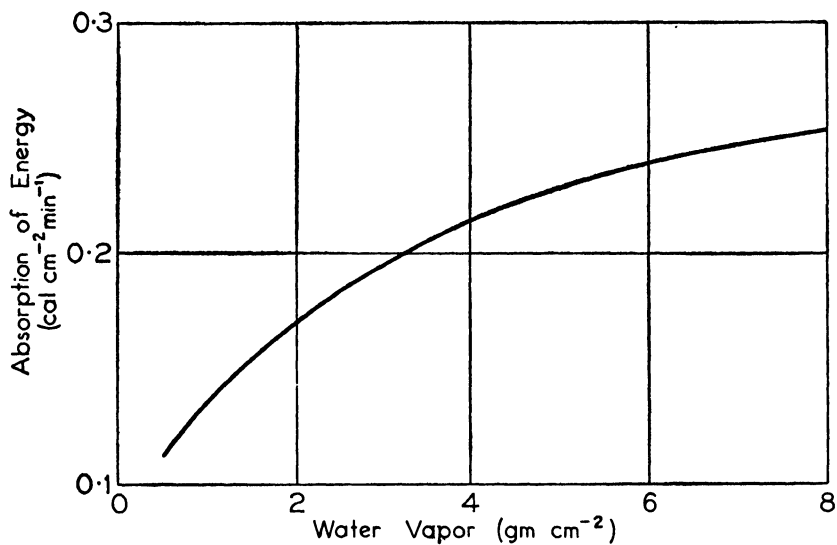


FIG. 23. Absorption of solar radiation by water vapor. (After Hoelper.)

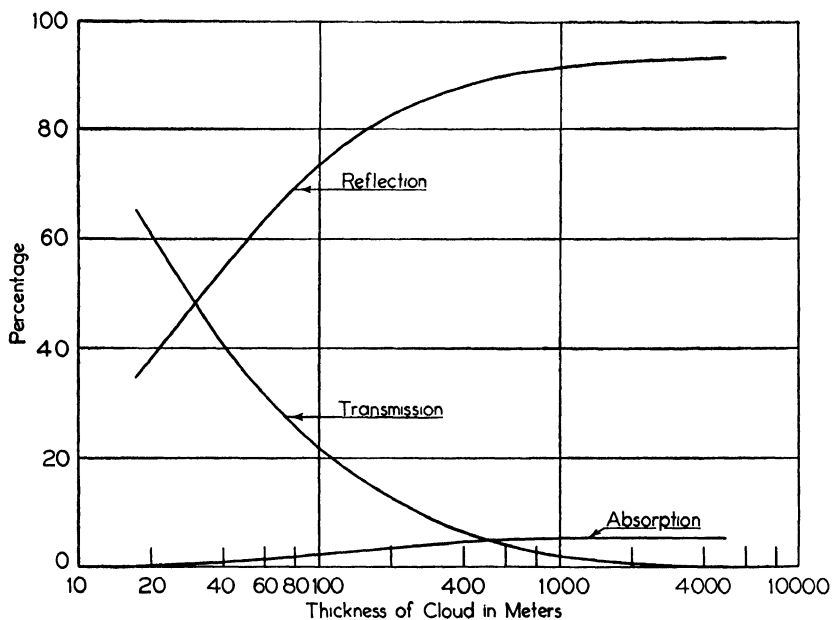


FIG. 24. The reflection, absorption, and transmission of solar radiation by clouds of varying thicknesses.

clouds. The reflecting power, or *albedo*, of clouds for solar radiation varies widely, depending mainly on the thickness of the cloud in question, and the amount of liquid water within it. It has been found, from theoretical considerations, that the albedo for thin, diffuse clouds may be as small as 0.1 or 0.2 (an albedo of 0.2 means that 20 per cent of the incident radiation is reflected), or for very thick, dense clouds it may be higher than 0.9. For clouds of average thickness and density, the albedo is about 0.8. The percentage of solar radiation reflected by clouds of varying thickness containing 1.0 gm of liquid water per m^3 is shown in Fig. 24. The maximum absorption of solar radiation in clouds is about 7 per cent of the incident radiation, which occurs in very thick, dense clouds. For thin, diffuse clouds the absorption is small, being less than 1 per cent. The variation of absorption with thickness of clouds having the same water content as above is shown in Fig. 24. The third curve in the figure gives the percentage transmitted. These curves are for cloud droplets of radius of 5×10^{-4} cm. There is some variation in the values given in the figure for clouds comprised of larger or smaller droplets. The nature of the relationship for clouds made up of ice crystals has not been determined.

Part of the solar radiation reaching the earth's surface is reflected, and the remainder is absorbed. Consider first the radiation incident on land masses. Most of the substances comprising the surface of the continents, such as rock and vegetation, have albedoes varying from 0.1 to 0.3. The only important exception is a snow surface, which has an albedo of about 0.8. The radiation which is not reflected is absorbed by the surface layer of the earth, raising its temperature, and this heated surface in turn warms the adjacent air. If the values of the specific heat and conductivity of the soil are high, the increase in temperature just at the surface is less than if they are low. Moist soils have a greater specific heat and conductivity than dry ones. For this reason moist sand, for example, does not become as warm as dry sand on a clear summer day. In the former case, part of the heat is used in evaporating the moisture, and this also prevents a marked increase in temperature.

Over the oceans, the albedo of the water surface varies with the altitude of the sun. With the sun near the horizon, the albedo of a smooth sea surface is about 0.4, whereas it is about 0.03 when the sun is near the zenith. The presence of waves causes little change with zenith sun, but produces an increase in the albedo when the sun is low. About 70 per cent of the incident radiation is absorbed in traversing the first meter of the ocean. The process of mixing, however, distributes this heat throughout a considerable layer of water, so that the

heating of the surface waters is very small. Not all this heat is effective in raising the temperature of the water, since about 30 per cent of the incoming energy is used in evaporating water. It has been estimated that about 2 mm of water per day are evaporated from the oceans.

29. Terrestrial and Nocturnal Radiation. Water vapor is much more effective in absorbing terrestrial radiation than in absorbing solar radiation. Carbon dioxide, which absorbs a negligible amount of solar radiation, is a strong absorber in several portions of the spectrum of

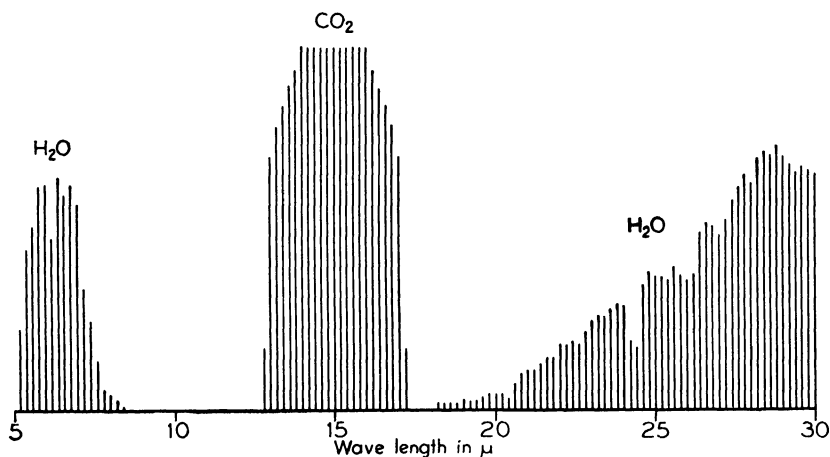


FIG. 25. The variation in the absorption of terrestrial radiation by water vapor and carbon dioxide. (After Elsasser.)

terrestrial radiation. As mentioned in section 27, the absorption by water vapor and carbon dioxide is by groups of lines and must be treated in a special manner. The absorption spectra of these two substances from 5 to 30 μ are shown in a schematic manner in Fig. 25. The absorption at any given wave length is proportional to the length of the vertical line at that wave length. From Kirchhoff's law, it follows that the radiation at the same wave length is also proportional to the length of the line. From the diagram it is seen that there is a strong band of water vapor absorption and radiation from 5 to 8 μ , and another commencing at 18 μ , and extending to greater wave lengths. At wave lengths greater than 30 μ , the absorption and radiation by water vapor are still more intense. There is a band of intense absorption and radiation by carbon dioxide extending from 13 to 17 μ , and a smaller band, not shown in the figure, centered at about 4.3 μ . A number of experimental determinations of the absorption at several regions of the spectrum have been made, and from these measured values, Elsasser has

computed the following values of the generalized absorption coefficient l .

Peak of the $6\ \mu$ band	$l = 125$
Region from 8 to $13\ \mu$	$l = 0.10$
Region near $21\ \mu$	$l = 17$
Peak of the band at $\mu > 30$	$l = 3000$

Using these values and a technique beyond the scope of this book, Elsasser constructed a radiation chart which permits the evaluation of the radiation currents in the atmosphere when the vertical temperature and water vapor distribution are known. In the following paragraphs a simpler method of obtaining the approximate heat loss of the surface of the earth or of clouds is developed.

Any given portion of the earth's surface may be assumed to radiate as a black body at the temperature of that portion. The distribution of energy emission with wave length at a temperature of 273°A is shown in Fig. 21a. It follows from what has been said in the preceding paragraph that the atmosphere also emits radiation in certain wave lengths. Part of the energy emitted reaches the earth's surface. Thus the net loss of heat at the surface is given by the difference between the upward beam of black-body radiation and the downward beam of radiation, of the black-body type in certain wave length intervals only. The difference between these two beams is known as the *nocturnal radiation*, and may be measured on a clear night by a radiation instrument with its radiating element placed horizontally. The instrument measures the difference between the black-body radiation emitted by its element and the radiation received on the element from the atmosphere above.

Two empirical formulas from which the nocturnal radiation may be computed have been given. The expression developed by Ångström has the form

$$\frac{R}{\sigma T^4} = A - B 10^{-\delta e} \quad (29.1)$$

where R is the downward radiation from the atmosphere, σT^4 is the black-body radiation at the surface temperature T , e is the vapor pressure at the surface in millibars, and A , B , and δ are constants having the values 0.81, 0.24, and 0.052. The second equation, given by Brunt, is

$$\frac{R}{\sigma T^4} = a + b\sqrt{e} \quad (29.2)$$

where $a = 0.44$, $b = 0.080$, and e is the vapor pressure in millibars. In general, the values obtained by the use of these two formulas are in

good agreement. It may be seen that these equations give valid results for the radiation only for limited ranges of values of e by assuming that the air at the surface is perfectly dry, i.e., $e = 0$. According to the expressions given, the downward radiation is then about one-half of the black-body radiation, an improbable result in view of the dependence of radiation by the atmosphere on water vapor.

The nocturnal radiation N is given by the expression

$$N = \sigma T^4 - R \quad (29.3)$$

Substitute for R from (29.2) and (29.3) becomes

$$N = \sigma T^4 (1 - a - b \sqrt{e}) \quad (29.4)$$

An expression similar to (29.4), but not involving the vapor pressure e , may be developed by considering the absorption spectrum of water vapor and carbon dioxide shown in Fig. 25. On the basis of the data given in this figure, it is possible to divide the spectrum of water vapor and carbon dioxide absorption into two main regions, as given below.

(a) Complete absorption.

By a small amount of water vapor from 5 to 8 μ ,

By a small amount of carbon dioxide from 13 to 17 μ ,

By a moderate amount of water vapor from 17 to 20 μ ,

By a small amount of water vapor for $\mu > 20$.

(b) Complete transmission.

By a large amount of water vapor or carbon dioxide from 8 to 13 μ .

A small amount of water vapor or carbon dioxide may be taken as the amount normally present in a vertical column of air near the surface, of unit cross section and a height of 50 m. A moderate amount of water vapor is that in a similar column 1 km high, and a large amount of water vapor or carbon dioxide is that in a column extending from the surface to the upper limit of the atmosphere. It follows that the layer of air extending from the surface to a height of 1 km will absorb the upward beam of black-body radiation from the earth's surface from 5 to 8 μ , and at wave lengths greater than 13 μ . From Kirchhoff's law, it follows that this layer radiates as a black body at its appropriate temperature at these same wave lengths. It may be assumed as a first approximation that this downward black-body radiation from the layer is equal in magnitude to the upward radiation from the earth at the same wave lengths. From 8 to 13 μ there is no absorption or radiation by the atmosphere, and the black-body radiation from the surface proceeds undiminished to outer space, and as a result the surface cools.

Now consider Fig. 26, which shows Planck's curve for black-body radiation at 273°A , which will be taken as the surface temperature: The hatched area under the curve represents the energy lost to outer space in the transparent band. At the other wave lengths, the surface receives as much energy from the atmosphere as it emits, and there is thus no net loss of energy in these wave lengths. It was assumed above that the black-body radiation downward from the atmosphere

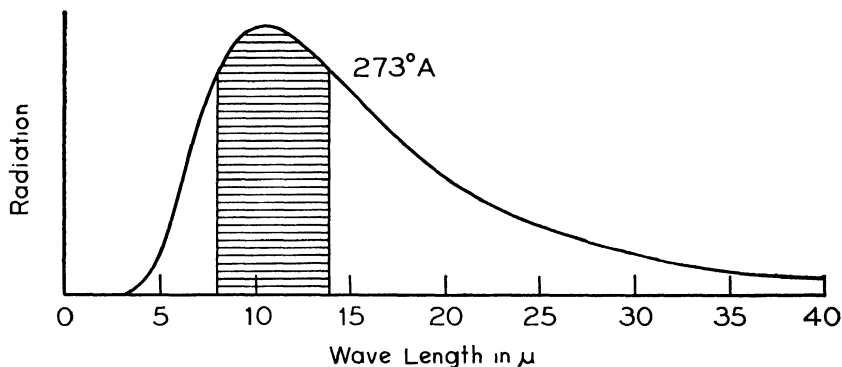


FIG. 26. Energy transmitted by and absorbed in the atmosphere.

to the surface was emitted at the same temperature as that radiated upward from the surface. For all absorbing wave lengths except those from 17 to $20\ \mu$, the absorption and radiation occur in the lowest $50\ \text{m}$ of the 1-km layer, and it is therefore valid to assume that there is no significant variation in temperature in this height interval. From 17 to $20\ \mu$, however, the downward radiation comes from a layer $1\ \text{km}$ in height, and the mean temperature of this layer will be, under average conditions, about 3°C lower than the surface temperature. There is thus a small net loss of energy in this interval. To allow for this loss without unduly complicating the diagram, the transparent band has been drawn as extending from 8 to $14\ \mu$, instead of from 8 to $13\ \mu$.

If now the ratio of the hatched area to the total area under Planck's curve is denoted by γ , it follows that the net loss of energy, or the nocturnal radiation, is given by $\gamma\sigma T^4$, since the area under the curve is proportional to σT^4 according to Stefan's law. Measurement of the areas by planimeter gives the following values of γ for various temperatures.

$T\ (^{\circ}\text{A})$	200	225	250	273	300	325
γ	0.22	0.27	0.32	0.35	0.37	0.39

The variation in γ in the range of surface temperatures from 250° to

300° A is small, and sufficient accuracy is obtained by assuming that γ is constant and equal to 0.35. The nocturnal radiation is then given by

$$N = \gamma \sigma T^4 = 2.85 \times 10^{-11} T^4 \text{ cal cm}^{-2} \text{ min}^{-1} \quad (29.5)$$

This equation gives results of the same order of magnitude as those given by the empirical relationship (29.4).

Since clouds radiate effectively as black bodies, this expression may also be used to determine the approximate radiational loss of heat at the top of a cloud. When the cloud is at medium or high altitudes, the absorbing layers are considerably thicker than 50 m and 1 km, since there is less water vapor present. As a result, the net loss of heat in the absorbing bands, and especially from 17 to 20 μ , is greater. Thus, although γ as given above decreases with temperature, the effective value of γ does not vary much from 0.35, as a more detailed study of the areas shows. Thus equation 29.5 may also be used without modification to obtain an estimate of the radiational heat loss from the top of clouds.

It must be emphasized that equations of the types (29.4) and (29.5), when applied to specific situations, give results which only roughly approximate the true values. If more accurate values are required, the vertical distribution of temperature and water vapor must be known, and more refined and complicated methods involving the use of a radiation chart, such as that developed by Elsasser, must be used.

A knowledge of the loss of heat at the surface by nocturnal radiation is important in forecasting minimum temperatures, in forecasting radiation fog (section 134), and for frost forecasting (section 172).

30. Radiation with Cloudy Skies. When clouds are present, the loss of heat from the surface by nocturnal radiation is reduced. Since clouds act as black bodies in absorbing and emitting long-wave radiation, it follows that the upward radiation in the transparent band from the earth's surface does not escape to outer space, but is absorbed by the base of the cloud layer. The cloud base also radiates as a black body in all wave lengths. In the absorbing bands, the radiation is absorbed by the air just below the cloud, and black-body radiation from this air returns to the cloud base. There is thus no net loss of heat in the absorbing bands. In the transparent band, the black-body radiation at the temperature of the cloud base reaches the earth's surface undiminished in intensity. The net loss of heat at the surface is then given by the difference between black-body radiation in the transparent band at the temperature T_s of the surface and that in the same

band at the temperature T_B of the cloud base. Thus, with cloudy skies

$$N = \gamma\sigma(T_S^4 - T_B^4) \quad (30.1)$$

It will now be shown that the loss of heat at the surface is approximately proportional to the height of the cloud. Denote the difference in temperature between the surface and the cloud base by ΔT . Thus

$$T_B = T_S - \Delta T \quad (30.2)$$

Substituting (30.2) in (30.1) gives

$$N = \gamma\sigma[T_S^4 - (T_S - \Delta T)^4] \quad (30.3)$$

By the binomial theorem

$$(T_S - \Delta T)^4 = T_S^4 - 4T_S^3\Delta T + \frac{4 \times 3}{2} T_S^2(\Delta T)^2 - \dots$$

If suitable values such as $T_S = 280^\circ \text{A}$ and $\Delta T = 10^\circ \text{A}$ are substituted in this equation, it is seen that sufficient accuracy is obtained by retaining only the first two terms on the right-hand side. Thus

$$(T_S - \Delta T)^4 = T_S^4 - 4T_S^3\Delta T \quad (30.4)$$

Substituting (30.4) in (30.3) leads to

$$N = 4\gamma\sigma T_S^3\Delta T = 4\gamma\sigma T_S^3(T_S - T_B) \quad (30.5)$$

Thus for any specified value of T_S

$$N \propto T_S - T_B$$

If it is assumed that the temperature in the atmosphere decreases linearly with height, the heat loss by nocturnal radiation is proportional to the height of the cloud. The general validity of this result is shown by measured values of the nocturnal radiation with clouds at various heights, given in Fig. 134, section 134. It is also of interest to note that for any given value of ΔT the loss of energy from the surface by radiation varies as the third power of the surface temperature when the sky is clouded, but when it is cloudless, the loss varies as the fourth power of the surface temperature. Dividing (29.5) by (30.5), it is seen that the radiational heat loss for the same surface temperature is

$\frac{T_S}{4\Delta T}$ times as great when the sky is clear as when it is clouded. If

$T_S = 280^\circ \text{A}$ and $\Delta T = 12^\circ \text{A}$, the heat loss is about six times greater for clear than for cloudy skies. This result is also of significance in forecasting the occurrence of fog and frost.

In a similar manner the net loss of heat by a cloud may be computed.

The same reasoning that showed that the loss of heat by the surface is given by (30.1) also indicates that the gain of heat at the cloud base is equal to

$$\gamma\sigma(T_S^4 - T_B^4)$$

If the temperature of the top of the cloud is denoted T_T , the loss of heat at the top is equal to

$$\gamma\sigma T_T^4$$

The net loss of heat by the cloud is then

$$\gamma\sigma(T_T^4 - T_S^4 + T_B^4)$$

In the lower troposphere a cloud always loses heat by radiation. To show this, consider the limiting case where the heat lost at the top is just equal to that gained at the base. This occurs when

$$\gamma\sigma(T_T^4 - T_S^4 + T_B^4) = 0 \quad (30.6)$$

or

$$T_T^4 + T_B^4 = T_S^4 \quad (30.7)$$

If the cloud is not very thick, it is possible to state, with sufficient accuracy, that

$$T_T^4 + T_B^4 = 2T_M^4 \quad (30.8)$$

where T_M is the mean temperature of the cloud. Substituting (30.8) in (30.7) obtains

$$T_M^4 = \frac{1}{2}T_S^4 \quad (30.9)$$

The mean surface temperature at latitude 50° N is approximately 281° A. Substituting this value in (30.9), and solving for T_M gives T_M equal to 236° A. This temperature is the average temperature in the atmosphere at a height of 7 km at latitude 50° N. Thus clouds of small or medium thickness below this height always lose heat by radiation. For thick clouds the loss is even more pronounced, for they extend to lower levels, and gain less heat at the base, while the heat loss at the top is undiminished.

31. The Heat Balance in the Atmosphere. Since there is no evidence of any significant increase or decrease in the mean temperature of the earth's atmosphere over a period of years, it is evident that the radiant energy received from the sun and that emitted by the earth and its atmosphere to outer space must be equal. The total amount of heat reaching the earth during a year may be computed without difficulty by using the value of the solar constant, 1.94 cal per cm^2 per min, and

remembering that the area intercepting solar radiation at any instant is the cross-sectional area of the earth. A simple computation shows that the earth receives energy from the sun at the rate of 130×10^{22} cal per annum.

The various transformations of this energy before it is radiated again to outer space are of interest and will be discussed in the following paragraphs. The discussion follows that given by Landsberg, with minor modifications based on the work of Baur and Philipps, and Möller. The unit of energy used is 10^{22} cal per annum. Of the 130 units received by the earth from the sun, clouds reflect 39 and the atmosphere scatters 12 back to outer space, the atmosphere absorbs 19, and 35 reach the earth's surface in the direct solar beam, and 25 reach it as diffuse sky radiation. There is an exchange of heat between the earth and its atmosphere by terrestrial radiation, by condensation and evaporation processes, and by turbulence. Heat is absorbed at the earth's surface in the process of evaporating water, the water vapor is carried upward, and when it condenses, this heat is released to the atmosphere. There is thus a transfer of heat from the surface to the atmosphere. Equation 53-11 shows that when the lapse rate of temperature is of the stable type, there is a transfer of heat downward by turbulence, and when the lapse rate is of the unstable type, there is a transfer of heat upward. The average lapse rate in the troposphere is about 6°C per km, and therefore stable, so there is on the average a transfer of heat from the atmosphere to the surface of the earth by turbulence.

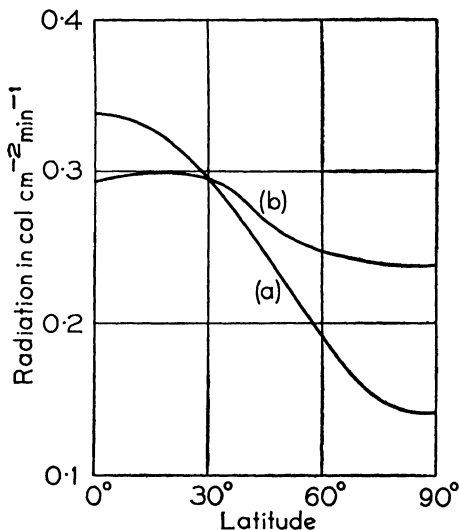


FIG. 27. The variation of (a) incoming and (b) outgoing radiation with latitude. (After Simpson, Baur and Philipps.)

The various amounts of heat transferred by these processes are given in the following table. The letter (S) indicates that the radiation is of the short-wave or solar type, and (L) shows that it is of the long-wave or terrestrial type. The upward and downward fluxes of energy through a surface at the outer limit of the atmosphere and through a

surface at mean sea level are given in the upper portion of the table. At the bottom the gain and loss of heat in the atmosphere between these two surfaces are indicated. The values given in the table are only approximate, but they indicate the order of magnitude of the several processes involved.

THE HEAT BALANCE IN THE ATMOSPHERE
Unit 10^{22} cal per annum

	The Downward Flux from the		The Upward Flux from the	
At the outer limit of the atmosphere	Sun	130	Clouds (S)	39
			Atmosphere (S)	12
			Atmosphere (L)	65
			Earth (L)	14
		130		130
At the earth's surface	Sun (direct) (S)	35	Earth to outer space (L)	14
	Sun (diffuse) (S)	25	Earth to the atmosphere	
	Atmosphere		By radiation (L)	146
	By radiation (L)	125	By evaporation	30
	By turbulence	5		
		190		190
The atmosphere	Gains by		Losses by	
	The absorption of radiation from the		The emission of radiation to	
	Sun (S)	19	The earth (L)	125
	Earth (L)	146	Outer space (L)	65
	Condensation	30	Turbulence	5
		195		195

The heat balance of the earth as a whole has been discussed above. Investigation of the average intensities of the incoming beams of solar radiation and outgoing beams of terrestrial radiation at various latitudes have also been carried out. Curve (a) in Fig. 27 shows the variation in intensity with latitude of the effective incoming solar radiation, according to Simpson. In obtaining this curve, allowance was made for the reflection of solar radiation from the atmosphere, including that from the average amount of cloud found at each latitude, and from the earth's surface. Curve (b) gives the variation in intensity with latitude of the outgoing terrestrial radiation, according to Baur and Philipps. This curve is computed on the basis of

assumed distributions of temperature and water vapor with height at each latitude. The figure shows that from the equator to latitude 30° the incoming radiation is greater than the outgoing radiation, whereas from 30° latitude to the pole the situation is reversed. It is evident from this that there must be a transport of heat from equator to pole if the mean temperature distribution over the earth is to be maintained. The significance of this transport of heat in the general circulation of the atmosphere is discussed in Chapter 12.

32. Radiative Equilibrium in the Stratosphere. In the troposphere the lapse rate appears to be controlled by mixing processes which occur with turbulent motion. An atmosphere in which the vertical temperature distribution is governed entirely by mixing is said to be in *convective equilibrium*. The effect of turbulent mixing in the troposphere is discussed in detail in sections 53 and 76.

It has been believed for some time that radiation plays an important part in maintaining that isothermal, or nearly isothermal, portion of the atmosphere known as the stratosphere. It was suggested in 1909 that *radiative equilibrium*, a condition in which each element of air gains as much energy by absorption of radiation as it loses by emission, accounted for the presence of the stratosphere. These early investigations depended on the assumption that water vapor in the atmosphere radiated and absorbed long-wave radiation as a gray body, i.e., that in all wave lengths it emitted and absorbed a fixed fraction of the black-body radiation at the appropriate temperature. The work of Simpson at a later date showed that this assumption is not valid, even as a first approximation. The wide variation of absorption with wave length is shown in Fig. 25. A further complication in the mathematical treatment is introduced by the fact that the radiation does not occur in parallel beams, but is diffuse. These early investigations were based on certain assumed vertical distributions of water vapor. For instance, an expression for the variation of the mean vapor pressure with height was given by Hann as

$$e = e_0 10^{-\frac{h}{6.3}}$$

where e_0 is the vapor pressure at the surface, and e is that at a height h in kilometers. Later work has shown that expressions of this type are not adequate. Progress in the investigation of radiative processes in the stratosphere has been hampered by the lack of instruments which are capable of providing accurate humidity measurements at the low temperatures encountered in the stratosphere.

Studies of the ozone distribution in the atmosphere have provided information which may prove useful in accounting for the presence of

the stratosphere. It has been shown that ultra-violet radiation from the sun is absorbed by ozone located at heights from 10 to 40 km, with a mean height of 22 km. It is estimated that from 4 to 6 per cent of the incident solar radiation is absorbed by this means. It is probable that the increase in temperature with height in the stratosphere in the tropics, and the more nearly isothermal conditions near the pole, shown in Fig. 3, are connected with the observed increase in ozone from equator to pole. The precise nature of the relationship between these two elements is not known, however.

Any complete explanation of the stratosphere must also take account of the advection, or horizontal transport of air, which takes place in the stratosphere. A satisfactory explanation of the stratosphere awaits the integration of the separate effects of solar and terrestrial radiation, ozone, and advection into a comprehensive and consistent theory.

PROBLEMS AND EXERCISES

1. The radius of the sun is 430,000 miles, and the radius of the earth's orbit is 93 million miles. Using the value of the solar constant, compute the temperature of the sun if it radiates as a black body.

2. According to the figures given in section 31, 39 per cent of the solar radiation incident at the outer limits of the atmosphere is reflected back to space. Keeping this in mind and using the value of the solar constant, compute the effective radiating temperature of the earth and its atmosphere taken as a unit if it radiates as a black body.

3. According to the figures given in section 31, 15 per cent of the solar radiation incident at the outer limits of the atmosphere is on the average throughout the year absorbed in traversing the atmosphere. Compute the average increase in temperature of the atmosphere for a 24-hour period attributable to the absorption of solar radiation. Assume that the mean pressure at mean sea level over the earth is 1013 mb.

4. Solar radiation of intensity $1 \text{ cal cm}^{-2} \text{ min}^{-1}$ falls on the top of a cloud extending from 800 to 700 mb. Assume that 6 per cent of this radiation is absorbed in traversing the cloud. The temperature at the top of the cloud is 5°C , that at the base of the cloud is 10°C , and the surface temperature is 18°C . Neglecting the specific heat of liquid water, $1 \text{ cal gm}^{-1} \text{ deg}^{-1}$, in comparison with the latent heat of condensation, approximately 591 cal gm^{-1} at the temperature of the cloud, compute the decrease in temperature of the cloud as a whole in 1 hour.

BIBLIOGRAPHY

- Brunt, D., *Physical and Dynamical Meteorology*, London, Cambridge University Press, 1939. Chapters 5, 6, 7.
- Haurwitz, B., *Dynamic Meteorology*, New York, McGraw-Hill Book Co., 1941. Chapter 5.
- Problems of Modern Meteorology*, London, Royal Meteorological Society, 1934. Number 7.

- Shaw, Sir N., *Manual of Meteorology*, London, Cambridge University Press. Vol. 3 (1930), Chapters 4, 5.
26. Cork, J. M., *Heat*, New York, John Wiley and Sons, 1933. pp. 145-170.
- 27, 29. Elsasser, W. M., *Heat Transfer by Infrared Radiation in the Atmosphere*, Harvard Met. Studies, No. 6, 1942.
28. Aldrich, L. B., "The Reflecting Power of Clouds," *Smithsonian Inst., Misc. Coll.*, **69**, No. 10, 1919.
28. *Ann. Astrophys. Obs. Smithsonian Inst.*, Washington, D. C., **2**, 1908; **3**, 1913; **4**, 1922; **5**, 1932.
28. Hewson, E. W., "The Reflection, Absorption and Transmission of Solar Radiation by Fog and Clouds," *Q. J. Roy. Met. Soc.*, **69**, 47-62 (1943).
28. Paranjpe, M. M., "Variations of the Solar Constant and Their Relation to Weather," *Q. J. Roy. Met. Soc.*, **64**, 459-474 (1938).
29. Brunt, D., "Notes on Radiation in the Atmosphere," *Q. J. Roy. Met. Soc.*, **58**, 389-418 (1932).
29. "Emission and Absorption of Radiation in the Atmosphere," *Q. J. Roy. Met. Soc.*, **68**, 197-214 (1942).
31. Baur, F., and H. Philipps, "Der Wärmehaushalt der Lufthülle der Nordhalbkugel," *Gerl. Beitr. Geophys.*, **45**, 82-132 (1935); **47**, 218-223 (1936).
31. Landsberg, H., *Physical Climatology*, State College, Pennsylvania State College, 1941. pp. 81-107.
31. Möller, F., "Bemerkungen zur Warmebilanz der Atmosphäre und der Erdoberfläche," *Gerl. Beitr. Geophys.*, **47**, 215-217 (1936).
31. Simpson, Sir G. C., *Some Studies in Terrestrial Radiation*, Mem. Roy. Met. Soc., **2**, No. 16, 1928.
- Further Studies in Terrestrial Radiation*, Mem. Roy. Met. Soc., **3**, No. 21, 1928.
- Distribution of Terrestrial Radiation*, Mem. Roy. Met. Soc., **3**, No. 23, 1929.

CHAPTER 6

ATMOSPHERIC MOTIONS UNDER BALANCED FORCES

The atmosphere is a fluid, and as such its motions may be analyzed by means of hydrodynamics. Using hydrodynamical principles, it is possible to set up equations of motion for a fluid on a rotating earth which are perfectly general in their application. If a perfectly general solution could be arrived at, it would then be possible to forecast the weather by means of the hydrodynamical equations. The complexities of the atmosphere are so great, however, that a number of simplifying assumptions are necessary before these equations can be solved. As a consequence, the equations of motion yield results of only limited applicability. The general equations of motion will not be derived, therefore, but attention will be focused on the simpler equations which result when secondary effects are neglected. In particular, in this chapter only steady motions, i.e., those not involving accelerations, of the air in question will be considered. If no net acceleration is present, the motion must be under balanced forces. Two of the most important of these forces will now be considered in detail.

33. The Pressure Gradient Force. Since the atmosphere is a fluid, the pressure in it will vary from one portion to another, but the variation is always continuous. Because of these variations in pressure throughout the atmosphere, both in the horizontal and vertical, there is a force acting on any given element of air.

The magnitude and direction of this force may be derived in the following manner. Consider a parallelepiped with the dimensions dx , dy , and dz , as shown in Fig. 28. Assuming the atmosphere to be a non-viscous fluid, then the pressure acts over any surface in a direction normal to that surface. The total force, then, acting on face $A E H D$ is $p \, dy \, dz$, since pressure is force per unit area, where p represents the average pressure over the face. Since this surface is parallel to the yz plane, the force acts in the x direction. If $\partial p / \partial x$ is the x component of the pressure gradient, the pressure over the face $B F G C$ is $p + \frac{\partial p}{\partial x} dx$, so the force on that face of the parallelepiped is $\left(p + \frac{\partial p}{\partial x} dx \right) dy \, dz$, acting in the negative x direction. The resultant force acting on the

volume $dx\,dy\,dz$ in the x direction is then

$$p\,dy\,dz - \left(p + \frac{\partial p}{\partial x}dx\right)dy\,dz = -\frac{\partial p}{\partial x}dx\,dy\,dz$$

In meteorology, as in hydrodynamics, unit mass of fluid is considered, so the expression must be divided by the mass in the volume element,

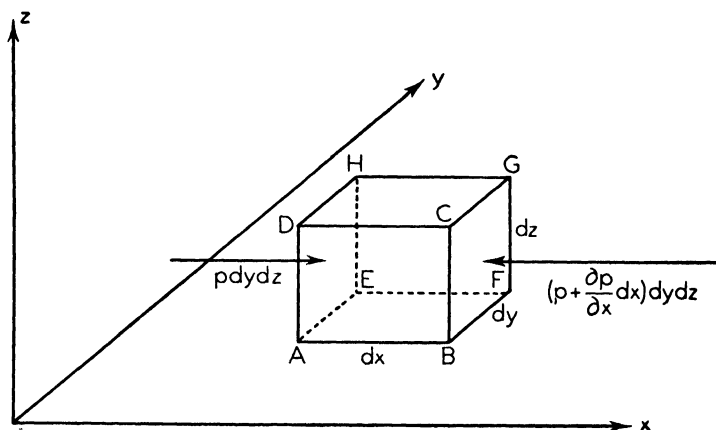


FIG. 28. The determination of the pressure gradient force.

which is $\rho\,dx\,dy\,dz$, where ρ is the mean density. The force per unit mass in the x direction is then

$$-\frac{1}{\rho}\frac{\partial p}{\partial x} \quad (33.1)$$

If p increases with x , then $\partial p/\partial x$ is positive, and the negative sign indicates that the pressure gradient force acts in the negative x direction, i.e., from high to low pressure. In a similar manner, it may be shown that the pressure gradient force in the y direction is

$$-\frac{1}{\rho}\frac{\partial p}{\partial y} \quad (33.2)$$

and in the z (vertical) direction it is

$$-\frac{1}{\rho}\frac{\partial p}{\partial z} \quad (33.3)$$

The resultant of $\partial p/\partial x$ and $\partial p/\partial y$ is known as the pressure gradient as the term is generally used in meteorology. If the vertical com-

ponent of the pressure gradient force (33.3) is exactly balanced by the acceleration of gravity g , it follows that

$$-\frac{1}{\rho} \frac{\partial p}{\partial z} = g \quad (33.4)$$

This is the fundamental statical equation already given in (9.1). This equation is highly accurate except when large vertical accelerations occur, as in strong convection currents.

The horizontal components of the pressure gradient force are of primary importance in the study of atmospheric motions, as will be seen in later sections.

34. The Deflecting Force of the Earth's Rotation (Coriolis Force).

The pressure gradient force, which has just been considered, is a true force. The second force is an apparent force which results from the rotation of the earth, rather than a true force. In the following discussion, motion with respect to two frames of reference, one being the solar system, or more simply space, and the other the rotating earth, will be considered. The Newtonian mechanics holds without modification in a stationary frame of reference, or in one moving with a constant velocity of translation, but not in a rotating frame of reference. The simple form of Newton's laws applicable in space does not therefore apply on the rotating earth, which is the frame of reference for atmospheric motions. It is, however, much more convenient to use Newton's laws in their simple form on the earth. The force under consideration in this section, known as the deflecting force, is one of two fictitious forces which, if included in the equations of motion of a particle on the rotating earth, permit the use of Newton's laws in their simple form for a fixed frame of reference.

Before proceeding with the mathematical treatment, an indication of the general nature of this fictitious force may be helpful. The portion of the earth's surface near the poles may, without serious loss of accuracy, be considered as a plane which rotates about the polar axis with the angular velocity of the earth. Only forces acting in the horizontal will be considered, so that the force of gravity which acts vertically does not have to be taken into account. It is assumed that frictional forces are absent.

A man stationed at the north pole throws a ball horizontally. To an observer in space the ball moves in a straight line with uniform velocity, while the earth rotates beneath it. To the man at the pole, however, the ball appears to curve to the right. Referring to Fig. 29, to the observer in space the ball thrown from O travels in a straight path and reaches P after time t . When the man at O throws the ball,

he is facing the point P . During the time t , however, he rotates with the earth through an angle ωt , where ω is the angular velocity of the earth, so that with respect to the space frame of reference he faces the point P_1 at the end of time t . He has not changed his position on the earth, and still faces in the same direction, since P and P_1 represent the same point on the earth's surface. To him, then, the ball has been deflected to the right, following the curved path shown in the figure. He naturally attributes this curved motion to a horizontal deflecting force. But no true force has been acting during the time t ; it only appears to the observer at the pole that a force has been acting. Just as the ball leaves O , its velocity is the same to both the observer in space and to the man at O . The time scale is the same in both frames of reference, so that to both observers it reaches point P after the time interval t . In the fixed frame of reference, the ball has traveled to P in a straight path with a uniform velocity in conformity with the Newtonian laws, since no external forces are acting. But to the man at O the ball has traversed the longer curved path in the same time, so that to him it has undergone an acceleration in the direction of motion, which he attributes to a force acting in that direction. It is clear, however, that no true force has been acting. This impression results from the operation along the direction of motion of a component of the second of the two fictitious forces mentioned, the centrifugal force.

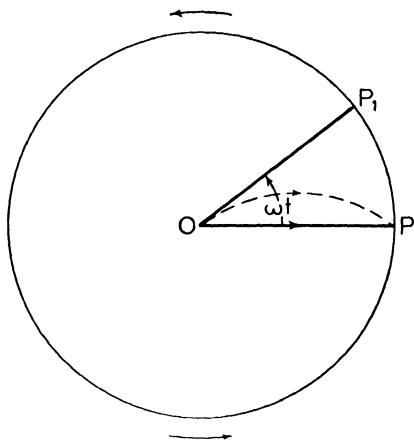


FIG. 29. The path of an object moving from the north pole.

The magnitudes of these two fictitious forces will now be determined mathematically. In Fig. 30a the xy system of axes is fixed in space, with the origin at the north pole. The x_1y_1 axes also have their origin at the north pole, but this system is fixed to the earth, so that it rotates about the polar axis with the angular velocity ω of the earth. At time $t = 0$ the two sets of axes coincide, so that after time t the angle between x and x_1 and between y and y_1 is ωt . Consider the motion of a unit mass at P as, for example, the ball of the previous paragraphs, or a unit mass of air, relative to the two coordinate systems.

It may be seen from Fig. 30a that the x_1 and y_1 coordinates of P

in terms of fixed coordinates x and y are given by

$$x_1 = x \cos \omega t + y \sin \omega t \quad (34.1)$$

$$y_1 = y \cos \omega t - x \sin \omega t \quad (34.2)$$

Now differentiate (34.1) with respect to time. In the following treatment a single dot above the coordinate symbol denotes the first deriv-

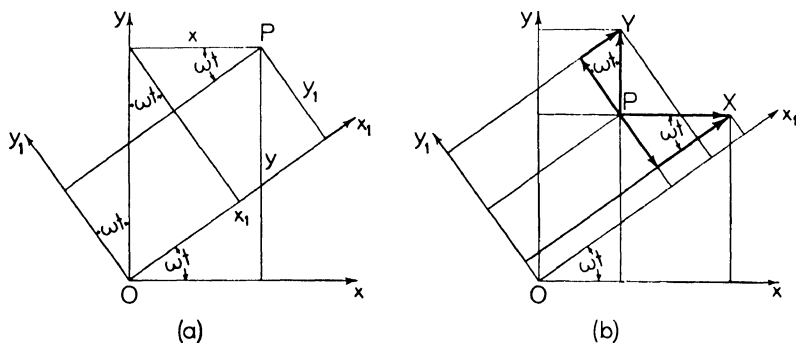


FIG. 30. Motion with respect to rotating frames of reference.

ative with respect to time; two dots denote the second derivative with respect to time.

$$\ddot{x}_1 = \ddot{x} \cos \omega t + \ddot{y} \sin \omega t - \omega \dot{x} \sin \omega t + \omega \dot{y} \cos \omega t \quad (34.3)$$

Multiplying (34.2) by ω and substituting in (34.3) lead to

$$\ddot{x}_1 = \ddot{x} \cos \omega t + \ddot{y} \sin \omega t + \omega \dot{y}_1 \quad (34.4)$$

Similarly,

$$\begin{aligned} \ddot{y}_1 &= \ddot{y} \cos \omega t - \ddot{x} \sin \omega t - \omega \dot{y} \sin \omega t - \omega \dot{x} \cos \omega t \\ &= \ddot{y} \cos \omega t - \ddot{x} \sin \omega t - \omega \dot{x}_1 \end{aligned} \quad (34.5)$$

Differentiating (34.4) with respect to time gives

$$\ddot{\ddot{x}}_1 = \ddot{\ddot{x}} \cos \omega t + \ddot{\ddot{y}} \sin \omega t + \omega \ddot{y}_1 - \omega \dot{x} \sin \omega t + \omega \dot{y} \cos \omega t \quad (34.6)$$

Multiply (34.5) by ω and substitute in (34.6). Then

$$\ddot{\ddot{x}}_1 = \ddot{\ddot{x}} \cos \omega t + \ddot{\ddot{y}} \sin \omega t + 2\omega \ddot{y}_1 + \omega^2 x_1 \quad (34.7)$$

Similarly,

$$\begin{aligned} \ddot{\ddot{y}}_1 &= \ddot{\ddot{y}} \cos \omega t - \ddot{\ddot{x}} \sin \omega t - \omega \ddot{x}_1 - \omega \dot{y} \sin \omega t - \omega \dot{x} \cos \omega t \\ &= \ddot{\ddot{y}} \cos \omega t - \ddot{\ddot{x}} \sin \omega t - 2\omega \ddot{x}_1 + \omega^2 y_1 \end{aligned} \quad (34.8)$$

In Fig. 30b the same coordinate systems are shown, with the X and Y components of the true forces on unit mass at P in the fixed frame of

reference shown as vectors by thick lines parallel to the x and y axes. A vector may be defined as any quantity which has both magnitude and direction. Velocities, angular velocities, and forces, for example, are vectors. The length of the line is proportional to the magnitude of the quantity, and the direction of the line denotes the direction of the quantity. Vectors may be combined according to the parallelogram law. As may be seen from the figure, the components in the rotating x_1y_1 system of these two components are given by

$$X_1 = X \cos \omega t + Y \sin \omega t$$

$$Y_1 = Y \cos \omega t - X \sin \omega t$$

Now since unit mass is being considered, $X = \ddot{x}$ and $Y = \ddot{y}$ in the fixed system. Thus

$$X_1 = \ddot{x} \cos \omega t + \ddot{y} \sin \omega t \quad (34.9)$$

$$Y_1 = \ddot{y} \cos \omega t - \ddot{x} \sin \omega t \quad (34.10)$$

By substituting (34.9) and (34.10) in (34.7) and (34.8), it follows that

$$\ddot{x}_1 = X_1 + 2\omega\dot{y}_1 + \omega^2 x_1 \quad (34.11)$$

$$\ddot{y}_1 = Y_1 - 2\omega\dot{x}_1 + \omega^2 y_1 \quad (34.12)$$

Now if

$$2\omega\dot{y}_1 = 2\omega v_1 = X'_1 \quad (34.13)$$

$$-2\omega\dot{x}_1 = -2\omega u_1 = Y'_1 \quad (34.14)$$

and

$$\omega^2 x_1 = X''_1, \quad \omega^2 y_1 = Y''_1 \quad (34.15)$$

equations 34.11 and 34.12 may be written

$$\ddot{x}_1 = X_1 + X'_1 + X''_1 \quad (34.16)$$

$$\ddot{y}_1 = Y_1 + Y'_1 + Y''_1 \quad (34.17)$$

G. Coriolis in 1831 called X'_1 and Y'_1 the components of the "force centrifuge composée" to distinguish them from those of the "force centrifuge ordinaire," X''_1 and Y''_1 . The former are the components of the deflecting force and the latter the components of the centrifugal force mentioned in the earlier general discussion.

The direction of these fictitious forces is shown in Fig. 31a. If the velocity V_1 denotes the resultant of the velocity components u_1 and v_1 , then it can be seen from (34.13) and (34.14) that the deflecting force acts perpendicular to and to the right of the direction of motion of the unit mass at P at any instant. If x_1 and y_1 are the components of the

radius r_1 from the center of rotation O to the unit mass at P , then the centrifugal force on P acts outward along r_1 according to (34.15).

From (34.16) and (34.17) it can be seen that if these two fictitious forces are added to the true forces present, then Newton's law that force equals acceleration for unit mass holds in the rotating frame of reference, the earth in this instance.

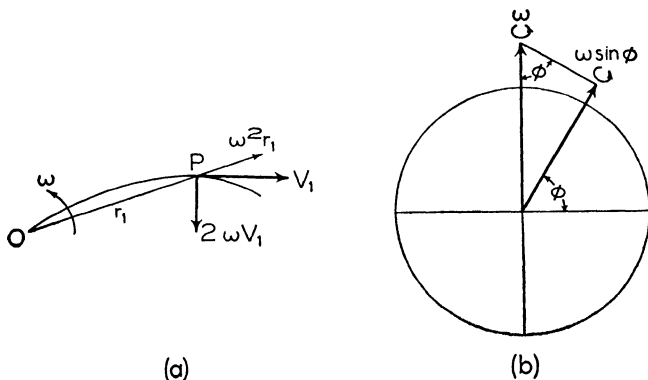


FIG. 31. (a) The direction of action of centrifugal and deflecting forces. (b) The component of the earth's angular velocity at latitude ϕ .

At the pole the centrifugal force is zero, since $r_1 = 0$. At a distance of, say, 100 m from the pole, it is very small, being 5.3×10^{-5} dyne. The deflecting force is, in general, much larger near the pole. For a velocity of 20 m sec^{-1} , it is 2.9×10^{-1} dyne. Thus in the situation depicted in Fig. 29 the centrifugal force may be neglected in comparison with the deflecting force.

The angular velocity of the earth about its polar axis is ω . The effective angular velocity about any other vertical axis is readily found since angular velocity is a vector.* The line representing the vector coincides with the axis about which the rotation occurs; the length of the line is proportional to the magnitude of the angular velocity; the direction of the vector is the direction of advance of a right-hand screw rotating in the same sense as the body. Thus in Fig. 31b the angular velocity of the earth is represented vectorially by the thick line coinciding with the polar axis of the earth. The angular velocity about a vertical axis at latitude ϕ is then, according to the figure, $\omega \sin \phi$. If this value of the angular velocity is substituted in (34.13) and (34.14), the horizontal components of the deflecting force at latitude ϕ are

$$X'_1 = 2\omega \sin \phi v_1 \quad (34.18)$$

$$Y'_1 = -2\omega \sin \phi u_1 \quad (34.19)$$

* J. H. Jeans, *Theoretical Mechanics*, Boston, Ginn and Company, 1907, p. 287.

If, as before, the velocity V_1 denotes the resultant of the velocity components u_1 and v_1 , then the magnitude of the deflecting force on unit mass of air moving over the earth's surface at latitude ϕ with velocity V_1 is

$$2\omega \sin \phi V_1 \quad (34\cdot20)$$

Since in meteorology the frame of reference is always the rotating earth it is not necessary to retain the subscripts. Equations 34·18 and 34·19 show that the deflecting force at any instant always acts perpendicularly to the direction of motion and to the right of it. In the southern hemisphere the magnitude of the deflecting force is the same, but it then acts to the left of the direction of motion. It follows then that the deflecting force tends to change the direction of motion of an air particle but not its speed.

A more extensive analysis of the motion of a particle in three dimensions shows that there is also a vertical component of the deflecting force. However, this component is extremely small in comparison with the force of gravity, and only rarely is it of significance. A situation in which this vertical component must be taken into account is discussed in section 38. The horizontal components of the deflecting force are of the same order of magnitude as the horizontally acting true forces in the atmosphere, such as the pressure gradient force discussed in the previous section, and they therefore form an essential part of any discussion of horizontal atmospheric motions.

The second of the two fictitious forces, the centrifugal force, is zero at the pole, and was therefore omitted from the previous discussion. However, for $\phi < 90^\circ$ it is of the same order of magnitude as the deflecting force. Since this force always acts perpendicularly to and outward from the axis of rotation of the earth, as shown in Fig. 31*a*, it follows that for $90^\circ > \phi > 0^\circ$ there is a horizontal component of the centrifugal force acting to the south in the northern hemisphere. This force acts whether the particle under consideration is moving or not. Accordingly, a unit mass initially at rest on the earth's surface should, if unrestrained, move toward the equator. This does not happen, however, since the earth is not a true sphere, and the attractive force of the earth's mass on the mass considered does not act in a direction exactly normal to the earth's surface. As a result of this, there is a component of gravity toward the north which exactly balances the southward component of the centrifugal force. The horizontal component of the centrifugal force is thus always balanced by an equal and opposite force, and it is not necessary to consider it in the analysis of horizontal atmospheric motions. A similar process of compensation operates in the southern hemisphere.

The centrifugal force discussed in this section must not be confused with the one introduced in section 37. In the latter the centrifugal force is that resulting from the circular motion of a mass of air about a center of rotation on the earth's surface, and is independent of the rotation of the earth. The centrifugal force in the present section results from the rotation of a mass of air around the polar axis of the earth, and the two are therefore entirely distinct. The shape of the earth has no effect on the centrifugal force on a mass of air rotating about a point on the earth's surface, and the force in this case is not, of course, zero.

35. The Geostrophic Wind Equation. The first of the atmospheric motions to be considered is that resulting when the pressure gradient force just balances the deflecting force. A mass of air at rest in a pressure field is acted upon only by the pressure gradient force. As soon as it commences to move as a result of that force, however, the deflecting force starts to operate, and the more rapid the motion, the greater the corresponding deflecting force becomes. It is clear, therefore, that air does not flow perpendicular to the isobars, from high to low pressure, but that it is subjected to a force which continually acts to deflect it to the right. In this case, however, there is no balance of forces and the air undergoes an acceleration. This situation is not, therefore, within the scope of this chapter.

The only situation in which the two forces may balance is that where the air is moving parallel to isobars which are themselves straight and parallel. The resulting wind is known as the *geostrophic wind*. The balance of forces may be seen with the aid of Fig. 32. The isobars are parallel to the y axis, with pressure increasing in the positive x direction. The pressure gradient force always acts in the negative x direction in this case, irrespective of the direction of motion of the air. The only direction of motion which permits a balance is that shown in the figure, the air flowing in the positive y direction. With a suitable value of v , then, the deflecting force will exactly balance the pressure gradient force and steady motion results. The geostrophic wind equation is, therefore,

$$2\omega \sin \phi v = \frac{1}{\rho} \frac{\partial p}{\partial x} \quad (35-1)$$

and v is the geostrophic wind velocity.

This equation may be used in any situation as long as the y axis is chosen parallel to the isobars. If the x axis is chosen parallel to the isobars, similar reasoning shows that the equation takes the form

$$2\omega \sin \phi u = -\frac{1}{\rho} \frac{\partial p}{\partial y} \quad (35-2)$$

When the isobars are parallel to neither x nor y axis, but have some intermediate orientation, the geostrophic wind velocity V may be considered as the resultant of the two component velocities u and v in

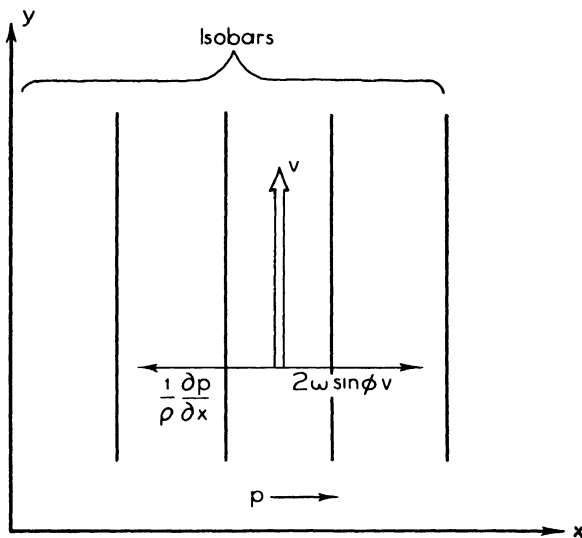


FIG. 32. The balance of forces for geostrophic motion.

the x and y directions respectively. In addition, $\partial p/\partial x$ and $\partial p/\partial y$ are then the components of the existing pressure gradient in the x and y directions, and the geostrophic motion is defined by two following equations.

$$2\omega \sin \phi v = \frac{1}{\rho} \frac{\partial p}{\partial x} \quad (35.3)$$

$$2\omega \sin \phi u = -\frac{1}{\rho} \frac{\partial p}{\partial y} \quad (35.4)$$

Buys Ballot's law follows directly: In the northern hemisphere an observer who stands with his back to the wind will have lower pressure to his left than to his right; in the southern hemisphere, the contrary holds.

It is assumed in the above treatment that no frictional forces are present, or if present, they are so small as to be negligible. This is an accurate statement of conditions in the atmosphere at heights greater than 2000 or 3000 ft above the surface. At lower levels, the frictional drag of the irregularities at the earth's surface on the moving air is

appreciable and leads to a decrease in velocity. The pressure gradient force is not affected thereby, but the deflecting force is reduced. This leads to air motion across isobars, from high to low pressure. Steady motion results, with the deflecting and frictional forces balancing the pressure gradient force. The flow across isobars may be noted on any surface weather map. This question is discussed further in section 52, and its practical significance in explaining diurnal variations of wind is brought out in section 123.

It has not been proved from theoretical considerations that air moves under the balanced conditions postulated above. Studies of air motions in the free atmosphere, however, have shown that masses of air frequently do move without appreciable acceleration for great distances over the earth's surface. This observed fact is the final justification for the use as a first approximation of the geostrophic wind relationship in meteorology. That the geostrophic wind is only an approximation is demonstrated by the fact, shown in section 47, that no pressure changes at the earth's surface are possible with simple geostrophic motion. Non-geostrophic motions are discussed in sections 46 and 121.

Representative values of the geostrophic wind velocity, computed by means of (35.1), are given in the following table. The density of the air is taken to be 1.1×10^{-3} gm cm⁻³, the average density at a height of 1 km above mean sea level.

GEOSTROPHIC WIND VELOCITY IN METERS PER SECOND

Latitude \ Pressure gradient	1 mb per 100 km	2 mb per 100 km	4 mb per 100 km
30°	12.5	25.0	50.0
45°	8.8	17.7	35.3
60°	7.2	14.4	28.8

A graph giving geostrophic winds corresponding to the distance between successive isobars is shown in Fig. 120, section 120. Such a graph facilitates the determination of geostrophic winds for forecasting purposes.

36. The Thermal Wind Component. Equation 9.1 shows that the rate of change of pressure with height is a function of the density only, if the small variations in the acceleration of gravity are neglected. It can be seen from this equation that the pressure decreases more rapidly with height in cold air than in warm air. Consider two points at the

earth's surface which have equal pressure, but with colder air above one than above the other. At a height of 1 km, say, the pressure in the colder air will therefore be less than that in the warm air. An isobar may join the two points at the surface, but cannot join the two points 1 km above these, since the pressures there are not the same. It follows that when a horizontal temperature gradient is present in the atmosphere, the pressure gradient and hence the geostrophic wind must vary with height. This variation may be a change in direction, in speed, or both. The geostrophic wind at 1 km may then be thought of as the resultant of two components, one the surface geostrophic wind, and the other component resulting from the horizontal temperature gradient. This latter component is known as the *thermal wind component*. The magnitude of this component is obviously proportional to the horizontal temperature gradient. Its direction is given by the following rule, which follows directly from the foregoing considerations: The thermal wind component blows around low temperature in the same sense that the geostrophic wind blows around low pressure, keeping low temperature to its left.

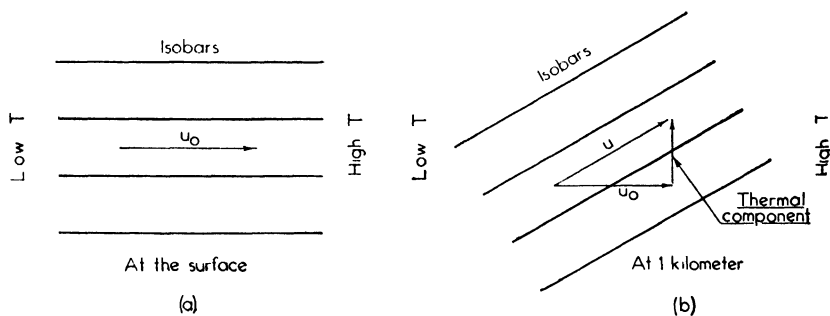


FIG. 33. Variation of geostrophic wind with height.

A typical variation of geostrophic wind with height is shown in Fig. 33. The pressure distribution and the geostrophic wind u_0 at the surface are shown in Fig. 33a. The air to the west is colder than that to the east. Conditions at 1 km are indicated in Fig. 33b. The thermal component, blowing from the south, is added vectorially to u_0 , giving the geostrophic wind u at 1 km. If colder air were to the north, the geostrophic wind would increase with height without undergoing any change in direction. The above considerations apply equally well to any levels in the atmosphere. If the geostrophic wind at 2 km is known, that at 3 km, or 4 km, can be found in this qualitative fashion, provided that the approximate direction and magnitude of the horizontal temperature gradient are known.

Equations for this variation of geostrophic wind with height may be derived. Using (7.7), the statical equation may be expressed as

$$\frac{1}{p} \frac{\partial p}{\partial z} = - \frac{g}{RT} \quad (36.1)$$

Differentiating (36.1) with respect to x and changing the order of differentiation give

$$\frac{\partial}{\partial z} \left(\frac{1}{p} \frac{\partial p}{\partial x} \right) = \frac{\partial}{\partial x} \left(\frac{1}{p} \frac{\partial p}{\partial z} \right) = \frac{\partial}{\partial x} \left(- \frac{g}{RT} \right) = \frac{g}{RT^2} \frac{\partial T}{\partial x} \quad (36.2)$$

Similarly, differentiating (36.1) with respect to y gives

$$\frac{\partial}{\partial z} \left(\frac{1}{p} \frac{\partial p}{\partial y} \right) = \frac{g}{RT^2} \frac{\partial T}{\partial y} \quad (36.3)$$

Substituting for ρ from (7.7) in (35.3) and (35.4), the equations for the geostrophic wind components u and v , leads to

$$\frac{v}{T} = - \frac{R}{l} \frac{1}{p} \frac{\partial p}{\partial x} \quad (36.4)$$

$$\frac{u}{T} = - \frac{R}{l} \frac{1}{p} \frac{\partial p}{\partial y} \quad (36.5)$$

where l is the Coriolis parameter $2\omega \sin \phi$. Differentiating (36.4) and (36.5) with respect to z gives

$$\frac{\partial}{\partial z} \left(\frac{v}{T} \right) = - \frac{R}{l} \frac{\partial}{\partial z} \left(\frac{1}{p} \frac{\partial p}{\partial x} \right) \quad (36.6)$$

$$\frac{\partial}{\partial z} \left(\frac{u}{T} \right) = - \frac{R}{l} \frac{\partial}{\partial z} \left(\frac{1}{p} \frac{\partial p}{\partial y} \right) \quad (36.7)$$

Substituting (36.2) and (36.3) in (36.6) and (36.7) respectively, gives

$$\frac{\partial}{\partial z} \left(\frac{v}{T} \right) = \frac{g}{l} \frac{1}{T^2} \frac{\partial T}{\partial x} \quad (36.8)$$

$$\frac{\partial}{\partial z} \left(\frac{u}{T} \right) = - \frac{g}{l} \frac{1}{T^2} \frac{\partial T}{\partial y} \quad (36.9)$$

Integration between the levels z_0 and z leads to the expressions

$$\frac{v}{T} = \frac{v_0}{T_0} + \frac{g}{l} \int_{z_0}^z \frac{1}{T^2} \frac{\partial T}{\partial x} dz \quad (36.10)$$

$$\frac{u}{T} = \frac{u_0}{T_0} - \frac{g}{l} \int_{z_0}^z \frac{1}{T^2} \frac{\partial T}{\partial y} dz \quad (36.11)$$

where u_0 and v_0 are the geostrophic wind components and T_0 the temperature at height z_0 . Rearranging gives

$$v = \frac{T}{T_0} v_0 + \frac{gT}{l} \int_{z_0}^z \frac{1}{T^2} \frac{\partial T}{\partial x} dz \quad (36-12)$$

$$u = \frac{T}{T_0} u_0 - \frac{gT}{l} \int_{z_0}^z \frac{1}{T^2} \frac{\partial T}{\partial y} dz \quad (36-13)$$

Several simplifying approximations may now be made. Since T and T_0 are not likely to differ widely and they are in degrees Absolute, the ratio T/T_0 may be taken as unity. In addition, T may be taken as the mean temperature of the layer from z_0 to z , and $\partial T/\partial x$ and $\partial T/\partial y$ may be assumed to be constant with respect to z . The integration of the right-hand terms of (36-12) and (36-13) is then straightforward, and leads to

$$v = v_0 + \frac{g}{lT} \frac{\partial T}{\partial x} (z - z_0) \quad (36-14)$$

$$u = u_0 - \frac{g}{lT} \frac{\partial T}{\partial y} (z - z_0) \quad (36-15)$$

The right-hand terms are the thermal wind components in the y and x directions and v and u are the geostrophic wind components at height z , expressed in terms of the geostrophic wind components v_0 and u_0 at height z_0 and the appropriate thermal components. These equations will be used in section 121 to derive a simple procedure for forecasting upper winds when direct observations of the latter are not available.

37. The Gradient Wind Equations. When isobars are curved, the motion of the air can no longer be linear, and the centrifugal force must also be considered. The centrifugal force has the magnitude v^2/r , where v is the velocity of the particle, and r the radius of curvature of its motion; it acts in the direction of increasing r . The air motion corresponding to a balance among the pressure gradient force, the deflecting force, and the centrifugal force is known as the *gradient wind*. The radius of curvature of the motion must be constant, if the motion is to be steady, and so the wind must blow in circular paths.

Consider a region of low pressure, having circular isobars, as indicated in Fig. 34. Since the pressure gradient force $-\frac{1}{\rho} \frac{\partial p}{\partial r}$ always acts at right angles to the isobars, while the deflecting force and centrifugal force always act at right angles to the direction of motion, it follows that the only direction of motion which permits a balance of forces is

that parallel to the isobars. Theoretically either clockwise or counterclockwise motion is possible. If clockwise motion is assumed, the centrifugal force must balance the sum of the pressure gradient and

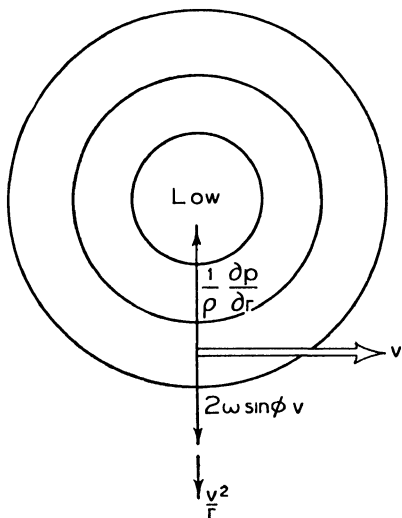


FIG. 34. The balance of forces in a cyclone.

deflecting forces. The centrifugal force is, however, considerably smaller than either of the other two under ordinary meteorological conditions. Only when r is small, ($r < 100$ km), does the centrifugal force approach the sum of the other two in magnitude. It is clear then that the hypothesis of clockwise motion around a low-pressure area must be discarded. The alternative, counterclockwise motion, as shown in Fig. 34, means that the pressure gradient force just balances the sum of the deflecting and centrifugal forces. No limitations of the above kind are present, and the balanced condition may hold for any value of the radius of curvature. This result is confirmed by an inspection of

weather maps, which show counterclockwise winds around low-pressure areas.

The balance of forces for the cyclonic case is given by

$$\frac{1}{\rho} \frac{\partial p}{\partial r} = lv + \frac{v^2}{r} \quad (37.1)$$

where l is, as in section 36, the Coriolis parameter $2\omega \sin \phi$. It follows from a comparison of (37.1) and (35.1) that the gradient wind in cyclones is less than the geostrophic wind for the same pressure gradient.

Solving the quadratic (37.1) leads to

$$v = -\frac{lr}{2} + \sqrt{\frac{l^2}{4}r^2 + \frac{r}{\rho} \frac{\partial p}{\partial r}} \quad (37.2)$$

The negative sign before the radical is rejected because if it is retained, $v \neq 0$ when $\partial p / \partial r = 0$, a result having no physical significance.

For an anticyclone, similar reasoning shows that the balance of forces may be expressed as

$$\frac{1}{\rho} \frac{\partial p}{\partial r} = lv - \frac{v^2}{r} \quad (37.3)$$

A comparison of (37.3) and (35.1) shows that the gradient wind in an anticyclone is greater than the geostrophic wind for the same pressure gradient. The velocity must have a maximum value since the balance of forces is destroyed if the centrifugal force becomes greater than the deflecting force.

The solution of the quadratic (37.3) also brings out this limitation of the possible velocity,

$$v = \frac{lr}{2} - \sqrt{\frac{l^2}{4}r^2 - \frac{r}{\rho} \frac{\partial p}{\partial r}} \quad (37.4)$$

The positive sign before the radical is rejected in this case, since if $\partial p / \partial r = 0$, $v \neq 0$, and the equation loses its physical significance.

The maximum possible velocity in an anticyclone occurs if the radical in (37.4) is equal to zero, i.e., if

$$\frac{1}{\rho} \frac{\partial p}{\partial r} = \frac{l^2 r}{4} \quad (37.5)$$

It is necessary, then, since this maximum cannot be exceeded, that the following conditions be obeyed in the anticyclone.

$$\frac{\partial p}{\partial r} \leq \frac{\rho l^2 r}{4} \quad (37.6)$$

Thus the pressure gradient over an anticyclone is subject to certain restrictions, if motion under balanced forces is to occur. If the pressure gradient at great distances from the center is as large, or nearly as large, as possible, according to the criterion given in (37.6), then the pressure gradient must become progressively smaller as r becomes less. Pressure charts show that that condition is fulfilled, and large pressure gradients are never noted in the central portions of anticyclones.

Representative values of the gradient wind velocity in meters per second at latitude 45° , when the pressure gradient is 1 mb per 100 km, are given in the upper portion of the following table. The density ρ is taken as 1.1×10^{-3} gm per cm^3 . In the last line of the table are shown the maximum possible values of the pressure gradient for the given values of r , computed from (37.6), using the same values of ρ and ϕ as above.

r (km)	100	300	500	1000
Gradient wind velocities (m per sec)				
Cyclone	5.7	7.2	7.7	8.2
Anticyclone	11.3	9.8
Maximum pressure gradient possible (mb per 100 km)	0.3	0.9	1.5	2.9

As for the geostrophic wind equations, the gradient wind equations apply only at heights greater than 2000 or 3000 ft above the surface where the effects of surface friction are negligible.

In the frictional layer there is a flow of air across the isobars from high to low pressure in both cyclones and anticyclones. The deflecting force is nearly always much greater than the centrifugal force, and a decrease in the former explains the observed flow of air from high to low pressure near the surface in both types of pressure distribution.

The gradient wind also varies with height if there is a horizontal temperature gradient in the atmosphere. The ideas given in section 36 to account for the variation of pressure gradient with height are equally applicable here. The variation of gradient wind with height may then be determined in the same qualitative fashion.

Strictly speaking, the radius of curvature of the moving air should be taken. However, it is often sufficient to take the radius of curvature of the isobar instead.

PROBLEMS AND EXERCISES

1. A small mass of air is set in motion with a velocity of 10 m per sec towards the east. It moves only in a region where the pressure gradient is everywhere zero, and friction is assumed negligible. Determine quantitatively the motion of the mass of air if it is set in motion at

(a) Latitude 80° N.

(b) Latitude 40° N.

(c) Latitude 0° .

2. Keeping in mind the data supplied in sections 2 and 3, how may one account for the general westerly drift of air in middle latitudes? How account for the fact that the velocity of these westerly winds usually increases with height?

3. Under what conditions might the pressure gradient force and centrifugal force be so great in comparison with the deflecting force that the latter could be neglected? Is it possible that motion under balanced forces in such circumstances ever occurs in the atmosphere? Name one type of atmospheric motion which might be included in this category.

4. Show that the maximum possible velocity of anticyclonic winds is twice as great as the geostrophic wind for the same pressure gradient.

BIBLIOGRAPHY

- Brunt, D., *Physical and Dynamical Meteorology*, London, Cambridge University Press, 1939. Chapters 8, 9.
- Haurwitz, B., *Dynamic Meteorology*, New York, McGraw-Hill Book Co., 1941. Chapters 6, 7.
- Koschmieder, H., *Dynamische Meteorologie*, Leipzig, Akad. Verlag., 1933. Chapter 6.
- Shaw, Sir N., *Manual of Meteorology*, London, Cambridge University Press. Vol. 4 (1931), Chapter 2.

CHAPTER 7

FRONTAL SURFACES

38. The Slope of Frontal Surfaces. It has been known for many years that currents of air at different temperatures and with different velocities could move side by side, the warmer overlying the cold, without appreciable mixing between the two air masses. The surface of discontinuity between two air masses is known as a *frontal surface*. In the atmosphere, frontal surfaces are nearly horizontal, their average slope being about 1 in 125. It will be shown that the slope depends on the differences of temperature and velocity in the two air masses. In

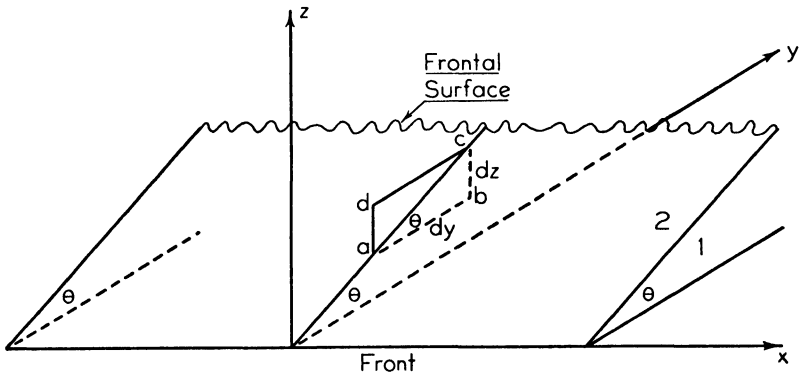


FIG. 35. The determination of the slope of a frontal surface.

the mathematical discussion that follows, it is assumed that a true mathematical surface separates the two currents of air. In the atmosphere, of course, there is actually a zone of transition of finite width. The horizontal extent of the zone varies from 10 or 20 miles for sharp frontal surfaces, to several hundred miles for diffuse ones. The line of intersection of a frontal surface with the earth's surface is known as a *front*. When the motion of a front is such that warm air replaces cold air at a fixed point when the front passes that point, it is said to be a *warm front*. Conversely, if cold air replaces warm air, it is known as a *cold front*. The general characteristics of fronts are discussed in section 108 and following.

Consider now a front lying in a line running from west to east, with the frontal surface sloping upward to the north. The situation is illustrated in Fig. 35, where the x axis is positive towards the east, the y axis

is positive towards the north, and the z axis is vertical. The angle which the frontal surface makes with the horizontal xy plane is denoted by θ . Consider the rectangle $abcd$, of length dy and height dz , lying in the yz plane. The subscript 1 denotes the denser air mass which lies under the frontal surface and north of the front. The subscript 2 denotes the lighter air, extending from south of the front up to and over the frontal surface.

Since the pressure is continuous at the frontal surface, it is immaterial whether the point a is approached from air mass 1 or air mass 2; the pressure attained on reaching a is the same in both. Similarly at c , so that

$$p_{c_1} - p_{a_1} = p_{c_2} - p_{a_2} \quad (38.1)$$

In addition

$$p_{c_1} - p_{a_1} = (p_{b_1} - p_{a_1}) + (p_{c_1} - p_{b_1}) = \frac{\partial p_1}{\partial y} dy + \frac{\partial p_1}{\partial z} dz \quad (38.2)$$

and

$$p_{c_2} - p_{a_2} = (p_{d_2} - p_{a_2}) + (p_{c_2} - p_{d_2}) = \frac{\partial p_2}{\partial z} dz + \frac{\partial p_2}{\partial y} dy \quad (38.3)$$

Substituting (38.2) and (38.3) in (38.1) and rearranging give

$$\left(\frac{\partial p_1}{\partial y} - \frac{\partial p_2}{\partial y} \right) dy = - \left(\frac{\partial p_1}{\partial z} - \frac{\partial p_2}{\partial z} \right) dz \quad (38.4)$$

Therefore

$$\tan \theta = \frac{dz}{dy} = - \frac{\frac{\partial p_1}{\partial y} - \frac{\partial p_2}{\partial y}}{\frac{\partial p_1}{\partial z} - \frac{\partial p_2}{\partial z}} \quad (38.5)$$

According to (33.4),

$$\frac{\partial p_1}{\partial z} = -g\rho_1 \quad \text{and} \quad \frac{\partial p_2}{\partial z} = -g\rho_2$$

and so

$$\tan \theta = \frac{1}{g} \frac{\frac{\partial p_1}{\partial y} - \frac{\partial p_2}{\partial y}}{\rho_1 - \rho_2} \quad (38.6)$$

Another form of the equation for the slope is obtained by substituting

for $\partial p_1/\partial y$ and $\partial p_2/\partial y$ from (35.4), giving

$$\tan \theta = \frac{2\omega \sin \phi}{g} \frac{(\rho_2 u_2 - \rho_1 u_1)}{\rho_1 - \rho_2} \quad (38.7)$$

Here u_2 and u_1 represent the components of the geostrophic wind parallel to the front. Substituting for ρ from (7.7) gives finally

$$\tan \theta = \frac{2\omega \sin \phi}{g} \frac{(T_1 u_2 - T_2 u_1)}{T_2 - T_1} \quad (38.8)$$

Various values of the slope of a frontal surface at latitude 45° for $T_1 = 273^\circ \text{A}$ and $u_1 = 10$ m per sec, when T_2 varies from 278 to 288°A and u_2 varies from 20 to 50 m per sec, are shown in the following table.

SLOPE OF A FRONTAL SURFACE				
When $T_1 = 273^\circ \text{A}$; $u_1 = 10$ m per sec				
T_2 ($^\circ \text{A}$) \diagdown u_2 (m per sec)	20	30	40	50
278	$\frac{1}{177}$	$\frac{1}{88}$	$\frac{1}{58}$	$\frac{1}{44}$
283	$\frac{3}{61}$	$\frac{1}{77}$	$\frac{1}{18}$	$\frac{1}{8}$
288	$\frac{1}{52}$	$\frac{1}{85}$	$\frac{1}{78}$	$\frac{1}{32}$

This table shows that the smaller the temperature difference and the greater the wind component difference between the two air masses, the greater is the slope of the frontal surface separating them. According to (38.8), the frontal surface becomes vertical when $T_1 = T_2$. A more rigorous analysis, however, taking into account the vertical component of the deflecting force, as well as the horizontal component, shows that the surface is not vertical for $T_1 = T_2$. Neglecting this vertical component introduces a significant error only for very small differences in temperature, and its omission in no way affects the accuracy of the values given in the table above. There is possibly, then, a small value of $T_2 - T_1$ which will give a vertical frontal surface between two air masses. Small portions of certain types of frontal surface are sometimes vertical, but from this it is not to be assumed that the temperature difference between the adjacent air masses is very small. Vigorous vertical motion, which is not geostrophic, frequently occurs near frontal surfaces, and when such vertical motion is present, equation 38.8 cannot be applied with any degree of accuracy.

39. The Pressure Trough at Fronts. From the results derived in section 38, it will now be shown that there must always be a discontinuity in the isobars at a front. Since pressure is continuous at the front, it follows that at the front

$$p_1 = p_2$$

and the horizontal pressure gradients parallel to the front at the frontal surface in the two air masses are related by the equation

$$\frac{\partial p_1}{\partial x} = \frac{\partial p_2}{\partial x} \quad (39.1)$$

The relationship between the horizontal pressure gradients normal to the front is given by (38.6). Since the warmer and lighter air overlies the colder and denser air, $\tan \theta > 0$ and also $\rho_1 > \rho_2$, so that

$$\frac{\partial p_1}{\partial y} > \frac{\partial p_2}{\partial y} \quad (39.2)$$

These facts are shown diagrammatically in Fig. 36, which is a two-dimensional representation of Fig. 35. As before, the x axis may be

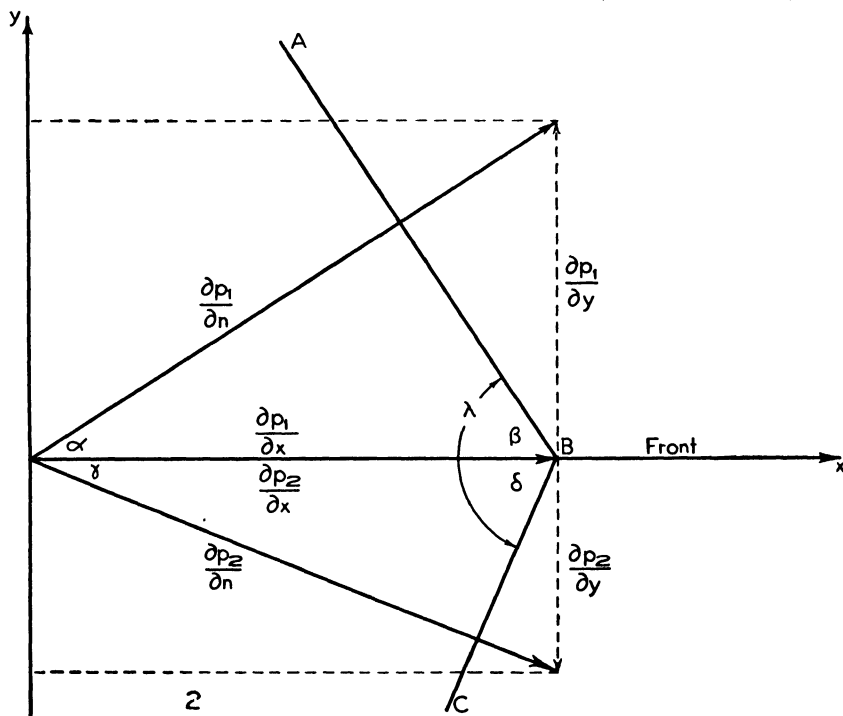


FIG. 36. The pressure trough at a front. (From Haurwitz, *Dynamic Meteorology*, McGraw-Hill Book Co.)

considered as positive towards the east, and the y axis as positive towards the north. The x and y components of the pressure gradient are indicated in the figure, and the resultant pressure gradients are denoted $\partial p_1/\partial n$ for air mass 1 and $\partial p_2/\partial n$ for air mass 2. By definition, the isobars are perpendicular to the pressure gradient. AB therefore represents an isobar in air mass 1 and BC an isobar in air mass 2. From this diagram it is seen that the isobars are always V-shaped at a front, with lower pressures within the V. The discontinuity in isobars at fronts may be seen in Fig. 109 of section 112.

It is also possible to develop a formula for the angle between the two arms of the V made by the isobars at a front. In Fig. 36, α represents the angle between the pressure gradient and the x axis in air mass 1 and γ represents that between the pressure gradient and the x axis in air mass 2. Similarly β and δ represent the angles between the x axis and the portions AB and BC of the isobar in the two air masses. Therefore

$$\tan \alpha = \frac{\frac{\partial p_1}{\partial y}}{\frac{\partial p_1}{\partial x}} \quad \text{and} \quad \tan \gamma = -\frac{\frac{\partial p_2}{\partial y}}{\frac{\partial p_2}{\partial x}}$$

The negative sign appears because the pressure in air mass 2 increases in the negative y direction. In addition

$$\tan \alpha = \tan \left(\frac{\pi}{2} - \beta \right) = \cot \beta$$

and

$$\tan \gamma = \tan \left(\frac{\pi}{2} - \delta \right) = \cot \delta$$

Thus

$$\cot \beta = \frac{\frac{\partial p_1}{\partial y}}{\frac{\partial p_1}{\partial x}} \tag{39.3}$$

and

$$\cot \delta = -\frac{\frac{\partial p_2}{\partial y}}{\frac{\partial p_2}{\partial x}} \tag{39.4}$$

If λ denotes the angle between the two portions of the isobar, then

$$\cot \lambda = \cot (\beta + \delta) = \frac{\cot \beta \cot \delta - 1}{\cot \beta + \cot \delta} \quad (39.5)$$

By substituting (39.3) and (39.4) in (39.5), rearranging, and remembering that $\partial p_1 / \partial x = \partial p_2 / \partial x$, it follows that the angle made by the two portions of an isobar at a front is given by

$$\cot \lambda = \frac{\left(\frac{\partial p_1}{\partial y}\right)\left(\frac{\partial p_2}{\partial y}\right) + \left(\frac{\partial p_1}{\partial x}\right)^2}{\frac{\partial p_1}{\partial x} \left(\frac{\partial p_2}{\partial y} - \frac{\partial p_1}{\partial y}\right)} \quad (39.6)$$

40. Pressure Tendencies below a Frontal Surface. There are several atmospheric processes which cause variations in pressure at a given point. One of these is the advective, or horizontal transport of air of a different density. If Fig. 35 is referred to, it can be seen that if the frontal surface depicted there moves northward, the pressure at a station in the cold air will fall, for the cold air aloft is being replaced by warm air. The pressure tendency, i.e., the pressure change at a fixed point during a specified interval of time, usually 3 hours, resulting from advection, may be obtained in an approximate manner in such a situation.

If no vertical motion occurs, the velocity v of the frontal surface is the same as that of the adjacent air masses. In time Δt , the frontal

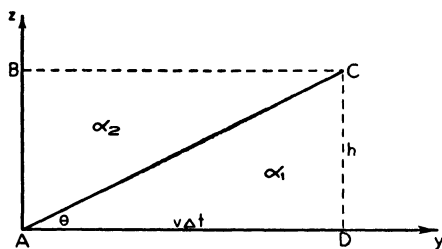


FIG. 37. The pressure tendency at a front.

surface moves a distance $v\Delta t$, i.e., the surface front initially at A , as shown in Fig. 37, has advanced to D . Regarding D as fixed, the pressure at D falls, since the air in the column of height h , of mean density ρ_1 , has been replaced by lighter air of mean density ρ_2 . It is assumed that the pressure in the warm air at height h is constant with respect to both space and time. The change of pressure in the time Δt , or the tendency at the surface, is then given by $p_A - p_D$. According to (9.9), the pressures at A and D are given by

$$p_A = p_B \left(1 - \frac{\alpha_2 h}{T_A}\right)^{-\frac{g}{R\alpha_2}} \quad (40.1)$$

and

$$p_D = p_C \left(1 - \frac{\alpha_1 h}{T_D}\right)^{-\frac{g}{R\alpha_1}} \quad (40.2)$$

where α_1 and α_2 represent the lapse rates in air masses 1 and 2, respectively. Thus, since $p_B = p_C$, it follows that

$$p_A - p_D = -p_D \left(1 - \frac{\alpha_1 h}{T_D}\right)^{\frac{g}{R\alpha_1}} \left[\left(1 - \frac{\alpha_1 h}{T_D}\right)^{-\frac{g}{R\alpha_1}} - \left(1 - \frac{\alpha_2 h}{T_A}\right)^{-\frac{g}{R\alpha_2}} \right] \quad (40.3)$$

Multiplying through leads to the form

$$p_A - p_D = -p_D \left[1 - \left(1 - \frac{\alpha_1 h}{T_D}\right)^{\frac{g}{R\alpha_1}} \left(1 - \frac{\alpha_2 h}{T_A}\right)^{-\frac{g}{R\alpha_2}} \right] \quad (40.4)$$

Expanding the terms on the right-hand side of (40.4) by the binomial theorem and neglecting terms of order higher than the first lead to

$$\begin{aligned} p_A - p_D &= -p_D \left[1 - \left(1 - \frac{gh}{RT_D} + \dots\right) \left(1 + \frac{gh}{RT_A} + \dots\right) \right] \\ &= -p_D \frac{gh}{R} \left(\frac{T_A - T_D}{T_A T_D} \right) \end{aligned} \quad (40.5)$$

But $h = v\Delta t \tan \theta$, and denoting $T_A - T_D$ as ΔT , and $p_A - p_D$ as Δp , it follows that

$$\Delta p = - \frac{p_D g v \Delta t \tan \theta \Delta T}{RT_A T_D} \quad (40.6)$$

Put in the values of the constants; assume that $p_D = 1000$ mb, that $T_A T_D = 273^2$, and that the slope of the warm front is 1 in 150. It then follows that the tendency

$$\frac{\Delta p}{\Delta t} = -0.033v\Delta T \text{ mb per 3 h} \quad (40.7)$$

when v is in meters per second and ΔT is in $^{\circ}\text{C}$.

If v is in miles per hour and ΔT in $^{\circ}\text{F}$, (40.7) becomes

$$\frac{\Delta p}{\Delta t} = -0.008v\Delta T \text{ mb per 3 h} \quad (40.8)$$

Cold fronts slope in the opposite direction from that shown in Fig. 37 and have a slope of about 1 in 75. Thus the tendency behind a cold

front is positive and is given approximately by

$$\frac{\Delta p}{\Delta t} = +0.066v\Delta T \text{ mb per 3 h} \quad (40-9)$$

if the units are meters per second and °C, or

$$\frac{\Delta p}{\Delta t} = +0.016v\Delta T \text{ mb per 3 h} \quad (40-10)$$

if the units are miles per hour and °F.

Advection and the other factors causing pressure changes are discussed in section 47. The difference between the actual tendency as observed at a station and that computed from one of the foregoing equations gives the magnitude of the factors, other than advection, which are also present. This knowledge is frequently useful in forecasting.

41. Frontogenesis and Frontolysis. Temperature Gradient Changes in a Wind Field. When new fronts and frontal surfaces develop in the atmosphere, *frontogenesis* is said to occur. The reverse process of the dissipation of fronts and frontal surfaces is known as *frontolysis*. Any given front usually persists for a considerable period of time, and especially persistent ones may be followed for a week or more as they cross the continents and oceans. As a frontal surface moves, it may be subjected to frontogenetical or frontolytical processes, which will cause an intensification or weakening of the contrast in properties across the frontal surface. In forecasting, it is necessary to consider the probable change in intensity of a front, as well as its change in position.

Since a frontal surface is not a true surface of discontinuity, the change of a property, such as temperature, from one side of this zone to the other is marked but not discontinuous in the mathematical sense at any point. The frontal zone is usually narrow enough to be indicated on a weather map as a line. If a contrast in temperature is taken as delineating the position of a frontal zone, then the frontal zone is, more specifically, a region of maximum value of $\left| \frac{\partial T}{\partial n} \right|$, where n indicates a horizontal direction normal to the isotherms. Any process which produces an increased value of $\left| \frac{\partial T}{\partial n} \right|$ is frontogenetical, while frontolytical processes produce a decrease in the value of $\left| \frac{\partial T}{\partial n} \right|$.

Any special distribution of winds which tends to bring masses of air with differing temperatures closer together is called a *deformation field*.

The simplest type of deformation field occurs when the wind velocity varies along the normal to the isotherms. The condition for frontogenesis or frontolysis in such a wind field may be seen from the following kinematical considerations. In this section, only the question of how frontogenesis occurs, not why it occurs, will be considered.

To determine whether frontogenesis or frontolysis is occurring, it is necessary to evaluate $\frac{d}{dt} \left| \frac{\partial T}{\partial n} \right|$. The total derivative with respect to time must be used since frontogenesis occurs in the moving air along a line denoting the position of the same particles, and not at a line fixed in space. It follows from the expression for a total derivative in terms of partial derivatives that

$$\frac{d}{dt} \left| \frac{\partial T}{\partial n} \right| = \frac{\partial}{\partial t} \left| \frac{\partial T}{\partial n} \right| + \frac{\partial}{\partial n} \left| \frac{\partial T}{\partial n} \right| \frac{dn}{dt}$$

Multiplying and dividing by $\partial T / \partial n$ give the form

$$\frac{d}{dt} \left| \frac{\partial T}{\partial n} \right| = \left(\frac{\partial^2 T}{\partial t \partial n} + \frac{\partial^2 T}{\partial n^2} \frac{dn}{dt} \right) \frac{\left| \frac{\partial T}{\partial n} \right|}{\frac{\partial T}{\partial n}} \quad (41.1)$$

Now evaluate $\partial^2 T / \partial n \partial t$. If T is invariant with respect to time

$$\frac{dT}{dt} = \frac{\partial T}{\partial t} + \frac{\partial T}{\partial n} \frac{dn}{dt} = 0$$

and so

$$\frac{\partial T}{\partial t} = - \frac{\partial T}{\partial n} \frac{dn}{dt}$$

Differentiating partially with respect to n gives

$$\frac{\partial^2 T}{\partial n \partial t} = \frac{\partial}{\partial n} \left(\frac{\partial T}{\partial t} \right) = - \frac{\partial^2 T}{\partial n^2} \frac{dn}{dt} - \frac{\partial T}{\partial n} \frac{\partial}{\partial n} \left(\frac{dn}{dt} \right) \quad (41.2)$$

Substituting (41.2) in (41.1) then gives

$$\frac{d}{dt} \left| \frac{\partial T}{\partial n} \right| = - \left| \frac{\partial T}{\partial n} \right| \frac{\partial}{\partial n} \left(\frac{dn}{dt} \right) \quad (41.3)$$

But dn/dt is v_n , the velocity along the normal, so that (41.3) becomes

$$\frac{d}{dt} \left| \frac{\partial T}{\partial n} \right| = - \left| \frac{\partial T}{\partial n} \right| \frac{\partial v_n}{\partial n} \quad (41.4)$$

The following conditions for frontogenesis and frontolysis may now be given.

If $\frac{\partial v_n}{\partial n} < 0$, then $\frac{d}{dt} \left| \frac{\partial T}{\partial n} \right| > 0$, and frontogenesis occurs.

If $\frac{\partial v_n}{\partial n} > 0$, then $\frac{d}{dt} \left| \frac{\partial T}{\partial n} \right| < 0$, and frontolysis occurs.

The application of these results to frontogenesis and frontolysis in various types of deformation fields is considered in detail in section 109.

PROBLEMS AND EXERCISES

1. The component of the pressure gradient normal to a front is + 4 mb per 200 km in the cold air mass, and + 4 mb per 400 km in the warm air mass. The component of the pressure gradient parallel to the front is + 4 mb per 300 km in both air masses. Compute the angle at the front between the two portions of an isobar.

2. A warm front lies in a north-south direction. The isobars, drawn at 4 mb intervals, are 200 km apart along the front, and extend westward in the warm air and northeastward in the cold air. Compute the slope of the frontal surface at the point where the 1000 mb isobar intersects it, when the surface temperature in the cold air is 0° C, and that in the warm air is 7° C.

BIBLIOGRAPHY

- Brunt, D., *Physical and Dynamical Meteorology*, London, Cambridge University Press, 1939. Chapter 10.
- Haurwitz, B., *Dynamic Meteorology*, New York, McGraw-Hill Book Co., 1941. Chapter 8.
- Koschmieder, H., *Dynamische Meteorologie*, Leipzig, Akad. Verlag., 1933. Chapter 6.
41. Petterssen, S., *Weather Analysis and Forecasting*, New York, McGraw-Hill Book Co., 1940. Chapter 5.
41. Petterssen, S., "Contribution to the Theory of Frontogenesis," *Geofys. Publ.*, **11**, No. 6, 1935.

CHAPTER 8

GENERAL KINEMATICS AND DYNAMICS OF AIR MOTIONS

42. The Movement of Significant Curves in the Pressure Field. It is frequently convenient to be able to determine the movements of certain significant points in the pressure distribution, such as the centers of highs and lows and of certain significant lines, such as fronts. Such determinations may be made readily from kinematical considerations, following Petterssen's method of procedure, providing certain conditions are met. It is well to keep in mind that the treatment is purely a kinematical one, and therefore that the equations developed in this and the next section indicate only how the motion is occurring, but not why it is occurring. The pressure field is chosen for analysis, rather than the temperature field or the moisture field, since pressure can be measured more accurately than any of the other meteorological elements. Certain effects accompanying high winds may give non-representative values of the pressure, as indicated in section 63, but these are of comparatively rare occurrence. The errors in correcting from station pressure to sea level pressure at high level stations are more serious, but if pressures at stations at lower altitudes only are used, this source of error is avoided. The following analysis applies not only to pressure itself but also to functions of pressure, such as the spatial and temporal derivatives of pressure.

The pressure distribution in a horizontal plane, as at mean sea level, is specified completely by the expression

$$p = p(x, y, t) \quad (42.1)$$

The isobars on a synoptic weather map give this distribution at the time when the observations were made. Thus the equation of one of the significant curves, the isobar, is

$$p(x, y, t_0) = \text{Constant}$$

If a curve joins points of equal pressure change in a specified interval, i.e., of equal tendency, this curve is known as an *isallobar*. The tendency is expressed by $\partial p / \partial t$, and is a function of x, y, t . The equation of an isallobar is then

$$\frac{\partial p}{\partial t} = \text{Constant}$$

Other curves, some of which will be discussed later, may be similarly specified.

A formula for the velocity of a significant curve will now be developed. The pressure itself will be discussed here, as the procedure is more readily understood using pressures, but the argument applies equally well to derivatives of the pressure, such as the tendency $\partial p/\partial t$ or the pressure gradient $\partial p/\partial x$. Since pressure in a horizontal plane is a function of x, y, t as indicated in (42.1), the total differential dp , expressed in terms of partials in the standard manner, is

$$dp = \frac{\partial p}{\partial t} dt + \frac{\partial p}{\partial x} dx + \frac{\partial p}{\partial y} dy$$

The x and y axes in this equation are fixed with respect to the earth. Then

$$\begin{aligned} \frac{dp}{dt} &= \frac{\partial p}{\partial t} + \frac{\partial p}{\partial x} \frac{dx}{dt} + \frac{\partial p}{\partial y} \frac{dy}{dt} \\ &= \frac{\partial p}{\partial t} + u_1 \frac{\partial p}{\partial x} + v_1 \frac{\partial p}{\partial y} \end{aligned}$$

Here dp/dt represents the pressure variation with time on a moving particle of air, and u_1 and v_1 represent the velocity components of the particle in the x and y directions. The term $\partial p/\partial t$ represents, then, the pressure variation with time at any fixed point at or above the earth's surface, i.e., it is the tendency. Orienting the axes so that the motion is in the x direction only, the equation reduces to

$$\frac{dp}{dt} = \frac{\partial p}{\partial t} + u_1 \frac{\partial p}{\partial x} \quad (42.2)$$

If the axes are moving with the pressure system, the pressure variation with time on the moving air particle is

$$\frac{dp}{dt} = \frac{\delta p}{\delta t} + u_2 \frac{\partial p}{\partial x} \quad (42.3)$$

In this equation, $\delta p/\delta t$ represents the pressure variation with time in the moving system and thus represents the deepening or filling of the system. The velocity u_2 is that relative to the axes moving with the pressure system. The terms dp/dt and $\partial p/\partial x$ are the same irrespective of whether the motion is referred to the fixed or the moving axes.

Equating (42.2) and (42.3) gives

$$\frac{\delta p}{\delta t} = \frac{\partial p}{\partial t} + (u_1 - u_2) \frac{\partial p}{\partial x} = \frac{\partial p}{\partial t} + c \frac{\partial p}{\partial x} \quad (42.4)$$

where c , being the difference between the velocity relative to the fixed axes and that relative to the moving axes, is the velocity of the pressure system relative to the axes fixed on the earth. Equation 42.4 cannot be solved as it stands, for there are two knowns, the tendency and the pressure gradient, and two unknowns, the deepening or filling term and the velocity. If only systems in which neither deepening nor filling occurs are considered, then solving for the velocity leads to

$$c = - \frac{\frac{\partial p}{\partial t}}{\frac{\partial p}{\partial x}}$$

This gives the velocity of an isobar. Since the development has been perfectly general, this equation applies not only to p , which is constant along an isobar, but also to any function of p , $f(p)$, the constancy of which specifies a significant curve of the pressure field. Thus the velocity of any significant curve of the pressure field is given by

$$c = - \frac{\frac{\partial f(p)}{\partial t}}{\frac{\partial f(p)}{\partial x}} \quad (42.5)$$

For example, an isallobar is a significant curve, being specified by

$$f(p) = \frac{\partial p}{\partial t} = \text{Constant}$$

The velocity of an isallobar is therefore, according to (42.5), given by

$$c = - \frac{\frac{\partial^2 p}{\partial t^2}}{\frac{\partial^2 p}{\partial x \partial t}}$$

The acceleration A of a significant curve is given by

$$A = \frac{dc}{dt} = \frac{\partial c}{\partial t} + c \frac{\partial c}{\partial x} \quad (42.6)$$

To obtain the acceleration, it is necessary to develop an expression for the term $\delta^2 p / \delta t^2$. According to (42.4)

$$\frac{\delta p}{\delta t} = \frac{\partial p}{\partial t} + c \frac{\partial p}{\partial x}$$

Since the operator $\delta/\delta t$ is, in terms of partials,

$$\frac{\delta}{\delta t} = \frac{\partial}{\partial t} + c \frac{\partial}{\partial x}$$

then

$$\begin{aligned} \frac{\delta^2 p}{\delta t^2} &= \frac{\delta}{\delta t} \left(\frac{\delta p}{\delta t} \right) = \frac{\partial}{\partial t} \left(\frac{\partial p}{\partial t} + c \frac{\partial p}{\partial x} \right) + c \frac{\partial}{\partial x} \left(\frac{\partial p}{\partial t} + c \frac{\partial p}{\partial x} \right) \\ &= \frac{\partial^2 p}{\partial t^2} + 2c \frac{\partial^2 p}{\partial x \partial t} + c^2 \frac{\partial^2 p}{\partial x^2} + \left(\frac{\partial c}{\partial t} + c \frac{\partial c}{\partial x} \right) \frac{\partial p}{\partial x} \end{aligned}$$

Substituting from (42.6), the equation becomes

$$\frac{\delta^2 p}{\delta t^2} = \frac{\partial^2 p}{\partial t^2} + 2c \frac{\partial^2 p}{\partial x \partial t} + c^2 \frac{\partial^2 p}{\partial x^2} + A \frac{\partial p}{\partial x} \quad (42.7)$$

Since there are two unknowns, $\delta^2 p/\delta t^2$ and A , in this equation, then it is possible to solve for A when $\delta^2 p/\delta t^2 = 0$. The term $\delta^2 p/\delta t^2 = 0$ when the rate of deepening or filling of the moving pressure system is constant. With this situation, the acceleration of the system is, from (42.7),

$$A = - \frac{\frac{\partial^2 p}{\partial t^2} + 2c \frac{\partial^2 p}{\partial x \partial t} + c^2 \frac{\partial^2 p}{\partial x^2}}{\frac{\partial p}{\partial x}}$$

The meaning of these terms is brought out in the next section when discussing the acceleration of a front.

The acceleration of any significant curve $f(p) = \text{constant}$ is, therefore, given by

$$A = - \frac{\frac{\partial^2 f(p)}{\partial t^2} + 2c \frac{\partial^2 f(p)}{\partial x \partial t} + c^2 \frac{\partial^2 f(p)}{\partial x^2}}{\frac{\partial f(p)}{\partial x}} \quad (42.8)$$

43. The Movement of Troughs, Wedges, and Fronts. The equation for the curve which characterizes a pressure trough may be obtained in the following manner. In order to simplify the discussion, a symmetrical trough, of the type shown in Fig. 38a, will be considered. The trough line may be defined as the line joining the points on successive cyclonically curved isobars at which the curvature is a maximum. The broken line in Fig. 38a denotes the trough line. If the x axis is chosen

perpendicular to the trough line, as shown in the figure, then the trough line is specified by the conditions that

$$\frac{\partial p}{\partial x} = 0 \quad (43.1)$$

and

$$\frac{\partial^2 p}{\partial x^2} > 0 \quad (43.2)$$

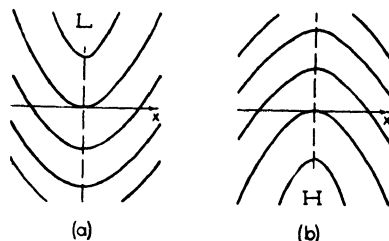


FIG. 38. Isobars at (a) a trough and (b) a wedge.

Then (43.1) is the equation of the trough line. Substituting $f(p) = \partial p / \partial x$ in (42.5), it follows that the velocity of a trough line in the x direction is

$$c = - \frac{\frac{\partial^2 p}{\partial x \partial t}}{\frac{\partial^2 p}{\partial x^2}} \quad (43.3)$$

The numerator represents the x component of the isalobaric gradient and may be evaluated from the isobars on the weather map. The denominator may be evaluated from the isobars, the sign of the term being given by (43.2).

A wedge line, shown in Fig. 38b, is specified by the conditions that

$$\frac{\partial p}{\partial x} = 0 \quad (43.4)$$

and

$$\frac{\partial^2 p}{\partial x^2} < 0 \quad (43.5)$$

The velocity of a wedge line in the x direction is, then,

$$c = - \frac{\frac{\partial^2 p}{\partial x \partial t}}{\frac{\partial^2 p}{\partial x^2}} \quad (43.6)$$

where the sign of the denominator is negative, as indicated by (43.5).

The movement of a cyclone in which no fronts are present may now be determined. Choose two axes, x and y , not necessarily at right angles, but intersecting near the center of the cyclone, in such a manner

that along the y axis $\partial p / \partial x_1 = 0$ and along the x axis $\partial p / \partial y_1 = 0$, where x_1 and y_1 are axes perpendicular to the y and x axes respectively. The velocity c_y of the y axis in a direction along the x_1 axis is given, according to (43.3), by

$$c_y = - \frac{\frac{\partial^2 p}{\partial x_1 \partial t}}{\frac{\partial^2 p}{\partial x_1^2}}$$

The velocity c_x of the x axis in the y_1 direction is given by

$$c_x = - \frac{\frac{\partial^2 p}{\partial y_1 \partial t}}{\frac{\partial^2 p}{\partial y_1^2}}$$

After an interval of time Δt , the y axis will have moved a distance $c_y \Delta t$ in the x_1 direction, and the x axis will have moved a distance $c_x \Delta t$ in the y_1 direction. The intersection of the x and y axes in their new positions then gives the location of the center of the cyclone at the end of the time interval Δt . The movement of an anticyclone may be found in a similar manner, using (43.6).

The formula for the acceleration of a trough or wedge line is obtained by substituting $\partial p / \partial x$ for $f(p)$ in (42.8).

In section 38 it was shown that, at the front separating air masses denoted 1 and 2, $p_1 = p_2$, since pressure is continuous. Thus a front is a significant curve of the pressure field, since $p_1 - p_2$ has the constant value zero along it. The function $f(p)$ characterizing a front is therefore given by

$$f(p) = p_1 - p_2 \quad (43.7)$$

Substituting (43.7) in (42.5) gives for the velocity of a front

$$c = - \frac{\frac{\partial p_1}{\partial t} - \frac{\partial p_2}{\partial t}}{\frac{\partial p_1}{\partial x} - \frac{\partial p_2}{\partial x}} \quad (43.8)$$

The tendency $\partial p_1 / \partial t$ at any given point on the front in air mass 1 is most accurately obtained by drawing the isallobars in air mass 1, as indicated in Fig. 39, and noting the value of the isallobar which intersects the front at the chosen point. Similarly, the isallobars in air mass 2 determine the value of $\partial p_2 / \partial t$ in that air mass. Typical dis-

tributions of isallobars in the vicinity of fronts are shown in Fig. 110 of section 112. The denominator of (43-8) is readily evaluated from the distribution of isobars in the two air masses. The exact method of procedure for evaluating the four terms of (43-8) is given in section 167, and an example is worked out in section 169.

The formula for the acceleration of a front is obtained by substituting (43.7) in (42.8). Thus

$$A = - \frac{\frac{\partial^2 p_1}{\partial t^2} - \frac{\partial^2 p_2}{\partial t^2} + 2c \left(\frac{\partial^2 p_1}{\partial x \partial t} - \frac{\partial^2 p_2}{\partial x \partial t} \right) + c^2 \left(\frac{\partial^2 p_1}{\partial x^2} - \frac{\partial^2 p_2}{\partial x^2} \right)}{\frac{\partial p_1}{\partial x} - \frac{\partial p_2}{\partial x}} \quad (43-9)$$

This acceleration formula is made up of three groups of terms. Denoting the portion of the acceleration arising from the first group as A_1 , that arising from the second group as A_2 , and that from the third group as A_3 , (43-9) may be expressed as

$$A = A_1 + A_2 + A_3 \quad (43-10)$$

Insufficient data are given on an ordinary weather map to permit the accurate determination of each of these groups, more particularly the first group, but the sign of each may be found in the following manner. Fig. 39 shows the distribution of isobars (full lines), isallobars (broken lines), and the barogram (curve abc at the bottom of the diagram) in the vicinity of a warm front. Curve abc is not the barogram trace at any one station, but represents rather a composite picture of the slopes of the barograms at stations along the x axis at any given instant of time. It is this curve which cannot be obtained accurately from the data given on weather maps.

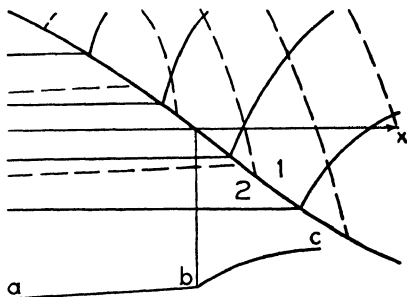


FIG. 39. Isobars, isallobars, and barogram at a warm front.

Since the x axis is chosen parallel to the isobars in the warm air, $\partial p_2 / \partial x = 0$, and the first term becomes

$$A_1 = - \frac{\frac{\partial^2 p_1}{\partial t^2} - \frac{\partial^2 p_2}{\partial t^2}}{\frac{\partial p_1}{\partial x}} \quad (43-11)$$

In addition, the tendency in the warm air is uniform, i.e., ab is a straight line, so that $\partial^2 p_2 / \partial t^2 = 0$. In the cold air ahead of the front the barogram trace bc is curved anticyclonically, using Petterssen's terminology, so that the magnitude of the negative tendencies increases with time, and therefore $\partial^2 p_1 / \partial t^2 < 0$. In the cold air the pressure increases in the positive x direction, so that $\partial p_1 / \partial x > 0$. Thus $A_1 > 0$.

The portion of the acceleration A_2 resulting from the second group is given by

$$A_2 = - \frac{2c \left(\frac{\partial^2 p_1}{\partial x \partial t} - \frac{\partial^2 p_2}{\partial x \partial t} \right)}{\frac{\partial p_1}{\partial x}} \quad (43-12)$$

In the cold air the isallobars are negative, and become less negative in the positive x direction, so that $\partial^2 p_1 / \partial x \partial t > 0$. In the warm air, since the isallobars are very nearly parallel to the x axis, $\partial^2 p_2 / \partial x \partial t \approx 0$ and may be neglected. Since the velocity c and $\partial p_1 / \partial x$ are both positive, it follows that $A_2 < 0$.

The acceleration A_3 contributed by the third group is given by

$$A_3 = - \frac{c^2 \left(\frac{\partial^2 p_1}{\partial x^2} - \frac{\partial^2 p_2}{\partial x^2} \right)}{\frac{\partial p_1}{\partial x}} \quad (43-13)$$

Since the pressure in the cold air increases in the positive x direction, but at a diminishing rate, as shown by the configuration of the isobars, then $\partial^2 p_1 / \partial x^2 < 0$. The isobars in the warm air are parallel to the x axis, and therefore $\partial^2 p_2 / \partial x^2 = 0$. As c^2 and $\partial p_1 / \partial x$ are both positive, it follows that $A_3 > 0$.

Thus A_1 and A_3 produce positive accelerations, and A_2 produces a negative acceleration, or a retardation. Assuming, as a first approximation, that the magnitude of the acceleration contributed by each term (43-11), (43-12), and (43-13) is the same, then the front experiences a small net acceleration in the positive x direction.

The sign of the acceleration of fronts with other barograms and distributions of isobars and isallobars may be evaluated in a similar manner. This qualitative method of analysis is used in section 112 to discuss the relative motion of the warm and cold fronts in four types of frontal depressions.

44. Streamlines and Trajectories. In a field of moving particles of air, the *streamlines* are defined as the curves to which, at a given instant of time, the velocity vectors for each particle are tangential. In Fig. 40, the curved line represents a streamline, with the tangent at one particular point indicated. The equation of the tangent line is

$$y = a + bx$$

where b represents the slope of the tangent line. Differentiating,

$$dy = b dx$$

or the slope b of the line is

$$b = \frac{dy}{dx}$$

But if V represents the tangential velocity, having components u and v in the x and y directions respectively, then the slope b is also given by

$$b = \frac{v}{u}$$

Thus the differential equation of the streamline is

$$\frac{dy}{dx} = \frac{v}{u} \quad (44.1)$$

Now consider the streamlines in geostrophic motion. By multiplying (35.3) by dx and (35.4) by dy and denoting the Coriolis parameter $2\omega \sin \phi$ by l , it follows that

$$lv dx = \frac{1}{\rho} \frac{\partial p}{\partial x} dx \quad (44.2)$$

$$lu dy = -\frac{1}{\rho} \frac{\partial p}{\partial y} dy \quad (44.3)$$

Subtracting (44.3) from (44.2) leads to

$$l(v dx - u dy) = \frac{1}{\rho} \left(\frac{\partial p}{\partial x} dx + \frac{\partial p}{\partial y} dy \right) \quad (44.4)$$

But

$$dp = \frac{\partial p}{\partial t} dt + \frac{\partial p}{\partial x} dx + \frac{\partial p}{\partial y} dy$$

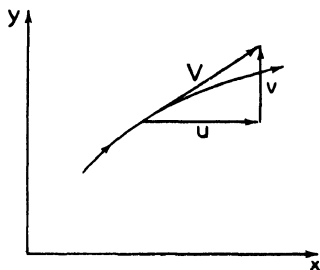


FIG. 40. The tangential velocity at a streamline and its components.

In section 47 it is shown that with geostrophic motion the pressure cannot vary with time, and therefore $\partial p / \partial t = 0$. Thus

$$dp = \frac{\partial p}{\partial x} dx + \frac{\partial p}{\partial y} dy \quad (44.5)$$

and (44.4) becomes

$$l(v dx - u dy) = \frac{dp}{\rho} \quad (44.6)$$

But, from (44.1)

$$v dx - u dy = 0$$

With geostrophic motion, therefore, $dp = 0$, and the streamlines coincide with the isobars.

A streamline gives an instantaneous picture of the motion of a group of particles. A *trajectory*, on the other hand, gives a picture of the motion of a single particle during a finite interval of time. The tra-

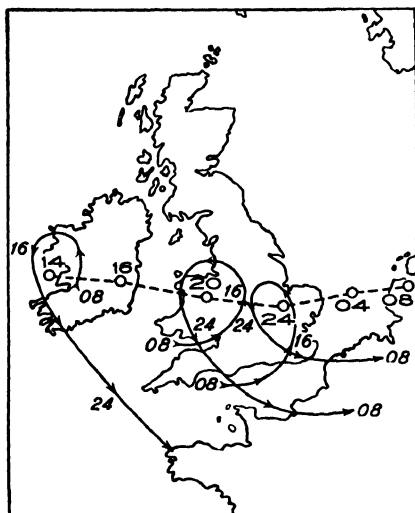


FIG. 41. The trajectories of air particles near a depression, September 10-11, 1903. (After Shaw and Lempfert.)

jectories of several particles of air in a depression near the British Isles are shown in Fig. 41. The motions indicated occurred during the interval from 08 h on September 10 to 08 h on September 11, 1903. The small circles connected by broken lines represent successive positions of the center of low pressure.

Only when the motion is stationary do the streamlines and trajectories coincide. Geostrophic motion is of necessity stationary, so that the streamlines and trajectories are the same. When a pressure system moves as a whole, there are usually very marked differences between the streamlines and trajectories, as, for example, in Fig. 41. This distinction

between streamlines and trajectories is important in forecasting air motions, especially in the vicinity of pressure centers. Unless the difference between the two is kept in mind, there is a tendency to use the streamlines, instead of the probable trajectories, in forecasting the position of a mass of air.

45. The Equation of Continuity. Divergence and Convergence.

One of the basic concepts of hydrodynamics is that nowhere in a system is fluid created or destroyed. This fundamental condition is expressed in the equation of continuity. Consider the rectangular parallelepiped shown in Fig. 42, with sides dx , dy , dz parallel to the x , y , z axes. The

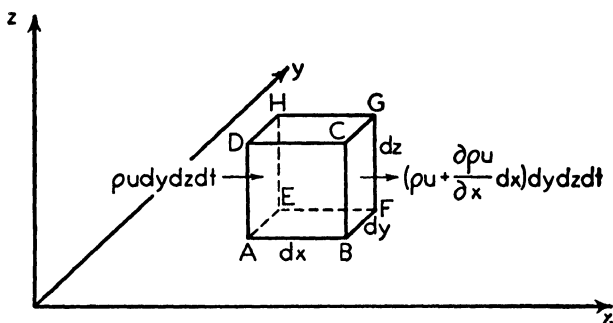


FIG. 42. The derivation of the equation of continuity.

velocities in the x , y , z directions are u , v , w , and the density of the fluid is ρ . The transport of fluid in the positive x direction through the face $AEHD$ in the time dt is $\rho u \, dy \, dz \, dt$, where ρu is the average value for the face, and that through the face $BFGC$ in the same direc-

tion is $\left(\rho u + \frac{\partial \rho u}{\partial x} dx \right) dy \, dz \, dt$. The increase in mass in the parallelepiped resulting from the x component of motion is then the amount entering through face $AEHD$ minus the amount leaving through face $BFGC$, or $-\frac{\partial \rho u}{\partial x} dx \, dy \, dz \, dt$. Similar expressions give the increase

in mass resulting from y and z components of the motion. The total increase in mass in the parallelepiped is then

$$-\left(\frac{\partial \rho u}{\partial x} + \frac{\partial \rho v}{\partial y} + \frac{\partial \rho w}{\partial z} \right) dx \, dy \, dz \, dt \quad (45.1)$$

Since the fluid is neither created nor destroyed and since the mass in a given volume increases, the density of the fluid must increase in

time dt from ρ to $\rho + \frac{\partial \rho}{\partial t} dt$. Thus the total increase in mass in the parallelepiped may also be expressed as

$$\frac{\partial \rho}{\partial t} dx \, dy \, dz \, dt \quad (45.2)$$

Equating (45.1) and (45.2) gives the *equation of continuity*

$$\frac{\partial \rho}{\partial t} + \frac{\partial \rho u}{\partial x} + \frac{\partial \rho v}{\partial y} + \frac{\partial \rho w}{\partial z} = 0 \quad (45.3)$$

If the fluid is incompressible, ρ is constant, and (45.3) reduces to

$$\frac{\partial u}{\partial x} + \frac{\partial v}{\partial y} + \frac{\partial w}{\partial z} = 0 \quad (45.4)$$

The equation of continuity is frequently used in this form in meteorology for certain types of computations. The variations in ρ in the horizontal are very small, but in the vertical there is a rapid decrease of ρ with height. If a layer of small vertical extent only is considered, however, it is permissible, as a first approximation, to assume that ρ is constant throughout the layer, and therefore to use (45.4).

The expression

$$\frac{\partial \rho u}{\partial x} + \frac{\partial \rho v}{\partial y} + \frac{\partial \rho w}{\partial z}$$

is known as the *divergence* of the transport. When it is positive, there is a decrease of mass per unit volume per unit time, according to (45.1). When this expression is negative, it is known as the *convergence*, for there is then an increase of mass per unit volume per unit time. Similarly, for an incompressible fluid, this divergence is

$$\frac{\partial u}{\partial x} + \frac{\partial v}{\partial y} + \frac{\partial w}{\partial z}$$

which equals zero, according to (45.4). The expression $(\partial u / \partial x) + (\partial v / \partial y)$ is often called the horizontal divergence, and $\partial w / \partial z$ the vertical divergence. From (45.4) it follows that

$$\frac{\partial u}{\partial x} + \frac{\partial v}{\partial y} = - \frac{\partial w}{\partial z} \quad (45.5)$$

Thus, in an incompressible fluid, the horizontal divergence equals the vertical convergence.

The method of using (45.5) for comparatively thin layers of air, in which ρ may be considered constant without introducing serious error, is given below. Assume that the air moves in the positive y direction, i.e., northward, so that $u = 0$. Then (45.5) becomes

$$\frac{\partial v}{\partial y} = - \frac{\partial w}{\partial z} \quad (45.6)$$

Expressing (45.6) in terms of finite differences gives

$$\frac{\Delta v}{\Delta y} = - \frac{\Delta w}{\Delta z} \quad (45.7)$$

or

$$\frac{v_1 - v_0}{y_1 - y_0} = - \frac{w_1 - w_0}{z_1 - z_0} \quad (45.8)$$

Assume that the xy plane shown in Fig. 43 coincides with the surface of the earth. The dimensions of the parallelepiped as drawn are x_1 , y_1 , and z_1 . Thus $y_0 = 0$ and $z_0 = 0$. Since the base of the parallelepiped coincides with the surface of the earth, $w_0 = 0$ also. Equation 45.8 then becomes

$$w_1 = - \frac{z_1}{y_1} (v_1 - v_0) \quad (45.9)$$

The same result is, of course, obtained by determining the net transport across the two faces in and parallel to the xz plane and equating this to the outflow across the horizontal plane at height z_1 . The vertical velocity at height z_1 , resulting from horizontal divergence or convergence, is thus obtained.

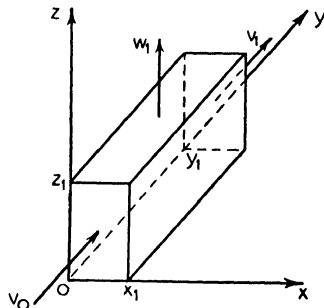


FIG. 43. The vertical velocity resulting from horizontal convergence in the atmosphere.

Consider the case in which straight and parallel isobars lie in a north-south direction at a given latitude, with pressure increasing to the east. The geostrophic wind is then south, of magnitude given by (35.1),

$$v = \frac{1}{2\omega \sin \phi \rho} \frac{\partial p}{\partial x}$$

The vertical velocity w_1 at a height of z_1 between latitudes ϕ_1 and ϕ_0 is then obtained by substituting (35.1) in (45.9). Providing that ρ and $\partial p / \partial x$ are constant with latitude, then

$$w_1 = - \frac{z_1}{2\omega \rho y_1} \frac{\partial p}{\partial x} \left(\frac{\sin \phi_0 - \sin \phi_1}{\sin \phi_1 \sin \phi_0} \right) \quad (45.10)$$

The distance y_1 over the earth's surface between latitudes ϕ_1 and ϕ_0 is given by

$$y_1 = \frac{\pi E}{180} (\phi_1 - \phi_0) \quad (45.11)$$

where E is the radius of the earth. Introducing (45-11) into (45-10) leads to the form

$$w_1 = - \frac{180z_1}{2\pi E \omega \rho \sin \phi_1 \sin \phi_0} \frac{\partial p}{\partial x} \left(\frac{\sin \phi_0 - \sin \phi_1}{\phi_1 - \phi_0} \right) \quad (45-12)$$

Horizontal convergence occurs since $\sin \phi_0 < \sin \phi_1$ and $\phi_1 > \phi_0$ and the air ascends between latitudes ϕ_1 and ϕ_0 .

If the geostrophic wind were north, there would be horizontal divergence and descending air motion. When straight and parallel isobars extend from ϕ_1 to ϕ_0 , but in a direction other than the north-south one, the vertical velocity is less than that given by (45-12), since y_1 then has a value greater than that given by (45-11).

An example of the application of (45-10) to an actual weather map is given in the latter part of section 119. The vertical velocities resulting from the variation of the gradient wind with latitude are also discussed in section 119. The horizontal divergence and convergence resulting from the variation in the curvature of the streamlines are discussed in section 141.

46. The Isallobaric Wind. In the equations of motion of an air particle given in sections 35 and 37, it was assumed that the forces acting on a moving air particle were balanced. When the forces are balanced in this manner, the motion of the air particle is not accelerated, but is steady. Brunt and Douglas studied the motion of an air particle when the forces are unbalanced, so that the particle experiences an acceleration. Sutcliffe's variation of Brunt and Douglas' treatment is given below.

According to section 35, there are two forces acting on an air particle moving in a straight line over the earth's surface. If the motion is northward, i.e., in direction y , and parallel to isobars which are themselves straight and parallel, the deflecting force of the earth's rotation acts in the positive x direction. Since pressure increases with x , the pressure gradient force acts in the negative x direction. If these two forces do not balance, the net force in the positive x direction is the deflecting force minus the pressure gradient force. According to Newton's law, force equals acceleration for unit mass. Thus the acceleration du/dt of unit mass of air in the positive x direction equals the net force in the same direction. These facts may be expressed in the form of an equation as

$$\frac{du}{dt} = lw - \frac{1}{\rho} \frac{\partial p}{\partial x} \quad (46-1)$$

If the motion is eastward, with the isobars lying in an east-west direc-

tion, similar considerations show that

$$\frac{dv}{dt} = -lu - \frac{1}{\rho} \frac{\partial p}{\partial y} \quad (46.2)$$

If u and v are the x and y components of velocity V , rather than two distinct velocities, then (46.1) and (46.2) together specify the motion of unit mass of air when the forces are not balanced.

Denoting the x and y components of the geostrophic wind velocity as u_g and v_g , and substituting for the pressure gradient force terms in (46.1) and (46.2) from (35.3) and (35.4), the former become

$$\frac{du}{dt} = l(v - v_g) = lv_i \quad (46.3)$$

$$\frac{dv}{dt} = -l(u - u_g) = -lu_i \quad (46.4)$$

where u_i and v_i are the departures of the wind components u and v from their geostrophic values u_g and v_g . Expressing the total differential du in terms of partials

$$du = \frac{\partial u}{\partial t} dt + \frac{\partial u}{\partial x} dx + \frac{\partial u}{\partial y} dy + \frac{\partial u}{\partial z} dz$$

and so

$$\frac{du}{dt} = \frac{\partial u}{\partial t} + u \frac{\partial u}{\partial x} + v \frac{\partial u}{\partial y} + w \frac{\partial u}{\partial z}$$

since

$$\frac{dx}{dt} = u, \quad \frac{dy}{dt} = v, \quad \text{and} \quad \frac{dz}{dt} = w$$

Since $u = u_g + u_i$, it follows that

$$\frac{du}{dt} = \frac{\partial u_g}{\partial t} + \frac{\partial u_i}{\partial t} + u \frac{\partial u_g}{\partial x} + u \frac{\partial u_i}{\partial x} + v \frac{\partial u_g}{\partial y} + v \frac{\partial u_i}{\partial y} + w \frac{\partial u_g}{\partial z} + w \frac{\partial u_i}{\partial z} \quad (46.5)$$

Brunt and Douglas have given some evidence to show that under ordinary atmospheric conditions the first term on the right-hand side is much greater than the remaining terms on that side, so that, as a first approximation, the latter may be neglected. Thus (46.3) and (46.4) become

$$\frac{\partial u_g}{\partial t} = lv_i \quad (46.6)$$

$$\frac{\partial v_g}{\partial t} = -lu_i \quad (46.7)$$

By differentiating (35.4) and (35.3) partially with respect to time and changing the order of differentiation, it follows that

$$\frac{\partial u_g}{\partial t} = -\frac{1}{l\rho} \frac{\partial}{\partial y} \left(\frac{\partial p}{\partial t} \right) \quad (46.8)$$

$$\frac{\partial v_g}{\partial t} = \frac{1}{l\rho} \frac{\partial}{\partial x} \left(\frac{\partial p}{\partial t} \right) \quad (46.9)$$

Substituting (46.8) and (46.9) in (46.6) and (46.7) then leads to

$$v_i = -\frac{1}{l^2\rho} \frac{\partial}{\partial y} \left(\frac{\partial p}{\partial t} \right) \quad (46.10)$$

$$u_i = -\frac{1}{l^2\rho} \frac{\partial}{\partial x} \left(\frac{\partial p}{\partial t} \right) \quad (46.11)$$

The terms $\frac{\partial}{\partial x} \left(\frac{\partial p}{\partial t} \right)$ and $\frac{\partial}{\partial y} \left(\frac{\partial p}{\partial t} \right)$ are the x and y components of the isallobaric gradient, and u_i and v_i are therefore known as the components of the *isallobaric wind*. It is seen from (46.10) and (46.11) that the isallobaric wind blows at right angles to the isallobars toward the lowest isallobars. The actual wind is obtained by adding vectorially the geostrophic and isallobaric winds.

Several attempts have been made to check these formulas, but without any decisive results, owing to the difficulties involved. It follows from the foregoing statements that there is horizontal divergence from an isallobaric high and horizontal convergence in an isallobaric low. Descending air motion therefore occurs in an isallobaric high, and ascending air motion in an isallobaric low. The essential validity of the results is attested by the observed fact that, in general, clear skies accompany an isallobaric high and clouded skies accompany an isallobaric low.

This isallobaric effect, however, does not always give a complete explanation of atmospheric developments. It appears that, in certain conditions, the terms in (46.5) which have been neglected assume importance. When this occurs, the mathematics becomes very involved, and a satisfactory method of solving the more complex equations has not yet been devised, although attempts in this direction have been made.

An example of an isallobaric wind obtained from the data on a weather map is worked out in section 121, and the significance of isallobaric winds in forecasting is discussed in Chapter 24.

47. The Origin of Pressure Changes. If it is assumed that the atmosphere is in statical equilibrium, a valid assumption except near cumulonimbus clouds where marked vertical accelerations often occur, it is possible to determine the several factors which cause pressure changes at any level. The pressure p at any height z may be found by integrating (9.1) from z to ∞ . Thus

$$p = \int_z^{\infty} g\rho \, dz \quad (47.1)$$

Differentiating partially with respect to time and assuming the acceleration of gravity g to be constant, it follows that the tendency at any level z is

$$\frac{\partial p}{\partial t} = g \int_z^{\infty} \frac{\partial \rho}{\partial t} \, dz \quad (47.2)$$

Substitute for $\partial \rho / \partial t$ from the equation of continuity 45.3, and (47.2) becomes

$$\frac{\partial p}{\partial t} = -g \int_z^{\infty} \left(\frac{\partial \rho u}{\partial x} + \frac{\partial \rho v}{\partial y} \right) dz - g \int_z^{\infty} \frac{\partial \rho w}{\partial z} dz \quad (47.3)$$

Then by carrying out the differentiation in the first term and rearranging, and integrating the second term, (47.3) takes the form

$$\frac{\partial p}{\partial t} = -g \int_z^{\infty} \rho \left(\frac{\partial u}{\partial x} + \frac{\partial v}{\partial y} \right) dz - g \int_z^{\infty} \left(u \frac{\partial \rho}{\partial x} + v \frac{\partial \rho}{\partial y} \right) dz + g(\rho w)_z \quad (47.4)$$

since $\rho = 0$ at $z = \infty$.

This equation shows that a pressure variation at height z can arise from the operation of one or more of three distinct processes. The first term represents the effect of horizontal divergence or convergence at all heights greater than z . The second gives the effect of horizontal advection of air of different density at heights greater than z . The last term represents the effect on p of vertical motion at the height z .

At the surface of the earth $w = 0$, so that the variation of pressure p_0 with time at any fixed point at the surface, i.e., the tendency at the surface, is

$$\begin{aligned} \frac{\partial p_0}{\partial t} &= -g \int_z^{\infty} \left(\frac{\partial \rho u}{\partial x} + \frac{\partial \rho v}{\partial y} \right) dz \\ &= -g \int_z^{\infty} \rho \left(\frac{\partial u}{\partial x} + \frac{\partial v}{\partial y} \right) dz - g \int_z^{\infty} \left(u \frac{\partial \rho}{\partial x} + v \frac{\partial \rho}{\partial y} \right) dz \end{aligned} \quad (47.5)$$

Thus the pressure at the surface can vary only as a result of horizontal divergence or convergence or of advection of air of different density at higher levels.

Although equations 47.4 and 47.5 are comparatively simple, the determination of the actual divergence or convergence and advection in the troposphere and stratosphere requires a quantity and accuracy of upper air data which have not yet been attained. Valuable deductions may be made, however, from special types of air motion which are frequently observed, such as that discussed in the next section.

When the air motion at all levels in the atmosphere is geostrophic, the tendency at the surface must be zero. The equations 35.3 and 35.4 may be expressed in the form

$$\rho v = \frac{1}{l} \frac{\partial p}{\partial x} \quad (47.6)$$

$$\rho u = - \frac{1}{l} \frac{\partial p}{\partial y} \quad (47.7)$$

Differentiating (47.6) partially with respect to y and (47.7) with respect to x obtains

$$\frac{\partial \rho v}{\partial y} = \frac{1}{l} \frac{\partial^2 p}{\partial x \partial y} \quad (47.8)$$

$$\frac{\partial \rho u}{\partial x} = - \frac{1}{l} \frac{\partial^2 p}{\partial x \partial y} \quad (47.9)$$

By substituting (47.8) and (47.9) in (47.5),

$$\frac{\partial p_0}{\partial t} = 0$$

Since no changes in surface pressure are possible in a geostrophic wind field, it follows that variations in the distribution of pressure at the surface can occur only with departures from geostrophic motion, such as, for example, the isalobaric wind components discussed in the previous section.

48. The Movement of Upper Troughs and Wedges. Investigations of the pressure field at high levels have shown that the isobars are distributed in a sinusoidal pattern, the general trend of the isobars being parallel to the parallels of latitude. The relationship between the resulting northward and southward motions at these levels and the surface centers of high and low pressure is discussed in section 113. The observed east or west motions of these upper troughs and wedges

may be accounted for by horizontal divergence and convergence in these systems.

A sinusoidal system of isobars approximating those often occurring in the upper air is shown in Fig. 44. At x_0 and x_2 the isobars are curved cyclonically. The gradient wind equation 37.2,

$$v_{0,2} = -\frac{lr}{2} + \sqrt{\frac{l^2}{4}r^2 + \frac{r}{\rho}\frac{\partial p}{\partial r}}$$

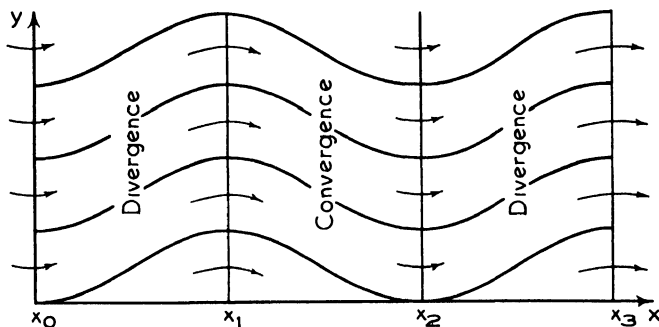


FIG. 44. Convergence and divergence with sinusoidal isobars.
(After J. Bjerknes.)

gives the velocity of the air motion at these values of x . At x_1 and x_3 the isobars are curved anticyclonically, and the gradient wind velocity is, according to (37.4),

$$v_{1,3} = \frac{lr}{2} - \sqrt{\frac{l^2}{4}r^2 - \frac{r}{\rho}\frac{\partial p}{\partial r}}$$

It was shown in section 37 that, for equal values of r , ρ , and $\partial p/\partial r$, when variations in latitude ϕ included in the Coriolis parameter l are neglected, $v_{1,3} > v_{0,2}$. Thus, as indicated in the figure, there is divergence between x_0 and x_1 , convergence between x_1 and x_2 , and divergence between x_2 and x_3 . If it is assumed that advection of air of different density and vertical motions are absent, the pressure falls, according to (47.4), between x_0 and x_1 and between x_2 and x_3 , and rises between x_1 and x_2 . This is equivalent to a motion in the positive x direction, i.e., eastward, of the system of isobars.

It is implied in the above treatment that the north-south amplitude of the isobars is not great, the variations in latitude ϕ being small enough to justify neglecting them. However, if an isobar extends over a considerable range of latitude, as sometimes happens, it is no longer permissible to assume that l is constant. The effect of introducing the

Thus the pressure at the surface can vary only as a result of horizontal divergence or convergence or of advection of air of different density at higher levels.

Although equations 47.4 and 47.5 are comparatively simple, the determination of the actual divergence or convergence and advection in the troposphere and stratosphere requires a quantity and accuracy of upper air data which have not yet been attained. Valuable deductions may be made, however, from special types of air motion which are frequently observed, such as that discussed in the next section.

When the air motion at all levels in the atmosphere is geostrophic, the tendency at the surface must be zero. The equations 35.3 and 35.4 may be expressed in the form

$$\rho v = \frac{1}{l} \frac{\partial p}{\partial x} \quad (47.6)$$

$$\rho u = - \frac{1}{l} \frac{\partial p}{\partial y} \quad (47.7)$$

Differentiating (47.6) partially with respect to y and (47.7) with respect to x obtains

$$\frac{\partial \rho v}{\partial y} = \frac{1}{l} \frac{\partial^2 p}{\partial x \partial y} \quad (47.8)$$

$$\frac{\partial \rho u}{\partial x} = - \frac{1}{l} \frac{\partial^2 p}{\partial x \partial y} \quad (47.9)$$

By substituting (47.8) and (47.9) in (47.5),

$$\frac{\partial p_0}{\partial t} = 0$$

Since no changes in surface pressure are possible in a geostrophic wind field, it follows that variations in the distribution of pressure at the surface can occur only with departures from geostrophic motion, such as, for example, the isalobaric wind components discussed in the previous section.

48. The Movement of Upper Troughs and Wedges. Investigations of the pressure field at high levels have shown that the isobars are distributed in a sinusoidal pattern, the general trend of the isobars being parallel to the parallels of latitude. The relationship between the resulting northward and southward motions at these levels and the surface centers of high and low pressure is discussed in section 113. The observed east or west motions of these upper troughs and wedges

may be accounted for by horizontal divergence and convergence in these systems.

A sinusoidal system of isobars approximating those often occurring in the upper air is shown in Fig. 44. At x_0 and x_2 the isobars are curved cyclonically. The gradient wind equation 37.2,

$$v_{0,2} = -\frac{lr}{2} + \sqrt{\frac{l^2}{4}r^2 + \frac{r}{\rho} \frac{\partial p}{\partial r}}$$

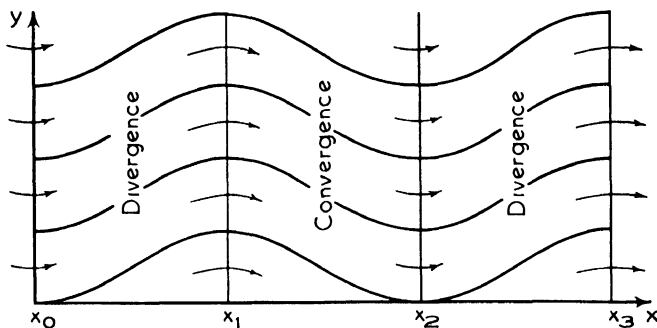


FIG. 44. Convergence and divergence with sinusoidal isobars.
(After J. Bjerknes.)

gives the velocity of the air motion at these values of x . At x_1 and x_3 the isobars are curved anticyclonically, and the gradient wind velocity is, according to (37.4),

$$v_{1,3} = \frac{lr}{2} - \sqrt{\frac{l^2}{4}r^2 - \frac{r}{\rho} \frac{\partial p}{\partial r}}$$

It was shown in section 37 that, for equal values of r , ρ , and $\partial p/\partial r$, when variations in latitude ϕ included in the Coriolis parameter l are neglected, $v_{1,3} > v_{0,2}$. Thus, as indicated in the figure, there is divergence between x_0 and x_1 , convergence between x_1 and x_2 , and divergence between x_2 and x_3 . If it is assumed that advection of air of different density and vertical motions are absent, the pressure falls, according to (47.4), between x_0 and x_1 and between x_2 and x_3 , and rises between x_1 and x_2 . This is equivalent to a motion in the positive x direction, i.e., eastward, of the system of isobars.

It is implied in the above treatment that the north-south amplitude of the isobars is not great, the variations in latitude ϕ being small enough to justify neglecting them. However, if an isobar extends over a considerable range of latitude, as sometimes happens, it is no longer permissible to assume that l is constant. The effect of introducing the

variations in $\sin \phi$ in l is to reduce the difference in velocity between x_0 and x_1 , and thus the eastward velocity of the system of isobars. For large ranges of latitude v_0 may equal v_1 , and when this happens, the isobaric system is stationary. This condition is met when (37.2) equals (37.4), or

$$-\omega r \sin \phi_0 + \sqrt{\omega^2 r^2 \sin^2 \phi_0 + \frac{r}{\rho} \frac{\partial p}{\partial r}} = \omega r \sin \phi_1 - \sqrt{\omega^2 r^2 \sin^2 \phi_1 - \frac{r}{\rho} \frac{\partial p}{\partial r}} \quad (48.1)$$

This equation may be solved for ϕ_0 and ϕ_1 by a graphical method, assuming certain values for r , ρ , and $\partial p/\partial r$. The values of ϕ_0 and ϕ_1 for stationary isobars when $\rho = 0.8 \times 10^{-3}$ gm per cm³, $\partial p/\partial r = 1$ mb per 100 km, and r equals in succession 500, 1000, and 1500 km are given in the following table. The distribution of isobars is symmetrical about latitude 45° in each case.

CONDITIONS FOR STATIONARY ISOBARS

r (km)	$v_0 = v_1$ (m per sec)	ϕ_0 (deg)	ϕ_1 (deg)	$\Delta\phi$ (deg)
500	12.5	31	59	28
1000	12.2	38½	51½	13
1500	12.2	41	49	8

When the radius of curvature is small, say 500 km, the distance $x_2 - x_0$, which may be called for convenience the wave length of the motion, will in general be small. For such isobaric systems to be stationary, a single isobar must extend through a large interval of latitude, 28° in the example in the table. Such a latitudinal variation with a short wave length rarely, if ever, occurs. Thus systems with short wave lengths generally move eastward. They are associated with the traveling highs and lows of middle latitudes. The variation in latitude required for stationary isobaric systems with greater radii of curvature and hence of greater wave lengths is considerably less, as indicated in the table. For example, for $r = 1000$ km, if $\Delta\phi < 13^\circ$, the system moves eastward; if $\Delta\phi > 13^\circ$ it moves westward. Since latitudinal variations of the order of 13° with longer wave lengths are of frequent occurrence, it follows that such systems tend to remain stationary, or nearly so. It is possible that considerations of this kind account, at least in part, for the motions of the semi-permanent centers of action in the atmosphere, such as the Aleutian and Icelandic lows, and the sub-tropical highs. The study of such isobaric systems may thus be useful in long-range forecasting techniques, discussed in section 170.

49. Circulation and Vorticity. The concept of circulation is fundamental in hydrodynamics, and has a number of applications in meteorology. The *circulation* around a closed curve is, by definition, the line integral of velocity around the curve. Defined mathematically, it is

$$C = \oint (u \, dx + v \, dy + w \, dz) \quad (49.1)$$

If the curve is in the xy plane, (49.1) becomes

$$C = \oint (u \, dx + v \, dy) \quad (49.2)$$

The circulation may also be expressed in polar coordinates. The circulation around the closed curve shown in Fig. 45 is obtained in the following manner. A and B are two points on the curve separated by a small distance ds , and V is the velocity at A , a distance r from the instantaneous center of rotation O . Since α is the angle between V and ds , the component of V along ds is $V \cos \alpha$. Thus the circulation corresponding to (49.2) is

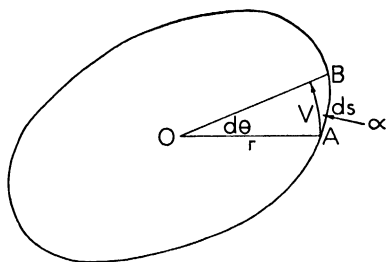


FIG. 45. The computation of circulation.

$$C = \oint V \cos \alpha \, ds \quad (49.3)$$

If the instantaneous angular velocity about O is $\frac{1}{2}\zeta$, then $V = \frac{1}{2}r\zeta$. In addition,

$$\cos \alpha = \frac{V \, dt}{ds} = \frac{r \, d\theta}{ds}$$

If substitutions are made for V and $\cos \alpha$ and the limits of integration are changed, equation 49.3 becomes

$$C = \int_0^{2\pi} \frac{1}{2} r^2 \zeta \, d\theta \quad (49.4)$$

But the integral

$$\int_0^{2\pi} \frac{1}{2} r^2 \, d\theta \quad (49.5)$$

gives the area enclosed by any plane curve. The quantity ζ , which is twice the angular velocity, is known as the *vorticity*. If ζ is constant

over the area, then by substituting (49.5) in (49.4), it is seen that circulation = area \times vorticity. Thus the circulation around a circle of radius r is given by

$$C = \pi r^2 \zeta$$

When vorticity is present in a fluid, the motion is called *rotational*. When vorticity is absent, the motion is *irrotational*. The term rotational as defined above does not always have the ordinary connotation of that word. One condition in which circular fluid motion may be irrotational is brought out in problem 4 at the end of this chapter. The rotation of a solid is rotational motion. The earth's atmosphere as a whole rotates as a solid, with the same angular velocity as the earth, so that the mean vorticity of the atmosphere is 2ω .

50. Rate of Change of Circulation. A knowledge of the rate of change of circulation, and thus of vorticity, with time is necessary for the discussion of a number of meteorological problems. Kelvin's circulation theorem, which gives the rate of change of circulation with time, may be derived in the following manner. If (49.1) is differentiated with respect to time

$$\begin{aligned} \frac{dC}{dt} &= \oint \left(\frac{du}{dt} dx + \frac{dv}{dt} dy + \frac{dw}{dt} dz \right) \\ &+ \oint \left[u \frac{d}{dt} (dx) + v \frac{d}{dt} (dy) + w \frac{d}{dt} (dz) \right] \quad (50.1) \end{aligned}$$

Since

$$\frac{dx}{dt} = u, \quad \frac{dy}{dt} = v, \quad \frac{dz}{dt} = w$$

the second term on the right-hand side may be written as

$$\oint (u du + v dv + w dw) = \frac{1}{2} \oint d(u^2 + v^2 + w^2) = 0$$

since the integration is that of a total differential carried out around a closed path. Thus Kelvin's circulation theorem

$$\frac{dC}{dt} = \oint \left(\frac{du}{dt} dx + \frac{dv}{dt} dy + \frac{dw}{dt} dz \right) \quad (50.2)$$

follows directly. By a slight modification of (46.1), (46.2), and (33.4),

the equations of motion become

$$\frac{du}{dt} = lw - \frac{1}{\rho} \frac{\partial p}{\partial x} + X \quad (50.3)$$

$$\frac{dv}{dt} = -lu - \frac{1}{\rho} \frac{\partial p}{\partial y} + Y \quad (50.4)$$

$$\frac{dw}{dt} = -g - \frac{1}{\rho} \frac{\partial p}{\partial z} + Z \quad (50.5)$$

The terms X , Y , Z represent external forces, such as those resulting from friction. Equation 50.5 gives the vertical acceleration when the gravity, pressure gradient, and external forces are not balanced. If (50.3), (50.4), and (50.5) are substituted in (50.2), the latter becomes

$$\begin{aligned} \frac{dC}{dt} = & - \oint \frac{1}{\rho} \left(\frac{\partial p}{\partial x} dx + \frac{\partial p}{\partial y} dy + \frac{\partial p}{\partial z} dz \right) + \oint (X dx + Y dy + Z dz) \\ & - \oint g dz - 2\omega \oint \sin \phi (u dy - v dx) \end{aligned} \quad (50.6)$$

Since, when there are no changes of pressure at a point,

$$dp = \frac{\partial p}{\partial x} dx + \frac{\partial p}{\partial y} dy + \frac{\partial p}{\partial z} dz$$

the first integral becomes

$$- \oint \frac{dp}{\rho}$$

The second integral may be written

$$W = \oint (X dx + Y dy + Z dz)$$

where W represents the work done by the external forces.

Since the integration is around a closed path, the third integral is zero. Thus,

$$- \oint g dz = 0$$

The fourth integral may be interpreted in the following manner. Consider a cyclonic circulation at latitude ϕ . At that latitude take the x axis positive to the east and the y axis positive to the north and project these axes on the equatorial plane of the earth. The pro-

jected axes are denoted x_1 and y_1 . The x and x_1 axes are parallel, so that

$$x = x_1, \quad dx = dx_1, \quad \text{and} \quad u = u_1$$

The y and y_1 axes are not parallel; the relationship between them may be seen from Fig. 46, which represents a cross section of the earth through the origin O of axes x and y and through the axis of rotation of the earth. It is apparent from this diagram that

$$y_1 = y \sin \phi$$

and hence $dy_1 = dy \sin \phi$ and $v_1 = v \sin \phi$.

The area F enclosed by the projection of the circulation at latitude ϕ on the equatorial plane is given by

$$F = \oint x_1 dy_1 \quad (50.7)$$

The rate of increase of area dF/dt is obtained by differentiating (50.7) with respect to time.

$$\frac{dF}{dt} = \oint (u_1 dy_1 + x_1 dv_1) \quad (50.8)$$

since $dx_1/dt = u_1$ and $d(dy_1/dt) = dv_1$. Dividing (50.8) into two integrals and subtracting $v_1 dx_1$ from the first and adding it to the second lead to

$$\frac{dF}{dt} = \oint (u_1 dy_1 - v_1 dx_1) + \oint (x_1 dv_1 + v_1 dx_1)$$

But

$$\oint (x_1 dv_1 + v_1 dx_1) = \oint d(x_1 v_1) = 0$$

since the integration is around a closed path. Thus

$$\frac{dF}{dt} = \oint (u_1 dy_1 - v_1 dx_1) \quad (50.9)$$

Substituting for u_1 , v_1 , dx_1 , and dy_1 in (50.9) leads to

$$\frac{dF}{dt} = \oint \sin \phi (u dy - v dx) \quad (50.10)$$

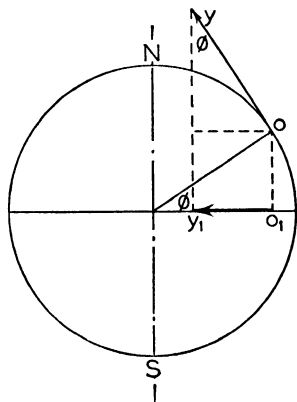


FIG. 46. The projection of axes with origin at latitude ϕ on the equatorial plane of the earth.

which is the fourth integral of (50.6). The latter may now be written

$$\frac{dC}{dt} = - \oint \frac{dp}{\rho} + W - 2\omega \frac{dF}{dt} \quad (50.11)$$

This equation gives V. Bjerknes' variation of Kelvin's circulation theorem, and the method of derivation gives precisely the same result as that in which the vertical components of the deflecting force are taken into account.

The circulation theorem as given in (50.11) has a number of applications to meteorology. For example, considering the last term only, if convergence occurs in the air motion over an area of low pressure at latitude ϕ , then in the equatorial plane $dF/dt < 0$, and $dC/dt > 0$. This agrees with the observed fact that the greater the convergence in the lower levels of a depression, the greater the cyclonic motion of the system becomes. In anticyclones, an increase in anticyclonic motion accompanies an increase in divergence in the lower levels.

This question may also be discussed quantitatively. Consider a system of air particles moving in horizontal circular paths about a center O . The rate of change of circulation around the circular path of radius r when divergence or convergence occurs may be obtained in the following manner. The circuit of particles around which the circulation is taken encloses an area πr^2 . If the area is sufficiently small that it may be considered as located at latitude ϕ , then the area F of its projection on the equatorial plane is given by

$$F = \pi r^2 \sin \phi \quad (50.12)$$

The change in area with time as divergence or convergence occurs is obtained by differentiating (50.12) with respect to time. Thus

$$\frac{dF}{dt} = 2\pi r \sin \phi \frac{dr}{dt} \quad (50.13)$$

and

$$\frac{dC}{dt} = -2\omega \frac{dF}{dt} = -4\pi\omega r \sin \phi v_r \quad (50.14)$$

where v_r denotes the radial velocity dr/dt . Since the length of the circuit is $2\pi r$, the mean acceleration around this circuit is, from (50.2),

$$\frac{\overline{dV}}{dt} = \frac{1}{2\pi r} \frac{dC}{dt} \quad (50.15)$$

Thus, by substituting in (50.15) from (50.14), it follows that

$$\frac{dV}{dt} = -2\omega \sin \phi v_r \quad (50.16)$$

The mean acceleration is thus that which results from the deflecting force of the earth's rotation, given by (34.20), and acts perpendicular to the radial velocity, and thus tangential to the circular motion. If convergence occurs in a cyclone, the motion is inward, $v_r < 0$, and $\frac{dV}{dt} > 0$, and the intensity of the cyclonic motion increases. If the radial velocity inward at any portion of the cyclone at 40° latitude is 1 m per sec, then

$$\frac{dV}{dt} = 9.4 \times 10^{-3} \text{ cm sec}^{-2}$$

If the mean acceleration is constant, at the end of an hour the tangential velocity V has increased by 0.34 m per sec.

If a cyclone in which little convergence is occurring moves southward, the projection on the equatorial plane of a circuit of air particles decreases, and the intensity of the cyclonic motion increases. Similarly the anticyclonic circulation decreases as a high-pressure system moves southward. The converse holds for northward motions. Rossby attributes the development of cyclonic curvature in southward-moving air at high levels and of anticyclonic curvature in northward-moving air to the influence of this term of the equation. The large-scale cyclonic and anticyclonic eddies which have been found from studies of the motions in isentropic surfaces are discussed briefly in section 166.

The rate of change of circulation resulting from the northward or southward movement of circular cyclonic or anticyclonic systems may be readily computed. Consider cyclonic motion with radius r . The projected area on the equatorial plane is given by (50.12),

$$F = \pi r^2 \sin \phi$$

If now the system as a whole moves northward with velocity v , r remaining constant, the projected area varies with time. Differentiating (50.12) with respect to time leads to

$$\frac{dF}{dt} = \pi r^2 \cos \phi \frac{d\phi}{dt} \quad (50.17)$$

Since

$$\frac{d\phi}{dt} = \frac{v}{E}$$

where E is the radius of the earth, then

$$\frac{dC'}{dt} = - \frac{2\omega\pi r^2}{E} \cos \phi v \quad (50-18)$$

Since the length of the circuit is $2\pi r$, the mean acceleration around this circuit is

$$\frac{dV}{dt} = - \frac{\omega r}{E} \cos \phi v \quad (50-19)$$

If the system moves southward at latitude 40° with a velocity of 10 m per sec, r having the constant value 400 km, then

$$\frac{dV}{dt} = 3.5 \times 10^{-3} \text{ cm sec}^{-2}$$

If the mean acceleration is constant, at the end of an hour the mean tangential velocity V has increased by 0.13 m per sec.

It must not be inferred from the foregoing that the cyclonic circulation of southward-moving depressions always increases, and similarly for the other motions discussed. It appears that the only term of those in (50-11) which produces an increase in horizontal circulation is $-2\omega(dF/dt)$. The effect of friction, included in the W term, is always to decrease either cyclonic or anticyclonic circulation. It has been shown by Brunt that the term $-\oint \frac{dp}{\rho}$ cannot produce closed horizontal

cyclonic circulations. In addition, atmospheric motions at the surface and those at higher levels are related, as shown in section 116, and developments in the upper air may offset or even reverse the changes which might be predicted on the basis of the discussion in this section.

If the circuit of air particles is in the yz plane, then $dF/dt = 0$ since F is at all times zero. In addition, this term is zero if the x , y , and z coordinates of every point on the circuit are constant, and if no change in latitude occurs. Equation 50-11 then reduces to

$$\frac{dC'}{dt} = - \oint \frac{dp}{\rho} + W \quad (50-20)$$

The circulation theorem in this form is used in section 71 in discussing the meridional circulation on a non-rotating globe. The method of evaluating the term $-\oint \frac{dp}{\rho}$ is given in that section. The process outlined there may also be used in studying slope and valley winds (section 124) and land and sea breezes (section 125).

PROBLEMS AND EXERCISES

1. A warm front extends from the northwest to the southeast. Isobars, equally spaced along the front, run northward ahead of the front and westward behind it. The barogram trace at a station just ahead of the front is curved cyclonically, and that at a station just behind the front is a straight line. In the cold air, the negative isallobars run parallel to the front, and become less negative with increasing distance from it. In the warm air, the isallobars run westward from the front. What is the sign of the acceleration of the front in this situation?

2. Equally spaced isallobars run from west to east over a portion of the earth's surface. The isallobar $+4$ mb per 3 h is found at latitude 40° N, and the isallobar $+1$ mb per 3 h is found at latitude 45° N. Assuming that this isallobaric gradient extends from the surface to a height of 2 km, and that the average density in this layer is 1.0×10^{-3} gm cm^{-3} , compute the average vertical velocity at a height of 2 km between latitudes 40° and 45° .

3. A layer of air extending from the surface to a height of 2 km moves from north to south. The velocity varies with latitude, but not with height. At a certain latitude, the north wind has a velocity of 10 m per sec, whereas 1000 km to the south it has a velocity of 11 m per sec. The layer has a uniform temperature of 7° C throughout, and the mean pressure of the air in the layer is constant, being 900 mb. Atmospheric conditions above 2 km cause no variations in surface pressure. Compute the pressure tendency in mb per 3 h at the surface under these conditions.

4. Air particles move in circular paths about a center O , with velocities given by $V = f(r)$. Compute the circulation about an area bounded by two radii which contain an angle θ and by two arcs subtending the angle θ . Under what condition will the circulation be zero?

5. A layer of air extending from the surface to a height h moves parallel to the x axis with a velocity which is constant with height, but which increases at a constant rate with x . The layer is isothermal both vertically and horizontally. If atmospheric conditions above the level h cause no variations in surface pressure, show that the pressure tendency at the surface is given by

$$\frac{\partial p_0}{\partial t} = \left(e^{\frac{-\rho_0 h}{RT}} - 1 \right) \left(p_0 \frac{\partial u}{\partial x} + u \frac{\partial p_0}{\partial x} \right)$$

BIBLIOGRAPHY

- Brunt, D., *Physical and Dynamical Meteorology*, London, Cambridge University Press, 1939. Chapters 8, 15.
- Haurwitz, B., *Dynamic Meteorology*, New York, McGraw-Hill Book Co., 1941. Chapters 6, 7.
- Koschmieder, H., *Dynamische Meteorologie*, Leipzig, Akad. Verlag, 1933. Chapter 10.
44. *Ibid.*, pp. 161-168.
- 42, 43. Petterssen, S., *Weather Analysis and Forecasting*, New York, McGraw-Hill Book Co., 1940. Chapter 9.
- 42, 43. Petterssen, S., "Kinematical and Dynamical Properties of the Field of Pressure with Applications to Weather Forecasting," *Geofys. Publ.* 10, No. 2, 1933.
44. Petterssen, S., *op. cit.*, pp. 224-227.

46. Brunt, D., and C. K. M. Douglas, *The Modification of the Strophic Balance for Changing Pressure Distribution and Its Effect on Rainfall*, Mem. Roy. Met. Soc., **3**, No. 22 (1928).
46. Sutcliffe, R. C., "On Development in the Field of Barometric Pressure," *Q. J. Roy. Met. Soc.*, **64**, 495-504 (1938).
48. Bjerknes, J., "Theorie der aussertropischen Zyklonenbildungen," *Met. Z.*, **59**, 462-466 (1937).

CHAPTER 9

TURBULENCE

51. Streamline and Turbulent Motion. There are two main types of air motion, streamline and turbulent. The nature of the difference between these types may be understood by considering the motion of water, which may be more readily observed. Streamline motion often occurs near the center of a slowly moving mill stream. At any instant the streamlines of the flow are parallel straight lines. Near the banks, however, the motion is irregular and broken into small eddies. This latter motion is turbulent. The irregularity of the flow is more noticeable in the rapids of a swiftly moving stream.

Turbulent motion in the atmosphere is made visible by smoke. For instance, the smoke leaving a burning cigarette in a quiet atmosphere ascends at first with streamline flow. There is an upward acceleration, however, and at a certain point the stability of the flow breaks down, and the motion becomes turbulent, as shown by the irregularity of the smoke pattern. A similar effect may be noted in smoke leaving a chimney.

No clear-cut physical picture of the nature of the eddies comprising turbulent motion can be visualized. This lack of rigid definition of the quantity to be studied has seriously hampered the development of adequate methods of analysis of turbulent flow in the atmosphere. The gusts and lulls shown on the records of certain types of wind-recording instruments indicate the presence of turbulent motion in the atmosphere but tell little of the nature of the eddies.

An adequate theory of turbulent motion must account for the observed variation of the wind with height near the surface, where the latter exerts a frictional drag on the air flowing over it. It must also account for the variation of temperature with height near the surface, and the diffusion of matter in the atmosphere. It has been shown that the effect of molecular movements is far too small to account for the observed variations in these elements.

So far, the main attempts to formulate a theory have been made on the basis that eddy motion in the atmosphere is completely analogous to molecular motion in a gas, the only difference being one of scale. Evidence mounts that this approach is not adequate, but no superior

method of attack on the problem has as yet been developed. Thus the transport of momentum, heat, and matter by eddy motion in the atmosphere is assumed to be similar to the transport of these quantities by molecular motion in a gas. The formulas developed in the following sections of this chapter are the same as those for molecular viscosity, conduction of heat, etc.

52. Turbulent Transfer of Momentum. The Wind Variation with Height in the Frictional Layer. The retardation of the air flow near the earth's surface is assumed to be due to a type of internal friction, known as eddy viscosity. This method of approach resulted from the work of Osborne Reynolds, who postulated that the system of eddy stresses caused by internal friction is a result of the deviations of the velocity from its mean value. The investigations of Taylor indicate that, if the instantaneous deviations from the mean wind velocity u , the x axis being oriented to coincide with the mean wind, are u' , v' , and w' in the x , y , and z directions respectively, then the mean values of u'^2 , v'^2 , and w'^2 are equal. This suggests that there is equipartition of the energy of the eddies in these three directions. Other investigations suggest, however, that the cross-wind component is greater than the vertical component. It is probable that the latter is a more accurate statement of conditions near the surface.

The frictional drag of a slowly moving air current on a more rapidly moving current adjacent to it is assumed to be a result of the transport of momentum from one current to the other by means of eddies. If a mass of air from the slowly moving current penetrates the rapidly moving current, conserving its initial momentum during the process, the result is a retardation of the faster current. Consider air flowing in the x direction with a mean velocity u , the instantaneous deviations from u being u' and w' in the x and z directions respectively. In

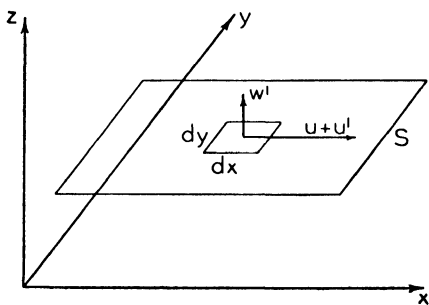


FIG. 47. Vertical transfer of momentum through turbulence.

Fig. 47 $dx dy$ represents an element of the horizontal area S . If w' is the instantaneous mean vertical velocity over the area $dx dy$, then the mass of air flowing upward across area $dx dy$ in unit time is

$$\rho w' dx dy$$

The amount of x momentum dI_x moving upward through area $dx dy$ in

unit time is then given by

$$dI_x = \rho w' (u + u') dx dy \quad (52.1)$$

since momentum equals mass times velocity. The amount of x momentum moving upward through the area S in unit time is, therefore,

$$\begin{aligned} I_x &= \iint \rho w' (u + u') dx dy \\ &= u \iint \rho w' dx dy + \iint \rho w' u' dx dy \end{aligned} \quad (52.2)$$

Since there is no net transfer of mass through the large area S during unit time, it follows that the first integral on the right-hand side of (52.2) is zero, and the equation becomes

$$I_x = \iint \rho w' u' dx dy \quad (52.3)$$

Now consider an eddy which starts from level z_0 with the mean x component of velocity u_{z_0} appropriate to that level. It arrives at level z with the same x component of velocity u_{z_0} . The mean velocity of the air motion at the new level z is u_z , so that the instantaneous deviation u' of the eddy motion from the mean velocity u_z at that level is $u_{z_0} - u_z$. The deviation u' at the level z is then given with sufficient accuracy by the expression

$$u' = \frac{\partial u}{\partial z} (z_0 - z) = - \frac{\partial u}{\partial z} (z - z_0) \quad (52.4)$$

Substituting (52.4) in (52.3) leads to

$$\begin{aligned} I_x &= - \iint \rho w' \frac{\partial u}{\partial z} (z - z_0) dx dy \\ &= - \frac{\partial u}{\partial z} \iint \rho w' (z - z_0) dx dy \end{aligned} \quad (52.5)$$

The quantity $\overline{w'(z - z_0)}$, where the bar indicates that the mean value of the product is to be taken, is known as the *coefficient of eddy diffusivity* and is denoted by K , using the notation introduced by Taylor. The units of K in the cgs system are $\text{cm}^2 \text{sec}^{-1}$, which are the same as those of the coefficient of heat conductivity κ and of the coefficient of kinematic viscosity ν for molecular processes. The coefficient K is an attribute of eddy motion over a large area for a considerable period of time, not one of eddy motion at a point at a given instant of time. The linear dimensions of the area should be at least 10 km and

the interval of time at least 5 min. The quantity $\overline{\rho w'(z - z_0)}$, or $K\rho$, was called the *Austausch* (exchange) coefficient A by Schmidt. The units of A in the cgs system are $\text{gm cm}^{-1} \text{sec}^{-1}$, the same as those of the coefficient of molecular viscosity μ . The mean value of $z - z_0$, denoted $\overline{z - z_0}$, was called by Prandtl the *Mischungsweg* (path of mixing).

The eddy transfer of x momentum upward through unit area may then be written, according to (52.5), assuming that K and ρ are mean values over the unit area,

$$I_x = -K\rho \frac{\partial u}{\partial z} \quad (52.6)$$

Now consider a disc of unit cross section and thickness dz . The amount of x momentum entering through the bottom is I_x and the amount leaving through the top is $I_x + \frac{\partial I_x}{\partial z} dz$. The net gain in x momentum in the disc is then $-\frac{\partial I_x}{\partial z} dz$ or, using (52.6),

$$\frac{\partial}{\partial z} \left(K\rho \frac{\partial u}{\partial z} \right) dz \quad (52.7)$$

The units of this expression are

$$\text{gm cm}^{-1} \text{sec}^{-2} = \frac{\text{gm cm sec}^{-2}}{\text{cm}^2}$$

The expression 52.7 then represents a force per unit area, or a shearing stress exerted by a moving current of air on a slower moving current adjacent to it. This expression thus gives the magnitude of the frictional forces acting in the atmosphere, which are most marked in the surface layers.

If unit volume is considered, $dz = 1$, so that (52.7) becomes

$$\frac{\partial}{\partial z} \left(K\rho \frac{\partial u}{\partial z} \right) \quad (52.8)$$

If the atmosphere is assumed to be incompressible, so that ρ is constant, the frictional force per unit mass is obtained by dividing by ρ . Thus, from (52.8), it is seen that the frictional force per unit mass resulting from eddy viscosity is

$$\frac{\partial}{\partial z} \left(K \frac{\partial u}{\partial z} \right) \quad (52.9)$$

When the mean velocity of the air stream has the components u and v ,

and when K is constant with height, the x and y components of the eddy frictional force are

$$K \frac{\partial^2 u}{\partial z^2} \quad \text{and} \quad K \frac{\partial^2 v}{\partial z^2} \quad (52-10)$$

It will be noted that several assumptions have been made in this derivation. In particular, it has been assumed that an eddy conserves its momentum as it moves from one level to another. Since the eddy moves through a varying pressure field as it ascends or descends, however, it is difficult to see how this condition can be obeyed. Nevertheless, the expressions in (52-10) give results which are approximately correct.

The general equations of horizontal motion given by (46-1) and (46-2) may now be expanded to include the effect of frictional forces resulting from turbulent air motion. The equations thus become

$$\frac{du}{dt} = fv - \frac{1}{\rho} \frac{\partial p}{\partial x} + K \frac{\partial^2 u}{\partial z^2} \quad (52-11)$$

$$\frac{dv}{dt} = -fu - \frac{1}{\rho} \frac{\partial p}{\partial y} + K \frac{\partial^2 v}{\partial z^2} \quad (52-12)$$

Under certain assumptions these equations may be solved to give the variation of wind with height in the surface layers where the frictional forces are large. The various steps leading to the solution are too lengthy and involved to be included here. A simpler analysis given by Guldberg and Mohn will be used instead.

When the isobars are straight and parallel, balanced motion occurs in the free atmosphere when the deflecting force exactly balances the pressure gradient force, as shown in section 35. It was also indicated in that section that in the lower layers of the atmosphere, up to heights of 2000 or 3000 ft, the action of frictional forces causes the air to flow across the isobars toward lower pressure. The retarding effect of friction causes a smaller velocity than in the free atmosphere, so that the deflecting force is smaller than the pressure gradient force. This situation is illustrated in Fig. 48. The isobars are parallel to the y axis, with pressure increasing in the positive x direction. Since the velocity V is not parallel to the isobars, and the deflecting force is perpendicular to the direction of motion of the air, while the pressure gradient force acts in a direction perpendicular to the isobars, it follows that these two forces do not act in opposite directions, and therefore cannot be balanced. Guldberg and Mohn assumed that the frictional force is proportional to the velocity, and hence is given by kV , where k is the

coefficient of friction, and acts in a direction opposite to that of the velocity. For a balance among deflecting, pressure gradient, and frictional forces, therefore, the frictional force must be equal to the resultant of the other two and oppositely directed. It follows then that the

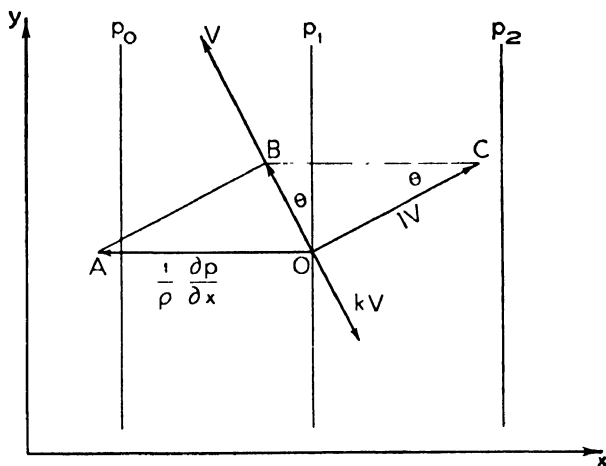


FIG. 48. Deviation of the wind by friction

resultant of these two, denoted by OB in the figure, must lie along the wind vector V . The frictional force kV , represented by a vector in the diagram, is equal in magnitude to OB . Since $AOCB$ is a parallelogram, $BC = AO = (1/\rho)(\partial p/\partial x)$. Considering triangle OBC , it follows that

$$(kV)^2 + (lV)^2 = \left(\frac{1}{\rho} \frac{\partial p}{\partial x} \right)^2$$

Thus

$$V = \frac{1}{\rho} \frac{\partial p}{\partial x} (k^2 + l^2)^{-\frac{1}{2}} \quad (52.13)$$

But, according to (35.1)

$$\frac{1}{\rho} \frac{\partial p}{\partial x} = lv_g$$

where v_g denotes the geostrophic wind velocity. Substituting in (52.13) then gives

$$V = lv_g (k^2 + l^2)^{-\frac{1}{2}} \quad (52.14)$$

If θ represents the angle which the wind vector makes with the isobars, then

$$\tan \theta = \frac{kV}{lV} = \frac{k}{l} \quad (52.15)$$

A more complete analysis shows that the assumptions of Guldberg and Mohn are only approximate. Nevertheless the equations 52.14 and 52.15 have the virtue of simplicity, while not deviating too far from accuracy. They are used in section 123 to account for the observed diurnal variation of wind in the lower levels.

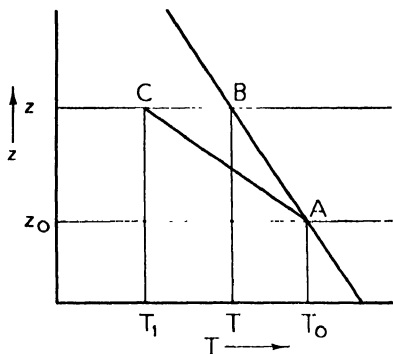


FIG. 49. Eddy transfer of heat.

53. Turbulent Transfer of Heat.

The following treatment of the vertical transfer of heat by eddy motion follows that given by Brunt. In Fig. 49, AB represents a portion of a stable environment curve plotted on a temperature-height diagram. The temperature of a particle of air at A at height z_0 is T_0 , while that of a particle at B at height z is T . Since the temperature decreases with height, it follows

$$T_0 = T - \frac{\partial T}{\partial z} (z - z_0) \quad (53.1)$$

Now consider an eddy initially at A which ascends from height z_0 to height z , its temperature decreasing at the dry adiabatic lapse rate Γ during the process. It arrives at C at height z with the temperature T_1 given by

$$T_1 = T_0 - \Gamma(z - z_0) \quad (53.2)$$

By substituting (53.1) in (53.2),

$$T_1 = T - \left(\Gamma + \frac{\partial T}{\partial z} \right) (z - z_0) \quad (53.3)$$

The heat content of the air comprising the eddy of mass m when the latter ascends through a horizontal surface at level z is therefore

$$mc_p \left[T - \left(\Gamma + \frac{\partial T}{\partial z} \right) (z - z_0) \right]$$

The total heat content of all the eddies ascending through unit area in unit time is then

$$\Sigma mc_p \left[T - \left(\Gamma + \frac{\partial T}{\partial z} \right) (z - z_0) \right]$$

or

$$c_p T \Sigma m - c_p \left(\Gamma + \frac{\partial T}{\partial z} \right) \Sigma m (z - z_0) \quad (53.4)$$

where the symbol Σ signifies a process of summation

Similarly, the total heat content of all the eddies descending from level z'_0 through unit area at level z in unit time is

$$c_p T \Sigma m' - c_p \left(\Gamma + \frac{\partial T}{\partial z} \right) \Sigma m' (z - z'_0) \quad (53.5)$$

The net upward transfer of heat by eddy motion, obtained by subtracting (53.5) from (53.4), is then

$$c_p T (\Sigma m - \Sigma m') - c_p \left(\Gamma + \frac{\partial T}{\partial z} \right) [\Sigma m (z - z_0) - \Sigma m' (z - z'_0)] \quad (53.6)$$

As much mass is transported upward across the surface as is transported downward across the same surface, so that $\Sigma m = \Sigma m'$, and the first term of (53.6) is zero. The net upward transfer therefore becomes

$$-c_p \left(\Gamma + \frac{\partial T}{\partial z} \right) [\Sigma m (z - z_0) - \Sigma m' (z - z'_0)] \quad (53.7)$$

Now consider two elements S_1 and S_2 of a large horizontal area S . Over the small area S_1 there is a mean upward eddying velocity w'_1 . The mass of air m passing upward through S_1 in unit time is $\rho w'_1 S_1$. Over S_2 there is a mean downward eddying velocity $-w'_2$. The mass of air m' passing downward through S_2 in unit time is then $-\rho w'_2 S_2$. Substituting these values in (53.7) gives for the upward transfer

$$-c_p \left(\Gamma + \frac{\partial T}{\partial z} \right) [\Sigma \rho w'_1 S_1 (z - z_0) + \Sigma \rho w'_2 S_2 (z - z'_0)] \quad (53.8)$$

Adding the contributions of all such small elements it follows that the net upward transfer of heat over the area S is

$$-c_p \left(\Gamma + \frac{\partial T}{\partial z} \right) [\Sigma_s \rho w' (z - z_0)]$$

or

$$-c_p \left(\Gamma + \frac{\partial T}{\partial z} \right) [\rho S \overline{w' (z - z_0)}]$$

where, as in the previous section, the bar denotes the mean value of the product, in this case the mean value over the area S . The net upward transfer through unit area is, therefore,

$$-c_p \left(\Gamma + \frac{\partial T'}{\partial z} \right) [\rho \overline{w'(z - z_0)}] \quad (53.9)$$

But the expression $\overline{w'(z - z_0)}$ is the coefficient of eddy diffusivity K , so that the net upward transfer of heat through unit area is

$$-K\rho c_p \left(\Gamma + \frac{\partial T'}{\partial z} \right) \quad (53.10)$$

If the rate of decrease of temperature with height of the environment, i.e., the lapse rate of the environment, is denoted α , so that $\partial T'/\partial z = -\alpha$, then the net upward transfer of heat is

$$-K\rho c_p (\Gamma - \alpha) \quad (53.11)$$

For a stable lapse rate $\Gamma > \alpha$, and the turbulent transfer of heat is downward. When $\Gamma = \alpha$ there is no vertical transfer of heat and when the environment is unstable, so that $\Gamma < \alpha$, the transfer is upward. This result has numerous applications in meteorology, both theoretical and applied, many of which will be noted in other sections of this book.

The assumptions made in obtaining this result should be noted. It was assumed that the density was uniform, that the air particles at z_0 and z'_0 were normal specimens of the air at those levels, and that the lapse rate of the environment was constant over the mixing length $z - z_0$.

From (53.10), the upward eddy transfer of heat Q through unit area in unit time is given by the expression

$$Q = -K\rho c_p \left(\Gamma + \frac{\partial T'}{\partial z} \right)$$

The units of this expression are, of course, $\text{cal cm}^{-2} \text{sec}^{-1}$. Now consider a disc of unit cross section and thickness dz . The amount of heat entering through the bottom is Q and the amount leaving through the top is $Q + \frac{\partial Q}{\partial z} dz$. The net gain of heat in the disc is then $-\frac{\partial Q}{\partial z} dz$, or using (53.10),

$$\frac{\partial}{\partial z} \left[K\rho c_p \left(\Gamma + \frac{\partial T'}{\partial z} \right) \right] dz \quad (53.12)$$

The rate of gain of heat in the disc may also be expressed as

$$\rho \, dz \, c_p \frac{dT}{dt}$$

or, with little error, by

$$\rho \, dz \, c_p \frac{\partial T}{\partial t} \quad (53.13)$$

Equating (53.12) and (53.13) gives, since c_p is a constant,

$$\rho \frac{\partial T}{\partial t} = \frac{\partial}{\partial z} \left[K \rho \left(\Gamma + \frac{\partial T}{\partial z} \right) \right] \quad (53.14)$$

Now Γ is a constant, and ρ and K may be assumed to be constant, so that finally

$$\frac{\partial T}{\partial t} = K \frac{\partial^2 T}{\partial z^2} \quad (53.15)$$

This equation gives the effect of turbulent transfer of heat only in causing changes in temperature. A knowledge of the radiative transfer of heat is also necessary for a complete determination of the rate of change of temperature.

Equation 53.15 has the same form as the equation for the conduction of heat by molecular motions, the latter having the coefficient of conductivity κ instead of K as in the former. The use of this equation in evaluating K is outlined in section 55.

Taylor has given a number of interesting applications of this equation to atmospheric processes. One of these was a discussion of the variations which occur in a mass of air when the surface temperature is suddenly lowered, as when in summer a current of air leaves a warm

land surface and moves over a relatively cold sea surface. The boundary conditions are as follows. As shown in Fig. 50, the air leaves the warm land surface with temperature T_0 at the level $z = 0$ and with temperature $T = T_0 - \alpha z$ at level z when $t = 0$. The lapse rate α is

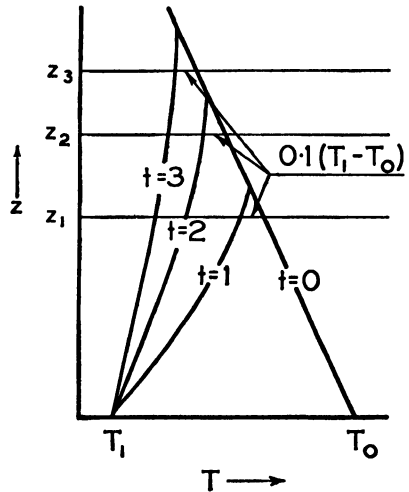


FIG. 50. Cooling of an air mass through turbulence.

assumed to be initially constant. At $t > 0$ and $z = 0$, $T = T_1$, the temperature of the cool sea surface. The solution of (53-15) with these boundary conditions is*

$$T = T_0 - \alpha z + (T_1 - T_0) \left[1 - \frac{2}{\sqrt{\pi}} \int_0^{z/2\sqrt{Kt}} e^{-\frac{z^2}{4Kt}} d\left(\frac{z}{2\sqrt{Kt}}\right) \right] \quad (53-16)$$

The sudden change in temperature of the surface air is given by $T_1 - T_0$. The term to the right is the probability integral discussed in section 59. Taylor showed from (53-16) that the time t required for a change of temperature of amount $0.1(T_1 - T_0)$ to occur at height z was specified approximately by the equation

$$\frac{z}{2\sqrt{Kt}} = 1$$

or

$$z^2 = 4Kt \quad (53-17)$$

He assumed that the change of temperature $0.1(T_1 - T_0)$ was sufficiently small to be considered as just the beginning of the change, so that (53-17) gives the approximate height to which the effect of the surface cooling extends at the end of time t . The heights of cooling at the end of times 1, 2, and 3 are shown in Fig. 50. The result is practically the same if the surface cooling is not instantaneous, but gradual. Radiational processes will tend to increase the height to which the cooling extends during any given interval of time. The use of this equation in indicating the height to which advection and radiation fog will extend is mentioned in section 134.

54. Turbulent Transfer of Matter. The equation for the vertical transfer of matter by eddy diffusion may be derived in a manner similar to that used to obtain the equation of heat transfer, given in the previous section. Consider any entity in the atmosphere the mass of which associated with unit mass of air does not vary with vertical motion. Such an entity might be, for example, atmospheric dust, carbon dioxide, or water vapor as long as the air remains unsaturated. Denote the mass of the entity in unit mass of air by the symbol χ . For water vapor the specific humidity s would be substituted for χ , since the specific humidity is defined as the mass of water vapor per unit mass of moist air.

* H. S. Carslaw, *The Conduction of Heat*, London, Macmillan Co., 1921, pp. 46-47.

The portion AB of the curve shown in Fig. 51 gives the rate of change of χ with height in the interval from z_0 to z . The entity has the value χ_0 at the point A at height z_0 and the value χ at the point B at height z . It follows, then, that

$$\chi_0 = \chi - \frac{\partial \chi}{\partial z} (z - z_0) \quad (54.1)$$

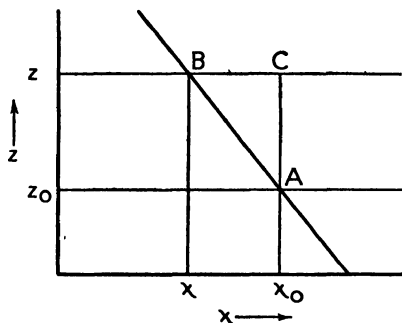


FIG. 51. Eddy transfer of matter.

An eddy of mass m ascends from A at level z_0 , conserving its initial value of χ_0 as it rises to C . The amount of the entity which passes upward through a horizontal surface at level z is $m\chi_0$, or, with (54.1),

$$m \left[\chi - \frac{\partial \chi}{\partial z} (z - z_0) \right] \quad (54.2)$$

The total mass of the entity contained in all the eddies rising through unit area in unit time is thus

$$\Sigma m \left[\chi - \frac{\partial \chi}{\partial z} (z - z_0) \right]$$

or

$$\Sigma m \chi - \Sigma m \frac{\partial \chi}{\partial z} (z - z_0) \quad (54.3)$$

Similarly, denoting the mass of each downward moving eddy by m' , the total mass of the entity carried downward through unit area in unit time by all descending eddies is

$$\Sigma m' \chi - \Sigma m' \frac{\partial \chi}{\partial z} (z - z'_0) \quad (54.4)$$

The net upward flux of the entity is then

$$\chi (\Sigma m - \Sigma m') - \frac{\partial \chi}{\partial z} \left[\Sigma m (z - z_0) - \Sigma m' (z - z'_0) \right] \quad (54.5)$$

Since $\Sigma m = \Sigma m'$, the first term is zero and the net upward flux becomes

$$- \frac{\partial \chi}{\partial z} \left[\Sigma m (z - z_0) - \Sigma m' (z - z'_0) \right] \quad (54.6)$$

The mass of air m passing upward in unit time through the small area

S_1 is $\rho w'_1 S_1$, while the mass m' passing downward in unit time through S_2 is $-\rho w'_2 S_2$. Substituting these values in (54.6) gives for the net upward flux

$$-\frac{\partial \chi}{\partial z} \left[\Sigma \rho w'_1 S_1 (z - z_0) + \Sigma \rho w'_2 S_2 (z - z'_0) \right] \quad (54.7)$$

The net upward flux over the large area S is then the sum of all such contributions

$$-\frac{\partial \chi}{\partial z} \left[\Sigma \rho w' (z - z_0) \right]$$

or

$$-\frac{\partial \chi}{\partial z} \left[\rho S \overline{w' (z - z_0)} \right]$$

where the bar denotes the mean value of $w' (z - z_0)$ over the area S . The net upward flux of the entity per unit area is thus

$$-\frac{\partial \chi}{\partial z} \left[\rho \overline{w' (z - z_0)} \right]$$

or

$$-K\rho \frac{\partial \chi}{\partial z} \quad (54.8)$$

The units of this expression are $\text{gm cm}^{-2} \text{sec}^{-1}$.

The assumptions made are similar to those in the previous section. It was assumed that the density was uniform, that an eddy was a normal sample of its environment when it started to ascend or descend, and that $\partial \chi / \partial z$ was constant over the mixing length.

The net upward flux of mass M of the entity per unit area per unit time is given by, according to (54.8)

$$M = -K\rho \frac{\partial \chi}{\partial z}$$

The amount of mass of the entity entering through the bottom of a disc of unit cross section and thickness dz in unit time is M and the amount leaving through the top is $M + \frac{\partial M}{\partial z} dz$. The net gain of mass in the

disc is then $-\frac{\partial M}{\partial z} dz$ or

$$\frac{\partial}{\partial z} \left(K\rho \frac{\partial \chi}{\partial z} \right) dz \quad (54.9)$$

The rate of gain of the entity χ in the disc may also be expressed as

$$\rho \, dz \, \frac{d\chi}{dt}$$

or, with sufficient accuracy, by

$$\rho \, dz \, \frac{\partial \chi}{\partial t} \quad (54.10)$$

Equating (54.9) and (54.10) and assuming that ρ and K are constant with height obtain

$$\frac{\partial \chi}{\partial t} = K \frac{\partial^2 \chi}{\partial z^2} \quad (54.11)$$

This equation, along with (54.8), is useful in determining the diffusion of water vapor through the atmosphere by turbulent mixing processes. It has the same form as the equation for the diffusion of the molecules of a gas.

55. Evaluation of the Coefficient of Eddy Diffusivity. The diurnal variation of temperature at the earth's surface may be expressed as a harmonic function of the time. The daily temperature period is not a true harmonic function, however, since the maximum and minimum of temperature do not occur 12 h apart. In general, the maximum occurs at 14 h while the minimum does not occur at 02 h but at sunrise. As a first approximation, however, the variation of surface temperature with time may be expressed as

$$T = T_0 + B \cos \frac{2\pi}{D} t \quad (55.1)$$

where T_0 is the mean temperature for the day, B is the amplitude of the surface temperature variation, and D is a period of 24 h. Time t is taken to be zero when the temperature is a maximum, so that the maximum temperature is $T_0 + B$.

When the above boundary conditions are satisfied, the solution of (53.15) is*

$$T = T_0 - \alpha z + B e^{-\lambda z} \cos \left(\frac{2\pi}{D} t - \lambda z \right) \quad (55.2)$$

where

$$\lambda = \sqrt{\frac{\pi}{DK}} \quad (55.3)$$

* H. S. Carslaw, *The Conduction of Heat*, London, Macmillan Co., 1921, pp. 47-50.

The $-\alpha z$ term makes allowance for the mean lapse rate during the period. It is seen from (55.2) that the amplitude of the temperature variation decreases exponentially with height, while the maximum temperature occurs after an increasing interval of time after the surface maximum is attained, as shown by the increasing lag of the phase angle λz with height. The ratio of the amplitudes at any two heights z_1 and z_2 is $e^{-\lambda(z_1-z_2)}$. If the amplitude of the diurnal variation at height z_1 is B_1 , while the amplitude at height z_2 is B_2 , then

$$e^{-\lambda(z_1-z_2)} = \frac{B_1}{B_2} \quad (55.4)$$

The method of determining the harmonic function which best fits the observed temperatures is given in section 62. The maximum deviation from the mean temperature is then the amplitude B . The value of λ , and so of K , can then be determined from (55.4) and (55.3).

It was assumed in deriving (53.15) that K is constant. However, it is known that K has marked daily and vertical variations. Since observations at different heights extending over a 24-h period at least are used in determining values of K by the above method, it must be realized that there may be wide divergences between values computed in this way and actual values of the eddy diffusivity at any given height and time.

Taylor, using this method, computed values of K from hourly temperature observations made during the five-year period 1890-94 on the Eiffel Tower at heights of 123, 197, and 302 m above the surface, and at a height of 18 m above the terrace of the Bureau Météorologique. The variations of K with height and during the year are shown in Fig. 52. It can be seen that, in general, K is greater in summer than in winter. In addition, it increases with height in summer, but decreases with height in winter. He found a mean value of approximately 10^5 for the height interval 18 to 302 m for the year. Using (53.17), Taylor found values over the ocean which were considerably less than these, of the order of 10^3 . Presumably the lapse rates in winter and over the ocean are smaller than over a land surface in summer so that the dimensions and activity of the eddies are less in the former than in the latter situations.

The effects of radiative as well as of turbulent diffusion of heat are included in the above results. It follows then that the separate contribution of eddy diffusion is somewhat less than suggested by the values given in the figure. More recent investigations, however, have shown that, even allowing for the effects of radiation, there are internal

discrepancies in the results obtained through the use of (53.15). The presence of these discrepancies suggests that the latter equation does

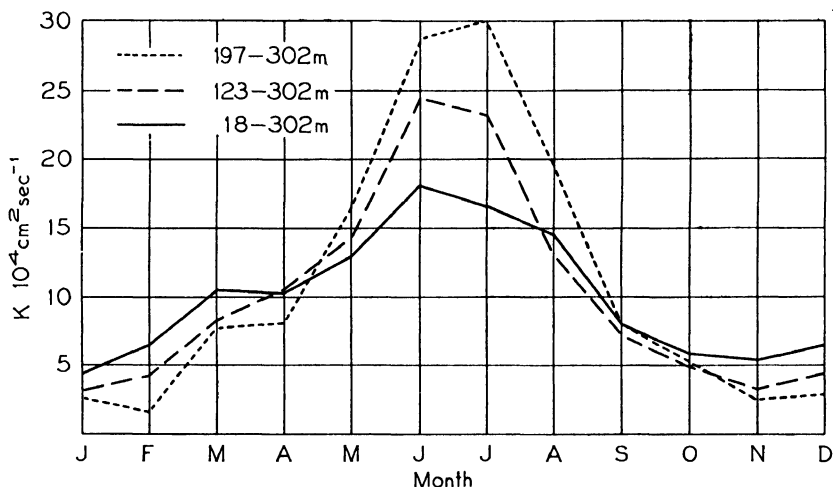


FIG. 52. Annual variation of the coefficient of eddy diffusivity. (After Taylor.)

not give a completely accurate description of eddy diffusion of heat in the atmosphere.

PROBLEMS AND EXERCISES

1. Show that the effect of turbulent transfer of heat in the atmosphere is always to smooth out irregularities in the lapse rate.

2. In winter a warm mass of air advances from a tropical sea surface over a cold continent. If K has the constant value $2 \times 10^4 \text{ cm}^2 \text{ sec}^{-1}$, how long, in days, will it take the surface cooling to extend to heights of (a) 1 km, (b) 2 km, and (c) 3 km?

3. Compute the mean change in the specific humidity between the pressures 950 and 650 mb during a 24-h period when the variation of specific humidity with height is constant during the period, being a decrease of 1 gm per kg of moist air per km at 950 mb and zero at 650 mb. The coefficient of eddy diffusivity has the value $6.8 \times 10^4 \text{ cm}^2 \text{ sec}^{-1}$, which is constant with height. The density of the air at 950 mb is $1.0 \times 10^{-3} \text{ gm cm}^{-3}$.

4. At heights greater than 1 km above a given aerological station the specific humidity varies inversely with height. At 3 km the specific humidity is 4 gm per kg of moist air. Assuming that K is constant with height and equal to $10^5 \text{ cm}^2 \text{ sec}^{-1}$, compute the rate of change of specific humidity with time at 3 km. Express the final answer in grams per kilogram of moist air per hour.

5. An isothermal winter air mass with temperature -10°C has a surface pressure of 1000 mb. If K at 500 mb is $10^3 \text{ cm}^2 \text{ sec}^{-1}$, compute the mean increase in temperature in the layer of air below during a 1-h period.

BIBLIOGRAPHY

- Brunt, D., *Physical and Dynamical Meteorology*, London, Cambridge University Press, 1939. Chapters 11, 12.
- Haurwitz, B., *Dynamic Meteorology*, New York, McGraw-Hill Book Co., 1941. Chapters 10, 11.
- Koschmieder, H., *Dynamische Meteorologie*, Leipzig, Akad. Verlag., 1933. Chapter 7.
- Problems of Modern Meteorology*, London, Royal Meteorological Society, 1934. Number 5.
- Shaw, Sir N., *Manual of Meteorology*, London, Cambridge University Press, Vol. 4 (1931), Chapter 4.
- Cowling, T. G., and A. White, "The Eddy Diffusivity and the Temperature of the Lower Layers of the Atmosphere," *Q. J. Roy. Met. Soc.*, **67**, 276-283 (1941).
- Lettau, H., *Atmosphärische Turbulenz*, Leipzig, Akad. Verlag., 1939.
- Taylor, G. I., Report by, in *Report on the Work Carried Out by the S. S. "Scotia," 1913*. London, H. M. Stationery Office, 1914. Pages 48-68.
- Taylor, G. I., "Eddy Motion in the Atmosphere," *Phil. Trans. Roy. Soc.*, **A215**, 1 (1915).
- Taylor, G. I., "Phenomena Connected with Turbulence in the Lower Atmosphere," *Proc. Roy. Soc.*, **A94**, 137-155 (1918).
- Taylor, G. I., "The Transport of Vorticity and Heat through Fluids in Turbulent Motion," *Proc. Roy. Soc.*, **A135**, 685-702 (1932).
- Taylor, G. I., "Turbulence," *Q. J. Roy. Met. Soc.*, **53**, 201-211 (1927).
- Schmidt, W., *Der Massenaustausch in freier Luft und verwandte Erscheinungen*, Hamburg, Henri Grand, 1925.

CHAPTER 10

STATISTICAL ANALYSIS OF METEOROLOGICAL DATA

56. The Purpose of Statistics. Meteorology is similar to many other sciences since, in its study, measurements are taken of different variables. To understand their significance, they must be condensed and analyzed. There are many ways of doing this, some graphical, some numerical. Thus the isobars on the synoptic weather chart show in a pictorial manner the values of the sea level pressures at the numerous reporting stations and their variation over the region, and thus permit the significant features of the pressure distribution to be grasped. The different methods whereby these data are condensed and analyzed form a part of the field of statistics. Therefore a knowledge of some of the elementary ideas of statistics is helpful to the meteorologist.

When the data are in numerical form, the significant features of the series can be summarized by choosing two or three values, which are then used to represent the series. Of these measures, two are used most often in meteorology. The first is a measure of central tendency, or an average, and the second is a measure of variability. The use and the method of calculation of these will be shown in the following sections.

57. Measures of Central Tendency. Computation of the Mean. When the amounts of annual precipitation for a station for a number of years are obtained, it is found that they vary from, say, 20 in. to 50 in. The selection of one number to represent all values, to be called the annual rainfall, might be made in different ways. From one point of view it would seem desirable to choose the number of inches of rain that was found to recur most often in the series. This would give the mode. Another way to select a value to represent the series is to choose the middle one after the numbers in the series have been arranged in increasing order of magnitude. This gives the median. A third way is to find the total rainfall during the period, and then divide by the number of years comprising the period. This value is called the arithmetic mean, or sometimes the mean. Other methods are used at times, but the mean, median, and mode are the most commonly used measures of central tendency.

The *mode* of a number of observations is that value for the variable x

which recurs most frequently. The table on page 163 presents a series of observations in a convenient form called a frequency distribution. The mean temperature for every April 13 from 1841 till 1940 for Toronto, Ontario, was obtained, and the values classified. Two values were found between 25.5 and 27.4° F, four between 27.5 and 29.4° F, etc. The number of values in each class is set forth in column 3. The mid-points of the class intervals are given in column 2.

According to column 3 of the table there were more days with mean temperatures in the class interval 37.5 to 39.4° F than in any other interval. Hence the modal class interval is 37.5–39.4° F, or, to use the midpoint of the interval, 38.5° F is the mode.

Since the mode is that value that occurs most frequently, it is a typical value for the series. It is used in meteorology in speaking of the region of the westerlies, or the northeast trade wind belt. For in certain regions of the earth these are the modal wind directions. The most frequent storm track is a mode of various tracks. Since, though, it presents difficulties in calculation in some series and since it fails to be typical except for series with many observations, the mode is reserved for particular series, such as those mentioned.

Another measure for the distribution is the median. If all the values of the variable x are arranged in numerical order, the *median* is the middle one of the series so arranged, or with an even number of observations the average of the middle two. It thus typifies the series since half the observations are on either side.

Although the meaning of the median is easily understood, its determination becomes more difficult when the number of observations is large. When the observations are grouped in classes, such as in the distribution given in the table, the assumption must be made that the values in any class interval are arranged at regular intervals. With this assumption, the median can be computed. The median for the distribution in the table is in the interval 39.5–41.4° F, since there are 47 of the 100 observations having values below those in that interval. On the assumption of an even distribution of the observations, the three additional values required to give one-half the observations will lie in the lower 3/13 of the class interval 39.5–41.4° F. The median, then, equals

$$39.5 + (\frac{3}{13} \text{ of } 2.00) = 39.5 + 0.46 = 39.96^\circ \text{ F}$$

The median is particularly useful in typifying a series with a small number of observations. The mode would seldom have meaning, and the mean value would be influenced greatly by one exceptional value. For example, if the series is 1, 1, 3, 4, 14, the median 3 is more representative of the numbers than the mode, 1, or the mean, 5. Such

COMPUTATION OF THE MEAN AND THE STANDARD DEVIATION

Frequency distribution of daily mean temperatures for
April 13th's, for Toronto, Ontario, during the period 1841-1940*

Class Interval	Midpoint	Frequency	Deviation from Arbitrary Origin		
°F	°F	f	d'	fd'	fd'^2
(1)	(2)	(3)	(4)	(5)	(6)
25.5-27.4	26.5	2	-8	-16	128
27.5-29.4	28.5	4	-7	-28	196
29.5-31.4	30.5	4	-6	-24	144
31.5-33.4	32.5	3	-5	-15	75
33.5-35.4	34.5	6	-4	-24	96
35.5-37.4	36.5	11	-3	-33	99
37.5-39.4	38.4	17	-2	-34	68
39.5-41.4	40.5	13	-1	-13	13
41.5-43.4	42.5	9	0		
43.5-45.4	44.5	9	1	9	9
45.5-47.4	46.5	7	2	14	28
47.5-49.4	48.5	4	3	12	36
49.5-51.4	50.5	5	4	20	80
51.5-53.4	52.5	2	5	10	50
53.5-55.4	54.5	1	6	6	36
55.5-57.4	56.5	2	7	14	98
57.5-59.4	58.5	1	8	8	64
Totals		100		-187	1220
				93	
				-94	

Correction to arbitrary mean, c (in class interval units) = $\frac{-94}{100} = -0.94$.

Correction to arbitrary mean (°F) = -1.88 .

Mean = $42.5 - 1.88 = 40.62^\circ \text{F}$.

s^2 (in class interval units) = $\frac{\Sigma fd'^2}{N} = \frac{1220}{100} = 12.20$.

σ^2 (in class interval units) = $s^2 - c^2 = 12.20 - 0.88 = 11.32$.

σ (in class interval units) = 3.36 .

σ (°F) = 6.72 .

* Richmond W. Longley, "The Frequency Distribution through the Year of Abnormally High and Low Daily Mean Temperatures at Toronto," *J. Roy. Astron. Soc. Can.*, **36**, 225-236 (1942).

series are found in the rainfall of some regions of the earth where rainfall is infrequent, but very heavy showers occur at irregular intervals. The mean annual rainfall, in such a region, would not give as correct an impression of the lack of rain as would the median value for the series. In general, though, the median is not used to any great extent in the field of meteorology, partly because of the difficulty of computation, and partly because the mean is more suitable in most meteorological series.

The most commonly used average is the *arithmetic mean*. It is defined as the sum of the values of the variable x divided by the number of observations, N . The arithmetic mean is expressed by the equation

$$M_x = \frac{x_1 + x_2 + \cdots + x_N}{N}$$

or

$$M_x = \frac{\Sigma x}{N} \quad (57.1)$$

where M_x is the arithmetic mean of the variable x , and Σ represents the process of summation.

With ungrouped data, the computation of the mean is done by adding the individual items and dividing by the number of items. Since in some series the number of items is large, this would become burdensome and, to avoid the excessive labor involved, the items are frequently grouped in classes according to their respective values. Thus the mean temperatures for Toronto for the different April 13th's were grouped in classes, which are given in the table. When this is done, the assumption is made that every item in an interval has the value of the midpoint of the interval. Thus it is assumed, referring to the table, that there were 2 days, mean temperature 26.5° F, 4 with mean temperature of 28.5° F, etc. To compute the mean, then, it is necessary only to multiply each midvalue by the number of times that that value was supposed to occur, add the products, and divide by the number of items. In terms of the figures given in the table, this would be represented as

$$M = \frac{(2 \times 26.5) + (4 \times 28.5) + (4 \times 30.5) + (3 \times 32.5) + \cdots + \text{etc.}}{100}$$

One method of avoiding the necessity for lengthy computations in the determination of the mean is by the use of an assumed mean, M' . The assumed mean is then subtracted from each value of the series,

resulting in a series of values of $(x - M')$. The algebraic average, c , of these is taken

$$c = \frac{\Sigma(x - M')}{N} = \frac{x_1 - M' + x_2 - M' + \cdots + x_N - M'}{N} \quad (57.2)$$

$$= \frac{\Sigma x}{N} - M' = M - M'$$

or

$$M = c + M' \quad (57.3)$$

Thus the arithmetic mean is obtained by adding the mean of the deviations to the assumed mean. An immediate corollary to this theorem is that the sum of the deviations from the real mean is zero.

A second method of avoiding excessive computation with grouped data involves the use of the class interval as a unit and then returning to the original units after the computation is finished. In the computation of the table, the assumed mean is taken as 42.5° F. The column headed d' gives the difference in class intervals of each class from the assumed mean, with negative signs for those less than the assumed mean. There are, then, 2 occurrences -8 class intervals from the assumed mean, 4 which are -7 class intervals away, etc. By multiplying these to give the figures in the column headed fd' and adding, it is found that the total is -94 class intervals. The mean of these values then, $-94/100 = -0.94$ class intervals. The mean according to (57.3) is -0.94 class intervals when the origin is at the assumed mean, or 1.88° F below the assumed mean of 42.5°. The mean of the distribution is, then,

$$42.5 - 1.88 = 40.62^\circ \text{ F}$$

The value of the mean, 40.62° F, gives a typical figure for the whole distribution, and it is frequently used as such. Its advantages over other measures of central tendency arise from, first, the ease with which its significance is understood, second, the simplicity with which it may be computed, and third, the possibility that it can be manipulated algebraically. Also it is affected by the value of every term of the series, but this is sometimes a disadvantage when an extreme value changes the mean by an unduly large amount.

In meteorology, as in other sciences, the mean is used extensively to typify a distribution. In climatological tables values are given for the mean monthly temperature, the mean annual rainfall, etc. Mean

pressures are given on mean pressure maps. Mean winds are given, too, on climatological maps. Here, though, the direction must be considered, and the mean wind is a vectorial average rather than a numerical average. For some series the mean is not completely satisfactory. Such a series is that representing the cloudiness over a station. The mean cloudiness may be computed as 0.6. This, though, could be an average of a series in which most of the observations are either overcast or clear. Thus the statement that the mean cloudiness is 0.6 says nothing about the probable weather at any time during the series. In that respect it is different from the mean value of 40.62°F for the series of temperatures, since most of the observations of temperature lie near the central part of the distribution, and so the mean gives a reasonable probable value for a member of the series. In a series such as cloudiness the mean is not a typical value, and when a mean of the series is given, it must be interpreted with that understanding.

58. Measures of Variability. Standard Deviation. A measure of central tendency, either the mean, the median, or the mode, represents one feature of the series of observations. The purpose of each is to represent a value around which, to a greater or less degree, the series is grouped. But they by no means completely typify a series. For example, the mean of the numbers 3, 5, 6, and 6 is 5. But 5 is also the mean of the four numbers 11, 5, 2, and 2. Yet in one case the numbers are grouped closely about the mean, and in the other the mean is close to only one of the individual figures of the series. In order to represent this difference between various series, some method of determining the spread of the series is desirable.

A graphical method for showing the variation in the wind direction and force is the *wind rose*, two of which are depicted in Fig. 53. Diagram (a) is for a place in the region of west-

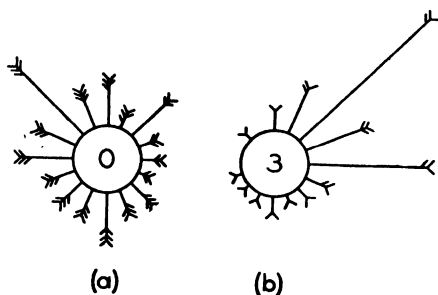


FIG. 53. Wind roses: (a) at 42.5°N , 47.5°W ; (b) at 7.5°N , 22.5°W .

erlies off the east coast of Newfoundland, and diagram (b) is for a region in the northeast trade wind belt off the west coast of Africa. The length of the line drawn in any direction is proportional to the frequency of the wind from that direction, while the number of feathers on the wind arrow indicates the average force of wind in the Beaufort scale, given in section 66, in that direction. The percentage of calms is entered inside the circle. Thus the extent to which the wind at a given place tends to blow in one direc-

tion, or to vary its direction, may be seen by an inspection of the wind rose.

Three numerical measures of the variability of a series are the range, the mean deviation, and the standard deviation. The *range* is merely the difference between the largest and the smallest value of the series. Thus it is easily understood, but has little real meaning. The statement of the maximum and minimum temperatures is one of the ways in which the range is used in meteorology and climatology. But it is quite possible to postulate a temperature variation for a day, such as might occur if a sharp cold front (section 38) passed the station shortly before midnight, in which the range failed to express satisfactorily the variation that occurred.

Another measure of the variability is the *mean deviation*. To obtain this, the difference between the mean and each of the observations of the series is taken. The mean of these differences is then calculated, the signs of the terms being disregarded. In this manner, a representative figure for the variation of the individual items from the mean value is obtained. The mean deviations of the two series in the first paragraph of the section are 1 and 3, respectively.

A more satisfactory measure of the variation from the mathematical point of view is the standard deviation. To obtain this, the differences are taken, as in the mean deviation, and then squared. The mean of these squared differences is found, and the square root of this mean is taken. Expressed in the form of an equation, the *standard deviation*

$$\sigma = \sqrt{\frac{\Sigma(x - M)^2}{N}} \quad (58.1)$$

By squaring the differences, the algebraic inconsistency of ignoring the signs, as is done with the mean deviation, is eliminated.

Of the two deviations, the standard deviation is used more frequently. However, the squaring of the differences allows a term of the series which is extreme in its value to influence the value of σ to a disproportionate degree. For that reason, the mean deviation is used at times for series in which an occasional extreme is likely to occur. Such a series is that giving the amount of annual rainfall at a station. So in computing the variability of rainfall, the mean deviation is used instead of the standard deviation.

In order to develop a formula with which to compute σ , square (58.1) to give

$$\begin{aligned} \sigma^2 &= \frac{\Sigma(x^2 - 2Mx + M^2)}{N} \\ &= \frac{\Sigma x^2}{N} - 2M \frac{\Sigma x}{N} + \frac{NM^2}{N} \end{aligned}$$

From (57.1), it follows that

$$\begin{aligned}\sigma^2 &= \frac{\Sigma x^2}{N} - 2M^2 + M^2 \\ &= \frac{\Sigma x^2}{N} - M^2\end{aligned}\quad (58.2)$$

Thus the standard deviation may be computed by squaring, not the deviations, but the original values, finding the mean of these, subtracting the square of the mean of the series, and then taking the square root. Thus in the series 11, 5, 2, and 2, given in the first paragraph of this section, the value of σ is found to be

$$\sigma = \sqrt{\frac{121 + 25 + 4 + 4}{4} - (5)^2} = \sqrt{\frac{154}{4} - 25} = \sqrt{13.5} = 3.7$$

As with the mean, the computation of the standard deviation is simplified by the use of an assumed mean, M' .

$$\begin{aligned}\sigma^2 &= \frac{\Sigma(x - M)^2}{N} \\ &= \frac{\Sigma[(x - M') + (M' - M)]^2}{N} \\ &= \frac{\Sigma(x - M')^2}{N} + 2(M' - M) \frac{\Sigma(x - M')}{N} + \frac{N(M' - M)^2}{N}\end{aligned}$$

But from (57.2)

$$\frac{\Sigma(x - M')}{N} = M - M'$$

Hence

$$\begin{aligned}\sigma^2 &= \frac{\Sigma(x - M')^2}{N} - 2(M' - M)^2 + (M' - M)^2 \\ &= \frac{\Sigma(x - M')^2}{N} - c^2\end{aligned}\quad (58.3)$$

The first term is the mean of the squares of the deviations from the assumed mean. From this is subtracted the square of the deviation of the real mean from the assumed mean. The square root of the difference is then taken. By transposition in (58.3)

$$\frac{\Sigma(x - M')^2}{N} = \sigma^2 + c^2$$

Hence the minimum value of $\frac{\sum(x - M')^2}{N}$ is found when $c = 0$, or the mean of the squared deviations is a minimum when the deviations are taken from the true mean.

The use of class interval units when the data are grouped is an aid in the computation of σ . Class interval units are used in the computation of σ for the distribution of the table of section 57. Column 6 gives the squares of the deviations, in class interval units, times the number of observations having that squared deviation, i.e., fd'^2 . The mean of these squared deviations, indicated by s^2 , is found by dividing the sum, 1220, by the number of observations, 100, giving 12.20. In addition, $c^2 = 0.88$. Hence, from (58.3)

$$\sigma^2 = 12.20 - 0.88 = 11.32$$

Therefore

$$\sigma \text{ (in class interval units)} = 3.36$$

Now returning to the original units, since the class interval is 2° F , it follows that

$$\sigma = 6.72^\circ \text{ F}$$

The meaning of this figure, 6.72° F , may be seen by comparing it with similar figures for other times in the year. Thus the standard deviation for the January 13 temperatures for Toronto for the same period is 10.07° F and for August 13 it is 4.99° F . Thus the mean temperatures in the middle of winter varied more from year to year than those in spring, while the mean temperatures in the middle of summer were the most uniform.

59. The Theory of Errors. The value of 40.62° F has been found for the mean of the mean temperatures for April 13, for Toronto. By using the average increase of the monthly mean temperatures from March to May it is found that at Toronto during April the mean daily temperature increases at the rate of 0.38° F per day. It seems reasonable to expect, then, that the mean temperature for April 14 would be $40.62 + 0.38$; for April 15, $40.62 + 2 \times 0.38$, etc. Calculation shows that these results are approximately correct, but the computed means show minor variations from the value that the hypothesis would indicate.

The causes of the irregularities found in the broad uniform trend in temperature are the factors other than the increasing amount of insolation received each day that contribute to the daily temperature. In any one year there are periods during which the temperature is below

normal, followed by periods with the temperature above normal. The variations are closely associated with the passage of cyclones and anticyclones. Yet there is no tendency for cold spells to recur at the same part of the month each year. Hence the variation from the normal rise in temperature is attributed to "chance," that is, to the sum total of a large number of causes, no one of which is predominant.

If the mean temperatures were taken for a long series of years, the effect of these chance factors would cancel out for any particular day. The computed mean would be the true mean for that day. For shorter periods the chance variations give a value for the computed mean which is not quite large enough in some instances, and too large in others. For example, it is possible that the April 13th's for the period 1841 to 1940 had more days colder than normal than would be expected if all April 13th's were considered, making the computed mean value of 40.62° F too small. How nearly correct can one assume this value to be?

If a large number of values for some variable x exists, take for consideration a fraction of these values. Choose the individual values entirely at random, that is, in such a manner that every value has an equal chance of being selected, and so that the choice of any one value has no influence on the choice of any other. The selection of five cards from a well-shuffled pack would be a random sample. If the means of sample after sample of the original series are found, these means will be grouped about the true mean in a standard pattern. For example, the true mean value of a pack of 52 cards is

$$\frac{4(1 + 2 + \cdots + 12 + 13)}{52} = 7$$

As the number of sample means increases, the distribution of mean values approaches more and more closely the mathematical curve given by the equation,

$$y = \frac{N'}{\sigma\sqrt{2\pi}} e^{-\frac{x^2}{2\sigma^2}} \quad (59.1)$$

where N' represents the number of samples, e is the base of the Napierian logarithms, and σ is a constant, the standard deviation of the distribution. The ordinate y gives the frequency of occurrence of a deviation x from the true mean. Thus the frequency of occurrence of a sample of mean value 5 or 9 from the pack is

$$\frac{50}{\sigma\sqrt{2\pi}} e^{-\frac{2}{\sigma^2}}$$

if there have been 50 sample selections made from the pack.

This curve is frequently called the *normal curve of error* or the *probability curve*. A graph of it is given in Fig. 54. The normal curve of error enters frequently in the field of statistics. For that reason it has been the basis for much study by students in this subject. For a complete discussion of the properties of the curve, reference should be made to any standard text in that field.

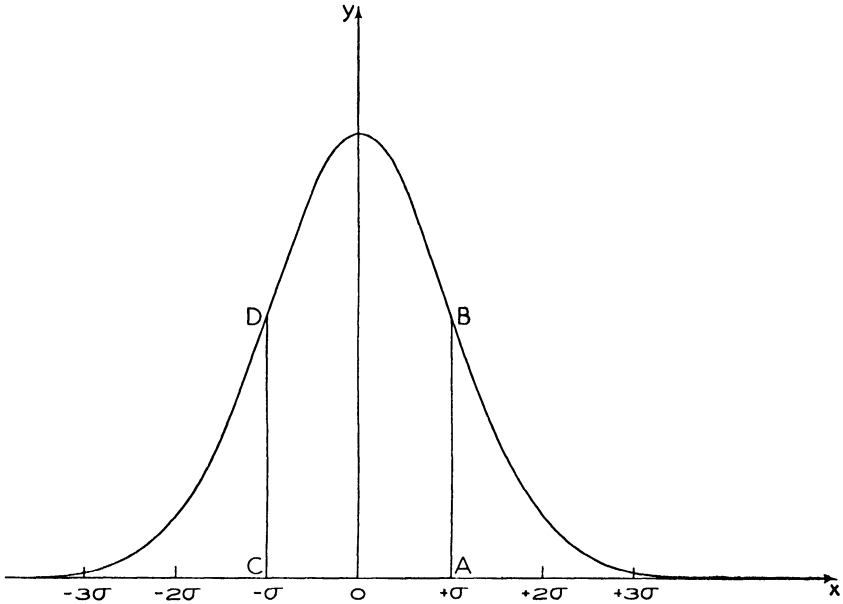


FIG. 54. The normal curve of error.

The following considerations show why this curve is known as the probability curve. If N possibilities are all equally likely, and if y of these N realize the event A , the probability p_A of the event A occurring is defined statistically as

$$p_A = \frac{y}{N}$$

Thus if a die is absolutely homogeneous, the probability of 4 dots, for example, turning up is $\frac{1}{6}$. In other words

$$p_4 = \frac{1}{6}$$

Thus, since as indicated above, y in (59.1) represents the frequency of occurrence of a deviation x from the true mean, it follows that the probability of a deviation x is given by

$$p_x = \frac{1}{\sigma\sqrt{2\pi}} e^{-\frac{x^2}{2\sigma^2}}$$

Since the distribution of means is given by a form of the normal curve of error, a computed mean can be expected to lie close to the true mean. The total area under the curve (59.1) is found to be N' . If N' , then, is taken as equal to 1, the proportion A of the total area which lies within the limits of $-x$ and $+x$ is given by

$$A = \frac{1}{\sigma\sqrt{2\pi}} \int_{-x}^x e^{-\frac{x^2}{2\sigma^2}} dx = \frac{\sqrt{2}}{\sigma\sqrt{\pi}} \int_0^x e^{-\frac{x^2}{2\sigma^2}} dx \quad (59.2)$$

This gives the probability that an observed value lies within x of the true value, provided that σ is known. Values of A in units of x/σ are given in statistical tables.

One important value of this function (59.2) is found when $x = \sigma$. Then

$$A = 0.6827$$

Thus the probability of an occurrence lying within σ of the true value is about $\frac{2}{3}$. For limits of 2σ , the probability is about $\frac{19}{20}$, and for 3σ , about $\frac{99}{100}$. The ordinates at $x = \pm\sigma$ are indicated by the lines AB and CD in Fig. 54.

In order to apply this discussion to the problem, it is necessary to know the standard deviations of the distribution. By statistical theory, it can be shown that

$$\sigma_M = \frac{\sigma}{\sqrt{N}} \quad (59.3)$$

where σ_M is the standard deviation of the frequency distribution of the means, σ the standard deviation of the total distribution from which the sample is taken, and N the number of observations in the sample. This value is sometimes called the *standard error* of the mean. For example, if it is assumed that the value of σ for the distribution of temperatures for all April 13th's is the same as the value of σ of the 100-yr sample studied, then

$$\sigma_M = \frac{6.72}{\sqrt{100}} = 0.67$$

Thus the computed mean of 40.62° F has a probability of $\frac{2}{3}$ of lying within 0.67° F on one side or the other of the true mean, a probability of $\frac{19}{20}$ of lying within $2 \times 0.67^\circ$ F of the true mean, and almost complete assurance of lying within $3 \times 0.67^\circ$ F of the true mean.

Consider the means for all the days in April. The true mean values for the daily temperatures of April should lie on a smooth curve, in-

creasing from the first till the end of the month. Of the thirty computed means, about twenty of them should lie within a value of 0.67° F of the smooth curve, and only one or two should lie farther than 1.34° F from this curve. Thus a line through the computed means will have irregularities, with the magnitude of these variations depending on the value of σ_M . To indicate that the value of a statistical magnitude is not uniform for all similar series, and to indicate the amount of variation expected in such series, the value of the standard error of the magnitude is included with the magnitude by the use of the sign \pm . The range thus indicated should, in two-thirds of the computations, include the true value of the magnitude. Thus the mean temperature for April 13 is $40.62 \pm 0.67^{\circ}$ F.

The accuracy of a measure is sometimes given in terms of a quantity which is 0.6745 times the standard error. This is called the *probable error*. Ordinates at $\pm 0.6745\sigma$ from the origin cut off one-half the area under the probability curve. Hence deviations from the mean greater than and less than the probable error are equally probable, thus explaining the name. Since practice in this respect is not uniform, care should be taken to ascertain which of the two, the standard error or the probable error, is being used.

The same considerations hold for σ as for M . The standard deviation of the frequency distribution of different values of σ is

$$\sigma_{\sigma} = \frac{\sigma}{\sqrt{2N}}$$

For the distribution in the table of section 57,

$$\sigma_{\sigma} = \frac{6.72}{\sqrt{200}} = 0.48$$

Hence

$$\sigma = 6.72 \pm 0.48^{\circ} \text{ F}$$

Further discussion of the standard errors of statistical magnitudes and their use other than to indicate the relative accuracy of the magnitude can be found in the standard texts on statistics. In meteorology and climatology, some observations have been made for a short period only. Reliance may be placed on means, etc., from such series, provided the computed values are approximately equal to the true values. The degree to which this is true can be learned from the standard errors. The standard errors are sometimes included in meteorological statistics but an even more extensive use of these would be helpful in interpreting the data.

60. Method of Least Squares. Column 1 of the table on page 175 gives a series of 25 values of the magnitude of the decrease with height of the wet-bulb potential temperature, θ_w , indicated by X , in the warm sectors of depressions over western Europe. (For a description of the

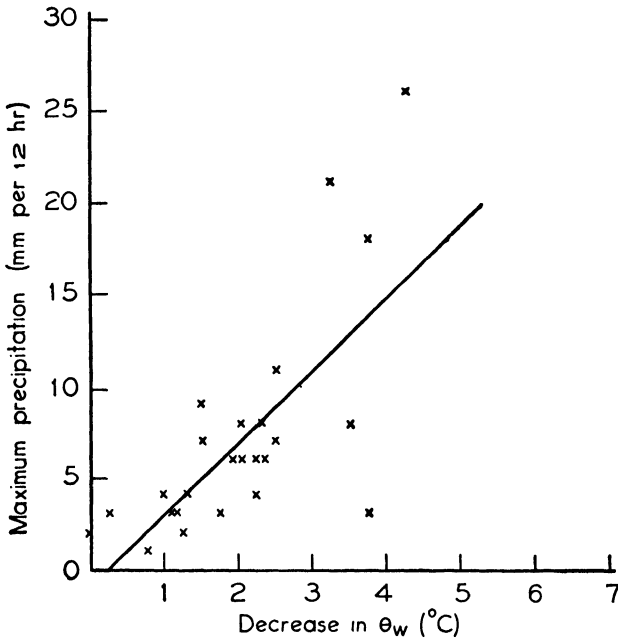


FIG. 55. The relation between decrease in θ_w with height and maximum rainfall.

warm sector of a depression see section 111.) Associated with each observation there is given in column 3 the maximum rainfall in millimeters per 12 h that occurred at any of the stations along the trajectory of the air during the 24-h period following the upper air sounding. Fig. 55 gives the same data plotted with the decrease of θ_w , X , as the abscissa, and the rainfall, R , as the ordinate.

Even a casual glance at the figures or the plotted points reveals that there is a tendency for large values of one to be associated with large values of the other and similarly for small values. It is desirable to express more exactly the relationship which exists between these two quantities. This may be done geometrically by drawing a straight line which best represents the relationship. The definition of a *line of best fit* could be given in several ways. It is usually defined in such a manner that the relation of the points to the line is the same as that of the individual observations of a series to the mean of the series. In

THE RELATIONSHIP BETWEEN THE DECREASE IN WET-BULB
POTENTIAL TEMPERATURE WITH HEIGHT AND SUBSEQUENT PRECIPITATION*

(1)	(2)	(3)	(4)	(5)	(6)
Decrease in θ_w ($^{\circ}\text{C}$) X	Decrease (Unit $\frac{1}{4}^{\circ}\text{C}$) x	Maximum rainfall (mm per 12 h) R	x^2	R^2	xR
0.75	3	1	9	1	3
1.5	6	9	36	81	54
2.0	8	6	64	36	48
1.0	4	3	16	9	12
2.25	9	8	81	64	72
1.0	4	4	16	16	16
2.0	8	6	64	36	48
1.25	5	2	25	4	10
3.25	13	21	169	441	273
2.25	9	6	81	36	54
2.25	9	4	81	16	36
1.75	7	3	49	9	21
0.0	0	2	0	4	0
3.5	14	8	196	64	112
1.0	4	3	16	9	12
3.75	15	3	225	9	45
2.0	8	8	64	64	64
3.75	15	18	225	324	270
2.5	10	11	100	121	110
4.25	17	26	289	676	442
2.25	9	6	81	36	54
0.25	1	3	1	9	3
1.5	6	7	36	49	42
1.25	5	4	25	16	20
2.5	10	7	100	49	70
	199	179	2049	2179	1891

$$179 = 25a + 199b$$

$$1891 = 199a + 2049b$$

$$a = -0.83 \quad b = 1.01$$

$$y = -0.83 + 1.01x$$

$$= -0.83 + 4.04X$$

other words, the best fitting line is the line such that the sum of the squares of the distances from the points to the line is a minimum.

Let a number N of paired values of variables $X_1Y_1, X_2Y_2, X_3Y_3, \dots, X_NY_N$ be given. It is desired to determine the best fitting straight line,

$$y = a + bX \quad (60.1)$$

for the values, where y indicates the ordinate of a point on the line.

* Data from E. W. Hewson, "Rainfall in Depressions," *Q. J. Roy. Met. Soc.*, **63**, 323-335 (1937).

For each value X there is a corresponding value of y on the straight line. By definition, the sum of all the values $(Y - y)^2$ is a minimum. If the value of y from equation 60.1 is used, it follows that there are N terms of the form

$$(Y_i - a - bX_i)^2 = Y_i^2 + a^2 + b^2X_i^2 - 2aY_i - 2bX_iY_i + 2abX_i \quad (i = 1 \dots N)$$

The sum is given by the expression

$$F(X, Y, a, b) = \Sigma Y_i^2 + Na^2 + b^2 \Sigma X_i^2 - 2a \Sigma Y_i - 2b \Sigma X_i Y_i + 2ab \Sigma X_i$$

The values of a and b are to be chosen such that this sum is a minimum. To satisfy this condition, the equations

$$\begin{aligned} \frac{\partial F}{\partial a} &= 0 \\ \frac{\partial F}{\partial b} &= 0 \end{aligned}$$

must be satisfied. Or,

$$\begin{aligned} 2Na - 2\Sigma Y_i + 2b\Sigma X_i &= 0 \\ 2b\Sigma X_i^2 - 2\Sigma X_i Y_i + 2a\Sigma X_i &= 0 \end{aligned}$$

Transposing

$$\begin{aligned} \Sigma Y_i &= Na + b\Sigma X_i \\ \Sigma X_i Y_i &= a\Sigma X_i + b\Sigma X_i^2 \end{aligned} \quad (60.2)$$

These equations are called the *normal equations*. By solving these for a and b , values are found which, substituted in the equation 60.1, give the best fitting line for the paired values (X, Y) .

In the table column 2 gives the values of X multiplied by 4, called x , to simplify the computations. Columns 4 and 6 are computed to aid in the determination of the line of least squares. Using the totals given in the table, the normal equations become

$$\begin{aligned} 179 &= 25a + 199b \\ 1891 &= 199a + 2049b \end{aligned}$$

By solving these,

$$a = -0.83 \quad b = 1.01$$

The equation of the line is

$$R = -0.83 + 1.01x$$

Since x is in quarter degrees, this becomes

$$R = -0.83 + 4.04X$$

This equation is plotted on Fig. 55. A glance at the figure shows that the line follows the distribution of points fairly well.

The line of least squares, or the *regression line* as it is sometimes called, can be used to obtain the approximate relationship between any paired numbers. One use of it in economics, and to a lesser degree in meteorology, is to determine the line of best fit of a time series. By this line a rate of increase can be determined, and by projecting into the future, this rate can be used for the prediction of future values. This is done on the assumption that the trend will continue in the future as in the past, an assumption which must be checked by a study of conditions, not by statistics.

61. Correlation. The straight line fitted to the data in section 60 is the best fitting line. Yet even the best fitting line may not be particularly good. Some measure of the closeness with which the line fits the data should be obtained to indicate *goodness of fit*.

Such a measure of the goodness of fit was derived by Karl Pearson, and is called the coefficient of correlation. Consider the same series of paired variables X_1Y_1, \dots, X_NY_N as was used in section 60. The standard deviation σ_Y of the dependent variable Y is a measure of the variability of Y from its mean. A similar measure can be obtained by considering the distances from the points to the straight line. Take the deviation for each observation of the variable Y_i from the line of best fit, square, add, and take the square root of the sum. The measure thus obtained, S_Y , indicates the variability about the straight line, $y = a + bX$, given in (60.1). If the line were through the mean M_Y of the series and parallel to the x axis, the deviations from the line would equal the deviations from the mean and $S_Y = \sigma_Y$. This would indicate the absence of any relationship between X and Y . Thus σ_Y would be the maximum value of S_Y . The line, though, was computed so that S_Y is a minimum, so generally $S_Y < \sigma_Y$. A comparison of S_Y and σ_Y gives a measure of the goodness of fit of the line.

The formula developed by Pearson is

$$r = \pm \sqrt{1 - \frac{S_Y^2}{\sigma_Y^2}} \quad (61.1)$$

where r is the *coefficient of correlation*. The sign used is the same as that for b , the slope of the regression line.

A study of this formula brings out some significant facts concerning r .

If the data fit perfectly along the line, $S_Y = 0$, and so $r = \pm 1$. This would be the maximum value for r . On the other hand, S_Y has for its maximum value that of σ_Y , so the minimum value of $r = 0$. Thus a value for r near 0 means that there is little relationship between the two variables. On the other hand, a value of r greater than 0.80 or less than -0.80 indicates that in general there is a close relationship between the variables. Since the sign corresponds with that of the slope of the regression line, a positive value for r indicates that large values of one variable are associated with large values of the other, while a negative value for r indicates that the two quantities vary in an opposite sense.

A value of r which might be considered satisfactory varies in the different fields in which statistics is applied because of the control which may be exercised over variables that might cause changes in the dependent variable under consideration. Experiments in physics keep constant as many factors as possible in order that some particular relationship may be studied. The correlation, then, should be high. In other fields the variables are less subject to control, and so smaller values of r may indicate a probable common variability. The following values of correlation coefficients were obtained by W. H. Dines* for different pairs of meteorological variables.

Pressure at mean sea level and surface temperature	$r =$ 0.16
Pressure at mean sea level and at 9 km	$r =$ 0.68
Temperature at 4 km and pressure at 9 km	$r =$ 0.82
Height of tropopause and temperature of tropopause	$r =$ -0.68
Height of tropopause and surface temperature	$r =$ 0.30

The determination of the correlation coefficient can be made from one of several formulas which have been developed. If the regression line (60.1) has been determined, the value of r can be obtained by the formula

$$r = \frac{\sigma_X}{\sigma_Y} b \quad (61.2)$$

Other formulas that are useful at different times are

$$r = \frac{\Sigma XY - NM_X M_Y}{N \sigma_X \sigma_Y} \quad (61.3)$$

and

$$r^2 = \frac{a \Sigma Y + b \Sigma XY - NM_Y^2}{\Sigma Y^2 - NM_Y^2} \quad (61.4)$$

where M_X , M_Y indicate the mean values for X and Y .

* W. H. Dines, *M. O. Geophys. Mem.*, Nos. 2 and 13.

Using the data of the table given in section 60, and substituting in (61.3),

$$M_R = \frac{179}{25} = 7.16 \text{ mm}$$

$$\sigma_R = \sqrt{\frac{2179}{25} - (7.16)^2} = 5.99 \text{ mm}$$

$$M_x = \frac{199}{25} = 7.96 \text{ quarter degrees C}$$

$$\sigma_x = \sqrt{\frac{2049}{25} - (7.96)^2} = 4.31 \text{ quarter degrees C}$$

it follows that

$$r = \frac{1891 - 25 \times 7.96 \times 7.16}{25 \times 5.99 \times 4.31} = 0.72^*$$

Since r is a dimensionless number, its value will be independent of the units used in its determination, provided that the latter are used consistently throughout.

The standard error for r

$$\begin{aligned} \sigma_r &= \frac{1 - r^2}{\sqrt{N}} \\ &= \pm 0.096 \end{aligned} \tag{61.5}$$

or

$$r = +0.72 \pm 0.096$$

The value of r for the 147 items from which this group of 25 was chosen was 0.78, which is within the range of the standard error of the computed value for r . The value of 0.78 indicates that there is a definite and reliable relationship between the decrease in wet-bulb potential temperature with height and the rainfall during the succeeding 24 h below the warm frontal surface.

62. Harmonic Analysis. Section 60 treated the problem of fitting a straight line to a set of points, on the assumption that the relationship between the sets of values could best be represented by a straight line. It is possible to extend the method in order to fit a polynomial of a higher degree to fit the data. Thus the best fitting parabola

$$y = a + bx + cx^2$$

* A shorter method for computing r is given in the Appendix.

may be determined, or the cubic equation may be used. These are seldom used in meteorology, although other branches of science find value in fitting non-linear functions to the data.

There is, though, in meteorology a large number of variables which have periodic fluctuations. Some of these, such as temperature and precipitation, are related to the seasons, thus showing an annual variation. Others, such as temperature, dew point, and pressure, have a

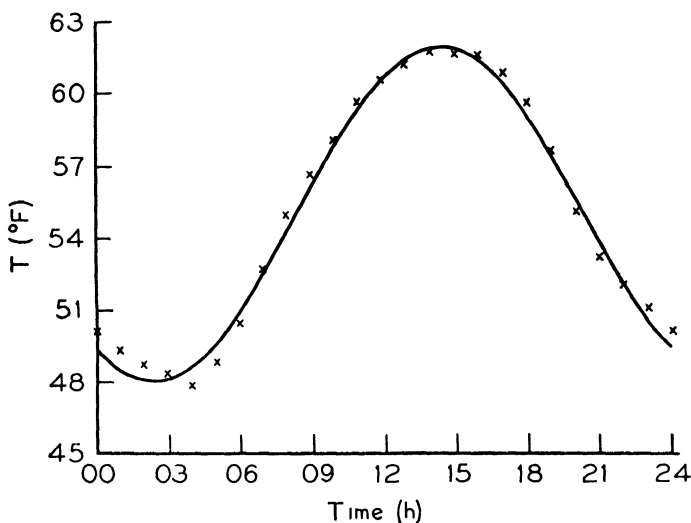


FIG. 56. Mean hourly temperatures for June at Leafield, England. (After Johnson and Heywood.)

daily period. Fitting a curve to such data requires the use of the trigonometric functions. The figures in column 2 of the accompanying table give the values for the temperatures at a height of 1.2 m averaged for each hour of the day for June for a period of five years at Leafield, England.* They are plotted in Fig. 56.

If t represents the time in hours after midnight and T the mean temperature at time t , then the relationship between T and t can be best represented by the cosine function,

$$T = T_0 + a \cos \left(\frac{\pi}{12} t - \phi \right)$$

or a similar sine function. With this function, the amplitude of the

* Data from N. K. Johnson and G. S. P. Heywood, "An Investigation of the Lapse Rate of Temperature in the Lowest Hundred Meters of the Atmosphere," *M. O. Geophys. Mem.*, No. 77, 1938.

THE EVALUATION OF FOURIER COEFFICIENTS

(1)	(2)	(3)	(4)
Hour t	Mean June Temperature T (°F)	$\cos \frac{\pi}{12} t$	$\sin \frac{\pi}{12} t$
24	50.1	1.000	0.000
01	49.3	0.996	0.259
02	48.7	0.866	0.500
03	48.3	0.707	0.707
04	47.8	0.500	0.866
05	48.8	0.259	0.966
06	50.4	0.000	1.000
07	52.7	-0.259	0.966
08	54.9	-0.500	0.866
09	56.6	-0.707	0.707
10	58.0	-0.866	0.500
11	59.6	-0.966	0.259
12	60.5	-1.000	0.000
13	61.4	-0.966	-0.259
14	61.7	-0.866	-0.500
15	61.6	-0.707	-0.707
16	61.5	-0.500	-0.866
17	60.8	-0.259	-0.966
18	59.6	0.000	-1.000
19	57.6	0.259	-0.966
20	55.1	0.500	-0.866
21	53.2	0.707	-0.707
22	52.0	0.866	-0.500
23	51.1	0.966	-0.259
<hr/>			
1321.3			

$$24A_0 = 1321.3 \quad A_0 = 55.05$$

$$12A_1 = -10.4 (1.000) - 20.6 (0.966) - 19.0 (0.866) - 16.7 (0.707) \\ - 13.5 (0.500) - 7.1 (0.259)$$

$$= -67.15$$

$$A_1 = -5.60$$

$$12B_1 = -3.6 (0.259) - 7.0 (0.500) - 9.9 (0.707) - 13.9 (0.866) - 16.9 (0.966) \\ - 9.2 (1.000)$$

$$= -48.99$$

$$B_1 = -4.08$$

$$T = 55.05 - 5.60 \cos \frac{\pi}{12} t - 4.08 \sin \frac{\pi}{12} t$$

variation in T is given by a . As t increases from 0 to 24 h, T passes through a complete cycle, returning to its original value when $t = 24$. ϕ is the angle of lag for the cycle. Expanding the expression above,

$$\begin{aligned} T &= T_0 + a \cos \phi \cos \frac{\pi}{12} t + a \sin \phi \sin \frac{\pi}{12} t \\ &= T_0 + A_1 \cos \frac{\pi}{12} t + B_1 \sin \frac{\pi}{12} t \end{aligned} \quad (62.1)$$

where

$$A_1 = a \cos \phi \quad B_1 = a \sin \phi$$

In this form, the expression gives three terms of the Fourier series

$$\begin{aligned} T &= A_0 + A_1 \cos \theta + A_2 \cos 2\theta + A_3 \cos 3\theta + \dots \\ &\quad + B_1 \sin \theta + B_2 \sin 2\theta + B_3 \sin 3\theta + \dots \end{aligned}$$

where $\theta = \frac{\pi}{12} t$, and $A_0 = T_0$.

Fourier's theorem states that, if T is a function of θ which is finite and has only a limited number of maxima and minima and of finite discontinuities within the range $0 < \theta < 2\pi$, then the function may be represented by the series, except at the points where the function is discontinuous. The constants are evaluated by the formulas

$$\begin{aligned} A_0 &= \frac{1}{2\pi} \int_0^{2\pi} T \, d\theta \quad \text{or} \quad \frac{\Delta\theta}{2\pi} \Sigma T \\ A_i &= \frac{1}{\pi} \int_0^{2\pi} T \cos i\theta \, d\theta \quad \text{or} \quad \frac{\Delta\theta}{\pi} \Sigma T \cos i\theta \\ B_i &= \frac{1}{\pi} \int_0^{2\pi} T \sin i\theta \, d\theta \quad \text{or} \quad \frac{\Delta\theta}{\pi} \Sigma T \sin i\theta \end{aligned} \quad (62.2)$$

The first form is used in the case where T is a continuous function. A complete evaluation of the constants permits any function to be fitted perfectly by the series. If, however, the series is evaluated only for an equal number, m , of sine and cosine terms, then the least squares solution for the periodic curve with $2m + 1$ constants is obtained. In the problem under discussion, the equation desired has three constants, T_0 , A_1 , B_1 , and one cosine and one sine term, according to (62.1).

The intervals are 1 h, and so $\Delta\theta = \pi/12$. Furthermore, $t = 0$ at 24 h.

Then from (62.2)

$$\begin{aligned}T_0 &= A_0 = \frac{1}{24} \sum_1^{24} T \\A_1 &= \frac{1}{12} \sum_1^{24} T \cos \frac{\pi}{12} t \\B_1 &= \frac{1}{12} \sum_1^{24} T \sin \frac{\pi}{12} t\end{aligned}$$

In the accompanying table, columns 3 and 4 give the values of the cosine and sine functions by which the values of T must be multiplied. Since, in this instance, the number of intervals is a multiple of 4, there is a repetition of certain numbers in these columns, with changes in sign. Here the amount of calculation is reduced by adding and subtracting the appropriate values of T before multiplication. When this is done, the following values are obtained.

$$\begin{aligned}T_0 &= \frac{1}{24} \times 1321.3 = 55.05 \\A_1 &= \frac{1}{12} \times (-67.15) = -5.60 \\B_1 &= \frac{1}{12} \times (-48.99) = -4.08\end{aligned}$$

The best fitting curve has the equation

$$T = 55.05 - 5.60 \cos \frac{\pi}{12} t - 4.08 \sin \frac{\pi}{12} t$$

This curve is plotted with the given data in Fig. 56.

By fitting a sine curve to a set of data in the above manner, significant facts about the variation of any meteorological element may be determined to aid in understanding the periodicities in the atmosphere. The amplitude of a sine curve which best fits the observed diurnal temperature variation, along with the amplitude obtained in a similar manner at a greater height (see problem 3 of this chapter) may be used in the manner outlined in section 55 to compute the value of the coefficient of eddy diffusivity.

PROBLEMS AND EXERCISES

1. The distribution of the annual precipitation for the period 1886-1938 for the states of New York and North Dakota is given in the following table.* Compute the means and standard deviations for the two distributions.

* Data from *Climate and Man*, 1941 Yearbook of Agriculture, U. S. Department of Agriculture, Washington, D. C.

NEW YORK		NORTH DAKOTA	
Amount of Precipitation (in.)	Number of Occurrences	Amount of Precipitation (in.)	Number of Occurrences
31.00-32.99	1	7.00- 8.99	1
33.00-34.99	3	9.00-10.99	2
35.00-36.99	7	11.00-12.99	2
37.00-38.99	15	13.00-14.99	6
39.00-40.99	12	15.00-16.99	11
41.00-42.99	6	17.00-18.99	18
43.00-44.99	6	19.00-20.99	11
45.00-46.99	1	21.00-22.99	2
47.00-48.99	1		
49.00-50.99	1		
Total	53		53

2. The following table* gives the height of 30 meteorological stations situated on the plateau and the eastern slope of the Rocky Mountain range between latitudes 35° and 49° N, and the mean temperature for these stations for July, 1940. Compute the line of least squares which gives the relationship between these two variables, and the coefficient of correlation.

Mean Temperature		Mean Temperature	
Altitude of Station (hundreds of feet)	July, 1940 (°F)	Altitude of Station (hundreds of feet)	July, 1940 (°F)
36	74.6	13	80.4
25	71.9	34	80.0
41	70.4	14	81.4
32	71.8	44	70.8
26	77.2	61	74.5
32	77.0	43	72.4
61	70.1	55	71.6
54	72.6	42	81.0
38	73.2	46	80.8
62	63.7	34	68.7
28	79.6	29	74.9
53	74.6	45	74.0
48	76.8	20	72.8
14	82.8	10	76.3
25	82.0	11	74.4

3. The mean values for the hourly temperatures for June for a height of 12.4 m at Leafeld, England, are given in the following table.† Fit a sine curve to the data. Compare the values of the amplitude and the time of maximum temperature with the results for 1.2 m analyzed in the text.

* Data from *Monthly Weather Review*, 68, 202-203 (1940).

† Data from N. K. Johnson and G. S. P. Heywood, *loc. cit.*

Time (<i>t</i>)	Temperature (°F)	Time (<i>t</i>)	Temperature (°F)
01	50.5	13	59.9
02	49.9	14	60.4
03	49.4	15	60.5
04	49.0	16	60.6
05	49.2	17	60.2
06	50.0	18	59.4
07	51.9	19	57.9
08	53.7	20	56.0
09	55.2	21	54.4
10	56.5	22	53.2
11	58.0	23	52.3
12	59.0	24	51.2

4. Mean values are given for the height of the tropopause over Sault Ste. Marie, Michigan, in different meteorological situations.*

	Height (km)
Rear of a low	10.28
Center of a low	10.75
Front of a low	11.08
Rear of a high	12.36
Center of a high	11.55
Front of a high	10.91

Assume that these are spaced at equal distances and fit a sine curve to the points. The significance of these data is discussed in sections 113 and 116.

5. Using the amplitudes of the sine curves fitted to the mean values of the hourly temperatures for June at Leafield at heights of 1.2 and 12.4 m, as given in section 62 and in problem 3, compute the mean value for June of the coefficient of eddy diffusivity between these levels. The method of procedure is outlined in section 55.

BIBLIOGRAPHY

- Brunt, D., *Combination of Observations*, London, Cambridge University Press, 1931.
 Mills, F. C., *Statistical Methods*, New York, Henry Holt & Company, 1924.
 Whittaker, E. T., and G. Robinson, *The Calculus of Observations*, London, Blackie and Sons, Ltd., 1924.
 Yule, G. Udny, and M. G. Kendall, *An Introduction to the Theory of Statistics*, London, Griffin, 1937.

* Data from C. M. Penner, "The Effects of Tropospheric and Stratospheric Advection on Pressure and Temperature Variations," *Can. J. Research*, A19, 1-20 (1941).

PART II. APPLIED METEOROLOGY

CHAPTER 11

METEOROLOGICAL INSTRUMENTS AND OBSERVATIONS

The raw material from which the weather map is made and by means of which the meteorologist makes his forecast consists of the reports of a number of observations and of readings of instruments from each of a large number of meteorological stations. Whenever possible numerical values of the weather elements are obtained, but with some of these elements, such as cloud types, the observer's judgment must be relied on. Brief descriptions of the most important instruments and of the methods of observing the several meteorological elements, along with the criteria used, are given in this chapter. However, complete instructions for taking observations are not given. Explicit directions for observers may be found in the handbooks supplied by official weather services to their observing stations.

A meteorological instrument must fulfil demands that are not made upon a laboratory instrument. It must continue to operate in all kinds of weather and with little or no care, or with the care of a tinkering amateur, which may be worse. A high degree of accuracy is sometimes sacrificed for simplicity in order to meet these demands. Usually, extremely accurate values of the meteorological elements are not representative, as that term is defined in section 77, of the atmospheric conditions over the area surrounding a station and thus have little value to a forecaster. The pressure is a representative property and so it is measured more accurately than the other elements.

63. Pressure. The pressure at any level in the atmosphere is the force exerted on unit area at that level by the vertical column of air extending to the outer limits of the atmosphere. A method of determining the pressure was discovered in 1643 by Torricelli. A replica of his barometer may be constructed in the following manner. Invert a glass tube about 36 in. long filled with mercury into a bowl of mercury. The mercury descends from the top of the inverted tube to a point where the weight of the column of mercury balances the weight of a column of air

extending from the surface of the mercury in the bowl to the top of the atmosphere. The mercury barometer is still the standard instrument for measuring pressure. Improvements in design have permitted more accurate measurements of the weight of the mercury column, but the basic principle remains the same.

Originally the weight of the air was given in terms of the length of the column of mercury in the barometer, in inches in the English system of units, and in millimeters in the metric system. Because this height depends on the temperature of the mercury and on the value of the acceleration of gravity, the height of the mercury as read is corrected to standard values of T and g . An equation showing the variation of g with latitude and height is given in section 8.

To eliminate the inconsistency of measuring a force on unit area by a unit of length, the air pressure is now measured for meteorological purposes in terms of a unit of 1000 dynes cm^{-2} called a millibar (mb). As indicated in section 6, the length units and the dynamic units are related as follows.

$$1 \text{ in. mercury} = 33.86 \text{ mb}$$

$$1 \text{ mm mercury} = 1.333 \text{ mb}$$

The length of the column of mercury as read on the barometer, even if the latter is calibrated in millibars, does not give the correct pressure. It must still be corrected for variations in T and g in order to obtain the correct value of the atmospheric pressure.

There are two types of barometers in general use. As the pressure changes, the level of the mercury in the cistern at the base of the mercury column, as well as that of the mercury near the top of the tube, rises and falls. In the *Fortin barometer* the tube and scale are fixed, but the level of the mercury in the cistern is adjusted for each reading of the barometer. The tip of an ivory cone, attached to the barometer case so that its point is just above the level of the mercury in the cistern, coincides with the zero point of the height scale. The cistern is made partly of leather, and the top of the mercury is made to coincide with the ivory point by adjusting a screw which raises or lowers the base of the leather bag, and thereby the level of the mercury in it. The height of mercury can then be measured on the scale.

A second method of measuring the height of the column of mercury is utilized in the *Kew barometer*. The construction of the cistern of the barometer is illustrated in Fig. 57. The cistern A is of cast iron or similar metal with a boxwood top D . This is held in place by means of a screw C . The barometer tube E is cemented into the boxwood to keep it steady. The metal flanges at B are provided to damp out the oscilla-

tions of the mercury when the barometer is transported. The pores of the boxwood provide a means whereby the pressure of the air in the cistern and that outside are equalized.

Since the total volume of the mercury is fixed, any given drop in pressure will cause the level in the tube to drop a fixed amount and that

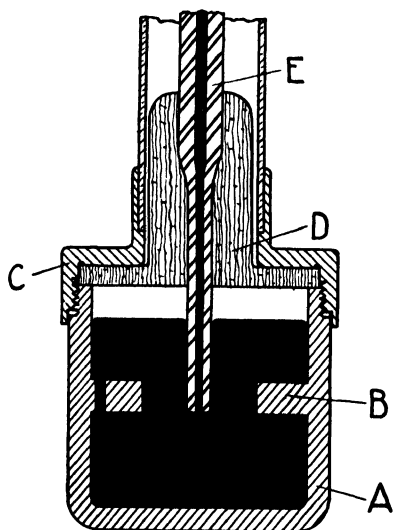


FIG. 57. The cistern of a Kew barometer. (From Middleton, *Meteorological Instruments*, University of Toronto Press.)

in the cistern to rise by a corresponding amount, depending on the cross-sectional areas of tube and cistern. Assume that the surface of the mercury in the tube is one forty-ninth of the surface of the mercury in the cistern. With a fall of 1 in. in the atmospheric pressure, the mercury in the tube will fall 0.98 in. and the mercury in the cistern will rise 0.02 in. Thus a distance along the tube of 0.98 in. can be treated as 1 in. in indicating a change in the atmospheric pressure. Knowing the exact ratio between the two surfaces in any barometer, the scale may be adjusted so that the actual height may be read off directly.

After the height of the mercury has been determined, the measured value of the pressure must be corrected for errors in the manufacture

of the instrument as well as for the temperature of the barometer and the value of the acceleration of gravity at the station as described above. The value of g is constant for any given station, and the value of the instrument correction is constant for any given barometer. The only variable which will change the value of the correction is the temperature. A correction card accompanies each barometer, giving the total correction corresponding to any temperature of the barometer.

An error in the reading of the barometer occurs at some stations with high winds. The level of the mercury in the barometer fluctuates because of a pumping effect resulting from the variations of the wind velocity. No adjustment can be made for this error. A similar error occurs with mercury barometers on shipboard through the motions of the ship.

Since pressure changes rapidly with altitude, the values of the station pressure determined as described above have little significance. For

pressures to be compared, they must be corrected to a standard level. This usually is mean sea level, although in plateaus and mountainous regions the standard may be nearer the general level of the terrain. To assume that there is a sea level pressure is equivalent to assuming that there exists a column of air from sea level to the height of the top of the atmosphere. An approximate value of the weight of an imaginary column of air between the level of the station and sea level can be determined if the height of the station and the mean temperature of the air column are known. An approximation to the mean temperature is found by averaging the temperature of the air at the station and the corresponding temperature twelve hours ago. The latter is included to provide a means of partially eliminating non-representative values for the current temperature. These corrections to sea level are calculated for each station with the values of the correction varying with the value of the mean temperature of the column of air. These corrections are added for all stations except those below mean sea level.

Another type of barometer is the *aneroid barometer*, the basic parts of which are shown in Fig. 58. This instrument consists of a partially evacuated thin metal cylinder *C*, whose circular sides are prevented from collapsing under the pressure of the atmosphere by a spring *S*. When the pressure increases, the top of the cylinder approaches the bottom

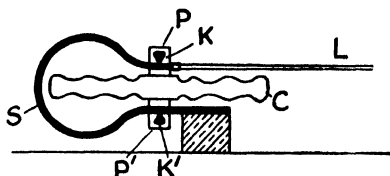


FIG. 58. A simple aneroid barometer. (From Middleton, *Meteorological Instruments*, University of Toronto Press.)

of the cylinder which is fixed to a base plate; as the pressure decreases, the top recedes. These motions are communicated to the spring and then to the lever *L* by means of the knife edges *K* and *K'* which pass through posts *P* and *P'* attached to the two circular faces of the cylinder at their center. The deflection of *L* is magnified by mechanical means not shown in the figure. The cylinder is very flexible and therefore the range of the deflection of *L* is governed almost entirely by the tensile characteristics of the spring. The instrument is calibrated by comparison with a standard mercury barometer.

The aneroid barometer is not so accurate an instrument as the mercury barometer, but it has the advantages of small size and the ease with which it can be transported without danger of being damaged. Since pressure is related to height in the manner specified by equations 9-5 and 9-9, the aneroid is installed in airplanes as a height-measuring instrument. When its scale is calibrated in height units such as feet or meters, it is known as an *altimeter*. An altimeter gives correct height

readings only under certain standard conditions. At other times a correction to the reading, depending on the surface pressure and the mean temperature of the air column below the aircraft, gives sufficient accuracy for the purposes of air navigation.

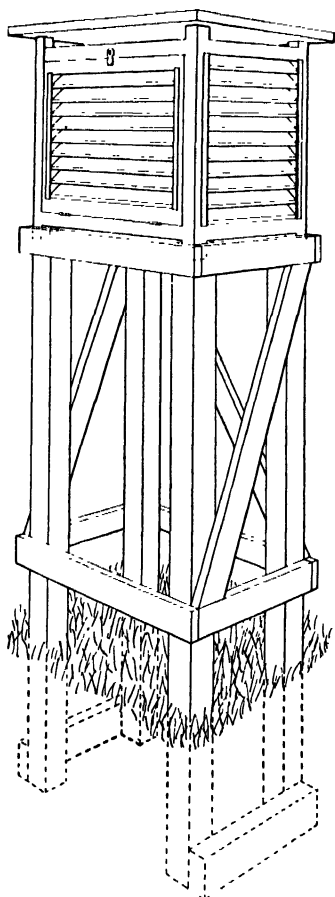


FIG. 59. Stevenson screen.
(From Middleton, *Meteorological Instruments*, University of Toronto Press.)

With other aneroids the pointer is replaced by a pen which records its movements on a revolving drum. After the instrument has been calibrated, the movements of the pen give a record of the pressure changes. This instrument is called a *barograph* and the pressure record which it makes is known as a *barogram*.

64. Temperature. In meteorological observations the temperature is measured on either the Fahrenheit or the Centigrade scale. The freezing and boiling points on these and on the Absolute scale, along with conversion equations, are given in section 6. The variations of usage for different purposes and in different countries are also discussed in that section.

The temperature of the air is measured by means of an ordinary mercury-in-glass thermometer, called a mercury thermometer. Such a thermometer rapidly assumes a temperature which represents an equilibrium with the environment, heat being transferred to and from the thermometer by conduction, convection, and radiation. When surrounding objects have approximately the same temperature as that of the air, the measured temperature will be representative of the air temperature at

the height of the thermometer. A thermometer exposed in the open would be heated by insolation during the day and would read too high, but during the night it would be cooled by terrestrial radiation (see section 29) and read too low. To eliminate as much as possible such errors resulting from the radiative transfer of heat, thermometers are housed in Stevenson screens made of wood, one of

which is shown in Fig. 59. Such screens vary in construction in different countries, but they must be designed so that little or no heat can be transferred by radiation from outside to inside, yet a free flow of air is impeded as little as possible.

Frequently conditions occur in which the temperature varies markedly within a short distance, or at one spot within a short interval of time. Thus during a partly cloudy afternoon a thermometer exposed in the open may vary as much as 5°F during a period of half an hour, or the difference between the temperature at the top and bottom of a hill may amount to $15\text{--}20^{\circ}\text{F}$ during a still winter night. Thus it is useless to attempt to determine the temperature of the air more accurately than to the nearest degree, although for the determination of the water vapor content as described in section 65, the readings should be taken to the nearest tenth.

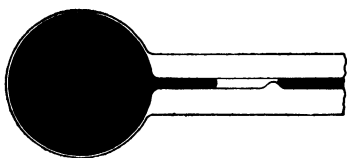


FIG. 60. Capillary on the maximum thermometer. (From Middleton, *Meteorological Instruments*, University of Toronto Press.)

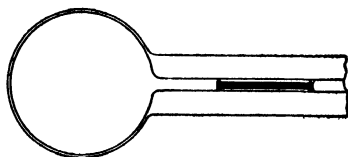


FIG. 61. Index of the minimum thermometer. (From Middleton, *Meteorological Instruments*, University of Toronto Press.)

To measure the maximum temperature a special type of thermometer is used in which there is a constriction in the capillary of the thermometer near the bulb, as shown in Fig. 60. With rising temperature the mercury is pushed past the constriction so that the thermometer gives the correct reading. When the temperature begins to fall, the mercury breaks at the constriction, leaving the mercury above to register the maximum temperature. The thermometer is reset by whirling it or swinging it while holding it at the end away from the bulb. This causes the mercury above the capillary to return past the constriction.

When the temperature falls below -39°C , mercury freezes, and so at lower temperatures mercury thermometers are no longer useful. At these temperatures organic liquids such as ethyl alcohol must be used, but because thermometers using such liquids are less accurate than mercury thermometers, they are not used in general practice except for minimum thermometers. In the capillary of a spirit thermometer which is used for a minimum thermometer there is a small index as shown in Fig. 61. The index slides easily along the capillary which is kept in a

horizontal position. When the temperature falls the surface tension at the free end of the liquid draws back the index as the liquid as a whole recedes. When the temperature rises the liquid flows past the index leaving it at the point of minimum temperature. The thermometer is reset by tapping it gently to allow the index to slide down till it comes again in contact with the surface of the liquid.

When two metal strips of different substances are clamped together, the difference in the coefficients of expansion of the two metals causes the combined strip to change its curvature as the temperature varies. This principle is used in the *bimetallic thermometer*. In the latter a pointer is attached to the strip which is in the form of a helical coil. As the temperature varies, the end of this pointer swings through an arc. This instrument is not stable enough for precision temperature measurements, but is sufficiently accurate for most purposes if calibrated frequently by comparison with a standard mercury thermometer. If a pen is attached to the end of the pointer so that the former makes a trace on a revolving drum, the instrument becomes a recording thermometer, or *thermograph*. In this form the bimetallic thermometer is widely used in meteorological work.

65. Humidity. The water vapor content of the atmosphere may be measured in several ways. Its value at the surface of the earth is reported by the dew point or by the relative humidity. These quantities are discussed in sections 10, 21, 81, and 82. Briefly, the *relative humidity* indicates how near the air is to being saturated. The *dew point* gives the temperature at which the air would be saturated if it cooled so that no change in water vapor content occurred in the cooling. A humidity-measuring instrument is known as an *hygrometer*.

The dew point may be determined directly, but in meteorological practice it is computed by using the ordinary thermometer, referred to for purposes of differentiation as the dry-bulb thermometer, and a wet-bulb thermometer. When the bulb of a thermometer is kept moist, evaporation occurs. The heat required for evaporation is taken from the air surrounding the wet bulb, and the thermometer registers a temperature lower than that shown by the dry-bulb thermometer in the same atmosphere. The difference is dependent on the amount of evaporation which in turn is determined by the relative dryness of the air. A discussion of the theory is given in sections 23 and 24. The basic features of the wet- and dry-bulb hygrometer are shown in Fig. 62. A piece of muslin covers the wet bulb, which is kept moist by the water which travels from the container along the wick to it. To obtain satisfactory readings of the wet-bulb temperature, it is necessary that a fresh supply of air should flow continually past the wet bulb. One method of

accomplishing this is used in the sling psychrometer. The wet- and dry-bulb thermometers are mounted on a frame which can be rotated rapidly. In another type of psychrometer the two thermometers are inserted in a duct or ducts through which air is drawn by means of an electric fan, thus ventilating the bulbs. When readings of the wet- and dry-bulb thermometers have been taken, the values of the dew point and of the relative humidity can be obtained from prepared tables.

When the temperatures are above freezing, the wet bulb is cooled by the evaporation of liquid water. At these temperatures the readings are fairly accurate. When the temperatures are below freezing, the bulb is kept damp by dipping it in water. Since the water freezes and

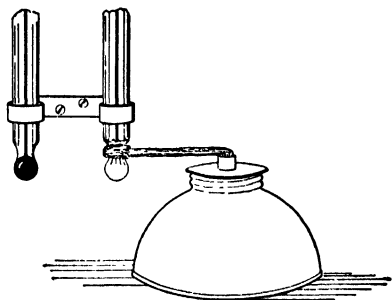


FIG. 62. A simple wet- and dry-bulb hygrometer. (From Middleton, *Meteorological Instruments*, University of Toronto Press.)

the rate of evaporation and the conductivity vary with the thickness of the ice coat, errors are greater. Furthermore, for a small change in the value of the wet-bulb temperature, there is a large change in the value of the dew point. For these reasons the dew point obtained by this method is not accurate for low temperatures.

The relative humidity of the air can be measured directly by an instrument which operates through the changes in the length of hair caused by changes in the humidity. When the relative humidity of the air increases, human hair increases in length slightly. These changes are magnified so that they can be read through the movements of a pointer along a scale or of a pen making a trace on a revolving drum. The scales are calibrated by comparison with values obtained through the use of a psychrometer. In spite of careful manufacture, the hair hygrometer does not give consistently accurate readings, and these instruments should be checked regularly by comparison with values for the relative humidity obtained by other means. The accuracy decreases with decreasing temperature, the lag being so great at temperatures below -20°C that the instrument is practically useless.

66. Wind. There are many methods of measuring the wind direction and velocity. A brief description of only a few of these will be given here.

An early method of indicating the velocity of the wind was that devised by Admiral Beaufort in 1805. He divided the wind velocities into thirteen classes according to their effect on objects about the sea.

This Beaufort scale has been adapted to land winds, and then the velocities determined in miles per hour corresponding to each of the classes. The following table gives the Beaufort scale, with the descriptive name, the corresponding velocity range, and the effect of the wind on common objects. With the aid of the descriptive material given in the last column, an estimate of the wind velocity can be made without the use of instruments. In comparing the values obtained by this means and those obtained from an anemometer, it should be remembered that the wind velocity changes rapidly with height near the surface of the earth.

BEAUFORT SCALE OF WIND VELOCITIES

Beaufort Number	Description of the Wind	Velocity (mph)	Effect of the Wind
0	Calm	Less than 1	Smoke rises vertically.
1	Light air	1 to 3	Wind direction shown by smoke drift but not by wind vanes.
2	Light breeze	4 to 7	Wind felt on face; leaves rustle.
3	Gentle breeze	8 to 12	Leaves and twigs in constant motion; wind extends light flag.
4	Moderate breeze	13 to 18	Raises dust and loose paper; small branches are moved.
5	Fresh breeze	19 to 24	Small trees in leaf begin to sway.
6	Strong breeze	25 to 31	Large branches in motion; whistling heard in telegraph wires.
7	Moderate gale	32 to 38	Whole trees in motion; inconvenience felt in walking against wind.
8	Fresh gale	39 to 46	Breaks twigs off trees; generally impedes progress.
9	Strong gale	47 to 54	Slight structural damage occurs.
10	Whole gale	55 to 63	Trees uprooted; considerable structural damage occurs.
11	Storm	64 to 75	Accompanied by widespread damage.
12	Hurricane	Over 75	

This is the scale used in weather reports to give the velocity of the wind at the reporting station.

The *cup anemometer* is one of the most widely used instruments for measuring the wind velocity. In this instrument hemispherical cups are attached to the ends of horizontal arms which extend outward radially from a vertical shaft. This shaft rotates readily, and the number of rotations during any given interval of time is counted by mechanical means.

When the cups are exposed in the open, the wind is caught by the inside of the cup. The force exerted causes the cups to rotate. By

calibration as, for example, in a wind tunnel, the number of rotations which the cups will make when a mile of wind goes by can be determined. From this value the number of miles of wind that pass during any time interval, and hence the velocity, can be obtained. The number of cups on a shaft varies. A shaft with two cups is not satisfactory since the force varies greatly, depending on the angle between the horizontal arms and the wind at any instant. Usually three or four cups are used. The number of rotations for a mile of wind will vary with the number of cups and their dimensions.

It will be noticed that the wind speed determined by means of the cup anemometer is obtained by counting the number of revolutions of the cups in any given time interval t . The result is then an average velocity over the interval. As t decreases the value of the velocity approaches more nearly the instantaneous velocity. When the wind is gusty its velocity changes rapidly; the inertia of the cups will then tend to keep them rotating at the same speed. The anemometer then fails to register the extreme values of the velocity. The tendency is for the readings to be too high with gusty winds for the cups accelerate with a gust more rapidly than they decelerate with a lull.

A second method of measuring the wind velocity makes use of the increased air pressure in a tube when a wind blows into the open end of the tube and the decreased pressure when a wind blows across the mouth. The anemometer using this principle was designed by W. H. Dines. The head of a *Dines anemometer* is shown in Fig. 63.

By means of the wind vane, the mouth A of a horizontal tube is kept facing the wind. Ball bearings at C permit the vane to rotate readily. The additional pressure in the horizontal tube is transmitted by means of slots at B through the stationary tube D and out through F . To insure efficient performance the fit between D and the rotating tube at E must be close so that the pressure is transmitted undiminished through this portion of the instrument.

A group of holes is located in the pipe at G . The suction of the wind blowing on these holes is transferred through H to the outlet J . The assembly is supported by means of the pipe mast M ; the cone and cylinder L form a covering for the pipe and connections. The rod K is attached to the vane, passes through the center of the anemometer tube, and actuates the direction-recording mechanism.

The tube F transmits the pressure increase from the horizontal tube to the interior of a float in a sealed water tank. The decrease in pressure at G causes a corresponding pressure decrease in the air space above the float. Thus both the pressure increase inside the float and the decrease in the air space above cause the float to rise. The design of

the float is such that its vertical displacement is directly proportional to the wind velocity. This displacement is recorded on a rotating drum. The Dines anemometer thus measures the effect of the wind at each instant and so permits the determination of the instantaneous velocity. It is therefore more suitable for measuring the maximum velocity and the gustiness of the wind.

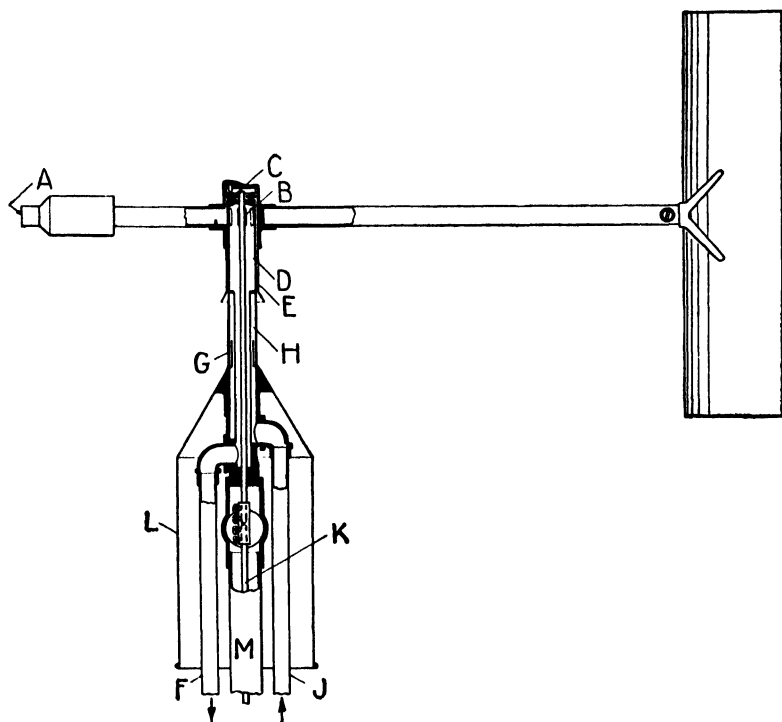


FIG. 63. The head of a Dines anemometer. (From Middleton, *Meteorological Instruments*, University of Toronto Press.)

The cup anemometer, as well as the Dines, can be designed to record the wind speed on a revolving drum. The record of wind direction is usually made at the same time.

Above the surface of the earth the direction and speed of the wind are obtained by observing the movements of a balloon which is free to move with the currents of air. A balloon is filled with a light gas, hydrogen or helium, and allowed to ascend. If the balloon is filled with a given amount of gas, the rate of ascent will be almost constant, and so the height above the earth at any instant can be calculated, using the length

of time since the balloon was released. The path of the balloon is followed by the observer with the help of a theodolite. At regular intervals the azimuth and elevation angles are determined. These two angles, with the height as given by the time elapsed since release, determine the position of the balloon. With the help of tables and a plotting board the observer is able to calculate the average horizontal velocity of the balloon for each time interval, and so the horizontal velocity and direction of air in the layer through which the balloon passed. By interpolation the velocity of the air and the corresponding direction at given levels are found, and these are reported to the forecast offices for use in analyzing the map and preparing the forecast.

The method of determining the wind velocity of the upper air with balloons has several sources of error. The most serious of the errors is caused by the assumption of a constant rate of ascent for the balloon. With light rain or snow falling, the buoyant force decreases and the balloon will not rise at the normal rate. Even if there is no precipitation, the presence of vertical air currents will cause the rate of ascent to vary and make calculations less reliable. This error can be eliminated by following the balloon with two theodolites placed at a distance from each other. The position of the balloon is then determined, using the azimuth and elevation angles as measured by the two theodolites.

Free balloons are also used in meteorology to determine the temperature, pressure, and moisture content of the upper air. A small lightweight box is suspended below a large balloon filled with hydrogen or helium. Within the box there are an aneroid barometer, a bimetallic thermometer, and an hygrometer. These are connected to a very small radio transmitter in such a manner that signals giving pressure, temperature, and humidity at various levels are radiated by the instrument as it ascends. These signals are picked up and recorded by a special receiving set at the station from which the balloon was released. An instrument of this type is known as a *radiosonde*. Using the values of pressure, temperature, and humidity received in this manner, the observer is able to compute the height of the balloon at any time by the method outlined in section 11. He then codes the values to send them off to the different forecast centers.

67. Clouds. Clouds and cloud types are classified according to a system introduced early in the nineteenth century. The standard for classification is laid down by the International Meteorological Organization and is presented fully in the International Cloud Atlas. This atlas also includes a large number of excellent plates of the different types of clouds.

The classification of clouds is very necessary to the forecaster. The

development of different types of clouds is the result of various processes taking place in the atmosphere, as shown in Chapter 20, so a knowledge of the cloud type aids the forecaster in determining the physical developments in an air mass. In many regions of the earth, owing to lack of upper air observations, this is the only method whereby the forecaster is able to learn something of the physical processes occurring in the air above the surface layers.

Cloud types are divided into two main divisions, cumulus (having the appearance of closely packed wool) type clouds, and stratus (layer) type clouds. A second basis of division is in terms of the height of the base of the cloud. The high clouds are called cirrus or have the prefix cirro- in their names. Middle clouds are distinguished by the prefix alto-. Low clouds have no distinguishing prefix. The prefix fracto- is used to indicate cloud which is a part of a larger cloud that has been broken by the wind. Nimbo- or nimbus included in the name of a cloud indicates that it is closely associated with precipitation.

The following table gives the names, levels, and abbreviations for the common types of clouds.

THE CLASSIFICATION OF CLOUDS

General Category	Mean Upper Level		Mean Lower Level		Type	Abbreviation
	km	ft	km	ft		
High	11	35,000	6	20,000	Cirrus	Ci
					Cirrostratus	Cs
					Cirrocumulus	Cc
Middle	6	20,000	2	6,500	Alto cumulus	Ac
					Alto stratus	As
					Strato cumulus	Sc
Low	2	6,500	0.1	300	Stratus	St
					Nimbostratus	Ns
					Cumulus	Cu
Clouds with vertical development	11	35,000	0.5	1,600	Cumulonimbus	Cb

The high clouds are seldom found below 15,000 ft, their height usually being between 20,000 and 35,000 ft. These clouds are very thin and white, and are composed of ice crystals. Cirrostratus (Fig. 64) is a thin veil which spreads over the sky, sometimes merely giving the sky a milky appearance. It frequently produces a halo about the sun or moon. Cirrus (Fig. 65) is similar, but is fibrous in nature, and is frequently seen with hooks at the ends of individual cloud elements.

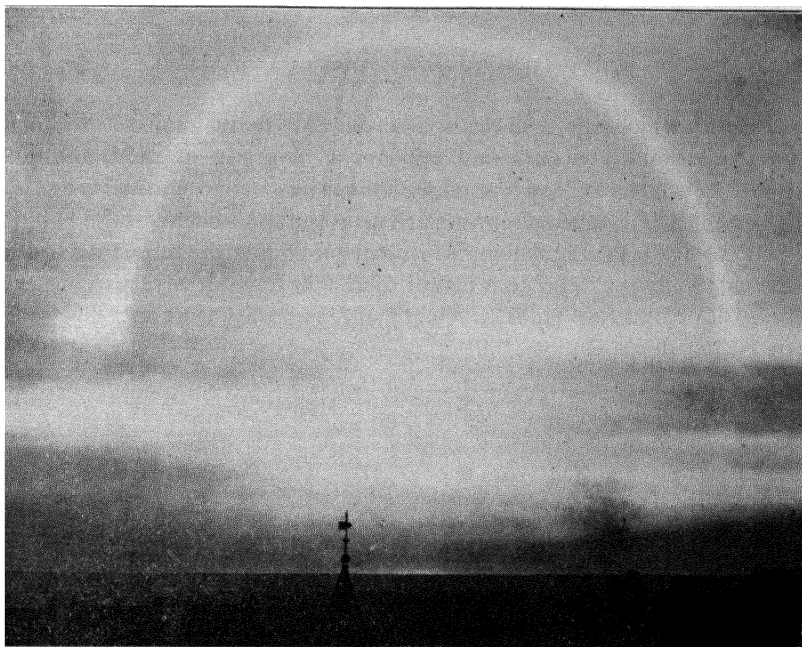


FIG. 64. Cirrostratus. (From *Cloud Forms and States of the Sky*, U. S. Weather Bureau.)



FIG. 65. Cirrus. (From *Cloud Forms and States of the Sky*, U. S. Weather Bureau.)

It is cirrus which the fishermen describe as "mares' tails." Cirrocumulus occasionally occurs and appears as a group of small rounded bunches of white cloud at the edge of a cirrus or cirrostratus layer.

The clouds of the middle levels are usually found between the heights of 6000 and 20,000 ft, although in a region of low pressure the tops of these clouds may extend to a height of 23,000 ft. Altostratus (Fig. 66) is grayish or bluish in color. When thin, it permits the sun's disc to be seen; when thick, it hides the sun or moon, or only allows their position



FIG. 66. Altostratus. (From *Cloud Forms and States of the Sky*, U. S. Weather Bureau.)

to be determined by a bright spot on the cloud. In the vicinity of a warm front, the base of an altostratus cloud descends to a height of 1000 to 2000 ft and is then called nimbostratus. This is a low cloud and is usually accompanied by rain or snow. Altocumulus clouds (Fig. 67) are formed of globular masses and are often thick. When they become closely packed, they may be distinguished from altostratus by the irregularities on the under surface of the cloud. They are white or gray in color. Sometimes they occur in a regular pattern to give a "mackerel sky." One species of altocumulus is altocumulus castellatus. In this type of cloud several tufts showing vertical de-

velopment extend upward in the shape of small turrets from an alto-cumulus cloud.

Low clouds may be found with their bases almost reaching the earth's surface while in other situations the base may be as high as 10,000 ft. Stratus is a thin gray cloud, usually occurring at a low level. Fog is



FIG. 67. Altocumulus. (From *Cloud Forms and States of the Sky*, U. S. Weather Bureau.)

a stratus cloud at the earth's surface. Fractostratus or scud is formed when a layer of stratus is broken by the wind or when a layer of stratus is in the process of formation. Stratocumulus (Fig. 68) closely resembles stratus since it is found in a layer, and is of a gray color. It is variable in thickness and has light spots over its surface or is formed of individual clouds with clear spaces between. Nimbostratus is a low



FIG. 68. Stratocumulus. (From *Cloud Forms and States of the Sky*, U. S. Weather Bureau.)



FIG. 69. Cumulus of fine weather. (From *Cloud Forms and States of the Sky*, U. S. Weather Bureau.)

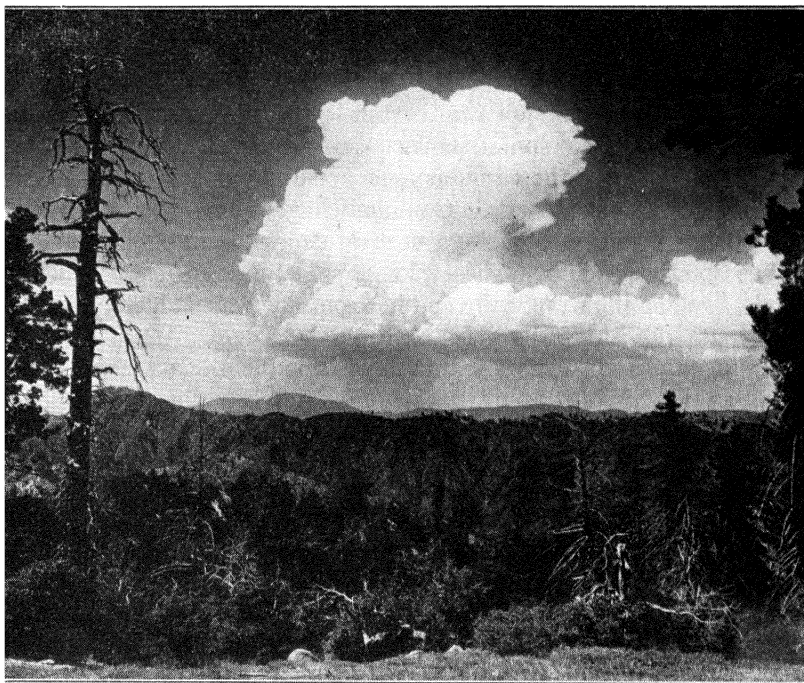


FIG. 70. Heavy cumulus. (From *Cloud Forms and States of the Sky*, U. S. Weather Bureau.)

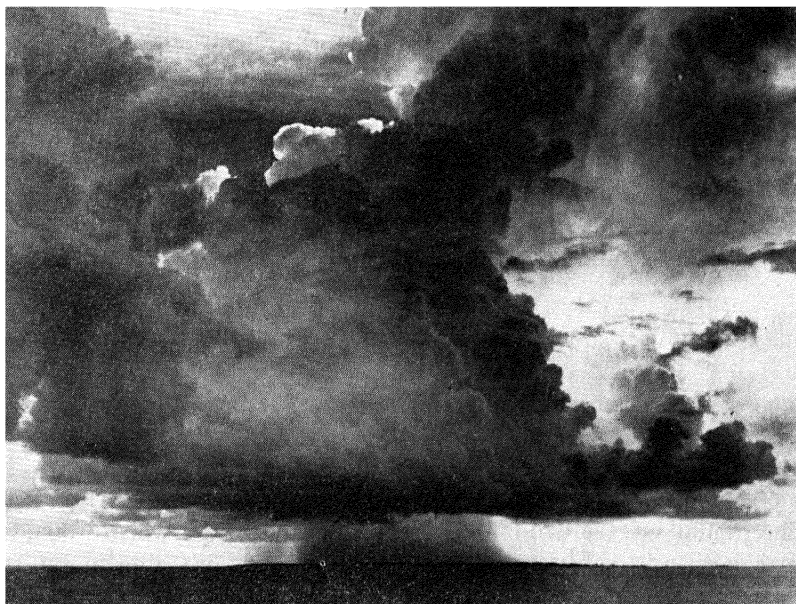


FIG. 71. Cumulonimbus. (From *Cloud Forms and States of the Sky*, U. S. Weather Bureau.)

cloud resulting from the downward extension of altostratus in the manner indicated in the discussion of the latter.

The low clouds of the cumulus type are usually easily distinguished from the low stratus clouds. Cumulus clouds (Figs. 69 and 70) may be small rounded clouds of slight vertical development, called cumulus, or fine weather clouds. These clouds sometimes develop into large clouds, swelling both vertically and horizontally to form heavy cumulus. Heavy cumulus clouds have definite rounded edges. When the edges about the top begin to form a fibrous veil, it has turned into a cumulonimbus cloud (Fig. 71). This formation indicates the presence of ice crystals at the top of the cloud. When the vertical development is inhibited by an isothermal layer, the cloud top spreads horizontally so that it resembles an anvil.

Sometimes the type of cloud is easily determined. On other occasions the cloud appears to be intermediate between two related cloud types. In such instances careful observation is necessary to classify the cloud properly.

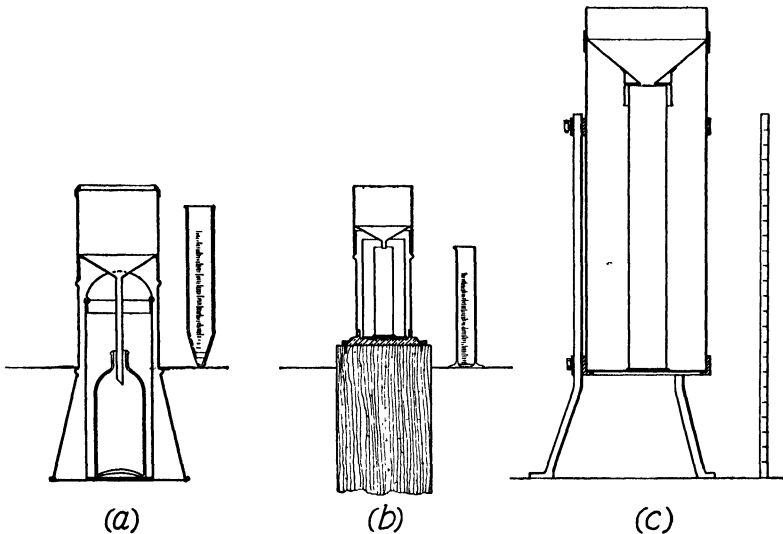


FIG. 72. Rain gages of (a) the British Isles, (b) Canada, (c) the United States. (From Middleton, *Meteorological Instruments*, University of Toronto Press.)

68. Precipitation. Rainfall is measured by means of a *rain gage*. The rainfall as recorded is the average depth of water which would fall on a level area. Three types of rain gages are illustrated in Fig. 72. The three gages shown are standard types used in (a) the British Isles, (b) Canada, (c) the United States. The rain gage consists, first, of a

large cylindrical vessel which is fixed solidly upon or just above the earth's surface; second, a metal funnel which fits firmly over the top of the vessel, and which has a strong beveled upper edge; third, a receiver to be placed inside the vessel and under the delivery tube of the funnel. The rain falling into the funnel is carried through the delivery tube into the receiver inside the vessel. Two methods of measuring the amount of rain which has fallen are used. In Canada and Great Britain, when the observer measures the rainfall, he removes the receiver from the vessel and empties the contents into a glass graduate. The area of the cross section of the glass graduate is a known proportion of the area of the top of the cylinder. Knowing this proportion, one is able to calculate the amount of rain per unit area, or the rainfall. Usually the glass graduate is calibrated to read off directly the depth of the rainfall. In the United States, on the other hand, the amount of rain is measured by dipping a thin measuring stick into the cylinder through the hole in the funnel, and noting the length of the graduated stick which is wetted.

In the types of rain gage described, the loss by evaporation is small, provided the funnel is fitted closely to the vessel. The possibility of rain splashing into or out of the funnel must be considered. The tops of the smaller rain gages are about 1 ft above the ground level to guard against the rain splashing in from the outside. The top of the larger gage of the United States Weather Bureau is usually about 2.5 ft above the ground. If the sloping sides of the funnel are several inches below the level of the rim, there is little danger that rain which has fallen into the gage will splash out again. Eddies will at times carry the falling rain away from the gage and thus make the reading inaccurate. With a careful choice of site this error can be minimized.

Several types of gages have been devised by which the rate of fall can be determined. In the tipping-bucket gage, when a unit of rain, as 0.01 in., collects in the bucket, it tips and empties while a companion bucket on the other side of the pivot is filling. The time at which the bucket tips is recorded on a revolving drum. The rainfall during any given interval of time is then readily determined. Float gages record the height of a float which ascends as the level of water in the vessel into which the falling rain is carried rises. When the vessel becomes full, a device such as a siphon acts to empty the vessel in a short time, after which the vessel again fills by the falling rain. These instruments do not give highly accurate values, and so are not used for primary measurement of rainfall. Furthermore they are not satisfactory for cold climates since the instrument may be ruined if the water in it freezes.

The accurate measurement of snowfall is more difficult than the

measurement of rainfall. When the fall is measured in a gage similar to a rain gage, the eddies about its mouth do not permit a representative amount of snow to fall into the gage. The effects of shields have been studied, but these do not fully eliminate the errors resulting from the eddies. Heating the gage will cause the amount measured to be smaller than the average fall since some of the moisture evaporates when melted.

The other common method of measurement of snowfall is by measuring the fall of snow at several places over a level area where there has been no drifting, and taking an average value of the measured depths. This necessitates the determination of the level of the old snow, a task which is sometimes difficult. The depth of snow is converted into equivalent rainfall by dividing by 10 or 12. This is only an approximation since the density of newly fallen snow varies widely. With snow pellets the density may be as high as 20 or 25 lb per cu ft. Thus any method of snowfall determination gives approximate values only.

69. Sunshine and Radiation. The measurement of neither of these two weather elements is as yet of direct interest to the weather forecaster. These elements are of interest, though, to the theoretical meteorologist and the climatologist. The theoretical meteorologist is concerned with the heat balance of the atmosphere, and so with the losses and gains in heat energy in the different layers of it. The climatologist prefers to use the continuous record of sunshine rather than the intermittent record of cloud observations in obtaining his value for the average cloudiness of the day.

Fig. 73 shows a *Campbell-Stokes sunshine recorder*. A glass sphere focuses the rays of the sun on a specially prepared card. When clouds do not impede the radiation from the sun, the heat concentrated at the focal point is sufficient to char the card. The focal point moves over the card as the sun moves across the sky, leaving a record on the card of the times when the sun was visible. Different slots are provided to care for the variation of the angle of elevation of the sun during the seasons. This instrument has many of the desirable features of the best type of meteorological instrument, such as simplicity, durability, lack of the need of adjustment, ease of understanding the results. There are some minor possibilities of error. One of these is in the exact determination of the time of passage of a cloud over the sun, for the burn spreads over the surrounding parts of the card. The use of the record to determine the cloudiness for any particular day is open to criticism since the sky can be covered with broken clouds only, and yet no sunshine may be recorded. Averages would tend to decrease the error produced by this effect.

The standard instrument for the measurement of solar radiation,

according to the International Meteorological Organization, is the *Ångström compensating pyrheliometer*. Solar radiation is received on two thin strips of metal coated with black. Sensitive thermojunctions are attached to the back of these strips, but electrically insulated from them. These are connected through a sensitive galvanometer. When desired either strip can be shielded from the sun and an electrical current passed through it. To make an observation one of the strips is shielded

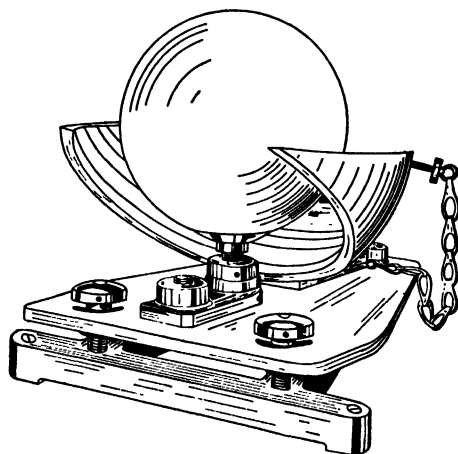


FIG. 73. Campbell-Stokes sunshine recorder.

and sufficient current is passed through it so that the temperatures of the two strips are the same. The energy absorbed by the unshielded strip is then equal to the electrical energy communicated to the other. This second can be measured, and so the first determined.

The *silver disc pyrheliometer* is another commonly used instrument for measuring the sun's radiation. Sunlight is allowed to fall on a silver disc for a stated time interval and the rise in temperature of the disc is carefully measured. The disc is mounted so as to minimize the transfer of heat to or from it by processes other than radiation. The instrument is simply designed and gives very accurate results.

70. Visibility. Visibility is defined as the distance in a horizontal direction at which objects can be distinguished. It is useful for the airman since he uses it in deciding whether he can land safely at an airport. To the forecaster the visibility is indicative of certain features of the atmosphere, such as the stability.

About any observing station a number of visibility marks are chosen and the distance of each from the observing tower determined. For daylight observations, the marks are prominent objects on the skyline.

For night observations, the marks are certain lights in the vicinity. The visibility of the lights is converted into daylight visibility by a comparison of the visibility before and after sundown in the same meteorological situation. The observer then makes his estimate of the visibility by noting the farthest visibility mark which he is able to see from the tower, and then noting whether the visibility in other directions is about the same. The reported visibility is the average visibility in all directions.

Care is necessary in the choice of visibility marks. They should stand out clearly against the skyline or against their background. At some stations there are no suitable visibility marks beyond a certain distance. The visibility, when it is greater than the farthest visibility mark, is then estimated by determining the clarity with which the farthest mark stands out. With practice this method gives a reliable measure of the visibility at the station.

BIBLIOGRAPHY

- Glazebrook, Sir Richard, *Dictionary of Applied Physics*, Vol. III, London, Macmillan and Co., 1923.
- Middleton, W. E. K., *Meteorological Instruments*, Second Edition, Toronto, University of Toronto Press, 1943.
- United States Weather Bureau Circulars*, Washington, D. C.
- Handbooks of the Meteorological Office*, London, H. M. Stationery Office.
- Handbooks of the Meteorological Service of Canada*, Toronto, Meteorological Office.
67. International Meteorological Committee, *International Atlas of Clouds and States of the Sky*, Paris, 1932.
70. Middleton, W. E. K., *Visibility in Meteorology*, Second Edition, Toronto, University of Toronto Press, 1941.

CHAPTER 12

THE GENERAL CIRCULATION OVER THE EARTH

71. Circulation on a Non-Rotating Globe. The movement of air over the earth's surface is affected by many different factors. It is easier to understand the final distribution of winds and pressure if the most important factors are considered separately.

If the atmosphere on a non-rotating globe were heated by contact with the uniformly heated surface of the globe, the only type of motion which might occur would be local convection currents. Equilibrium in the system is reached when the total outgoing radiation is equal to the input of energy. Since, though, some of this heat would be lost from the upper atmosphere, the unstable temperature distribution would persist, and the convection currents continue to develop.

If now the sun is assumed to revolve around the non-rotating globe, the heating is not uniform and the situation is more complex. Curve (α) in Fig. 27 (section 31) shows the variation in intensity with latitude of the effective incoming solar radiation. This curve thus gives the relative amount of energy received at the different regions of the non-rotating globe. It is clear from this diagram that the equatorial region receives much more solar energy than the polar regions, and the air at the equator will become warmer than that at the poles. As a result of this heating, the air will expand and rise. Near the upper limit of the atmosphere the amount of air above some given height will exceed the amount of air above the same altitude in the colder regions, and so the pressure will be greater. A pressure gradient will be produced, and the resulting pressure gradient force (see section 33) will move the heated air at higher levels toward the colder parts of the earth. Here the total weight of the atmosphere will increase and the weight of the air at the equatorial part of the globe will decrease. Hence a pressure gradient will be produced at the surface from warm to cold regions. A complete circulation (see Fig. 74) will result, with air rising over the region heated most strongly by the sun, moving in the upper atmosphere to the polar regions, subsiding there, and traveling near the surface to its starting point.

In section 49 the idea of circulation was defined. In general terms, the circulation C about a closed curve measures the flow along that curve,

and is obtained by multiplying the velocity V for every small part of the curve ds by ds , and summing the products. The rate of growth of circulation is, according to (50.20),

$$\frac{dC}{dt} = - \oint \frac{dp}{\rho} + W$$

or, with (7.7)

$$\frac{dC}{dt} = - \oint RT d(\log p) + W$$

In this equation t represents time, R is the gas constant for dry air, T the temperature in degrees Absolute, p the pressure, and W the term for the external forces. The rate of change of circulation around the closed curve $ABDC$ shown in Fig. 74 may now be computed. This closed curve

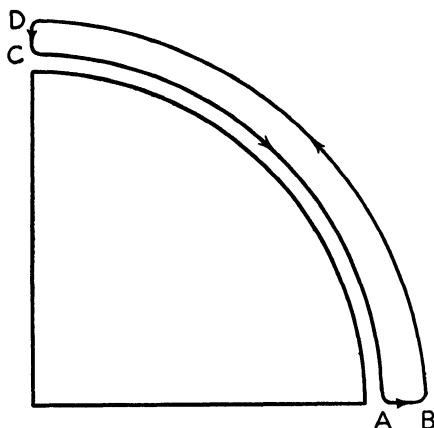


FIG. 74. Circulation on a non-rotating globe.

may be specified as comprising two vertical lines, one above the equator, and the other above the pole, which are joined by the two isobars, $p = 300$ mb and $p = 1000$ mb. Along BD and AC

$$d(\log p) = 0$$

and so the contributions to $\frac{dC}{dt}$ are zero. If T_E is the mean temperature of the column AB ,

$$\int_A^B RT d(\log p) = RT_E \log \frac{3}{10}$$

Similarly if T_P is the mean temperature of CD ,

$$\int_D^C RT d(\log p) = RT_P \log \frac{10}{3}$$

If no external forces are acting, so that $W = 0$, then

$$\frac{dC}{dt} = - RT_E \log \frac{3}{10} - RT_P \log \frac{10}{3} = R (T_E - T_P) \log \frac{10}{3}$$

Assume that the difference in mean temperature between equator and pole is 30° C. Then the magnitude of the circulation at the end of 3 h

$$C = 11.2 \times 10^{11} \text{ cm}^2 \text{ sec}^{-1}$$

The length s of the curve is approximately 2×10^4 km. Hence the average velocity at the end of 3 h

$$V = \frac{C}{s} = 5.6 \text{ m per sec}$$

The accelerating force is still present, and V would continually increase but for two counteracting forces. As the velocity increased, the transport of the cold air to the equator and the heated air to the poles would also increase, and the temperature difference could not be maintained. The accelerating force then decreases proportionately to the decrease in the difference in temperature. Another force results from the retarding effect of friction. The computations assumed external forces zero, but such forces are actually present and the surface air moving toward the equator would be retarded by the friction between the air and the globe's surface. The velocity would not, then, increase indefinitely. On a non-rotating globe these forces would finally reach an approximate balance, with deviations being minor departures from the general circulation.

72. The Effect of the Earth's Rotation. The preceding section discussed the circulation that would develop on the earth if the sun revolved about the earth rather than the earth revolving on its axis. When the rotation of the earth is considered, another force is exerted on the moving particles of the atmosphere.

As explained in section 34, there is an apparent force acting on all particles moving over the earth's surface which tends to change the direction of motion to the right in the northern hemisphere, and to the left in the southern hemisphere. The force has no effect on the speed of the particles. In the discussion that follows only the northern hemisphere will be considered. A similar discussion would be true for the southern hemisphere, except that the directions mentioned would, at times, differ.

The magnitude of the force arising from the earth's rotation, called the deflecting or Coriolis force, is $2\omega \sin \phi V$, where ϕ is the latitude, and ω is the angular velocity of the earth. If, in the circulation discussed in section 71, the air particle starts in the upper air toward the north pole, it is not affected by the deflecting force immediately since at the equator the force is zero. But as the air advances northward, the deflecting force increases as ϕ increases, and, by the time that it has reached latitude 20° or 30° N, the motion will have a marked eastward component. At this latitude there is an accumulation of air which leads to a high-pressure region at the earth's surface. At the surface on the southern side of this high-pressure area the winds blow toward the equator, but

again they are affected by the deflecting force. Thus they become northeast winds, rather than northerly winds, and form the northeast trade winds shown in Figs. 5 and 6 of section 3. The high-pressure belt in the vicinity of 30° N, often referred to as the horse latitudes, is called the sub-tropical high.

A similar thermally produced circulation is found in the vicinity of the poles. The air subsiding as a result of cooling in the lower layers at the poles moves toward the equator in diverging currents. These northerly winds are deviated to the right by the deflecting force as they advance southward, and thus become east winds. When the air motion is in this direction the deflecting force and the pressure gradient force balance and the motion is steady. The air slowly becomes heated and rises, returning aloft to the pole.

On the northern side of the sub-tropical high-pressure belt the winds blow from west to east, giving the westerlies of the temperate zone.

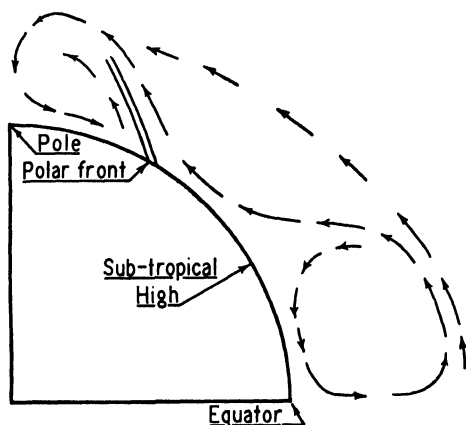


FIG. 75. Longitudinal cross section of the atmospheric circulation on the earth.

Near the surface, the slow movement of the air across the isobars results in a northward flow of air which transports the heat of the equatorial regions toward the poles. At the northern edge of the temperate zone it meets the polar air moving westward. A low-pressure trough forms at the junction of these two currents. At times the warm moist westerly current rises over the colder polar air, giving widespread precipitation. The warm air now continues northward at high levels to

subside over the poles. The accumulation of air there which would result from this transport of air in a northward direction is prevented by occasional outbreaks from the polar high which carry the surplus air southward into the region of westerlies, and so down to the sub-tropical high-pressure region. A diagram of the general circulation, showing the above features on a vertical section of one-quarter of the earth, is given in Fig. 75. The wind distribution at the earth's surface is given in Figs. 5 and 6, section 3.

The foregoing discussion attempts to describe and explain the circulation of air that is observed upon the earth. That this attempt leaves

something to be desired is well understood by the authors. There has been as yet no completely satisfactory exposition of certain of the major features of the general circulation. Why do the sub-tropical high-pressure belts occur at about 30° from the equator? Precisely how does the air which gradually moves from the equator to the poles find its way back again to the equatorial regions? Why is the circulation from equator to pole divided into three cells? These and other questions still await a satisfactory answer from meteorologists.

73. The Influence of the Land Masses. On a globe with a uniform surface the effect of the apparent movement of the sun north and south with the seasons, which occurs as a result of the inclination of the earth's axis, would not be pronounced. The heat equator, and so the equatorial low-pressure region, would follow the sun slowly, and the major centers of pressure would move in the same direction. The polar high would decrease in intensity during the summer as a result of the large amount of heat that is received during the polar day. At the other end of the globe's axis, the long, cold, polar night would intensify the high-pressure region there. This describes to a large extent the seasonal changes which actually occur in the southern hemisphere, since there are no large land masses there to modify appreciably the general circulation.

An anomaly exists in the southern hemisphere in that the air of the Antarctic continent contains less oxygen than the air over the remainder of the earth (see section 5). This fact suggests that the exchange of air between that continent and the surrounding area is small. The sub-polar low-pressure trough of the southern hemisphere coincides closely with the boundary of that continent. This trough, then, would be the outer limit to a closed polar circulation. The air that moves slowly across the isobars from the sub-tropical high must return to tropical latitudes without penetrating this great polar cell.

The same conditions do not exist in the northern hemisphere. It appears likely, then, that the southward-moving outbreaks of air across the continents, which extend almost to the pole, permit a complete mixing of the air near the north pole and the air from more southerly regions.

In the northern hemisphere the proportion of land and sea is more nearly equal, and both land and water masses extend from the tropical regions to the Arctic. There is a difference in the heating effect of the sun on sea and on land. Both the specific heat and the conductivity of soil are lower than for water, and as a result the heat absorbed produces a greater increase in temperature in the surface layers of soil than in those of water. Thus in summer the water is cool relative to the land. The air above the water is cooled, and the high-pressure areas over the

oceans are intensified in this manner. Over the land the heat gained by the air from the warm surface causes the air to expand, so that there is a smaller mass of air over a given area, resulting in a decrease in the surface pressure. For these reasons, the sub-tropical high-pressure belt does not extend continuously around the earth in summer, but becomes indistinct over the heated continents, and more extensive and pronounced over the ocean areas. Meanwhile the sub-polar lows become prominent and develop over the land areas. The low over Asia is especially marked. The circulation about this low, moving counter-clockwise, gives the monsoon, an extensive flow of air from the Indian Ocean over India, and from the Pacific over China (see Fig. 5, section 3). The low over North America is not quite so prominent; yet the mean winds for the summer months show a definite monsoonal effect.

During the winter the difference between land and sea is reversed. The snow surface over the northern portions of the continents reflects most of the incident solar radiation since the albedo of snow is high (section 28). On the other hand, the loss of heat by long-wave radiation from the earth's surface is pronounced, and since the conductivity of snow is very small, a large fall in temperature of the snow surface is the result. The air just above is in turn cooled. (Note the crowding of the isotherms over the land areas in winter, Fig. 2, section 1.) When the surface water loses heat by long-wave radiation, it is replaced by warmer waters from below, and the oceans remain relatively warm. As a result high-pressure areas develop over the continents and the sub-tropical highs become less extensive over the oceans. In the region of 60° N the sub-polar low becomes prominent over the oceans, appearing as the semi-permanent Aleutian and Icelandic lows during the winter (see Fig. 6, section 3). The monsoon circulation becomes predominant over Asia, but now the air motion is clockwise about an extensive high-pressure system, and the winds blow from the land over the water, giving cold, dry winds during the winter season.

Aloft these features are less noticeable. The continental highs and the polar high of winter have disappeared at the 2 km level, but the sub-tropical high may still be detected. The general trend of the isobars is in concentric circles about the low-pressure area at the pole. During the summer the continental lows extend to greater heights than their winter counterparts, the anticyclones, but have disappeared by 4 km. Above that height the polar low and the remnants of the sub-tropical highs are the chief features of the pressure distribution.

74. Air Masses and Their Source Regions. In the center of a high-pressure system, such as the Azores high, the air subsides slowly, and the winds are light. The underlying surface is water having a nearly

uniform temperature over extensive areas. As the air subsides, that near the surface will assume a uniformity of properties as it comes in contact with the water surface below. These properties will be transferred upward through turbulent and convective eddies. The result is that the air throughout the anticyclone is nearly uniform in any horizontal layer, and these properties change in all vertical columns at about the same rate.

When, after having acquired the properties of a region, part of the air flows to other regions, it retains for a certain period of time its former characteristics. It can be identified, and its trajectory can be inferred from these. This traveling anticyclone, or portion of one, is called an *air mass*, and the region from which it derived its properties is called its *source region*. Adjectives are added to the term air mass to describe some of the most prominent characteristics of each. Thus the terms equatorial, maritime, and polar are a few of those used to describe different types.

As suggested above, the traveling air mass must be extensive, with uniform or nearly uniform properties in the horizontal. If a true air mass is to develop, the underlying surface must be uniform, and the air must be stagnant over it long enough to assume the characteristics of the source region.

The principal source regions are the areas where pronounced anticyclones develop, as described in sections 3 and 73. The source region for a tropical maritime air mass in the northern hemisphere is either the Atlantic or Pacific Ocean, in the vicinity of latitude 30° N, where the sub-tropical highs occur. That for a tropical continental air mass is the Sahara Desert. An Arctic type of air develops over the Arctic and Greenland high-pressure regions. In winter, polar continental air masses develop in high-pressure systems over Siberia and northwest Canada.

An area of the earth's surface may be so large and so uniform in its properties that a body of air traveling over it becomes modified until it takes on definite properties characteristic of the surface. It is also described as an air mass. Such regions having sufficiently uniform characteristics are located in the north Pacific and northeast Atlantic oceans. Moving over these regions, a body of air may become modified to a point where it can be described as a polar maritime air mass. The same process takes place over polar continental regions during the summer, producing summer polar continental air masses. A third region of modification is on the southern edge of the sub-tropical high, where air masses to which the term "equatorial" is applied form.

Chapter 15 describes the air masses from the several source regions

that affect North America and Europe. The air masses of the southern hemisphere have not been the subject of study to the same degree as those of the northern hemisphere. Nevertheless, similar considerations would permit some of the conclusions about source regions and air mass types given in this section and in Chapter 15 to be applied to the region south of the equator.

BIBLIOGRAPHY

- Brunt, D., *Physical and Dynamical Meteorology*, London, Cambridge University Press, 1939. Chapter 19.
- Haurwitz, B., *Dynamic Meteorology*, New York, McGraw-Hill Book Co., 1941. Chapter 13.
- Petterssen, S., *Weather Analysis and Forecasting*, New York, McGraw-Hill Book Co., 1940. Sections 63–72.
- Problems of Modern Meteorology*, London, Royal Meteorological Society, 1934. Number 2.
- Shaw, Sir N., *Manual of Meteorology*, London, Cambridge University Press. Vol. 2 (1936), Chapter 7.
- Bjerknes, V., and collaborators. *Physikalische Hydrodynamik*, Berlin, Verlag. Julius Springer, 1933. Page 680.
- Rossby, C.-G., in *Climate and Man*, 1941 Yearbook of Agriculture, Washington, U. S. Department of Agriculture, 1941. Pages 599–654.

CHAPTER 13

TEMPERATURE AND HUMIDITY IN THE ATMOSPHERE

75. The Temperature of the Air at the Earth's Surface. Any small mass of air, referred to for convenience as a particle of air, is subject to physical processes which tend to change its properties. It is desirable to study in detail these different processes and the changes resulting from them. The first property to be studied is the temperature of a particle of air near the surface of the earth.

Radiation is one process which causes wide variations in the surface air temperature. There are two ways in which radiation may act to cause a variation in properties. During the daytime the short-wave radiation from the sun, sometimes referred to as insolation, passes through the earth's atmosphere with very little absorption, as indicated in section 28, and thus without appreciably warming it. The surface of the earth absorbs a large fraction of this radiation, and radiates it as long-wave radiation. The incoming short-wave radiation, especially on a clear day, is greater than the outgoing long-wave radiation, so the temperature of the ground increases. Consequently the temperature of the air in contact with the ground also increases. During the night, on the other hand, there is no insolation, and when the sky is clear the ground cools by means of long-wave radiation to outer space, as explained in section 29. The air in the lower layers which has been in contact with the ground will therefore cool.

Insolation and nocturnal radiation may produce marked variations. Fig. 76 shows typical variations of temperature with height, i.e., *lapse rates*, during the day and night. The type of lapse rate usually found during the daytime is shown by curve (a) of Fig. 76. There is a more or less steady decrease in temperature with height, which on the average amounts to 6° or 7° C per km. During a cloudless night, when the wind velocity is not high, the surface of the ground cools by means of nocturnal radiation, and the temperature of the air just above also decreases. This cooling may be sufficient to produce near the surface an *isothermal layer*, i.e., a layer in which there is no variation in temperature with height, or an *inversion*, a condition where temperature increases with height. An inversion in the lower levels is shown by curve (b) of Fig. 76. The degree of inversion which may develop in any given

region depends on a large number of local features and conditions. During the night, therefore, the temperature of the surface air may show

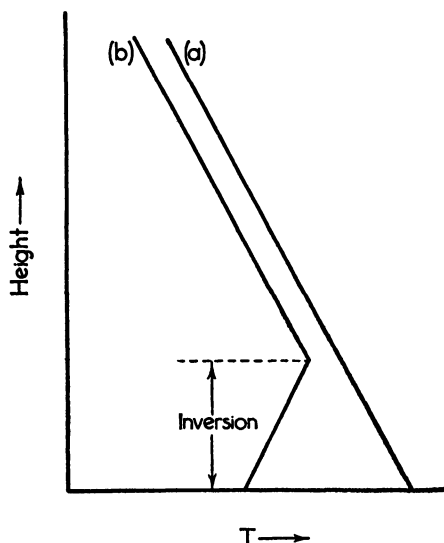


FIG. 76. Temperature variations with height of the air near the earth's surface.

wide variations in a given air mass. In these ways radiation causes the temperature of the surface air to change.

The processes of evaporation and condensation sometimes cause a change in temperature. Evaporation of water from water or moist earth surfaces requires heat. If the source of this heat is the water or ground, the evaporation will not cause any appreciable change in the temperature of the air. This is the usual situation because of the large thermal capacity of the water or moist ground compared with that of air. If the supply of heat, though, were to come from the air, cooling

would take place. Conversely, condensation supplies heat. Thus if the air cools, as, for example, by radiation, to the point where some of the water vapor condenses, the latent heat of condensation is released. Thereafter the rate of decrease of temperature is retarded.

At the earth's surface mixing of air of different temperatures occurs as, for example, in coastal regions. The resulting temperature will be a weighted average of the two original temperatures.

76. Temperature in the Free Air. Above the lowest layers the direct influence of the earth's surface on the temperature is not present. Insolation, which passes with little absorption through the atmosphere, according to section 28, imparts to it a very small amount of energy. As indicated in section 29, the water vapor in any given layer of air absorbs long-wave radiation from the earth's surface and from other layers. The water vapor in the layer also radiates energy, and since under average conditions the energy radiated is always greater than that absorbed, a decrease in temperature results.

This exchange of energy is illustrated by the diagrams of Fig. 77. These give, considered separately and then together, the rate of heating by the absorption of solar radiation, and the rate of cooling resulting from terrestrial radiation processes as computed by Möller for the air

over Lindenberg. From Fig. 77a it is seen that with clear skies the net result is a decrease in temperature of approximately 1°C per day. With cloudy skies, condensation of water vapor supplies heat to the atmosphere, the effect of which is allowed for in the balance illustrated in Fig. 77b. Here, too, the net result is a gradual cooling except in the lowest 3 km. More recent data on the absorption of terrestrial radiation in the atmosphere will change the numerical values on which these

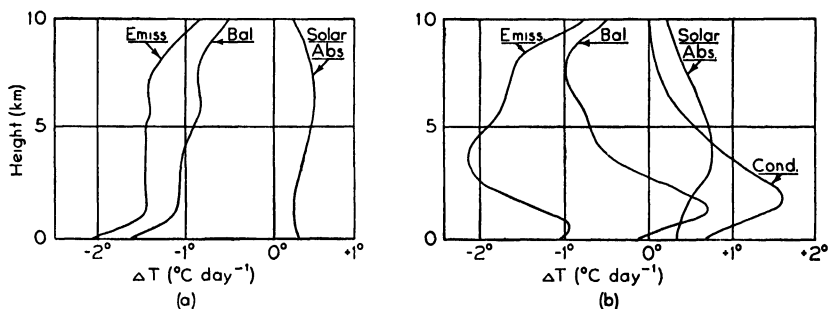


FIG. 77. The loss and gain in energy in the free atmosphere (a) with clear skies, (b) with cloudy skies. (After Möller.)

figures are based. Nevertheless the final result will differ only in degree from that illustrated. The net cooling resulting from radiation in the atmosphere is a function of the water vapor content. In the troposphere when the sky is clear, it varies from 2° to 3°C per day in air from polar regions to about 1°C per day in air from the tropics. The effect of insolation during the day and terrestrial radiation at night is to produce a large diurnal variation of temperature of the earth's surface. The air from the surface to about 1 km experiences a similar variation, since heat is transported in the vertical by turbulence. During the day, then, there is an increase in temperature in the lower layers and a slight decrease at higher levels. During the night the temperature at all levels decreases, but the cooling at upper levels is small compared with that just above the surface of the earth. The gradual cooling by radiation at the upper levels is in part compensated for by a transfer of energy from the surface layers by means of rising currents of air.

In the free atmosphere evaporation takes place from water droplets. The heat content of these is insufficient to supply the latent heat of vaporization required. This heat comes from the surrounding air, cooling it. The opposite process of condensation, which takes place in the formation of clouds, heats the air by releasing the latent heat of condensation.

In the free atmosphere the air particles do not always remain at the

same level. If the change in level occurs without transfer of energy to or from the environment, i.e., adiabatically, the ascent and descent of air cause large changes in free air temperature. As long as the air remains unsaturated, the variation of temperature with pressure is given by equation 13.2

$$T = T_0 \left(\frac{p}{p_0} \right)^\kappa$$

where T = the temperature of the air at pressure p .

T_0 = the temperature of the air at initial pressure p_0 .

$\kappa = AR/c_p = 0.288$.

The temperature variation with ascent or descent given by a slightly modified form of this formula is known as the *dry adiabatic lapse rate*, Γ , and amounts to approximately 1°C per 100 m, or 5.4°F per 1000 ft, as shown in section 14.

If the ascent of the air continues beyond the saturation point, water vapor condenses, and the latent heat of condensation is taken up by the air, warming it. The temperature of the ascending air then decreases at the *saturated adiabatic lapse rate*, Γ' , which is discussed in section 20. The saturated adiabatic lapse rate is not constant, as the dry adiabatic lapse rate is, but shows wide variations. At high temperatures, where the water vapor content of saturated air is great, the saturated adiabatic lapse rate is much less than the dry adiabatic, being only about 0.4°C per 100 m. The water vapor content is small at low temperatures, and consequently the amount of latent heat released with ascent is small. The saturated adiabatic lapse rate is therefore very nearly equal to the dry adiabatic under such conditions. Actual values at various pressures and temperatures may be seen in the table in section 20.

One phenomenon of nature can be explained by the difference between the dry and the saturated adiabatic lapse rates. When moist air flows up the side of a mountain range, the temperature drops at the dry adiabatic lapse rate until it becomes saturated, and after that at the saturated adiabatic. After saturation, part of the water vapor which condenses falls as rain or snow. When the air, which has lost much of its moisture during ascent, subsides on the other side of the mountain, the temperature rises at the dry adiabatic lapse rate after the clouds have evaporated. Because of the difference between the two lapse rates, the air on the lee side of the mountain will be warmer than it was at the same level on the windward side. The extent of the increase will depend on the temperature and moisture content of the air initially, the height to which it is lifted, and the fraction of liquid water precipi-

tated. With a lift of 8000 ft the increase will amount to about 10° F under average conditions. This phenomenon occurs on the southern side of the Alps, producing the Föhn winds of northern Italy, and on the eastern side of the Canadian Rockies, producing the Chinook winds which warm the prairie provinces. Less famous examples of the same phenomenon are found in other regions.

Turbulent mixing in the vertical may produce large temperature changes in an air mass. According to (53.11), the net upward flux of heat across a horizontal unit area in unit time is

$$-K\rho c_p(\Gamma - \alpha),$$

where K = a quantity denoting the intensity of the turbulent motion, known as the coefficient of eddy diffusivity.

ρ = the density of the air.

c_p = the specific heat of dry air at constant pressure.

α = the lapse rate of the environment.

It can be seen from this formula that the flow of heat which is due to eddy motion is downward if $\alpha < \Gamma$, and upward if $\alpha > \Gamma$. It therefore follows that the effect of vertical mixing is always to make the actual lapse rate more closely approach the dry adiabatic if the air is unsaturated, or the saturated adiabatic if the air is saturated. The only case where vertical mixing causes no change in temperature is that in which the actual lapse rate is equal to the dry adiabatic. For all other lapse rates the free air temperature changes with vertical mixing processes. As long as the air remains unsaturated the changes in water vapor content of the air mass resulting from mixing do not appreciably affect the temperature.

77. Conservative and Representative Properties. In the last two sections the physical processes of radiation, evaporation and condensation, ascent and descent, and turbulent mixing have been studied with respect to air temperatures. In general, as a result of these processes, the temperature changes. However, there are exceptions to this generalization. For instance, if the heat of vaporization during evaporation is supplied by an outside source, the temperature remains constant.

The term *conservative* is applied to any property which remains constant when the body is acted upon by some process. Thus the temperature of an air particle is conservative with respect to evaporation when the heat of vaporization is supplied by an outside source. In the air the magnitude of all properties changes slowly, so conservatism in the air is relative. If the magnitude of the property remains constant within the range of error of the observation for a period of 12 h at the

earth's surface, or from 24 to 48 h in the free atmosphere, it is said to be conservative.

To be of value a property must be not only conservative but also representative. A *representative* property is one which characterizes an extensive region of the atmosphere adjacent to the point of observation. For example, the temperature at any level in a uniform air mass is representative. On the other hand, the temperature at the surface below a nocturnal inversion varies with the cloudiness and wind and so cannot be considered a representative property.

Conservative and representative properties are useful in analyzing and classifying various masses of air. In the succeeding sections of this chapter the different properties of an air particle will be defined and discussed and their conservatism or lack of it determined under the influences mentioned above.

78. Lapse Rate and Stability. It was indicated in sections 14 and 20 that the lapse rate of an air column and its stability are closely related. It will be shown in Chapter 15 that each air mass has a representative lapse rate. When adiabatic ascent or descent of a layer occurs, the lapse rate changes but not rapidly, as shown in section 16. Similarly, since cooling by radiation takes place throughout the column, the lapse rate does not change appreciably above the surface layers. The intensity of turbulence varies inversely with the stability of the air, so that stable lapse rates in the free air change only very slowly, since the amount of turbulence is small. In an unstable layer the turbulence is marked and tends to change the equilibrium to the neutral type. The most rapid change takes place near the surface of the earth. In general, since the lapse rate changes but slowly, it is relatively conservative, and so is frequently used in identifying air masses.

79. Diurnal Temperature Variations. In Fig. 78, curve (a) represents the temperature variation with height in a column of air which is nearly in neutral equilibrium, and curve (b) represents that in a column of air which has great stability. The dotted lines represent the dry adiabatic lapse rate. If these two curves represent the lapse rates in two different air masses in the early morning, then after the sun rises insolation will increase the temperature of the earth's surface and hence that of the air just above. When the lapse rate becomes greater than the dry adiabatic, the air becomes unstable (section 14) and vertical currents develop which readjust the temperature distribution. Thus as long as the surface temperature is increasing, the lower layers will have a lapse rate close to the dry adiabatic.

Assume that the surface temperature increases by the same amount for the two columns. The limiting dry adiabatic line will intersect the

original curve at a higher level for the unstable column than for the stable column. A thicker layer of air must then be heated in the unstable column for the same increase of surface temperature, requiring the input of more energy. Or, if equal amounts of energy are available, the surface temperature will rise farther in the stable column than in the unstable column, but the increase will extend to a greater height in

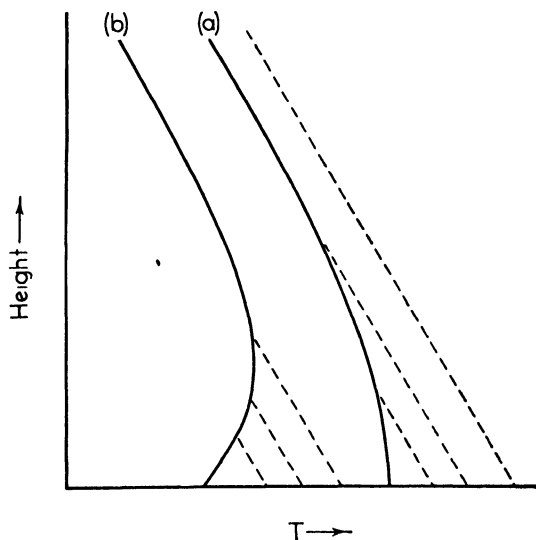


FIG. 78. Temperature increase through insolation.

the unstable column of air. An additional increase of the surface temperature, after the early morning rise, requires the heating of a thick layer and so the input of a large amount of heat. Therefore the maximum temperature for the day varies little from day to day in the same air mass when the sky is clear, but differs from one air mass to another. The maximum temperature is then a representative and conservative property.

The cooling at night is decreased by a cloud cover, and the daily range of temperature is consequently small. But even with clear skies, the minimum temperature varies with the location. A thermometer in a hollow into which cold air from nearby slopes drains readily, and in which the wind cannot keep the air stirred, will register a lower minimum temperature than one in a more exposed location. Thus the minimum temperature and so the range of temperature are neither representative nor conservative properties of an air mass, but they vary with local conditions.

80. Potential Temperature. The potential temperature of a mass of air is defined as the temperature which that air would attain if brought dry adiabatically to a standard pressure, usually 1000 mb. By referring to equation 13-5, it is seen that the temperature corresponding to the standard pressure 1000 mb, i.e., the potential temperature θ , is given by

$$\theta = T \left(\frac{1000}{p} \right)^\kappa$$

The equation shows that the potential temperature of a given mass of air is a function of its temperature and pressure. It is therefore not conservative with respect to radiation, evaporation (except when the heat of vaporization comes from an external source) and condensation, and turbulent mixing (heat) processes, since the temperature of the air is changed by all these. But dry adiabatic ascent and descent are reversible processes, and hence it follows that, as long as there is neither evaporation nor condensation, the temperature of a specified air particle brought adiabatically to 1000 mb will always be the same, no matter how much or how often the air ascends or descends before reaching that pressure. If that condition is fulfilled, therefore, ascent and descent produce no changes in the potential temperature (see section 13). Any change in water vapor content resulting from turbulent mixing will produce no significant variation in the potential temperature.

81. Water Vapor Content. There are four methods by which the amount of water vapor in the atmosphere may be expressed.

Absolute humidity, a , is defined as the mass of water vapor per unit volume of air. Its value is, according to (10-6),

$$a = \epsilon \frac{e}{RT} \text{ gm per cm}^3$$

where $\epsilon = 0.622$.

e = the vapor pressure in dynes per cm^2 .

If e is expressed in millibars, then

$$a = 217 \frac{e}{T} \text{ gm per m}^3 \quad (81.1)$$

The absolute humidity is not at all conservative, since all the processes listed in section 77 may produce large variations in either e or T . This measure of atmospheric humidity has therefore a limited use in meteorology.

Specific humidity, s, may be defined as the mass of water vapor per unit mass of moist air. From equation 10-10, it is seen that

$$s = \epsilon \frac{e}{p - (1 - \epsilon)e} \text{ gm per gm}$$

or

$$s = 622 \frac{e}{p - 0.378e} \text{ gm per kg}$$

Since the specific humidity is a ratio between two masses, neither of which is changed by a change in temperature, it is conservative for those processes involving a variation in temperature. It is not, though, conservative for those changes involving a change in water vapor content, i.e., for evaporation and condensation and turbulent mixing processes. Specific humidity thus finds a wide use in meteorological analysis.

Humidity mixing ratio, x, is the mass of water vapor per unit mass of dry air. It can be expressed by the equation 10-8

$$x = \epsilon \frac{e}{p - e} \text{ gm per gm}$$

or

$$x = 622 \frac{e}{p - e} \text{ gm per kg}$$

The numerical difference between the values of the specific humidity and mixing ratio for any given particle of air is very small, and in practice the two are used interchangeably. The values of these elements are given with sufficient accuracy by the formula 10-11

$$x = s = \epsilon \frac{e}{p} \text{ gm per gm}$$

It follows from the foregoing, of course, that the mixing ratio has the same degree of conservatism and the same range of use as the specific humidity.

Relative humidity, f, is defined as the ratio of the actual vapor pressure to the saturation vapor pressure at the same temperature. Its value is given by the equation 10-7,

$$f = \frac{e}{e_s}$$

where e_s is the saturation vapor pressure at the given temperature. If the relative humidity is expressed as a percentage, the equation takes the form

$$f = 100 \frac{e}{e_s}$$

By combining (10·7), (10·11), and (10·12), it is seen that the relative humidity can also be expressed as the ratio of the actual specific humidity to the specific humidity of air saturated at the same temperature. The same relation holds if the mixing ratio is used instead of the specific humidity. Thus, the relative humidity may also be computed from the equation

$$f = 100 \frac{s}{s_s} = 100 \frac{x}{x_s} \quad (81·2)$$

where s_s and x_s indicate the values required for saturation.

Since the saturation vapor pressure is a function of temperature as shown by (21·4), and the actual vapor pressure may undergo changes as a result of evaporation, and of turbulent mixing processes, it follows that the relative humidity varies with all the processes considered in section 77. It is therefore not a conservative element, but nevertheless it has a wide range of use in many phases of meteorological theory and practice.

82. Dew Point. The dew point of a particle of air is the temperature to which the air must be cooled at constant pressure and constant water vapor content in order to become saturated. Either the saturation vapor pressure or the amount of water vapor per unit volume required for saturation, i.e., the saturation value of the absolute humidity, is a single-valued function of the temperature as given by the equation 21·4

$$e_s = 6.11 \times 10^{8.573 - \frac{2340}{T}} \text{ mb}$$

or by (81·1). Therefore the dew point is a single-valued function of the amount of water vapor per unit volume. For that reason, then, any process changing the amount of water vapor per unit volume changes the dew point. Thus the dew point of a particle of air is not conservative for evaporation and condensation, nor for turbulent mixing with air of a different water vapor content. It is, though, conservative for radiational heating or cooling to the point of saturation, or for turbulent mixing when the mixing masses of air differ only in temperature.

Changes of pressure cause variations in the vapor content of a given volume since the volume varies inversely with the pressure at constant

temperature, as shown by (7.6). Thus the dew point also changes. With ascent the mass of water vapor per unit volume decreases, lowering the dew point. This change with ascent is small, being about one-sixth the change of temperature under dry adiabatic conditions. The variation of dew point with height in adiabatically ascending air is given by (21.8).

Several types of thermodynamic charts used in the analysis of upper air data are described in section 22. One of the most widely used of these is the tephigram. This chart is shown in Fig. 17, section 22, and a full-scale copy is provided at the back of the book. In the tephigram the abscissa is temperature on a linear scale and the ordinate is entropy on a linear scale, which is equivalent, according to (18.7), to potential temperature on a logarithmic scale. The path of a particle of air moving dry adiabatically is then given by a horizontal line of the diagram. Lines of equal pressure slope upward to the right, and lines of equal saturation mixing ratio are dotted lines which are almost parallel to the isotherms but slope upward to the left. A fifth set of lines slopes upward to the left and gives the saturated adiabatic lapse rates.

On the tephigram the dew point of a particle of air can be found by noting the intersection of the constant-pressure line and the humidity mixing ratio line corresponding to the moisture content of the air. The temperature at this point of intersection is the dew point. For example, from the full-scale tephigram it is seen that the dew point of air with temperature 5°C , pressure 800 mb, and mixing ratio 2.5 gm is -9°C . There is no change in the moisture content of air rising dry adiabatically, and so the dew point will always lie on the same mixing ratio line. For this reason these saturation mixing ratio lines are frequently called dew-point lines. When the air has been lifted until the temperature and the dew point coincide, saturation is attained. The level at which this occurs is called the *condensation level*, or the *lifting condensation level* to distinguish it from another type of condensation level described later.

83. Wet-Bulb Temperature. The wet-bulb temperature of a given mass of air may be defined as the lowest temperature to which that air may be cooled by evaporating water into it. In practice it is measured directly by means of a ventilated wet-bulb thermometer as indicated in section 65. It is denoted by the letter T_w .

It has been shown by Normand that, to a high degree of approximation, the dry adiabat through the dry-bulb temperature, the saturated adiabat through the wet-bulb temperature, and the saturation mixing ratio line through the dew-point temperature all meet at a point. The proof of this proposition is given in section 24. This relationship is

shown on the tephigram given in Fig. 79 in which A represents the dry-bulb, D represents the wet-bulb, and B represents the dew-point temperature. The three lines intersect at C , the condensation level. Thus if any two of these quantities and the pressure are known, the other two may be obtained directly with the aid of an adiabatic chart such as the tephigram.

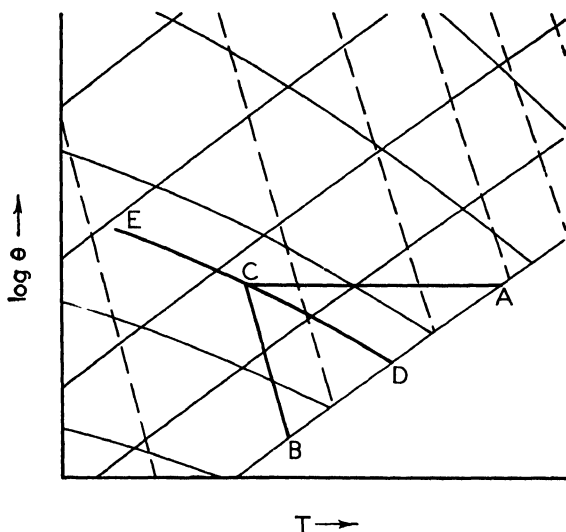


FIG. 79. Determination of the wet-bulb temperature.

This relationship is useful in many ways. For instance, if the temperature, pressure, and relative humidity of a mass of air are known, the wet-bulb temperature may be obtained readily from the tephigram. The saturation mixing ratio for the air is given by the saturation mixing ratio line through the dry-bulb temperature A on the tephigram. According to (81.2), the actual mixing ratio is found with sufficient accuracy by multiplying the saturation mixing ratio by the relative humidity expressed as a fraction. Proceed horizontally along the dry adiabat from A until the mixing ratio line corresponding to the actual mixing ratio is reached at C . Follow the saturated adiabat through this point until it meets the pressure line through A at D . The temperature at D is then the wet-bulb temperature of the air. For example, if the particle of air has pressure 950 mb, temperature 3°C , and relative humidity 60 per cent, the dew point is -4°C , and the wet-bulb temperature is 0°C . Because of the approximations in Normand's treatment, the value found in this manner is not exactly the same as the

actual reading of a wet-bulb thermometer in the air in question. However, the difference is so small that it may be considered negligible for all practical purposes.

The wet-bulb temperature changes if radiational cooling occurs. It follows from Fig. 80 that if the dry-bulb temperature decreases through radiational cooling from A to E , the condensation level will descend from B to F . Remembering the relationship between dry-bulb, wet-bulb, and dew-point temperatures as given by Normand, it can be seen that the wet-bulb temperature will decrease from C to G .

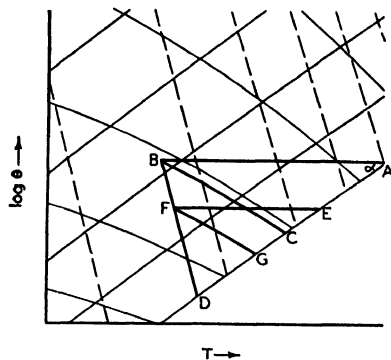


FIG. 80. Change of wet-bulb temperature through radiation.

The relationship between the decrease in dry-bulb temperature with radiational cooling and the corresponding decrease in wet-bulb temperature may be shown in the following manner.

In Fig. 80, EFD and ABD may be taken, with sufficient accuracy for present purposes, as similar triangles. Then

$$\frac{FD}{BD} = \frac{ED}{AD}$$

Triangles FDG and BDC are also similar, so that

$$\frac{FD}{BD} = \frac{GD}{CD}$$

Thus

$$\frac{GD}{CD} = \frac{ED}{AD} \quad \text{and so} \quad \frac{CD - GD}{CD} = \frac{AD - ED}{AD}$$

or finally

$$\frac{CG}{CD} = \frac{AE}{AD}$$

If α represents the angle BAD , then

$$\frac{(T_{w_1} - T_{w_2}) \sec \alpha}{(T_{w_1} - T_{d_1}) \sec \alpha} = \frac{(T_1 - T_2) \sec \alpha}{(T_1 - T_{d_1}) \sec \alpha}$$

where the subscript 1 refers to initial values, and the subscript 2 refers

to values after the radiational cooling has taken place. Thus

$$T_{w_1} - T_{w_2} = \frac{T_{w_1} - T_{d_1}}{T_1 - T_{d_1}} (T_1 - T_2) \quad (83.1)$$

The fraction $(T_{w_1} - T_{d_1})/(T_1 - T_{d_1})$ is a constant for any given situation. The value of this fraction for surface pressures is approximately 0.4 at 20° C, 0.6 at 0° C, and 0.9 at -20° C.

It follows from the definition given at the first of this section that the wet-bulb temperature is invariant for processes of evaporation and condensation. For if the evaporating is done in two or three stages, as suggested in section 24, it can be seen that the wet-bulb temperature does not change during the process. The air can still be cooled only to the same temperature, so the wet bulb must remain the same.

Using a method similar to that above, the change of the dew point during evaporation can be related to the change in temperature. Referring to Fig. 81, the initial temperature, condensation level, wet-bulb temperature, and dew point are denoted by A, B, C, and D respectively.

FIG. 81. Change of dew point with evaporation.

After the process of evaporation postulated has occurred, they are denoted by E, F, G, and D respectively. Using similar triangles as before, it follows that

$$\frac{CG}{CD} = \frac{EC}{AC}$$

and so

$$\frac{GD}{CD} = \frac{AE}{AC}$$

If α indicates angle BAD, then the increase in dew point resulting from the evaporation is given by

$$\frac{(T_{d_2} - T_{d_1}) \sec \alpha}{(T_{w_1} - T_{d_1}) \sec \alpha} = \frac{(T_1 - T_2) \sec \alpha}{(T_1 - T_{w_1}) \sec \alpha}$$

or

$$T_{d_2} - T_{d_1} = \frac{T_{w_1} - T_{d_1}}{T_1 - T_{w_1}} (T_1 - T_2) \quad (83.2)$$

The fraction is constant for any one situation. Its value for surface pressures is approximately 0.6 at 20°C , 1.5 at 0°C , and 6 at -20°C .

Normand's treatment brings out the fact that the wet-bulb temperature varies at the saturated adiabatic lapse rate as air ascends or descends. Thus if air originally at a pressure of 1000 mb ascends to the condensation level, the wet-bulb temperature, as indicated in Fig. 79, will decrease from D to C . At C the dry-bulb, wet-bulb, and dew-point temperatures coincide, and with further ascent all three move along the same saturated adiabat, CE . For example, if air with $p = 800$ mb, $T = 10^{\circ}\text{C}$, $T_w = 4^{\circ}\text{C}$, $T_d = -2^{\circ}\text{C}$ ascends, it can be seen from the tephigram that the condensation level is reached at

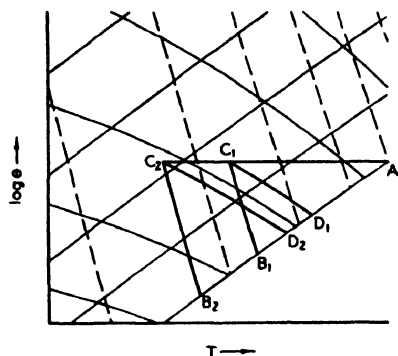


FIG. 82. Change of wet-bulb temperature with change in moisture.

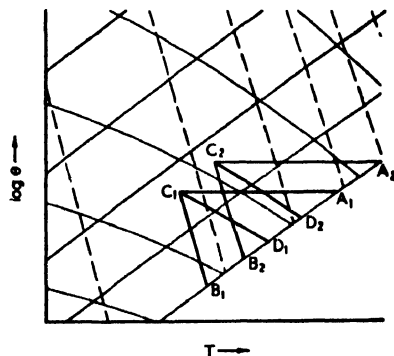


FIG. 83. Changes in dry-bulb, wet-bulb, and dew-point temperatures with turbulent mixing.

a pressure of 670 mb, and if ascent continues to a level where the pressure is 500 mb, the three elements are identical at this level, being -19.5°C . It is therefore obvious that wet-bulb temperature is not a conservative property in processes which involve ascent and descent of the air.

The result of temperature changes caused by turbulent mixing of different air masses is exactly the same as that caused by radiational heating and cooling, provided the actual moisture content does not change with the mixing. The corresponding changes in wet-bulb temperature are therefore also the same and may be seen from Fig. 80. If there is a change in water vapor content with the turbulent mixing, but no change in temperature, the type of variation is shown in Fig. 82. A decrease in mixing ratio was the result of turbulent mixing, the dew point decreasing from B_1 to B_2 , and the wet-bulb temperature decreasing from D_1 to D_2 .

Turbulent mixing usually, however, results in changes in both temperature and moisture content. In Fig. 83 the dry-bulb temperature increases from A_1 to A_2 , and the dew point increases from B_1 to B_2 . Under these conditions, the wet-bulb temperature increases from D_1 to D_2 .

Wet-bulb temperatures may be used very conveniently in conjunction with dry-bulb temperatures in the analysis of upper air data, as on the tephigram. The advantages of the use of this element are discussed in the next chapter.

84. Wet-Bulb Potential Temperature. The wet-bulb potential temperature of an air mass, denoted by θ_w , is defined as the wet-bulb temperature of that air when brought adiabatically to a standard pressure, usually 1000 mb (see section 24).

It was indicated in the previous section that the wet-bulb temperature of ascending or descending air changes at the saturated adiabatic lapse rate. The wet-bulb potential temperature is therefore obtained by noting the temperature at the point of intersection of the saturated adiabat through the wet-bulb temperature with the 1000-mb line. The various saturated adiabats on a tephigram are frequently specified by their corresponding wet-bulb potential temperatures, in the manner shown on the full-scale tephigram. For example, it may be found with the aid of the tephigram that air with $p = 700$ mb, $T = 3^\circ \text{C}$, and $f = 44$ per cent has a wet-bulb potential temperature of 14°C .

It follows by definition that wet-bulb potential temperature is conservative for processes of ascent and descent, even if condensation occurs during ascent. Like the wet-bulb temperature, it is also conservative for evaporation and condensation. It is not conservative for processes of radiation and transfer of heat and water vapor by turbulent mixing. These latter, however, are usually of secondary importance in the free air above the region of influence of surface friction. Thus wet-bulb potential temperature is one of the most conservative elements which may be used in the analysis of upper air data.

85. Equivalent and Equivalent Potential Temperatures. According to section 25, the equivalent temperature T_e is the temperature of absolutely dry air whose wet-bulb temperature is T_w .

There are two methods of defining the equivalent temperature. The first defines it as the temperature attained if all the water vapor in the air is condensed, and the latent heat of condensation so released is added to the air, the whole process being carried out at constant pressure. The equivalent temperature is then given by the equation 25.2.

$$T_e = T_w + \frac{L_w x_{sw}}{c_p}$$

where L_w = the latent heat of condensation at temperature T_w .

x_{sw} = the saturation mixing ratio at T_w .

It can be seen that the second term on the right-hand side of the equation represents the increase in temperature resulting from the release of the latent heat of condensation.

It may also be defined as the temperature attained by a mass of air which ascends until all the moisture in the air condenses and is precipitated, and which then descends dry adiabatically to the original pressure. Thus in Fig. 84, air with dry-bulb temperature A and wet-bulb

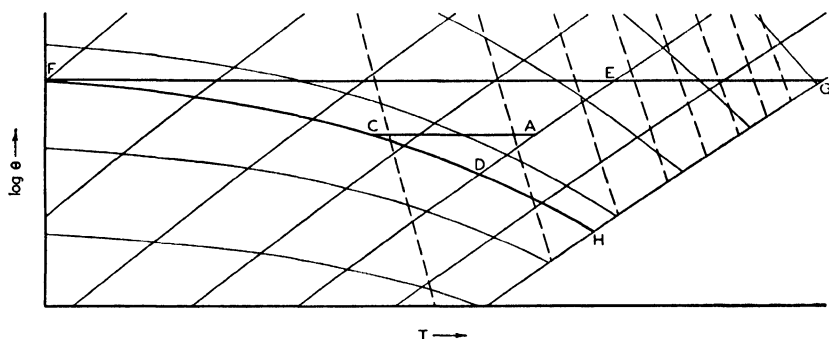


FIG. 84. Equivalent, equivalent potential, and wet-bulb potential temperatures.

temperature D ascends to the condensation level C . The air continues to ascend to F , the moisture condensing and being precipitated during the ascent. All the water vapor has been removed by the time the air reaches F , and it then descends dry adiabatically to the original pressure at E . The temperature at this latter point is then the equivalent temperature.

These two methods of definition give values of T_e which are ordinarily very nearly the same. For example, consider air at 900 mb pressure, with dry-bulb temperature 4°C , and relative humidity 80 per cent. Substituting appropriate values in the equation 25.2 gives

$$T_e = 15\frac{1}{2}^\circ\text{C} \quad \text{approximately}$$

By using the other definition, and with the aid of the tephigram, the value obtained is

$$T_e = 16^\circ\text{C} \quad \text{approximately}$$

Different values are obtained by the two definitions because in one the removal of the moisture is assumed to be carried out at constant pres-

sure, whereas in the other the pressure and temperature vary greatly during the process.

It can be seen from Fig. 84 that the saturated adiabat through the wet-bulb temperature is asymptotic to the dry adiabat through the equivalent temperature, i.e., the equivalent temperature is a single-valued function of the wet-bulb temperature. It therefore follows that the equivalent temperature is conservative or non-conservative in exactly the same sense as the wet-bulb temperature is. Thus it is conservative for evaporation and condensation, but not for the other processes discussed in section 77.

The *equivalent potential temperature* θ_e (section 25) of an air mass may be defined as the equivalent temperature of that air if brought adiabatically to a standard pressure, usually 1000 mb.

There are several ways in which this property may be defined. The first defines it as the temperature attained if the air is brought dry adiabatically to a pressure of 1000 mb, then all the water vapor in the air is condensed, and the latent heat released in the process is added to the air, raising its temperature. From equation 13-5 it can be seen that the equivalent potential temperature may also be given by the equation

$$\theta_e = T_e \left(\frac{1000}{p} \right)^\kappa$$

The value of θ_e obtained will depend on which value of T_e is used. The values of θ_e obtained by using the two definitions of T_e are very nearly equal.

A value of θ_e may readily be found with the aid of the tephigram. As shown in Fig. 84, it is obtained by descending dry adiabatically from E to the 1000-mb line at G . In the example given, using $T_e = 16^\circ\text{C}$, the value of θ_e is 25°C .

It will be remembered that the value of the wet-bulb potential temperature may be obtained by noting the temperature at the point of intersection of the saturated adiabat through the wet-bulb temperature with the 1000-mb line, indicated by H in Fig. 84. Thus, since FH and FG are asymptotic, θ_e is a single-valued function of θ_w , and θ_e exhibits exactly the same degree of conservatism as θ_w . θ_e is therefore conservative for processes of ascent and descent, and evaporation and condensation, but not for radiation and turbulent mixing.

In actual practice θ_w is more convenient to use than θ_e . The former may be obtained from any adiabatic chart, whereas θ_e cannot be found at high temperatures if the pressure lines on the chart do not extend to values lower than 400 or 500 mb. Furthermore, θ_w values may be

obtained directly if the wet-bulb curve is plotted on a tephigram on which the saturated adiabats are appropriately labeled.

86. Summary of Degree of Conservatism of Properties. The results of the discussion of the comparative conservatism of properties outlined in the previous sections are summarized in the following table.

DEGREE OF CONSERVATISM OF VARIOUS PROPERTIES

Property Conservative for Processes of	Radiation	Evapora- tion and Condensa- tion	Ascent and Descent	Turbulent Mixing	
				Heat	Water Vapor
Dry-bulb temperature	No	No	No	No	Yes ¹
Absolute humidity	No	No	No	No	No
Specific humidity	Yes ¹	No	Yes ¹	Yes ¹	No
Mixing ratio	Yes ¹	No	Yes ¹	Yes ¹	No
Relative humidity	No	No	No	No	No
Potential temperature	No	No	Yes ¹	No	Yes ¹
Dew-point temperature	Yes ¹	No	No	Yes ¹	No
Wet-bulb temperature	No	Yes	No	No	No
Wet-bulb potential temperature	No	Yes	Yes	No	No
Equivalent tempera- ture	No	Yes	No	No	No
Equivalent potential temperature	No	Yes	Yes	No	No

¹ As long as condensation does not occur.

PROBLEMS AND EXERCISES

1. A particle of air has a mixing ratio of 3 gm per kg. By means of the tephigram, determine the difference between T and T_c . How much variation is there in this value for different original temperatures and pressures? Repeat the process for 1.5 gm per kg. How can the equivalent temperature of a particle of air, $T = 27^\circ \text{C}$, $p = 950 \text{ mb}$, $x = 15 \text{ gm per kg}$, be evaluated using the results obtained?

2. A mass of air with temperature T becomes stationary over a water surface of temperature T_1 . What changes will take place in T and T_w before equilibrium is reached? Consider this situation both when $T_1 < T_w$ and when $T_w < T_1 < T$.

3. Which of the properties of the surface air mentioned in the summary are conservative as air moves over a dry surface which has a temperature higher than that of the air?

BIBLIOGRAPHY

- Byers, H. R., *Synoptic and Aeronautical Meteorology*, New York, McGraw-Hill Book Co., 1937. Chapter 1.
- Petttersen, S., *Weather Analysis and Forecasting*, New York, McGraw-Hill Book Co., 1940. Chapter 1.
- Shaw, Sir N., *Manual of Meteorology*, London, Cambridge University Press. Vol. 2 (1936), Chapters 4, 5.

CHAPTER 14

STABILITY AND INSTABILITY

87. General Considerations. The conditions for stability of air are the same as those for a solid body. To illustrate these conditions, consider the result if a force is applied to a body. If the body is in stable equilibrium, it will return to its original position when the force is released; if in unstable equilibrium, it will move farther away from its original position; and if in neutral equilibrium, it will not change its position after the force is released. Thus a cube resting on a horizontal surface is stable, a cone balanced on its point is unstable, and a sphere on a horizontal surface is in neutral equilibrium. The complexity arising when the stability of air is considered is due partly to the compressibility of the gas, and partly to the variable amount of water vapor present in the atmosphere.

There are several assumptions involved in the treatment which is to be given in the following sections. One of the most important of these is the assumption that an ascending or descending mass of air may be thermally segregated from the surrounding atmosphere, so that there is no transfer of heat from one to the other. This assumption represents only a rough approximation to what happens in the atmosphere. Actually, of course, the motion is not truly adiabatic, since there must be some mixing between the ascending air and that air constituting the environment. It can therefore be seen that the temperature of vertically moving air does not change at exactly the dry or saturated adiabatic lapse rate. Furthermore, it follows that this mixing also produces changes in the actual lapse rate of the environment. No suitable method of allowing for this mixing has yet been developed, and so its effect cannot be taken into consideration directly. However, the error introduced by neglecting this factor is not usually great.

88. Conditions Required for Stability. The conditions for stable, unstable, or neutral equilibrium were found for dry air in section 14, for unsaturated moist air in section 15, and for saturated air in section 20. The results can be expressed briefly as follows. If the observed lapse rate is less than the adiabatic lapse rate, the air is stable; if greater, the air is unstable; and if equal to the adiabatic lapse rate, the air is neutral. For dry and for moist unsaturated air until saturation is reached, the

dry adiabatic lapse rate is to be used. For saturated air, the saturated adiabatic lapse rate is to be used. The conditions previously derived can be summarized as follows.

	FOR DRY AIR, OR MOIST, UNSATURATED AIR	FOR SATURATED AIR
Stable equilibrium	$\alpha < \Gamma$	$\alpha < \Gamma'$
Unstable equilibrium	$\alpha > \Gamma$	$\alpha > \Gamma'$
Neutral equilibrium	$\alpha = \Gamma$	$\alpha = \Gamma'$

89. The Stability of Moist, Unsaturated Air. When the possibility of saturation occurring in unsaturated air is considered, the question of its stability is much more complicated than for either dry or saturated air because the stability may depend not only on the vertical temperature distribution, but also on the vertical water vapor distribution. When a particle of moist but unsaturated air is lifted in the atmosphere, its lapse rate changes at the point of saturation. Before saturation the temperature falls at the dry adiabatic lapse rate, and after saturation the fall is at the saturated adiabatic lapse rate. Thus it is possible, when the lapse rate of the environment lies between the two adiabatic lapse rates, that a rising particle of air will be cooler than the environment for the first part of the ascent, but warmer than the environment at a higher point. Thus air may be stable if it undergoes only a small vertical displacement, but may become unstable for large vertical displacements.

This suggests three main headings under which the stability of unsaturated air may be discussed:

- (a) $\alpha < \Gamma'$, absolute stability.
- (b) $\alpha > \Gamma$, absolute instability.
- (c) $\Gamma > \alpha > \Gamma'$, conditional instability.

Since the least decrease of temperature with height in a particle rising adiabatically is Γ' , then when $\alpha < \Gamma'$ the particle will never be warmer than the environment, and the air can never become unstable. Similarly, when $\alpha > \Gamma$, the rising particle will always be warmer than its environment, and the air will be absolutely unstable. When the lapse rate is greater than the saturated adiabatic but less than the dry adiabatic, the stability is said to be of the *conditional* type, for the stability is conditional on the water vapor content. This type of stability will be discussed in considerable detail in the following sections.

90. Conditional Instability. Upper air observations plotted on a tephigram are shown in Fig. 85. Dry-bulb temperatures are shown by the curve *AHB*, and corresponding wet-bulb temperatures are indi-

cated by the broken curve CD . Consider now a particle of air at the surface, with dry bulb A and wet bulb C , and assume that it is given an upward displacement. The dry-bulb temperature decreases at the dry adiabatic rate, and the wet-bulb temperature decreases at the saturated adiabatic rate. The air becomes saturated on reaching E , and its temperature drops at the saturated adiabatic rate with further ascent. At point F the temperature of the ascending air is the same

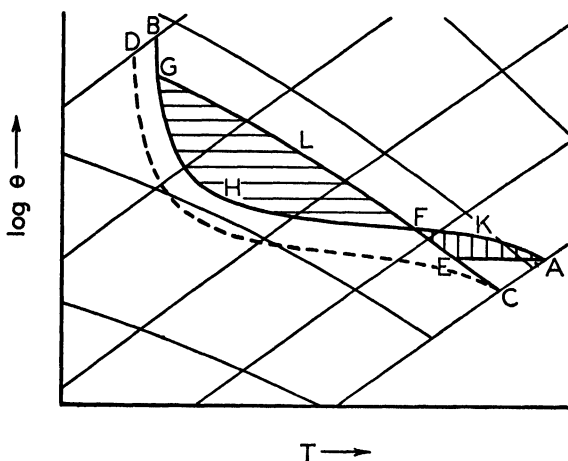


FIG. 85. Conditional instability.

as that of the environment. In the ascent from the surface to F , the rising air has, at each level, been colder than the surrounding air and therefore denser. It is clear, then, that energy from some outside source must have been supplied to move the air from the surface to F . The construction of the tephigram and of adiabatic charts in general is such that the amount of this energy is proportional to the area enclosed on the lower side by the line (AEF in Fig. 85) traced out by the rising air and on the upper side by the line (AKF in the figure) denoting the environment (see section 22). This area is shown by vertical hatching in Fig. 85. As the particle of air in question ascends to levels above F , it will be warmer and therefore less dense than the surrounding air. The ascent along the saturated adiabat will therefore continue until the temperature of rising air and environment become equal again, as at G . In this case, the energy necessary to move the mass of air from F to G is supplied by the environment itself and is proportional to the area $FHGL$, indicated by horizontal hatching in the figure.

Thus it can be seen that if the vertical displacement of the air by some outside agency does not carry it to a height as great as F , the air

will tend to sink back to its former position as soon as the displacing force is removed. In other words, the air is stable for small displacements. On the other hand, if the air is carried only a short distance above F by outside forces, it then ascends to greater heights by means of the energy supplied by the environment. Here the air is unstable for displacements to heights above F , i.e., for large displacements. Summarizing, it may be said that the air at the surface is stable for small displacements, but unstable for large displacements. This is a typical example of conditional instability.

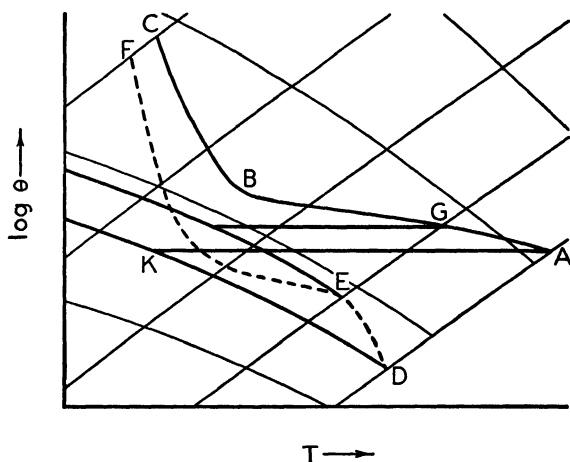


FIG. 86. Stable type of conditional instability.

91. Stable Type of Conditional Instability. If one defines conditional instability by saying that it exists if the actual lapse rate is intermediate in value between the dry and saturated adiabatic rates, there is one case included in this category in which instability cannot possibly occur. The air in such a situation cannot therefore be considered in any real sense to be conditionally unstable, since it is absolutely stable for all displacements. It has been called by Normand the *stable type of conditional instability*, although in rigorous terminology the adjective "conditional" would not be used at all. An example of this type is given in Fig. 86. The curve ABC shows the dry-bulb temperatures and the broken curve DEF gives the corresponding wet-bulb temperatures. Now consider that a parcel of the surface air is given an upward displacement. In the ascending air the dry-bulb temperature decreases at the dry adiabatic rate, and the wet-bulb at the saturated adiabatic rate, until the condensation level K is reached. Thereafter both decrease at the saturated adiabatic lapse rate. It can be seen from the

figure that the temperature of the rising surface air is less than that of the environment at all levels. The surface air is therefore stable for all displacements. If the air at each level is considered in the same manner, it can be seen that the air in the whole column is stable for all displacements, both large and small. Inspection of the curves shows that the air with dry-bulb temperature G and wet-bulb temperature E comes nearest to actual instability. The air which most closely approaches instability in this manner is always that which in the lower levels has the maximum wet-bulb potential temperature. It can readily be shown that the air with temperature G has the maximum value of θ_w .

The criterion for deciding whether the stable type of conditional instability is present or not is as follows: If no saturated adiabat through the wet-bulb curve cuts the environment curve at a higher level, the air is stable, even if $\alpha > \Gamma'$.

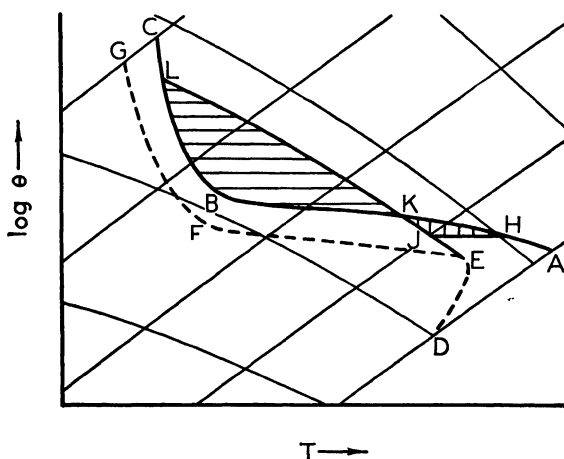


FIG. 87. Latent instability.

92. Latent Instability. Another type of conditional instability is known as latent instability. This type is illustrated in Fig. 87. The dry-bulb temperatures are represented by ABC , and the wet-bulb temperatures by $DEFG$. It can be seen that the surface air, with dry bulb A and wet bulb D , is stable, since the saturated adiabat through D does not cut the environment curve at a higher level, and ascending air will therefore always be cooler and denser than the surrounding air. But consider air with dry bulb H and wet bulb E . If this air is displaced to a height above K , in the manner outlined in section 90, it will then be warmer and less dense than the surrounding air, and will con-

tinue to rise until its density becomes equal to that of the environment at L . The energy which must be supplied from external sources is proportional to area HJK , while the amount of energy derived from the environment is proportional to area KBL , as shown in section 22.

Latent instability has been subdivided into two types:

- (a) Real latent instability, area $KBL >$ area HJK .
- (b) Pseudo latent instability, area $KBL <$ area HJK .

Where the area KBL is much greater than the area HJK , strong ascending currents will result from only a small input of energy from external sources. Thunderstorms frequently accompany such strong ascending

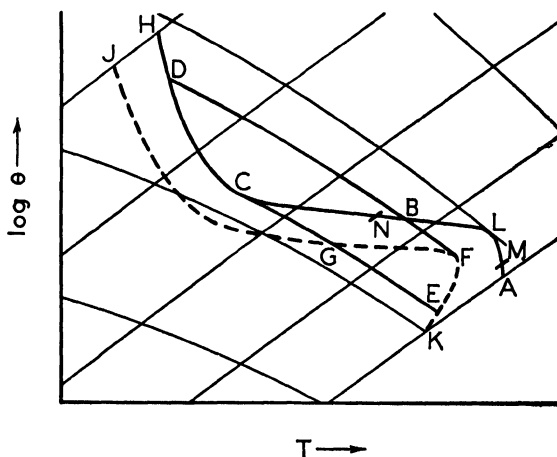


FIG. 88. Layer having latent instability.

currents. However, in pseudo latent instability, the initial input of energy required to bring the air to the point K is great. Such large amounts of energy from outside sources are rarely available, so that the air is, in effect, stable, and ascending currents rarely occur.

The presence or absence of latent instability is readily determined from the dry-bulb and wet-bulb curves plotted on a tephigram. Such curves are denoted by ACH and KGJ in Fig. 88. The saturated adiabat CGE tangential to the dry-bulb curve at C gives the layer in which latent instability exists. This layer, as can be seen from the figure, is that which has wet-bulb temperatures given by the curve EF , E and G being the points of intersection of the tangential saturated adiabat and the wet-bulb temperature curve below C . Thus particles of air in the layer MN between the pressures corresponding to points E and G are said to have latent instability. A paradoxical situation

exists in the portion ML of the layer MN , for particles of this layer are absolutely stable for small displacements according to the criterion of section 89; yet for large displacements the particles will realize latent instability. The saturated adiabat DBF tangential to the wet-bulb curve at F shows the layer which has *liability*, for it is in the layer BD that energy will be released to force the rising particles to ascend further.

The determination of the boundary between the layer showing real latent instability and that showing pseudo latent instability can be made only by trial and error. It is seldom important, though, for the greatest value to be derived from an analysis of the data comes from determining the presence or absence of real latent instability in the column, and so the probability of vertical currents.

93. Potential Instability. In the previous sections, one main type of stability has been considered, that of a particle in an undisturbed environment. Another main type, the stability of a particle of air immersed in a layer of air which moves as a whole, will now be examined. A particle of air might be described as a mass of air whose three dimensions are of the same order of magnitude. In the atmosphere, the dimensions of a particle are usually small, ranging up to lengths of perhaps two miles. In the case of a layer of air, however, the vertical extent of the mass is very much less than the horizontal extent. For example, a layer might be half a mile in thickness but might extend for a thousand miles in the horizontal. In the following treatment, the layer of air does not ascend or descend through an undisturbed environment, but the whole air mass, or a large section of it, ascends or descends. The air above and below the layer therefore undergoes the same vertical motion as the layer itself.

Consider a layer of air between 800 and 900 mb, whose dry-bulb temperature varies from A to B , and whose wet-bulb temperature varies from C to D , as shown in Fig. 89. There is, of course, air both above and below this layer, but in order to simplify the diagram its lapse rate is not shown. The air is unsaturated, and since the lapse rate is less than the dry adiabatic the air in this layer is stable. Now let the whole air mass ascend until the air which originally extended from 900 to 800 mb (layer AB) is saturated. It can be seen from the figure that the air in this example becomes saturated after an ascent of 200 mb. But the lapse rate is greater than the saturated adiabatic, and since the air is saturated, the air in that layer will be absolutely unstable as indicated in section 88. It is, however, not usual for the air at each level in the layer to become saturated after an ascent through the same pressure interval, such as 200 mb, as suggested in Fig. 89. The relative humidity at the base of the layer is often considerably

greater than that at the top, with the result that the air at the base becomes saturated before that at the top. Thereafter, with further ascent, the air in the lower portion of the layer cools at the saturated adiabatic rate, while the drier air near the top cools at the greater dry adiabatic rate. Hence the difference in temperature between bottom and top will become greater, and so instability will develop. The breakdown of the unstable layer will, in general, be accompanied by

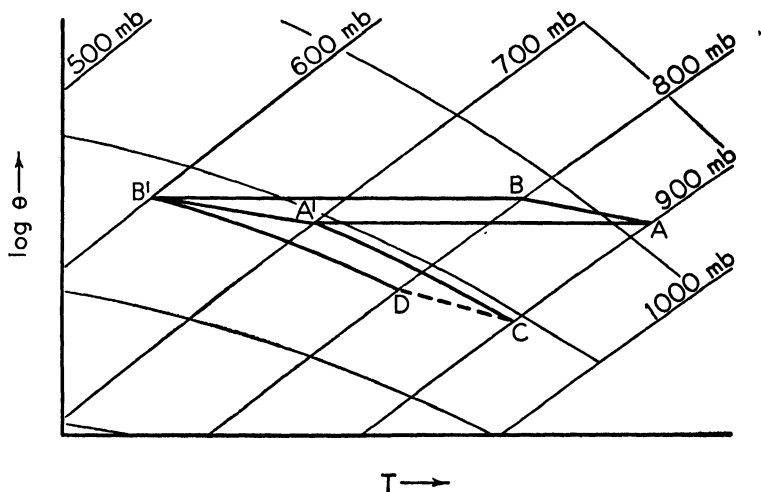


FIG. 89. Potential instability.

strong vertical air movements in the layer and in the air just above and below it. It can readily be seen from a study of several cases that if the lapse rate of wet-bulb temperature in a given layer is greater than the saturated adiabatic lapse rate, that layer will eventually become unstable if it is lifted far enough. Thus a layer may be said to have *potential instability* if the lapse rate of wet-bulb temperature in that layer is greater than the saturated adiabatic lapse rate. This type is sometimes referred to as convective instability.

Potential instability may also be realized by evaporation. If a potentially unstable layer lies under a warm frontal surface, then the evaporation from the falling rain drops will saturate the layer, cooling the air at each level in the layer to the appropriate wet-bulb temperature which will remain constant in the process. The lapse rate will then be greater than the saturated adiabatic and so the layer will be unstable.

As an example, consider the meteorological ascent in which the following values of pressure, temperature, and humidity were recorded.

Pressure	1000	900	800	700	600	mb
Temperature	15	12	6	2	-3	°C
Relative humidity	62	51	58	11	15	per cent

It will be seen after plotting the dry- and wet-bulb temperatures on a tephigram that there is potential instability in the layer from 700 to 800 mb. The air at 800 mb will become saturated after an ascent of 90 mb, while that at 700 mb must ascend 250 mb before reaching saturation. The realization of the potential instability will then commence in the lower part of the layer after an ascent of over 90 mb, but the potential instability of the whole layer will not be realized until it has ascended 250 mb.

94. The Relationship between Latent and Potential Instability. For latent instability to be present, a saturated adiabat through a point on the wet-bulb curve must intersect the dry-bulb curve at a higher level. When such a situation exists, it is necessary that the slope of the wet-bulb curve be greater than that of the saturated adiabat. Hence potential instability must be present in part of the air column.

The reverse situation need not be true. The wet-bulb curve may have, at times, a slope greater than that of the saturated adiabat, even though the air column itself is stable. So the presence of potential instability does not mean that latent instability is also necessarily present, although it often is.

These statements can readily be verified if a number of examples are plotted on the tephigram. For instance in the latter part of section 93 there is a numerical example in which potential instability is present, but without latent instability.

95. The Development of Potential and Latent Instability. Using again the criterion for potential instability, that the lapse rate of the wet-bulb curve must be greater than the saturated adiabatic lapse rate, it follows that any process raising the wet-bulb temperature in a lower layer while lowering it in a higher layer favors the development of potential instability. Any process raising the wet-bulb temperature in a lower layer while lowering the dry-bulb temperature at higher levels favors the development of latent instability.

It follows from section 83 that the wet-bulb temperature at lower levels rises under the following circumstances.

(a) It rises when heat is added to the air near the surface on a sunny afternoon through radiation and turbulent mixing.

(b) It always rises in the lower layers of an air mass which passes from a land surface to a water surface whose temperature is greater than the dry-bulb temperature of the air. If the temperature of the water surface lies between the dry- and wet-bulb temperatures of the

air, the wet-bulb temperature of the air near the surface first decreases, and then increases, becoming the same as that of the water surface when saturation is reached. The foregoing statement holds only if the dry-bulb temperature decreases to that of the water surface very rapidly, and the process of evaporation from the surface which produces saturation proceeds more slowly. The wet-bulb temperature is always higher when the final, steady state is reached. If the surface temperature of the water is less than the wet-bulb temperature of the air, the latter always undergoes a decrease.

(c) There is an increase in wet-bulb temperature in the lower layers of air moving over warm, moist soil, in exactly the same manner as if the air were moving over a water surface.

(d) If there is turbulent mixing of the air mass in question with a moister air mass of the same temperature there will be an increase in wet-bulb temperature of the former.

The dry- and wet-bulb temperatures of air at upper levels are lowered by means of advection of cold, dry air, usually from northern latitudes. Thus it can be said that, in general, a southerly wind at lower levels with a northerly one at upper levels favors the development of potential and latent instability, while reverse winds inhibit the development of these types of instability. Even in the situation where the velocity of a southward-moving current of air increases with altitude, potential and latent instability may result, since such a wind field will increase the lapse rate of an air column.

A second means of development of latent and potential instability is through the action of radiational cooling. The top of a cloud layer will lose the maximum amount of heat during the night, as shown in section 30, lowering both the dry- and wet-bulb temperatures, which at this point will be equal. This occurs frequently above the cloud bank above a warm front, giving rise to vertical currents and thunderstorms in the overrunning air at night.

There is another process which develops and increases latent instability, but not potential instability. This process is the ascent of a whole air mass, as in flowing over an extensive mountain range. Referring to Fig. 90, the dry-bulb temperature before ascent is given by *ABC*, while the corresponding wet-bulb curve is denoted by *DEF*. No saturated adiabat through the wet-bulb curve cuts the environment curve at a higher level, so that there is no latent instability present at this stage. Now assume that the whole column has ascended 100 mb, the dry-bulb temperature of the air originally at 1000 mb decreasing from *A* to *G*, and the corresponding wet-bulb temperature decreasing from *D* to *K*, and similarly with the air at higher levels. The dry-bulb

- (2) Latent instability: A saturated adiabat through the wet-bulb curve intersects the environment curve at a higher point.
- (i) Pseudo latent instability: The energy released by the moving particle is less than the energy necessary to move it to a point of instability.
- (ii) Real latent instability: The energy released by the moving particle is greater than the energy necessary to move it to a point of instability.
- (d) Potential instability: The lapse rate of the wet-bulb temperature is greater than the saturated adiabatic lapse rate.

PROBLEMS AND EXERCISES

The following tables give the values of the pressure p , the temperature T , and the mixing ratio x , for different meteorological ascents. After plotting the data on the tephigram, determine the types of instability present and the layers in which each is present.

1.	p	987	936	863	825	741	680	591	533	514	473	408	mb
	T	21	21	16	14	10	6	-1	-6	-5	-8	-16	°C
	x	15.2	15.6	13.2	12.3	9.8	7.1	6.0	4.7	3.7	2.2	1.4	gm per kg
2.	p	1011	955	909	864	834	755	719	632	598	mb		
	T	16	12	7	5	9	6	6	1	0	°C		
	x	8.1	7.0	7.0	6.0	5.7	3.8	4.2	2.6	2.2	gm per kg		
3.	p	979	921	805	684	570	457	mb					
	T	19	18	11	4	-4	-16	°C					
	x	13.7	13.0	9.8	5.3	2.3	1.2	gm per kg					

4. Plot on a tephigram the dry- and wet-bulb curves for the data below. If the layer is lifted 50 mb, plot the resulting dry- and wet-bulb curves. What changes in stability have taken place as a result of the lifting?

p	1020	961	905	854	757	mb
T	15.8	15.7	12.9	10.7	7.0	°C
x	9.9	9.6	8.3	6.9	4.0	gm per kg

BIBLIOGRAPHY

- Byers, H. R., *Synoptic and Aeronautical Meteorology*, New York, McGraw-Hill Book Co., 1937. Chapter 2.
- Pettterssen, S., *Weather Analysis and Forecasting*, New York, McGraw-Hill Book Co., 1940. Sections 27-54.
- Shaw, Sir N., *Manual of Meteorology*, London, Cambridge University Press. Vol. 3 (1930), Chapter 7.
- Normand, C. W. B., "On Instability from Water Vapor," *Q. J. Roy. Met. Soc.*, **64**, 47-66 (1938).

CHAPTER 15

CHARACTERISTIC PROPERTIES OF DIFFERENT AIR MASSES

97. Systems of Classification. As indicated in section 74, air which remains for several days over a uniform surface acquires certain characteristics typical of that region. An understanding of these characteristics is useful since it helps explain the weather associated with the air mass at the source region and as it leaves that region.

Air masses are identified by two different features of their source region. The first distinction is made on the basis of the latitude of the region. Thus one speaks of equatorial, tropical, polar, and Arctic air. Equatorial air, denoted *E*, is very warm, moist, and unstable. Its source region lies between the two trade wind belts. Tropical air, *T*, has its source region in the sub-tropical high-pressure belts. In general it is not as moist in the upper layers as equatorial air, but it is very warm. Polar air, *P*, in spite of its name, has its source region in latitudes from 45° to 70°. The term Arctic, *A*, is applied to air which comes from the polar high. It is very cold and stable in the winter, with the temperatures increasing somewhat in the summer. In this chapter equatorial and Arctic air will not be discussed. Equatorial air is very similar to moist tropical air; Arctic air sometimes appears over northern Europe, but rarely over northern Canada. In general the differences between Arctic air and polar air are relatively unimportant.

The second differentiating feature is the type of underlying surface. The two kinds of surface are maritime, *M*, and continental, *C*. A third distinction is sometimes made by comparing the surface temperature of the air mass after it leaves its source region and that of the underlying surface. Thus *W* indicates that the air is warmer than the surface, and so is becoming more stable, while *K* indicates that the air is colder than the underlying surface, with instability developing. For example, *P_M* indicates polar maritime air, and *_MT_W* indicates tropical maritime air that is moving over a relatively cold surface.

Another method of classification uses the same latitudinal differentiation of tropical, polar, etc., but it uses more specific terms to indicate the source regions. For example, the polar maritime air masses are divided into polar Pacific and polar Atlantic, indicated by the letters *P_P* and *P_A*. Modified air masses are indicated by the letter *N*, as *NP_P*.

Similarly distinctions are made in the other types of air masses. In general the method of classification based on latitude and underlying surface will be used in this text although significant differences between similar source regions will be noted.

98. Polar Continental (P_C) Air Masses in Winter. The main sources of P_C air in winter are the polar anticyclones over northwest Canada and over Russia. The surface temperatures are very low in these regions. The subsiding air in these anticyclones tends to dissipate any cloud present, and the resulting clear skies permit rapid cooling of the snow surface by radiation to outer space. Large inversions, often as great as 20°C , develop over these cold snow surfaces. The cooling in the layers just above the surface is often sufficient to cause the deposition of frost on the snow surface. In this manner the moisture content of the surface air decreases. Turbulent mixing of this dry air with moister air at higher levels, although a slow process in such circumstances, ultimately leads to an appreciable drying of the whole air mass. At the outer edges of the anticyclone, where the wind velocities and therefore mechanical turbulent mixing are greater, inversions and isothermal layers are not so frequently found. Mean dry- and wet-bulb temperature conditions in P_C air during the winter at Ellendale, North Dakota, are shown in Fig. 91. This figure also gives the mean free air temperatures above Fort Smith, Northwest Territories, Canada, for the month of January, 1937. This curve represents the average of all ascents, irrespective of air mass type. Nevertheless most of the ascents are in P_C air, and other types of air mass, if present, would have become modified greatly by the time they reached Fort Smith. It will be noted that there is no major difference in the two temperature curves, except for the lower temperatures and greater inversion found near the surface at Fort Smith. An inversion of about 6°C at Ellendale and of about 8°C at Fort Smith from the surface to 800 mb can be noted from the diagram. The lapse rate from 800 to 600 mb is not large.

It can thus be seen that the air is absolutely stable. The moisture content of the air is very low, the humidity mixing ratio varying from about 0.3 to 0.6 gm per kg. The relative humidity in these air masses averages about 80 per cent in the lower layers. The depression of the wet bulb is very small at these low temperatures, because the maximum possible moisture content of the air is so small. Conditions are very similar over northern Russia. Mean temperatures at the surface are about the same, but at higher levels, say about 600 mb, temperatures are lower and lapse rates steeper. The moisture content of the air is about the same at both source regions.

Observations in Antarctica indicate that cooling at the upper levels

takes place slowly by radiation leading to extremely low temperatures of the order of -80°C at a height of 12 km during the winter night. For comparison purposes average winter temperatures for Antarctica are given in Fig. 91.

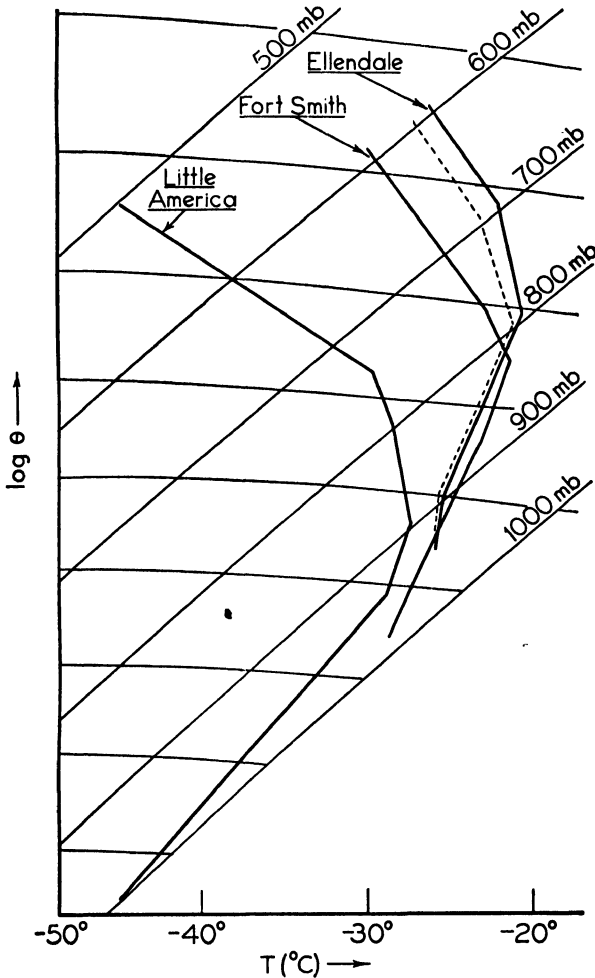


FIG. 91. Temperature curves in typical winter P_C air masses.

As a result of the stability, marked turbulent air motion and clouds are absent in the source region. The visibility is good, since there are few sources of impurities. However, the relative humidity is high so that at the edge of an anticyclone clouds form with the mechanical turbulence, and snow flurries sometimes occur.

When a winter anticyclone becomes stationary to the east of the Rocky Mountains, P_C air may extend as far south as Texas with little modification. The surface layers become warmer through insolation, but subsidence and horizontal divergence of air cause the inversion to become more pronounced, as shown in section 16. If, for example, the air at Ellendale, shown in Fig. 91, were to descend adiabatically so that the air originally at 800 mb subsided 50 mb, and that at 700 mb subsided 100 mb, the layer in which initially the temperature decreased slightly with height would now have an inversion of 4°C . Flying conditions in general are good, with few clouds. With such stable lapse rates, turbulence is slight, the coefficient of eddy diffusivity K is small, so that according to (54-8), the vertical transport of atmospheric impurities such as smoke is inhibited. Thus near industrial regions the products of combustion are concentrated in the surface layers as a result of the inversion, causing poor visibility.

A second important modifying process for winter polar continental air over North America is the movement of the air over the Great Lakes. The lakes present a surface of open water with a temperature greater than 0°C , and thus are a source of heat and water vapor. The temperature of the air crossing the lakes increases, sometimes as much as 15°F , and the surface mixing ratio often increases from 0.5 gm to 2.5 gm per kg. These modifications generally extend to a height of only 2 km, but they are sufficient to produce conditional instability of the latent type in the air mass. Cumulus clouds are frequent over the lakes and on the lee shore where the land surface produces mechanical turbulence in the air stream to set off the instability. These give frequent snow flurries, producing "snow belts" to the lee of the lakes. The water vapor that does not condense here is carried to the Appalachian range where orographic lifting causes condensation of at least some of the remainder.

99. Polar Maritime (P_M) Air Masses in Winter. Since there are no high-pressure regions over the northern oceans in winter, there are no true source regions for polar maritime air. Outbreaks of polar continental air from Siberia or Alaska move southward to the west of the Aleutian low and are carried in the circulation about that low into a westerly current to the coasts of British Columbia, Washington, and Oregon. A similar situation exists for Europe, with the P_C air moving from the North American continent or Greenland, around the Icelandic low to western Europe. In both cases the ocean surface is highly uniform in temperature and the path over the ocean is long enough for the air to acquire definite characteristics.

The P_C air which moves out over the ocean is cold and stable. Ad-

vancing over the warmer water, there is a rapid increase in the moisture content and temperature of the air in the lower layers. This is similar to the modification of P_C air moving over the Great Lakes, but the time spent over the water surface is much longer, and so modifications extend to greater heights, such as 3 to 4 km. Fig. 92 illustrates polar Pacific air just as it leaves its source region and reaches Seattle, Washington. The surface temperature is 30°C warmer than in P_C air in winter, and the moisture content at the surface is about 5 gm per kg.

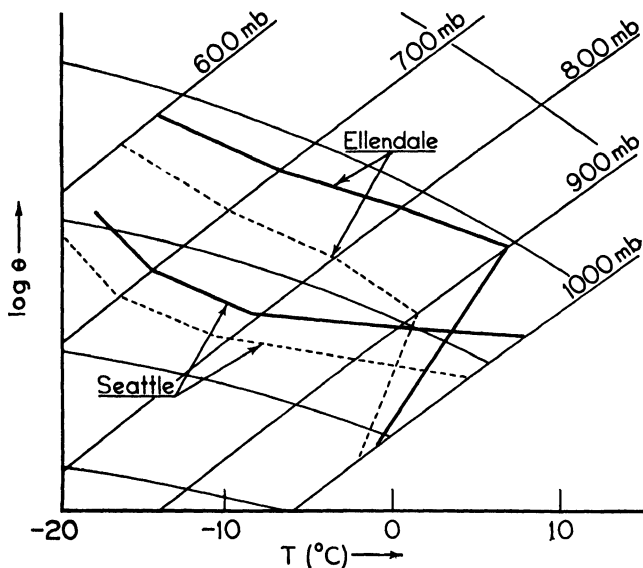


FIG. 92. Temperature curves for typical fresh and modified winter P_P air masses.

Potential instability and conditional instability of the pseudo latent type are present in the lowest 200 mb. The condensation level is low, so that low clouds of the cumulus type develop frequently.

When polar Pacific, P_P , air flows over the mountains, the potential instability present is often realized, and the pseudo latent instability develops into real latent instability through orographic lifting in the manner outlined in section 95. Heavy cumulus and cumulonimbus clouds develop on the windward side of the ranges, giving heavy rains and thunderstorms.

When polar Pacific air crosses the Rockies it undergoes a number of modifications. There is a marked increase in temperature, and a decrease in moisture content. These changes can be seen in the dry- and wet-bulb temperature curves for modified polar Pacific air over Ellendale, shown in Fig. 92. These upper air observations were made

in the early morning hours, and nocturnal radiation accounts for the inversion in the lowest 100 mb. The lapse rate in that layer is much greater during the day. The increase in temperature from Seattle to Ellendale is partly due to the fact that the temperature of the air ascending the western slope of the Rockies decreases during the latter part of the ascent at the saturated adiabatic rate, with the condensed moisture being precipitated, and then descends the eastern slope at the

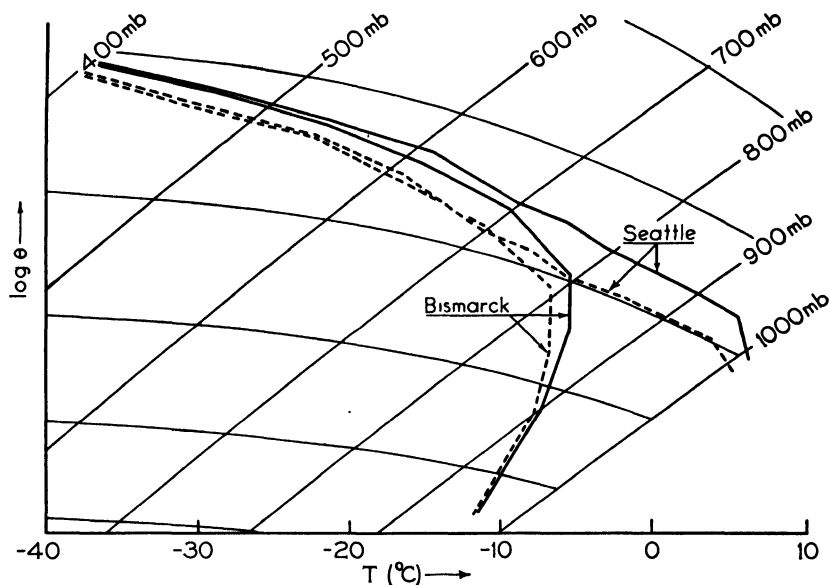


FIG. 93. Mean temperature curves for Bismarck and Seattle, January, 1941.

dry adiabatic lapse rate. That does not account for all the difference between the two curves, and other factors such as subsidence and turbulent mixing must be in operation. Farther east, these modified polar Pacific air masses are warm, dry, and stable.

The previous paragraphs have described the characteristics of polar maritime air from the Pacific Ocean. Over western Europe the lapse rate and moisture conditions in polar maritime air from the Atlantic are practically identical with those at Seattle. The modifications in this air will not be the same as those in P_P air over North America because of the absence of a mountain barrier, such as the Rocky Mountains. Over Europe polar maritime air tends to be modified by cooling in the lower layers, with a consequent increase in stability.

When a low-pressure area is situated south of Newfoundland, the easterly current north of the low brings air from the Atlantic over

Quebec, and at times as far west as New England. This polar Atlantic, P_A , air was previously polar continental air, but had a short trajectory over the northern Atlantic. Since the time over the ocean is shorter than that for polar Pacific air on the other side of the continent, the modifications do not extend above 1 to 2 km. In this lower layer the relative humidity is high and conditional instability is present. Turbulence clouds of the stratocumulus type are frequent with light precipitation. Above this low layer of clouds the sky is cloudless.

The similarity of P_C and P_M air aloft is shown in Fig. 93. One pair of curves gives the mean dry-bulb and wet-bulb temperatures over Bismarck, North Dakota, for January, 1941, and the other pair gives the same data for Seattle. No attempt was made to separate ascents into groups of those taken either in P_C or P_M types of air masses, but the resemblance of the Bismarck curve to typical P_C air given in Fig. 91 suggests that there was very little variation in air mass type over this station for this month. The average for Seattle was a few degrees warmer and slightly more stable in the lower layers during this month than for average polar Pacific conditions. It is readily seen that above 700 mb the average conditions were almost identical.

100. Tropical Maritime (T_M) Air Masses in Winter. Tropical maritime air masses have their source regions in the large sub-tropical anticyclones of the Atlantic and Pacific oceans at 30° N latitude. The light winds, uniform underlying surface, and subsidence permit the development of a uniform air mass. Air from both these source regions influences the weather over the North American continent.

The tropical Pacific air which enters North America by way of the southern Pacific coast of the United States is very similar to the tropical Atlantic air from the Atlantic anticyclone over southwest Europe. Fig. 94 gives mean values for tropical Pacific air at San Diego, California, and for tropical Atlantic air at Trappes, Dijon, Lyon, and Chateauroux in France. The temperature shown by the latter is less by about 10° C, since France is farther north than San Diego, and the relative humidity is correspondingly greater, but the stability conditions are about the same in both regions.

The air in general is warm throughout, with moisture decreasing gradually with height. There is some conditional instability of the stable type, but little potential instability. The absence of real latent instability is probably due to subsidence in the layers aloft. Since this air moves into California and France from more southerly regions, inversions resulting from the advance of the air over a cooler surface and from subsidence are sometimes found, with accompanying stratus type clouds.

Tropical maritime air from the Atlantic region is called tropical Gulf (T_G), or tropical Atlantic (T_A) air. T_G air comes from the Caribbean or Gulf of Mexico region, while T_A air comes from a region farther north in the vicinity of the Sargasso Sea. In practice it is found that they are indistinguishable and in the following discussion the symbol T_G will be used to denote both. At times the tropical Gulf air found over the southeastern states is just P_C air which has left the continent, become rapidly modified over the warm waters, and has returned to the continent.

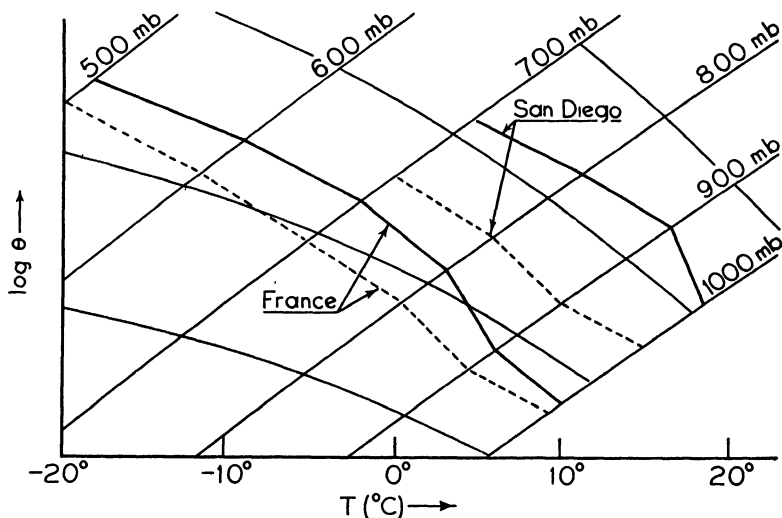


FIG. 94. Temperature curves for typical winter T_M air in California and France.

The mean values of winter temperatures and wet-bulb temperatures in T_G air over Groesbeck, Texas, are given in Fig. 95. The most outstanding features are the very moist layer in the lowest kilometer, with a relative humidity of 90 per cent, and the dry layer, with the relative humidity less than 40 per cent, above. In the lower layer there is conditional instability of the stable type and slight potential instability. With strong winds, the mechanical turbulence frequently produces a layer of stratocumulus cloud at night, but without precipitation. The insolation during the day causes this layer to dissipate.

The extremely dry layer aloft tends to make the air more stable, although the small amount of moisture at these levels causes marked potential instability in the whole air mass. Since, though, this potential instability is released only after the ascent of the layer through a

pressure interval of 200 mb, it is not likely to be realized except with ascent at a frontal surface.

The warm dry layer aloft is of a type known as Superior air, designated by *S*. This air has no known surface source region, but is thought to come from the upper portions of the tropical anticyclones. Air with similar properties is sometimes found above a layer at P_C or P_M air. Its extreme dryness is explained then by subsidence. At times, particularly in summer, it appears at the surface of the earth, giving extremely hot and dry weather.

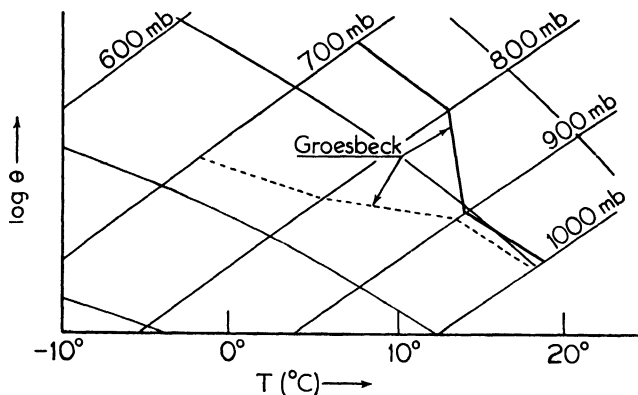


FIG. 95. Temperature curves for typical winter T_G air masses.

Modifications occur as the T_G air moves northward over the continent. These are especially marked by the time the air reaches the northeast portion. The observations over Boston show that near the surface the temperature and moisture content values are lower than at Groesbeck. On the other hand, the moisture content at higher levels is greater. This suggests that T_G air which reaches the northeast coast may not be from exactly the same source region as that over Groesbeck. It may be air which has had a more recent polar origin, in which moisture has been carried up to higher levels by turbulence. An alternative explanation is that the air has become thoroughly mixed during its northward movement to the vicinity of Boston, producing a decrease in moisture content at lower levels and an increase at higher levels. As modified T_G air proceeds northeastward over the cold ocean surface to the vicinity of Newfoundland, dense fogs frequently develop. These affect the coastal regions of the eastern provinces of Canada.

101. Tropical Continental (T_C) Air Masses in Winter. There is only one source of tropical continental air in the northern hemisphere, that being over north Africa. There are not sufficient upper air obser-

variations in this air mass to be able to obtain the average conditions of temperature and moisture content. Some general conclusions may be reached, however, from surface data. The air is warm, stable, and very dry. The cooling by nocturnal radiation is very great, and large inversions develop in the early morning hours.

102. Polar Continental (P_C) Air Masses in Summer. Polar continental air masses are quite different in summer from those in winter. There is no snow cover over the source region, and the heating of the ground by radiation from the sun produces a greater lapse rate in the lower levels. As indicated in a previous section, there are no well-marked anticyclones over northwest Canada or Russia in summer, so

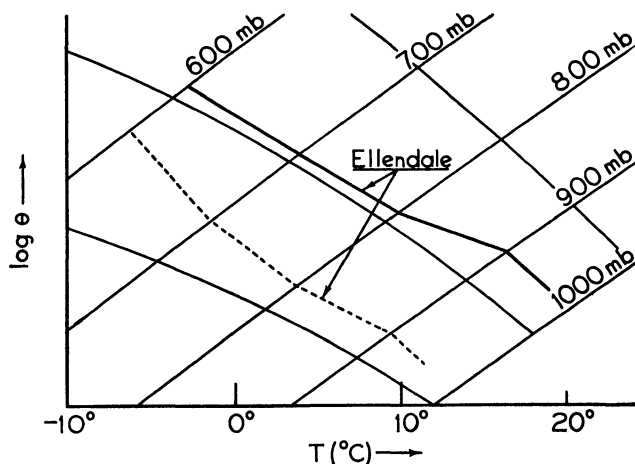


FIG. 96. Temperature curves for typical summer P_C air masses.

that the summer P_C air masses do not form in the same manner as the winter ones do. Average upper air conditions in P_C air masses in summer over Ellendale are shown in Fig. 96. It can be seen from the diagram that the moisture content, especially in the lower levels, is small. The air near the surface is far from saturation, the relative humidity being only about 45 per cent. This lack of moisture in the lower levels permits large diurnal temperature variations, sometimes as great as 15°C . The stability is to be classified as the stable type of conditional instability. The figure shows that on the average there is no potential instability in summer P_C air at the time of observation. These curves represent average conditions during the early morning hours only. The situation is different during the day, however, when radiation from the sun heats the earth's surface. The dry-bulb and wet-bulb temperatures of the surface air rise, frequently producing

latent and potential instability. The condensation level of the surface air is high, and only a few high clouds of the convective type form. If the moisture content of the lower air increases, convective processes are more pronounced, and thunderstorms may occur. Air to the east of Ellendale is usually colder because of the influence of the cool waters of Hudson Bay. Near the Gulf of Mexico summer P_C air is warmer and more moist at all levels than that at Ellendale.

Summer P_C air in western Europe is slightly cooler and much more moist than that at Ellendale. This suggests that P_C air reaching western Europe has generally had a recent oceanic trajectory. The temperature in P_C air over eastern Europe is about the same as that over western Europe, but the moisture content of the air is slightly less.

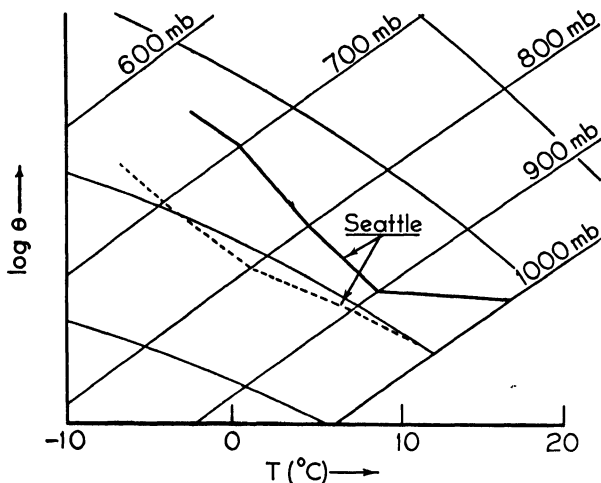


FIG. 97. Temperature curves for typical summer P_P air masses.

103. Polar Maritime (P_M) Air Masses in Summer. In summer the comparatively cold ocean surfaces increase the intensity of the sub-tropical high-pressure systems. In the Pacific the ridge of high extends north to the Aleutians. The resulting pressure gradient between this high and the continental low brings air from Alaska over the Pacific and to the west coast of North America in a northwest current. This air becomes modified sufficiently in its trajectory over the Pacific to acquire typical properties and is called polar Pacific air.

Fig. 97 gives average conditions in this type of air mass over Seattle. Turbulence in the moderate winds produces a lapse rate close to the dry adiabatic in the lowest kilometer. Thus conditional instability of the stable type is found here, and a layer of stratocumulus frequently

forms during the night at the top of this layer. Above this layer the lapse rate is close to the saturated adiabatic, but there is little potential instability. The temperature of the air, since it has come directly from the north over relatively colder water, is lower than that of P_C air. In spite of its southerly trajectory, it frequently becomes more stable as it passes over the cold coastal waters. The condensation level lowers and fogs develop. As P_M air passes over the mountains, it acquires heat in the lower layers and rapidly becomes modified so that it is indistinguishable from P_C air.

Over western Europe summer polar Atlantic air is slightly cooler and more moist than P_M air observed at Seattle.

Along the east coast of North America a return circulation occasionally develops, bringing over the continent air which has passed over the north Atlantic. This circulation develops most frequently in spring and early summer. The waters of this region are cold for their latitude, and so the polar Atlantic air is moist with low temperatures. Low turbulence clouds form in this current, but above this layer the air is clear and flying conditions are good.

104. Tropical Maritime (T_M) Air Masses in Summer. As noted in the discussion of P_M air in summer, the air trajectory at the eastern boundaries of the oceans is from the north, and for the same reason the return circulation gives southerly winds at the western boundaries. For this reason the tropical maritime air reaching California and southwest Europe is dry, stable, and relatively cool, whereas the tropical maritime air along the southeast coast of the United States is moist and unstable. Fig. 98 gives average conditions in this air mass at Miami, Florida.

It will be readily noted that the relative humidity is high throughout, with temperatures also high. The lapse rate is of the conditionally unstable type, with real latent and potential instability. A small lift of 50 mb is sufficient to release the potential instability; or even the diurnal heating over the warm land will set off strong convective currents. Thunderstorms are, then, frequent in this air mass. This T_G air is more nearly of the equatorial type than of the tropical type. It is practically identical in properties with air over Batavia, Java, at 6° S latitude.

In the spring and early summer, when as sometimes happens T_G air has moved northward and over the cold waters of the Great Lakes, it is cooled in the lower layers. Because of the abundant moisture present, fogs frequently develop in this air at the north shore of the lakes. The modifications along the Atlantic coast are very marked. Moving northeastward parallel to the east coast of the United States, it leaves

the Gulf Stream to move over the cold waters of the Labrador Current. Rapid cooling in the lower layers causes dense fogs over the Newfoundland Banks and adjacent waters during this season.

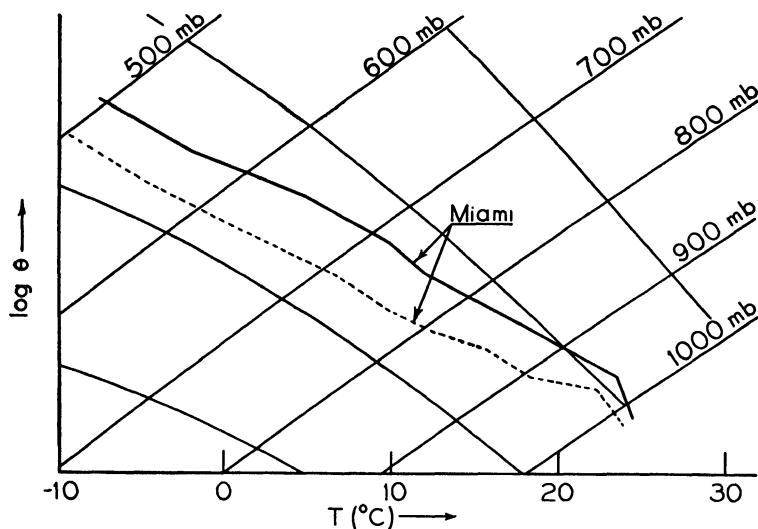


FIG. 98. Temperature curves for typical summer T_G air masses.

105. Tropical Continental (T_C) Air Masses in Summer. This type of air mass develops over north Africa and west Asia. The air is so dry, and subsidence is so prevalent, that condensation forms do not develop, despite the steep lapse rate which occurs during the daytime. If it moves northward or northeastward, it takes up considerable moisture in the lower portion of the air mass, and convective clouds and showers, and sometimes thunderstorms, develop over southeastern Europe and southwestern Asia.

No tropical continental air is found over North America in summer since there is no source region on this continent.

106. The Rossby Diagram as an Aid to Classification of Air Masses. The various types of air masses may be conveniently identified by means of the Rossby diagram. In this diagram, discussed briefly in section 25, the ordinate is partial potential temperature on a logarithmic scale, and the abscissa is the mixing ratio on a linear scale. Partial potential temperature is obtained in the customary manner, but the partial pressure of the air, $p - e$, is used instead of the ordinary pressure p . Partial potential temperature has very nearly the same value as ordinary potential temperature, and in practice, the two may be used interchangeably. A Rossby diagram is shown in Fig. 99. The

lines sloping downward from left to right are lines of constant equivalent potential temperature. Pressure and temperature lines are sometimes shown on the diagram, but their usefulness is limited, since they are applicable only if the air is saturated. Average winter conditions in P_C air at Ellendale (Fig. 91), in P_P air at Seattle (Fig. 92), and in T_G air at Groesbeck (Fig. 95) are shown in Fig. 99. The different types of air masses may be readily distinguished. If the actual lapse rate is equal to the dry adiabatic, and if the moisture content is the same at all

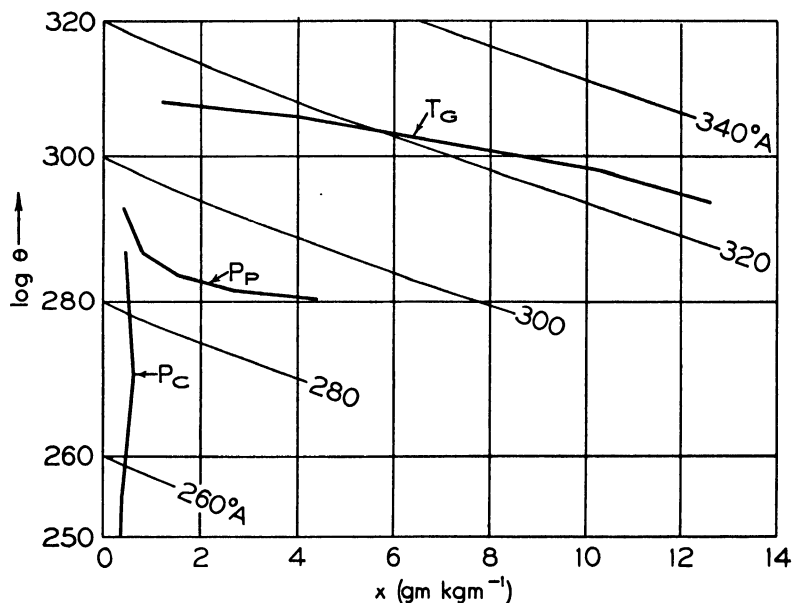


FIG. 99. Typical winter air mass curves on a Rossby diagram.

levels, the ascent curve becomes a single point. An ascending or descending particle of air will be represented by a single point on the diagram as long as processes of evaporation and condensation do not occur. The equivalent potential temperature at each level may be readily determined, since lines of constant equivalent potential temperature are drawn on the diagram. The presence or absence of potential instability in a layer may therefore be determined directly, since it is present if the equivalent potential temperature decreases with height in that layer. It can be seen that the T_G air has potential instability, but the P_C has not.

The chief use of the Rossby diagram is in identifying air masses. However, the tephigram, with both dry- and wet-bulb temperatures

plotted on it, may also be used for this purpose. The lack of pressure coordinates on the Rossby diagram is inconvenient, and the tephigram is much better for the study of stability.

107. Comparison of Air Masses. The following table presents a comparison of the typical air masses of North America at their source regions. These are for average conditions, from which, of course, variations will occur in particular cases.

AIR MASS TYPES OF NORTH AMERICA

Season	Type of Air Mass	Surface Temperature	Stability	Cloud Forms	Precipitation	Flying Conditions
Winter	P_C	-26°C	Very stable	None	None	Smooth
	P_C modified over Great Lakes	-1°C	Conditional instability in lowest 2 km	Stratocumulus with cumulus	Snow flurries	Turbulence in lowest layers; moderate rime icing
	P_P	7°C	Potential and pseudo latent instability	Cumulus and cumulonimbus over mountains	Showers and thunderstorms over mountains	Severe turbulence; severe icing over mountains
	T_P	18°C	Stable	Some stratus	None	Moderate visibility
	T_G	19°C	Potential instability realized with ascent at fronts	Stratocumulus at night	Drizzle	Visibility poor at times
Summer	P_C	$15-25^{\circ}\text{C}$	Real latent during the day; stable at night	High level cumulus	None	Moderately turbulent during day
	P_P	17°C	Stable type of conditional instability at surface	Stratocumulus with low tops at night	None	Smooth; poor visibility
	T_G	24°C	Real latent and potential instability	Heavy cumulus and cumulonimbus	Thunderstorms	Extremely turbulent

PROBLEMS AND EXERCISES

1. The mean conditions in winter P_C air at Boston, Massachusetts, modified as it has moved eastward, are as follows.

Height	0.0	1.0	2.0	3.0	4.0	km
T	-6.3	-14.3	-18.0	-23.0	-29.0	°C
x	0.9	0.6	0.5	0.3	0.2	gm per kg

As this air moves out over the waters of the Atlantic, which are at a temperature of 2° C, what changes will take place? To what height will the turbulent currents extend? What clouds and weather can be expected when P_C air in winter moves off the continent over the warmer ocean?

BIBLIOGRAPHY

- Admiralty Weather Manual*, London, H. M. Stationery Office, 1938. Chapter 20.
- Byers, H. R., *Synoptic and Aeronautical Meteorology*, New York, McGraw-Hill Book Co., 1937. Chapter 7.
- Byers, H. R., and V. P. Starr, "Circulation of the Atmosphere at High Latitudes during Winter," *Monthly Weather Review*, Supplement 47, Washington, D. C., 1941.
- Chang-Wang Tu, "Chinese Air Mass Properties," *Q. J. Roy. Met. Soc.*, **65**, 33-51 (1939).
- Namais, J. et al, *An Introduction to the Study of Air Mass Analysis*, Fifth Edition, Milton, Mass., American Meteorological Society, 1940.
- Schinze, G., "Troposphärische Luftmassen und vertikalen Temperaturgradient," *Archiv deut. Seewarte*, **52**, No. 1, 1932.
- Showalter, A. K., "Further Studies in American Air Mass Properties," *Monthly Weather Review*, **67**, 204-218 (1939).
- Willet, H. C., "American Air Mass Properties," *Mass. Inst. of Tech., Papers in Physical Oceanography and Meteorology*, **2**, No. 2, Cambridge, Mass., 1934.

CHAPTER 16

CYCLONES AND ANTICYCLONES

108. General Characteristics of a Front. One characteristic of an air mass is its uniformity. Properties of the air in an air mass change little if any in the horizontal direction. When, though, two air masses lie side by side there is a rapid change in properties from one air mass to the other. Fig. 100 illustrates this in terms of the isotherms when one air mass is warmer than the other. This region of discontinuity between the air masses is called a *frontal surface* or a *front*. The term frontal surface is used for the surface of discontinuity between the two air masses when it is desirable to make a distinction between the discontinuity at the earth's surface

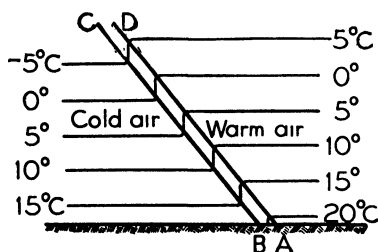


FIG. 100. Isotherms across a frontal zone.

and that above it. The term front refers then to the line of discontinuity at the ground.

As a result of turbulent mixing between the air masses, there is no discontinuity in the mathematical sense across the frontal surface, but rather a narrow zone of transition. The limits of this zone are indicated by AD and BC in Fig. 100. The

discontinuity is usually one of temperature, but at times the contrast in moisture content across the surface is as marked as that of temperature.

When two liquids of unequal density, such as oil and water, are put into the same vessel, equilibrium is reached when the lighter liquid rests above the heavier. In the atmosphere there is a tendency for the warmer, and therefore lighter, air to lie above the colder and heavier air. But as a result of the rotation of the earth, the equilibrium condition is reached when the frontal surface intersects the ground at a small angle. As shown in equation 38-8,

$$\tan \theta = \frac{2\omega \sin \phi}{g} \frac{(T_1 u_2 - T_2 u_1)}{T_2 - T_1}$$

where θ is the angle between the frontal surface and the ground, as-

sumed horizontal, ω the angular velocity of the earth, ϕ the latitude, g the acceleration of gravity, T_1 , u_1 represent the temperature and the component parallel to the front of the geostrophic wind in the cold air, and T_2 , u_2 the corresponding quantities in the warm air. The angle θ increases with increasing difference in velocity, and also increases with decreasing difference in temperature across the frontal surface.

Since a front is a boundary between two air masses, it must move when the air masses move. Thus the successive positions of the front may be determined from the velocity components normal to the front of the air on the two sides of the front. Some mixing does, at times, take place to decrease the sharpness of the discontinuity, although in other situations the front may become more distinct. The wind distribution in the vicinity of a front is closely related to the changes both in the position and the sharpness of the front.

109. Frontogenesis and Frontolysis in Deformation Fields. As mentioned above, there is not a mathematical discontinuity at a front, but a zone of transition. This zone of transition is a region in which the temperature changes rapidly with distance, or, in other words, where the temperature gradient is large. Such a zone does not keep the same width at all times. Mixing will change the temperature gradient, as will a difference in the directions of the winds. When this zone of transition is becoming sharper, *frontogenesis* is said to be taking place; the reverse situation is called *frontolysis*. These processes are closely associated with the distribution of the wind.

If n represents the direction of a horizontal line perpendicular to the isotherms, the temperature gradient is given by the rate of change of temperature with n , i.e., $\partial T / \partial n$. Near a front $|\partial T / \partial n|$ is a maximum, the absolute value being used since n may be in the direction of rising or of falling temperatures. For frontogenesis, $|\partial T / \partial n|$ must increase with time, and for frontolysis it must decrease with time. As given in equation 41.4

$$\frac{d}{dt} \left| \frac{\partial T}{\partial n} \right| = - \left| \frac{\partial T}{\partial n} \right| \frac{\partial v_n}{\partial n}$$

where v_n represents the velocity in the direction of n . For any particle of air, T is assumed to be invariant with time. Therefore frontogenesis occurs when the velocity decreases along the normal and frontolysis occurs when the velocity increases along the normal.

It may be shown that if the velocity is given by a linear function of the space coordinates, it can be compounded of one or more of six primary fields of motion. These are

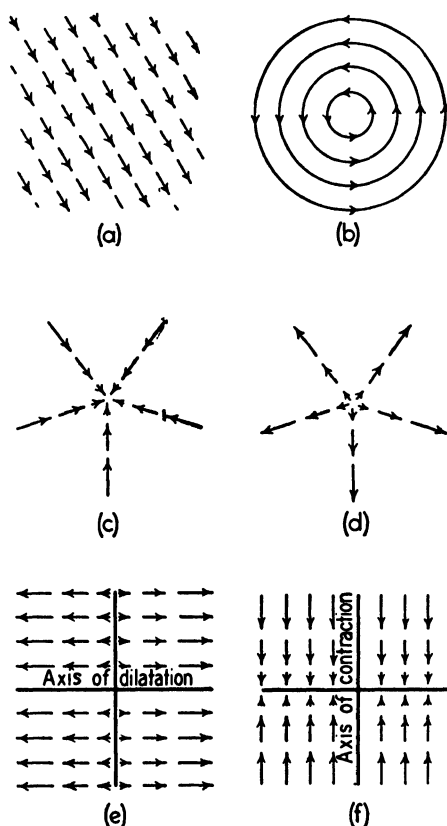


FIG. 101. Primary fields of motion.

from B to A decrease in value, become negative, and then have increasing negative values. Then, according to (41.4), frontogenesis takes place in such a wind field. Since the wind field is symmetrical with respect to the central point, the orientation of the isotherms does not alter this conclusion.

With a divergence field, the method of analysis is similar. The velocity components then increase along the normal to the isotherms, and hence there is frontolysis.

- (a) Translation.
- (b) Rotation.
- (c) Convergence.
- (d) Divergence.
- (e) Dilatation.
- (f) Contraction.

These fields of motion are illustrated in Fig. 101.

When the velocity field is one of pure translation or of pure rotation, there is no tendency for particles of air to approach or to separate from one another. Hence there will be no tendency for either frontogenesis or frontolysis.

Frontogenesis in a convergence field is illustrated in Fig. 102. T_1, T_2 , etc., are isotherms, and the line AB is a normal to these. Thin arrows indicate the velocity. The components of velocity along the normal AB are indicated by thick arrows. As can be seen from the diagram, the velocity components

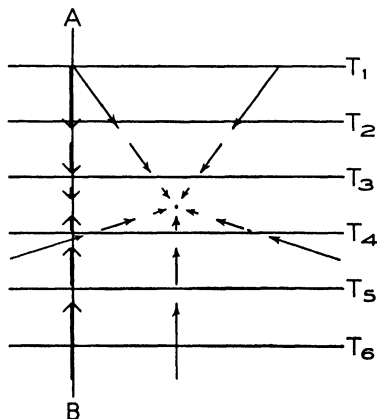


FIG. 102. Frontogenesis with convergence.

Frontolysis in a dilatation field may be understood by reference to Fig. 103. The velocities are parallel to the axis of dilatation, and are indicated by thin arrows. The isotherms are indicated by T_1, T_2 , etc.; AB is normal to them. The thick arrows along the direction AB indicate the velocity components along the normal. In the situation illustrated, the velocity from B to A increases from large negative values to small negative ones, then to small positive, and finally to

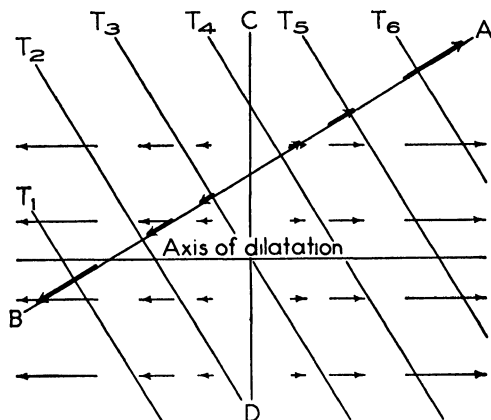


FIG. 103. Frontolysis with dilatation.

large positive values. Thus $\partial v_n / \partial n$ is positive and, according to (41.4), frontolysis is taking place. If, though, the isotherms are parallel to the axis of dilatation, the velocity along the normal is zero, and so neither frontogenesis nor frontolysis occurs.

Since the particles on the line CD , from which the particles are diverging, are not moving, the point of intersection of an isotherm with CD is fixed. On either side the particles on the isotherm are moving away from CD . Hence the direction of the isotherm is changing in such a manner that the angle of intersection with CD increases, approaching 90° as a limit. Frontolysis is then no longer taking place.

A similar discussion of a contraction field shows that contraction causes frontogenesis unless the isotherms are parallel to the axis of contraction. With this exception the velocity field changes the direction of the isotherms, causing the angle between the isotherms and the axis of contraction to increase. This change of direction increases the tendency to frontogenesis.

An example of a specific contraction field in the earth's atmosphere will now be given. Consider the situation in which straight parallel

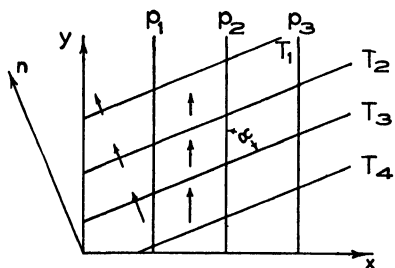


FIG. 104. Frontogenesis in air with a northward component of motion.

isobars run in a north-south direction, as illustrated in Fig. 104. Here x is positive to the east, and y is positive to the north. The geostrophic wind is south, of magnitude given by (35.1),

$$v = \frac{1}{2\omega \sin \phi \rho} \frac{\partial p}{\partial x}$$

The isotherms are also straight and parallel, and make an angle α with the isobars, as indicated in the figure. The velocity component in the direction n normal to the isotherms is then

$$v_n = v \sin \alpha$$

Thus

$$v_n = \frac{\sin \alpha}{2\omega \sin \phi \rho} \frac{\partial p}{\partial x} \quad (109.1)$$

Assuming that ρ is constant, only the latitude ϕ varies with n . Differentiating (109.1) partially with respect to n gives

$$\frac{\partial v_n}{\partial n} = \frac{\sin \alpha}{2\omega \rho} \frac{\partial p}{\partial x} \frac{\partial}{\partial n} (\sin \phi)^{-1} = - \frac{\sin \alpha \cos \phi}{2\omega \rho \sin^2 \phi} \frac{\partial p}{\partial x} \frac{\partial \phi}{\partial n} \quad (109.2)$$

Substituting (109.2) in (41.4) leads to

$$\frac{d}{dt} \left| \frac{\partial T}{\partial n} \right| = \left| \frac{\partial T}{\partial n} \right| \frac{\sin \alpha \cos \phi}{2\omega \rho \sin^2 \phi} \frac{\partial p}{\partial x} \frac{\partial \phi}{\partial n} > 0$$

since both $\partial p / \partial x$ and $\partial \phi / \partial n > 0$. The temperature gradient increases with time, so that the wind field is of the frontogenetical type.

It must not be inferred from this that frontogenesis always occurs in northward-moving air when the isotherms are as shown, although it frequently does. Variations in the pressure gradient or in the density may be sufficient to reverse the sign of $\frac{d}{dt} \left| \frac{\partial T}{\partial n} \right|$. Furthermore, non-geostrophic components, of the type discussed in section 46, may be so large that it is no longer valid to use the geostrophic wind, even as a first approximation.

A similar process of reasoning shows that if the geostrophic wind is north, rather than south, the wind field is of the dilatational type, and hence produces frontolysis.

When contraction and dilatation velocity fields are superimposed, the result is as illustrated in Fig. 105. AB is the axis of dilatation and CD the axis of contraction. Thin arrows give the velocity components and thick arrows the resultant velocities. The streamlines are given by the smooth curves. These streamlines are similar to the isobars near

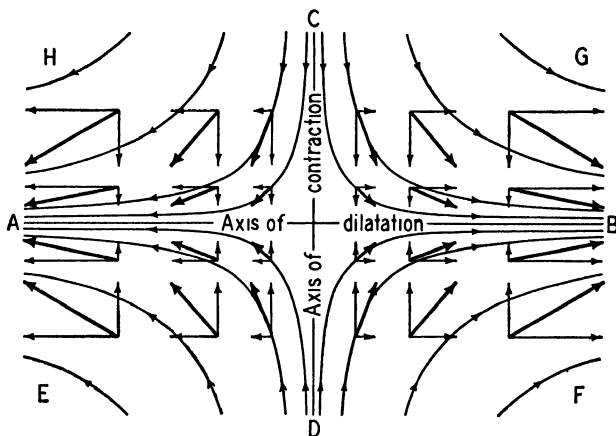


FIG. 105. Resultant of contraction and dilatation velocity components.

a col as given on a weather map, where high-pressure areas are situated near the points F and H and lows near E and G . Because of the direction of movement of the particles, AB is sometimes known as the axis of outflow, and CD the axis of inflow. A velocity field which is compounded of a dilatation and a contraction field is known as a *deformation field*.

In a deformation field, if the isotherms are parallel to the axis of contraction, no frontogenesis results from the contraction component, but frontolysis results from the dilatation component. Similarly, if the isotherms are parallel to the dilatation axis, frontogenesis results along the axis of dilatation. For isotherms in intermediate directions, the result depends upon the relative strengths of the frontogenetical and frontolytical tendencies. If the angle which the isotherms make with the axis of dilatation is less than 45° , frontogenesis will occur, but if it is greater than 45° , frontolysis will result.

As shown above, both contraction and dilatation tend to rotate the isotherms into a position parallel to the axis of dilatation. This rotation would result in frontogenesis along the axis of dilatation. In actual situations, though, the structure of the pressure system will rarely remain constant long enough for this to occur.

A deformation field may be compounded with any one of the other types of velocity fields, although not all possible combinations are found on actual weather maps. Fig. 106 gives one resultant field that is frequently found on synoptic charts. It is a combination of a deformation field and a rotation field. In this situation the axes of inflow and outflow CD and AB are not perpendicular to each other, and the axes of contraction and dilatation are not readily obtainable. The axes of contraction and dilatation may be defined as follows. In a wind velocity field consider a flexible circular ring attached to the particles of air at any given moment. After an interval of time, the circle will be deformed until it has approximately the shape of an ellipse.

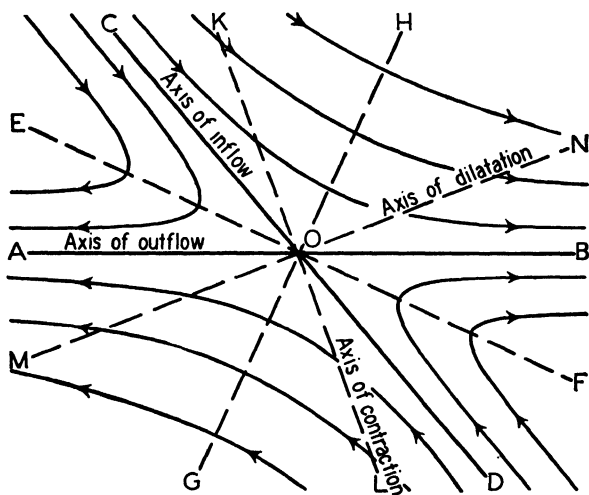


FIG. 106. The determination of the axes of contraction and dilatation.

The major axis, along which the particles are spreading apart most rapidly, is the *axis of dilatation*. The minor axis, along which the particles are approaching one another most rapidly, is the *axis of contraction*.

These axes may be found in Fig. 106 most readily by the following steps. Bisect the angles AOC and BOC by the lines EOF and GOH . Bisect the angles EOG and FOG by the lines MON and KOL . The line MON , nearer the axis of outflow, is the axis of dilatation and the line KOL is the axis of contraction. Frontogenesis, when it occurs, will be along the axis of dilatation. The rule, as determined above, that frontogenesis will occur when the isotherms make an angle of 45° or less with the axis of dilatation is still useful, although the angle varies slightly depending upon the extent of convergence or divergence.

Contraction and convergence are the two types of wind fields which lead to frontogenesis. Contraction is found in the region of cols, and convergence is prominent in the regions of low pressure. For that reason, temperature gradients near either of these two types of pressure distributions should be watched closely for the possible development of fronts. Also, since high-pressure areas are regions of divergence, fronts will dissipate near the center of an anticyclone or across a ridge.

110. Frontal Zones. Frontogenesis between Air Mass Source Regions. Frontogenesis is especially likely to occur near the coastline of a continent. If the air moves parallel to the coast for a long period, so that one portion of the air mass has an extended continental trajectory, while adjacent air has a long oceanic trajectory, even a small amount of deformation or convergence may produce frontogenesis. This would occur, for example, if the isobars over the east coastal waters of the United States were parallel to the coast line. Rapid transformation of the air over the ocean would lead to the formation of a front along the boundary of the Gulf Stream. This is a frequent cause of frontogenesis, and such a development must be allowed for in forecasting.

The main sources of the temperature differences which lead to frontogenesis are:

- (a) The north-south temperature gradient.
- (b) The contrasts between air masses over continents and those over oceans.

Deformation fields usually produce the fronts, aided occasionally by convergence. The zone of frontogenesis nearly coincides with the region of maximum temperature gradient of the underlying surface. In general, it may be said that frontogenesis occurs most readily near the east coasts of northern continents.

In winter there are five main regions where frontogenesis occurs. There is one zone near the east coast of North America, and another near the east coast of Asia. There is another zone in the north Pacific, nearer to North America. This is a result of the division of the north Pacific sub-tropical high into two cells. The deformation field between the two cells leads to frequent frontogenesis in this region. Another zone of frontogenesis lies to the east of Greenland, in the general region of the Icelandic low. The last main zone is found extending in an east-west direction along the Mediterranean.

In summer there are only three main zones of frontogenesis. The temperature contrast between air of continental origin and that of oceanic origin is small in summer, especially in middle latitudes. The contrasts between cool Arctic air and warm continental air are larger, and therefore the summer frontal zones are found at higher latitudes.

One zone extends across Canada, another across northern Europe, and the third extends from northeast Russia to Alaska.

111. Air Masses and Cyclones. The first attempt to study physical processes in a depression from the air mass point of view was made by

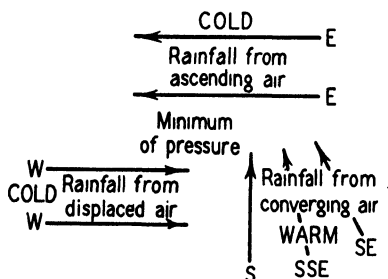


FIG. 107. Motion of air near a center of low pressure. (After Shaw.)

Shaw and Lempfert in 1906. They studied the trajectories of air in cyclones with the aid of one- and two-hourly weather maps. Some of the results of this investigation are shown in Fig. 107, taken from one of Shaw's later papers. The interaction of the warm and cold air masses is indicated clearly. The similarity with later models of a depression in its early stages, as developed by the Norwegians, may be readily seen.

Helmholtz, late in the nineteenth century, suggested that two currents with different properties could flow side by side, separated by a surface of discontinuity. A number of meteorologists, such as Bigelow, Hanzlik, Von Ficker, and Shaw and Lempfert suggested early in the present century that cyclones tend to form at surfaces between warm and cold air. These earlier ideas were developed by Norwegian meteorologists, notably V. and J. Bjerknes. The former studied the question from the mathematical standpoint, considering a depression as a wave on a surface of discontinuity. J. Bjerknes, the son, investigated physical processes at fronts, and applied his findings to map analysis and forecasting.

112. Life History of a Frontal Depression. The development of a depression forming at a front, as visualized by Bjerknes, is shown in Fig. 108. At first there is a front separating cold air, denoted 1, moving westward or slowly eastward, from warm air, denoted 2, moving more rapidly eastward, as indicated in Fig. 108a. Then a bulge appears in the front, the warm air advancing from the south and the cold air retreating to the north, as shown in Fig 108b. This bulge is similar to a wave, but the exact nature of the generating cause for the wave along the front is not known. This stage in the development is preceded and accompanied by more rapidly falling pressures in the neighborhood of the wave than elsewhere, and by increasing cloudiness caused by ascent of the warm air over the cold.

The kinematics of this northward advance of warm air mass 2 may be discussed in the following manner. Draw an axis y positive to the north through point B on the stationary front, as shown in Fig. 108a.

Since the front is stationary, the velocity c of the front is zero, and the acceleration A of the front becomes, according to (43.9),

$$A = - \frac{\frac{\partial^2 p_1}{\partial t^2} - \frac{\partial^2 p_2}{\partial t^2}}{\frac{\partial p_1}{\partial y} - \frac{\partial p_2}{\partial y}} \quad (112.1)$$

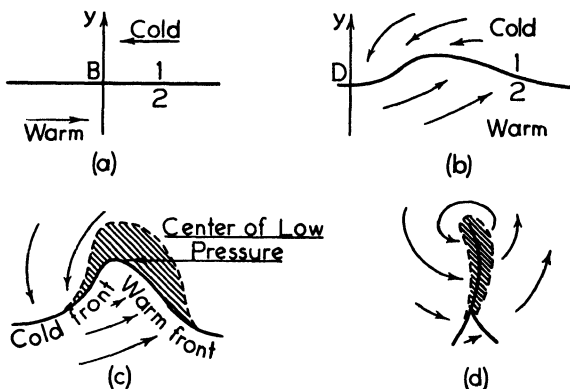


FIG. 108. Life history of a cyclone.

where the subscripts refer to air masses 1 and 2. According to (39.2),

$$\frac{\partial p_1}{\partial y} - \frac{\partial p_2}{\partial y} > 0$$

Now if the falling pressure tendencies are becoming greater more rapidly with time in cold air mass 1 than in warm air mass 2, it follows that

$$\frac{\partial^2 p_1}{\partial t^2} - \frac{\partial^2 p_2}{\partial t^2} < 0$$

The front then has a positive acceleration northward, as shown by (112.1) and the bulge develops, as indicated in Fig. 108b.

The bulge becomes more marked, with the overrunning causing precipitation, and a low-pressure area forms at the point where the warm air has advanced the greatest distance into the cold. This stage is illustrated in Fig. 108c, the hatching indicating the extent of the precipitation area. Now consider a point D on the front farther to the west, where the front is still stationary, as shown in Fig. 108b. Here the falling tendencies usually increase less rapidly with time in air mass 1 than in air mass 2, or in the former the pressure may even be

rising. Under such conditions

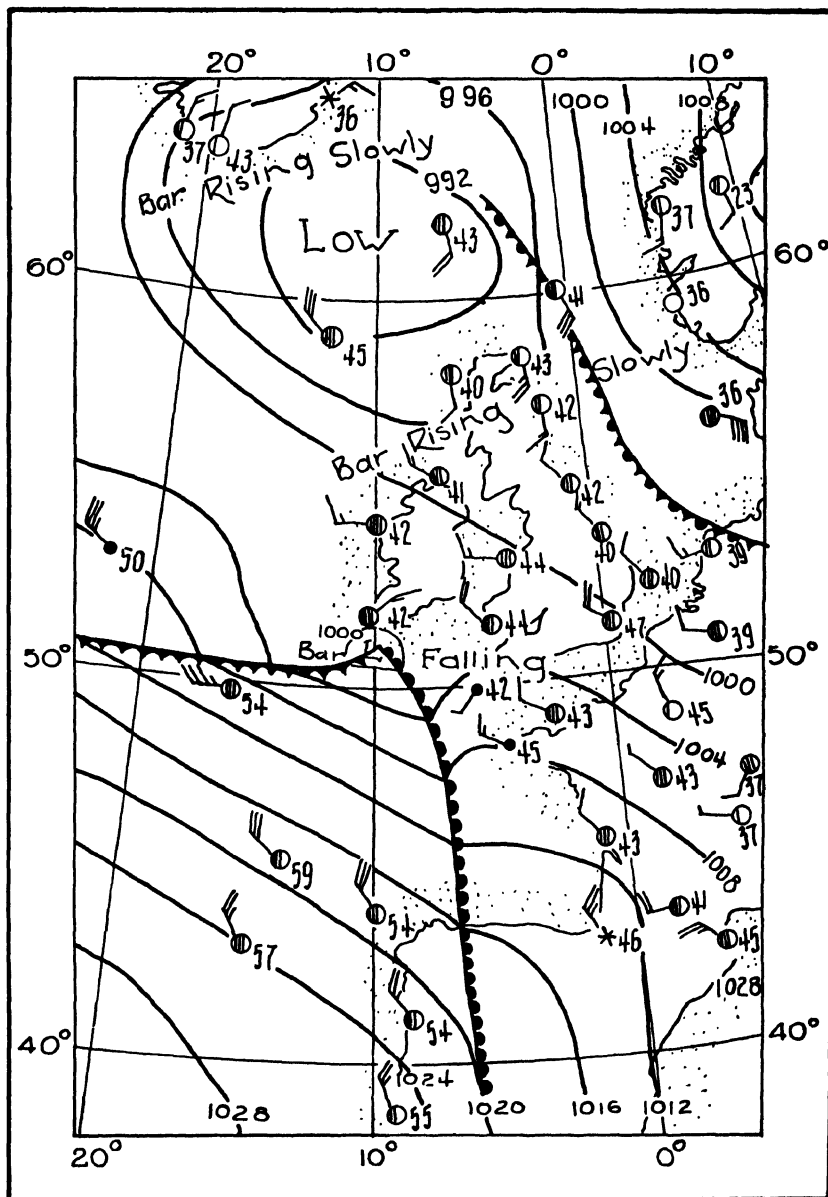
$$\frac{\partial^2 p_1}{\partial t^2} - \frac{\partial^2 p_2}{\partial t^2} > 0$$

and, according to (112.1), this portion of the front has a southward acceleration. The advance of this section of the front to the south is shown in Fig. 108c.

The portion of the depression having warm air at the surface is called the *warm sector*. The air to the west of the center of low pressure that has formed advances southward and southeastward, as indicated above, replacing the warm air at the ground. This section of the front is called a *cold front*. On the other side of the low the warm air replaces the cold, and this portion of the front is known as a *warm front*. The isobars in the warm sector are usually nearly straight. This stage is accompanied by falling tendencies ahead of the warm front, becoming steady in the warm sector, and rising back of the cold front. The wind veers, i.e., its direction changes in a clockwise manner at each front. The temperatures in the warm sector are fairly uniform with contrasting temperatures across the fronts.

The wave sometimes moves rapidly along the original front during stages (b) and (c), never developing beyond stage (c). The rate of movement is dependent on the velocities of the air on either side of the front. As the wave travels eastward, the area just north of the front will have a short spell of cloudy weather with precipitation, accompanied by rapidly changing winds. This development is to be expected if falling tendencies occur to the east of the crest of the wave, and to the west of the crest the pressure is rising.

The other possible development is a deepening of the center of low pressure, accompanied by an increase in the amplitude of the wave, the movement of the system in the direction of the isobars in the warm sector, and the overtaking of the warm front by the cold. This stage is shown in Fig. 108d. The fronts now form one line at the surface, known as an *occlusion*. As the process of occlusion occurs, the cold and dense air pushes underneath the warm air, the cold front advancing at the same rate as the wind in the cold air behind the front. On the other hand, at the warm front the warm air overrides the cold air. Hence the warm air does not displace the cold air with the speed of the air in the warm sector but at a speed which varies with different situations but averages about 60 per cent of that of the warm sector air. Since, then, with the same pressure gradient, the cold front moves more rapidly than the warm front, it overtakes the warm front, driving aloft the warm air that is trapped between the two.



information plotted for each reporting station is the wind, the amount of sky covered, and the temperature. The sky cover is indicated by the amount of shading within the circle representing the station. The wind direction is given by the shaft from the station circle, the wind blowing along this line toward the station. The force of the wind is indicated by the number of feathers on the shaft, each feather representing two points of the Beaufort wind scale described in section 66. The full lines give the sea level isobars, with pressures as indicated.

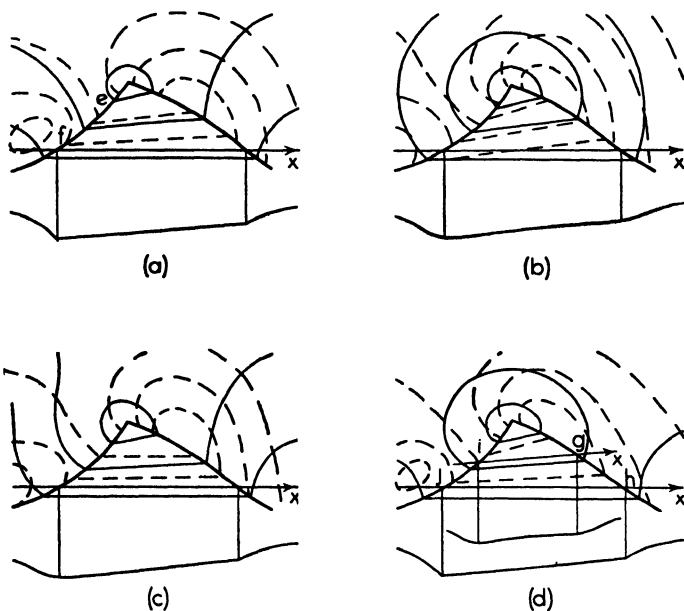


FIG. 110. Types of isobars, isallobars, and barogram curves about low-pressure areas. (After Petterssen.)

The warm front is given by a curve with semicircular black areas on it. Triangular black areas mark the cold front, and alternate triangles and semicircles designate an occlusion. An example of an occlusion is found in the upper right-hand portion of the diagram.

The warm sector is located in the low situated south of Ireland. Note the change of wind across both the warm and cold fronts, as well as the difference in temperature. This system never reached stage (d) of Fig. 108, as frontolysis occurred shortly after the time of the map in Fig. 109. Near Iceland there is a low-pressure area which is now filling, and out of which extends an occlusion. Note the wind shift across the occlusion, as well as the difference in temperature. During the occlusion process, the low at the end of the occlusion deepens and moves

much more slowly. When the occlusion process is complete, the warm air has been pushed aloft, and at the surface there is a core of cold air. The center fills, the occlusion is subjected to frontolysis and finally disappears.

If the method of analysis adopted by Petterssen is used, the rate of occlusion in several types of frontal depressions may be discussed qualitatively with the aid of the formula for the acceleration of a front given in section 43. It was shown in that section that the acceleration A of a front is made up of three components, A_1 , A_2 , and A_3 . According to (43.10)

$$A = A_1 + A_2 + A_3$$

The nature of each component is indicated in section 43. For any given distribution of isobars, isallobars (lines of equal pressure tendency), and any type of barogram curve, the sign of each of these components in the x direction may be determined by the method indicated in section 43. Four types of frontal depressions, differentiated by the distribution and curvature of isobars, isallobars, and barogram curves in each, are shown in Fig. 110. The full lines represent isobars and fronts, broken lines represent isallobars, and the curve at the base of each diagram represents the barogram curve. Applying the procedure of section 43 to each, the results given in the table are obtained. Al-

SIGNS OF THE VARIOUS ACCELERATION COMPONENTS
FOR WARM AND COLD FRONTS

Type of Depression	Front	Components of Acceleration		
		A_1	A_2	A_3
(a)	Warm	+	-	+
	Cold { At e At f	-	+	-
		-	-	-
(b)	Warm	-	-	-
	Cold	+	-	+
(c)	Warm	+	-	+
	Cold	+	-	+
(d)	Warm { At g At h	-	-	-
		+	-	+
	Cold { At i At j	+	-	+
		+	-	+
		-	-	-

though the magnitudes of the three components will vary from one depression to the next, to facilitate the following discussion it will be assumed that each component has the same magnitude, the only difference being one of sign.

It can be seen from the table that in type (a) depression the warm front has a small net acceleration to the east. Near the center of low pressure, at *e*, the cold front has a small net retardation, and farther south, at *f*, it has a large net retardation. It follows, then, that this type will not tend to occlude, but rather to move as a stable wave. Systems of this kind frequently travel for hundreds of miles as a stable wave. The system shown in Fig. 109 appears to be of this type. As mentioned before, it did not occlude but dissipated as a result of frontolysis.

In type (b) the warm front is strongly retarded at all points, while the cold front has a net acceleration towards the east. A cyclone of this type is therefore likely to occlude rapidly.

There is a small net eastward acceleration of both fronts in type (c). With this configuration, then, the system may move as a stable wave, or if it occludes, the rate of occlusion will not be rapid. It is intermediate between types (a) and (b).

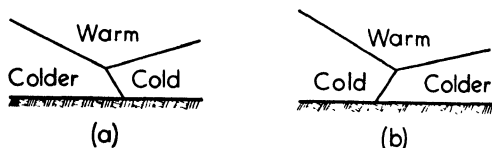


FIG. 111. (a) Cold and (b) warm front types of occlusions.

An examination of the table shows that type (d) occludes rapidly near the center of low pressure at *g* and *i*, but only very slowly, if at all, farther south, near *h* and *j*. The result is that the northern portion of the warm sector occludes rapidly in the early stages of development. The process of occlusion then ceases, leaving an occlusion extending northwestward from the tip of the warm sector to the center of low pressure. This type of depression is of frequent occurrence. If a fresh supply of warm moist air flows into the warm sector, providing a new source of energy for the system, a secondary low may form at the junction of the warm and cold fronts. When this happens, the original low becomes less prominent with the development of the second depression.

Two types of occlusions occur, and are illustrated in Fig. 111. Originally the portions of air on the two sides of the occlusion were from the same air mass and therefore nearly identical in properties. But in moving over different underlying surfaces and in other ways, slight differences in properties across the occlusion develop. When the air behind the occlusion is colder, the occlusion is of the cold front type, illustrated by Fig. 111a. When the air behind is warmer, the occlusion

is of the warm front type, illustrated by Fig. 111*b*. The difference in temperature is seldom as large as that between one of the cold air masses and the warm air mass. Hence, according to (38·8), the slope of the occlusion surface below the trough of warm air is steeper than the slope of either the cold or the warm frontal surface. At times, with a warm front type occlusion, the passage of the upper trough of warm air can be determined at a station by means of a change in the rate of fall of the barometer or by an increase in the precipitation arising from the lifting of the warm air at the upper cold front at this point.

With some fronts several waves will develop, one after another. The average length of time between the development of successive waves is about 24 h. When a front has become stationary the passage of a family of these waves may cause the front to shift back and forth several times across a station which lies near the front.

There may be secondary cold fronts behind the main cold front. These sometimes occur in rapidly moving polar air as it flows southward over a warmer land surface. These secondaries continue as long as the wind velocity remains high. The distance between secondary cold fronts in any given depression is nearly equal, but this distance shows wide variations in different depressions. They may be anywhere from 50 to 400 mi apart, and moving with velocities from 25 to 40 mph. A continuous succession of these secondaries may pass, some being marked and others very weak. Their passage is usually characterized by gusty, shifting winds, and a short period of rain, with hail and thunder on occasion. It is often impossible to determine the positions of these secondary cold fronts from ordinary synoptic weather maps, and autographic records must be used in conjunction with the maps if their exact location is desired. It is obvious, therefore, that discretion must be used in plotting secondary fronts on the map. Only the most marked of these can safely be plotted unless sufficient time and data are available to permit exhaustive analysis.

Seclusion of the warm sector air, instead of occlusion, sometimes occurs under certain orographic conditions. The process of seclusion is shown in Fig. 112. The motion of the lower portion of the warm front is retarded, as indicated in Fig 112*a*, by high hills or a range of mountains. The cold front overtakes the warm front first at this point, leaving an island of warm air secluded farther to the north, as shown in Fig. 112*b*. This development sometimes occurs on the west coast of Norway, where the coastal range juts westward in the southern part of the country, retarding advancing warm fronts at this point.

The changes in the weather elements that occur with the approach and passage of a front vary widely. The variations result from differ-

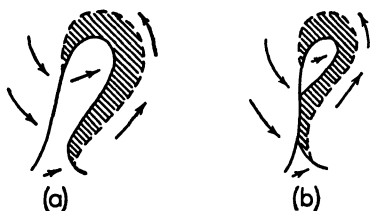


FIG. 112. The development of a seclusion.

ences in the air masses, in the rates of motion of the fronts, in the amount of overrunning, in the rate of deepening, and other causes. The following table gives the changes normally expected in the vicinity of cold and warm fronts. Yet, owing to the differences between individual fronts, each of these changes should

be taken as the average one only, and not as invariably accompanying every front. The changes which occur at an occlusion are not as clearly defined as those taking place when a warm or a cold front passes.

USUAL CHANGES ACCOMPANYING THE PASSAGE OF FRONTS

Type of Front	Property	Ahead of Front	At Frontal Passage	After Frontal Passage
Warm	Pressure	Steady fall	Fall ceases	Not much change; perhaps slow fall
	Temperature	Slow rise	Rise ceases	Not much change
	Humidity	Gradual rise	Rise ceases	Not much change
	Wind	Back, and increase	Veer and decrease	Not much change
	Cloud	Ci, Cs, As, Ns in succession	Low Ns and Fs	Perhaps St or Sc
	Weather	Steady precipitation	Precipitation decreases	Fair or drizzle, perhaps intermittent
	Visibility	Good, except in rain, decreasing with approach of front	Poor; sometimes mist or fog	Poor; mist or fog often persist
Cold	Pressure	Fall, usually slow	Sudden rise	Rise continues more slowly
	Temperature	Not much change	Sudden fall	Fall continues slowly
	Humidity	Not much change	Sudden decrease	Low
	Wind	Slight backing, increasing	Sudden veer, perhaps squall	Not much change; further veering perhaps
	Cloud	Perhaps Cu or Cb	Cu and Cb, perhaps Ns	Sometimes As, then Cu
	Weather	Possibly rain	Heavy rains, sometimes thunder and hail	Showers
	Visibility	Poor	Sudden improvement	Good

A discussion of the types of clouds normally associated with a frontal depression will be given in section 137. The occurrence of fog in the vicinity of fronts is discussed in section 131 and following, and the extent of the areas of frontal precipitation is indicated in section 129.

113. Upper Air Conditions above Frontal Depressions. In the early stages of a depression, when the warm sector is broad, closed isobars occur at the surface, but do not usually extend to heights as great as 3 km. As the depression intensifies, however, closed isobars extend upward to greater heights, and in the later stages even the isobars at 7 or 8 km frequently have cyclonic curvature, as shown by the motion of cirrus clouds near a depression.

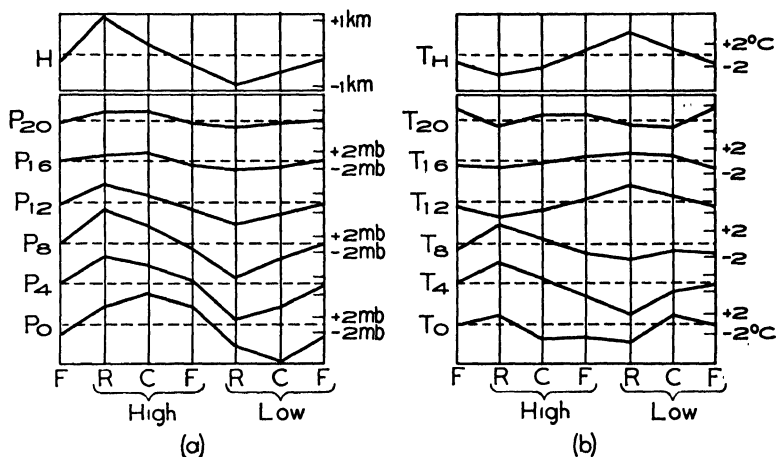


FIG. 113. Variation (a) of pressure at various heights in kilometers and of the height of the tropopause, and (b) of temperature at the same heights and at the tropopause with the passage of high- and low-pressure areas. (After Penner.)

Since the air on the west side of a low is colder than that in the warm sector, the rate of decrease of pressure with height is greater in the former than in the latter. The center of lowest pressure at higher levels is found, then, on the west side of the surface depression. This deduction is substantiated by the movement of cirrus clouds, which have a cyclonic trajectory about a point to the west of the center at the earth's surface.

Further support for this deduction is found in the data illustrated in Fig. 113. In Fig. 113a curves are given showing the variation in the mean pressure p_z at the level z in kilometers for the areas at the east or front (F) side of a low, at the west, or rear (R) side, of a high, at the center (C) of a high, at the east side of a high, at the west side of a low,

and at the center of a low. Also included is the variation in the height of the tropopause, H , for the same areas. Fig. 113*b* gives the corresponding variation in mean values for the temperature T_z . These curves were computed from the radiosonde reports from Sault Ste. Marie, Michigan.

It will be noticed that at 4 and 8 km and at the tropopause (about 10 km) the lowest pressure is at the rear of a low. The tropopause is highest and coldest at the rear of a high. As the diagram shows, a wave on the tropopause is associated with the surface low-pressure area.

Under average conditions the tropopause is high and cold over the equator, whereas at the poles it is low and relatively warm, as shown in Fig. 3, section 2. Thus the conditions at the tropopause over the rear of a high, i.e., over the warm frontal surface, correspond to those occurring on the average at the tropopause a few degrees of latitude to the south, but over the rear of a low, i.e., over the cold front, the conditions are similar to those a few degrees to the north. These considerations suggest the presence of a horizontal north-south wave motion of the tropopause, which in turn produces a vertical wave motion of the latter. The cyclonic motion in the cold and warm air in the troposphere thus extends above the tropopause into the stratosphere, as manifested by a movement north and south of the tropopause in the vicinity of a surface low-pressure area.

The exact nature of the relationship between the wave motions of the tropopause and surface low-pressure areas is not known. Some meteorologists believe that the upper wave is induced by the variations near the surface. Others hold the opposite view, that the decrease in pressure in the stratosphere results in a corresponding decrease in pressure below, at the surface of the earth. The truth probably lies somewhere between these two opinions. More study of individual depressions is needed before these questions can be answered with assurance. However, it is probable that no single picture is applicable to all depressions.

114. Other Types of Depressions. All depressions do not have the structure outlined in the previous sections. Because of the unequal heating over the earth's surface, there is a tendency for *thermal depressions* to develop over warmer regions. Of course influences other than surface heating are significant, such as upper air conditions, but sometimes this factor is predominant. The summer monsoon low of south Asia (Fig. 5, section 3) is the most notable example of this type. The winds flow in the usual manner about the center of low pressure, but extensive cloud systems are not always present. On the contrary, long periods of clear weather often occur in regions where there are no large

ranges of hills or mountains. It cannot be said, therefore, that cyclones always bring disturbed weather conditions.

The development of some cyclones may be due to instability within the air mass. These are called *instability depressions*. They sometimes develop in polar air masses as they move over warmer portions of the earth's surface. A depression of this type sometimes forms in winter and early spring in an extensive mass of polar continental air which becomes stagnant over the Great Lakes and acquires heat and thus instability from the underlying warm water. Instability is pronounced under such conditions. These depressions initially have no discernible frontal structure, although fronts may develop in them later.

Orographic depressions sometimes form in the lee of mountain ranges. There is a slight tendency for compression of the air to the windward to occur, producing a ridge of high pressure, and for rarefaction on the lee side, producing a shallow depression there. Orographic cloud and rain may occur over the windward slope of the mountain, while descending motion of the air to the lee may prevent the formation of cloud in the shallow depression. These depressions will, at times, move from the region of their formation and into the general west to east track of extra-tropical cyclones.

115. Tropical Hurricanes. Tornadoes. Tropical hurricanes, as their name suggests, are violent storms developing over the tropical portions of the oceans. These storms do not occur near the equator, since the deflecting force of the earth's rotation (section 34) is not sufficiently strong there to produce cyclonic motion. They develop only at latitudes greater than 5° or 6° .

As these storms form over the ocean in tropical latitudes where there are few weather reports from ships, there is some doubt as to the manner of their formation. Two main suggestions have been put forward. The Norwegian meteorologists and some others associate their development with an "inter-tropic front." They believe that this inter-tropic front lies between the trade wind systems of the northern and southern hemispheres. The trade wind systems move northward and southward with the seasons. The maximum northward displacement occurs during the months of August, September, and October. Also during these months the difference in temperature across the front between the air of the northern hemisphere and that of the southern hemisphere is at a maximum. For these reasons, the maximum number of hurricanes occurs during these months. Other meteorologists believe that tropical hurricanes develop whenever high temperature and moisture content in the surface air coincide with suitable upper air conditions. This may

occur when fresh polar continental air has moved from the continent and has become rapidly modified in the lower layers, producing instability of the real latent type.

There are a number of characteristic features of a tropical hurricane. One of the most striking of these is the presence of what is known as the *eye* of the storm. In the eye there are higher temperatures and lower humidities than in the outer portions of the storm region, few clouds, nearly calm conditions, and a pressure minimum. The diameter of the eye of the storm varies from 5 to 50 mi. The foregoing facts suggest that there is subsiding air in the central portion of the storm. Air may be brought down from above as a result of the extremely low pressure. In the area outside the eye there are very high winds and heavy rainfall.

It is generally thought that the latent heat released by condensation provides the energy of the storm. It is difficult to understand how the air ascending from below is removed at upper levels. Several hypotheses have been put forward, but no entirely satisfactory explanation has been developed as yet.

Fortunately only a small number of tropical hurricanes reach continental areas. The usual path of tropical hurricanes in the Atlantic is shown in Fig. 114. The storm develops to the south of the Atlantic anticyclone and moves westward. Generally its path is approximately parallel to the isobars of the sub-tropical high. It acquires a north-westward component, then moves northward and finally northeastward. The storm is said to *recurve* when it acquires an eastward component of motion. The storm decreases in intensity as it moves to higher latitudes, and it may continue thereafter with all the characteristics of an ordinary depression of middle latitudes. However, if the hurricane does not recurve, it may move along the eastern coast of the continent, doing great damage. If the hurricane moves inland, its energy is rapidly dissipated, but it may give very heavy rainfall even in its later stages.

The region of the western Atlantic from the West Indies north to Bermuda is frequently visited by these storms. They are found, too, in the western Pacific along the China coast, where they are called *typhoons*. Relatively few occur in the southern hemisphere.

A *tornado* has many features of a tropical hurricane but is of much smaller dimensions. It is a violent whirlwind several hundred yards in diameter, moving rapidly and destroying everything in its path. They occur most frequently in the United States and Australia. They develop in air of great instability and are frequently associated with cold fronts at the leading edge of an outbreak of fresh polar continental

air in the spring and early summer. They are usually accompanied by thunderstorms and heavy rain, and at times hailstorms.

The tornado is intermediate in size between phenomena such as dust devils on the one hand, and tropical hurricanes on the other. It is

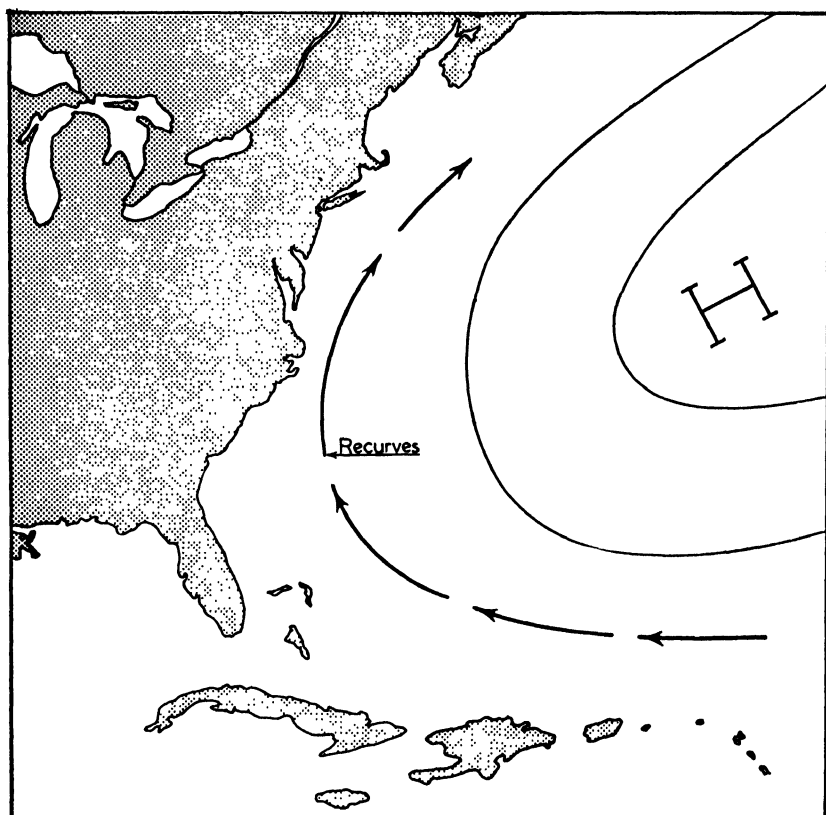


FIG. 114. The path of a tropical hurricane over the western Atlantic.

essentially a cyclone with a center of low pressure (see problem 3, chapter 6), and winds moving as specified by Buys Ballot's law. The horizontal dimensions of a tornado are too small for it to be shown by isobars on a weather map.

116. Comparison of Upper Air Conditions above Cyclones and Anticyclones. It might be thought that convergence of air in the lower levels would lead to high pressure. Just the reverse is true, however, for there is divergence from anticyclones, which are high-pressure systems. The winds move in a clockwise manner around the center of high pressure in such a manner that the deflecting force just balances

the sum of the centrifugal force and that arising from the pressure gradient (section 37). There is descending motion of the air in the anticyclone, as indicated by the divergence at the surface. A common misconception, widely held, is that the air at upper levels above an anticyclone is colder than that at the same levels above a cyclone. Fig. 115 shows that the reverse is true. The two curves give mean values of the temperature distributions with height in cyclones and

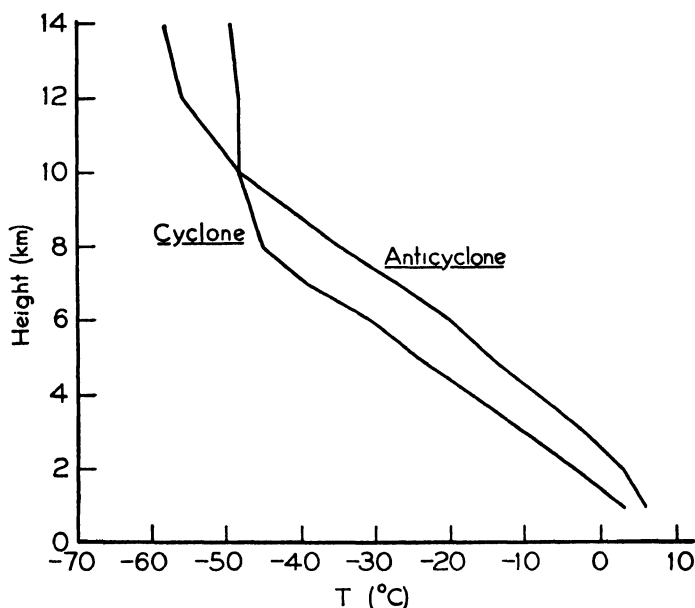


FIG. 115. Mean temperature curves in cyclones and anticyclones over England. (After Dines.)

anticyclones. A similar comparison can be made between the temperatures in anticyclones and cyclones by noting the temperatures for the center of a high and the center of a low as given in Fig. 113*b*, section 113. These diagrams show two significant features. The first is that, at nearly all levels of the troposphere, air in anticyclones is warmer than that in cyclones. In the lowest 2 km the evidence is conflicting. This difference is probably due to the relative development of the cyclones. When the cyclone is occluded, the surface air at the center of the cyclone will be colder than in a cyclone which has an open warm sector. Thus in the lowest levels the mean temperature depends on whether the majority of observations are taken before or after occlusion. The second point of interest is that the stratosphere is higher and colder above anticyclones than above cyclones.

The pressure at the base of an air column is proportional to the density of the air above, and so is less with air columns with high temperatures. The weight of the air in the troposphere over a center of high pressure is, then, less than that over a center of low pressure. The higher pressure at the surface must, for this reason, be the result of heavier and therefore colder air in the stratosphere. A statistical analysis by W. H. Dines reveals the close relationship among these variables. Between the pressure at the surface and the pressure at 9 km, the coefficient of correlation is 0.68. Between the pressure at 9 km and the temperature at 4 km, the coefficient of correlation is 0.82. Between the pressure at 9 km and the mean temperatures from the surface to 9 km, it is 0.95. Between the pressure at 9 km and the height of the tropopause, it is 0.84.

The warm air found in the troposphere above the center of high pressure may be explained by the subsidence that accompanies the divergence.

The low temperatures in the stratosphere may be explained as a result of the wave motion of the tropopause discussed in section 113. The horizontal movement in the stratosphere which accompanies the surface pressure variation carries northward in the region above the anticyclone the colder air of the southern stratosphere. At the same time there is a southward movement of the warm air of the northern stratosphere above the center of low pressure. Further evidence to support this explanation is found in the distribution of ozone mentioned briefly in section 5. In the normal distribution the ozone, which is found chiefly in the region from 20 to 40 km, increases with latitude. But near a depression the ozone content is greater than the normal for the latitude, while near an anticyclone the amount is less than normal.

117. The Cold Anticyclone. Variations from the mean temperature values discussed in the previous section are found in individual anticyclones. Certain high-pressure systems exist, not because of cold air in the stratosphere, but because of a shallow layer of very cold air near the surface of the earth. These are called cold anticyclones. Semi-permanent anticyclones of this type are found over Greenland and over the Antarctic continent. Rapid subsidence occurs with air diverging horizontally from the ice caps. The cold air is shallow, though, and warm air moves in above the cold dome.

A similar situation exists over Siberia and over northwest Canada during the winter. The underlying snow surface, being very cold as a result of long-wave radiation, cools the adjacent air. The air is cold only in the lowest few kilometers, and warm air lies above it. Fig. 116 illustrates a west-east cross section of an anticyclone of this type over

North America. The exact determination of the upper boundary of the cold dome is not easy, owing to the mixing that takes place. The eastern boundary is a steep cold frontal surface, while to the west the warm P_P air ascends the warm frontal surface.

In North America these air masses are frequently so shallow that they are prevented from extending to the west coast of the continent by the Rocky Mountain barrier. They then follow a southeasterly path changing to easterly as they leave the continent and move over

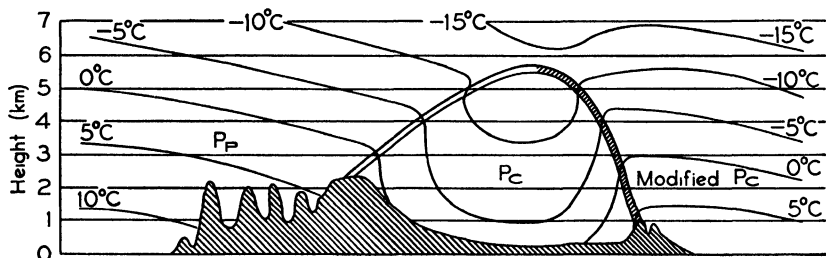


FIG. 116. A vertical cross section through a cold anticyclone.

the Atlantic Ocean. In Europe there is no extensive mountain barrier and the cold Siberian anticyclone is free to move to the west. Thus western Europe in the winter is more often under the influence of a continental type of climate than the Pacific coast of North America.

As a cold anticyclone becomes heated during its advance to lower latitudes, the pressure at times decreases, and such a weakened cold dome frequently collapses as a center of low pressure moves toward it. Another change sometimes occurs. If the cold anticyclone becomes stationary in middle latitudes, the pressure above the cold dome frequently increases as a result of advection of cold air at that level. Thus the decrease of pressure resulting from the increase in temperature at the surface is compensated for by an increase in pressure aloft, and the cold anticyclone is transformed into a warm anticyclone.

118. The Warm Anticyclone. Warm anticyclones, such as those comprising the sub-tropical high-pressure belts, have high surface pressures in spite of their high surface temperatures. These anticyclones extend, then, to great heights. This type of anticyclone is also found in the temperate zone. If one of the sub-tropical high-pressure cells divides, one of the component parts of the system may penetrate the region of westerlies and move in the general westerly circulation. Also, as indicated in the previous section, at times a cold anticyclone which has become stagnant in middle latitudes is transformed into a warm anticyclone.

The warm anticyclone is more stable than a cold anticyclone. A cyclone moving eastward toward one of the former will become stagnant on the western boundary of the anticyclone or will move in the anticyclonic circulation about the center of high pressure.

As shown by the variation of pressure at 8 km indicated in Fig. 113a, section 113, the wedge of high pressure at that level is found above the rear of the surface high-pressure system. Above the center of high pressure at the surface the clouds at the cirrus level move from the northwest along the eastern edge of the ridge of high at that level. In a warm anticyclone the cirrus clouds sometimes disappear above the high-pressure system at the surface. This fact suggests that the subsidence in the anticyclone extends up to the cirrus level.

119. Convergence and Divergence in Cyclones and Anticyclones.

Some of the weather occurring in cyclones and anticyclones is the result of convergence and divergence in these systems. In all portions of a cyclone there is horizontal convergence in the frictional layer near the surface, which accounts in part for the cloudiness which occurs in low-pressure areas. Similarly, horizontal divergence in the frictional layer accounts in part for the clear skies associated in general with anticyclones. However, frictional inflow and outflow do not explain the variations in weather from one section of a cyclone or anticyclone to another.

Convergence and divergence resulting from the variation of the gradient wind with latitude account for many of these variations in weather. The gradient wind velocity v in a cyclone with circular isobars is, according to (37.2),

$$v = -\omega r \sin \phi + \sqrt{\omega^2 r^2 \sin^2 \phi + \frac{r}{\rho} \frac{\partial p}{\partial r}}$$

since the Coriolis parameter $l = 2\omega \sin \phi$. In this equation r represents the radius of curvature of the motion. Consider now a cyclone centered at latitude ϕ . The gradient wind v_0 at ϕ_0 and v_1 at ϕ_1 may be computed, if r , ρ , and $\partial p / \partial r$ are known. With the horizontal convergence or divergence found in this manner, the resulting average vertical velocity w_1 at height z_1 between ϕ_0 and ϕ_1 is obtained by substituting for $v_1 - v_0$, y_1 , and z_1 in (45.9), where y_1 is the arc of a circle of radius r extending from ϕ_0 to ϕ_1 . Remember that the length of the chord subtended by angle θ is

$$2r \sin \frac{\theta}{2}$$

and it may readily be shown that the length of the arc between ϕ_0 and ϕ_1 is

$$\frac{\pi r}{90} \text{ arc sin } \frac{\pi E (\phi_1 - \phi_0)}{360r}$$

where E is the radius of the earth.

The following example shows the order of magnitude of the vertical velocities at a height of 1 km above the surface at varying distances from the center of low pressure, when the latter is at 45° N latitude,

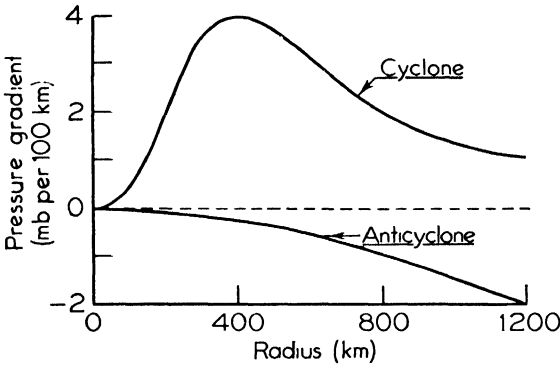


FIG. 117. Variations of pressure gradient with distance from the centers of cyclones and anticyclones.

when $\phi_0 = 42.5^\circ$, $\phi_1 = 47.5^\circ$, $\rho = 1.1 \times 10^{-3}$ gm per cm^3 , and the variation of the pressure gradient $\partial p / \partial r$ with r is as given by the curve marked cyclone in Fig. 117. The positive direction of r is taken as outward from the center. The results of the computation are given in the upper part of the following table. The positive velocities indicate

VERTICAL VELOCITIES AT 1 KM RESULTING FROM
THE VARIATION OF THE GRADIENT WIND VELOCITY WITH LATITUDE

Type of Pressure System	Radius (km)	v_0 (m per sec)	v_1 (m per sec)	Vertical Velocity w_1 (cm per sec)	
				East of Center	West of Center
Cyclone	400	23 2	22 2	+0 16	-0.16
	800	15.4	14 5	+0.16	-0.16
	1200	8 6	8 0	+0 11	-0.11
Anticyclone	400	1 9	1 8	-0 02	+0.02
	800	10 6	9 5	-0 19	+0.19
	1200	22 8	19.9	-0 52	+0 52

that the air is ascending, while the negative ones show that it is descending. The vertical velocities at 2 km will be twice as great as those at 1 km, shown in the table, provided that the field of motion extends to 2 km.

A similar computation for an anticyclone may be carried out by using the equation 37.4 for the gradient wind in the anticyclonic case

$$v = r\omega \sin \phi - \sqrt{r^2\omega^2 \sin^2 \phi - \frac{r}{\rho} \frac{\partial p}{\partial r}}$$

and the appropriate values for $\partial p/\partial r$ as given by the curve designated anticyclone in Fig. 117. In deriving this equation, the positive direction for r was taken as inward toward the center of high pressure, so that the negative values of $\partial p/\partial r$ shown in Fig. 117 are positive when substituted in the equation. The vertical velocities obtained in this manner are given in the lower portion of the table.

The distributions of $\partial p/\partial r$ with r shown in the figure are representative of those in many cyclones and anticyclones, so that it is permissible to make a number of generalizations on the basis of the values shown in the table. The vertical velocities are always small except at the eastern and western outer limits of an anticyclone. Here the vertical velocities of about 0.5 cm per sec at 1 km and 1 cm per sec at 2 km are sufficient to account for, at least in part, the cloudiness and light precipitation often observed near the western edge of an anticyclone, and the clear skies near the eastern edge. The values of vertical velocities given in the table are the maxima to be expected at 1 km from this cause in cyclones and anticyclones, since the variation of ϕ and so of $\sin \phi$ for any given length of arc is a maximum to the east and west of the center. Near the north-south axis of a cyclone or anticyclone, the vertical velocities are much smaller than indicated in the table, since the variation of ϕ along the arc is slight, and they become zero at the axis where the variation of ϕ along the arc is zero. The weather occurring at the northern and southern edges of an anticyclone must thus be accounted for in other ways, perhaps by variations in the curvature of the air motion, as outlined in section 141.

The distribution of vertical velocities in a frontal depression resulting from the variation of the gradient wind with latitude and pressure gradient is shown in Fig. 118a. The circular lines are streamlines of the air motion at distances of 400, 800, and 1200 km from the center. Since the wind in the warm sector is approximately west when the latter is in the position shown, the vertical velocity is very nearly zero. If the warm sector is oriented so that the air has a considerable north-

ward component of motion, horizontal convergence and ascending motion occur, the approximate magnitude of which may be computed with the aid of (45-10). Fig. 118*b* gives the distribution of vertical velocities in an anticyclone, based on the figures given in the above table.

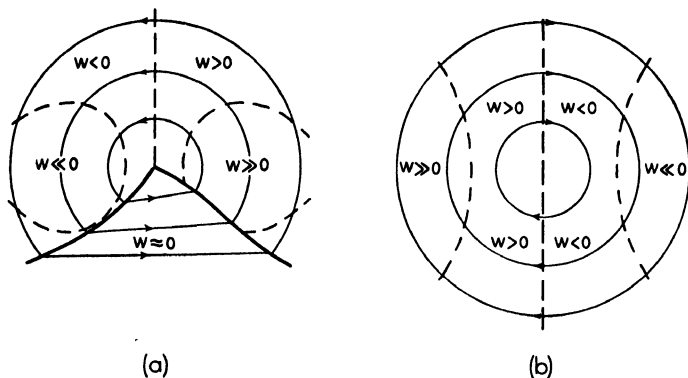


FIG. 118. Vertical velocities resulting from latitudinal convergence and divergence in (a) cyclones and (b) anticyclones.

According to (47-4), ascending motion at any level results in increasing pressure at that level, whereas descending motion results in decreasing pressure. On the basis of the above results alone, then, the pressure at a height of 1 km should rise ahead of a cyclone and fall behind it. The reverse actually happens, however. This apparent anomaly is resolved because the pressure at any level also depends on the convergence or divergence and advection at higher levels, as shown in section 47. The effect of vertical velocity is, in this case, overcompensated by the convergence and divergence at greater heights in the warm sector air, of the type discussed in section 48, and by advection. Similar considerations apply to the pressure variations ahead of and behind an anticyclone.

The anticyclone that dominated the eastern portion of Canada and the United States at 01.30 h EST on November 5, 1942, is shown in Fig. 119. Since the isobars on the western edge of the system are practically straight, the variation of the geostrophic wind with latitude may be used in determining the horizontal convergence. By using (45-10), the average velocity of ascent at 2 km between latitudes 40° and 55° is found to be 0.5 cm per sec. The average velocity of ascent of the warm sector air in an occluding frontal depression, which produces thick cloud systems and moderate to heavy precipitation, is about 4 cm per sec. Thus the computed vertical velocity of 0.5 cm per

sec is sufficient to account for the cloud development and light precipitation that occurred at the western edge of the anticyclone, as shown in Fig. 119.

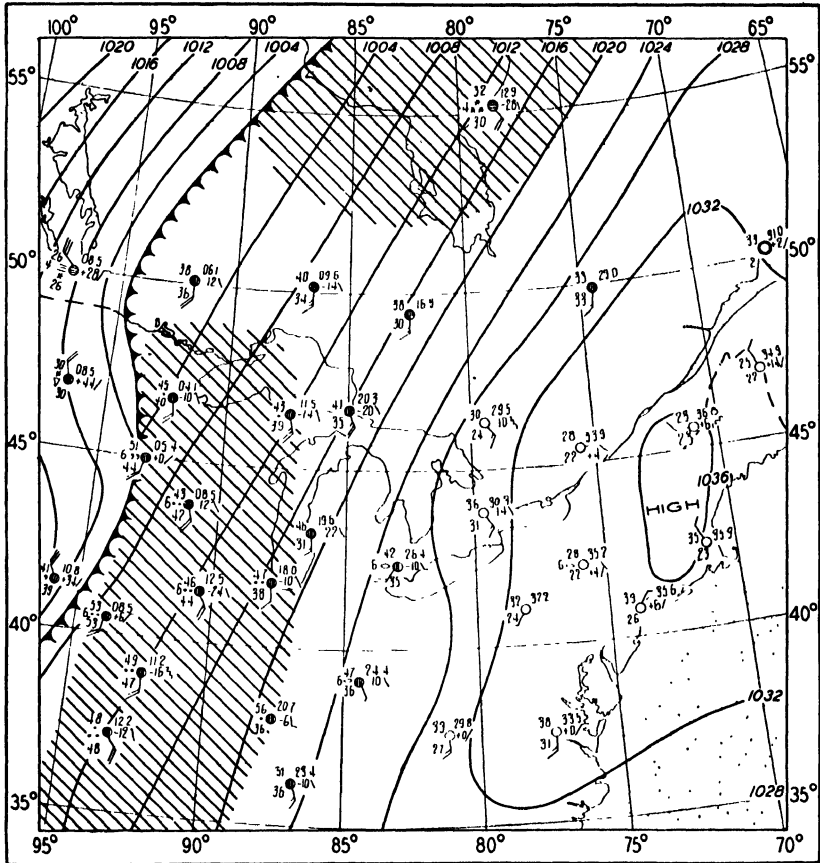


FIG. 119. The weather map for 01.30 h, November 5, 1942, illustrating the horizontal convergence in air with a northward component of motion.

PROBLEMS AND EXERCISES

1. An airport is in the cold air 250 mi east of a warm front lying in a north-south direction. The front is moving eastward at 15 mph. A plane is 300 mi west of the airport and is flying at 3000 ft above the surface eastward at 100 mph. Assuming that the warm frontal surface has a slope of $\frac{1}{200}$, at what distance from the station will the plane pass through the frontal surface?
2. If a cold front passed a station at 10.00 h, moving at the rate of 25 mph, at what time would the winds at 2000, 5000, and 10,000 ft veer with the frontal passage if the frontal surface is assumed to have a slope of $\frac{1}{50}$?

3. A warm front, slope $\frac{1}{150}$, lies 400 mi from a station at 08.30 h and is moving toward the station at a speed of 20 mph. At what times will the wind at 4000 and 8000 ft veer as a result of the passage of the frontal surface?

4. The warm sector air of a depression overruns the cold air ahead. The warm air at the surface has a temperature of 67° F and a dew point of 55° F. If the front has a slope of $\frac{1}{200}$, at what distance ahead of the surface front will the air become saturated?

BIBLIOGRAPHY

- Admiralty Weather Manual*, London, H. M. Stationery Office, 1938. Chapters 18, 19.
- Brunt, D., *Physical and Dynamical Meteorology*, London, Cambridge University Press, 1939. Chapters 17, 18.
- Byers, H. R., *Synoptic and Aeronautical Meteorology*, New York, McGraw-Hill Book Co., 1937. Chapters 5, 12.
- Haurwitz, B., *Dynamic Meteorology*, New York, McGraw-Hill Book Co., 1941. Chapter 15.
- Petterssen, S., *Weather Analysis and Forecasting*, New York, McGraw-Hill Book Co., 1940. Chapters 4, 5, 6.
- Problems of Modern Meteorology*, London, Royal Meteorological Society, 1934. Numbers 1, 9.
- Shaw, Sir N., *Manual of Meteorology*, London, Cambridge University Press. Vol. 2 (1936), Chapter 8.
109. Bergeron, T., "Über die dreimensional verknüpfende Wetteranalyse," *Geofys. Publ.*, 5, No. 6, Oslo, 1928.
109. Petterssen, S., "Contribution to the Theory of Frontogenesis," *Geofys. Publ.*, 11, No. 6, Oslo, 1934.
111. Shaw, W. N., and R. G. K. Lempfert, *The Life History of Surface Air Currents*, London, Meteorological Office, M. O. 174, 1906.
112. Bjerknes, J., "On the Structure of Moving Cyclones," *Geofys. Publ.*, 1, No. 2, Oslo, 1918.
112. Bjerknes, J., "Practical Examples of Polar Front Analysis over the British Isles in 1925-26," *Geophys. Mem.*, No. 50, London, 1930.
112. Douglas, C. K. M., "Some Aspects of Surfaces of Discontinuity," *Q. J. Roy. Met. Soc.*, 55, 123-147 (1929).
112. Gold, E., "Fronts and Occlusions," *Q. J. Roy. Met. Soc.*, 61, 107-157 (1935).
113. Bjerknes, J., "Exploration de quelques perturbations atmospherique à l'aide de sondages rapprochés dans le temps," *Geofys. Publ.*, 9, No. 9, Oslo, 1932.
113. Bjerknes, J., "Investigations of Selected European Cyclones by Means of Serial Ascents, Case III," *Geofys. Publ.*, 11, No. 4, Oslo, 1934.
113. Bjerknes, J., and E. Palmén, "Investigations of Selected European Cyclones by Means of Serial Ascents, Case IV," *Geofys. Publ.*, 12, No. 2, Oslo, 1937.
- 113, 116. Penner, C. M., "The Effects of Tropospheric and Stratospheric Advection of Pressure and Temperature Variations," *Can. J. Res.*, A19, 1, 1941.
115. Mitchell, C. L., "West Indian Hurricanes and Other Tropical Cyclones of the North Atlantic Ocean," *Monthly Weather Review*, Supplement 24, Washington, D. C., 1924.
115. Tannehill, I. R., *Hurricanes*, Princeton, Princeton University Press, 1942.

CHAPTER 17

WINDS

120. Geostrophic and Gradient Winds. When a hole is made near the bottom of a cask full of water, a force acts upon the liquid inside the cask to cause the water to flow out the hole. This force arises from the difference in pressure on the two sides of the hole, that on the inside resulting from the weight of the water and the air above the water, and that on the outside resulting from the weight of the air only. Since the pressure inside is greater, the water is forced out. In a similar manner the variations in the pressure of the air at different points in a horizontal plane in the earth's atmosphere give rise to forces which tend to make the particles of air move from regions of high pressure to regions of low pressure. This force is called the *pressure gradient force*, and always acts normal to the isobars toward low pressures. As shown in section 33, its value on a unit mass of air is

$$-\frac{1}{\rho} \frac{\partial p}{\partial n}$$

where n is measured in the direction along the normal to the isobars.

Another force acts on any particle moving relative to the surface of the earth. It is caused by the rotation of the earth and is called the *Coriolis force*, or the *deflecting force* of the earth's rotation. Its value for unit mass, as shown by (34.20), is

$$2\omega \sin \phi V$$

In this expression V is the total velocity. The deflecting force acts normal to the velocity, to the right in the northern hemisphere, and to the left in the southern hemisphere. Since this force is normal to the velocity it affects the direction of the air motion but not its speed.

When the pressure gradient force exactly balances the deflecting force on a mass of air, the motion is said to be *geostrophic*. This situation is illustrated in Fig. 32, section 35, with the pressure gradient force acting toward low pressure being just equal to the deflecting force acting in the opposite direction. It follows that, since the pressure gradient force acts in a direction normal to the isobars, the motion of the air, or the wind, must be parallel to the isobars when the motion is

geostrophic. Such winds are known as geostrophic winds. Numerous investigations have shown that, above the heights where the surface friction exerts an influence, winds do blow parallel to the isobars most of the time and therefore these two forces are usually balanced. If these two forces are equated, it follows that the geostrophic wind velocity

$$V_g = \frac{1}{2\omega\rho \sin \phi} \frac{\partial p}{\partial n} \quad (120-1)$$

If then on a weather chart the isobars are drawn for fixed intervals of pressure, the geostrophic wind velocity for a given latitude is inversely proportional to the distance between the isobars. In any given situation V_g may be computed by substitution of the proper values in (120-1). Values of V_g obtained in this manner are given in the table in section 35. The necessity of doing this calculation each time may be eliminated by the use of a scale such as the one shown in Fig. 120. This scale

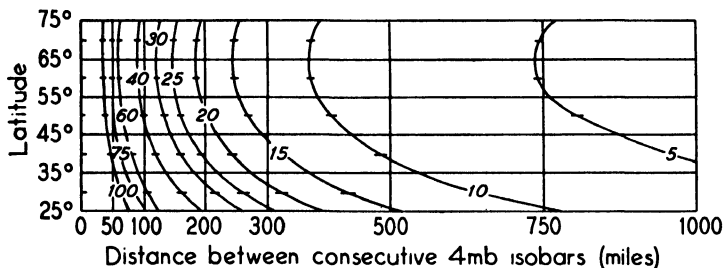


FIG. 120. Geostrophic wind scale for 4-mb isobar intervals.

was computed for isobars drawn at intervals of 4 mb and for $\rho = 1.163 \times 10^{-3} \text{ gm cm}^{-3}$, which is the average density at 2000 ft. The abscissa is the distance in miles between two consecutive 4-mb isobars and the ordinate is latitude. The curves are lines of equal geostrophic wind velocity in mph. The geostrophic wind for any given spacing of isobars and at any latitude from 25° to 75° may thus be obtained directly. For example, if the isobars are 200 mi apart the geostrophic wind is 20 mph at 50° latitude and 32 mph at 30° latitude. The scale may readily be adjusted for use with isobars drawn at intervals other than 4 mb. Thus with 2-mb isobars the distance between every second isobar may be taken.

When the scale of distances for the geostrophic wind scale is made to correspond to the scale of distances on the weather map, the value of the geostrophic wind velocity may be determined directly. Measure the distance between consecutive isobars and apply this to the geo-

strophic wind scale at the appropriate latitude, reading off the answer. Allowance must be made for the type of map projection used, since the distance between two points on a map may not be the same as the true distance between the points. For instance, in a conformal conic projection having standard parallels at 30° and 60° , measured distances are true distances only at these two latitudes, although the error at intermediate latitudes is not large. As the equator or the pole is approached, however, the error becomes progressively greater.

The scale may be used not only to determine the geostrophic wind velocity but also the component of the velocity in any direction. Thus if a front intersects the isobars but not at right angles, the geostrophic wind has one component parallel to the front and one normal to the front. The latter, useful in determining the velocity of the front, is obtained by measuring the distance between the intersections of consecutive isobars with the front and using that distance to determine the desired component of the geostrophic wind.

When the direction of motion of the particle of air is not straight but curved, the centrifugal force acts upon the air. The magnitude of this force is V^2/r , where r is the radius of curvature of the path, and is directed outward along the radius of curvature. When the motion is such that there is a balance among the pressure gradient force, the deflecting force, and the centrifugal force, the wind is known as the *gradient wind*. As shown in section 37, when the isobars are cyclonically curved the nature of the balance among the three forces is different from that when the isobars are anticyclonically curved. The equations for the gradient wind, as given by (37.2) and (37.4), are

$$v = -\frac{lr}{2} + \sqrt{\frac{l^2 r^2}{4} + \frac{r}{\rho} \frac{\partial p}{\partial r}}$$

for cyclonic curvature, and

$$v = \frac{lr}{2} - \sqrt{\frac{l^2 r^2}{4} - \frac{r}{\rho} \frac{\partial p}{\partial r}}$$

for anticyclonic curvature, where l is the Coriolis parameter $2\omega \sin \phi$. When the curvature is cyclonic the gradient wind is less than the corresponding geostrophic wind; for anticyclonic curvature the gradient wind is larger. The difference increases as r decreases. Thus in a tropical hurricane at latitude 30° and at a distance of 200 km from the center of rotation the gradient wind is 21 m per sec when the geostrophic wind is 50 m per sec for the same pressure gradient.

121. Thermal Winds. Isallobaric Winds. The geostrophic and gradient winds are closely related to the magnitude and direction of the pressure gradient. As shown in section 36, there is a tendency for low-pressure areas to form aloft above cold regions, and high-pressure areas to form above warm regions. These changes in the pressure gradient with height result in corresponding changes in the geostrophic wind with height. The vector difference between the geostrophic winds at two levels is called the *thermal wind* in that height interval. The thermal wind blows about an area of low temperature in the same direction that the geostrophic wind blows about an area of low pressure. The additional component of equations 36.14 and 36.15 which is due to the horizontal thermal gradient between the levels z_0 and z is

$$V_t = \frac{g}{lT} \frac{\partial T}{\partial n} (z - z_0) \quad (121.1)$$

where $\partial T/\partial n$ is the rate of change of temperature in the direction n , normal to the isotherms, and T the mean temperature of the layer. The geostrophic wind, (120.1), is given by

$$V_g = \frac{1}{l\rho} \frac{\partial p}{\partial n'}$$

where n' represents the direction of the pressure gradient. If the distance between isotherms is equal to the distance between isobars, it follows that

$$\frac{V_t}{V_g} = \frac{g\rho\Delta T(z - z_0)}{T\Delta p} \quad (121.2)$$

where finite differences are substituted for differentials. The right-hand side of (121.2) can be evaluated approximately. Assume that $\rho = 1.2 \times 10^{-3}$ gm cm⁻³, $\Delta T = 5^\circ$ F, $z - z_0 = 1000$ ft, $T = 273^\circ$ A, $\Delta p = 4$ mb. After converting these to cgs units where necessary, it follows that

$$V_t = 0.0914V_{gt}$$

where V_{gt} indicates the wind velocity obtained from the geostrophic wind scale, using the spacing of the isotherms drawn at intervals of 5° F. With sufficient accuracy for forecasting purposes, the constant may be remembered as one-tenth for every 1000-ft interval for which the wind is to be calculated. Thus if the height interval is 5000 ft, the thermal component is one-half of the value read from the geostrophic wind scale.

The method of using the thermal wind is illustrated in Fig. 121.

Isobars at level z_0 are indicated by $p, p + 1, p + 2$, and the geostrophic wind at the point P is V_{g0} . Mean isotherms for the layer z_0 to z are indicated by $T, T + 1, T + 2$. The thermal wind, calculated by (121.1) or by (121.2), is indicated by V_t and is drawn as a vector from the point P parallel to the isotherms with low temperatures on the left. The resultant of V_{g0} and V_t, V_g , is the geostrophic wind for level z .

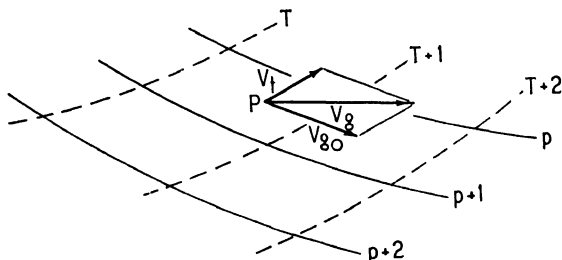


FIG. 121. The application of the thermal wind.

The behavior of the thermal wind may be described by four rules.

(a) If low temperatures are associated with low pressures, the wind increases with height.

(b) If low temperatures are associated with high pressures, the wind decreases with height.

(c) If the wind blows from high temperatures to low, it will veer with height.

(d) If the wind blows from low temperatures to high, it will back with height.

The thermal gradient from pole to equator is a permanent feature of the troposphere. The resultant thermal wind component causes the winds in the temperate latitudes to acquire a westerly component with increasing height, and finally produces the west to east flow found in the upper troposphere and the lower stratosphere.

A second cause for a variation in the winds of the free atmosphere is the changing pressure distribution. As shown in section 46, in a region of falling pressure there is a component of the wind toward the center of the isallobaric low, and in a region of rising pressure there is a component away from the isallobaric high. The *isallobaric wind*, as it is named, differs fundamentally from the thermal wind. The thermal wind is a component added to or subtracted from the geostrophic wind at one level to obtain the geostrophic wind at another level. The isallobaric wind is a correction to the geostrophic wind at any given level where there is no longer a balance of forces.

The value of the isallobaric wind, as obtained from equations 46.10

and 46.11 is, dropping the negative sign which indicates only the direction of the motion,

$$V_i = \frac{1}{l^2 p} \frac{\partial}{\partial n} \left(\frac{\partial p}{\partial t} \right) \quad (121.3)$$

where the normal n is taken with respect to the isallobars, and where the direction of the isallobaric wind is along the normal toward an isallobaric low. The tendencies plotted on the weather map may be used to obtain the values of $\partial p / \partial t$ and so to draw the isallobars. Dividing (121.3) by (120.1) obtains

$$\frac{V_i}{V_{gi}} = \frac{\Delta(\partial p / \partial t)}{l \Delta p t}$$

where V_{gi} is the value obtained from the geostrophic wind scale using the spacing of isallobars. If $\partial p / \partial t$ is in millibars per 3h, Δp is in millibars, t is the time in seconds for which tendencies are computed, and if again finite differences are substituted for differentials, the right-hand side may readily be evaluated. Thus if isobars are drawn for 4-mb intervals, and isallobars for intervals of 1-mb change in 3 h, then

$$V_i = \frac{0.16}{\sin \phi} V_{gi} \quad (121.4)$$

In practice the isallobaric wind cannot be obtained as accurately as the geostrophic wind. Because of this, a sufficient degree of accuracy in middle latitudes is obtained if the constant of proportionality is taken as one-quarter, which is the value at 40° latitude with 4-mb isobars and 1-mb isallobars.

The diagram in Fig. 122, a weather map for a portion of the southern United States for March 12, 1941, at 07.30 h, EST, shows the evaluation and use of the isallobaric wind. The method of plotting and drawing up the map is given in section 162. The broken lines are the isallobars and the full lines are the isobars. Consider the area about point A first, which is just to the south of the center of an isallobaric high. The isallobaric gradient about the center is nearly symmetrical with the mean value of 1 mb per 3 h per 80 mi. A distance of 80 mi at latitude 31° corresponds to a velocity V_{gi} of 75 mph, as can be seen from the geostrophic wind scale. Substituting this value in (121.4) the isallobaric wind is found to be 23 mph. Since the isallobaric wind blows outward from the isallobaric high, and since the point A lies to the south of the center of the high, the isallobaric wind is nearly north, as shown by the vector AP . The geostrophic wind, 46 mph, is represented by the vector AQ . The resultant is given by the vector AR . Since AR has a com-

ponent at *C*, just to the south of the front, is represented by the vector *CB*, and the isallobaric wind is 33 mph. The geostrophic wind at *C*, 22 mph, is represented by the vector *CD*. The vector *CE* represents the resultant. The component of this vector normal to the front is about 17 mph. If the front in the region *A* to *C* moves with a constant velocity, then the cold air is undercutting the warm air and causing some ascent of the latter.

122. Monsoon Winds. As was described in section 3, the distribution of land and sea produces a deviation from the general distribution of pressure which would occur on a globe with a uniform surface. This deviation is not constant but varies from winter to summer. In winter high-pressure areas develop over the land masses, and the low-pressure areas over the ocean deepen. The situation is reversed in the summer season, with the high-pressure areas over the ocean becoming more intense and low-pressure areas developing over the land.

These pressure variations are reflected in the winds (see Figs. 5 and 6, section 3). During the winter the winds blow anticyclonically about and outward from the continental high-pressure areas. With the development of the summer continental low during the spring months, the winds reverse, blowing cyclonically from the ocean toward the land areas.

These circulations are most pronounced over the eastern half of the Eurasian continent where they are known as the monsoons. Similar circulations, but on a smaller scale, are discernible over North America, Africa, and Australia. They can be observed also around the shores of large inland bodies of water, such as the Caspian Sea and Lake Superior, if the mean winds are used in order to eliminate variations produced by passing highs and lows.

It will be noted that the direction of the monsoon wind differs in different coastal regions. Thus in China the winter monsoon is northwest, but in India it is northeast, with a similar difference in the summer monsoon.

The monsoon wind is a striking feature of the general circulation. Yet it is a result of the general pressure distribution, and as such its velocity is determined by the pressure gradient existing at the time.

123. The Effects of Friction. Diurnal Variations. The winds which have been discussed in the last three sections are winds which exist in the free atmosphere. In the following three sections, winds which occur near the surface of the earth and are affected by local influences are treated.

The friction between the moving air and the surface of the earth causes the winds to deviate from the geostrophic wind value and to blow

across the isobars toward the low-pressure region. The effect of friction on the surface wind is discussed in section 52. There, under the simplifying assumption that the frictional force acts in a direction opposite to the wind and is proportional to the velocity, it is shown, according to (52.14) and (52.15), that the velocity

$$V = \frac{l}{\sqrt{k^2 + l^2}} v_g$$

and that

$$\tan \theta = \frac{k}{l}$$

In these formulas, k is the constant of proportionality, or the coefficient of friction, and θ is the angle at which the wind blows across the isobars, as shown in Fig. 48, section 52.

It will be noted that, with decreasing values of k , the velocity increases and the angle between the wind and the isobars decreases. Thus, over the sea where the frictional forces are small, the actual wind is much the same as the geostrophic wind in both magnitude and direction. For this reason reliable wind reports from ships and from island stations may be used to determine the direction and the spacing of the isobars, provided that isallobaric effects are absent. The isobars should be placed so that the surface wind is about 70 per cent of the geostrophic wind, and blowing at an angle of about 20° across the isobars.

Over the land areas the frictional force varies, depending on the underlying surface. Over plains the effect of friction is only slightly greater than over the sea. Hence the winds in such areas, when the velocity is greater than 12 mph, may be used with confidence in drawing the isobars. Over mountain areas the friction is great and surface winds give little help in drawing up a weather map unless the effect of the local topography on the wind at a given station is known.

The coefficient of friction is dependent not only on the nature of the underlying surface but also on the stability of the air. When the air is in neutral equilibrium or has little stability, little energy is needed to lift a particle over an obstacle at the surface of the earth. When, though, the air is very stable, as in an inversion, more energy is needed to lift a particle against the stabilizing factors of the environment. It follows that k , the coefficient of friction, is large with stable air, and small with unstable air.

The dependence of k on the stability of the air is shown in the diurnal variation of the wind at the surface of the earth. Curve (a) of Fig. 123

gives the mean values of the hourly wind velocities at Winnipeg, Manitoba, for the month of July, 1942, and curve (b) gives the values for an individual day, July 26, 1942, during which the wind remained constantly in the sector west to northwest. It is seen that the wind speed decreases until about 06 h, at which time the stability of the air caused by nocturnal radiation (see section 29) is a maximum. Thereafter the wind increases until 14–15 h, during which period the insolation from the sun exceeds the radiation from the earth, and as a result the air becomes

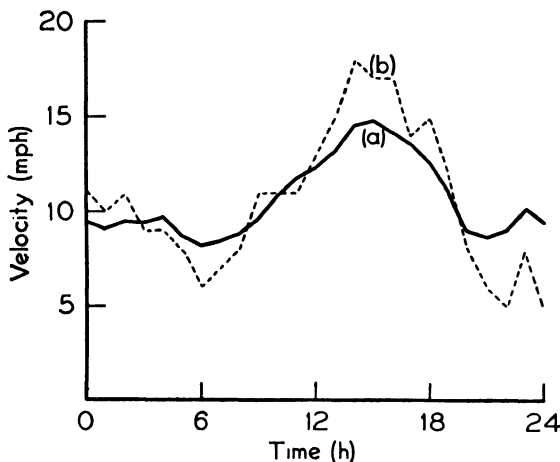


FIG. 123. (a) Mean hourly values of the wind velocity at Winnipeg, July, 1942; (b) wind velocities for Winnipeg for July 26, 1942.

increasingly less stable. After 15 h the increasing stability is accompanied by decreasing winds. Curve (b) shows that the diurnal variation is more pronounced on some individual days than it is when values are averaged over a number of days. This is to be expected since variations in the stability of the air occur from day to day. Thus on a day with a thick overcast sky, radiation from the sun has little effect at the surface of the earth, and so there is little increase in the wind velocity during the day. On the other hand, with a clear sunny day the marked changes which take place in the stability of the air are reflected in the changes of the surface wind.

The diurnal variations of the wind are superimposed on the other variations. Thus in forecasting winds, the changes in the pressure gradient and the time of day must be considered together. If the pressure gradient near a given station is decreasing during the morning, the diurnal increase may counteract the smaller value of the geostrophic wind. If,

instead, the pressure gradient is increasing, then the effect will be to superimpose the one increase upon the other.

Observations have shown that the friction between the earth's surface and the moving air affects the wind velocity in the layer from the surface to a height of about 1 km. Because of the stability such as occurs with

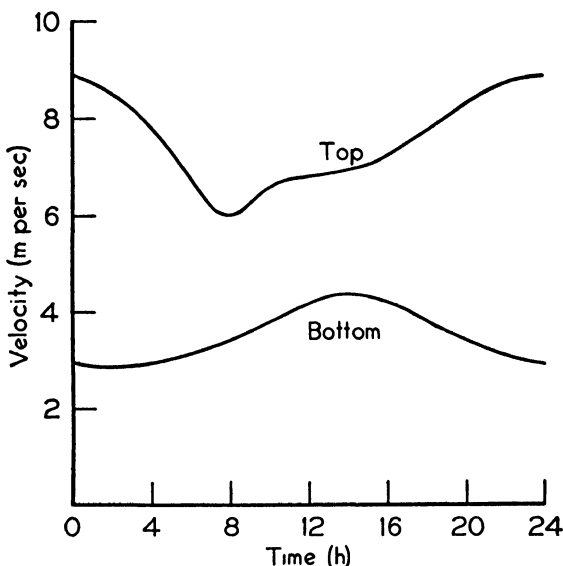


FIG. 124. The diurnal wind variation at the Eiffel Tower, Paris.

an inversion, the turbulent air motion is restricted to a thin layer near the earth's surface. Hence the decrease of winds which takes place during the early morning occurs only in the lower 300 m, while above this level the winds tend to be close to the geostrophic value. But during the time of maximum turbulence, the effect of friction is distributed over a thicker layer of 500 to 1000 m. This results in a wind variation in the upper levels of the frictional layer with a maximum at these levels during the night and a minimum in the early afternoon associated with the maximum that occurs at the ground at that time. At an intermediate level there is a tendency for two maxima, one in the early morning when the turbulence does not extend to that level, and one in the afternoon when the maximum at the ground extends to that height. These facts are brought out in Fig. 124, which gives the wind speeds for the bottom and top of the Eiffel tower (height about 300 m) in Paris. Observations have shown that these variations in the wind velocity are associated with backing or veering of the wind as k varies, as would be indicated by equations 52-14 and 52-15. Thus the winds at the surface back and

decrease during the night and veer and increase during the day. At the top of the frictional layer the winds back slightly as they decrease during the day and veer and increase during the night.

124. Slope and Valley Winds. A second type of wind that is associated with local topography is known as the slope wind. Nocturnal radiation on the side of a hill cools the air just above the slope, while the air at the same level at a considerable height above the ground farther down the hill experiences but little cooling. The air just above the slope is thus denser than its environment and subsides along the slope. The reverse process takes place during the day if the slope is strongly heated by the sun. The air in contact with the side of the hill becomes lighter than the environment and rises, resulting in a flow of air up the slope.

A large-scale example of this type of wind is found along the coasts of Greenland. The air in contact with the ice cap that covers that continent is cooled and a high-pressure area forms over the region. The pressure gradient force combined with the force of gravity gives rise to currents of air descending to the sea through the fjords and ravines along the coast. This current is only shallow but its velocity is often high, sometimes reaching gale force. The return current appears as a lighter on-shore wind at higher levels. Winds of this type are also known as *katabatic* winds. When the air flow is up a slope the wind is known as an *anabatic* wind.

A similar wind occurs in mountain districts. Consider a mountain river valley with steep sides. Here there are two slopes to be considered. At night the air just above the valley sides cools and sinks in the manner outlined above. This air subsides to the lowest portion of the valley. But the valley itself forms a slope, as shown by the flow of water in the river. The denser air from the valley sides therefore flows downstream under the influence of gravity just as the water comprising the river does. During the day the valley sides are heated by insolation, the air over these sides rises, and there is also a flow of air upstream along the length of the valley.

These air motions may also be discussed in terms of the pressure gradient force. Consider two points at the bottom of the valley, the elevation of the first above m s l being 1500 ft and the second downstream being 1200 ft above m s l. At night the density of the air just above the 1500-ft level is greater at the first point because of radiational cooling than at the second since, at the latter, air 300 ft above the valley bottom is being considered and there is little radiational cooling at that height above the surface. Since the weight of the air above a given level governs the pressure at that level, according to the statical equation 9-1, it follows that the pressure at the first point is greater than that at the

second. There is thus a pressure gradient directed up the valley and therefore a pressure gradient force acting down the valley, as shown by (33.1), giving rise to the downstream flow of air. It also follows that the mean density of the air in the height interval 1500 to 3000 ft, for instance, is greater over the first point than over the second, so that, as shown in section 36, the pressure above the first point at 3000 ft is less than that above the second point at the same height. At this and adjacent levels, therefore, the pressure gradient and thus the wind are opposite in direction to those at 1500 ft. There is thus a circulation in a vertical plane, changes in which may be computed with (50.20), using the method given in section 71. The up-valley flow extends through a considerable height interval, and the velocities are therefore small.

The effect of friction must be considered, even if only in a qualitative fashion. When the velocity increases to the point that the retarding effect of friction W just equals the value of the term $\oint \frac{dp}{\rho}$ in (50.20)

then the expression dC/dt becomes zero and steady conditions are attained. During the day the pressure gradient force acts up the valley and the wind is upstream. In the foregoing it was assumed that the mean pressure gradient along the valley for the day was zero. If the general pressure distribution over the mountain region is such that there is a component of the pressure gradient along the valley, this diurnal variation is superimposed on it, leading to a local diurnal variation in the magnitude of the pressure gradient. Thus the wind may not be down river at night but up river with a smaller velocity than during the day.

If the valley sides are steep so that the flow of air is generally either up or down river, the deflecting force of the earth's rotation need not be taken into account because it always acts perpendicularly to the direction of motion and is not strong enough to deflect the air up and over the sides of the valley to any significant extent. If mountains extending above the general level of the terrain are situated near the valley, large-scale eddies formed in the lee of these may further complicate the air motions. The air motions in valleys may be very complex, and the effects mentioned above are best seen from mean values of the wind rather than individual values.

A detailed study of the winds in the Columbia River Valley in southern British Columbia near the city of Trail has been made. The results of a large number of pilot balloon observations made at Columbia Gardens, which is near the center of the valley and about 4 mi north of the international boundary, are shown in Figs. 125 and 126. The mean wind values given in the figures are based on approximately one thousand

pilot balloon observations made at successive 2-h intervals during portions of the summers of 1938, 1939, and 1940. At Columbia Gardens the valley runs in a north-south direction, descending to the south. In Fig. 125 are shown the mean north- and south-wind components throughout the day from the valley floor at a height of about 1500 ft above m s l to a height of about 5000 ft above m s l. The curves on the figure are isolines of velocity, expressed in miles per hour. Mean north components are indicated by hatched areas and mean south components by unhatched areas. Since the sides of the valley extend up to heights of

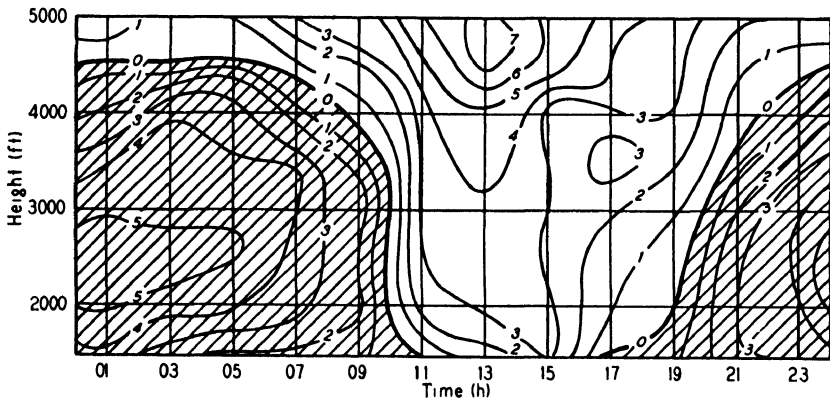


FIG. 125. The diurnal variation of the north-south wind components in the Columbia River valley near Trail, B.C.

4000 to 4500 ft above m s l, it can be seen that the prevailing wind above the valley has a south component. In the valley itself the mean wind is down valley until 10 h, although at higher levels the north wind ceases somewhat earlier than this. From 10 to 17 h the wind is up the valley. By 17 h the sun is no longer heating the valley floor and radiational cooling has commenced, as indicated by the beginning of a down-valley flow at that time. As cool air descends from the valley sides causing an increase of density at greater and greater heights, the wind gradually shifts from up to down valley until by midnight all the air in the valley is moving down valley.

The east-west or cross-valley components are shown in Fig. 126. As in the previous figure the curves give velocities in mph. Hatched areas indicate an east component of wind and unhatched areas a west component. Since it was desired to study the effects of the sun's heating, only velocity components of 5 mph or less were included. The inclusion of a number of components of 25 or 30 mph arising from other causes would tend to mask the effect of insolation. It can be seen that above

the valley the prevailing wind has a west component. In the valley itself during the night the wind generally has an east component. This may be due to the deflecting force acting on the air as it moves down valley and giving it a small westward component of motion, or it may be a manifestation of a large-scale eddy motion in the vicinity, since there is an opposite current above.

As the sun rises it heats the west side of the valley but not the east side. This unequal heating sets up a pressure gradient across the valley and thus a pressure gradient force acting from east to west. This pres-

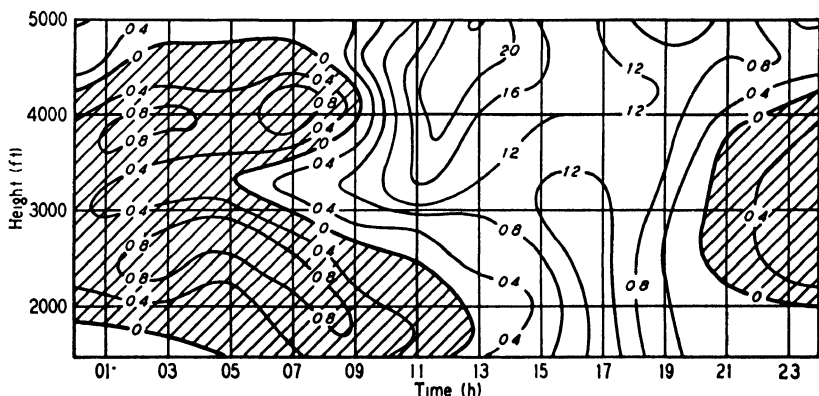


FIG. 126. The diurnal variation of the east-west wind components in the Columbia River valley near Trail, B.C.

sure gradient force reinforces the east component of wind which prevails during the night so that from 06 to 08 h there is a maximum of 0.8 mph at 4000 ft. This reinforcement of the east component probably starts at about 05 h when the insolation reaches the upper portion of the west side of the valley. The west component which appears at 3300 ft at 05 h may be regarded as a part of the return circulation of the air flow above. Near the surface the east component continues until noon. It is interesting to note that the direction of the cross-valley component changes as the sun passes the zenith and commences to heat the east slope of the valley more strongly than the west side. The west component continues strongly until 21 h when the east component characteristic of the night commences at intermediate levels. It would appear that the greater heating of the east slope during the afternoon causes a slight difference in temperature to persist during the night so that a small west component continues near the surface until 05 h.

The wind pattern on individual days may vary widely from that shown above. In the small but steep side valleys extending from the main

valley, however, the air flow at the surface is often much more regular. Surface wind observations for the month of October, 1938, in a small side valley extending upward to the east from the main valley near Columbia Gardens are summarized in Fig. 127. Wind directions in the sector northeast through east to southeast were considered as down-valley winds, while those in the opposite sector, southwest, west, to northwest were up-valley winds. The number of occurrences of the wind in these two sectors at each hour of the thirty-one days of the month is shown in the figure. The regularity of the down-valley motion at night and the up-valley motion during the day is striking. For example, the air flow at 19 h was down valley on thirty days.

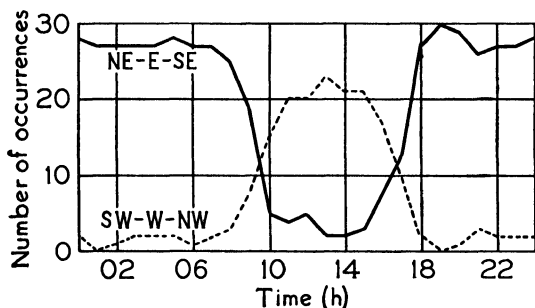


FIG. 127. Number of up-valley and down-valley winds in a side valley of the Columbia in October, 1938.

The strength and regularity of such katabatic and anabatic winds varies with the locality. A knowledge of the winds of this type in the vicinity is important in understanding local variations in the distribution of ground fog. This factor is discussed further in section 134.

125. Land and Sea Breezes. The unequal heating of land and water by the sun's rays causes one other type of local wind. During a day when the insolation is large, in a coastal area the land surface becomes warmer than the adjacent ocean. The heating of the surface air over the land results in the development of a pressure gradient and hence of a pressure gradient force acting normal to the coast line. This produces a wind blowing from the sea to the land. At higher levels the direction of the pressure gradient is reversed and the wind blows from land to sea. There is thus a circulation of air the magnitude of which may be computed with the aid of (50-20), using the method outlined in section 71. As the velocity increases during the day the deflecting force acting on the air becomes greater, so that by late afternoon the wind may be blowing nearly parallel to the coast line. During the night the radiational cooling reverses the situation, and the surface current now blows from

land to sea. In this manner the land and sea breezes, which are well known to inhabitants of coastal regions, are produced.

In the tropics these winds blow with great regularity. In the temperate zone the effect is often not strong enough to do more than modify slightly the gradient wind resulting from the general pressure distribution. If the general pressure distribution is weak, the sea breeze will develop during the late morning, dying down an hour or two before sundown. The night breeze off the land is generally light. These wind systems are limited in extent, reaching only a few miles inland. They are also surface phenomena, limited to the lower levels of the atmosphere. Above the surface layers the air motion is under the influence of the general circulation in the region.

PROBLEMS AND EXERCISES

1. At 2000 ft the wind is 15 mph from the northwest. At 10,000 ft the wind is 39 mph west southwest. If these are the geostrophic winds at these two levels, what is the direction of the mean isotherms for the layer from 2000 to 10,000 ft, and what is the temperature gradient? Assume latitude 45° and the mean temperature of the layer 273° A .
2. The isobars around the point of a trough line have a radius of curvature of 250 km. What is the value of the gradient wind if the geostrophic wind for the same pressure gradient is 20 m per sec, the latitude being 45° ?
3. On a summer day the mean temperature of a vertical column of air over a land surface at a distance of 5 km from an adjacent coast line is 24° C . The column extends from 1000 to 900 mb. The mean temperature of a similar column of air over the sea surface at a distance of 5 km from the coast is 22° C . The height of both columns may be assumed to be 1 km. If the effect of friction is neglected, compute the mean velocity of the circulation around this circuit 1 h after this temperature difference was set up, assuming that the latter remains constant during the 1-h period.

BIBLIOGRAPHY

- Admiralty Weather Manual*, London, H. M. Stationery Office, 1938. Chapter 8.
- Brunt, D., *Physical and Dynamical Meteorology*, London, Cambridge University Press, 1939. Chapter 13.
- Petterssen, S., *Weather Analysis and Forecasting*, New York, McGraw-Hill Book Co., 1940. Chapter 4.
- Shaw, Sir N., *Manual of Meteorology*, London, Cambridge University Press. Vol. 2 (1936), Chapter 6.
124. Heywood, G. S. P., "Katabatic Winds in a Valley," *Q. J. Roy. Met. Soc.*, **59**, 47-57 (1933).
124. Wagner, A., "Neue Theorie des Berg- und Talwindes," *Met. Z.*, **49**, 329-341 (1932).
125. Sutcliffe, R. C., "The Sea Breeze at Felixstowe, A Statistical Investigation of Pilot-Balloon Ascents up to 5,500 Feet," *Q. J. Roy. Met. Soc.*, **63**, 137 (1937).

CHAPTER 18

CONDENSATION AND PRECIPITATION

126. Saturation. The saturation pressure of water vapor is defined as the maximum pressure which water vapor can exert when in contact with a plane surface of pure water. In the atmosphere the water surfaces under consideration are not usually plane, but spherical. In addition, the water is not pure.

First to be considered is the nature of the surface of the liquid. Atmospheric condensation takes place chiefly in the form of water droplets. Owing to the surface tension of a curved water surface, the saturation pressure e'_s with respect to a water droplet is larger than the saturation pressure e_s with respect to a plane water surface which appears in the expression 10.7 for the relative humidity. It was shown by Kelvin that the logarithm of the ratio e'_s/e_s is inversely proportional to the radius of the droplet. In order for small droplets to form directly in the atmosphere, it would therefore be necessary that the vapor pressure increase considerably over the saturation value e_s with respect to a plane surface. The state in which the actual vapor pressure is greater than e_s is called supersaturation. Small supersaturation seems to occur in the atmosphere sometimes but never on a scale which would permit the direct formation of water droplets.

The saturation relative humidities for water droplets of various diameters are given in the following table.

VARIATION OF SATURATION RELATIVE HUMIDITY WITH DROPLET SIZE

Diameter (cm)	10^{-6}	10^{-5}	10^{-4}	10^{-3}
Relative humidity (per cent)	126	102.4	100.23	100.02

The second factor in causing the vapor pressure to vary is the material dissolved in the water. When there is a salt or an acid dissolved in the water, the saturation vapor pressure is reduced by a factor $(1 - kc)$ where k is a constant depending on the nature of the solute and c is the molecular concentration of the solution. The relative humidities for water vapor over a plane surface of sulphuric acid of various concentrations, when the temperature is 0°C , are shown below.

SATURATION RELATIVE HUMIDITY OVER VARIOUS CONCENTRATIONS
OF H_2SO_4 AT 0°C

Concentration (per cent)	10	20	30	40	50	60	70
Relative humidity (per cent)	95.5	87.6	74.8	55.6	33.8	15.0	3.4

Over a saturated solution of NaCl at 10°C the relative humidity is 22 per cent less than that over pure water. It is not certain if these relationships apply to small droplets, but they certainly do to large ones. It can be seen, therefore, that condensation would occur on large drops of a saturated solution of a salt with a relative humidity less than 100 per cent. This effect may be of fundamental importance in the early stages of the development of a droplet, especially if condensation commences on a small grain of the salt which acts as a nucleus.

A study of the effect of electrical charges on the saturation vapor pressure over small drops indicates that it would be significant only if the number of charges were very great. However, there is seldom more than one electrical charge on a nucleus of condensation, so that this effect is negligible in the early stages.

These various effects counteract one another. The final result in any part of the atmosphere is indeterminate. Yet the variation in the relative humidity in vertically ascending air is so great that for practical purposes it can be assumed that condensation begins when the relative humidity is 100 per cent, in other words when the air is saturated with respect to a plane surface of pure water.

127. Condensation on Nuclei. It was shown in the first table in the previous section that the saturation relative humidity over a droplet of pure water of diameter 10^{-6} cm is 126 per cent. But since relative humidities as great as this never occur in the atmosphere, condensation can commence only if there are already particles present, known as *condensation nuclei*, of diameter greater than 10^{-6} cm. Since supersaturation of only slightly more than 2.4 per cent will cause condensation on particles 10^{-5} cm in diameter, it appears that the condensation nuclei must be at least as large as this. Water molecules themselves cannot act as nuclei, as their diameters are of the order of 4×10^{-8} cm, and 5000 of them would have to come together to form a drop even 10^{-6} cm in diameter. It is difficult to visualize any process by which a number of molecules would coalesce to form a water droplet.

By means of an instrument devised by Aitken, the number of nuclei in a given volume of air can be obtained. The Aitken counter and others of a similar type operate by creating a very high degree of supersaturation in a chamber containing the sample of air to be analyzed. Such supersaturation causes droplets to form about particles in the air which,

because of their small size, would not act as nuclei in the free atmosphere. All the nuclei counted by such instruments are therefore not involved in ordinary condensation processes. There is a wide range in the number of nuclei present in unit volumes of air in different localities. Some representative values are given in the following table.

AVERAGE NUMBER OF NUCLEI PER cm^3

Locality	Average Number
City	147,000
Country (inland)	9,500
Ocean	940
Mountain (2 km)	950

The most important nuclei are composed of water-soluble salts. It is not yet certain if ordinary dust particles act as nuclei of condensation, although it is believed that they may function as nuclei for sublimation in the process of formation of ice crystals. One of the most common types of hygroscopic nuclei is composed of NaCl, carried into the atmosphere by the evaporation of ocean spray. Sulphuric acid particles in the air, formed through the oxidation of sulphur dioxide by the action of sunlight and union with water vapor, may act as nuclei for condensation. Other products of combustion found near industrial areas may also act as nuclei. Since condensation occurred long before the present industrial era, however, it is obvious that other substances must also act as nuclei. Nitrous acid, HNO_2 , is formed during natural processes, such as lightning discharges, and particles composed largely of this acid may therefore be present in the atmosphere to act as nuclei.

Condensation continues on the small droplet until the salt nucleus is dissolved. Thereafter the condensation reduces the concentration of the solution. An equilibrium situation will be reached with a large number of small droplets. Thus in country fogs the average droplet has a radius of from 4×10^{-4} to 3×10^{-3} cm. In clouds the radius of droplets may be as great as 10^{-2} cm. Since the average radius of raindrops under different conditions varies from 10^{-2} to 0.2 cm, some process or processes must be in operation to cause the droplets found in clouds and fogs to develop into drops large enough to fall as rain.

128. The Formation of Rain Droplets. According to a theory proposed by Bergeron, the most common cause of the formation of rain from cloud droplets is the difference in vapor pressure over water and over ice at the same temperature. This difference is shown in the upper portion of Fig. 139, section 135. When the air is above the freezing level, the water droplets become supercooled. At the same time some

ice crystals will form by sublimation on ice crystal nuclei. With both ice and water present, there will be a vapor pressure gradient from the ice crystal to the water droplet. Evaporation will take place from the droplet, with further sublimation on the ice crystal. This will continue until the ice crystal becomes large enough to sink. It will continue to increase in size as it falls, by coalescence with water droplets with which it collides, by further sublimation while it remains in the freezing zone, and by condensation after it falls below the freezing level and melts. Researches into the temperature distribution in the upper air when rain is falling, carried out by means of airplane ascents, have tended to confirm this theory, for in general the tops of the clouds have extended above the freezing level.

Since, though, light rain has been observed from clouds at temperatures above the freezing point, at times raindrops must form from cloud droplets by some other process. Bergeron further suggests that the difference in temperature between different drops can explain the increase in size. The vapor pressure increases with temperature. Hence when two drops of different temperatures are adjacent to one another, equilibrium conditions for the drop with the higher temperature will give supersaturation for the colder drop. Condensation will take place on the cold drop, with evaporation from the warmer drop. With temperatures near freezing this difference in vapor pressure is small for a small difference in temperature. But when the temperature is above 12°C , a difference of 0.5°C between droplets will lead to a difference in vapor pressure of 0.5 mb or more. This difference is greater than the maximum difference in vapor pressure between ice and water, and so would readily explain the increase in the size of the droplets. This difference in temperature between adjacent droplets could be caused by turbulent motion in the cloud which might bring droplets of different temperatures into proximity. This difference may also be explained at times by the cooling of the drops at the top of the cloud by long-wave radiation, in the manner indicated in section 30. After the drop has increased in size sufficiently to begin to fall, it will continue to increase in size through collision with other cloud droplets.

129. The Types of Rainfall. Precipitation is associated with clouds, and the different types of clouds produce different types of precipitation. The types of clouds and the causes of their formation are discussed in Chapter 20. In general clouds are formed by the cooling of the air below the saturation point. But precipitation of any considerable quantity falls from only those clouds which are produced through the lifting of a mass of air.

One region of widespread lifting of air is in the neighborhood of a

frontal depression. Above the warm frontal surface of a depression the lifting is extensive and gradual and leads to *frontal rainfall*. The area of precipitation, illustrated in Fig. 108, section 112, may extend 200 or 300 mi ahead of the surface front. The precipitation ahead is usually nearly continuous until the warm front passes. The amount of warm front precipitation shows wide variations from one depression to another, however. There appears to be a correlation between the degree of potential instability in the warm sector air before its ascent and the subsequent rainfall. The analysis in section 61 of the data given in section 60 shows a coefficient of correlation of 0.72 ± 0.096 . With a larger number of observations, the figure is even higher, 0.78. If there is little or no potential instability, the rainfall will be light, while if the potential instability is great, the precipitation may be heavy. Of course in the latter case, if there is insufficient ascent to permit the realization of the potential instability, the rainfall will not be great. The turbulence accompanying the realization of the potential instability may permit a more rapid ascent of the warm sector air, or it may produce larger raindrops. In either case the result will be the occurrence of heavier rainfall than if the ascending air were stable at all levels.

There is a small diurnal variation in both the amount and in the width of the band of warm front rainfall, the maximum being reached during the early morning. As suggested by R. V. Dexter, this may be accounted for by radiational heating of the warm sector air near the surface during the day, which increases its wet-bulb temperature and hence its potential instability. This air then ascends over the warm frontal surface and by the early morning sufficient ascent has occurred to cause saturation in the layer and the realization of the potential instability. The air which ascends during the day has been cooled at the surface by radiation during the preceding night, and so its potential instability is decreased.

The ascent of such large masses of air is a dynamical as well as a thermodynamical problem, and the part played by each factor is not clearly understood. For example, it is not clear why the air should converge and rise on the warm side of the front, either on theoretical grounds or from a study of surface winds. The dynamical aspect is often marked in the early stages of development of a depression. Extensive rainfall may occur when the bulge in the front is just developing, well before the depression has commenced to occlude, at the stage illustrated by Fig. 108b, section 112.

Precipitation also occurs at the cold front, but it does not last as long as that ahead of the warm front, nor is it as steady. It is generally of a showery nature, and in amount it may be either light or heavy. It was

shown in section 95 that latent instability may develop or increase when a mass of air is lifted bodily, as at a cold front. The precipitation may, on occasion, extend as far as 100 mi ahead of the cold front. No entirely satisfactory explanation has yet been advanced to account for the presence of ascending air currents so far ahead of the cold front. There is a diurnal maximum in the amount of cold front rainfall. This maximum is found in the afternoon, when insolation renders the air less stable and so makes instability showers at the cold front more probable.

Occlusion rainfall shows no well-defined characteristics. Generally speaking, if the occlusion is of the warm front type, the rainfall will resemble warm front rainfall in some respects, and similarly with cold front type occlusions. Heavy rainfall frequently accompanies either type.

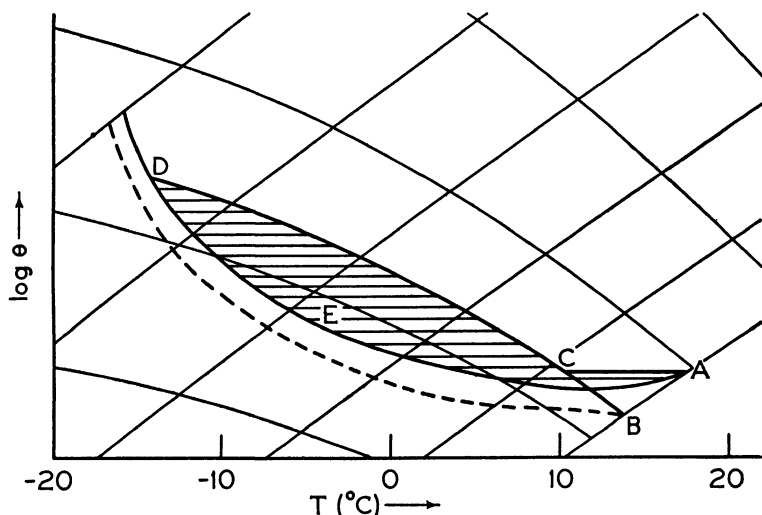


FIG. 128. A lapse rate favorable for convective rain.

Depressions of the middle latitudes are more intense and also more frequent in winter than in summer, so that there is a maximum of precipitation of the frontal type during the winter.

Convective rain is of frequent occurrence. This type is found when strong convection currents develop in an air mass. Individual masses of air may ascend until they reach their condensation level; if the lapse rate conditions are favorable for further strong ascent to greater heights, convective precipitation of the showery type usually results, especially if the top of the cloud extends above the freezing level. Upper air conditions favorable to the development of convective precipitation are shown on the tephigram in Fig. 128. Since the lapse rate near the sur-

face is greater than the dry adiabatic, any slight perturbation will start an upward motion in that portion of the air which is subjected to the perturbation. If the dry-bulb temperature of the surface air is A , and the corresponding wet-bulb temperature is B , the portion of this air which ascends will become saturated at C , and thereafter its temperature will decrease at the saturated adiabatic lapse rate with further ascent. In the example shown, the air will rise to a height at which the

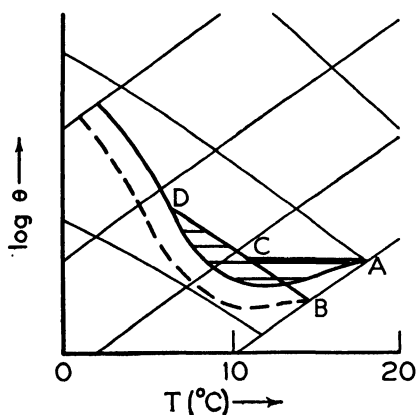


FIG. 129. A lapse rate unfavorable for convectional rain.

pressure is about 550 mb, denoted by D . The area $ACDE$ is a positive one, and represents the work done by the environment on the mass of air in question. This is, therefore, a case of absolute instability and latent instability of the real type (section 96). Strong ascent to considerable heights will occur in such circumstances, and convectional or instability showers are almost certain to develop. Instability of this type is likely to occur under conditions which have been outlined in section 95.

It will be remembered that such

instability tended to develop on warm, sunny afternoons in summer, and in cold air masses moving over warm, moist soil and over warm ocean surfaces.

Showers do not necessarily occur, however, when absolute or real latent instability is present. Fig. 129 is an illustration of absolute instability, but where convectional precipitation is not to be expected. The ascent beyond the condensation level in such a situation will not be sufficient to produce precipitation, although cumulus clouds will form. It has been observed that rain does not usually start to fall until the rising currents extend above the freezing level. The appearance of a swelling cumulus cloud, having an anvil-shaped top with mantle, indicates the formation of ice crystals and suggests that rain is about to start.

Another kind of precipitation which is of importance is *orographic rainfall*. Such precipitation occurs when air ascends in flowing over a range of hills or mountains. Orographic rainfall occurs frequently over the western slope of the Rockies, when moist air from the Pacific moves eastward over the continent. It can be seen that orographic rainfall has many points of similarity with warm front rainfall. It may be steady, or it may be of the showery type, depending on lapse rate con-

ditions. Although there may be no latent instability present as the air flows over the ocean, marked latent instability may develop through the ascent along the mountain slope, and heavy showers may occur. If the lapse rate before ascent is such that no latent instability will develop, even after ascent, the precipitation will be steady in character.

As explained in sections 119 and 141, horizontal convergence of air produces vertical currents in regions near cyclones and anticyclones. These currents are a contributing factor or at times the major cause of precipitation in some areas. When convergence is the predominating factor the rainfall is of the *convergence type*. The horizontal convergence resulting from isallobaric and frictional inflow of air across the isobars will give precipitation in some warm sectors. Also the latitudinal convergence on the west side of a ridge of high pressure may produce rain over a wide area. At times, although not always, the frontogenetical field associated with this convergence is sufficiently strong to cause the development of a well-marked front. Usually the ascent with convergence is slow and the rainfall is light.

130. Other Types of Precipitation. *Snow* occurs under the same general meteorological conditions as rain, except, of course, that the transition from the vapor to the solid state occurs at temperatures lower than 0°C . Sublimation of water vapor is believed to take place on special non-hygroscopic types of nuclei, generally referred to as ice crystal nuclei. The ice crystals increase in size as sublimation proceeds and start to fall slowly through the air. These ice crystals are found in an unlimited variety of forms and are completely symmetrical about a hexagonal base, as shown by numerous microscopic examinations of such crystals. Large snowflakes are aggregates of crystals, usually moist, and are usually found when the temperature is only slightly below the freezing point. At lower temperatures the crystals do not combine in this manner, and such large snowflakes do not develop. The name *sleet* has been given to two entirely different types of snow or ice structure. In Great Britain, sleet refers to the transitional type between rain and snow, and it may be either a mixture of rain and snow, or partially melted snow. It occurs only when the temperature is very near the freezing point, usually just above it. In North America the name sleet is given to pellets of ice which are initially small raindrops but which freeze during their descent. This latter type of precipitation occurs when rain falls from overrunning warm air which is at a temperature above 0°C into colder air below, which has a temperature lower than 0°C . If the water drops do not freeze during descent but become supercooled they will freeze upon striking the ground to form *glaze*.

The formation of *hail* is associated with the development of strong

convection currents. In order that the hailstone may grow to any considerable size, the ascending current must be sufficiently strong to prevent it from falling too rapidly to the ground. A current of such magnitude is to be found only in the process of realization of marked latent instability. It will be well to discuss the process of formation of hailstones in some detail. An ice crystal may form at high levels, and when it becomes heavy enough it will fall, increasing in size as it descends, and especially so if it falls through a cloud of water droplets. If there is sufficient upward motion of the air to keep the growing ice crystal from falling rapidly, it may develop to large proportions, and fall to the ground as a hailstone. If the greater part of its growth has occurred at temperatures well below the freezing point, it will be composed chiefly of snow which is loosely packed and often referred to as white ice. Such a particle is known as a *snow pellet*. A pellet of this type may not fall to the surface, however, but may be carried upward from lower levels by a rising current of air. While at temperatures near the freezing point a layer of clear ice may form on the core of white ice through collisions with supercooled water drops. As it ascends to greater heights again, white ice will form over the layer of clear ice. If the particle makes a number of vertical excursions in this manner, alternate layers of white and clear ice will form, until it finally drops to the ground as hail. Not all hailstones have such a structure, however. Many grow to large dimensions without undergoing a number of vertical excursions, and fall to the surface as a lump of clear ice.

The formation of large hailstones requires ascending currents strong enough to support the hailstone until it can grow to large dimensions. It is known that vertical velocities as great as 3000 ft per min are not uncommon in well-developed thunderstorms, and vertical velocities of even 5000 ft per min have been reported under extremely unstable conditions. Clouds which are extensive in the vertical are necessary for hailstone development, and will form when the air is very unstable. Hailstones as great as 4 in. in diameter and weighing nearly 2 lb have been found. Studies of the aerodynamics of hailstones suggest that the maximum weight of hailstones is about $1\frac{1}{2}$ lb.

The distribution of hail over the United States is shown in Fig. 163, section 151.

Drizzle is a form of precipitation in which the droplets are small, and fall very slowly to the ground. Because of the large number of the droplets per unit volume, drizzle tends to reduce the visibility more than ordinary raindrops. When it occurs, it generally falls from stratus and stratocumulus clouds.

BIBLIOGRAPHY

- Problems of Modern Meteorology*, London, Royal Meteorological Society, 1934.
Numbers 13, 14.
- Bergeron, T., *On the Physics of Clouds*, Memo. Met. Assoc., Intern. Union for Geodesy and Geophysics, Lisbon, 1933.
- Findeisen, W., "Die Kolloidmeteorologische Vorgänge bei der Neiderschlagsbildung," *Met. Z.*, **55**, 121-133 (1938).
- Simpson, Sir G. C., "On the Formation of Clouds and Rain," *Q. J. Roy. Met. Soc.*, **67**, 99-133 (1941).
- Stickley, A. R., "An Evaluation of the Bergeron-Findeisen Precipitation Theory," *Monthly Weather Review*, **68**, 272-280 (1940).
- Wright, H. L., "Atmospheric Opacity: a Study of Visibility Observations in the British Isles," *Q. J. Roy. Met. Soc.*, **65**, 411-439 (1939).

CHAPTER 19

FORMATION AND DISSIPATION OF FOG

131. The Effect of Evaporation. *Fog* is defined as a cloud which envelops the observer and reduces the horizontal range of visibility to less than 1 km. It is formed through the condensation of water vapor from saturated air. At least 0.5 gm of liquid water per kg of air must be present in the atmosphere before the visibility is reduced sufficiently to permit the classification of the condition as fog. With dense fog the amount of condensed water may amount to as much as 5.0 gm per kg.

There are four ways in which air near the surface of the earth may become saturated:

- (a) Evaporation of water into the air.
- (b) Turbulent mixing.
- (c) Adiabatic cooling.
- (d) Non-adiabatic cooling.

These four processes will be studied in some detail.

Evaporation of water is a frequent cause of fogs, especially of frontal fogs. There are three separate cases to be considered, depending on whether the temperature of the air in contact with the water is less than, equal to, or greater than that of the water. The source of the heat which is required for the evaporation of the water must also be considered in assessing the probability of fog formation. The following list of symbols will be used in the ensuing discussion.

- T = the temperature of the air.
- T_l = the temperature of the liquid water.
- e_{sl} = the saturation vapor pressure at the temperature of the water.
- e_s = the saturation vapor pressure of the air.
- e = the actual vapor pressure of the air.
- T_w = the wet-bulb temperature of the air.
- e_{sw} = the saturation vapor pressure at the wet-bulb temperature of the air.

(a) *Heat of Vaporization Supplied by the Body of Water.* This situation will exist most frequently at the surface of the earth over a large body of water, or over a moist land surface. During the evaporation,

the vapor pressure e increases, but the temperature of the air will be considered constant.

First, consider the result if $T > T_l$. In this case, equilibrium will be reached when $e = e_{sl}$. Then $e < e_s$, and so saturation is not reached, and thus no fog forms.

Second, if $T = T_l$, equilibrium will be reached when $e = e_{sl} = e_s$. Hence saturation will be reached, but no condensation occurs and thus no fog forms.

The third condition is specified by $T < T_l$. Equilibrium with respect to the water surface would be reached when $e = e_{sl}$. But this would require supersaturation of the air at temperature T , since e would then be greater than e_s and so condensation will occur if suitable nuclei are present. If the difference in temperature is great, the condensation may be sufficient to produce a fog. The vapor will condense immediately above the water surface, giving the appearance of steam leaving the surface of hot water before it boils. Hence fogs of this type are often called *steam fogs*.

When this situation exists the underlying warm surface will supply heat as well as moisture to the adjacent air. This addition of heat will induce instability in the air and hence will cause rising currents. These ascending currents will carry the fog upward where it will evaporate in drier air aloft, thus causing the dissipation of the fog. Such fogs are frequent over the open waters in the Arctic in the winter season, where the difference in temperature between air and water is great. Because of their appearance they have become known as *Arctic sea smoke*. If an inversion is present aloft to dampen the vertical currents, these fogs will persist in the surface layers, rather than being carried aloft. Steam fogs are also found frequently in temperate latitudes over lakes in the autumn, when these bodies of water are still warm while the air is cool.

(b) *Heat of Vaporization Supplied by the Air.* This situation will occur in the free atmosphere, the evaporation taking place from falling rain. The heat is supplied by the air since the heat content of the falling drop is too small to permit any extensive evaporation. With the heat being derived from the air, the temperature T of the latter will fall and the vapor pressure e will rise, but, as was shown in sections 24 and 83, T_w will remain constant.

When $T_w > T_l$, equilibrium will be reached when $e = e_{sl}$. Then $e < e_{sw}$, and saturation will not occur. When $T_w = T_l$, equilibrium conditions will prevail when $e = e_{sw} = e_{sl}$. In this situation, saturation will exist, but no condensation occurs, and thus no fog forms.

If $T_w < T_l$, equilibrium over the water surface would exist only if $e = e_{sl}$. This would require a decrease of the air temperature to T_w ,

so that $e > e_{sw}$ and the air would be supersaturated. The additional moisture would then condense to form cloud or fog. This condition arises when rain falls from a layer of warm air lying over a layer of cold air at a warm front. If the wet-bulb temperature of the surface air is less than the air temperature of the warm air aloft as shown in Fig. 130a,

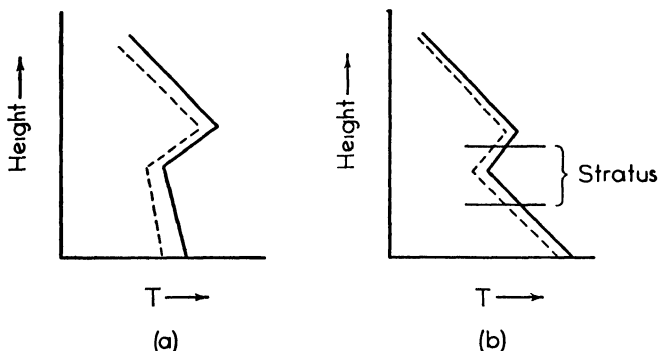


FIG. 130. Lapse rate conditions above and below a frontal surface with which (a) prefrontal fog will form, (b) stratus will form.

condensation will take place at the surface, giving a *frontal fog*. If the wet-bulb temperature of the air in the lower layers is greater than the temperature of the overrunning warm air, as indicated in Fig. 130b, then the cloud will build down from the frontal surface to the level where the temperature of the raindrops equals the wet-bulb temperature of the air, forming a layer of stratus cloud. The likelihood of frontal fog is readily determined if upper air observations, as shown in Fig. 130, are available. However, in the absence of such observations, upper air data in the warm sector or even surface data may be of use. Consider the case of fog just ahead of a warm front. Assume that a sharp front divides the warm sector air with a surface temperature at 50°F from the cold air ahead which has a temperature at the surface of 40°F . The surface air in both masses is saturated. The warm air flows up over the cold air, its temperature in this case decreasing at the saturated adiabatic lapse rate. It can be seen that fog may occur until the lower portion of the warm sector air has ascended to a height where its temperature has become less than 40°F . Saturated air at 1000 mb with a temperature of 50°F ascends to 880 mb before its temperature decreases to 40°F , as can be seen from the tephigram. Under average conditions this represents an ascent of about 3400 ft. If the slope of the warm frontal surface is 1 in 200, the fog may extend as far as 130 mi ahead of the warm front. Low stratus cloud, formed as indicated in Fig. 130b, may extend ahead of the band of fog, as shown in Fig. 131. In this

manner, a rough approximation to the horizontal extent of the fog may be obtained. Since a considerable difference in temperature between

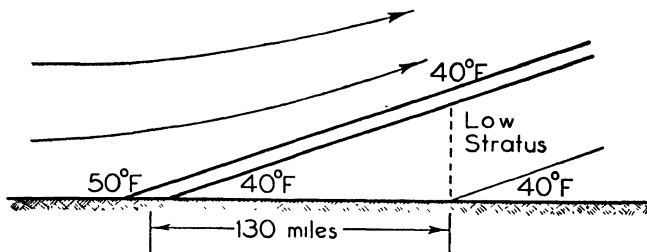


FIG. 131. The computation of the distribution of fog and stratus cloud under a warm frontal surface.

water and air is necessary before sufficient condensation to produce fog will occur, the actual width of the fog belt will be less than 130 mi.

132. Turbulent Mixing. Turbulent mixing in the vertical plays only a minor part in the formation of fog, perhaps carrying the effects of evaporation from warm rain down to the surface. Mixing usually inhibits the formation of fog. Before mixing takes place, the humidity mixing ratio will ordinarily decrease with height, as shown by the curve (a) in Fig. 132. The effect of vertical turbulent transfer of water vapor is, according to (54.8), to make the distribution of mixing ratio more nearly constant with height, as indicated by curve (b), Fig. 132. There is a tendency for condensation at higher levels, since the moisture content increases there, whereas there is less likelihood of condensation at lower levels, where the moisture content decreases. Turbulent mixing between the surface layer and the layer above promotes, then, the development of low stratus cloud, but retards the formation of fog.

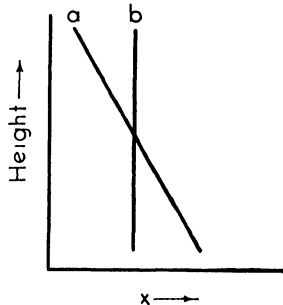


FIG. 132. The vertical distribution of moisture (a) before, (b) after vertical mixing.

Mixing between air of adjacent air masses, such as occurs at a front, will at times increase the relative humidity of the colder air. The equation for the increase of saturation vapor pressure with temperature (21.4) is not linear, as shown by Fig. 133. Mixing will give a mean value in temperature and in moisture content. Thus it would be possible for two air masses, both with relative humidity near 100 per cent, to mix and give supersaturated air. Yet the amount of water vapor that will

condense is never great enough to form a fog. Thus horizontal mixing alone will not cause the formation of a fog. Yet the process will aid in the saturation of air, and so will assist in the formation of fog when some other fog-forming process, such as radiation, is present.

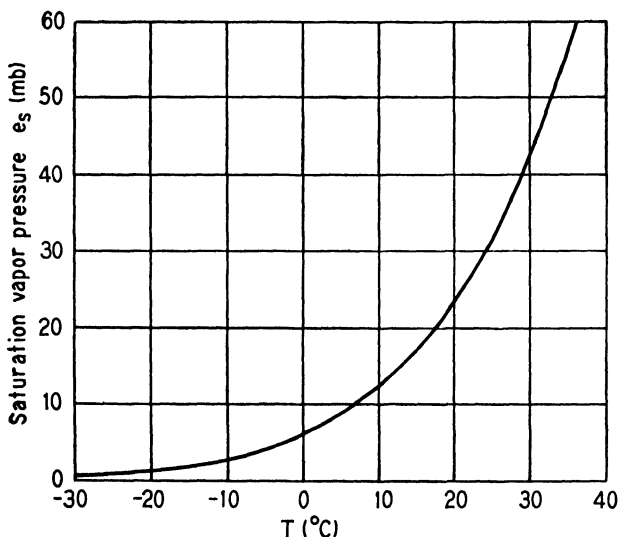


Fig. 133. The variation of saturation vapor pressure with temperature.

133. Adiabatic Cooling. Adiabatic cooling is the cause of *upslope fog*, which forms when the air is forced to rise above its condensation level as it ascends the side of a hill or mountain. Such fogs will form only if the air is stable, if the amount of turbulence is small, and if the relative humidity is high. Fog will not develop if there is potential instability in the air which would be released by the ascent. If there is sufficient ascent, the turbulent mixing resulting from the release of the potential instability will prevent the formation of fog.

134. Non-adiabatic Cooling. Two types of fog, radiation and advection fog, result from non-adiabatic cooling of surface air.

(a) *Radiation or Ground Fog.* The formation of radiation fog is favored by a number of conditions:

- (1) Clear sky.
- (2) High relative humidity.
- (3) Increasing moisture content with height.
- (4) Slight turbulence, but not completely calm.
- (5) Not too stable stratification.

Long-wave radiation to outer space proceeds most rapidly when there are no clouds in the sky, as indicated in sections 29 and 30. Radiation fogs are, therefore, most likely to occur on cloudless nights. It was shown in section 30 that there is a relationship between the amount of long-wave radiation to outer space and the height of cloud. This relationship is that the net nocturnal radiation from the ground is roughly proportional to the height of the cloud. Actual average values as determined by Asklöf are given in Fig. 134. The type of cloud present at each level at the time at which the observations were made is indicated

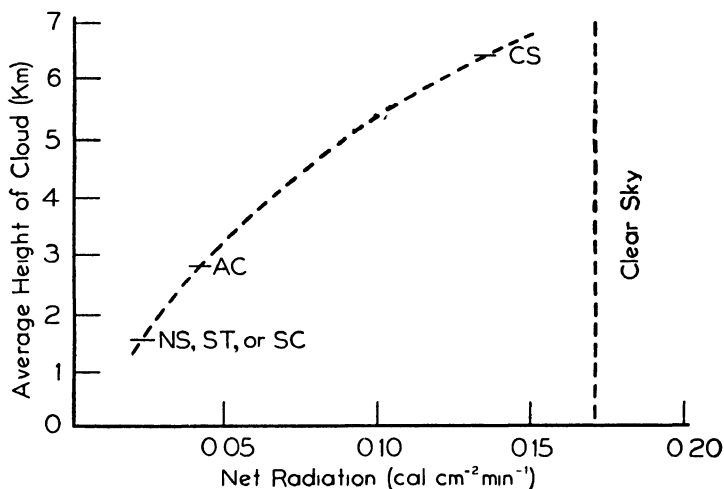


FIG. 134. Nocturnal radiation with cloudy and clear skies. (After Asklöf.)

in the figure. When the sky is covered with high cloud, the net loss of heat from the ground is almost as great as when the sky is clear. On the other hand, when the sky is covered with low cloud the net loss of heat from the ground is only about one-seventh as great as the loss when the sky is cloudless. It follows, therefore, that the fall in temperature at night when the sky is overcast with high cloud will be nearly as great as if conditions were cloudless, but will be only about one-seventh of this amount if the sky is overcast with low cloud.

It can be readily seen that high relative humidity favors the development of radiation fog. Under such conditions, the dew-point temperature is nearly as great as the dry-bulb temperature, and cooling of only two or three degrees may be sufficient to produce saturation. If the relative humidity is low, a much greater decrease in temperature, say ten degrees, will be necessary before the air becomes saturated. If it is assumed that a further decrease in temperature of three degrees is

required for sufficient condensation to produce a fog, a total cooling of six degrees with the high relative humidity, and thirteen degrees with the dry air will be necessary for fog formation. Thus if the temperature drop during the night is nine degrees, fog will form in the one situation, but not in the other.

Increasing moisture content with height assists in the formation of radiation fog. As indicated previously, turbulent mixing always acts in such a manner as to make the moisture distribution more nearly uniform vertically in the layer in which the mixing occurs (see Fig. 132, section 132). Thus turbulent mixing tends to increase the moisture content of air near the surface if the moisture content originally increased with height. Such a moisture distribution therefore facilitates the development of radiation fog. By the same reasoning a decrease in moisture with height retards the formation of radiation fog.

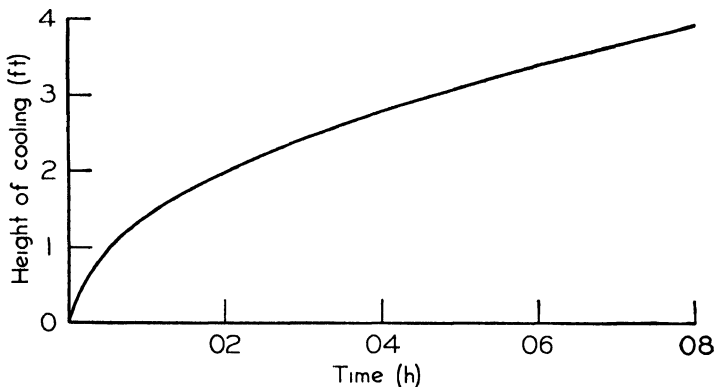


FIG. 135. The height of cooling by molecular conduction. (After Taylor.)

A slight amount of turbulence is necessary if radiation fog is to form. The height to which cooling will extend upwards from the surface as the latter cools during the night, if only the molecular conductivity of the air is taken into account, has been computed. These computations show, as indicated in Fig. 135, that 8 h after the ground temperature starts to fall the cooling of the air has extended up to a height of about 4 ft only. Molecular conductivity alone, therefore, will produce only very shallow ground fogs. Since it is known that cooling extends to much greater heights than this, it is clear that some heat-diffusing agency, other than conductivity, must be in operation. Radiational cooling of the air itself doubtless plays a part in this cooling process, but turbulent mixing is probably the main agent in diffusing heat. According to (53·17), the rate at which the cooling extends upward from the

surface by turbulent transfer of heat is given by

$$z^2 = 4Kt$$

where z is the height to which the cooling extends during time t , and K represents the coefficient of eddy diffusivity. The interval of time t commences when the surface temperature begins to fall. The coefficient K is of the order of 10^3 cm² per sec on a clear night when the wind is light. Thus with this value of K , and assuming that the temperature decrease at the ground commences at 20 h, the cooling extends to a height of about 75 m by midnight. Thus a certain amount of turbulence is necessary if a fog bank of any considerable depth is to form. The turbulence must not be too great, however, or the water droplets that form near the surface will be dispersed by the turbulence, preventing the development of radiation fog. The degree of turbulence accompanying a 2- to 8-mph breeze seems to be the most favorable for the development of this type of fog.

It was indicated in sections 53 and 76 that the eddy transfer of heat is downward when the lapse rate in the air is less than the dry adiabatic. The greater the stability of the air, the greater will be the downward transport of heat for a given value of K . Thus the effect of the cooling of the earth's surface by radiation to outer space in producing a surface inversion will be retarded by the downward turbulent transport of heat from higher levels. If the inversion becomes very marked, the turbulent transfer of heat from air above to that near the surface may be sufficient to prevent the formation of fog under certain conditions.

Radiation fogs occur most frequently in air of maritime origin after it has become stagnant over a cold continent. Accurate forecasting of such fogs is most essential, and useful methods to achieve this have been developed. Taylor constructed a chart for predicting radiation fogs which has been found very helpful. He took all cases of radiation fog at Kew Observatory, in England, which occurred during a five-year period, and studied the preceding temperature and humidity conditions. He found, for instance, that if the depression of the wet-bulb temperature below a given dry-bulb temperature exceeded a certain critical value as shown by the 20-h observations, radiation fog very rarely formed subsequently. These critical values were plotted in a manner similar to that indicated in Fig. 136. Thus in forecasting radiation fog at Kew, the dry-bulb temperature at 20 h would be plotted against the accompanying depression of the wet-bulb temperature. If the point so determined lies above the line sloping upward to the right, no radiation fog is to be anticipated; if the point lies below this line, fog may occur, but not necessarily so. In the latter case, other criteria must be

used in judging whether or not radiation fog will result. Another type of chart was constructed by George for ground fogs at Chattanooga, Tennessee. This chart, shown in Fig. 137, was constructed from obser-

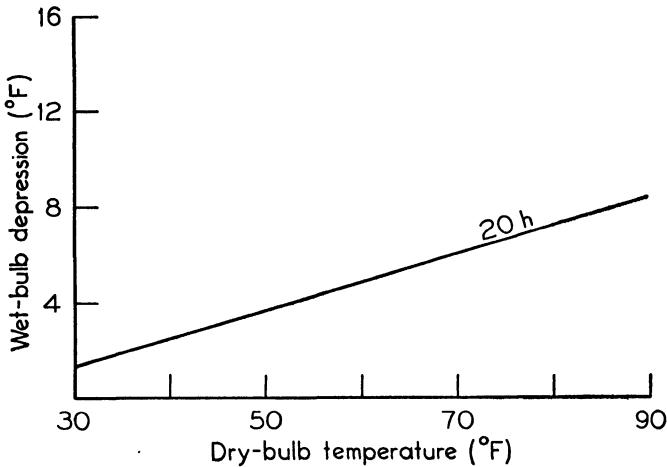


FIG. 136. The critical value of wet-bulb depression for various air temperatures at 20 h, for radiation fog formation at Kew, England. (After Taylor.)

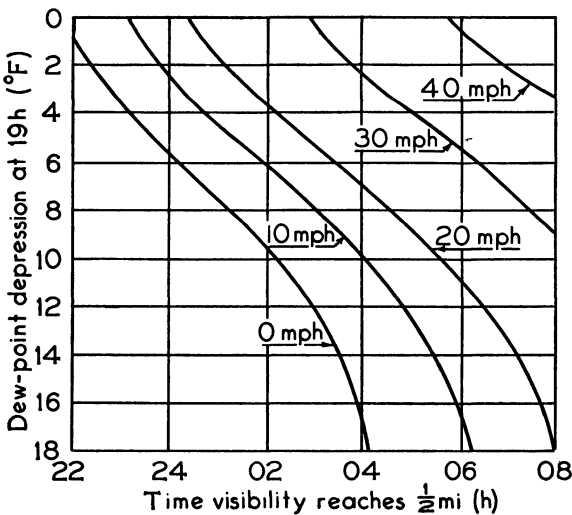


FIG. 137. Radiation fog formation at Chattanooga, Tenn. (After George.)

ventions of the gradient wind and the time of formation of the fog during the night for the months of March, April, and May. Similar charts were constructed based on observations made during the other seasons

of the year. This graph could be used at Chattanooga to assist in forecasting. The dew-point depression at 19 h is noted. Then along the horizontal line corresponding to that value, interpolation would be made for the computed gradient wind. Moving vertically, the expected time of occurrence of ground fog could be read from the scale on the horizontal axis. But in the use of these or any similar charts, all contributing factors must be kept in mind, including cloudiness, turbulence, and the vertical distribution of temperature and water vapor. The exact position of the limiting lines in such diagrams may be different for different localities, and it must be determined for each area for which fog forecasting is undertaken. There are other factors which must be kept in mind when forecasting fog of any description and which must be taken into account in the forecasting of radiation fog.

The first of these is the necessity of an adequate supply of condensation nuclei. Such a supply is nearly always present, but the number and type of nuclei will in part determine the density of the fog. Visibility observations provide, on occasion, an indication of the quantity of nuclei present. If the visibility is reduced to 4 to 6 mi by haze, not dust, it is probable that there are enough nuclei available to produce a dense fog when other conditions are appropriate. However, radiation fogs do sometimes form when the visibility is initially greater than 6 mi, and too much reliance should not be placed on visibility observations in fog forecasting.

If the forecasting is for fog over a comparatively small area, such as an airport, the topography of the surrounding country must be taken into account. Air cooled by coming in contact with sloping ground which is being cooled by nocturnal radiation will tend to flow down the slope, even if the incline is only very small. In this manner cold air tends to flow into declivities, and if the cooling is sufficient, radiation fog may form there. Fog is not so likely to occur on the slope itself. The conditions under which fog forms at a given locality depend so much on the topography that an individual study of conditions at each place at which fog forecasting is to be carried on extensively must be made if the maximum accuracy is to be attained.

A third factor which must be kept in mind is the possibility of a decrease in dew-point temperature, perhaps 2 or 3° C during the night, resulting from the deposition of dew. Dew, instead of fog, does frequently form under certain conditions, and especially when the air is calm and there is practically no turbulence. The dew-point temperature decreases when fog forms and increases again as it evaporates after being warmed by insolation.

Also to be considered is the depression below the dew point necessary

to provide sufficient condensed moisture to form a fog. As mentioned in section 131, 0.5 gm of liquid water per kg of air is necessary in order to reduce the visibility sufficiently for fog. When the amount of liquid water present is not so great as this, the atmospheric condition is known as *mist*. Since the curve of saturation vapor pressure with temperature is not linear, as shown by (21-4), the amount of moisture which would condense for one-degree drop in temperature varies. For saturated air with a temperature of 30° C, the amount of cooling required to form fog is less than $\frac{1}{2}$ ° C. For a temperature of 10° C, the corresponding cooling is 1° C; for -10° C, it is 3° C. Hence the amount of cooling necessary for fog formation is dependent on the temperature of the air as well as the dew-point depression.

The cloud cover during the day and the following night must be considered, too, in estimating the possibility of fog formation. If there has been an overcast during the day, the heating effect of the sun has been small. A clear sky during the night will then permit the air to cool rapidly to the dew point and so lead to the formation of fog. Such fogs are found at the rear of cold fronts. The surface air has acquired a high humidity in passing over a warm surface which has become moist through showers and rain. Clear skies during the night will give rise at times to a *mixing-radiation* type of fog.

The presence or absence of a surface snow cover also determines, in part, whether or not radiation fog will develop. The influence of a snow cover will be discussed in the next section.

(b) *Advection Fog*. Advection fog is another type which results from the non-adiabatic cooling of surface air. The development of this type of fog is favored by the following conditions:

- (1) High relative humidity initially.
- (2) Increasing moisture content with height initially.
- (3) Medium wind velocity.
- (4) Stable stratification initially.
- (5) Large temperature difference between air and underlying surface, the former being the warmer.

Items (1), (2), and (4) promote the formation of advection fog in the same manner as they promote the development of radiation fog. Advection fog will develop more readily in warm air as it moves over a colder surface when the relative humidity is high than when it is low. With regard to item (3), it can be seen that strong winds, with the accompanying marked turbulence and vertical mixing, tend to prevent the development of fog. If the wind is low, on the other hand, the warm air does not advance rapidly enough over the underlying surface, which

must have a marked horizontal temperature gradient to maintain the fog. For instance, fog may form in air flowing from a warm land surface over a cooler ocean surface. If the water does not become progressively cooler, however, with increasing distance from the shore, fog will form in the air when it first reaches the water surface, but as it blows farther out to sea, the fog will be dissipated by turbulent mixing. Thus a medium wind velocity is essential for the development of extensive advection fog. A large difference between the temperature of the air and that of the underlying surface is necessary, of course, to ensure sufficient cooling to produce a fog. Items (3) and (5) are the most important ones in the production of advection-type fogs.

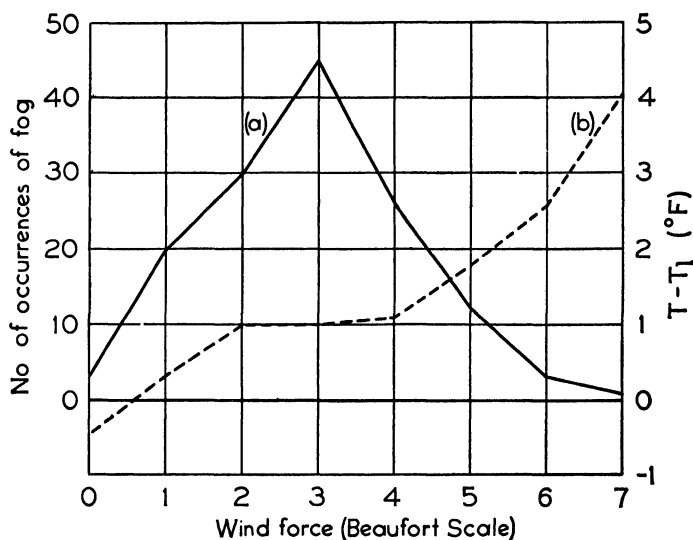


FIG. 138. The variation in (a) the number of occurrences of fog, and (b) the difference between the air and the sea temperature during fog with different wind velocities on the Grand Banks of Newfoundland. (After Taylor.)

G. I. Taylor has investigated the conditions under which advection fogs form over the Grand Banks of Newfoundland. Large horizontal gradients in the sea surface temperature occurring in this region, resulting from the proximity of cold water from the Arctic seas and the warm water of the Gulf Stream, make this one of the foggiest areas to be found on the earth. Some of his results are shown in Fig. 138. Curve (a) of the diagram indicates the frequency of fog formation with various wind velocities. Fogs formed most frequently when the wind was force 3 on the Beaufort scale (8 to 11 mph). Curve (b) of the diagram shows how various differences between air and water temperatures are related to

wind force. It can be seen that the great majority of fogs, about 72 per cent, occur when the air is approximately 1°F warmer than the sea surface and the wind is force 2, 3, or 4. Fogs rarely form when the temperature difference is great. Such large differences occur only when the air is moving rapidly over progressively cooler water, and the turbulent motion accompanying such winds prevents the development of fog. Low stratus clouds may form under such conditions. The vertical extent of advection fogs may be computed from (53-17) in the same manner as for radiation fogs.

There are several types of advection fogs. *Tropical air fogs* occur in tropical air as it moves gradually northward over the ocean surface which has, of course, a latitudinal temperature gradient. Fogs of the land and sea breeze type occur near sea coasts. These tend to form over the land adjoining the coast in winter, because the land mass is cooler than the ocean at that season. The temperature gradient is oppositely directed in summer and the fogs form over the cooler ocean.

In closing this section, it must be added that over a land surface advection fogs are usually difficult to distinguish from radiation fogs, and the characteristics of the former may best be determined from a study of fog formation over the ocean. Radiation fogs do not form over the ocean, of course, because of the very small diurnal variation in the temperature of the water.

135. The Dissipation of Fog over a Snow Surface. The processes taking place in a fog consisting of water droplets over a snow surface will be considered, following Petterssen, under two general headings: first, when the air temperature is below the freezing point, and second, when the air temperature is above the freezing point.

(a) $T < 0^{\circ}\text{C}$. Under these conditions, fog does not readily develop over a snow surface, owing to the lowering of the saturation vapor pressure over ice. The amount of this lowering may be seen from the upper portion of Fig. 139 in which Δe_s represents the difference in saturation vapor pressure over water and over ice. The maximum difference occurs at a temperature of about -12°C . If the relative humidity of the air at such a temperature is sufficiently high, the vapor pressure in the air will be greater than the saturation vapor pressure over ice or snow, and sublimation on the snow surface will result. This will prevent the air from becoming saturated with respect to a water surface, and only under exceptional circumstances will a water droplet fog result. For example, at -10°C the saturation vapor pressure over water is 2.87 mb, while over ice it is 2.60 mb. Thus if air at -10°C has a relative humidity of 91 per cent, the actual vapor pressure of the air is exactly equal to the saturation vapor pressure over ice. If the snow sur-

face and the air above it cool to a temperature lower than -10°C , sublimation on the snow surface will start, preventing saturation with respect to water and rendering the development of a water droplet fog unlikely. The lower portion of Fig. 139 gives the limiting values of relative humidity at which sublimation will start if further cooling occurs. Not only will fog not form under such conditions, but also water fogs transported from other regions will be dissipated if brought over

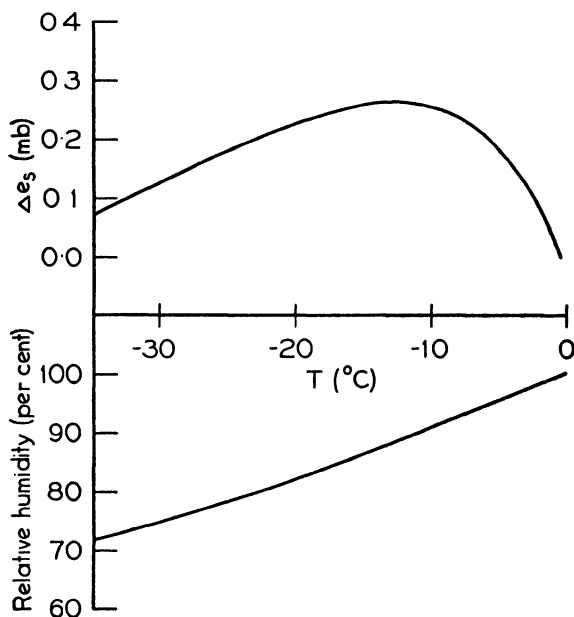


FIG. 139. The difference between saturation vapor pressure over water and over ice, and the relative humidity with respect to water for saturation over ice.

such snow surfaces. When the air temperature is only slightly below the freezing point, the difference in saturation vapor pressures is small, and if the cooling is rapid, fog may develop. However, sublimation on the snow surface will reduce the amount of liquid water, for the above-mentioned reasons, and the fog will dissipate unless the cooling proceeds steadily, or unless sufficient water vapor is brought down from the air above by turbulent transfer. If the air cools to a temperature of -10 to -15°C , Δe_s increases to its maximum, and fogs are much less likely to form. Those which are transported over the snow surface from other regions will dissipate rapidly.

The diurnal range over snow, at low temperatures, is small and nocturnal radiation alone rarely produces fog. Advection is the main cause

of the water fogs frequently found over the cold continental areas in winter. Most of such fogs are very diffuse, and do not reduce the visibility to any great extent. This difference in saturation vapor pressure accounts, to a large extent, for the fact that water fogs are comparatively rare over the cold snow-covered portions of the continents, even when moist polar maritime air flows over them. This is in marked contrast to the behavior of similar air when it flows over a surface which is not snow covered, such as an ocean, which may be only five or ten degrees cooler than the air. Dense fogs develop in such circumstances, and may persist for considerable periods.

(b) $T > 0^\circ \text{C}$. If the air temperature is above the freezing point, it will be taken for granted that the snow is melting. The air in contact with the melting snow will have a temperature of approximately 0°C , and a relative humidity of 100 per cent. The saturation vapor pressure is thus 6.11 mb just at the snow surface. Now assume that the air at 2 m above the surface has a temperature of 6°C and a relative humidity of

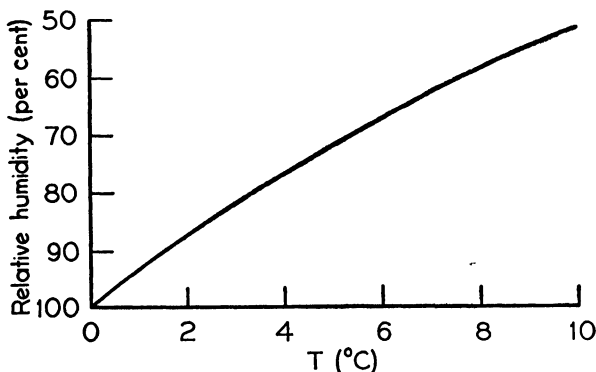


FIG. 140. The relative humidity for condensation on a melting snow surface.

100 per cent. The vapor pressure is then 9.35 mb. There is thus a vapor pressure gradient of approximately 1.6 mb per m, and part of the water vapor of the air will condense rapidly on the melting snow surface. This condensation will continue until the vapor pressure at 2 m decreases to 6.11 mb, i.e., until the relative humidity falls to 66 per cent. If the relative humidity is initially less than 66 per cent, water from the melting snow surface will evaporate into the air until the relative humidity reaches 66 per cent, which is the equilibrium value. It follows, therefore, that condensation occurs on the snow if the relative humidity is greater than a limiting value, in this case 66 per cent. The magnitude of this limit depends on the air temperature some distance above the

snow surface. The relative humidity of the air above the ground is usually greater than this limit, and therefore condensation of water vapor on the melting snow surface occurring in the spring after the air temperature has risen is the usual development. The limiting values of relative humidity for various temperatures of the overlying air are indicated in Fig. 140. It can be seen from the foregoing discussion that the greater the temperature at some distance above the ground, the more readily fog dissipates.

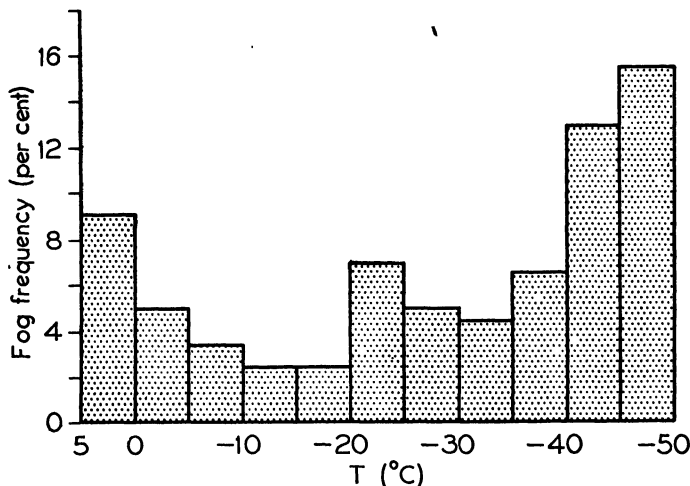


FIG. 141. Winter fog frequency on the lowlands of Siberia. (After Petterssen.)

Thus fog is formed and maintained to any large extent over a snow surface only when the temperature is slightly above or slightly below the freezing point. Fogs over snow surfaces are most prevalent during the spring of the year.

Sublimation on sublimation nuclei is the normal occurrence at temperatures from -20 to -50°C . Such sublimation processes produce *ice crystal fogs*. Since both the fog and snow surface are of an ice structure, there is no difference in saturation vapor pressure over the fog particles and the snow surface. There is, therefore, no tendency for such ice crystal fogs to dissipate, and they may persist for long periods.

The frequency of fog formation at various temperatures over ten meteorological stations in the lowlands of Siberia (lying to the east of the Ural Mountains) is shown in Fig. 141. The ordinate in the diagram is fog frequency in per cent, found from the expression $100(f/F)$, where f represents the frequency of the development of fog in each temperature interval, and F represents the frequency of occurrence of air tempera-

tures within each temperature interval. It can be seen that the fog frequency decreases rapidly as the air temperature falls below 0°C . This decrease continues until about -20°C , when a secondary maximum in the distribution occurs. This irregularity in the curve may be due to the fact that both water droplet and ice crystal fogs may occur in that temperature interval. There is a further slight decrease, and then an increase as the temperature drops to -50°C . A decrease at even lower temperatures is to be expected, because of the very small amount of water vapor available for sublimation processes at such low temperatures.

136. The Forecasting of Fog. According to the previous analysis, fogs can be classified according to their method of formation into steam fogs, pre-warm frontal fogs, upslope fogs, radiation fogs, and advection fogs. In general, a fog is frequently the result of two or more of these processes acting at once. For instance, fog will form at a coastal airport with an easterly wind blowing off the adjacent water, the easterly wind being associated with the pressure gradient under a warm front lying to the south of the airport. Such a fog is due to advection and pre-warm frontal conditions. Hence, although the causes for fog may be classified, any particular fog may be the result of several contributing factors.

The occurrence of fog is very variable, even in a small district. A widespread advection fog may fail to blanket some region owing to adiabatic heating. Hence satisfactory forecasting of fog demands the study of its occurrence at individual localities. Such studies have been made for a number of airports, and the conclusions are helpful in understanding the general causes of fog, as well as local peculiarities. The general conclusions are also helpful in understanding the occurrences in other localities. But a knowledge of the local variations at an airport will be of value only in forecasting for that particular airport. Such a study should include investigations of the general meteorological situation, the cloud cover, the gradient and surface winds, the dew-point depression, the temperature, the nocturnal cooling, the possible sources of moisture, and the general topographic features of the neighborhood. One airport may have fog chiefly as the result of the adiabatic cooling which occurs when the air from the adjacent river valley is carried upward to the airport, as the wind increases in the early morning, after being cooled all night by nocturnal radiation. Another airport may be in the bottom of a valley where light winds from one direction will continue to carry fresh air into the valley and so give no opportunity for nocturnal cooling to reduce the temperature of the air in the bottom of the valley, while higher winds from another direction will leave a calm at the valley floor

and so allow cooling to take place in the stagnant air. Studies of the causes contributing to fog at an airport, with the extent of the contribution of each, will aid in the forecasting for that locality.

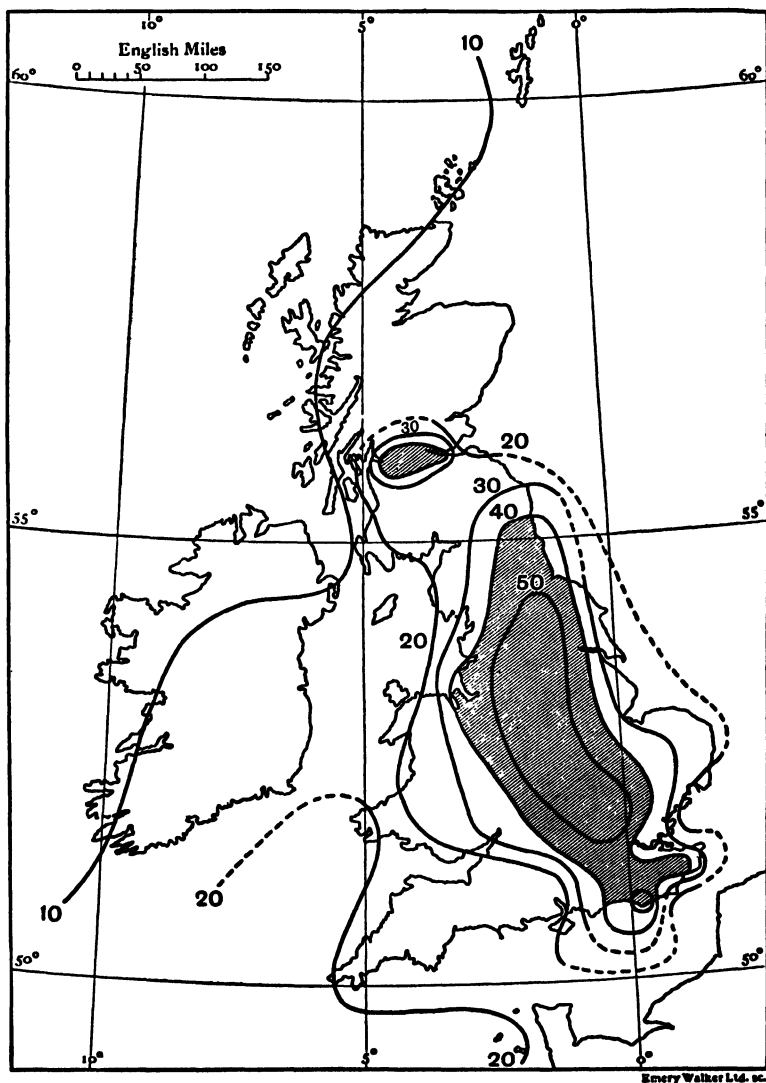


FIG. 142. The distribution of fog over the British Isles. (From Bilham, *The Climate of the British Isles*, Macmillan and Co.)

An examination of the distribution of fog over the British Isles, shown in Fig. 142, brings out a number of significant points for the forecaster.

The most striking feature of this chart is the location of the two maxima of fog frequency, the larger one extending northwestward from London over the Midlands and beyond, and the other over the Clyde Basin. Both of these regions are highly industrialized, and the correlation between fog and atmospheric pollution by processes of combustion is striking. It is probable that these impurities not only increase the obscurity themselves but also provide a plentiful supply of nuclei for condensation. The location of these areas suggests that radiational cooling is the predominant cause of fog formation over the British Isles, and that advection fog is of secondary importance. The lack of advection fog over the west coasts of the two main islands is especially surprising, but it is probably due to the strong turbulent mixing accompanying the unstable motion in the air coming from the Atlantic. The high incidence of fog at the northeast coast of England is to be attributed to advective transport of moist, stable air from the North Sea. Little upslope fog is shown in the figure since only data from stations at levels lower than 500 ft above m s l were used in constructing the diagram.

Fig. 143 gives the distribution of fog over the United States. Maxima are found over the western coastal regions, over the western slopes of the Appalachians, off the New England coast, and over the Great Lakes district. These maxima arise through different causes. The time for maximum frequency of fog over the west coast is during the summer months. Off California at this time, there is an upswelling of cool water along the coast which cools the surface air whereas an inversion at higher altitudes prevents mixing with dry subsiding air aloft. Farther to the north the fogs develop in currents of tropical air cooled on their trajectory northward. East of the Mississippi, fogs are most prevalent when in the winter a current of moist air from the Gulf of Mexico is carried north-northeastward and becomes stable as it moves over the cold surface. The region of maximum frequency is found where adiabatic cooling by lifting on the slope of the Appalachians aids advection in the formation of fog. Fogs over the Great Lakes during the spring months are associated with the stabilizing effect of the cool waters of the lakes, and in the autumn consist of radiation and steam fogs. Off Nantucket fog is most prevalent during the early summer. The area around Nantucket is part of the region of maximum fog occurrence extending from New England eastward to the Grand Banks of Newfoundland shown in Fig. 166, section 154. Much of this fog occurs in tropical Atlantic air which is carried over the cool waters of the Labrador current. Some fog near the coast lines occurs in the air leaving the continent during the summer. This air is cooled as it flows over the adjacent water.

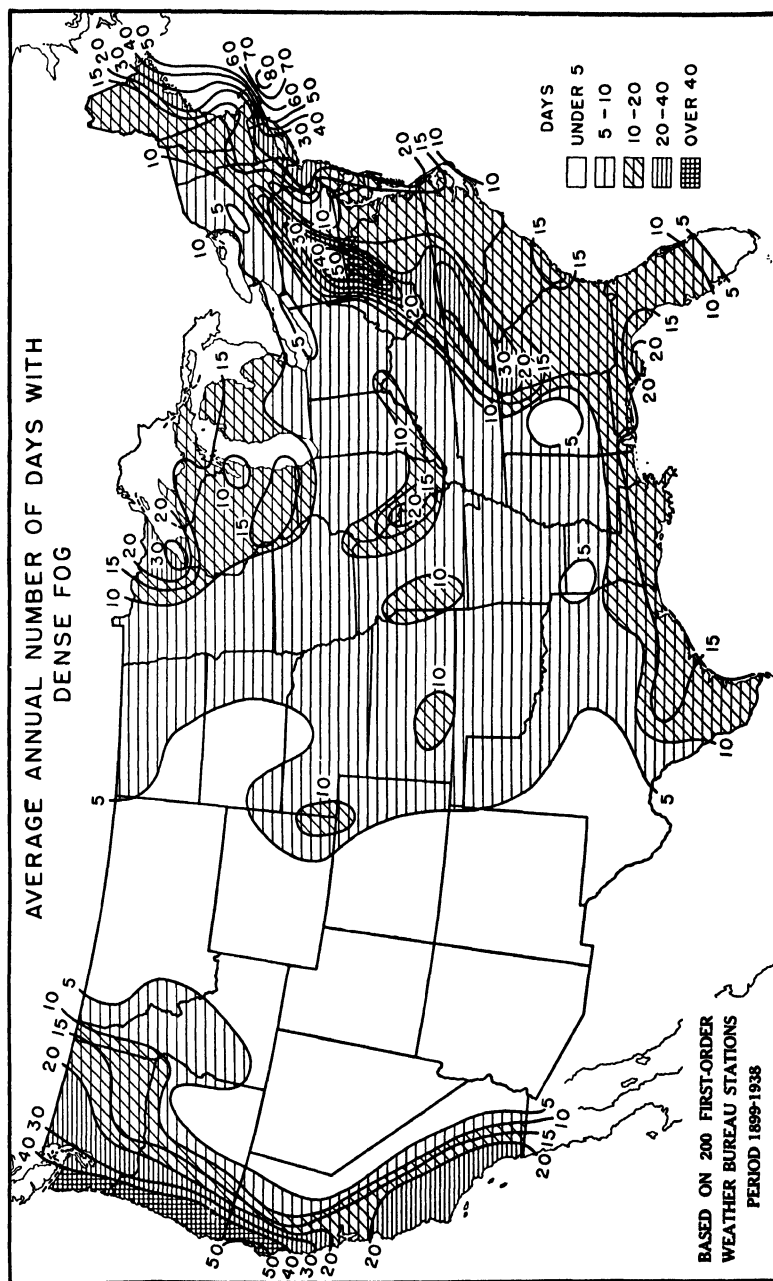


FIG. 143. The number of days with dense fog per year over the United States. (From *Climate and Man*, U. S. Dept. of Agriculture Yearbook for 1941.)

Fog, thunderstorms, and icing form the triad of major dangers to air travel. Fog is included in this category partly because it may blanket a wide area and thus increase the difficulties of air navigation, and partly because it may cover a particular landing field so completely and so rapidly without a great deal of warning. Hence the forecaster must be continually on the alert to detect the earliest signs of its occurrence.

PROBLEMS AND EXERCISES

1. An air mass had the following properties just as it left a continental area and was about to move over an ocean surface.

p	1000	950	900	800	mb
T	15	16	14.5	13	°C
f	93	75	70	70	per cent

The temperature of the water surface near the coast was 12° C, and decreased at the rate of 1° C per 100 mi in a direction normal to the coast line. Indicate what factors in this situation promote the formation of advection fog, and those which tend to prevent it.

2. There is a spread of 6° F between temperature and dew point at 18 h near the center of a high-pressure area, with clear skies expected for the night. The temperature is (a) 72° F in August, (b) 35° F in October, (c) 14° F in January. What factors make ground fog more probable in one situation than in another? What else would it be advantageous to know, in order to evaluate the probability of the occurrence of ground fog, and under what conditions should it be forecast for the coming night?

BIBLIOGRAPHY

- Admiralty Weather Manual*, London, H. M. Stationery Office, 1938. Chapter 9.
- Byers, H. R., *Synoptic and Aeronautical Meteorology*, New York, McGraw-Hill Book Co., 1937. Chapter 11.
- Petterssen, S., *Weather Analysis and Forecasting*, New York, McGraw-Hill Book Co., 1940. Chapter 2.
- Taylor, G. F., *Aeronautical Meteorology*, New York, Pitman Publishing Corporation, 1938. Chapter 14.
- George, J. J., *Fog, its Causes and Forecasting with Particular Reference to the Airports at Chattanooga, Tenn., Camden, N. J., Richmond, Va., Louisville, Ky., and San Antonio, Tex.*, New York, Met. Dept., Eastern Air Lines, Inc., 1939.
- George, J. J., "Fog, its Causes and Forecasting with Special Reference to Eastern and Southern United States," *Bul. Am. Met. Soc.*, **21**, 135-148; 261-269; 285-291 (1940.)
- Petterssen, S., "Some Aspects of Formation and Dissipation of Fog," *Geophys. Publ.*, **12**, No. 10, 1939.
- Taylor, G. I., "The Formation of Fog and Mist," *Q. J. Roy. Met. Soc.*, **43**, 241-268 (1917.)

CHAPTER 20

CLOUDS

137. Frontal Clouds. When the air in the vicinity of a depression, as, for example, that in the warm sector, ascends above its condensation level, condensation of water vapor commences and clouds form. Owing to variations in the stability and rate of ascent in different parts of a frontal depression, different types of clouds develop throughout the region. Some of the various cloud types encountered are indicated in Fig. 144. Diagram (*b*) shows a frontal depression as seen on a weather chart, with the frontal system beginning to occlude. *AB* and *DE* indicate the lines along which the vertical cross sections given in diagrams (*a*) and (*c*) are taken. Diagram (*c*) gives a cross section along a line which intersects both the cold and warm fronts and passes through the warm sector. Diagram (*a*) gives a cross section along a line which intersects the occlusion. As illustrated the occlusion is of the warm front type.

Warm front clouds are, in general, of the stratus type. When a warm front approaches a station, cirrus cloud is first noted, and then cirrostratus. With the nearer approach of the front, altostratus is next observed, with its base at medium heights, and this merges into low nimbostratus as the front itself passes. The cloud systems become more complicated if there is either actual or potential instability in the adjacent air masses. If there is potential instability in the warm air, ascent of the air may lead to its realization, and to the formation of cumuloform clouds embedded in the nimbostratus or altostratus. In such a situation, cumulus or cumulonimbus clouds may extend through and tower above the altostratus cloud as shown in Fig. 144c. If the slope of the frontal surface can be estimated, it will be possible to determine where the potential instability will be realized, and the cumulus type clouds form. If there is actual instability in the cold air mass, there will also be cumuloform clouds just below the warm frontal surface. It can thus be seen that stability conditions in the air masses must be considered when forecasting the types of warm frontal clouds that will develop.

Underneath the warm frontal surface the clouds will build downward in the cold air as explained in section 131. Near the front these clouds may extend to the surface and give a pre-warm front fog. Frequently too the precipitation falling through the cold air evaporates and increases

the relative humidity in the lower layers. Turbulence will then cause a layer of fractostratus or stratocumulus cloud to form which, near the front, merges with the nimbostratus cloud.

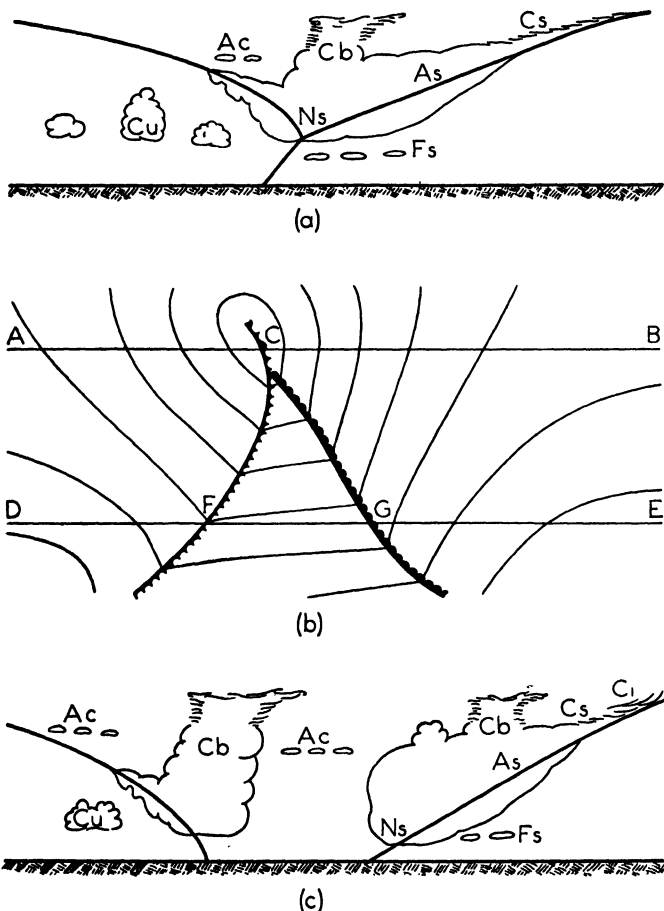


FIG. 144. Typical clouds in a frontal depression of the type shown in (b); (a) cross section through the occlusion, (c) cross section through the warm sector.

Because of the friction between the earth and the surface layers, the cold air behind a cold front moves more rapidly at a height of 3000 to 5000 ft than it does at the surface. The cold frontal surface, which is the leading edge of the cold air mass, tends to have a steep slope near the ground and with some fronts the frontal surface up to 5000 ft overhangs the front at the ground (see Fig. 192, section 177). The overrunning nose then traps warm air underneath it. With either a steep front or an

overrunning nose, the forward movement of the cold air gives to the warm air ahead of the cold front a vertical velocity which is much greater than that along the warm frontal surface. In addition, when cold air overlies warm air as suggested above, the disposition of air is unstable, and violent overturning takes place. The cold nose therefore forms, breaks down, reforms, and so on.

Cold front clouds are, then, predominantly of the cumulus type, and occur most frequently near the front. These clouds may be of great vertical extent if there has been marked potential instability in the warm air, and if the slope of the cold frontal surface is steep and its movement rapid. Line squall clouds of the cumulonimbus type occur under conditions of extreme instability. With some fronts subsidence occurs in the warm air above the cold front. In this situation the development of vertical currents producing cumulus and cumulonimbus clouds at the cold front is inhibited. The clouds then are of small vertical extent, or in situations with marked subsidence they may be entirely absent.

The type of cloud which forms in the cold air back of the cold front depends upon the characteristics of the fresh cold air. In moving over the surface warmed by the air of the warm sector and moistened by showers, the air behind the cold front quite frequently develops instability. Then cumulus of fine weather or turbulence stratocumulus forms. With strong outbreaks of polar continental air this instability is often sufficient to cause a showery type of precipitation. When, on the other hand, the air behind the cold front is already modified to some degree it remains stable, and no clouds develop. With a cold front of this type there is rapid clearing after the frontal passage.

Clouds associated with an occlusion may be of either the stratus or the cumulus type, depending on whether the occlusion is of the warm or the cold front type. Since the air has already been lifted some distance from the ground, any latent instability initially present has usually been released. Strong vertical currents are then unlikely except at the upper cold front of a warm front type occlusion where the cool air behind the occlusion ascends over the cold air ahead of the occlusion.

138. Convection Clouds. Convection clouds are of the cumulus type. Such clouds develop under various conditions, one of the most important of which is the heating of the air near the earth's surface on a sunny day. The forecasting of cumulus clouds which develop as a result of surface heating will now be discussed in detail, following a method developed by Poulter.

It is possible to forecast the approximate time and height at which cumulus cloud will form, and also the amount of cloud to be expected. The method of procedure for forecasting the height of the base of the

cloud is illustrated by Fig. 145. The dew-point temperature as observed in the early morning is represented by *A*. It is assumed that the dew-point temperature undergoes no significant increase as the surface air

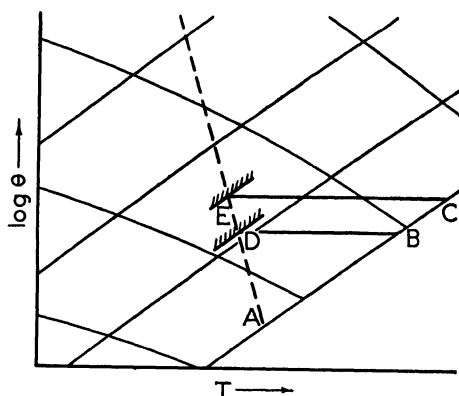


FIG. 145. The variation of the condensation level through insolation.

warms during the day, and by the time that the dry-bulb temperature at the surface has increased to *B*, the base of the cumulus cloud will be at the condensation level *D*. As the temperature rises, the height of the base of the cloud will increase, and the maximum height of the base may be forecast by forecasting the maximum temperature which the surface air will attain during the afternoon.

In the figure, *C* represents the maximum temperature expected, and *E* gives the corresponding maximum height of the cloud base. This method of cloud forecasting is chiefly of use in very homogeneous air masses, such as anticyclones. Very erroneous forecasts will result unless great care is exercised in choosing only homogeneous air masses. The cloud amount which will occur can be estimated by noting the relative humidity of the air at the level at which cloud is expected to form. If the air is near saturation at that level, the cloud droplets will evaporate slowly, and the amount of cloud cover will be large. On the other hand, if the relative humidity in the surrounding air is low, the cloud droplets will evaporate rapidly, and only a few tenths of cloud will develop. A linear relationship would suggest that if the relative humidity at the level where cloud is expected to form is 40 per cent, there will be $\frac{4}{10}$ of cloud; if 70 per cent, $\frac{7}{10}$ of cloud and so on. This rule holds only for relative humidities above 30 per cent.

The manner in which this method can be used is best shown by means of the example given in Fig. 146. *ABDF* gives the dry-bulb curve of an early morning radiosonde ascent, *GH* the wet-bulb curve, and *C* the dew point at the surface. The relative humidities and mixing ratios are plotted on the curve. The average mixing ratio in the lower layers is approximately 7.5 gm. The intersection of the 7.5 gm mixing ratio line with the environment is at *D*, at a level of 815 mb. This level is called the *convective condensation level*. It is the level at which the surface air will become saturated by adiabatic ascent and cooling, when the energy

necessary to carry the air to that level is obtained by surface heating. Dry adiabatic descent from *D* gives the point of intersection with the surface pressure line at *E*. The temperature at *E* gives the surface temperature which must be attained during the course of the day in order that convective currents may rise to the level *D* and form clouds.

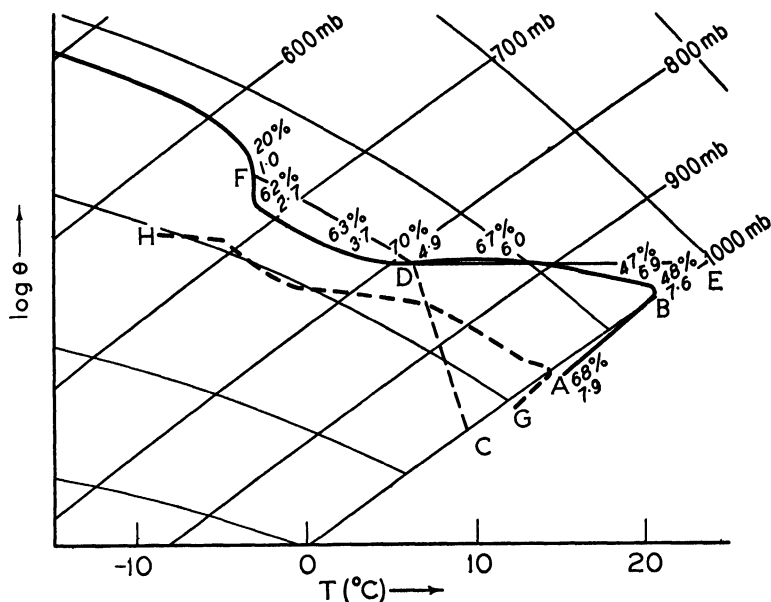


FIG. 146. Forecasting cumulus clouds.

In Fig. 146 the surface heating required is 9°C . But since the area between the ascent curve *ABD* and the adiabat *DE* is small, and near the level *D* there is a small layer of absolutely unstable air, it would be expected that the required heating would take place rapidly, and that the clouds would develop early in the morning. Further increase above the temperature at *E* by insolation would be unlikely since any increase in temperature above *E* would be accompanied by a corresponding increase in temperature throughout the turbulence layer. Another method of determining whether to expect a certain increase of temperature during the day is to observe the maximum temperature of the previous day in the same air mass. Since the maximum temperature is conservative, this will give a reliable approximation. The moist adiabat through *D* in the diagram intersects the environment curve again at the isothermal layer at *F*, 660 mb, at which point the air is again in equilibrium with the environment. The clouds of vertical development would

siderable heights locally. In Fig. 149b, the temperature in the cloud is greater than 0°C at all levels, and therefore no ice crystals will form. As the cloud extends upward, either of two things happens, depending on circumstances. It may reach a region where the wind increases or

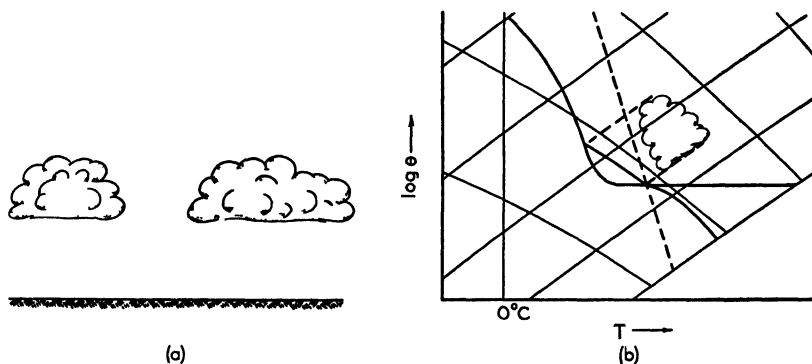


FIG. 148. (a) Cumulus humilis, and (b) lapse rate conditions favorable for its development.

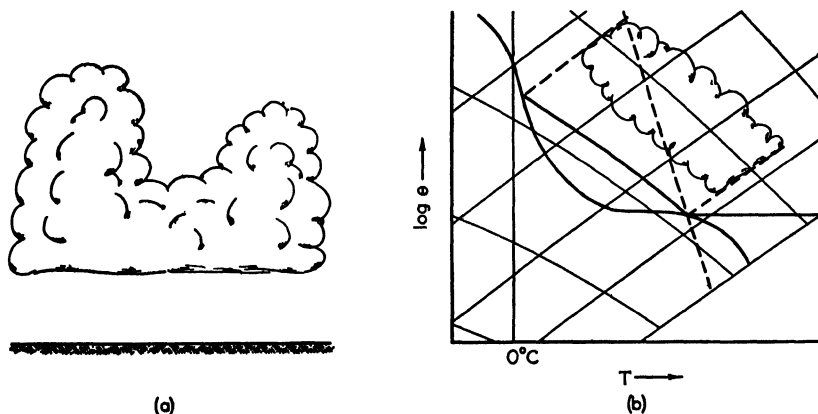


FIG. 149. (a) Cumulus congestus, and (b) lapse rate conditions favorable for its development.

changes direction rapidly with height, and the top of the towering cloud will be dissipated by mixing, and its vertical growth halted. If some such process does not take place, the top of the cloud will extend upward until it reaches equilibrium with its environment. If there is an isothermal or inversion layer at this level, the upward motion of the air will cease abruptly, and the cloud will spread laterally, giving a typical anvil type of cumulus cloud.

(c) *Cumulonimbus*. Cloud of the cumulonimbus type forms when the upper portion of the cloud penetrates into the region where ice crystals form. This region is at high levels during the warm portion of the year, when convection processes are most active. Marked instability must be present before cumulonimbus clouds will develop. A cumulonimbus

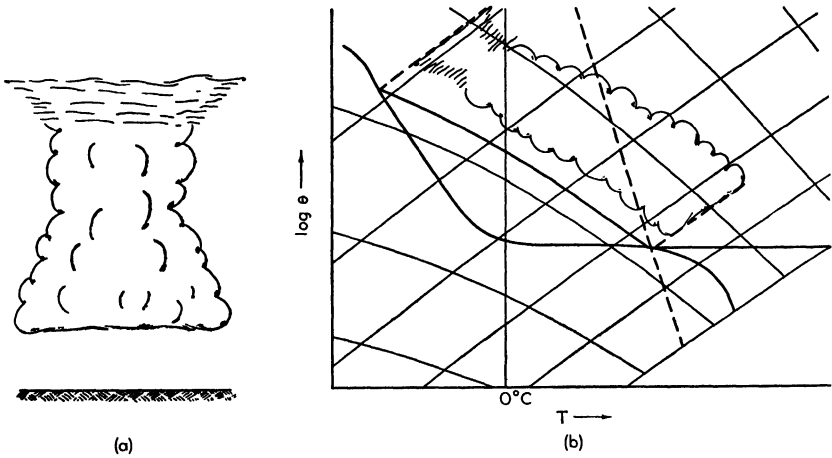


FIG. 150. (a) Cumulonimbus, and (b) lapse rate conditions favorable for its development.

cloud, with anvil and mantle, the latter composed of ice crystals, is sketched in Fig. 150a. Fig. 71, section 67, is a photograph of a cloud of this type. The appearance of the mantle heralds the beginning of precipitation from the cloud. Violent convection currents occur with cumulonimbus cloud, and, in addition, thunderstorms and hailstorms frequently develop. Typical upper air conditions are shown in Fig. 150b, with the upper portion of the cloud at temperatures well below 0°C . Cloud droplets do not usually freeze as soon as they reach a temperature of 0°C . The temperature often decreases to -5 or -10°C before ice crystals begin to form.

139. Turbulence Clouds. Turbulent air motion is found at any level in the atmosphere but occurs with the greatest frequency and intensity near the surface in the frictional layer, which extends to a height of about 2000 ft on the average. It was shown in section 54 that in a turbulent layer the upward flux of any property χ which does not change owing to vertical motion is given by the formula

$$-K\rho\frac{\partial\chi}{\partial z} \quad (54.8)$$

where K , the coefficient of eddy diffusivity, is a constant in any given situation. When equilibrium is reached, so that there is no transfer upward or downward, $\partial\chi/\partial z$ must equal zero, or the property χ must be uniform with height. Hence in the turbulent layer the specific humidity s or the mixing ratio x must become uniform with height. Similarly, equilibrium in the vertical temperature distribution is attained when the dry adiabatic lapse rate is reached, according to section 53. Fig. 151 illustrates the distribution of moisture, temperature, and relative humidity

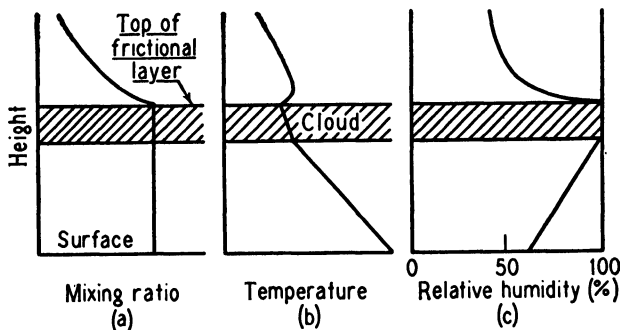


FIG. 151. The distribution of (a) moisture, (b) temperature, (c) relative humidity in and just above the turbulence layer.

humidity after equilibrium has been reached. If the layer is thick enough for the relative humidity to become 100 per cent, a layer of cloud will form at the level at which this occurs, extending to the top of the turbulent layer. Since during the mixing that has taken place heat has been transported from the top of the turbulent layer downward, as shown by (53.11), but has left unchanged the temperature above the layer, an inversion will frequently be found above the cloud top.

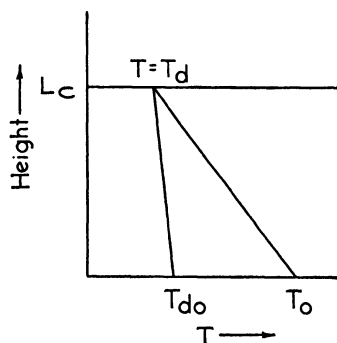
The height of the cloud base is given by the lifting condensation level of the air at the surface after complete mixing has occurred. According to (21.8), the rate of decrease of the dew point T_d in adiabatically ascending air is given by the equation

$$-\frac{dT_d}{dz} = 6.35 \times 10^{-8} \frac{T_d^2}{T} \text{ } ^\circ\text{C cm}^{-1}$$

since $\bar{T} \approx T$. But by (14.2) the corresponding decrease in temperature is

$$-\frac{dT}{dz} = 9.8 \times 10^{-5} \text{ } ^\circ\text{C cm}^{-1}$$

Consider a mass of air with temperature T_0 and dew point T_{d_0} at the



surface ascending to the lifting condensation level L_c , where $T = T_d$. The rates of change of temperature and dew point with height, given by the above equations, are shown in Fig. 152. It follows directly, then, that

$$T = T_0 + \frac{dT}{dz} L_c \quad (139.1)$$

and

$$T_d = T_{d_0} + \frac{dT_d}{dz} L_c \quad (139.2)$$

FIG. 152. The decrease of temperature and dew point with adiabatic ascent.

Since $T = T_d$, (139.1) and (139.2) may be equated to give

$$T_0 - T_{d_0} = \left(-\frac{dT}{dz} + \frac{dT_d}{dz} \right) L_c \quad (139.3)$$

Substituting from (14.2) and (21.8) in (139.3) leads to

$$T_0 - T_{d_0} = \left(9.8 \times 10^{-5} - 6.35 \times 10^{-8} \frac{T_d^2}{T} \right) L_c$$

or

$$L_c = \frac{T_0 - T_{d_0}}{9.8 \times 10^{-5} - 6.35 \times 10^{-8} \frac{T_d^2}{T}} \quad (139.4)$$

By assuming values for T and T_d , the fraction may be evaluated. Assuming $T = 280^\circ \text{A}$, $T_d = 270^\circ \text{A}$

$$L_c = 1.23 \times 10^4 (T_0 - T_{d_0}) \text{ cm}$$

or, with sufficient accuracy for evaluation purposes,

$$L_c = 125 (T_0 - T_{d_0}) \text{ m} \quad (139.5)$$

When the temperature and dew point are measured in degrees Fahrenheit,

$$L_c = 225 (T_0 - T_{d_0}) \text{ ft} \quad (139.6)$$

When the moisture content is indicated by the relative humidity f , an approximate relationship is given by

$$L_c = 70 (100 - f) \text{ ft} \quad (139.7)$$

Thus, if the temperature is 59° F, the dew point 51° F, the relative humidity is found to be 75 per cent. From (139.6) $L_c = 1700$ ft; from (139.7), $L_c = 1750$ ft.

There are two conditions essential for the development of turbulence cloud:

(a) The relative humidity in the air near the surface must be great enough to produce a low condensation level.

(b) The turbulence must extend to this condensation level.

If the lapse rate in the surface layer approaches the dry adiabatic, and the mixing ratio is constant with height in the same layer, the following method may be used to assist in determining if turbulence cloud will form. First, it is necessary to estimate the height to which turbulence will extend during the period for which the forecast is intended. Some general rules may be given which will be of assistance in determining this height. There are five general considerations which must be kept in mind:

(a) The time of day.

(b) The season of the year.

(c) The wind velocity.

(d) The stability conditions in the lower levels.

(e) The nature of the underlying surface.

During the night turbulence usually extends only about 500 ft above the surface, and often not that high. The maximum height is reached during the afternoon, when marked turbulence is frequently found at 1500 or 2000 ft above the surface. The turbulence layer is, in general, shallower in winter than in summer. The intensity and vertical extent of turbulence are directly related to the wind velocity, increasing as the velocity increases. Vertical motion occurs in the atmosphere more readily when the air is unstable, or nearly so, than when it is stable. Turbulence therefore extends to greater heights when the air is unstable. Finally, the topographical features of the underlying surface exert a large influence on the vertical extent of the turbulence layer. Over an extensive plain, or over the ocean, the turbulent layer is usually comparatively shallow. Over mountainous country, on the other hand, turbulence may extend to great heights, especially if the wind is strong. Thus the motion of air flowing rapidly over a mountainous region on a sunny afternoon in summer will be very turbulent. Under such conditions it is not unusual for the turbulence layer to be 5000 ft in thickness. Of course, it will be realized that these five factors are not independent of each other, but each should be kept in mind when estimating the vertical extent of the turbulent layer.

Once the height to which turbulence will extend has been estimated, the lifting condensation level should be computed from (139-6) or (139-7). When the condensation level is at 1500 ft, but turbulence extends only to 1000 ft, no turbulence cloud will form. If the turbulent layer extends to 2000 ft, however, turbulence cloud will form in the height interval from 1500 to 2000 ft.

The foregoing procedure must be modified somewhat if the actual lapse rate is not approximately the dry adiabatic or the mixing ratio is not constant with height. The temperature and moisture distribution after sufficient mixing to produce an equilibrium condition has occurred may be estimated in the following manner. The dry adiabatic lapse rate is 5.4°F per 1000 ft. After mixing, the difference in temperature between the bottom and top of a turbulent layer extending to 2000 ft will therefore be 11°F . If, during the morning before turbulence has developed, the surface temperature is 55°F , while that at 2000 ft is 50°F , with the intermediate lapse rate nearly constant, the effect of the vertical transfer of heat by mixing as the turbulence increases during the morning will be to increase the surface temperature to 58°F and decrease the temperature at 2000 ft to 47°F , so that the difference becomes 11°F . If the mixing ratio varies uniformly from 8.3 gm at the surface to 7.7 gm at 2000 ft, after equilibrium conditions are attained the mixing ratio in the column has the constant value 8.0 gm, which is the average for the column and which corresponds to a dew point of 51°F at the surface. Substituting $T_0 = 58^{\circ}\text{F}$ and $T_{d_0} = 51^{\circ}\text{F}$ in (139-6) gives the condensation level to be expected after the mixing occurs.

Another condition must also be kept in mind. If turbulence cloud is to form, the lapse rate above the condensation level should not be greater than the saturated adiabatic. If such unstable lapse rate conditions extend to any considerable height, the saturated air will be unstable, and towering cumulus clouds will develop. The lapse rate above the condensation level is usually considerably less than the saturated adiabatic, and indeed, when the cloud occurs as an extensive and persistent layer, there is nearly always a strong inversion of temperature just above it. Such an inversion is often maintained, and even intensified, through cooling of the upper portion of the cloud by means of long-wave radiation. The absorption of insolation by a cloud of this type is small, and may be neglected, as indicated in section 28.

Turbulence cloud sometimes appears as fractostratus, or as a thick layer of stratus or stratocumulus. Cloud of this type develops frequently in tropical maritime air when it arrives in temperate latitudes, owing to the surface cooling and the consequent increase in relative humidity. If the amount of turbulence is only small, fog may form

instead of turbulence cloud. Surface cooling in continental anticyclonic areas in winter proceeds rapidly, and this process increases the relative humidity of the air near the ground. Turbulence cloud frequently develops under such conditions, especially in England, where most of the surface is not snow covered. A snow cover, at temperatures below the freezing point, tends to reduce the relative humidity because of the difference in saturation vapor pressure over water and over ice, as pointed out in section 135.

140. Orographic, Billow, and Artificial Clouds. Clouds are produced when air ascends over a mountain range in much the same manner as warm front clouds develop. The chief differences between the two types arise from the fact that orographic cloud is of necessity stationary, or very nearly so, while the warm front cloud system moves with the front. Cloud which is purely orographic in character is of the stratus type, with a flat base. Its vertical thickness may vary considerably, depending on the height of the obstruction over which the air is flowing. Adiabatic warming of the air as it descends on the lee side of the mountain causes rapid dissipation of the cloud.

It has been shown previously that, if an air mass ascends, latent instability may develop within the air. If latent instability develops, or is intensified through ascent, and is then realized, clouds of the convection type will develop in addition to the essentially orographic cloud of the stratus type.

If there is a layer of moist but unsaturated air at a medium height over the lower ground, orographic ascent may produce condensation in this layer, and descent on the lee of the mountain will result in evaporation of the cloud droplets. In this manner, a stationary cloud may form at some height above the top of the mountain or hill. Clouds of this kind are of the orographic type, and are known as *lenticular clouds*. These clouds may form in the vertical currents which develop over the slope of a mountain heated by the sun, as described in section 124. The *banner clouds* which are seen about high mountain peaks are of this type.

Billow clouds form at the surface between two layers of air. Across such a surface there frequently is found a change in the direction or speed of the wind. This wind shear gives rise to vertical motions of the air particles. If the lower layer of air is near saturation, the air particles become saturated at the highest point in their path and form a cloud. Such clouds form in a regular pattern across the sky.

Another type of cloud is observed frequently behind aircraft flying in air at a low temperature. The clouds are formed by the passage of the airplane, but their cause is not fully understood. Sometimes they develop through the adiabatic cooling arising from the decrease in pres-

sure back of the wing tips. More frequently they are observed back of the engine exhaust and are caused by the additional moisture or condensation nuclei emitted by the exhaust. They always form in a layer of air of high relative humidity. Sometimes such *condensation trails* persist for considerable periods of time while at other times they dissipate rapidly.

141. Convergence Clouds. When horizontal convergence occurs near the surface, there is a corresponding ascent of the air, as shown in section 45. Similarly, descending motion accompanies horizontal divergence. The vertical air motions associated with convergence and divergence resulting from the variation of the gradient wind with latitude around cyclones and anticyclones were discussed in section 119. It was shown there that the computed velocity of ascent is great enough to account for the development of cloud, and even of light precipitation.

The horizontal convergence and divergence arising from variations in the radius of curvature of the air motions and the effect of the resulting

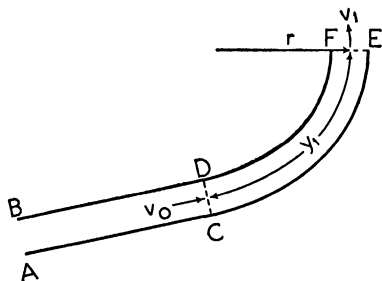


FIG. 153. Horizontal convergence resulting from the variation in the curvature of air motion.

vertical motion on cloud formation and dissipation will now be discussed. In order to simplify the computations the gradient wind where $r = \infty$, i.e., the geostrophic wind, is compared with the gradient wind for the same pressure gradient and for various finite values of r . Consider, for example, the distribution of isobars shown in Fig. 153. BDF and ACE represent parallel isobars, straight from B to D and from A to C , but developing curvature between CD and EF , the mean radius of curvature at the latter being r . The velocity of inflow at CD is v_0 ; the velocity of outflow at EF is v_1 . According to (45.9), the vertical velocity w_1 , resulting from horizontal convergence or divergence, is

$$w_1 = -\frac{z_1}{y_1}(v_1 - v_0)$$

where now y_1 represents the distance between CD and EF along the curved path and z_1 represents the height at which the vertical velocity is computed.

Assume that the streamlines and isobars coincide, an approximation giving sufficient accuracy for present purposes. This is equivalent to assuming that at each instant there is a balance among the pressure

gradient force, the deflecting force, and the centrifugal force. In the situation shown in the figure, since the pressure gradient force is constant, it follows that the centrifugal force must increase and the deflecting force must decrease in such a manner that their sum remains constant. Thus

$$\frac{v^2}{r} + 2\omega \sin \phi v = \text{Constant} \quad (141.1)$$

By differentiating with respect to time, it follows that

$$\frac{2v}{r} \frac{dv}{dt} - \frac{v^2}{r^2} \frac{dr}{dt} + 2\omega \sin \phi \frac{dv}{dt} = 0 \quad (141.2)$$

neglecting the variations in the latitude. Rearranging, the acceleration of the motion

$$\frac{dv}{dt} = \frac{v^2}{2r(v + r\omega \sin \phi)} \frac{dr}{dt} \quad (141.3)$$

Since $dr/dt < 0$ in the figure, and all the other terms on the right-hand side are positive, $dv/dt < 0$, and there is horizontal convergence and ascending motion along the path y_1 . From (35.1) and (37.2)

$$v_0 = \frac{1}{l\rho} \frac{\partial p}{\partial n}$$

and

$$v_1 = -\frac{lr}{2} + \sqrt{\frac{l^2}{4}r^2 + \frac{r}{\rho} \frac{\partial p}{\partial r}}$$

where $\partial p/\partial n = \partial p/\partial r$. Substituting in (45.9) and dropping the subscripts, it follows that

$$w = -\frac{z}{y} \left(-\frac{lr}{2} + \sqrt{\frac{l^2}{4}r^2 + \frac{r}{\rho} \frac{\partial p}{\partial r}} - \frac{1}{l\rho} \frac{\partial p}{\partial n} \right) \quad (141.4)$$

The values for w obtained by substituting various values of the radius and the pressure gradient in (141.4) are given in the upper portion of the following table. The latitude is assumed to be constant with the value 47.5° , and the density ρ has the value $1.1 \times 10^{-3} \text{ gm cm}^{-3}$. The height $z = 1 \text{ km}$ and the distance $y = 600 \text{ km}$. In the situation illustrated in Fig. 153 the air ascends, i.e., the vertical velocities are positive. If the wind entering the volume is the gradient wind, while that leaving is the geostrophic, the magnitude of the vertical velocity is the same, but the sign is opposite, i.e., negative, and the air descends. The distribution of

vertical motion in the vicinity of a trough of low pressure, based on these figures, is shown in Fig. 154.

VERTICAL VELOCITIES IN CENTIMETERS PER SECOND				
Radius (km)	200	400	800	1200
Pressure Gradient				
Cyclonic curvature				
4 mb per 100 km	2.8	2.0	1.3	1.0
2 mb per 100 km	1.0	0.7	0.4	0.3
1 mb per 100 km	0.3	0.2	0.1	0.1
Anticyclonic curvature				
2 mb per 100 km	1.0	0.5
1 mb per 100 km	...	0.5	0.2	0.1

The table shows that the maximum vertical motion occurs when the pressure gradient is large and the radius of curvature small. These conditions are found near the center of a well-developed occluding depression. The maximum vertical velocity shown in the table is 2.8 cm per sec, which is the same order of magnitude as the rate of ascent of

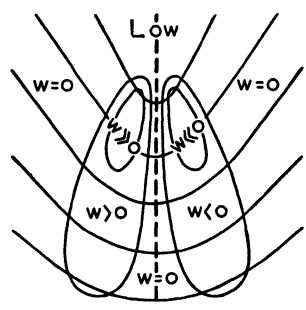


FIG. 154. Vertical currents at a trough line.

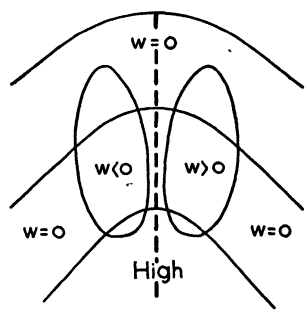


FIG. 155. Vertical currents at a wedge line.

air over a warm frontal surface in a rapidly occluding depression. In the latter, the vertical velocities usually range from 3 to 5 cm per sec. A rate of ascent of 2.8 cm per sec is therefore sufficient to produce dense cloud and medium precipitation. A trough accompanied by cloud and precipitation is frequently found in the rear portion of an occluding depression. There has been a tendency to place a back-bent occlusion, i.e., an occlusion extending outward from the center of low pressure and to the rear of it, in such a trough. No sound physical reason has been put forward to account for such an outward growth of an occlusion, and the foregoing analysis explains the weather of a frontal nature which

occurs in a trough near the center of a low without invoking any surface of discontinuity.

As shown in Fig. 154, there is a region of subsiding air just ahead of the trough line, in which the cloud would tend to decrease, the precipitation to cease, and the temperature to rise. Thus as the trough line approaches a station the cloud becomes less dense, the precipitation diminishes or stops, and the temperature rises. Then just after the trough line passes, the clouds become thicker, the precipitation starts again, and the temperature falls, which is precisely the sequence of weather to be expected with a cold front type of occlusion. The presence of an area of subsiding air and one of ascending air in such close proximity, both extending nearly parallel to the trough line, thus accentuates the impression that a cold front type of occlusion has passed, although in fact none has. The wind speed across the trough line is frequently greater than the speed of the trough itself in such situations, which is a further indication that no front lies in the trough. Even with smaller pressure gradients and larger radii of curvature, the vertical velocities shown in the upper portion of the table are sufficient to account for the formation of cloud near the outer limits of a trough.

The vertical motions associated with a wedge of high pressure may be computed from an equation similar to (141.4). By using the same values of ϕ , ρ , etc., as before, the vertical velocities calculated are shown in the lower portion of the table. The values for anticyclonic curvature are greater than those for cyclonic curvature for the same values of r and $\partial p / \partial n$, but owing to the upper limit on the pressure gradient in an anticyclone, discussed in section 37, the maximum vertical velocities attained are not so great as for cyclonic curvature.

The distribution of vertical velocities near a wedge line is shown in Fig. 155. There is horizontal convergence and ascending motion ahead of the wedge line, horizontal divergence and subsidence behind it, neither of which is as great as near a trough. Thus the cloud near a wedge tends to be concentrated just ahead of it when the latter is in the position shown in Fig. 155. Convergence and divergence of this type frequently account for the cloud distribution near the portion of an anticyclone where the curvature of the isobars changes rapidly.

The cloud resulting from isallobaric convergence, discussed in sections 46 and 121, belongs in the same category.

Convergence cloud is thus associated with horizontal convergence arising from variations in latitude and curvature, from isallobaric deviations from the geostrophic wind, and from frictional inflow during the motion of the air. Horizontal convergence arising from more obscure causes also occurs. •

In general, convergence cloud is of the stratus type. If marked latent or potential instability is present, however, the vertical motion accompanying the horizontal convergence may be sufficient to realize the instability, resulting in the development of clouds of the cumulus type as well.

PROBLEMS AND EXERCISES

1. The following are values of temperature and mixing ratio obtained during a radiosonde ascent.

<i>p</i>	994	960	823	768	692	611	540	517	429	mb
<i>T</i>	26	29	18	14	10	4	-2	-2	-11	°C
<i>x</i>	16.4	17.9	10.4	8.6	4.0	2.4	1.1	1.6	1.0	gm per kg

What cloud development is probable during the following day if it is expected that the surface temperature will rise to 93° F? What clouds and weather are to be anticipated if a cold front passes during the day?

2. Consider the same questions as in Problem 1 for the following ascent if the maximum temperature expected is about 83° F.

<i>p</i>	989	982	954	854	824	750	713	653	582	470	406	mb
<i>T</i>	15	19	20	13	14	11	9	6	-1	-9	-18	°C
<i>x</i>	10.1	13.5	7.0	5.4	2.9	8.3	7.8	4.1	2.6	1.1	0.7	gm per kg

3. The following table gives the values of the temperature and mixing ratio for an air column during the night.

<i>p</i>	950	861	774	710	623	588	423	mb
<i>T</i>	18	14	7	3	-4	-4	-19	°C
<i>x</i>	8.6	7.6	5.0	4.2	2.7	1.2	0.8	gm per kg

If the maximum temperature expected at the surface during the following day is 75° F, what cloud forecast should be made? If this were an ascent in the warm sector of a depression, what clouds would be expected as this air ascends the warm frontal surface?

BIBLIOGRAPHY

- Byers, H. R., *Synoptic and Aeronautical Meteorology*, New York, McGraw-Hill Book Co., 1937. Chapter 5.
- Petterssen, S., *Weather Analysis and Forecasting*, New York, McGraw-Hill Book Co., 1940. Chapters 2, 6.
- Shaw, Sir N., *Manual of Meteorology*, London, Cambridge University Press. Vol. 3 (1930).
- Douglas, C. K. M., "Physical Processes of Cloud Formation," *Q. J. Roy. Met. Soc.*, **60**, 333-341 (1934).
138. Poulter, R. M., "Cloud Forecasting — The Daily Use of the Tephigram," *Q. J. Roy. Met. Soc.*, **64**, 277-292 (1938).
139. Krick, I. P., "Forecasting the Dissipation of Fog and Stratus Cloud," *J. Aero. Sc.*, **4**, 366-371 (1937).

CHAPTER 21

ICING ON AIRCRAFT

142. Types of Ice Deposit. There are four types of ice which form on aircraft in flight:

- (a) Carburetor ice.
- (b) Hoar frost.
- (c) Rime ice.
- (d) Clear ice.

Carburetor ice is a type that occurs in the carburetor of the engine, arising from the condensation of part of the moisture present in the air when the latter expands rapidly. It occurs with outside temperatures as high as 70° F, and no method of forecasting its occurrence has as yet been developed. The elimination of icing of this kind is a problem for the aeronautical engineer rather than for the forecaster.

Hoar frost is the product of the sublimation of water vapor upon the surface of the aircraft. It is similar to frost that is deposited on the ground and occurs when the surface of the plane is colder than the dew point of the air. Hoar frost develops on a plane when it flies from cold air to warm. As the plane takes on the temperature of the new environment the frost evaporates. It is not, then, a serious hazard to the plane when it is in flight. Yet if a plane has been left outside during a clear frosty night, the radiational cooling of the surface of the plane may be sufficient to cause a deposit of frost. If the pilot attempts to take off before this is removed, the change in the aerodynamic properties of the wings may be so great that the plane is difficult to control, and the process of taking off dangerous. The development of hoar frost in this manner is not the concern of the meteorologist, however. Also, a coating of frost on the windshield sometimes develops when a plane descends rapidly from a high altitude for a landing, and interferes with the vision of the pilot.

Rime ice is white, opaque, and of a granular structure consisting of small ice pellets. This type of ice forms principally on the leading edges of the aircraft. It is seldom dangerous, since it does not alter the aerodynamic properties of the wings to a serious extent. A typical formation of rime ice is shown in Fig. 156a. Furthermore, because of its granular structure, it is frequently dislodged by vibration.

Clear ice is smooth and glassy in appearance and is dislodged only with difficulty. It forms near the leading edge of the airfoil or strut, usually in a mushroom shape as in Fig. 156b. This is the most dangerous type since it alters the aerodynamic properties of the wings, and the extra weight added to the plane may produce a serious loss of lift.

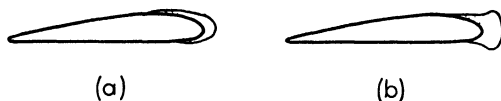


FIG. 156. The deposition of (a) rime ice, (b) clear ice on the wing of an airplane.

The last two types of icing are serious hazards to the aircraft, and the remainder of the chapter will be devoted to a discussion of the physical processes in operation and the meteorological conditions present when such ice forms.

143. Process of Deposition. It was indicated in section 128 that water droplets exist in the free atmosphere at temperatures below 0°C . These supercooled water droplets have been observed by Wegener in Greenland at temperatures of -35°C and by Haines in Little America at -26 , -30 , and -44°C . The extent of the supercooling can be accounted for by one of or all the following factors: the surface tension of the drop, the fact that the drop is not of pure water but is composed of a salt in solution, or the effect of the electrical charges on the drop. It has not been decided as yet which one of these factors is fundamental in permitting such a degree of supercooling in the atmosphere.

When a supercooled water droplet begins to freeze, its temperature rises instantaneously to 0°C , the heat necessary to raise the temperature being obtained by the release of the latent heat of fusion. If the supercooled water droplets are at a temperature of $-T^{\circ}\text{C}$, then f , the fraction of water frozen, is given by

$$80f = T \quad \text{or} \quad f = \frac{T}{80}$$

The latent heat is taken as 80 cal per gm. It can be seen that the fraction of water frozen is directly proportional to the degree of supercooling. Thus if $T = -8^{\circ}\text{C}$, 10 per cent will freeze immediately. Since the remainder of the drop is at a temperature of 0°C , evaporation can take place into the cool air stream, or heat can pass by conduction from the drop to the surrounding air or the plane. The heat of fusion is thus dissipated by any of or all these methods and the remainder of the drop will freeze.

The manner of freezing depends on the size and number of the drops. When the droplets are small so that each one freezes as a unit almost immediately on coming in contact with the plane, the ice which is deposited has little cohesion and there are small air pockets embedded in it. This ice, of the rime type, forms in a uniform layer along the leading edge of the wing so that it does not materially reduce the lift. Since it is made up of a large number of small crystals, it can be dislodged easily by ice-removing devices on the wings and other parts of the plane. For both these reasons rime ice does not endanger the aircraft.

When the drops which the plane strikes are large, considerable water is left after the initial freezing, and this is carried backward in the wind-stream over the edge of the wings. The ice that is formed as this water freezes extends over a considerable area of the plane as a solid and tenacious mass. If, before the drops are completely frozen, other drops come in contact with them, the mass of ice grows as a unit and becomes even more difficult to dislodge from the wings of the plane. This is the method of formation of clear ice. Because of its adhesive and cohesive properties, its rapid rate of accumulation, and the change which it causes in the shape of the wing, it is a major hazard to aviation.

144. Variation of Ice Deposits with Temperature and Season. The amount of ice formation varies greatly with temperature. In general, it may be said that the greatest deposits of ice occur at temperatures just below the freezing point. At lower temperatures the rate of accretion of ice is much less. Data on the dependence of icing on temperature over the

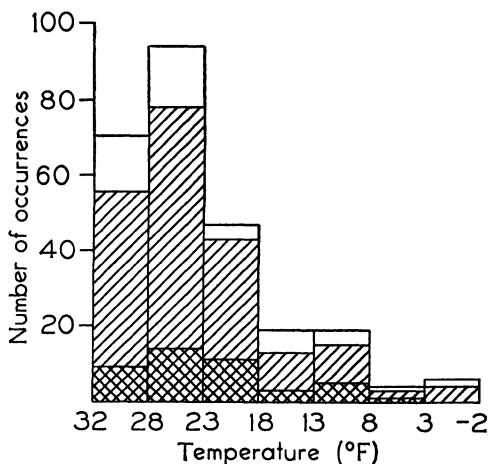


FIG. 157. Variation of icing with temperature in the British Isles: clear areas, flights without icing; single hatching, light icing; double hatching, heavy icing. (After Bigg.)

British Isles are available and are shown in Fig. 157. The total height of each column is proportional to the total number of occasions when the temperature was within the limits shown and ice formation might be expected. The unhatched portions of the columns in the diagram represent the number of cases without icing, whereas the

hatched areas of the columns indicate the number of cases of icing of all types in each temperature interval. Double hatching indicates the number of occurrences in which icing was heavy. For example, out of a total of 94 flights when the temperature was between 28 and 23° F, there was no ice formation during 16 and some icing occurred during the remaining 78 flights. Of the latter there were 14 cases of heavy icing. In addition to the values shown, there were five cases of icing at temperatures below -2° F, but no cases of heavy icing at temperatures below this. This diagram shows that the maximum icing of both heavy and all types occurs in the temperature interval 28 - 23° F. As can be computed from the values given in the chart, 82 per cent of all icing occurs in the interval 32 - 18° F, and 79 per cent of the cases of heavy icing occurs in this interval.

Similar data, although less in amount, have been obtained in the United States, and the analysis of these indicates that icing occurs under the same general conditions. The results of the analysis of 66 observations of icing are given in the table in which it can be seen that

OCCURRENCE OF CLEAR AND RIME ICING

Temperature range (°F)	Type of Ice	
	Clear	Rime
35 to -7		29 to -20
Mean temperature (°F)	20	12
Percentage at temperatures above 18° F	78	36

rime ice occurs at lower temperatures than clear ice. This is to be expected, as rime results from the freezing on impact of small supercooled water droplets, which are prevalent at lower temperatures. The large droplets which give clear ice are found at higher temperatures.

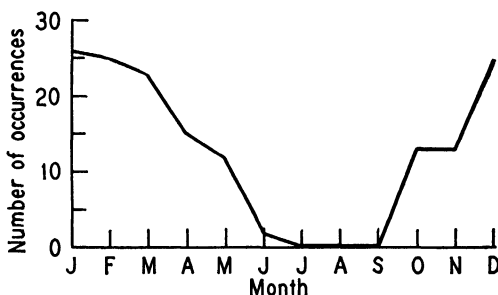


FIG. 158. The annual distribution of icing in the United States.

The seasonal variation of icing on aircraft over the United States is indicated in Fig. 158. The great majority of ice deposits occurred during the late autumn, winter, and spring months. These variations

are, of course, largely due to the variation in the height of the freezing level during the year. In winter the level is low, and aircraft often encounter sub-freezing temperatures. In summer the freezing level is high, and only under exceptional conditions will aircraft be flying at such levels. Conditions over the British Isles are essentially the same as those shown in Fig. 158.

145. Icing, Cloud Forms, and Stability. The deposition of ice occurs where there are supercooled water droplets, and the larger the amount of liquid water in a given volume, the greater the icing hazard. When saturated air at -5°C and 800 mb cools to -10°C , 1 gm of water vapor per kg of dry air condenses. If the air had been saturated at 5°C , and cooled to 0°C , the mass of water vapor condensed would have been 2 gm per kg. Thus the amount of water vapor which is condensed is dependent on the dew point of the air before condensation commenced as well as on the degree of cooling below that dew point.

Another factor to be considered is the length of time the cloud particles have been above the freezing level. As described in section 128, condensation occurs in the form of water droplets when the temperature is above freezing, and in the form of ice crystals or water droplets or both when the temperature is below freezing. When both ice crystals and water droplets exist at temperatures below 0°C , the state is unstable, as indicated in section 128, and the ice crystals grow at the expense of the water droplets. It follows that the longer the cloud particles stay above the freezing level the less the icing hazard becomes since an increasing proportion of the condensed moisture will be in the form of ice crystals. Thus the most serious icing in clouds occurs when the latter form in air which is initially warm and moist, and when the clouds have recently developed or have recently ascended above the freezing level.

In clouds of the cumulus type, icing is both probable and dangerous. The clouds are formed in vertical currents which carry air from near the surface of the earth to great heights. The amount of cooling below the dew point is considerable; the initial temperature and moisture content of the air before ascent are usually comparatively high; the time interval during which the cloud has existed above the freezing level is short; and the turbulence produces large water droplets. All these features aid in explaining the relatively high frequency of occurrence of heavy icing on aircraft in this type of cloud.

Altostratus and nimbostratus clouds are formed in the warm, moist overrunning air at a warm front. But the rate of ascent is small compared with that in a cumulus cloud. If then the cloud is far above the freezing level, more of the condensed moisture will be in the form of ice

crystals than of liquid water. A long flight in the cloud will lead to a considerable deposit of rime ice when the temperatures are below -8°C (18°F). The portions of the cloud at temperatures 0 to -8°C will have been above the freezing level for only a short time, and sufficient liquid water will be present to lead to clear icing, which will sometimes be heavy. If actual or latent instability is present, a cumulus cloud with heavy icing in its top portion may develop in the nimbostratus.

Turbulence stratus and stratocumulus clouds may persist for a considerable time. Since, however, the cloud droplets are continually evaporating and forming in the vertical currents just below the cloud base, water droplets will persist in these clouds. In stratus the droplets are usually small and rime ice will be deposited. When, as sometimes happens, the moisture content of the clouds is sufficient to give freezing drizzle, the accumulation of ice may be large if the aircraft persists in the cloud for any length of time. Since, though, stratus cloud is usually thin, flying can be done above the cloud and thus the hazard is eliminated.

Icing in stratocumulus is similar to that in stratus except that the turbulent eddies are stronger, and the drops are larger. In the stratocumulus clouds that form through the instability that develops in polar air behind a cold front, the amount of moisture may be sufficient to give a clear ice deposit at a moderate rate if the temperatures are above -8°C . In other situations, or with temperatures below this, the icing that occurs will be of the rime type.

The temperature at the altocumulus level is usually low enough that any icing that takes place there will be light and of the rime type. Observations in general have tended to confirm this deduction. Heavy clear icing in altocumulus occasionally occurs and may be due to the presence of strong turbulent eddies arising from the instability at that level which produces altocumulus congestus clouds.

Clouds at the cirrus level are formed of ice crystals and so do not lead to ice deposits.

In the foregoing discussion the clouds which give serious icing are distinguished from those that give light icing largely on the basis of the stability of the air. Thus rapid icing is found in cumulus, cumulonimbus, cumulus embedded in nimbostratus, and in stratocumulus behind a cold front. Stratus type clouds do not in general lead to rapid ice accretion. Investigations have confirmed this conclusion to a certain extent, the stability being evaluated in terms of the saturated adiabatic lapse rate. Further investigations of the relationship between instability and the rate of ice accretion are needed. *

146. Ice Formation by Supercooled Raindrops. The formation of ice on an aircraft as it flies through a cloud of supercooled droplets has been discussed in the previous section. Very serious ice accretion may also occur during flight beneath cloud, if the aircraft encounters supercooled raindrops as they are falling to earth. Such icing is likely to be especially serious beneath frontal and orographic cloud, because of the great extent of the cloud, both horizontal and vertical, and the difficulty in reaching a region free from supercooled rain. Rapid deposition of ice frequently occurs under such circumstances, and the airplane may be forced to land unless there is a layer below in which the temperature is greater than 0°C in which it can fly.

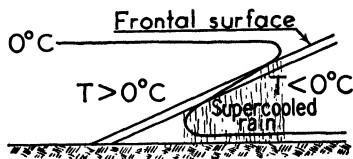


FIG. 159. Region of icing below a warm frontal surface.

At a warm front, the situation is serious if rain falls from warm front cloud through cold air below, the temperature of which is below the freezing point. The region of maximum danger below the warm frontal surface is indicated in Fig. 159.

At a cold front, conditions may be similar, but there are significant differences. Because of the fact that the slope of a cold front is usually greater than that of a warm front, and the cloud system associated with the former is often discontinuous, the area in which icing conditions occur is not so extensive in the horizontal as near a warm front. Since the amount of ice accretion is in part dependent on the length of time that the aircraft remains in the region where ice accretion occurs, it is clear that ice deposition will, in general, be less serious at a cold front than at a warm one. On the other hand, a slowly moving cold front often exhibits icing conditions similar to those at a warm front. In addition, cumulonimbus clouds are frequently associated with cold fronts, and icing in these is likely to be serious.

At occlusions serious icing may occur. The situation is similar to that at a warm front, for aloft there is a trough of warm air from which precipitation falls. If the temperature of the warm air is greater than 0°C , and that of the cold air masses below is less than 0°C , a wide area exists in which icing will occur rapidly.

Icing may also occur on an aircraft flying under a precipitating cloud of the cumulus type, such as cumulonimbus. However, such clouds are usually isolated, and it is possible on most occasions to avoid the regions where supercooled rain may be falling.

147. Means of Avoiding Deposition of Ice. The deposition of ice will be prevented if aircraft avoid ice-forming clouds and regions where

supercooled rain is falling. If ice begins to form on the plane, then the pilot must immediately estimate its rate of accretion, and leave the region, usually by ascent or descent, if the icing is going to be too heavy for continued navigation. Rules for avoiding serious icing can be summarized as follows:

(a) Avoid, at all times, flying in air cooler than 0°C into which rain is falling from above. If the plane cannot fly below the freezing level, it may be able to turn back out of the rain and climb above the region of serious icing. Otherwise the plane should land.

(b) Avoid, at all times, flying in cumulus and cumulonimbus clouds above the freezing level. Since these are usually isolated, it is usually possible to avoid these clouds.

(c) Avoid flying in nimbostratus and altostratus clouds when the temperature is between 0 and -8°C (32 and 18°F). If the air is unstable, or likely to become so, avoid these clouds in the layer between 0 and -14°C (32 and 7°F). Since these layers normally are about 4000 ft thick for stable air, and 8000 ft thick for unstable air, it is frequently possible to choose between flying above or below them to avoid the region of serious icing.

(d) Avoid extensive flying in stratus, stratocumulus, and altocumulus clouds in the temperature range 0 to -8°C (32 to 18°F). Since these clouds are usually thin, it is possible to get out of the cloud either by ascending or descending.

148. Forecasting the Deposition of Ice. The forecasting problem is considerably simplified if upper air temperatures are available. Determine the heights at which temperatures of 0 and -14°C (32 and 7°F) occur. If clouds are expected in the layer between, then icing is a possibility. If cumulonimbus clouds are expected, anticipate ice accretion at any level in the cloud. If no upper air temperatures are available, the height of the bottom and top of the region of serious icing can be obtained by approximate methods. Knowing the surface temperatures, a rough estimate of these levels may be obtained by assuming an average lapse rate of 6°C per km or 1°F per 300 ft. If there is a surface inversion, allowance must be made for this. If the inversion is due to a frontal surface, then the heights of the top and bottom of the region of serious ice accretion above the frontal surface may be calculated by assuming adiabatic ascent of the surface air in the warm sector. The height of the freezing level, or of the freezing levels when two air masses are present, should be available for pilots.

Since instability increases the danger of icing, an evaluation of this should be made. In lieu of upper air ascents, it is sometimes necessary to deduce its presence or absence by means of the types of precipitation that are reported at the observing stations.

PROBLEMS AND EXERCISES

1. Weather reports before, at, and after the passage of a cold front gave the information found in the table.

Time	14. 30	15. 30	15. 45	16. 30	17. 10	17. 30	h
Low cloud	Type	Sc	Sc	Sky	Sky	Sc	Sc
	Height	2000	2500	obscured	obscured	1500	2000
	Amount	6	7			9	7
Type of middle cloud	As	As	As	As	
Total cloud amount	10	10	10	9	tenths
Temperature	42	42	32	32	°F
Dew point	33	33	32	28	°F
Wind	Direction	SW	SSW	WSW	W	W	W
	Speed	25G ¹	25G	35G to 62	30G	35G	37G
Visibility	6	6	$\frac{1}{2}$	$\frac{1}{2}$	6	8	mi
Weather	Haze	Haze	Heavy sleet	Mod. sleet	Haze	..	

¹ Gusty.

From this information, what deductions may be made concerning the levels unfavorable for flying in the vicinity of the front?

2. The following values were obtained by an upper air sounding through a quasi-stationary front.

<i>Ht</i>	0	26	42	60	93	130	100's of ft
<i>p</i>	1000	900	850	800	700	600	mb
<i>T</i>	2	-1.5	-3	1	-6	-12	°C

The relative humidity throughout was over 70 per cent. Precipitation was falling at the station, and in the vicinity rolling hills reached an altitude of 600 ft. What routes are possible for a pilot who wishes to fly normal to the front from a point 200 mi on one side of the station to 200 mi on the other side?

BIBLIOGRAPHY

- Byers, H. R., *Synoptic and Aeronautical Meteorology*, New York, McGraw-Hill Book Co., 1937. Chapter 13.
- Bigg, W. H., *Ice Formation in Clouds in Great Britain*, Prof. Notes, No. 81, London, Meteorological Office, 1937.
- Jordanoff, H., *Safety in Flight*, New York, Funk and Wagnalls, 1941.
- Lacey, J. K., "A Study of Meteorological Factors Affecting the Formation of Ice on Airplanes," *Bul. Am. Met. Soc.*, **21**, 357-367 (1940).
- McBrien, R. L., "Study of Icing Problems of Transport Aircraft," *Canadian Aviation*, **14**, 21 (1941).
- Minser, E. J., "Studies of Synoptic Free-Air Conditions for Icing on Aircraft," *Bul. Am. Met. Soc.*, **19**, 111-122 (1938).
- Simpson, Sir G. C., *Ice Accretion on Aircraft*, Prof. Notes, No. 82, London, Meteorological Office, 1937.
- Sutcliffe, R. C., *Meteorology for Aviators*, London, H. M. Stationery Office, 1940. Pages 138-143.
- Taylor, G. F., *Aeronautical Meteorology*, New York, Pitman Publishing Corporation, 1938. Pages 313-318.

CHAPTER 22

THUNDERSTORMS

149. The Potential Gradient. Electrical Charges in the Atmosphere.

In fine weather there exists a difference in electrical potential between the earth and the atmosphere, or a vertical potential gradient. This potential gradient was first measured by Franklin by means of kites and vertical rods. It is still the object of innumerable measurements. During fine weather the gradient is positive upward with the earth acting as a negatively charged conductor.

The average value of the potential gradient over the ocean and over level land areas is about 100 volts per m. Individual values vary widely from this, however. During thunderstorms it reaches at times the value of 10,000 volts per m. Over the sea, where local factors are not significant, there is a diurnal variation, but the time of maximum is the same for all parts of the earth, being about 17.30 h GMT. There seems to be a close correspondence between the variation of the potential gradient and of the total number of thunderstorms that are occurring over the surface of the earth. This suggests that each thunderstorm adds a positive charge to the upper atmosphere which is carried rapidly over the earth.

The presence of clouds overhead changes the value and frequently the sign of the potential gradient. With the arrival of warm frontal clouds the gradient generally changes to negative. The gradient in the vicinity of a thunder cloud fluctuates rapidly, but it is generally negative below the edges of the cloud and strongly positive under the center of the cloud. With shower clouds the gradient is usually negative.

Measurements of the charges within thunder clouds were made by Simpson and Scrase between 1935 and 1939. This was done by attaching to a balloon an instrument, which they called an alti-electrograph, and permitting it to rise through the cloud to be studied. The average distribution of charge found in different parts of the thunder clouds investigated is illustrated in Fig. 160. At the top of the cloud, in the portion extending to heights greater than the level of the -10°C isotherm, the charge was found to be positive. In the middle portion of the cloud, between the -10°C and 0°C isotherms, the charge was

negative. In the base of the cloud a center of strong positive charge was at times measured, below which heavy rain occurred at the surface of the earth.

Measurements of the charge on raindrops falling to the earth have shown that these are electrically charged. The investigations indicated that during any one storm some drops carry negative charges, while others carry positive charges. Nevertheless the average charge carried to the earth in rain from thunder clouds is positive, that from shower clouds is negative, and that from frontal rain is positive.

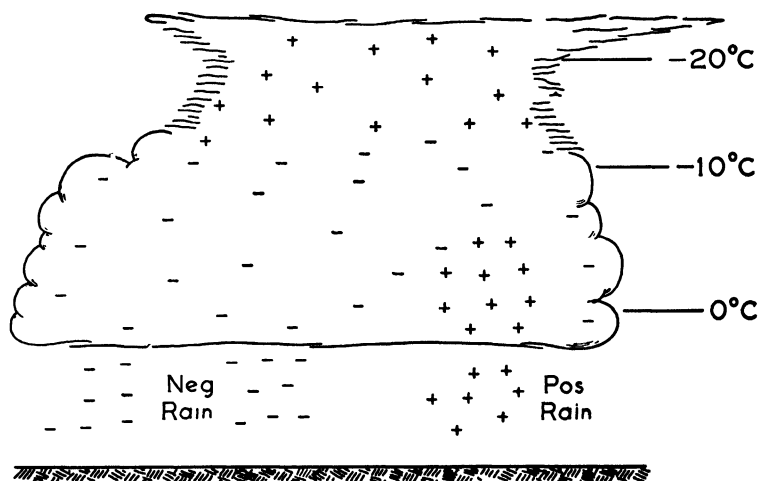


FIG. 160. The average distribution of charge in a thundercloud, according to Simpson.

During dust storms and snow storms there is a separation of electrical charges. The air becomes positively charged, while the dust or snow particles become negatively charged. The gradient developed during these storms is sometimes very great.

150. The Origin of Thunderstorm Electricity. Two main theories are current to account for the development of the great electrical fields which accompany thunderstorms.

(a) *The Breaking-Drop and Impact-of-Ice-Particles Theory.* In 1892 Lenard showed that pure water splashing against a solid object causes electrification, the water becoming positively charged. In 1908 Simpson showed that the same separation of charge takes place when water drops are broken up by a rapidly moving stream of air. Using this fact as a basis, Simpson developed a theory to account for thunderstorm electricity. He had found that the separation of charge occurred when the water droplets were broken by a stream of air moving at a speed

greater than 8 m per sec. Vertical currents with velocities greater than this occur in the lower front portion of a thunder cloud, producing a separation of charge in that region. The raindrops there become positively charged, and the negative charges become attached to the cloud particles and are carried by the turbulent currents through the cloud. With the discovery of the positively charged region in the top of the cloud, Simpson modified his theory. At the top of the cloud, which is usually at a temperature lower than -10°C , the ice particles are in turbulent motion. Collisions between them cause a separation of charges, with the ice crystals becoming negatively charged and the atmosphere positively charged. The ice particles increase in size and descend, leaving a positive charge at the top of the cloud, while at lower levels the preponderance of negatively charged ice crystals gives a negative charge to that part of the cloud. When the ice crystals fall below the freezing level, they become raindrops. The strong vertical currents cause most of these to break, during which process they are stripped of their negative charges and finally take on a positive charge. The drops which are not subjected to sufficiently strong vertical currents to be broken up carry their charges to the ground. By this theory both the distribution of charge in clouds and the differing charges on drops reaching the surface are explained. The theory also explains the charge on rain in showers, where the vertical currents are not as strong as in thunderstorms.

(b) *Influence Theory.* According to this theory, put forward by C. T. R. Wilson, the charges are separated by the influence of electrical fields, hence the name. Wilson assumes the ordinary fine-weather positive potential gradient and considers how a separation of charge may occur. He takes the case of raindrops falling through a cloud when such a positive field exists as is illustrated in Fig. 161. The positive charges aloft and the negative charges at the surface are used to denote the positive potential gradient of the earth's field. A drop falling in such a field will have negative charges induced at the top of the drop and positive ones at the bottom. Negative ions in the air will be attracted to the lower portion of the drop while positive ones will be attracted to the upper part of it. But because the drop is falling, negative ions will be readily drawn to the bottom and will neutralize the induced positive charge there. On the other hand, positive ions will have difficulty in overtaking the falling drop, especially in view of their small mobility, and there will be little neutralization of charge at the top of the drop. This will leave a net negative charge on such drops and a net positive charge on the air above from which negative ions have been removed. In this manner, according to Wilson, the separation of charge is effected.

As originally proposed, this theory explained the positive charge at the top of the thunder cloud and the negative charge over most of the base, which were known to exist when the theory was put forward. If the possibility of the separation of charges by impacts of ice crystals is accepted, it can be modified to explain the positive charge at the base. Below the freezing level, i.e., below the strong negatively charged layer from 0°C to -10°C , the ice crystals melt and fall as raindrops. Each

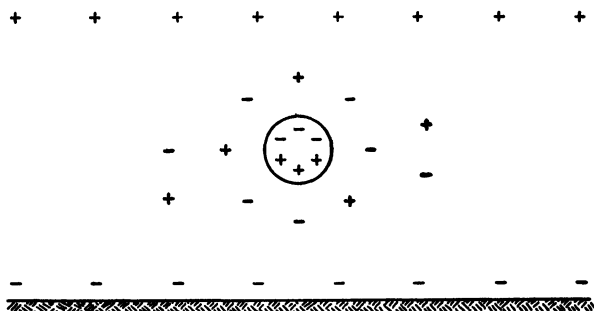


FIG. 161. The development of an electrical charge on a raindrop falling in an electrical field, according to Wilson.

drop is now falling through a region which has negative charges above and positive charges at the earth's surface and will then acquire a positive charge through the influence of the electrical field. The influence theory, however, fails to bring out the close connection between strong electrical fields and vertical currents since the potential gradient is present during all types of rain.

Neither theory satisfactorily explains the preponderance of positive charge found in warm frontal rain with stable conditions. A fully satisfactory theory for the development of atmospheric electricity has not yet been proposed.

151. Variations in Time and Place of Occurrence of Thunderstorms.

Thunderstorms are associated with strong vertical currents and so are most frequently found in regions of great instability. The vertical distribution of temperature and moisture which leads to thunderstorms is the same as that which leads to the development of cumulonimbus clouds, discussed in section 138.

Thunderstorms are most frequent over the moist, humid regions of the equatorial low-pressure belt. They are comparatively rare in the subtropical high-pressure belt except at the western edge of a cell where the southerly winds bring moist air from the equatorial regions. Over the temperate zone there is an annual variation, with the number of

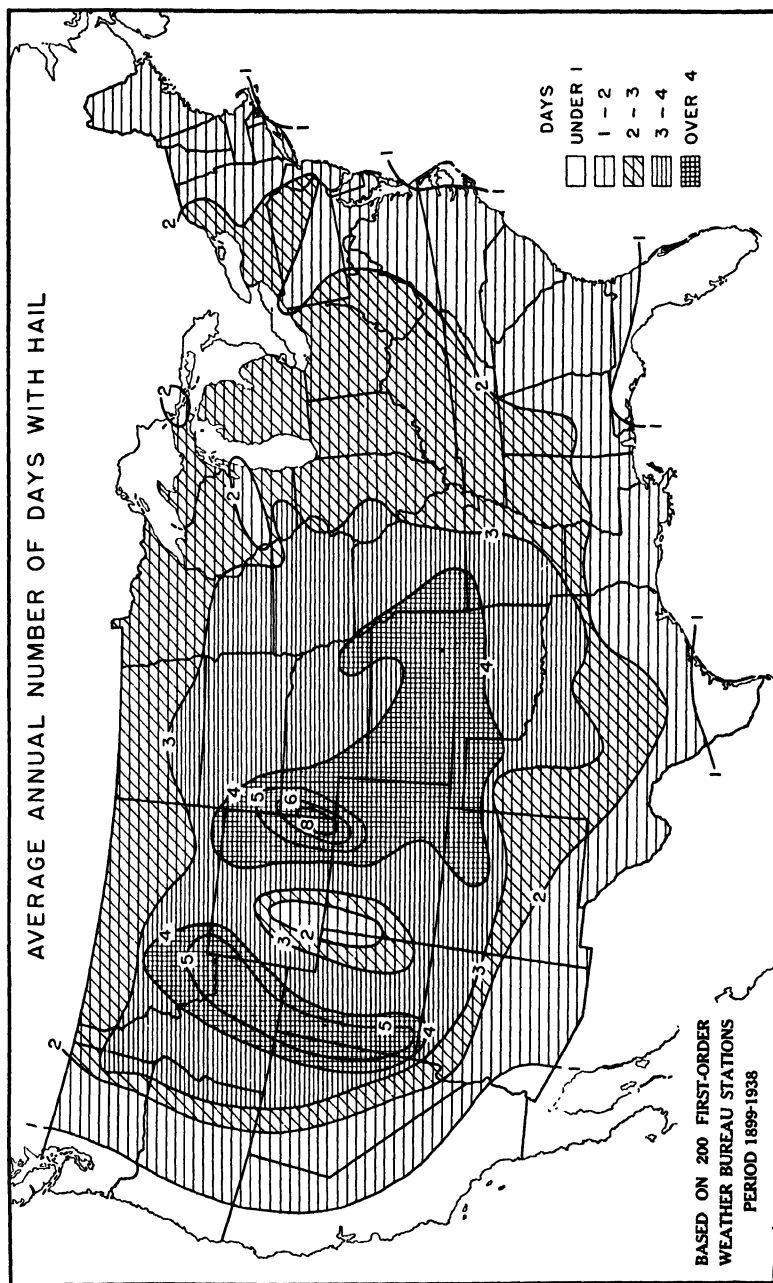


Fig. 163. The number of days with hail over the United States. (From *Climate and Man*, U. S. Dept. of Agriculture Yearbook for 1941.)

storms decreasing with increasing latitude. Very few occur in the polar regions.

In the temperate zone the time of most frequent occurrence of thunderstorms is during the months of June, July, and August. Very few thunderstorms occur over the ocean, but the time of maximum frequency of those reported is during the winter. There is a similar difference in the time of occurrence of maximum thunderstorm activity during the day over land and over ocean surfaces. Over the land most of the storms occur during the period 14 to 18 h, whereas over the ocean the maximum is from 24 to 04 h. This contrast is explained by the effects of surface heating. Over the land the time of maximum heating is during the afternoon in summer. The surface of the sea has a relatively constant temperature. Hence it is warmest with respect to the air moving off the land when that air is coldest, that is during the winter and during the night. The maximum instability over the ocean develops then, and with it the maximum of thunderstorm activity.

The effect of a water surface in decreasing instability must be kept in mind when forecasting for some land stations. When the trajectory of the air is over an extensive water surface during the summer, the instability that may be present originally will frequently decrease, leading to a cessation of thunderstorm activity as the air moves again over the land. The average distribution of thunderstorms over the United States is shown in Fig. 162. The region of maximum occurrence is over western Florida where the moist air from the Gulf develops instability through surface heating. A second maximum is found over New Mexico and Colorado. Fig. 163 gives the average distribution of hailstorms over the United States. Although there is some similarity in the distributions of hail- and thunderstorms, the storms near the Gulf are seldom accompanied by hail. The greatest proportion of storms with hail is found over the plains where on the average one storm in ten is accompanied by hail.

The effect of insolation in causing thunderstorms is well illustrated by the distribution of thunderstorms over the British Isles, shown in Fig. 164. During the summer months the prevailing winds are westerly. As the air leaves the ocean and advances over the land surface, which has been heated by insolation during the day, the lower layers in turn become heated. When the air at higher levels is cold, while that near the surface is particularly moist, this surface heating may be sufficient to produce marked real latent instability by the time the air reaches the Midlands, resulting in the observed maximum of thunderstorms there. This analysis is confirmed by the fact that the area of maximum thunderstorm activity coincides approximately with the region of maximum temperature during the summer months.

152. Thunderstorm Forecasting. The forecasting of thunderstorms has its own peculiar difficulties. Thunderstorms are local phenomena,

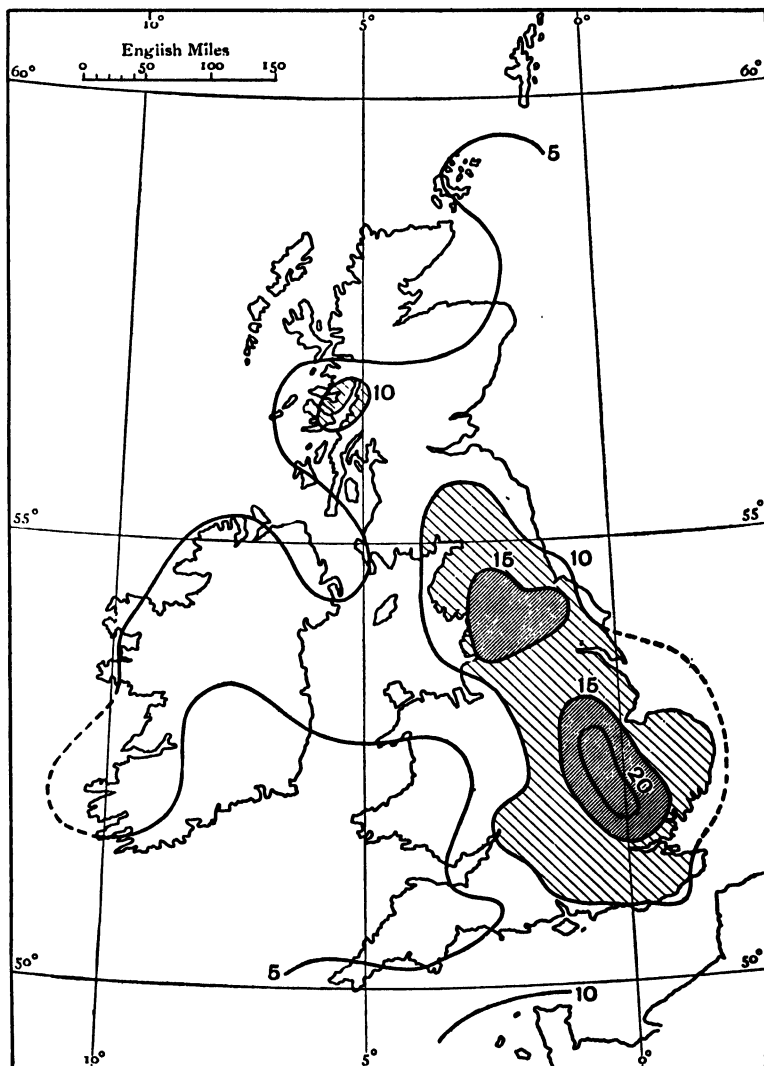


FIG. 164. The distribution of thunderstorms over the British Isles. (From Bilham, *The Climate of the British Isles*, Macmillan and Co.)

with diameters of 8 to 12 mi. Even in a district where thunderstorm activity is pronounced, there will be sections in which none occur. This difference is probably a result of the local topography, since a slight

orographic lift may be necessary to release the instability present. After a center of convective activity forms, it tends to persist and to move off in the direction of motion of the current of air at 4000 to 6000 ft. But since these storms are local, it is not possible to forecast their occurrence at a given station with assurance, although they can be expected in a given district.

There are several types of thunderstorms which must be kept in mind when forecasting.

Air mass thunderstorms may develop in several ways. Heating of the air near the surface is the most frequent cause of this type of storm, although advection of cold air in the middle layers is also occasionally a contributing factor. Insolation heating of the earth's surface will produce a steep lapse rate in the lower layers. If, in addition, the moisture content of the air near the surface is high, as in tropical maritime air masses, thunderstorms are likely to develop, especially when upper air conditions are such that a large positive area extending to great heights is shown on the tephigram. The development of these areas is discussed in section 138 in connection with the development of convection clouds. Air mass thunderstorms may also occur as a result of the heating in the lower levels of a cold air mass, such as a polar continental air mass, as it moves over a warmer surface. Very steep lapse rates will develop near the surface in this manner.

Possible changes in the upper air should be considered. If the air is becoming colder because of a wind shear at higher levels, or if the air near the surface is becoming more moist, instability may develop where it was previously absent. On the surface pressure map the region of thunderstorm activity frequently coincides with a weak low-pressure area, although the latter may be missed because of the weak pressure gradient usually existing over the continent during the summer.

There are several local indications that thunderstorms will develop. The occurrence of altocumulus castellatus, that is, altocumulus with turrets of cloud associated with it, during the early morning is an indication of instability in the upper levels which may increase as the surface layers are heated. Later in the day towering cumulonimbus clouds with warm, moist conditions at the surface suggest that thunderstorms will occur.

Frontal thunderstorms are of frequent occurrence. Latent instability in the warm air mass is developed or increased by lifting of the air mass in the manner outlined in section 95, and this increase in latent instability makes thunderstorm development more probable. Perturbations of the air motion, arising from the vertical motions sometimes occurring near a front, may also start the process of realization of the

latent instability. Thus thunderstorms frequently occur 100 mi. or so ahead of a cold front. Most frontal thunderstorms over North America occur in warm, moist tropical Gulf air. The base of a cold front thunder cloud is usually near the surface of the earth. On the other hand, warm front thunderstorms frequently occur 200 to 300 mi ahead of the surface position of the front at a high level at the point where the instability is released. Summer thunderstorms are very frequently associated with old occluded fronts which have taken on the characteristics of active cold fronts. Diurnal heating of the surface air tends to intensify frontal thunderstorms, especially those of the cold front type. The time of maximum occurrence of these is during the afternoon.

Orographic thunderstorms have many characteristics similar to those of warm frontal thunderstorms. The ascending motion of the air increases the latent instability, and the accompanying turbulence near the surface may be sufficient to start the process of release of the instability. An interesting feature of some orographic thunderstorms is their tendency to remain almost stationary. Mountain slopes which are nearly normal to the direction of the sun's rays may be very strongly heated, and intense thunderstorms often develop over such slopes.

BIBLIOGRAPHY

- Admiralty Weather Manual*, London, H. M. Stationery Office, 1938. Chapter 12.
- Byers, H. R., *Synoptic and Aeronautical Meteorology*, New York, McGraw-Hill Book Co., 1937. Chapter 12.
- Problems of Modern Meteorology*, London, Royal Meteorological Society, 1934. Number 3.
- Shaw, Sir N., *Manual of Meteorology*, London, Cambridge University Press. Vol. 2 (1936), Chapter 2; Vol. 3 (1930), Chapter 9.
- Brancato, G. N., *The Meteorological Behavior and Characteristics of Thunderstorms*, Washington, D. C., U.S. Department of Commerce, 1942.
- Byers, H. R., *Non-Frontal Thunderstorms*, University of Chicago, Inst. of Met., Misc. Reports, No. 3, 1942.
- "Discussion of Thunderstorm Problems," *Q. J. Roy. Met. Soc.*, **67**, 327-361 (1941).
- McEachern, K. B., and K. G. Patrick, *Playing with Lightning*, New York, Random House, 1940.
- Simpson, Sir G. C., "The Electricity of Clouds and Rain," *Q. J. Roy. Met. Soc.*, **68**, 1-34 (1942).

CHAPTER 23

CLIMATOLOGY

153. Importance of Climatology to the Meteorologist. Meteorology, as a science, deals with the daily weather, and more particularly with the variations that occur, and the influences that cause these variations. Climatology, too, is a study of the weather, but from the standpoint of assessing and explaining the average conditions. For example, the climatologist is interested in the statement that the average wind at a station is westerly. The meteorologist is concerned with understanding what conditions will produce, for example, easterly or southerly winds at the same station, and why. The forecaster's aim is to specify what changes are to be expected in the weather in the future. The work of the climatologist is to determine the average weather conditions which have occurred in the past.

To a large extent the statistical facts presented by the climatologist are not vital to the forecaster. Yet an understanding of some of the climatologist's findings is valuable in assessing the weather changes that may be expected.

Very frequently a forecaster remains in one district for a considerable period and learns the variations in the weather in that district only. If he moves to another district, it requires from one to six months for him to learn the broad trends and local anomalies of the weather, a thorough knowledge of which is necessary for accurate forecasting. If the climates of the two regions are similar, the minimum period only is required; if the climates are markedly dissimilar, so that his past experience no longer aids him when forecasting abnormal atmospheric conditions, the full period of six months is necessary to obtain a grasp of the climatology of the region. A study of climatological data giving, for example, average maximum and minimum temperatures and average limits of rainfall during the months of the year, is helpful. A study of climatology also aids in understanding the problems of the forecaster in other regions so that an exchange of ideas can take place more freely.

Even in the region in which the forecaster is primarily interested, a knowledge of climatic types is desirable. No region is so small that variations in the climate cannot be observed. Thus the climate in one part of the region may be continental in character; another part may be

under the moderating influence of lakes; another part may be on the lee side of hills where descending air is relatively dry and rain is less frequent. An understanding of the general significance of these factors will aid the forecaster in modifying a forecast to suit each portion of the region. The forecaster may learn this by experience as he analyzes the maps day after day. A more objective analysis by a statistical summary of the weather for the different parts of the forecast region would correct some of the ideas that the forecaster may have. It would also aid a new forecaster coming into the district in distinguishing the different climatic regions of the country. For example, studies of a climatological character of the conditions which precede the formation of radiation fog at various airports, of the types shown in Figs. 136 and 137 of section 134, are an aid to both the experienced and the inexperienced forecaster.

154. The Factors Governing Climate. The elements which, taken together, vary over the earth's surface and constitute climate, when they vary in any one place, produce weather. These are temperature, precipitation, clouds, moisture content of the air, and wind. Pressure varies, but changes in pressure are noted only because of corresponding changes in one of the other weather elements.

The distribution of temperature over the earth is shown in Figs. 1 and 2, section 1, and the winds of the earth in Figs. 5 and 6 of section 3. Fig. 165 gives the world distribution of precipitation. The variation of fog for June, July, and August over the north Atlantic is shown in Fig. 166. Fogs in this region are of the advection type, as shown by the fact that the area of maximum fog frequency, off the coast of Newfoundland, coincides with the area of maximum temperature gradient of the ocean surface. Several other climatic maps are given in other sections. Thus, the distributions of fog over the British Isles and the United States are shown in Figs. 142 and 143, section 136; of thunderstorms in Figs. 162 and 164, section 151; and of hail over the United States in Fig. 163, section 151.

Two regions have differences in climate because of differences in one or more of the following:

- (a) Latitude.
- (b) Altitude.
- (c) Topographic features.
- (d) Relation to the general pressure distribution.
- (e) Prevailing winds.
- (f) Nearness to ocean.
- (g) Relation to ocean currents.

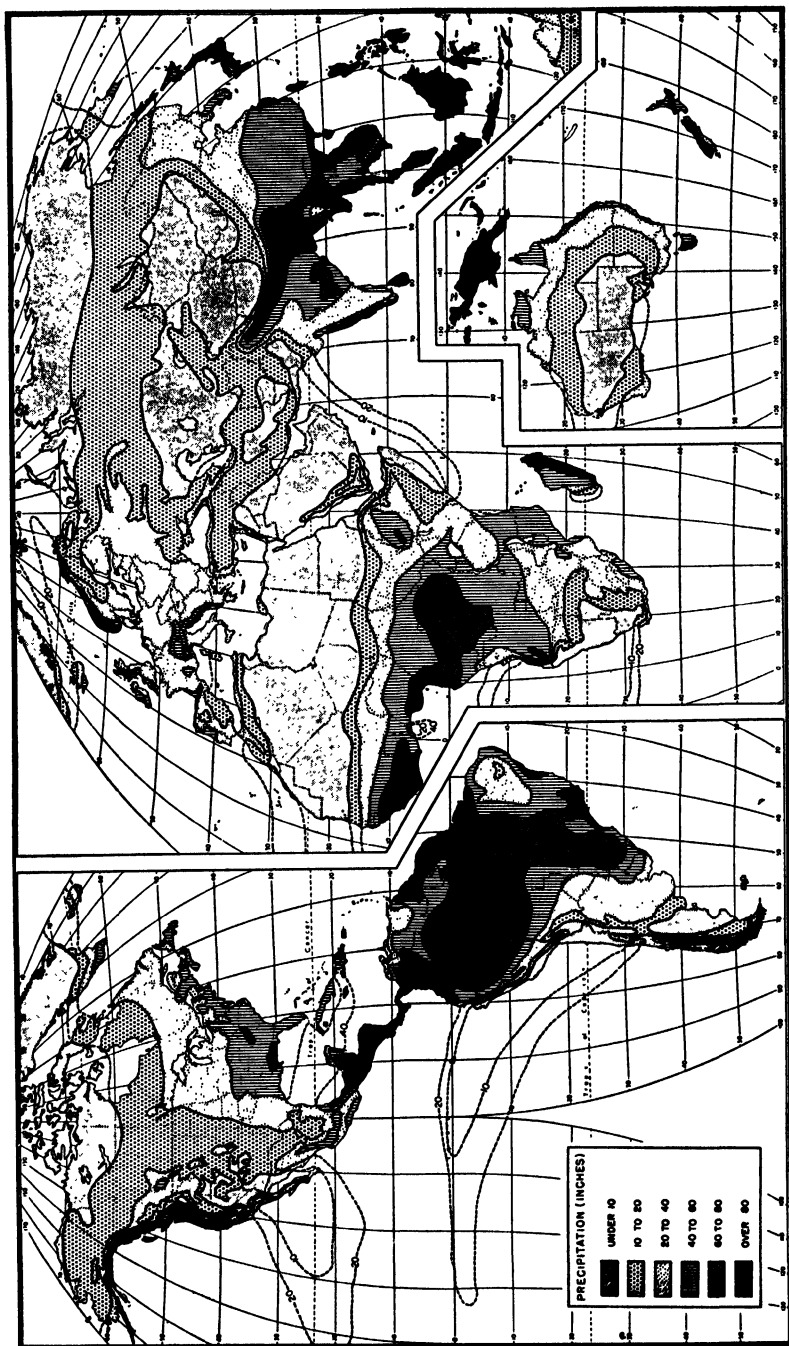


FIG. 165. The world distribution of precipitation. (From *Climate and Man*, U. S. Dept. of Agriculture Yearbook for 1941.)

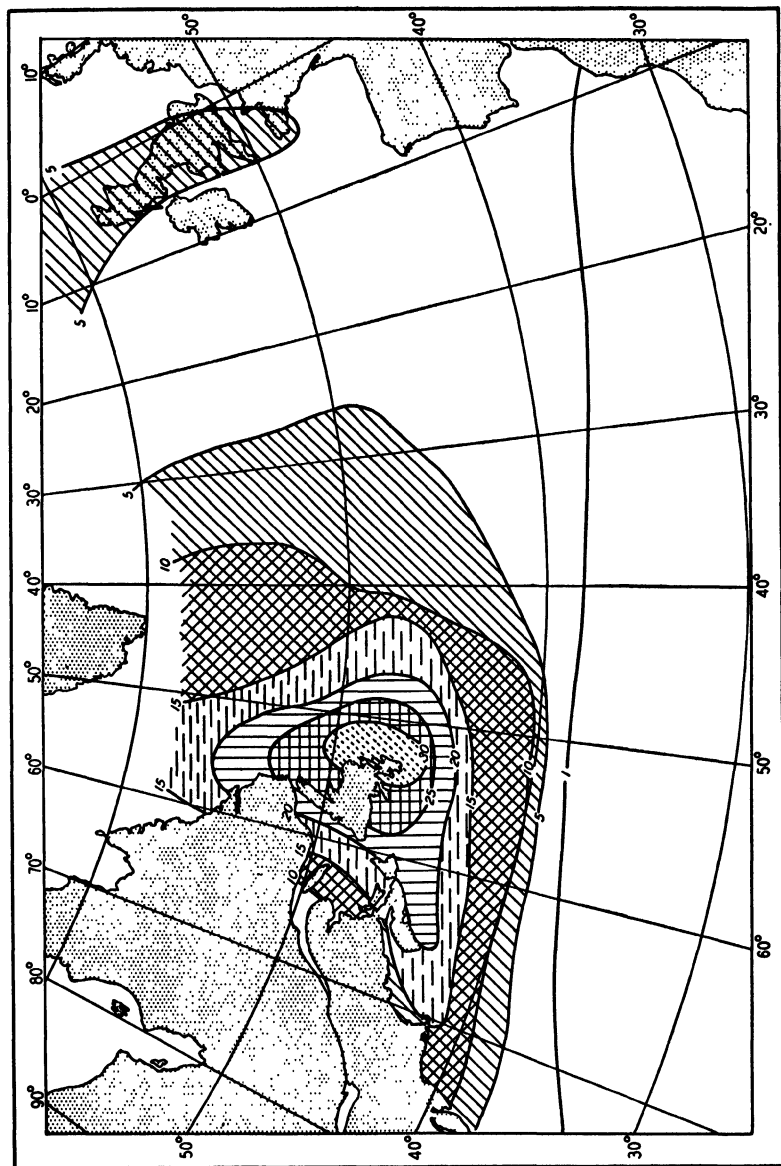


FIG. 166. The distribution of fog over the north Atlantic for June, July, and August. (From *Atlas of the Climatic Charts of the Oceans*, U. S. Weather Bureau.)

These climatic controls are not independent. Thus the general pressure distribution varies with latitude and, since the former has a controlling influence on the prevailing winds and the ocean currents, these also vary with latitude.

The weather, and particularly the temperature, varies markedly with latitude. This variation arises because the distance from the equator determines the amount of heat received directly from the sun, as shown in Fig. 27, section 31. The tropical regions, on which the sun shines nearly vertically throughout the year, are the warmest portions of the earth, and the polar regions, which receive considerable insolation during the summer, but none during the winter, as indicated in section 28, are the coldest. In order to be able to assess the other factors governing temperature, climatologists at times eliminate the latitudinal effect by drawing charts of temperature anomalies, i.e., maps showing the variation from the average for that latitude.

The temperature in the atmosphere decreases with altitude at a fairly regular rate, so that the mean temperature at any given point at the earth's surface is in part determined by the altitude of that point (see problem 2, Chapter 10). The altitude and the proximity to mountains also help determine the amount and type of precipitation. On the windward side of the mountain the air rises, giving orographic clouds and precipitation. On the lee side and sometimes on plateaus and in valleys the air is dry and little rain falls. Regions, such as these, which have less precipitation because of a mountain to the windward, are said to be in the mountain's *rain shadow*.

As described in Chapters 12 and 15, the general pressure distribution determines the characteristics of air masses and the frequency of their occurrence at any location. Hence regions differently located with respect to these will have differences in weather. For example, Florida, on the western edge of the Azores high, with southerly winds, has an annual rainfall of 52 in.; Rio de Oro, on the African coast with the same latitude but on the eastern edge of the Azores high, where northerly winds prevail, has an annual rainfall of less than 10 in. Since the prevailing winds are closely associated with the general pressure distribution, the effects of each on climate cannot be separated.

The ocean currents are an effective means of transferring heat from equator to pole and so of aiding in the maintenance of the terrestrial heat balance. Their influence is not spread uniformly and in some regions an adjacent current of warm water from the equatorial regions gives mild temperatures and abundant moisture. Other regions of the same latitude have a raw, cold climate because of the proximity of a current from the Arctic. The variations over the ocean areas of the

mean isotherms, as shown in Figs. 1 and 2, section 1, bring out clearly the effects of the ocean currents.

The sea exerts a moderating influence on the weather of the land areas about its borders. The summers are not so hot, and the winters not so cold as they are farther inland. Also the air is moist, so precipitation is usually abundant and uniform throughout the year, and droughts do not occur. With increasing distance from the sea these influences become less effective and a continental regime of less uniform precipitation and greater variations in temperature is in control. The extent to which the influence of the ocean reaches inland varies with the topographic features and the direction of the prevailing wind. In Europe, Sweden, lying to the east of the Scandinavian mountain range, is continental in climate, but farther south the influence of the Atlantic extends inland over the plain of northwest Europe as far east as Poland.

155. Köppen's Classification of Climate. Several different classifications of the climates of the world have been devised. The classification of Köppen, first published in 1918, has been widely accepted by climatologists, and will be described here. It has a numerical method of dividing the climatic zones, using combinations of letters to distinguish different regions. Each letter is rigorously defined, and these definitions are so well known by climatologists that the climatic types are often given by letters, rather than by more descriptive terms.

Köppen's classification divides the world into the following five major climatic divisions.

A climates. The moist tropical climates. The temperature of the coldest month is greater than 18°C (64.4°F). This is the climate of the hot, rainy, equatorial belt. Its two chief divisions are:

(a) *Af*, signifying regions where there is no dry season, the driest month having at least 6 cm (2.4 in.) of precipitation.

(b) *Aw*, denoting regions where there is a distinct dry season, one month with precipitation less than 6 cm (2.4 in.).

B climates. The arid climates. In these regions the evaporation exceeds the precipitation. Although the principal arid climates are found in the sub-tropics, this type also occurs farther north in certain parts of the world. There are two subdivisions of this type:

(a) *BW*, or the desert climates.

(b) *BS*, or the climate of the steppes.

A further subdivision distinguishes the sub-tropical deserts (*h*), with an average annual temperature of 18°C (64.4°F) or more, from the

middle latitude deserts (*k*), with an average annual temperature of less than 18°C (64.4°F).

C climates. The warm temperate rainy climates. The average temperature of the coldest month is less than 18°C (64.4°F) and greater than -3°C (26.6°F); the average temperature of the warmest month is over 10°C (50°F). Three distinct types are recognized, which are:

(a) *Cf*, with at least 3 cm (1.2 in.) of precipitation in the driest month and the difference between the wettest and driest month less than for *Cw* and *Cs*.

(b) *Cw*, with a winter dry season, and at least ten times as much precipitation in the wettest month of summer as in the driest month of winter.

(c) *Cs*, with a summer dry season, and at least three times as much rain in the wettest month of winter as in the driest month of summer, and in addition the driest month of summer having less than 3 cm (1.2 in.) of precipitation.

D climates. The cold temperate climates. The average temperature of the warmest month is above 10°C (50°F) and that of the coldest month is below -3°C (26.6°F). The two chief divisions are *Df* and *Dw* where *f* and *w* are defined as in *C* climates.

E climates. The polar climates. The average temperature of the warmest month is under 10°C (50°F). There are two subdivisions:

(a) *ET* (tundra), with an average temperature of the warmest month above 0°C .

(b) *EF* (frost), with no month with a temperature above 0°C .

To subdivide more closely, Köppen used a third set of letters defined as follows:

a (hot summer) average temperature of the warmest month over 22°C (71.6°F).

b (cool summer) average temperature of the warmest month under 22°C (71.6°F).

c (cool, short summer) less than 4 months over 10°C (50°F).

d average temperature of the coldest month below -38°C (-36.4°F).

g (Ganges) hottest month before the summer solstice.

i (isothermal) range of temperature between the warmest and coldest month less than 5°C (9°F).

k' temperature of warmest month under 18°C (64.4°F).

m (monsoon) short dry season, but sufficient moisture to give wet ground throughout the year.

n (Nebel, fog) frequent fog.

w' rainfall maximum in autumn.

w'' two distinct rainfall maxima.

The main features of the geographical distribution of the different climatic types as defined by Köppen are given in Fig. 167.

156. The Tropical Rainy Regions. The regions with this type of climate are those without a winter. They lie in the region of the equatorial low-pressure belt, generally within 20° of the equator. Along the eastern boundaries of the continents the moist, unstable, equatorial air is carried poleward around the sub-tropical high-pressure systems over the oceans and the adjacent land areas, and so along these coasts the tropical rainy climates extend farther northward.

The temperature in these regions remains high throughout the year. The maximum temperature is not so high as it is in the sub-tropical high-pressure belts and even farther north, but the average temperature is greater. The region is characterized by uniformity of temperature accompanied by high relative humidity which results in a minimum of radiative cooling at night near the surface.

Precipitation is generally abundant, although on the borders it decreases, approaching the precipitation regime of the dry climates. In these border regions there is a definite dry season followed by abundant moisture during the time of high sun, i.e., the summer season.

The air has real latent instability and the strong insolation assists in the release of this. Hence precipitation is usually in the form of thunder-showers. The sky is clear during the early morning, but cumulus clouds form with the heating of the surface layers by the sun during the morning and these frequently develop into cumulonimbus by mid-afternoon. Gusty winds and heavy thunder accompany the rain showers. These clouds dissipate during the evening. Although this is the usual type of precipitation, weak low-pressure areas sometimes develop and persist, giving periods of dull, gray skies and steady rain.

In some regions a belt of calm exists between the northeast and southeast trade winds. In other regions this belt becomes very narrow or disappears, and the winds observed are the constant trade winds. Nevertheless the winds, although steady, are not strong. The constancy of the trades is shown by the wind rose in Fig. 53*b*, section 58. Along the sea coast the sea breeze is a regular occurrence. Fogs rarely occur in this climatic region.

Figs. 168 and 169 illustrate the variation of the temperature and precipitation in the moist, humid regions. The solid line shows the variation of temperature and the dotted line that of precipitation. (This

practice is followed in other diagrams of this type.) Belem, Brazil, at the mouth of the Amazon in the *Af* regions, has a very uniform temperature regime and no dry season, although the amount of rain is not large in September, October, and November. Darwin (Fig. 169) on the north coast of Australia, with a dry season in the months of May to September, lies in the *Aw* climatic zone.

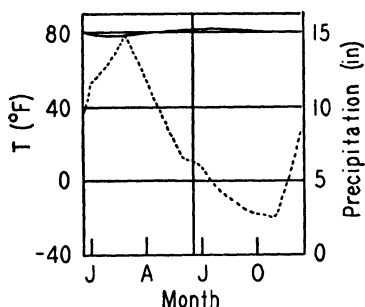


FIG. 168. The annual variation of temperature and precipitation at Belem, Brazil (1° S, 48° W).

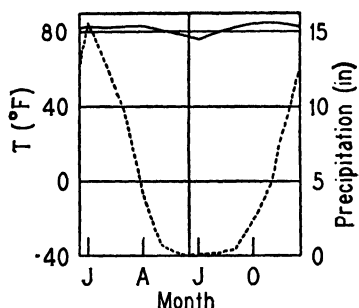


FIG. 169. The annual variation of temperature and precipitation at Darwin, Australia (12° S, 131° E).

157. The Arid Regions. The sub-tropical arid climates, *BSh* and *BWh*, are found in the regions of the sub-tropical high-pressure belts, which extend from about 15 to 30° latitude. In the western hemisphere the land areas at these latitudes are small, and the most extensive regions with this climate are found in Africa, Asia, and Australia.

On the eastern boundaries of the continents the trade winds of the general circulation carry moisture inland, so the arid regions do not extend to these coasts. Along the western boundaries the winds are off shore and directed toward the equator around the cells of the sub-tropical high. For this reason the western shores tend to be dry. Thus in South America the arid regions include the coastal strip on the west from latitude 35° S to 5° S. On the east the arid coastal regions extend only a short distance at 10° N, and a somewhat greater distance in the region of the westerlies, i.e., they are middle latitude deserts, at 40° S to 50° S.

Middle latitude arid regions *BWk* and *BSk* are located along the eastern slopes of the Rocky Mountains, lying in their rain shadow, and in central Asia, far from any source of moisture.

Since these arid regions extend over such a wide range of latitude, no general statement can be made about their average temperature. The clear, dry air with few clouds permits rapid changes in surface temperature through the action of both solar and terrestrial radiation. Both the daily and the annual ranges of temperature are large. Thus in the

desert the temperature during the day may reach 85° F, then fall to 40° F by sunrise the following morning.

In the sub-tropics the air is dry and, in spite of the high surface temperatures, relatively stable. This stability is caused, in the manner outlined in section 16, by the subsidence that occurs in the upper atmosphere. Turbulent eddy motion develops, but the influence of this does not generally extend to the condensation level, and clouds are few. Less cloudiness occurs in these regions than in any other part of the world.

Precipitation is infrequent and variable. That which falls is usually in the form of thundershowers in unstable air that has invaded the area. In the hot desert regions a heavy shower may occur after several dry years. Because of the irregularity of occurrence of these showers they provide little aid to vegetation.

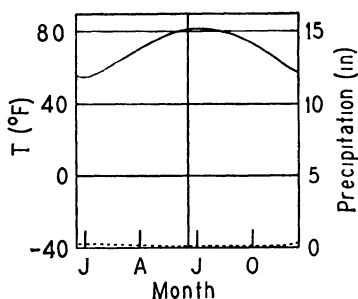


FIG. 170. The annual variation of temperature and precipitation at Cairo, Egypt (30° N, 31° E).

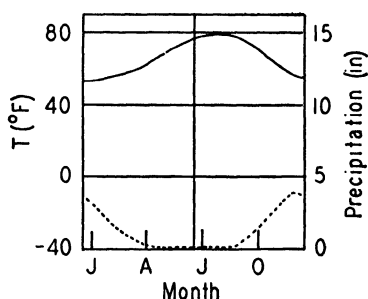


FIG. 171. The annual variation of temperature and precipitation at Tripoli, Libya (32° N, 13° E).

The variation of temperature and precipitation at a typical station in the *BW* climatic zone is shown in Fig. 170. This gives the value of these elements for Cairo, Egypt. As will be observed, the amount of precipitation is small, and it occurs at irregular intervals.

On the edges of the regions of *B* type climate the precipitation is slightly more regular. On the equatorial boundary of the sub-tropical deserts the precipitation occurs during the season when the sun is high, and on the side near middle latitudes it occurs when the sun is low, as the rains of the temperate regions extend to lower latitudes during that season.

Tripoli, Libya (Fig. 171), is an example of a station lying in the *BS* climatic zone on the poleward side of the desert region. The precipitation falls at the time of low sun, when the storms of the westerlies move farther south and nearer the station.

Since strong pressure gradients are not found in this region, the winds

are light. Nevertheless the instability that develops in the lower layers produces at times strong, gusty, surface winds accompanied by dust storms. Land and sea breezes are common along the coasts. Fogs are absent except along the west coastal regions where the stability and moisture content of the air increase over the relatively cool water.

The arid climates of the middle latitudes are a result of topographic features. They are found in Patagonia, in central Asia, and on the plateaus and eastern slopes of the Rockies. The climates of this type in South and North America are a result of the extensive mountain ranges to the westward which cause the westerly winds of these latitudes to lose a large part of their moisture as they ascend the western slopes and become drying winds after they have descended the eastern slopes. The district in Asia is inland and the winds which enter the continent have lost most of their moisture by the time they have reached the interior.

The temperature varies widely with latitude. As in the regions of the sub-tropical highs, the lack of clouds permits marked radiational heating and cooling near the surface. Hence the temperatures are more extreme, and the range is greater than at other places the same distance from the equator.

These areas are not without precipitation. The rains and cloud forms of the winter season are associated with low-pressure areas that move across these regions; but these cyclones are not well developed, and the amounts of precipitation are small. Instability developing in the cold air behind a cold front provides another source of winter precipitation in the form of the "blizzard" storms of the North American plains. Summer precipitation occurs in the form of thundershowers when the diurnal heating in the polar continental air is sufficient to release latent instability and form cumulonimbus clouds.

Turbulence in the mid-afternoon along with the pressure gradient which develops around the Asiatic low-pressure area produce, in the manner described in section 123, gusty, strong summer winds over the deserts in Asia. The winds about the winter anticyclone tend to be more moderate. In North America the winds are strong in the air current flowing down the eastern slopes of the Rockies as well as in the blizzards back of a traveling low-pressure system.

158. The Warm Temperate Rainy Regions. The limits set in the definition of the warm temperate climate restrict it to the temperate zone between the arid regions and the region of a snow cover. Some of the equatorial plateaus of Africa fall under this type by definition, since their coldest month has a mean temperature of less than 18°C , but their climate corresponds with that of the tropical rainy regions.

The normal region for this type of climate is between 30° and 40°

latitude, but topographic features and ocean currents are responsible for a much wider distribution than that. Along the western shores of the continents the moderating influence of the warm ocean currents permits this type to extend northward to Alaska, and to the Arctic Circle in Norway as well as to include most of western Europe. In Asia, parts of northern India and of southeast China are of this climatic type.

One distinct division of the warm temperate climates is the Mediterranean or *Cs* climate. This, by definition, has a dry summer and a moist winter. An example of this type of climate is shown in Fig. 172. In Lisbon, Portugal, there is no absolutely dry month, but the maximum precipitation occurs during the winter. The mean temperature never falls below 40° F. During the summer season the regions having this type are under the influence of the subtropical high-pressure belt and enjoy clear, warm days with cooling at night. During the winter the displacement toward the equator of the westerlies of middle latitudes brings the region under the influence of the traveling cyclones of the middle latitudes which give spells of variable weather and the winter rains. This type of climate is found around the Mediterranean, at the southern coasts of Australia, in central Chile, and along the western coast of the United States.

In summer these areas have a climate similar to that of the subtropical deserts. Clouds are few and rain is infrequent. As winter approaches, the influence of the low-pressure areas of the temperate zones becomes more prominent and the average cloud amount increases. The centers of cyclonic motion do not extend to these areas, however, and so the clouds are neither so thick nor so persistent as in regions where the ascending currents are more pronounced. The rain that falls is more of a showery type even when these regions are under the influence of the cyclones and the clouds tend to break up rapidly.

With the development of the winter cyclones and anticyclones, the winds increase in strength and veer with the passage of fronts. In summer the winds are lighter, but along the coasts sea breezes occur regularly. Fogs along the western shores are frequent and result from the same causes as those which produce fog along the western coasts of the arid regions. •

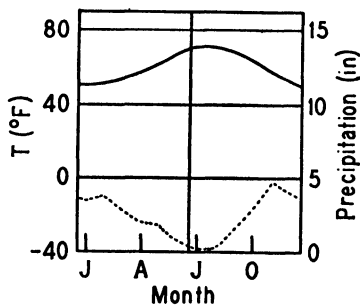


FIG. 172. The annual variation of temperature and precipitation at Lisbon, Portugal (39° N, 9° W).

In the other major division of the warm temperate climates, classified as *Cf*, the precipitation is distributed more uniformly throughout the year. One district is in the eastern United States extending north to the fortieth parallel. Summer rains are caused by the monsoon winds off the Gulf of Mexico. Another region with this type of climate is in western Europe north of the Mediterranean coast lands, including the British Isles, France, Germany, the northern Balkans, and the coast of Norway to the Arctic Circle. The westerly flow of moist air from the warm Gulf Stream accounts for the precipitation and moderate temper-

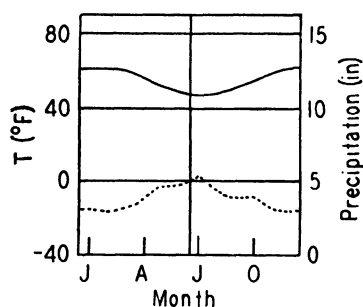


FIG. 173. The annual variation of temperature and precipitation at Wellington, New Zealand (41° S, 175° E).

atures for this region. A third district is found along the China coast, the monsoon off the Pacific providing the summer rains. Inland the winter precipitation is light and the region is classified as *Cw*.

An example from a fourth region is shown in Fig. 173. New Zealand and parts of Southern Australia lie in this climatic zone.

The temperatures of these regions vary according to the latitude, but the ocean control and the high relative humidity modify the temperature so that the diurnal and annual ranges are not so great as in other districts at the same distance from the equator. All regions experience cold periods during the winter when outbreaks of polar continental air from its source regions occur, and of course they are subject to the rapid changes in temperature associated with frontal passages.

Precipitation in winter occurs with frontal low-pressure systems. The warm sector air of these depressions is usually of maritime origin, and so precipitation is abundant. In the summer the air from the oceans becomes unstable in moving over the heated land and releases its moisture in the form of showers and thunderstorms. Winter is the time of cloudiness, the typical clouds being altostratus, nimbostratus, and stratus. In the summer, even though the amount of precipitation may be greater, the cloudiness is less, the clouds being more frequently of the cumulus type. In the winter the maritime air moving over the cold land surface becomes stable, and fogs of the advection type are frequently widespread. In summer the most common type of fog is that caused by radiation, but these fogs dissipate with the solar heating of the morning.

Besides being affected by the frontal depressions of the winter season,

the coastal regions of China and the southeastern United States are close to the path of the tropical hurricanes. Although these storms occur relatively infrequently, the high winds associated with them cause extensive damage along their path. The tornadoes of the United States also occur in the region which belongs to this climatic type.

159. The Cold Snowy Forest Regions. The cool, temperate climates lie to the northward of the warm temperate zone in North America and Eurasia. No continent of the southern hemisphere extends far enough to the south to have regions with a *D* type climate. By definition, there must be one month with an average temperature below freezing, and so snow will lie on the ground for at least a short period. The northern boundary coincides with the northern boundary of forest. In North America it extends from the fortieth parallel to, but does not include, the coastal regions of the Arctic and neighboring waters, except for the coastal region along the Pacific and an arid region in the rain shadow of the Rockies. In Eurasia, it includes Russia in Europe, and Asia north of the fortieth parallel, except for the coastal areas along the Arctic and the arid regions in the center of the continent.

In general the regions with this type of climate are continental in character. They include the east coasts of the continents, but, since the prevailing wind is westerly, these coasts are not under the influence of the adjacent ocean as much as the regions along the west coast. Hence the former have a climate which resembles the continental regime. With the radiational cooling that takes place during the long nights from the snow cover, the winter temperatures are low. It is in these areas that the polar continental air in winter derives its characteristics of low temperature and extreme stability. During the summer the radiation from the sun is large and, lacking the moderating influence of the ocean, the mid-day temperatures are high. Thus the annual range of temperature is large. The temperature changes rapidly as the wind shifts with the passage of the fronts associated with the traveling cyclones. Thus these regions experience successive warm and cold waves.

The annual precipitation over most of these areas is not great, more falling on some of the arid regions than over a large part of the cold temperate regions. But the evaporation is relatively much less, and moisture is sufficient for vegetation. During the winter the average position of the polar front lies to the south, and the precipitation falls from overrunning air. In the summer the front lies along the northern half of the region, and although some of the precipitation is caused by frontal phenomena, more falls in convective showers. The maximum for the year is during the early summer, at which time the growing crops

get the most benefit from the rain. In general the winter with its frontal clouds and low ceilings has the maximum cloudiness. But in the center of Siberia, under the influence of the Eurasian anticyclone, the average cloudiness is less in winter than in summer.

Leningrad, in European U.S.S.R. (Fig. 174), and Olekminsk, Siberia (Fig. 175), illustrate the regime of the cold, snowy climates. At these stations the continental influence is seen in the wide variation of temperature between summer and winter, and the tendency to a summer maximum of precipitation.

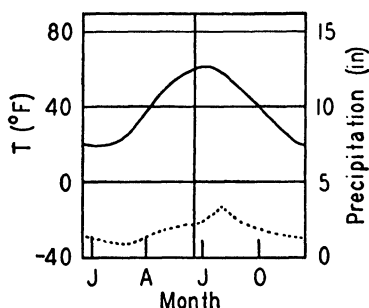


FIG. 174. The annual variation of temperature and precipitation at Leningrad, U.S.S.R. (60° N, 30° E).

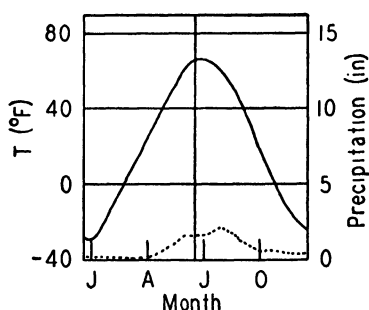


FIG. 175. The annual variation of temperature and precipitation at Olekminsk, U.S.S.R. (60° N, 120° E).

Most of the usual storm tracks of the extra-tropical cyclones cross the cold temperate regions, although they may lie slightly to the south of them during the winter months. These cyclones pass with some regularity, the average period during the winter months being about three days and during the summer about six days. They give rise to fresh to strong winds with their passage, but the winds are not so strong as those occurring about these lows after they move off the east coast over the water areas.

160. The Polar Regions. The polar regions include the ice-covered continents of Greenland and Antarctica, and also the coastal regions of North America and Eurasia, bordering along the Arctic Ocean. Radiational cooling during the long winter night causes extreme cold. Over the ice caps the temperature does not rise much above freezing even in summer, but in the other regions the temperature rises rapidly during the short summer, the maximum being greater than 70° F along the Canadian Arctic coast. An example of the temperature and precipitation variation is given in Fig. 176, showing the average values of these for Godthaab, Greenland.

The moisture content of the air is low, even during the summer, and precipitation is light. Over the ice caps of Greenland and Antarctica the cooling above the cold surface causes a semi-permanent anticyclone to form and little precipitation falls from the air which is usually subsiding. During the winter season the continental high-pressure systems produce a similar condition over the Arctic coastal regions, but during the summer weak low-pressure systems give some light precipitation. Some stratus clouds occur even in winter, but summer is the time of maximum cloudiness.

In general the winds are light, although the katabatic winds off the ice caps are strong and steady. In addition, the Icelandic low is adjacent to regions with this type of climate, and the strong pressure gradients about this system cause high winds and gales along some of the coasts in the vicinity. Inland fogs are rare but along the coastal regions fogs are frequent in summer.

The climates of the world can be classified by types to aid in understanding and remembering them, yet borderlines are indefinite, since there are no discontinuities in climate except those produced by orographic features. There is, in each climatic zone, a gradual change from place to place so that the climate of each blends smoothly with the climate of the next zone at the boundary. This fact must not be forgotten in any study of climates.

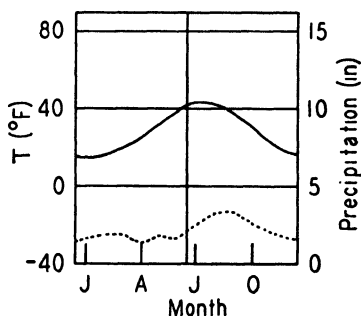


FIG. 176. The annual variation of temperature and precipitation at Godthaab, Greenland (64°N, 52°W).

BIBLIOGRAPHY

- Trewartha, G. T., *An Introduction to Weather and Climate*, New York, McGraw-Hill Book Co., Second Edition, 1943.
- Kendrew, W. B., *The Climates of the Continents*, Oxford, Clarendon Press, 1937.
- Conrad, V., *Fundamentals of Physical Climatology*, Milton, Mass., Harvard University, Blue Hill Meteorological Observatory, 1942.
- Bilham, E. G., *The Climate of the British Isles*, London, Macmillan and Co., 1938.
- Köppen, W., and R. Geiger, *Handbuch der Klimatologie*, Berlin, Verlag von Gebrüder Borntraeger, 1936.
- Brooks, C. E. P., *Climate*, Second Edition, London, Benn, 1932.
- Landsberg, H., *Physical Climatology*, State College, Pennsylvania State College, 1941.
- Climate and Man*, 1941 Yearbook of Agriculture, Washington, U.S. Department of Agriculture, 1941.

CHAPTER 24

MAP ANALYSIS AND FORECASTING PROCEDURE

161. Material Available for the Forecaster. The previous chapters have described the elements that make up the weather and discussed the causes for their variations. This chapter will attempt to show how the forecaster applies these facts when working with the synoptic weather chart. Yet no study of books will take the place, in the development of a forecaster, of training and experience with actual weather maps.

A large amount of data obtained from observing the weather elements is available to the forecaster as he prepares his forecasts. This material is collected at central points by telegraph, telephone, and radio, and it is then distributed by teletype to the different forecast centers where it can be used by the meteorologist. He then selects for analysis only that part of the data which is pertinent to the particular forecast which he must make.

The most significant material is contained in the synoptic weather reports, which give a fairly complete description of the current weather with some information about the past weather. The information is put into code form to save time in transmission. The code changes from time to time and a description of the current code is always available at the weather offices, so it will not be described here. The report usually contains the following data:

- (a) Sea level pressure.
- (b) Temperature.
- (c) Dew point or relative humidity.
- (d) Barometric tendency, i.e., the amount of rise or fall of pressure during the three-hour period preceding the time of observation, along with the type of change.
- (e) The total cloud amount.
- (f) Types of cloud present in the sky.
- (g) The height of the cloud base.
- (h) Visibility.
- (i) Present, and sometimes past, weather.
- (j) Wind direction and speed.

Other supplementary information, such as the amount of precipitation, the temperature of the sea, etc., is sometimes included. These synoptic

observations are taken four times a day at stated times, which are approximately uniform over the globe, at fixed stations on land, and on a large number of ships. They are sent to the forecast offices where they are plotted on a map, which is called the synoptic weather chart, ready to be analyzed by the meteorologist.

At airports the current weather is very important, and so more frequent observations are taken and relayed to neighboring airports and forecast centers where the information is of value. These "airways sequences," as they are called in North America, include a large part of the same type of information that is given in the synoptic weather report. These observations are usually taken every hour with special observations taken when the weather is changing rapidly.

At a number of stations a small balloon is released at regular intervals, and its path followed by a theodolite. Using the data in the manner described in section 66, the wind speed and direction are computed for different levels of the atmosphere, and this information passed by teletype to the forecast centers. Here the values are plotted on maps, a different one for each level, or sometimes by means of colored inks on the synoptic weather chart.

In a fourth set of data available for the forecaster are the values of the temperature and moisture content at the different levels in an air column above a small number of widely distributed stations. As indicated in section 66, a light-weight set of instruments called a radiosonde, containing a radio sending set, a bimetallic thermometer, an aneroid barometer, and an hygrometer, is released and carried aloft by means of a balloon. The transmitter sends back to the receiving set at the station the values for the pressure, temperature, and relative humidity. A report of these is sent to various forecast centers interested in the data. Here the information is plotted on adiabatic charts, such as the tephigram included at the back of this book, or evaluated by other means.

162. The Plotting of Data on the Surface Chart. In order to be able to include on a map all the data of the synoptic weather reports a system of shorthand has been devised. Some data are entered by figures. These include the sea level pressure, in millibars with the hundreds' digits missing, barometric tendency amount in tenths of millibars, temperature, dew point, amount of precipitation, cloud height, and visibility. These last two are reported and entered according to a standard scale which is accepted for general use by international agreement. The wind direction is given by a shaft drawn from the station circle, the wind blowing along the shaft toward the circle, and the force is given by the number of feathers drawn from the end of the shaft, each feather representing two units and a half feather representing one unit

on the Beaufort scale given in section 66. The remaining data are given by means of symbols.

Because of the lack of space on the reduced maps given in the text, the symbols for the different cloud types are not included on these maps. For that reason and since they are available with complete definitions at any forecast office, they will not be described. The total cloud amount is indicated by the amount of shading inside the station circle, with four vertical lines indicating an overcast sky. A sky obscured is denoted by three horizontal lines. The pressure tendency characteristic is given by means of one of a set of symbols, each of which resembles the shape of a particular barograph curve. Thus the symbol \searrow means that the pressure has been falling and is beginning to rise. There are 96 different symbols for the different types of weather which are defined by the international code, except the weather types defined as clear, partly cloudy, cloudy, and overcast. These are built up from a number of basic symbols. The most frequently used symbols with their meanings are:

Rain	•	Smoke	◊
Snow	*	Shower	▽
Drizzle	,	Thunder	⚡
Fog	≡		

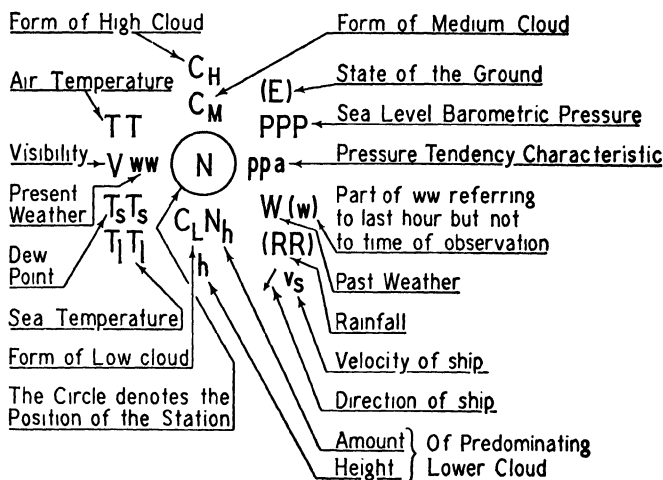
Various combinations of these and other symbols are used to differentiate the types of weather.

Each of these weather elements has a definite position about the station circle, as specified by the international plotting model. These positions are shown in (a) of Fig. 177. Diagram (b) shows a completely plotted station. The information given in diagram (b) is as follows: sky overcast with breaks in the overcast of stratocumulus cloud at 2000 to 3000 ft and cirrus cloud visible through the breaks; wind ENE 7-12 mph; pressure 1019.0 mb, which has risen 1 mb and then steadied during the past three hours; temperature -6° F; dew point -12° F; visibility between $12\frac{1}{2}$ and 31 mi; weather, light continuous snow which began 1-2 h ago, the total precipitation being 0.05 in. in rain equivalent during the past six hours.

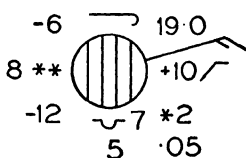
163. Construction of Isobars. When the meteorologist has a fully plotted map for analysis, he begins drawing the isobars, i.e., the lines of equal pressure, and the fronts. Since these two sets of lines are interdependent, the choice of drawing fronts or isobars first is a matter of personal preference with the forecaster.

The isobars are drawn for certain given pressures at regular intervals. The intervals and the pressures are determined by convention within

each forecasting service, the interval usually being 2, 3, or 4 mb depending upon the scale of the base map. In the diagrams given here the isobars are drawn for every 4 mb, starting from 1000 mb. If the reported pressures were accurate, the drawing of the isobars would be merely a



(a)



(b)

FIG. 177. The international station plotting model.

matter of drawing a smooth curve through points obtained by interpolation between the given pressures. Errors arise, though, at the observing station because of errors in observation or calculation, because the observations are not made at the specified time, or because the method of reducing the pressure to sea level may not give accurate results. Sometimes the pressures recorded on the map are wrong because of errors in transmission of the data from the observer to the plotted map. Errors in observation, calculation, and transmission must be expected occasionally. If the pressure for six hours ago is known, this error can be detected at times by computing from the tendencies on the

two maps an approximate value for the present pressure. Sometimes with ships at sea the error is not in the transmitted pressure but the transmitted position of the ship. The pressure and wind will sometimes check with those to be anticipated at a position 5 or 10° of latitude or longitude from the position as given. In that case the ship should be considered as reporting from this alternative position. Yet ship pressures are not so accurate as those for land stations since the motion of the ship does not permit the level of the mercury to assume a steady position, and so they cannot be relied upon as fully.

The correction to sea level is based on the assumption that a column of air of a specified temperature distribution exists from the level of the station to mean sea level. The temperature distribution is calculated from the present temperature and the temperature twelve hours ago. When the station is not over 1000 ft above sea level, the errors in this correction are small. For higher altitudes the correction to be added is large, being about 100 mb for 3000 ft, so that if the temperatures used happen to be non-representative of those for the air mass as a whole, the correction to sea level pressure will be inaccurate. Sometimes an error arising from this cause may be detected by noting if the temperature of the reporting station is lower or higher than representative temperatures for the district. When a front lies along a mountain ridge the correction to sea level will often produce a fictitious pressure gradient along the front, since in the cold air the corrections to sea level will be larger than those in the warm air. This pressure gradient does not exist at the surface of the earth and cannot be used in computing the gradient wind and the motion of fronts.

Because of the errors in the plotted pressures, the isobars based on them will be irregular. It is reasonable, however, to assume that in the free air the isobars are simple curves except at fronts, so that, except when the pressure gradient is weak, irregularities in an isobar should be eliminated, unless the adjacent isobars show a similar irregularity. In weak pressure systems, an intermediate isobar will sometimes show whether an irregularity is real or fictitious. The isobars should be drawn so that the gradient is approximately uniform or so that there is a regular decrease in distance between adjacent isobars as one goes from a high-pressure region to a low-pressure region. Along a front the isobars should be drawn with care, and to bring out the trough that exists at a front, as shown in section 39. If possible they should be drawn to show whether the isobars have a cyclonic or anticyclonic curvature at the front, especially in the vicinity of a frontal depression, since this in part determines the rate of occlusion (see section 112).

The wind direction and speed are very helpful in drawing the isobars,

particularly in the analysis of ocean weather maps, if the wind force is strong enough to be representative of the pressure gradient. Over the ocean the winds should blow across the isobars toward low pressure at an angle of about 20° , and the distance between isobars should correspond to a geostrophic wind one-quarter or one-third higher than the reported wind. Over land the angle at which the wind blows across the isobars should be about 30 or 40° , and the gradient should correspond to a geostrophic wind half as strong again as the surface wind.

If a complete map of the pressure distribution over the whole world were drawn, each isobar would be a closed curve. Since the maps drawn are for only a portion of the globe, parts of some of these closed curves extend beyond the map. Remembering this, and also the features of the general distribution of pressure over the world, as shown in Figs. 5 and 6 of section 3, it is possible to extend the isobars some distance beyond the recorded pressures with some justification. It is sometimes helpful to remember that when going along an isobar, high pressures remain always on one side and low on the other.

164. The Identification of Air Masses and the Location of Fronts.

The identification of air masses from an individual surface map is very difficult and is almost impossible unless something about the usual sequence of weather expected over the district is known. In this latter case an estimate of the probable sequence of developments that preceded the current map may be made, and from that a reasonable estimate of the types of air masses to be expected in the different sections obtained. Upper air data are more conservative and more representative and are thus very helpful. By plotting the data on a Rossby diagram or a tephigram, and comparing the curve with the typical curves for the different types of air masses as given, for example, in Chapter 15, the types of air masses present may be ascertained with reasonable accuracy. Even when the previous history of atmospheric developments is available, it is desirable to check by means of the upper air ascents. The best method is to combine the study of the upper air ascents with a review of the paths the air has taken during the past 48 to 96 h. Knowing the trajectory, the source region and the amount of modification that has taken place are readily determined.

Similarly the location of any given front is best determined from the history of the motion of the front and a comparison of the upper air ascents to locate the regions where a rapid change of temperature or moisture in the horizontal is present. After the analysis of a map is complete, the forecast position of the fronts at the time of the next map is usually indicated. When drawing up the latter, this extrapolated position from the previous map is useful as a starting point for locating

the actual position of the front. A study of the previous analysis tells the forecaster the extent of the contrast across the front and which weather elements reveal the position of the front most clearly. A search for the same contrasts will aid in the exact location of the new position of the front.

Although a front is a line across which the temperature changes rapidly, or more rapidly than in other regions, the surface temperatures do not always bear out this generalization. Temperature is not a conservative property, and at times the position cannot be located by means of temperature. The second table in section 112 gives some changes that should take place with a frontal passage, but only rarely are all these well marked. Because of the varying weight that may be given to different weather elements, two forecasters analyzing the same map may not agree on the precise position of a front, but usually the difference between the two positions will not be large. One of the most reliable indicators is the wind shift that occurs with a frontal passage. Another indicator which is reliable with many fronts is the comparative stability of the two air masses as indicated by cloud types, strength of winds, and types of precipitation. The line of zero pressure change cannot be considered the front, but a comparison of the amounts of pressure change often gives a good indication of the frontal position, provided the analyst remembers that stations which the front passed during the past 3 h will not show a representative tendency for that side of the front. During the summer the dew point is quite reliable since it is conservative for radiational heating. With temperatures below freezing the evaluation of the dew point is less accurate and so it cannot be used with the same degree of assurance. In regions where the observing stations are few and upper air data not available, frontal passages may sometimes be determined by means of the temperature changes during the past 24 h. If the comparison is attempted for a shorter period, the diurnal temperature variation must be allowed for. This is large in the northland where such a method is usually needed; it is difficult to estimate accurately, and for this reason the use of the 24-h period is preferred. All these changes must be considered, with attempts to explain them by causes other than the passage of the front, before the position of the front is finally decided.

Considerable assistance in locating fronts and determining their speeds may be obtained from the special airways reports. These give the values of the weather elements at more frequent intervals than are given by the synoptic weather reports. Since the position of the front is known from the last synoptic chart, the weather changes at those stations in the vicinity of the front can be noted from hour to hour. The

time of the frontal passage can often be determined quite accurately, and, knowing the time of the passage at two stations and the distance between them, the speed of the front can be computed. By studying the reports at the various stations, those changes which occur before, at, and after the passage of the front can be distinguished.

Besides finding the location of those fronts which were present on the past map, it is also necessary to investigate the possibility of frontogenesis in other regions of the map. As shown in section 109, the areas where cols and troughs are present are those in which frontogenesis is most probable, although fronts may form in other regions. The characteristics of the developing front will be the same as those discussed previously except that the indications are less well defined. If the front that appears to be developing will not affect the forecast for the region under consideration, the meteorologist at times will leave it for further observation before indicating its position on the weather chart.

165. The Use of Upper Air Data. The wind speeds and directions as obtained by means of pilot balloons have several different uses. At 2000 ft above the surface of the earth, the winds are not affected greatly by surface friction. These give approximately the gradient wind, or the resultant of the gradient and the isallobaric winds. If there is no isallobaric component these winds will be parallel to the isobars and will indicate the pressure gradient at the station. Thus, except in regions where the tendencies vary and therefore marked isallobaric components are present, the velocity at this level is helpful in drawing the isobars. In the neighborhood of a front a shift in the wind at 2000 ft above the surface is more significant than a shift in the surface wind, since the former wind is more representative of general conditions in the air mass than the latter. Furthermore, the motion of a warm front may be determined approximately by noting the component of wind speed at 2000 ft normal to the front in the cold air ahead of it; similarly the speed of the cold front is given by the component of motion normal to it in the cold air behind the front. Vertical motions are frequently too large in the warm sector to permit the use of pilot balloon data for this purpose in that portion of a depression. A further use of the wind reports can be found in certain instances. Usually near a warm front the cloudiness is too great to get satisfactory pilot balloon reports. Yet sometimes the balloon can be followed as it ascends through the frontal surface, and the height of the latter is then found by means of the wind shift. Having this information and also the position of the front at the ground, the slope of the front may be obtained with reasonable accuracy.

The pilot balloon reports assist the forecaster in telling the pilot of an aircraft the wind to be expected at every level. With the wind re-

ports available, the forecaster still has the task of forecasting the changes. With the wind reports missing, he must estimate the direction and spacing of the mean isotherms for the air above the surface and from these and the surface geostrophic wind compute, in the manner indicated in section 121, the value of the geostrophic wind at each level, and, using these values, forecast the changes expected.

Further information about conditions in the upper air comes to the forecaster through the radiosonde reports. As described above in section 164, the plotted reports assist the forecaster to determine the air mass type present in the different regions of the weather map. Also the plotted data are easily analyzed to give information about the stability of the air, as shown in Chapter 14. With this information available, the forecaster is able to estimate the possibility of the development of cumulus cloud, and its amount and height. When used in conjunction with the weather map the likelihood of the development of instability in the air as it passes over a warm surface can be assessed. For example, the meteorologist can decide if instability stratocumulus is likely to develop in a fresh outbreak of polar continental air.

In the neighborhood of a front, a comparison between representative values of temperature and moisture content in the two air masses may be made by observing the differences at the various levels between ascents made on both sides of the front, or between ascents made at the same station before and after the frontal passage. In this manner the analysis of the map from the surface data may be assisted and verified. This comparison may be made, using the data as plotted on a tephigram or on any of the other adiabatic charts. Another method, which permits the comparison of several ascents at once, is through the use of a cross section of the atmosphere. A cross section is taken in a vertical plane which intersects the earth's surface in a line near which radiosonde ascents are made. The values of the weather elements as determined by these ascents are plotted on the cross section. An example is given in Fig. 183, section 169. The vertical scale is greatly expanded in comparison with the horizontal scale. For each aerological station the temperature, the potential temperature, the relative humidity, and the mixing ratio are plotted for various chosen levels in the ascent. By comparing the values of these elements from station to station it is possible to decide whether or not frontal surfaces lie between the several stations. The actual intersections of the ascents with the frontal surfaces are usually manifested by a change in the lapse rate, frequently to an inversion or an isothermal layer, accompanied by an increase in the mixing ratio. The fronts are drawn on the cross sections by broad lines, blue for a cold and red for a warm front, to indicate the mixing zone.

The lines of equal potential temperature, or sometimes temperature, and of equal mixing ratio are drawn by colored lines. The heights of these lines will change at the frontal zones since these zones are regions of discontinuity for temperature and mixing ratio. By using the heights of the intersection of the frontal surface over two stations which are on a line perpendicular to the front, or the intersection at one aerological station and at the ground, the slope of the front may be determined.

When evaluating radiosonde data, inversions other than at fronts will be found frequently. During the night a ground inversion is to be expected. Subsidence in a stable cold air mass often causes an inversion, in the manner indicated in section 16, and another is sometimes found at the top of a cloud layer, the inversion arising from the turbulence in the cloud and the radiation from the cloud top. These last two types will be dry inversions, i.e., inversions in which the moisture content decreases with height. In studying radiosonde ascents it will be observed that the relative humidity sometimes does not go above 85 or 90 per cent in regions where cloud should be expected or is reported. This is partly explained through the failure of the instrument to register correctly because of a lag in the hygrometer. It is also possible that condensation has occurred at relative humidities less than 100 per cent owing to the lowering of the saturation vapor pressure over salt crystals and other hygroscopic nuclei (see sections 126 and 127).

Upper air pressure charts may also be used in analyzing radiosonde data. With a close network of aerological stations, isobars may be drawn at specified levels, such as 5000, 10,000, and 20,000 ft. If temperature and moisture observations are included, the motions of fronts and pressure systems at the several levels may be followed. A slight modification of this procedure has been extensively used in Germany, where contour lines of certain fixed isobaric surfaces have been drawn. The results obtained by the two methods will, of course, be essentially the same.

166. Isentropic Analysis. Another system of upper air analysis has been developed in the United States. The entropy of dry air is constant during adiabatic motions, since heat is neither added to nor taken from the air. Thus, in the absence of non-adiabatic processes, dry air always moves with constant entropy, i.e., along an isentropic surface. The study of such isentropic motion is the subject matter of isentropic analysis.

Isentropic surfaces are also surfaces of constant potential temperature, as shown by (18-7), and in practice the surfaces are labeled by their potential temperatures rather than their entropy. The isentropic surfaces chosen for study must be far enough above the ground to be

reasonably free from the operation of non-adiabatic processes such as turbulent mixing and radiational heating and cooling, yet not so high that they are at heights where the moisture content of the air is very small and humidity measurements inaccurate. The potential temperatures of the three standard isentropic surfaces used in the United States during the various months of the year are given in the following table.

ISENTROPIC SURFACES IN USE THROUGHOUT THE YEAR

Months	Potential Temperature (°A)		
	First Surface	Second Surface	Third Surface
January–February	290	296	302
March–April	296	302	308
May–June	302	308	314
July–August	308	314	320
September–October	302	308	314
November–December	296	302	308

Either of two groups of data may be plotted on the isentropic surface, depending on the personal preference of the analyst. Pressure, mixing ratio, and saturation mixing ratio may be included, or alternatively, pressure and condensation pressure, i.e., the pressure at which saturation is attained if the air ascends adiabatically, may be used. In either case isobars at 50-mb intervals are drawn for the isentropic surface. The moisture content of the air may be represented by lines of constant mixing ratio, or alternatively by isobars of condensation pressure, again at 50-mb intervals.

If the isentropic surface moves much less rapidly than the air itself, it is possible to determine whether vertical motion is occurring, as long as condensation has not commenced. Thus, if the wind blows normal to the isobars in the isentropic surface and toward low pressures, the air is ascending; if it blows toward high pressure, the air is descending. However, since the isentropic surface may be almost stationary, or may move with the speed of the wind, or at any intermediate speed, this criterion is not a satisfactory one. A more useful means of determining vertical motions is through an examination of the spacing between mixing ratio and corresponding saturation mixing ratio lines, or isobars and corresponding condensation isobars for successive charts. The method is illustrated in Fig. 178. The isobars are shown by full lines and the condensation isobars by broken lines. The distribution of isobars and condensation isobars on the preceding isentropic chart is shown in diagram (a). If the spacing of the two sets of lines has changed in the interval between charts in such a manner that at the time of the contemporary chart the distribution is as shown in diagram (b), i.e., isobars

and corresponding condensation isobars closer together, then ascending motion has occurred between the two maps. If the ascent continues, cloud and perhaps precipitation will develop. If the change is as shown in diagram (c), subsidence of the air is occurring, and cloud at adjacent levels where the air is saturated will tend to dissipate.

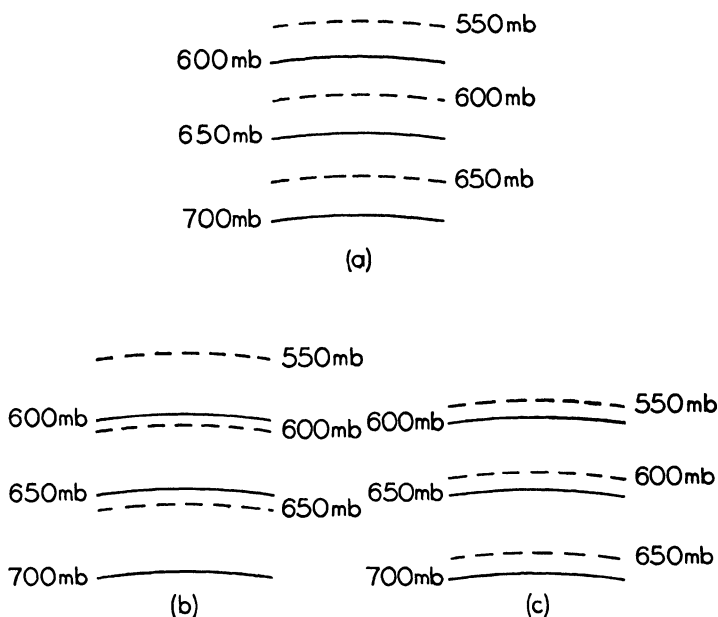


FIG. 178. Isobars and condensation pressure isobars in an isentropic surface.

Considerable evidence has been produced by Rossby and others that there is large-scale mixing, known as lateral mixing, along isentropic surfaces. The lateral transport of an entity, such as water vapor, by this means appears to be at times much greater than that resulting from small-scale eddy motion of the type discussed in Chapter 9. Large tongues of moist air, others of dry air, may often be noted on the isentropic chart. The diffusion of moisture from such moist tongues into the surrounding drier air is frequently rapid.

In general, the isentropic surfaces near a frontal surface lie parallel to the latter and close together, as indicated by cross sections. If, however, the isentropic surfaces intersect the frontal surface, the lateral mixing between the two air masses may be sufficient to cause the frontal surface to dissipate. Frontolysis in the free atmosphere may sometimes be forecast on this basis.

Isentropic charts usually show the presence of a moist tongue of air

advancing from the southwest in the warm sector of a frontal depression. On some occasions this moist tongue splits into two portions, one with a motion having cyclonic curvature, the other with anticyclonic curvature. When this happens a secondary center of low pressure often develops at the tip of the warm sector.

Three non-adiabatic processes tend to destroy the conservatism of isentropic surfaces. The first of these is cooling of the free atmosphere by long-wave radiation, which produces a decrease in temperature, and so of the potential temperature, of the order of 1° to 2° C per day. Convection, including vertical mixing, also produces changes in potential temperature. The third and most serious cause of variation is the process of evaporation or condensation. The cooling resulting from the evaporation of precipitation falling from overrunning air may be great, as when the relative humidity in the air through which the precipitation falls is initially low. As soon as condensation has started in the ascending warm sector air of a depression, the isentropic surface no longer coincides with the same layer of air particles and the method breaks down.

Several deficiencies have prevented the widest possible utilization of this method of upper air analysis. In the first place, little is known of just how and why isentropic surfaces move under various specified conditions. If the motions of the isentropic surfaces themselves could be forecast with reasonable accuracy, the value of the method would be greatly enhanced. Secondly, an adequate statement has not as yet appeared of the exact manner in which isentropic analysis can be used in conjunction with the surface analysis to augment the information provided by the latter. In order to realize the full potentialities of the method, it appears to be necessary to work with isentropic charts for a considerable period of time. Many meteorologists do not have the time available for this and so have been unable to utilize the method. This is in contrast with the method of frontal analysis, the advantages and limitations of which can be comprehended in a comparatively short period of time.

167. Forecasting Positions of Pressure Fields and Fronts. After the synoptic weather chart has been analyzed, with the fronts and isobars entered on the chart, it is ready to be used for forecasting. First to be forecast are the movements of the centers of high and low pressure and of the fronts, since the motions of these govern to a large extent the changes in the weather throughout the forecast region.

One of the easiest methods for forecasting the behavior of fronts and pressure centers is to extrapolate their positions in the direction and at the speed with which they have been moving during the period since the last map. In order to do this readily, the previous positions of the signi-

ficant points and lines are often entered upon the current weather map by colored dots or lines. Very little justification can be given for this method of forecasting, except that the processes which were active in the immediate past may continue to operate in the same manner in the future. This is often true, and the method can give reasonable first approximations for the movement of fronts and pressure systems. Care must be taken, though, to see that no significant changes have taken place or are taking place to make the forecast erroneous. Thus rapid deepening of a low may be occurring, indicating that occlusion of the fronts is imminent; or an active low-pressure area may be advancing toward one quadrant of a large anticyclone; or a long trough may have developed along the front; or some other development may have occurred, any one of which indicates that the system will not continue to move with the previous velocity.

The kinematical method of forecasting the motion of fronts, centers, etc., as given by Petterssen, was described in a general manner in sections 42 and 43. This treatment is mathematical in derivation and use, the movement being obtained by substituting into a formula values of certain functions of the pressure, such as the pressure gradient and tendency, at different points on the map. The formulas are in terms of partial derivatives. To use them, it is necessary to replace the derivatives by finite differences. An example of this computation will be given, using the formula for the velocity of a wedge. The formula for the velocity c normal to the wedge line is, according to (43.6),

$$c = - \frac{\frac{\partial^2 p}{\partial x \partial t}}{\frac{\partial^2 p}{\partial x^2}}$$

In this formula, x is taken in the direction perpendicular to the wedge line.

Fig. 179 shows a wedge, with AB denoting the line of the wedge and CD perpendicular to the line AB . By using finite differences in the above formula,

$$\begin{aligned} c &= - \frac{\frac{1}{\Delta x} \left(\frac{\Delta p}{\Delta t} \right)}{\frac{1}{\Delta x} \left(\frac{\Delta p}{\Delta x} \right)} \\ &= - \frac{\frac{\Delta T}{\Delta x}}{\frac{1}{\Delta x} \left(\frac{\Delta p}{\Delta x} \right)} \end{aligned}$$

where T represents the value of the tendency. Now $\Delta T/\Delta x$ may be evaluated from the map for any length Δx by taking values of the tendency at points Δx apart. Since these points should be centered on the line AB of which the velocity is to be determined, they should each be a distance $\frac{1}{2}\Delta x$ on either side of AB . The value of $(1/\Delta x)(\Delta p/\Delta x)$

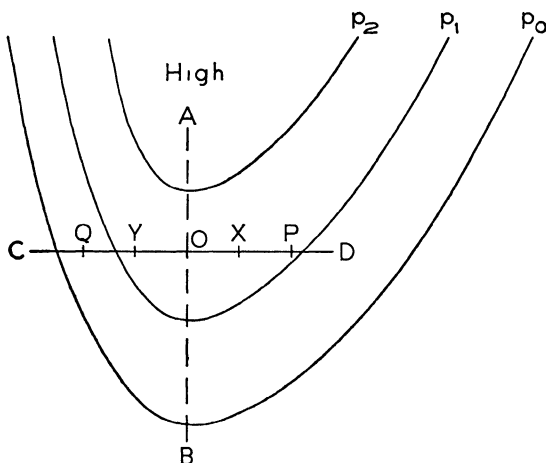


FIG. 179. The velocity of a wedge by the kinematical rules.

may be obtained by finding the values of $\Delta p/\Delta x$ for two lengths which extend for a distance of Δx in both the positive and negative x directions from the line AB , subtracting the values obtained, and dividing by Δx . In the diagram, let $\Delta x = OP$, and let $OQ = OP$ be measured on the other side of O on the line CD . Let X and Y be the midpoints of OP and OQ respectively. Then

$$\begin{aligned}\frac{\Delta T}{\Delta x} &= \frac{T_X - T_Y}{\Delta x} \\ \frac{1}{\Delta x} \left(\frac{\Delta p}{\Delta x} \right) &= \frac{1}{\Delta x} \left(\frac{p_P - p_O}{\Delta x} - \frac{p_O - p_Q}{\Delta x} \right) \\ &= \frac{(p_P - p_O) - (p_O - p_Q)}{(\Delta x)^2}\end{aligned}$$

Hence, if $\Delta x = OP = L$

$$c = - \frac{L(T_X - T_Y)}{(p_P - p_O) - (p_O - p_Q)}$$

This can be put in the more general form

$$c = - \frac{L(T_{+L} - T_{-L})}{(p_L - p_0) - (p_0 - p_{-L})} \quad (167.1)$$

Since the tendencies are given on the map for 3-h intervals, this formula gives the velocity of the wedge in miles per 3 h if L is expressed in miles. The displacement of the wedge line in miles during a 6-h period, for example, is obtained by doubling the answer obtained from (167.1).

Care must be exercised in selecting a suitable value for the length L . It is advantageous to draw tendency and pressure profiles along the x axis to aid in this selection. The maximum accuracy is attained if L is chosen so that at distances of $\frac{1}{2}L$ and $-\frac{1}{2}L$ from the wedge line, the tendency profile is nearly a straight line having a maximum slope. The slope of the pressure profiles should be regular and representative at distances of L and $-L$ from the wedge line.

In a similar manner the velocities of troughs, highs, and frontless lows may be determined as indicated in section 13.

Referring to section 42, it is seen that an absence of deepening or filling of the pressure system was assumed in deriving the formula for the velocity of an isobar. Similarly, the velocity formula when applied to a wedge is strictly accurate only when the x component of the pressure gradient in the moving system is invariant with time. The formula should be applied only to those wedges in which this condition is fulfilled.

A similar method is applicable to the motion of a front. Thus, using (43.8),

$$c = - \frac{L(T_a - T_r)}{(p_L - p_0) - (p_0 - p_{-L})} \quad (167.2)$$

where the distances L and $-L$ are now measured from the front, and T_a and T_r are tendencies just in advance and to the rear of the front. These latter are best obtained by drawing the isallobars and noting the tendencies in the two air masses just at the front. The formula should be applied only when deepening or filling of the pressure system is absent or is uniform on both sides of the front.

By using the formulas one assumes that the tendency profile of the moving pressure system will continue into the future. Thus again the method is to extrapolate the effects of the forces already present into the future, but the data used here are nearer the current situation, being pressure changes during the last 3 h, and so are more reliable for forecasting purposes. These formulas, then, will give a forecast which is more accurate than one obtained by the former method in a situation in which changes in the pressure field have taken place recently but are now no longer occurring. The forecasts of the motion from these formulas are most accurate for periods of 6 or 12 h in the future. Owing to the frequent development of accelerations, both positive and negative, only rarely will they predict displacements accurately for a full day in

advance. Acceleration formulas have been developed in section 43 for the significant points and lines of the pressure field, but the evaluation of these is very complicated and the results seldom justify the time spent.

A third procedure uses the pressure field of the current map and is simply applied. It is based on the fact that a frontal surface is the edge of an air mass, and so must keep ahead of the air that is moving behind it. Since there can be no overrunning of the cold air, a cold front must move with the speed of the winds behind it. Friction retards the surface wind, but a representative value is given by the wind at 2000 ft above the surface. After the component of wind at this height normal to the front has been expressed in miles per hour, the motion of the front in miles during a 6-h period, for example, is obtained by multiplying the above velocity component by the time interval, 6 h.

Another value of the speed of the front is found from the component of the geostrophic wind velocity normal to the front in the cold air, adjusted for the curvature of the isobars. The cold front can be assumed to move at a speed of 90 to 100 per cent of this adjusted value. Along the warm front the warm air may override the colder air underneath. Hence the warm front does not move with the speed of the warm air winds, but with the speed at which the cold air under the front advances in a direction normal to the front. This speed can be obtained approximately by noting the component of the velocity normal to the front of either the 2000 ft or the gradient wind in the cold air. The computation of the speed of an occlusion would depend on whether it was of the cold or warm front type. The method of computation for the velocity of a cold front would apply for a cold front type occlusion, and that of a warm front for a warm front type occlusion. Frequently, though, an occlusion lying along an extended trough moves very slowly and dissipates while a new pressure center forms at the junction of the cold and warm fronts.

The method as described in the last paragraph assumes that there is little or no change occurring in the pressure field. If there is a large isallobaric gradient, then the velocity will have to be obtained from the gradient wind compounded with the isallobaric wind in the manner explained in section 121. The observed 2000-ft wind already gives the adjusted value.

This last method is a valid one for obtaining the instantaneous velocity. It uses the current pressure gradient, adjusting it for the isallobaric system. It utilizes the present motion to determine the future displacement and does not allow for any changes in the pressure field. This method cannot be used for pressure centers, troughs, and wedges.

There is frequently very little difference among the values obtained by the three methods of forecasting displacement, and an average of the distances obtained from two of them gives a fairly reliable forecast. When there is a marked difference, then the value obtained by either of the last two methods is more reliable than that obtained by the first method, since they both take into account recent changes that have taken place in the pressure distribution and the effects of the isallobaric field.

Besides the methods outlined above for forecasting displacement, there are rules, some empirical and others that can be explained by reference to the tendencies, which tell the forecaster the direction in which pressure centers are likely to move. A frontal depression will move slightly to the left of the direction of the isobars in the warm sector until it begins to occlude. After occlusion, it tends to become stationary and to fill. A center of low pressure tends to move in the direction of the most rapidly falling tendencies, and a center of high pressure in the direction of the most rapidly rising tendencies. Near the periphery of a large semi-permanent warm anticyclone a low-pressure center tends to move in the circulation around the anticyclone.

Forecasting involves not only the prediction of the motion of the pressure centers and fronts but also of the increase or decrease in their intensity. With fronts it is necessary to decide whether frontogenesis or frontolysis is occurring. This can be determined by a study of the existing wind field, as shown in section 109.

For pressure systems, the variation in intensity is most readily determined by noting the changes occurring in the pressure at the center of the system. The deepening or filling that is occurring at the time of the map is indicated by the tendencies at the centers of the highs and lows. If it is assumed that these tendencies will continue, a high will become stronger if the tendency at the center is positive and will become weaker if the tendency at the center is negative. In a similar manner the filling or deepening of a cyclone can be determined. In a frontal depression the deepening or filling is determined by the tendencies in the warm sector. Allowance should be made when using these rules for the small pressure rise at certain periods of the day and the small fall at other periods according to the diurnal pressure wave mentioned in section 3.

Other empirical rules are useful in determining the probability of deepening or filling. Thus an occluding center deepens, and when the occlusion process is complete, the center begins to fill. When a secondary low forms, the primary low begins to fill. When in winter a low-pressure system moves off the land and over the ocean, the low will tend to deepen and become more active.

As shown in section 50, horizontal convergence in the wind field is

associated with increasing cyclonic circulation around a low and decreasing anticyclonic circulation around a high; with divergence the converse holds. Other things being equal, the cyclonic motion increases as a low moves southward and decreases as it moves northward; the converse is true for a high.

Many of the foregoing methods of forecasting assume that the atmospheric processes in operation at the time of the map are going to continue in the future. These conditions usually do persist for a period, but they gradually change. To extrapolate beyond the period during which the conditions as outlined on the map will persist cannot be justified. Over land reliable forecasts of frontal positions are limited to 12 to 24 h; over the sea the period may be extended to 24 to 48 h. With experience a meteorologist learns to anticipate developments in the weather with certain pressure configurations and learns to extend his forecast beyond the periods mentioned. Thus, as a front moves off the east coast of North America in winter, at times a center of low pressure develops on it and then moves northeastward along the coastal regions. This results from the inflow of warm air from over the Gulf Stream into the system, providing a fresh supply of energy for the circulation. But there may be no evidence of this development in the configurations of the isobars and the isallobars from which many of the above rules and methods were derived. With experience the forecaster is thus able to suggest the probable weather for three days, but the forecast for the third day is not too reliable. Methods of forecasting for a period longer than three days will be discussed in section 170.

168. Forecasting Condensation Phenomena. The different types of clouds are discussed in Chapter 20, and of precipitation in sections 129 and 130. The forecasting of clouds and precipitation is, of course, based on the determination of the circumstances in which these are likely to occur. These circumstances can be determined when the positions of the fronts and centers of high and low pressure have been forecast.








There is a diurnal variation in frontal precipitation, consisting of an increase in the intensity and area of occurrence of warm frontal precipitation during the night and a decrease during the day; at a cold front showers are more widely distributed during the day. As mentioned in section 129, the amount of frontal precipitation depends to a large extent on the amount of potential instability in the warm sector air. By a determination of the changes in the latter, it is possible to forecast the subsequent variations in the frontal precipitation. Variations in the amount of cloudiness and precipitation will also arise through a change in the intensity of the circulation about the low-pressure area.

Modifications in the air masses too will change the extent and intensity of the precipitation. If the air has a trajectory over a warm water area rather than over land, there will be an increase in the amount of moisture in the air mass and also a change in the stability. As a result of both these changes a difference in the cloudiness and precipitation is to be expected. Variations in the air trajectory over mountainous country will result in variations in the amount and extent of orographic cloud and precipitation.

169. An Example of Map Analysis. To learn to analyze a weather map satisfactorily, it is necessary to work with a number of maps under the supervision of an experienced analyst. Yet it is desirable to show how the foregoing discussion can be applied to an actual weather situation.

Certain symbols have been recommended by the International Meteorological Organization for indicating the details of the analysis. These are given in the accompanying table.

SYMBOLS TO INDICATE THE RESULTS OF THE ANALYSIS

	On working chart	On printed map
Surface cold front	Continuous blue line	
Surface warm front	Continuous red line	
Surface occlusion	Continuous purple line	
Upper cold front	Broken blue line	
Upper warm front	Broken red line	
Upper occlusion	Broken purple line	
Stationary front	Alternate red and blue line	
Areas of continuous precipitation	Continuous green area	Hatched area
Area of fog	Continuous yellow area	Fog symbols
Showers	Green triangles	

Figs. 180, 184, and 185 give the weather maps for a small section of North America for 19.30 h, November 17; 07.30 h, November 18; and 19.30 h, November 18, 1941. All times mentioned throughout the discussion are Eastern Standard Time. Because of the difficulty of giving the names of the reporting stations, a station will be referred to by its coordinates of latitude and longitude when necessary, as will areas to which it is desirable to refer. The only data plotted on the maps are: wind, pressure, tendency, temperature, dew point, and present weather. For a satisfactory analysis, information about cloud types and heights is necessary, but this information has been omitted because of lack of space on the printed map.

Previous to the evening of November 17, a ridge of high pressure had been centered along the Alleghenies. In addition, a center of low

pressure had been located at about (42, 107) with a cold front to the west moving rapidly southeastward and an almost stationary warm front extending to the southeast. By 19.30 h on November 17, occlusion had occurred, with the junction of the warm and cold fronts at (41, 106). The warm front extended to the eastward, and frontogenesis had taken place in the southerly current of returning polar continental air from (40, 103) to (46, 90). South of this front the polar continental air was much more modified than the air lying to the north of it.

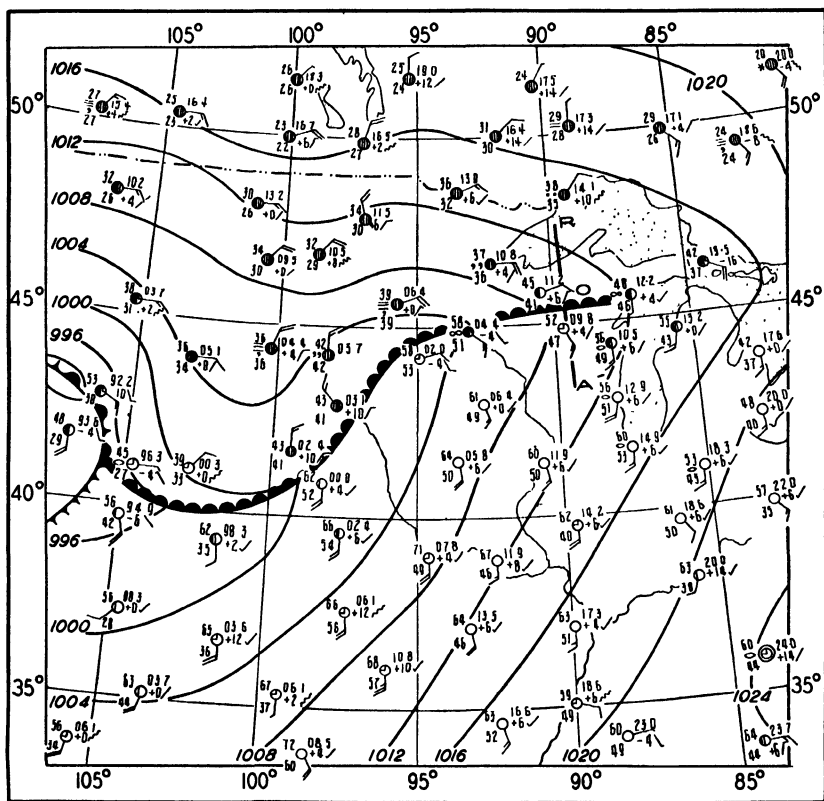


FIG. 180. Weather map for 19.30 h, November 17, 1941.

The placement of the front as shown in Fig. 180 can be explained in terms of winds, temperatures, and dew points. South of the front from longitude 88° to 100° the dew point of the air ranges from about 48° to 55°, whereas north of the front, the dew point decreases from 41° in the neighborhood of the front to 26° farther north where no precipitation has occurred. West of longitude 100° the air has had a trajectory over the dry lands west of the Gulf of Mexico, and the dew points are not

so high. Yet there is a difference in temperature across the front of about 20° in these longitudes decreasing to about 8° where the front has recently formed. Near the western portion of the front there is a decided difference in wind direction from southerly on the south side of the front to northerly on the north side of the front. In the region south of Lake Superior the wind shift is only from easterly to southerly across the front.

As is usual with a stationary front, there is little difference in tendency across the front. The motion of the air in the cold air mass governs the motion of the front, as mentioned in section 167. To the west the gradient wind near the front in the cold air is weak, but becomes stronger south of Lake Superior. However, in the latter region there is a weak isallobaric gradient directed northward, and therefore a small isallobaric wind component to the south. The resultant of this and the east south-east gradient wind is an east wind parallel to the front. Thus the front is almost stationary, with the warm air overrunning the cold in this region. In general there are rising tendencies along the front. But at (45, 95) the tendencies are falling, suggesting that a wave may be forming in the vicinity.

South of the front the weather is clear. North of the front in the cold air there is considerable cloudiness and precipitation, caused partly by the overrunning and partly by the slight orographic lift in the easterly current. Some clearing is occurring in the ridge of cold air at (42, 103).

There are not enough data given in the vicinity of the occlusion on which to base a forecast, although in general it would be expected that an old occlusion would remain almost stationary and dissipate. In the vicinity of (42, 98) the difference in the tendencies on the two sides of the front is not large. Thus, according to the kinematical rules, the motion of the front is small, a deduction that agrees well with that given by the previous motion and the geostrophic wind criterion. The wave at (45, 95) has not developed sufficiently to permit a forecast of the motion, but that development will lead to more extensive overrunning and so more precipitation and cloudiness to the north. At longitude 90° , a computation by the kinematical rules can be made. The line AOR is normal to the front at O and is considered positive to the south. The unit distance L is $OA = OR$. The tendencies at the front are 0.4 mb per 3 h in the warm air and 0.6 mb per 3 h in the cold air. Substituting into (167.2) gives

$$c = - \frac{0.4 - 0.6}{(1011 - 1009) - (1009 - 1013)} OA$$

$$= \frac{1}{30} OA$$

This gives the motion in 3 h. The movement in 12 h is south $\frac{4}{30}$ of OA . The displacement is small, and the front can be assumed to be stationary.

With the development of the wave, the gradient wind will increase slightly, but very little motion of the front is to be expected in this situation for the coming 12-h period. During the succeeding 12-h period the wave may move along the front. If that occurs, the motion of the front will be irregular with cloudy weather and precipitation north of the front. West of the moving center of low pressure the front will move south as a cold front. The other possibility is that the wave will remain almost stationary and occlude. In that event, increased overrunning will continue to give precipitation to the north, but the gradient wind will increase sufficiently to cause the front to move northward.

At 23.00 h, November 17, information on the upper air conditions was obtained at a number of stations by means of radiosondes. The ascents which are of interest in the present analysis are those taken at Sault Ste. Marie (46, 85), St. Paul (45, 93), Bismarck (47, 101), and Great Falls (48, 111). Great Falls is not on the part of the map given in Fig. 180 but is slightly to the west of the western boundary. The figure shows that Sault Ste. Marie is in the zone of frontogenesis, St. Paul is in the warm sector, and Bismarck and Great Falls in the cold air, although Bismarck is a short distance from the front and to the northwest of the developing wave. The upper air ascents for St. Paul and Bismarck are shown plotted on a tephigram in Fig. 181, and for Sault Ste. Marie and Great Falls in Fig. 182. The ascent at St. Paul is entirely in warm air, but the graph shows that the air is not completely uniform, having an isothermal layer at 800 mb as well as a nocturnal inversion near the surface. This lack of uniformity would be expected in polar continental air which has become modified to varying degrees depending on the extent of the southward excursion of the air. The air at Great Falls is almost saturated, as is that in the lower layers at Bismarck. The air at both stations is lying to the north of the front and is being carried westward and so being lifted because of the topography of the country. The air in the warm sector contains more water vapor, but the relative humidity is lower than in the cold air, and it will require a lift of 2000 or 3000 ft to saturate it. At Sault Ste. Marie the non-uniformity of the warm air is again apparent, since the developing frontal surface intersects the ascent where the increase of moisture and temperature occurs, from 950 to 900 mb, and the air above this level shows an inversion and an isothermal layer. The frontal surface is not delineated sharply in this region since the front is still developing.

The ascents at different aerological stations may be compared by means of their graphs on tephigrams. Another method, as described in

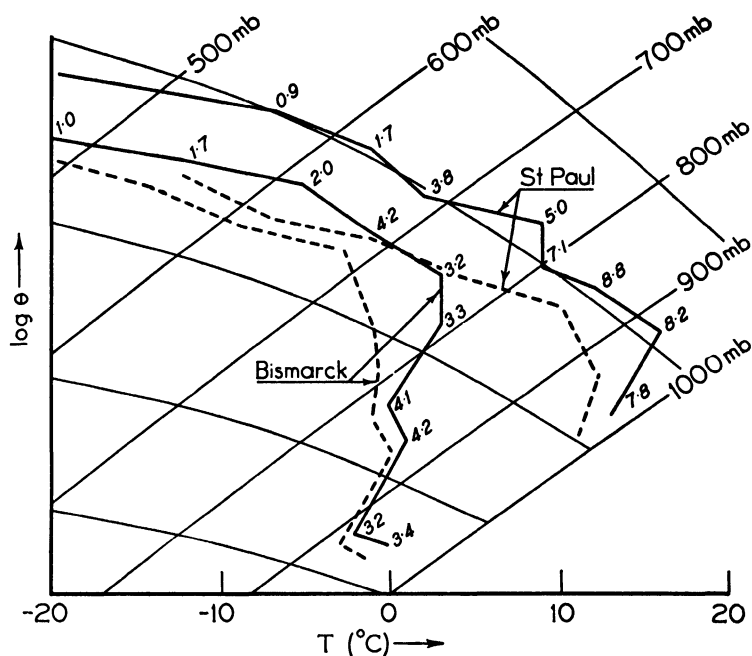


FIG. 181. Upper air ascent curves for St. Paul and Bismarck, 23.00 h, November 17, 1941.

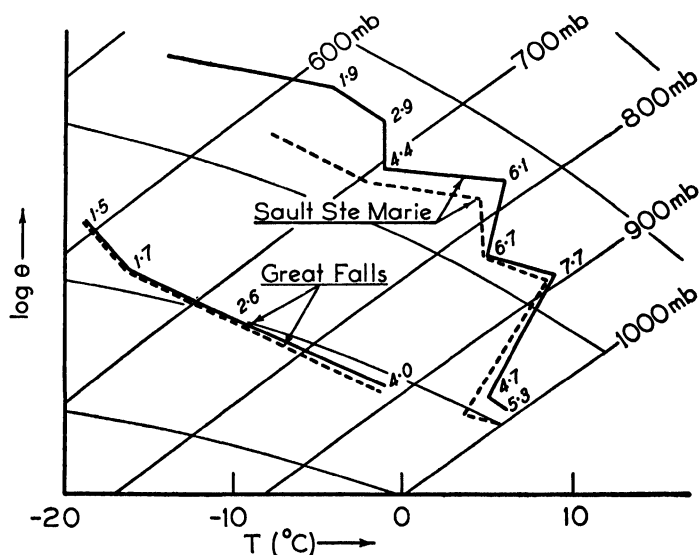


FIG. 182. Upper air ascent curves for Sault Ste. Marie and Great Falls, 23.00 h, November 17, 1941.

section 165, is to take a cross section of the atmosphere. Fig. 183 shows a cross section with data from these four stations plotted. The data included are temperature, potential temperature, relative humidity, and mixing ratio. By comparing the values of the potential temperature and the mixing ratio for the ascent at St. Paul with those at Bismarck and Sault Ste. Marie it is seen that there is only a small difference near the upper portions of the ascents, but near the surface the differences

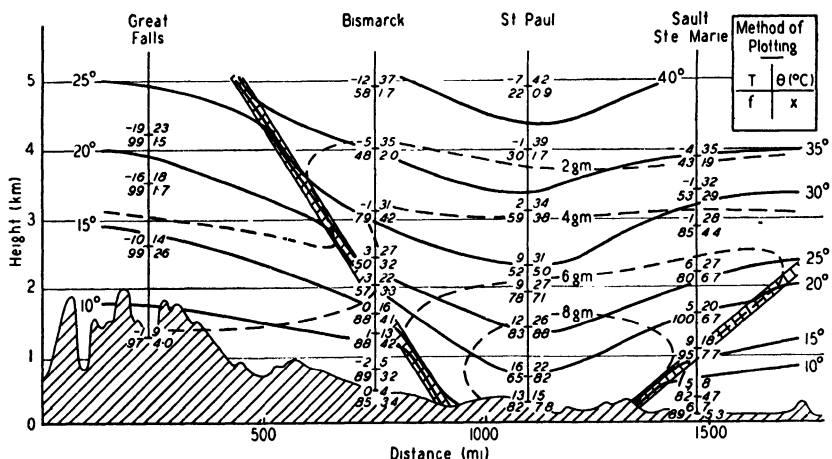


FIG. 183. Cross section for 23.00 h, November 17, 1941.

are marked. Similarly, comparing the ascent at Bismarck with that at Great Falls, it is apparent that at higher levels, above 2 km, the values are not similar, but near the surface the variation is less, although even here there is a difference, showing that the air mass is not quite uniform. On the basis of these facts, the cold frontal surface has been drawn to intersect the ground between St. Paul and Bismarck, and the Bismarck ascent at about 2 km. The warm frontal surface intersects the ground to the east of St. Paul and the Sault Ste. Marie ascent at about 1 km. Lines of equal potential temperature for the values of 10, 15, 20, . . . °C and for values of the mixing ratio of 2, 4, 6, . . . gm per kg have been drawn on the chart. Since the fronts are lines of discontinuity for these variables, on the chart the lines for the same value of the variable meet the frontal surface at different points of the two sides of the front. By using the position of the cold frontal surface at the ground and the point of intersection at Bismarck, the slope of the cold front is found to be $\frac{1}{150}$. The surface position of the warm front near Sault Ste. Marie is too indefinite to use for determining the slope of the front.

Fig. 184 shows the weather map for 07.30 h, November 18. In general there has been little change in the surface pressure distribution. The occlusion has moved slowly to the northeast, passing stations at (40, 105), (41, 105), and (43, 106), as shown by the strong rising pressures, by the shift in the winds from those with easterly to those with westerly components, and by the drop in temperature and dew point.

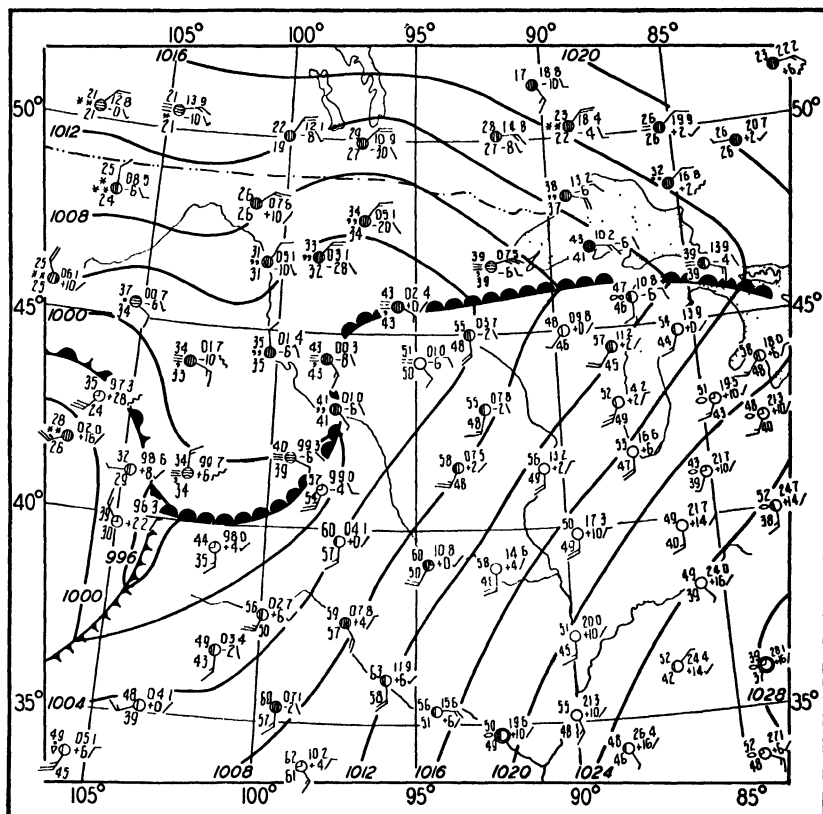


FIG. 184. Weather map for 07.30 h, November 18, 1941.

The temperature has decreased at other stations owing to the diurnal variation, but, in general, the drop at these stations which the front has passed has been more than that to the east of the front. The center of low at the tip of the occlusion has filled about 5 mb, and with the filling the weather has improved. Near the junction of the warm and cold fronts the pressure is rising slowly, as indicated by the rising pressure at (39, 102). Although some of this filling is attributable to the diurnal pressure variation, a good deal of it is a result of the general filling of the

low-pressure system. The cold front has moved to the southeast, although the rate of motion cannot be determined by the data plotted on the map. The warm front has apparently passed no stations. The developing low, presaged by the falling pressures along the front on the previous map, is shown by the 1000-mb pressure of (44, 98). The temperature at the reporting station continues to be representative of that of the cold air, but the wind has shifted from north to southeast. As will be seen when the hourly weather reports for (46, 95) are discussed, the wind shifts when the frontal zone reaches the station, and thus before the warm air actually arrives. A bulge has now developed on the front to form a wave. To the east there has been little change, although the wind shift at (46, 95) of 90° with a rise in temperature against the diurnal variation suggests that the frontal zone is approaching that station. Frontogenesis has occurred farther to the east, as seen by the difference in cloudiness, wind, and temperature between the stations (46, 85) and (45, 85).

The most important changes in the frontal positions will be related to the developing wave. The occlusion will continue to dissipate with the filling of the low-pressure area, and the warm front will not change its position much since the geostrophic wind normal to it is light and marked isallobaric gradients are absent. With the falling pressures on all sides of the newly developed low-pressure system, the cyclone should deepen and occlude during the succeeding 12-h period. With the occluding and deepening, the wave will tend to take its own path rather than move along the front. The motion to be expected is in the direction of the most rapidly falling tendencies around (48, 97). With the deepening that is occurring, the fronts, and especially the cold one, will accelerate. Hence any values obtained for the forecast displacements of these will be approximations only. By using the kinematical rules for the velocity of the warm front, the computed position of the latter at the end of 12 h is found to be at the forty-seventh parallel in the vicinity of Lake Superior, swinging northward to the forty-ninth parallel at longitude 97° . But with the eastward movement of the cold front to the south of the low, the western portion of the warm front will be occluded.

With the development of the wave, the precipitation to the north of the front will become more extensive during the succeeding period. The cold front south of the center will become more active and the lift at the frontal surface will probably release the potential instability which is present in the air over St. Paul and which will increase through the diurnal heating in the surface layers. Thus light to moderate showers should be expected with the cold frontal passage. •With the movement

of the low-pressure system to the region about (49, 97), the circulation over the Canadian prairie provinces will be northeasterly. This direction of wind carries the air over higher ground, and so the orographic drizzle and cloud will continue. Southwest of the center the air motion will have a north to northwest direction and will no longer be subjected to an orographic lifting process. Clearing is expected in this region.

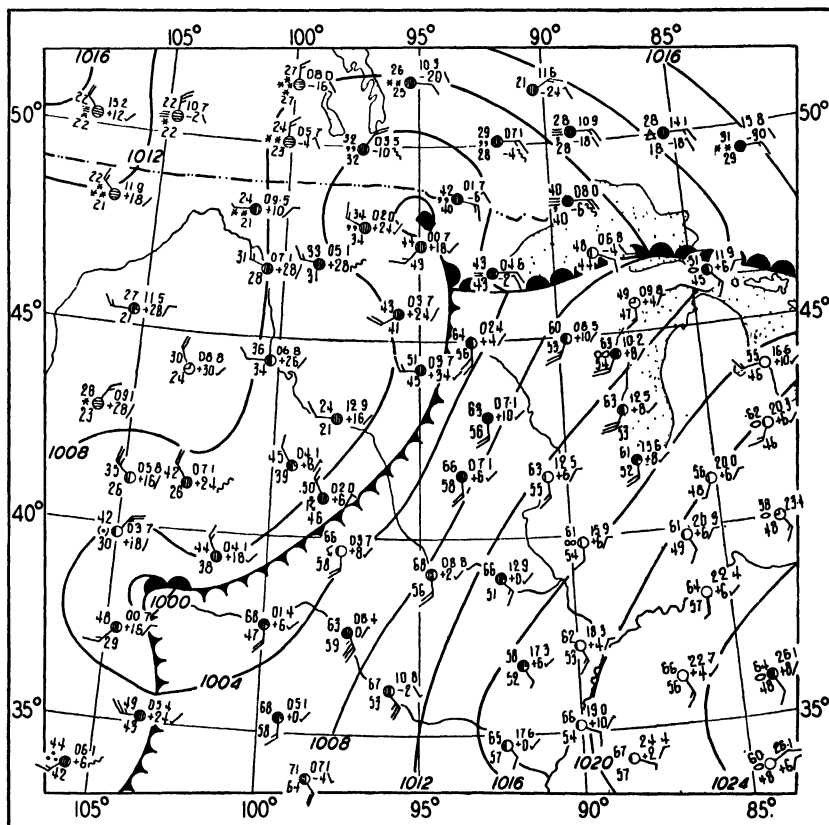


FIG. 185. Weather map for 19.30 h, November 18, 1941.

Fig. 185 shows the weather map for 19.30 h, November 18. Significant changes have taken place in the frontal construction. The occlusion near (41, 104) has now dissipated, and a weak low-pressure system is centered at (38, 104) and is filling, as shown by the tendency at (38, 100). The low which on the 07.30-h chart was at (44, 98) has moved northeasterward to (48, 95), as was indicated by the tendencies.

The position of the front is approximately as suggested by the analy-

sis of the 07.30-h map. In the southern portion, in the vicinity of (35, 103), the stronger rising tendencies behind the front than ahead of it help in placing it. Behind the front the winds are southwest or west. To the east of the front the winds are south, corresponding to the direction of the isobars. The dew points to the east of the front are 47° to 58° , whereas in the drier air to the west the dew points are 44° near the front and decrease with increasing distance from the front. A similar but more marked difference exists in temperature. Along the front lying in the trough between the two low-pressure areas, the difference in temperature and dew point across the front is ten degrees or more, with the values of these elements in the air behind the front decreasing rapidly with distance from the front. This situation is quite common. The warm air in the warm sector is usually nearly uniform in temperature and dew point. The main change in these elements occurs in the cold air under the warm frontal surface and behind the cold front. Owing to the small velocity of the front at (41, 97), the tendency contrast is small across it, but in the vicinity the thunderstorm reported and the distant lightning are both evidence of the proximity of the cold front. In the vicinity of Lake Superior the warm front did not move quite so far as was forecast. The rapid increase at (46, 85) of temperature and dew point as compared with that at (47, 88) shows that the front has passed the former but not the latter. Although there has been some increase in temperature in the vicinity of the low at (48, 95), at no point is there evidence of warm sector air. The increase in temperature can be explained by the heating produced by the precipitation falling from the trough of warm air aloft. As yet there is little difference in temperature across the occlusion, which in this situation is placed on the basis of the wind shift from easterly to southwesterly, and the rapidly rising tendencies to the west and southwest of the front. During the 12 h between the two maps, the pressure at the center of the low-pressure system decreased, with the lowest pressure at 13.30 h being 999.0 mb. Since that time the pressure has risen, and the center is filling, as shown by the mean tendencies in the region. This indicates that the occluding process is complete, and from now on the occlusion will dissipate.

The next problem is to forecast the motion of the fronts. In the southern portion at longitude 103° , the geostrophic wind criterion gives the front a velocity of 40 mph. But the filling of the low during the succeeding 12 h will cause this value to decrease during that period. As a result of the very weak trough in the isobars at the front, the denominator of the fraction in (167.2) giving the motion by the kinematical criterion is small. Any inaccuracy in the numerator will be magnified

when the distance the front is expected to move is computed. . Furthermore, the tendencies as recorded west of the front are very irregular, so it is difficult to draw isallobars. A computation on the thirty-sixth parallel places the front in 12 h at the ninety-seventh meridian, but this should be checked by the previous motion, or by a more accurate determination of the tendency field west of the front. Along the cold front between the two lows there is no geostrophic wind normal to the front, but in the cold air the pressures are rising more rapidly than in the warm air. The trough with the cold front will then move slowly eastward during the succeeding 12-h period. A motion of about 100 mi for 12 h might be expected. This agrees with the past motion south of the center of low pressure on the previous map. This center should move slowly toward the region of most rapidly falling pressures, that is to the northeast, and fill slowly. With the rapidly falling pressures to the north, the previous motion will not be reliable for a forecast of the displacement of the warm front. Moving it at 70 per cent of the geostrophic wind of 26 mph would put it at latitude 49° in the Lake Superior region. The same forecast position is reached by the use of the kinematical rules at longitude 87° . It would be expected then that at the end of 12 h the two fronts will meet in a center of low pressure at about (49, 92), with a short occlusion to the northwest, and the cold front extending southerly and then southwesterly in a weak trough.

The most extensive area of precipitation will extend to the north of the warm front, where overrunning is supplemented by orographic lift from the lakes region to the ridge to the north. The precipitation about the occlusion will become less pronounced, and to the west neither orographic lifting nor instability should cause much precipitation. Some local showers and thundershowers are to be expected with the cold frontal passage to the south. Data beyond the edge of the map will tell whether the current of air from the south has a trajectory over the Gulf of Mexico. If its moisture content is increasing as it flows over the Gulf, then convergence in the south-north current may give rise to cloud east of the frontal region.

Further data about the position and motion of fronts can be obtained from the hourly weather reports. Some of the information contained in the hourly reports from 01.30 to 21.30 h on November 18 from the station at (46, 95) is given in Fig. 186. The values for the pressure, temperature, and dew point are plotted, the latter two being coincident until 13.30 h. Underneath are given the wind directions and speeds in miles per hour, the height of the low cloud in hundreds of feet, and the visibility in miles. The low cloud layer formed an overcast except when noted. On the chart for 19.30 h of November 17, this station was in the

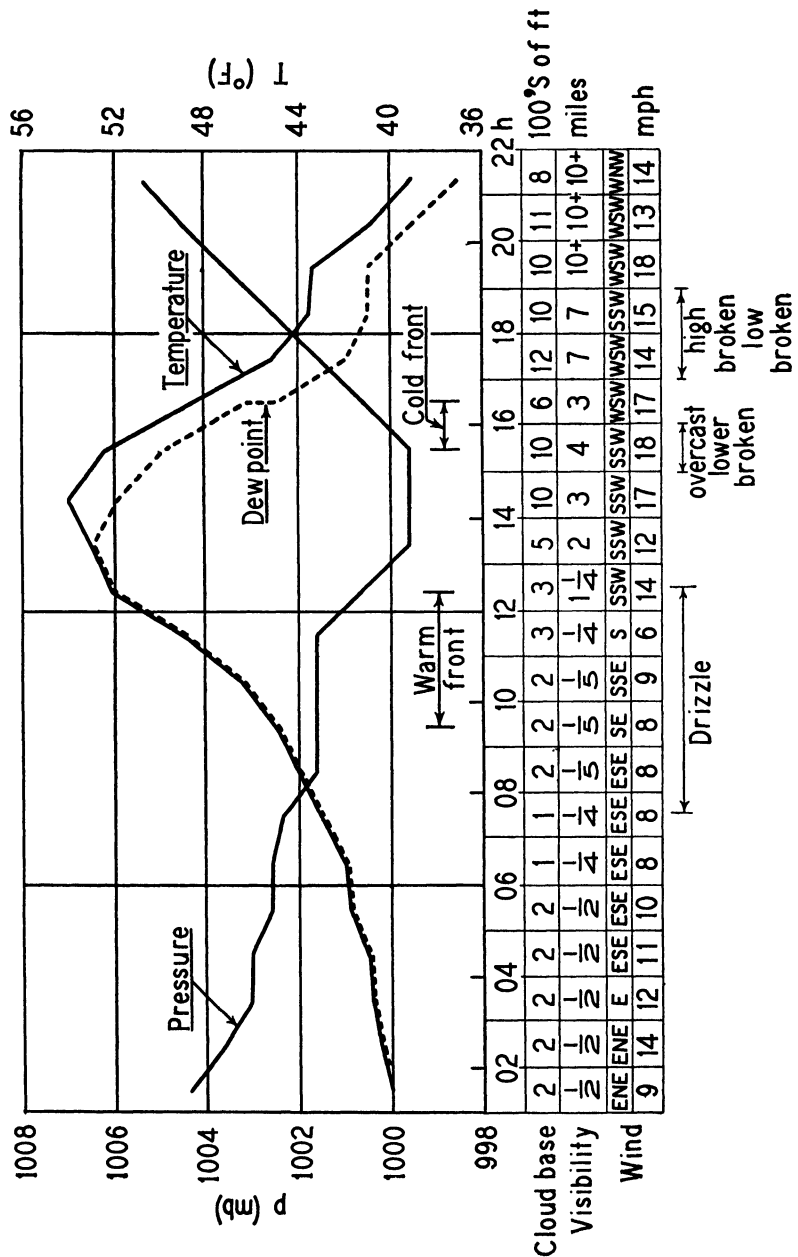


Fig. 186. Weather changes at Alexandria, Minn., (46, 95), November 18, 1941.

cold air under the warm frontal surface, and was still there at the beginning of the period illustrated. This is seen by the wind direction, the fog which was present north of the warm front, and the temperature. The drizzle later in the period was an indication of the approach of the front. The first sign that the station was in the frontal zone appeared at 09.30 h, at which time the wind shifted to the southeast. The temperature then began to rise more rapidly, but did not reach the temperature of the warm air until 12.30 h, when it became 52°. At this time the wind was south southwest, and the visibility had improved, showing that the drizzle was ceasing. The latter stopped and an increase in the ceiling took place during the next few hours. For 3 h, from 09.30 till 12.30 h, the station was in the frontal zone. Since the front was moving with a speed of about 5 mph, this indicates a frontal zone of 15 mi, which is not an exceptional width. The pressure decreased while the front was approaching, became steady with the arrival of the frontal zone, and then decreased again in the warm sector as the center of low approached the station. The center passed close to this station since the minimum pressure recorded of 999.7 mb was close to the minimum, 999.0 mb, at the center of the system.

The passage of the cold front was more sudden. Between 15.30 and 16.30 h the pressure began to rise, the temperature dropped 4° with an equal drop in the dew point, the wind veered through 45°, the ceiling and visibility decreased for one observation, but both improved after the frontal passage. After the cold air advanced past the station, the pressure continued to rise, and the temperature and dew point to drop until the end of the period illustrated. All these variations are of the type to be expected in a situation of this kind.

170. Long-Range Forecasting. A complete discussion of the procedure of long-range forecasting is beyond the scope of this book. A short description only of the methods by which this problem is being attacked will be given.

One method of attempting to solve the problem is by a study of possible variations of the energy output of the sun (see section 28). Since the sun is the source of energy for the earth, any variation in its output should have an effect on terrestrial weather. The atmosphere absorbs and scatters some of this solar energy, and so the best place for its measurement is on high mountains where there is less atmosphere and also less atmospheric pollution above the observers, and very few clouds. The Smithsonian Institution of Washington maintains observatories taking measurements of the energy from the sun at Mount Wilson, California, and in the Andes, and at a number of other stations. These measurements suggest that there are variations amounting to about

2 per cent of the total energy. It has been contended that these variations are not random but cyclic. The correction for the absorption and scattering by the atmosphere is on the average about 25 per cent of the total energy received at the outer limits of the atmosphere, and it is not yet clear if these variations mentioned above represent real variations in the energy output of the sun, or if they result from an incorrect allowance for the effect of the atmosphere. It has been further claimed that a correlation exists between the energy output of the sun and the world weather. Thus, for example, the eleven-year cycle of the sun's energy output is reflected in an eleven-year weather cycle on the earth. Some attempts to forecast for a period of a month in advance have been made, but as yet the method has not proven its value.

Another method of forecasting is the result of the study of a large number of meteorological series. By means of computing correlation coefficients (see section 61), meteorologists have been able to show that variations in the values of some series have been followed by corresponding variations in other series. Simultaneous variations are not uncommon. Thus if the pressure in Iceland falls, the pressure gradient over the North Atlantic increases, the transport of air to western Europe from the southwest is greater, and the temperature there rises. Subsequent variations are more rare. Yet it has been found by Walker that the summer rainfalls of India, Australia, and South Africa are related to the distribution of pressure of the previous season in the South Pacific and Indian Oceans. By using a combination of the values of several variables, a formula has been obtained by which to calculate the summer rainfall in these districts. The value of the latter has a correlation of from 0.7 to 0.82 with the actual rainfall. This formula gives a fairly reliable, although not perfect, estimate of the rainfall for the following six months.

Similar attempts have been made to find series, especially for the temperate zone of the Northern Hemisphere, which can be used to predict future values of the weather elements, but so far without success.

Baur has developed a method of forecasting for Germany for ten-day periods. His forecasts are based on observations in the stratosphere and high troposphere. According to Baur and his associates, the changes in pressure at the earth's surface are controlled by atmospheric movements at levels of 4 km and higher, the process whereby this occurs being known as "steering." This group of meteorologists has shown that the 24-h isallobaric highs and lows at the surface follow the direction of the wind in the upper atmosphere. Since the meteorological conditions at and above 4 km change only slowly, the air motion at these levels can be predicted with a degree of accuracy and thus also the movement of isallo-

baric centers at the surface. Knowing the current pressure system, Baur is therefore able to use the future position of the isallobaric systems to draw a forecast map of the pressure distribution. From this map he makes a forecast of the weather in the different districts. His forecasts have been highly regarded in Germany.

A method of forecasting for a period of five days has been developed by Rossby and collaborators. Rossby has shown that the positions of the semi-permanent centers of high and low pressure are related to the strength of the circulation in the free atmosphere in the region of westerlies. The changes in this circulation are less variable than those in the values of the weather elements at the surface. Thus by forecasting the value of the circulation, Rossby is able to forecast the positions of the pressure centers and so the general weather distribution. By this method forecasts for the subsequent five days are being made for the United States at the present time.

Because of the value that accurate long-range forecasts would have to various industries, many more or less reliable forecasts have been issued. Some of these methods operate in the realm of folk lore, using the position of the moon, the thickness of the fur on wild animals, the sunshine on Candlemas Day, etc. A few of these simple rules for forecasting for the immediate future have stood investigation.

Other forecasts are made for periods of a week to a month by meteorologists in which they combine changes arising from the annual variation of the weather with the average weather variations accompanying the passage of high- and low-pressure areas. As such they are valuable since they instruct those interested in the normal changes that can be expected. Yet it has not been proven that such methods are capable of forecasting the abnormal variations which comprise the most interesting part of the weather.

BIBLIOGRAPHY

- Admiralty Weather Manual*, London, H. M. Stationery Office, 1938. Chapters 17, 21.
- Byers, H. R., *Synoptic and Aeronautical Meteorology*, New York, McGraw-Hill Book Co., 1937. Chapters 8, 9.
- Problems of Modern Meteorology*, London, Royal Meteorological Society, 1934. Numbers 4, 6.
- Weightman, R. H., *Forecasting from Synoptic Weather Charts*, U.S. Department of Agriculture, Misc. Publications, 236. Washington, D. C., 1936.
- The Weather Map*, Third Edition, London, H. M. Stationery Office, 1939.
- Starr, V. P., *Basic Principles of Weather Forecasting*. New York, Harper & Bros., 1942.
170. Baur, F., "Die Bedeutung der Stratosphäre für die Grosswetterlage," *Met. Z.*, 53, 237-247 (1936).

170. Walker, Sir G. T., "Ten-Day Forecasting as Developed by Franz Baur," *Q. J. Roy. Met. Soc.*, **63**, 471-475 (1937).
170. Walker, Sir G. T., "Seasonal Weather and Its Prediction," *Smithsonian Report for 1935*, Washington, D. C. Pages 117-138.
170. Weightman, R. H., "Preliminary Studies in Seasonal Weather Forecasting," *Monthly Weather Review*, Supplement No. 45, 1941.
170. Willett, H. C., *Report of the Five-Day Forecasting Procedure*, Mass. Inst. of Tech. Papers in Physical Oceanography and Meteorology, **9**, No. 1, Cambridge, Mass. 1941.

CHAPTER 25

METEOROLOGY APPLIED TO VARIOUS HUMAN ACTIVITIES

Meteorology owes a great deal to the demand put upon its facilities by the development of aircraft, as well as to the additional information that the aircraft has provided for the study of the free atmosphere by the meteorologist. In return the meteorologist has given a great deal of his time and thought to the special problems of air transportation.

But climate and weather affect the other occupations of mankind. Climatic factors help determine, for example, the location of certain types of hospitals, the choice of agricultural crops, and the strength of a steel bridge. The information necessary for the solution of these problems is obtained from a study of climatological data, and the short-range forecast provides little assistance. Yet persons engaged in different occupations can use the information available from the forecaster to help do more efficiently the task at hand. To serve such persons best, it is necessary for the forecaster to understand the problem which he is helping to solve. He can thus give more readily the information desired.

Engineers to whom some of these forecasts will go are accustomed to accuracy in their data. Care must be taken to make certain that they understand that, at present, forecasts cannot be relied upon completely and that a margin of safety must be left when using the meteorologist's forecast. On the other hand, the forecaster should learn to give a statement which is more specific than the general forecast of "fair and colder," and one which is useful in planning the activities of the next few days.

171. Transportation. Weather forecasts have for years played an important part in maintaining the safety of ocean travel. The major point of interest to the navigator is the strength of the wind. Moderate gales may cause difficulty in keeping the course as well as damage to the ship. For the benefit of ships at sea the weather services issue storm warnings which tell the position and direction of motion of storms, with the result that a ship is sometimes able to change its course in order to avoid the worst part of the storm area. Freezing rain or drizzle hinders the work and movements about the ship, and the presence of fog frequently necessitates a decrease in the speed of the ship. These are the weather factors which the officers of the ship wish to have the meteorologist forecast.

Water travel on lakes and coastal waters is affected by the same weather elements as ocean travel. The direction of the wind and the times for wind shifts have more significance for ships plying inland waterways than for those over the ocean, however. Thus, for example, when ice is floating about, the direction of the wind may determine the availability of a particular harbor.

With all transportation systems that handle freight, the extremes of temperature have significance at times. These tell the responsible authorities the possibility of danger to the cargo through exposure to temperatures which would injure it. This is of particular significance with respect to freezing temperatures during periods of the transport of fruit, although other commodities as well are affected by temperature extremes.

Poor visibility caused by fog or precipitation leads to slowing down of railroad transportation. In this case, though, it is not greatly beneficial to the engineer to have this information beforehand. The railroad management, however, will be able to place its equipment better for keeping the tracks clear if it has advance information of the approach of a severe storm or of a high wind which would drift snow into the cuts along the track. Also if it knew of the approach of flood conditions along the route, plans could be made to repair any possible damage.

The meteorologist can assist the highway engineer, too, in planning the removal of snow. A previous knowledge of the approach of a snow-storm will provide the manager with an opportunity to assign his equipment to the best advantage for handling the clearing of the roads. Not only is he interested in the amount of snow but also the type. A heavy, wet snow is more difficult to handle than a dry, powdery snow. The wind direction during and after the snowfall is of interest since this will inform the engineer as to the routes along which drifting will be serious and those along which it will be light. Snow removal is necessary during and after periods of drifting snow as well as after periods of snowfall, since such drifting snow will fill up the cuts in the snow banks which have been made to permit road travel. Hence the engineer continues to be interested in the direction of wind and in any shift of it.

The occurrence of freezing rain on roads slows traffic and causes many accidents. The greatest danger occurs on hills. A notice of the approach of a sleet storm, even a couple of hours in advance, provides the highway engineer with an opportunity to send out trucks with gravel to these hills and so have the equipment ready to keep the danger at a minimum.

Ice storms affect the electrical contacts made by a street car with an overhead wire. Considerable time may be saved, and inconvenience

avoided if the cars are fitted out to cope with this difficulty before they leave the car barns. Hence the management of such transportation systems can make use of a forewarning of the approach of these storms.

172. Agriculture. Agricultural activities are affected greatly by the weather and the climate. The distribution of crops is determined by the length of the growing season, the amount of precipitation, etc. Average figures for these in the different districts of the country may be determined from climatological data. If it were possible to forecast the values of these for a particular year, agriculturalists would be able to adapt the crops to the weather expected. This is done in India where the monsoon rainfall is forecast at the beginning of the season, and an adjustment of crops is made on the basis of the forecast. This is not yet possible over most of the world.

Farmers have learned through experience to make a fairly accurate forecast covering the succeeding 12 to 24 h from the appearance of the sky and the direction of the wind. A forecast covering the succeeding 12 h is definitely helpful to them in planning their work, for some of it requires two fine days to complete satisfactorily. Drying of hay and of fruit is done much more easily if no rain falls during the drying period. A farmer finds a forecast useful when planning to plow clay soil, since the latter must be neither too dry nor too damp.

One special type of service which is saving the farmers time and money is the forecasting of minimum temperatures and frost. When the temperature is expected to fall below freezing, fruit growers are able to save their fruit by lighting smudge fires and keeping the temperature from falling so low in the orchards. Cranberry growers flood their bogs to save the cranberries from frost. These operations would be too expensive if no forecasts were available and they had to be carried out every night. Sheep breeders, too, are interested in knowing the minimum temperatures during the lambing and shearing seasons.

A common method of forecasting minimum temperatures is through a statistical analysis. Previous records are taken for the vicinity. The relative humidity or another function of the moisture content of the evening is plotted against the difference between the dew point of the evening and the succeeding minimum temperature. If the points fall along a straight line, as frequently happens, the line of least squares is determined for the data in the manner shown in section 60. By using the equation of the line and the relative humidity or the dew point of the evening, a reliable forecast for the minimum temperature of the night can be made. For example, the equation determined for San Diego, California, is

$$y = -6.6 + 0.62(T - T_d)$$

BURNING INDEX METER

For use on the Forests of the Northern Rocky Mountains

*Northern Rocky Mountain Forest and Range Experiment Station
Missoula, Montana
Model 1, April 1942*

Calendar		Date
August 21 to 31	Relative Humidity Stations having hygrometers use the minimum for the Others use the 4, 5, or 6 p. m.	
" 16 " 20		1 to 5 September
" 11 " 15		
" 6 " 10		6 " 10 "
" 1 " 5		
July 26 " 31		11 " 15 "
" 21 " 25		
" 11 " 20		16 " 20 "
" 1 " 10		21 " 25 "
June 16 " 30		15 to 24 26 " 30 "
" 1 " 15		10 to 14 1 " 10 October
May 16 " 31		Under 10 11 " 20 "
" 1 " 15		21 " 31 "

How to use this meter,—

First, set the slide so that the proper humidity is on line with the current date. Second, on reverse side in the column for current fuel moisture and on the line for concurrent wind, find the Burning Index or "BI"

Season,—

The net effect of four factors of forest inflammability changes with the calendar date brackets above. These are, (1) hours of sunshine, (2) intensity of solar radiation, (3) percentage of vegetation green, curing, or cured, and (4) cumulative drying or wetting of heavy fuels especially under dense timber or on steep north slopes.

Humidity,—

The above allowances are for an average fuel type, they are insufficient for pure grass or weed types and are too great for dense green timber stands.

Half-inch sticks,—

These represent a fuel common wherever there is any tree growth. Their moisture content is the most dependable single index of the inflammability of dead wood

FIG. 187. Burning index meter, side A, set for relative humidity 20 per cent on June 25. (After Gisborne.)

Wind Velocity		Half-inch stick moistures															
Average for afternoon, 20 feet above open level ground		Exposure 10" above ground, under standard shade, and measured ½ hour or more before sunset															
		Percentage of oven dry weight															
		25	21	18	15	13	11	9.5	8.5	7.5	6.5	5.5	4.5	3.4			
		to	to	to	to	or	or	10	9	8	7	6	5	4			
		+	24	20	17	14	12	10	9	8	7	6	5	4			
2.5 or less		3	5	7	8	11	13	16	19	22	25	28	32	35	39		
3.6		3	4	6	8	10	12	15	18	21	24	27	31	34	38	42	
4.5		4	5	7	9	11	14	17	20	23	26	30	33	37	41	45	
5.5		5	5	7	10	12	15	18	22	25	28	32	35	39	43	47	
6.6		6	6	8	11	13	17	20	23	27	31	34	38	42	46	50	
7.6		7	7	9	12	15	18	22	25	29	33	36	40	44	48	52	
8.6		8	8	10	13	16	20	23	27	31	35	39	43	47	51	55	
etc		9	9	11	14	17	21	25	29	33	37	41	45	49	54	58	
10		10	10	12	15	19	23	27	31	35	40	43	48	52	56	61	
11 or 12		11	11	13	16	20	25	29	33	37	42	46	50	55	59	64	
13 or 14		12	12	14	18	22	27	31	35	40	44	48	53	58	62	67	
15, 16, 17		13	13	16	19	23	28	33	37	42	47	51	56	60	65	70	
18, 19, 20		14	14	17	21	25	30	35	39	44	49	54	58	63	68	73	
21 to 24		15	15	18	22	27	32	37	41	46	52	56	61	66	71	76	
25 or more		16	16	20	24	29	34	39	43	49	54	59	64	70	74	80	

BURNING INDEX or 'BI'

Significance.-

Burning Index expresses the result of several conditions to which a forest is exposed. It supplies the need for a numerical scale for reporting the fire character of a day, a month or a season. A BI of say 50 will mean a different rate of spread of fire in different fuel types, just as a certain heat of fire in a forge, say 658°C., will turn lead to a liquid, will almost melt aluminum, but will leave iron still hard. The BI expresses intensity of conditions affecting all fuel types adjacent to the station where BI is measured. As derived here it is not expected to represent a particular instant. It is intended to rate an area and a fire-day as a whole. It is the first, but not total basis for rating daily and seasonal fire danger.

FIG. 188. Burning index meter, side B; for a velocity of 10 mph and fuel moisture 8 per cent the meter reads 40. (After Gisborne.)

where y gives the excess of the minimum temperature over the evening dew point in °F and values of T and T_d are those of the evening. The equation varies with different localities. In some instances, the relationship is best expressed by a parabolic equation connecting y and f , the evening relative humidity.

In general the wind velocity is not a major factor with agriculturalists when making their plans. They are interested in this element, though, during the seasons when spraying their orchards or field crops is necessary. With high winds a great deal of the spray is wasted since it is carried away by the wind. If rain is expected the following day, they may feel that immediate spraying is worth while since some of the fungi and insects will be destroyed. If, on the other hand, the following day is going to be fine and with light winds, the farmer will often prefer to postpone his spraying for a day till better weather has come. In such situations the agriculturalist will desire an accurate forecast of winds.

In these and in many other ways the farmer can make use of the forecaster's services to plan his work more efficiently.

173. Forestry. Forest fires are the greatest hazard to the conservation of forests. Since the possibility of fires starting and the rate at which a fire will spread are dependent upon atmospheric conditions, those in charge of forest conservation are vitally interested in various weather elements and forecasts of these elements.

Six factors are significant when assessing the danger of fires starting and spreading:

- (a) The season of the year.
- (b) The wind velocity.
- (c) The relative humidity.
- (d) The fuel moisture content.
- (e) The visibility.
- (f) The recent occurrence of lightning.

Although the visibility does not affect the starting or the actual spreading of the fires, it can hinder lookout men from observing a fire readily, thus giving the fire an opportunity to break away. Two factors, season and fuel moisture content, are not weather elements, although the moisture in the underbrush is closely related to the past weather of the region. Gisborne has combined these factors in such a manner that the relative danger of fire in the northern Rocky Mountain region of Montana is assessed. The computation is carried out by means of two meters, the burning index meter and the fire danger meter. The two sides of the burning index meter are shown in Figs. 187 and 188. By sliding the movable card, the relative humidity for the day is placed

on a line with the current date. As illustrated in Fig. 187, it is adjusted for a relative humidity of 20 per cent on June 25. Then, reversing the card, one reads off the burning index corresponding to the current wind velocity and fuel moisture. As shown in Fig. 188, for 8 per cent fuel moisture and a wind velocity of 10 mph, the burning index is 40. With the fire danger meter (not shown) this value is adjusted slightly for visibility and recent lightning. The forest executive uses this fire

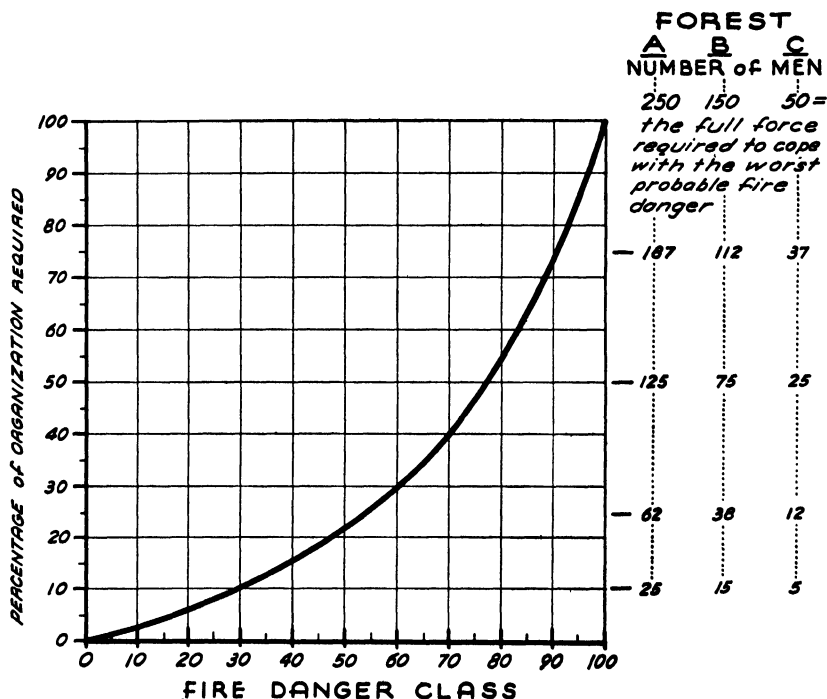


FIG. 189. The dependence of organization size on fire danger. (After Gisborne.)

danger rating in conjunction with the chart shown in Fig. 189 to determine the number of men required for a proper protection of the district. In the example only 15 per cent of his organization is necessary to be on guard against fires.

It must be emphasized that the weights given to the several meteorological elements will vary from one region to another. Thus the burning index meter shown in Figs. 187 and 188 may be used only in the northern Rocky Mountain area. The use of a meter of this type is permissible in another region only after investigations of the relative influence of the several factors in that region have been made and an appropriate meter constructed.

A somewhat similar method of determining the forest fire danger for various parts of Canada has been developed by Wright and Beall. This system is based on measurements of rainfall, evaporation, relative humidity, and wind velocity. On the basis of statistical analyses of these elements, tables of a fire hazard index for various periods of the fire danger season and for various types of timber stands have been constructed. In applying this method to assess the fire danger, daily values of these four elements are plotted on a fire hazard chart, and with the aid of the tables the current hazard index is determined.

The forest ranger not only uses the meteorological elements themselves, but he may also use forecasts of these. The forecast values of these weather elements may be used in place of the current values in assessing the expected fire danger. In this regard, the forest rangers have found it necessary to adjust the wind speeds as forecast on the Beaufort scale to allow for the decrease of wind in the forest where their own observations are made.

Forest executives use the forecasts also in planning for the fighting of fires. The defense that they plan must be adjusted to allow for any increase in wind speed or any change in wind direction. For instance, they may be able to use even a brief shift in the wind, if warned of its coming, to prepare a back-fire to stop the main conflagration.

174. Heavy Industry. There are a number of ways in which weather forecasts may be used to facilitate the operation of heavy industries. In this section, however, attention will be focused on one particular phase to which meteorological principles have been applied.

One of the problems arising from the operation of heavy industry is the atmospheric pollution which frequently results from the various processes employed in the plant operations. Sulphur dioxide, for instance, is frequently produced, and if released to the atmosphere, may damage vegetation in the vicinity. Damage to crops in the state of Washington occurred, for example, through the action of sulphur dioxide fumes emitted by the smelter of the Consolidated Mining and Smelting Company of Canada, Limited, located in the Columbia River valley at Trail, British Columbia, which is about seven miles north of the international boundary. The fixing of compensation for injury involved a good deal of international litigation until, under the authority of an Arbitral Tribunal set up by the governments of the United States and Canada in 1935, a control regime based largely on meteorological criteria was established in 1941.

The development of this regime was possible only after a comprehensive investigation of meteorological conditions in the Columbia River valley near the international boundary, some of the results of which are

given in section 124. The regime adopted is based largely on the wind direction and speed and on the atmospheric turbulence in the valley. The importance of the former in preventing the encroachment of smelter fumes on the territory of the state of Washington will be obvious. It is shown in section 54 that matter is diffused throughout the atmosphere by turbulence. Thus equation 54.11 gives the rate of diffusion of an entity x , in this case sulphur dioxide expressed as the number of parts of sulphur dioxide per million parts of air. Owing to the difficulty of obtaining mean values of the coefficient of eddy diffusivity for a period of half an hour (the minimum period required for the method given in section 55 is 24 h), a direct method of measuring the turbulence was developed.

For this purpose a special instrument called a bridled-cup turbulence integrator was designed by G. C. Gill. This consists essentially of an anemometer with 22 cups. The vertical shaft is bridled to prevent continuous rotation such as occurs in the ordinary cup anemometer described in section 66, and is so constrained that its angular displacement from the zero position for no wind is directly proportional to the wind velocity. When the air motion is turbulent the angular displacement of the anemometer increases as the gusts grow in intensity and decreases as the gusts die away. Each change of the velocity by 2 mph is recorded by electrical means on a rotating drum. The degree of gustiness or turbulence during a half-hour period, for example, is then obtained by counting the number of deflections recorded during that period. The number of deflections per half hour varies from zero when the atmosphere is very stable, as during the early morning hours, to 2000 or 3000 during a hot summer afternoon. The diffusion of the gas is closely related to the turbulence determined in this manner.

The maximum permissible sulphur emission depends on the time of the year since the possibility of damage is, of course, much greater during the growing than during the non-growing season. Allowance must also be made for the fact that crops are more susceptible to injury by sulphur dioxide during the day when exposed to sunlight than at night. The period of maximum danger is just after sunrise, which also coincides with the time when the concentrations of sulphur dioxide tend to be greatest.

The maximum sulphur emission in tons of sulphur per hour (one ton of sulphur corresponds very nearly to two tons of sulphur dioxide) permitted by the control regime laid down by the Tribunal is given in the table. Favorable winds are those from the north, east, south, and southwest, and intermediate directions, provided that they have a speed of 5 mph or more and have persisted for 30 min at the point of observation. All other winds are unfavorable. Most of the other provisions

of the regime are non-meteorological in character and will not be discussed here.

MAXIMUM PERMISSIBLE SULPHUR EMISSION

(Tons of sulphur per hour)

Time of Day	Season	Turbulence (Deflections per Half Hour)						
		0-74		75-149		150-349		350 and above
		Wind						
		Un-fav.	Fav.	Un-fav.	Fav.	Un-fav.	Fav.	Either unfav. or fav.
Midnight to 3 A.M.	Growing	2	6	6	9	9	11	11
	Non-growing	2	8	6	11	9	11	11
3 A.M. to 3 h after sunrise	Growing	0	2	4	4	4	6	6
	Non-growing	0	4	4	6	4	6	6
3 h after sunrise to 3 h before sunset	Growing	2	6	6	9	9	11	11
	Non-growing	2	8	6	11	9	11	11
3 h before sunset to sunset	Growing	2	5	5	7	7	9	9
	Non-growing	2	7	5	9	7	9	9
Sunset to midnight	Growing	3	7	6	9	9	11	11
	Non-growing	3	9	6	11	9	11	11

Few heavy industries have the flexibility of operation necessary to follow such a regime while maintaining full production. At Trail the plant installations were enlarged to permit such flexibility. The portion of the sulphur dioxide which cannot be discharged to the atmosphere during periods of poor diffusion is used in the manufacture of elemental sulphur and sulphuric acid.

Fig. 190 is a photograph of the smelter at Trail, taken from a point about a mile downstream from the smelter at 21 h on June 9, 1940. Although the sun had set, the smoke can still be seen above the stacks. The diffusion of the smoke at this time was slow. The bridled-cup turbulence integrator showed 65 deflections per half hour during the preceding hour and 10 deflections per half hour during the following hour. The wind at the stack was south 2 mph. The rate of emission of sulphur dioxide was low, having been 2.5 tons of sulphur per hour from 17 to 19 h; it was then increased to 3.5 tons per hour at 19 h and to 4.5 tons per hour at 21 h. The latter rate of emission is slightly greater than

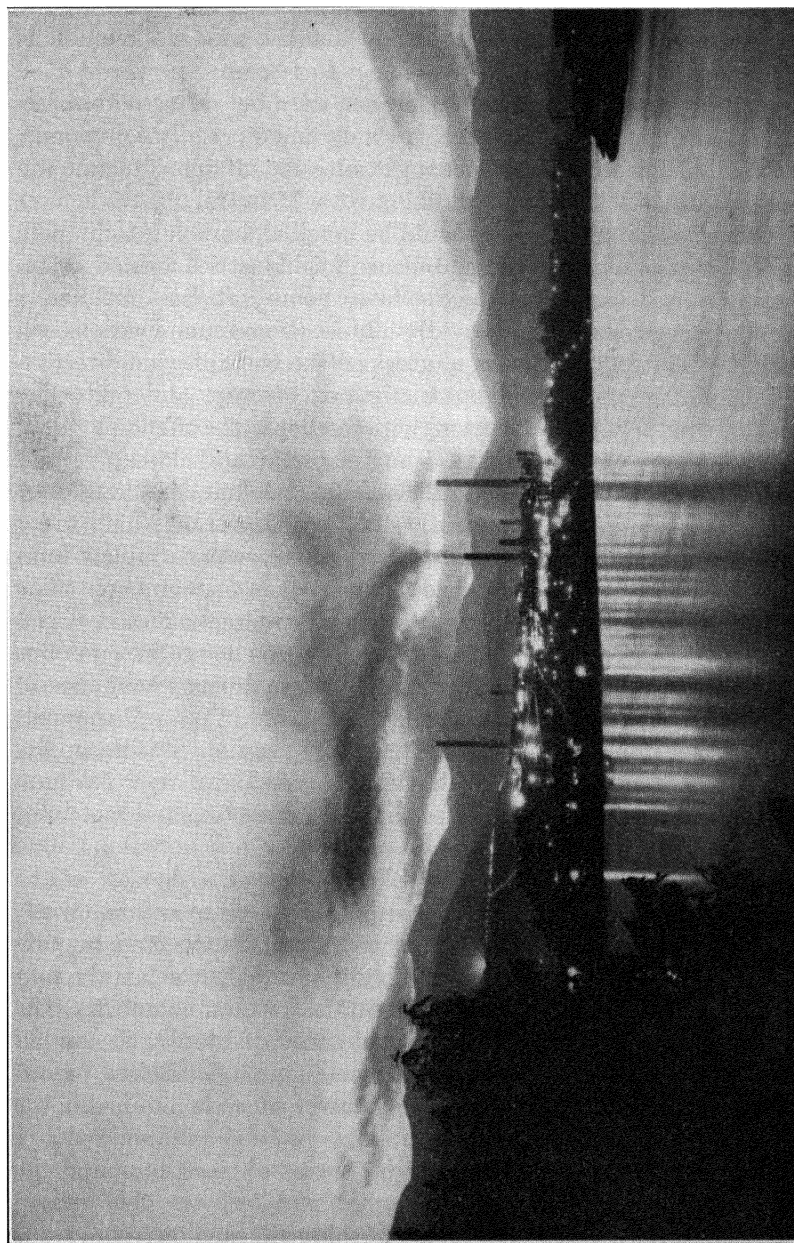


FIG. 190. The diffusion of smoke by turbulence at Trail, British Columbia. (From Dean and Swain, *Report Submitted to the Trail Smelter Arbitral Tribunal*, U. S. Bureau of Mines, Bulletin 453.)

the maximum permitted at a later date by the ruling of the Tribunal. According to the table the maximum from sunset to midnight during the growing season when the turbulence is low and the wind unfavorable is 3 tons of sulphur per hour.

The above regime is not based on forecast data but on current observations. The difficulties of forecasting winds, and especially light winds, and also turbulence in a valley located in such mountainous terrain are so great that it has not yet been possible to base a control regime on forecast weather developments. It should be possible, however, to prepare adequate forecasts of wind and turbulence for industries located where local topography does not introduce so many complications. Even near industrial areas which are so located that international complications will not arise, the control of emission of gases on the basis of wind direction may be helpful in preventing the fumigation of crops and centers of population lying in various directions with respect to the offending plant.

175. Hydrology. Hydrology and meteorology are closely related sciences, since they are concerned with two separate but complementary phases of the same cycle. The study of the processes by which water vapor in the atmosphere condenses, the resulting water droplets form clouds, and then fall to the ground as rain is basic in meteorology. The hydrologist takes up the water cycle at the point where the meteorologist stops and investigates what happens to precipitation before it evaporates and returns to the field of meteorology. The hydrologist's studies of the flow of water over and through the ground and in natural channels have numerous applications in the fields of irrigation, water supply, hydroelectric power, soil conservation, flood control, and river forecasting. The relationship between river or flood forecasting and meteorology is so close that it will be considered briefly here.

The river forecaster makes use of observations of a number of the meteorological elements such as precipitation, temperature, wind, evaporation, and humidity. Of these precipitation is the most important since it is used directly in determining the run-off, which is the portion of the precipitation which reaches the stream channels. The remainder of the precipitation which is not accounted for by the run-off is known as the loss and is determined by subtracting observed run-off from average rainfall. The loss occurs in water which is retained in the top soil and in that which percolates to lower layers of the soil; part of the loss is water which is intercepted by leaves of trees, etc., and the remainder is precipitation caught in ditches, puddles, etc. The run-off occurs either at the surface or by means of subterranean flow.

The problem of flood forecasting may be considered as made up of two parts. The first part is the prediction of the rate of outflow of

water from the headwater basins within the river district. The second is the problem of translating the flow from the headwaters to the lower limits of the river districts.

In headwater forecasting it is necessary to predict both the probable volume of run-off and the time distribution of this run-off at the out-flow station. One method of estimating the former is by the use of a chart of the type shown in Fig. 191 for a given basin. The run-off for any given value of the average rainfall is read off directly for any type of antecedent conditions. By the latter is meant the combined effect of rain, snow, temperature, humidity, wind, and other elements upon the run-off characteristics of a basin during the period just before a storm. In practice it is impossible to compute the effects of all these, and the flood forecaster estimates the antecedent conditions as very dry, dry, etc. Thus when the average rainfall for the basin to which Fig. 191 applies is 6 in., the run-off will be 4 in. when the antecedent conditions are very wet, but only 1.5 in. if they are very dry. The flow of the stream at the beginning of the rain may also be used to determine the antecedent conditions. The net peak flow resulting from a storm of specified duration is a function of run-off and is determined in a similar manner.

The rate of outflow at one station along the river is determined by the inflow at the next station upstream, plus the measured inflow from tributary streams along the reach of the river between the two stations, plus the unmeasured local inflow from other sources along the reach. The process of translating the flow from the headwaters to the lower reaches of the stream consists of combining the inflow from all three sources and distributing the total with respect to time at the downstream station. The most commonly used method of predicting the outflow at a lower station is based on a study of crest stages (heights) of numerous floods at two stations. Crest stages at the upstream station are plotted against corresponding crests at the downstream station, and a curve of best fit is drawn through the points. The flood forecaster, knowing the actual or predicted crest upstream, may then estimate the crest downstream. The time required for the crest to traverse any given

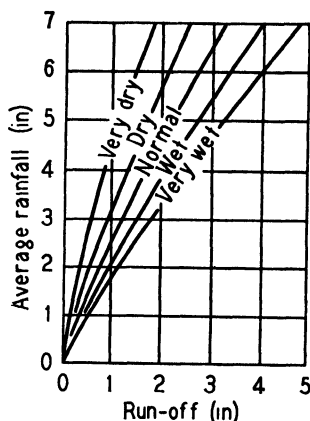


FIG. 191. The relation between precipitation and run-off for varying antecedent conditions. (From Linsley, *River Forecasting Methods*, U. S. Weather Bureau.)

reach, in addition to any backwater effects, must also be estimated.

The relationship between snow cover and the occurrence of floods varies. If a thin layer of snow melts during a severe storm, the flow of water may be augmented. On the other hand, a heavy blanket of snow may absorb a large proportion of the rainfall and thus reduce the flood hazard.

If snow or ice is to melt, the necessary latent heat of fusion, 80 cal per gm, must be supplied by some external source. The two most effective sources are the condensation of water vapor on the snow surface and solar radiation. For example, if there is an inversion in saturated air lying just above a snow surface at the freezing point, a vertical vapor pressure gradient will be present. Thus, if the temperature at 2 m above the surface is 4° C, the saturation vapor pressure at that level is 8.13 mb while that at the surface is 6.11 mb; the vapor pressure gradient is then 1 mb per m, and rapid condensation on the snow surface occurs. Since the latent heat of condensation, 595 cal per gm at 0° C, is about 7.5 times greater than the latent heat of fusion of ice and must be taken up by the ice, melting it, the condensation of 1 gm of water vapor results in the production of 8.5 gm of liquid water at the surface. Rapid melting occurs when the supply of saturated air is maintained either by advection or by turbulent mixing with moist air at higher levels and may be sufficient to increase the flood hazard.

The effect of solar radiation may also be estimated. The albedo of fresh clean snow is high, about 0.8 as indicated in section 28. If the solar radiation falling on a snow surface is $0.8 \text{ cal cm}^{-2} \text{ min}^{-1}$, only 20 per cent of this, $0.16 \text{ cal cm}^{-2} \text{ min}^{-1}$, will be absorbed, the remainder being reflected. Under such conditions 1 gm of ice will be melted in 8 h if its temperature is initially 0° C. If the snow is dirty, its albedo is lower and less time is required to melt 1 gm.

The melting effect of warm air is not great since the specific heat of air is small, $0.24 \text{ cal gm}^{-1} \text{ deg}^{-1}$. Thus the height of the column of air of 1 sq cm cross section which must cool from 10° to 0° C in order to provide sufficient heat to melt 1 gm of ice is approximately 260 m.

The estimation of the daily run-off resulting from the melting of snow requires complete data on wind, temperature, humidity, and cloudiness from representative stations within the basin. Empirical relations based on the correlation between observed run-off and certain combinations of meteorological factors during past years may also be used. A prediction of the seasonal run-off requires a somewhat different technique. The simplest procedure is to measure the deviation from normal of the water content of the snow field at the beginning of the season and then to forecast a corresponding deviation in the run-off.

At present, flood forecasting is done almost entirely on the basis of contemporary observations, including those of some of the weather elements. The warning of approaching flood conditions could be provided much earlier if forecast quantities were substituted in the equations and charts rather than observed ones. For example, since the rainfall in frontal depressions is closely related to the potential instability in warm sector air as shown in sections 60, 61, and 129, it should be possible to devise a chart similar to that shown in Fig. 191, but with the amount of decrease of wet-bulb potential temperature with height, i.e., the degree of potential instability, as ordinate instead of average rainfall. In this manner the probable run-off could be predicted even before the precipitation started. Other forecast procedures might be similarly adopted.

176. Public Utilities. Companies which supply power to the general public can make use of several features of the weather forecast. For instance they, along with telephone companies, telegraph companies, etc., have wires strung from pole to pole throughout the continent. These wires are sometimes damaged by lightning and by sleet storms. Lightning with its excessive voltage may injure the wire as it uses it while seeking a path to the ground, or it may enter through the power lines into one of the buildings and injure some of the equipment there. The power companies prepare for lightning before it arrives by installing protectors about its lines and its buildings. Yet the possible damage to the lines makes it desirable for those who control the power distribution to know the regions in which storms are occurring. They are able to do more to protect their lines during a sleet storm than they can during a lightning storm. The freezing rain and drizzle cause a ring of ice to form about the lines. This becomes so heavy in severe storms that it breaks the lines, particularly if strong winds accompany the storm. By routing extra power through the lines the engineers in charge are able to heat the wires sufficiently to prevent the layer of ice from forming. Being warned of the approach of such a storm a few hours in advance, they can plan their distribution to allow for this extra load on some of their lines. Thus the maintenance divisions of such public utilities are interested in advance knowledge of the occurrence of these storms.

With an accurate forecast of the month's rainfall at the beginning of the month, the hydroelectric power companies could plan the use of the available power more efficiently. Without it, they have to keep water in reserve to allow for possible dry periods. Although the short term forecasts do not provide them with all the desired data, even the advance information that these forecasts can give about the amount of

rainfall during the next few days is a help to them in determining the amount of water that they may use with safety.

The power companies with the aid of the forecast offices can help in decreasing the damage caused by floods. These companies always have a reserve supply of water dammed up in their lakes along the rivers. When a big storm is expected, they may release beforehand a part of this supply. Thus the run-off of the storm must first fill the partially emptied basins before the overflow starts down the river as a flood. In this manner the power companies can spread the abnormal supply of water over a longer period of time and lower the crest of the flood water. This is possible because of advance information that the forecast office supplies to the companies.

Companies which supply gas for heating and lighting can also use forecast information. The demand for gas varies with the temperature, and to a certain extent with the brightness of the day. It is necessary to have enough gas on hand to meet the demand. With some companies the source of supply is a long distance from the city. These will have a reserve supply to care for slight increases in the requirements, but which may not be adequate to meet a demand that continues for a long period. Since an interval of time must elapse between the time an extra supply is put into the pipes at the source and the time it reaches the city, it is necessary for the company to foresee the additional load in time to permit the gas to reach the city. By learning from the forecaster the variation in temperature that is expected, the distribution manager can adjust his supply of gas to care for the increased demand if the temperature drops. The demand for electricity varies in a similar manner, but there is no lag between the supply of more power at the generators and its arrival at the city. If, though, the demand for more power can be answered only by the use of one of the auxiliary generators which these electric power companies usually have in reserve, then an interval of time elapses between the demand and the provision of the additional supply. Forewarning in terms of a forecast of temperature changes is helpful to such companies as well as to those which supply gas.

177. Sports. Suitable weather is necessary for the various types of outdoor sporting events. A large number are private events, and the participants can learn from the general forecast whether the weather will be suitable in time to arrange a postponement if necessary. For some of the larger tournaments, such as football games, there is no change in plans, even if unsatisfactory weather is probable. Baseball games may be postponed because of rain, and so the managers of these games can make use of short-period forecasts to help decide whether to change their plans.

With the increase in popularity of skiing during the past few years, a new demand has been made on weather forecasters. Skiing trips usually last for two or three days, but will be spoiled if the weather is going to be unsatisfactory. The information that skiers desire includes the type of snow surface, the amount of new snow that is expected and its type, and the wind velocity. The facts about the present snow surface may be gathered from observers at the ski resorts. Modifications in the surface will take place under different conditions of cloud and temperature. In addition, the weather forecaster must adjust his forecast for the different districts and altitudes in the region covered, for orographic effects will vary over the region, and the temperature will change with altitude. These will make a difference in the type of the snow that will fall on the different parts of the district. The U.S. Weather Bureau has met the demand for this type of forecast in New England by broadcasting special forecasts regularly during the skiing season.

The first successful gliding in the ascending air stream over a hill slope was achieved by Lilienthal in Germany during the last two decades of the nineteenth century. Annual gliding competitions were started over the Wasserkuppe in the Rhon mountains in Germany in 1920. There, from 1926 to 1929, the art of soaring flight developed with the discovery by Nehring, Kronfeld, Hirth, and others that flights to considerable heights and for great distances could be made by utilizing convection currents in an unstable air mass or at a cold front. Since that time the sport of soaring has spread to other countries and the number of experienced sailplane pilots now runs into the thousands.

The sailplane pilot is interested in four aspects of the weather, the wind speed and direction, the degree of instability of an air mass, the proximity of cold fronts, and, in certain mountainous localities, the presence of standing waves.

The wind direction governs to a large extent the direction in which a flight may be made. Although a sailplane may fly with a cross-wind component of motion, the greatest distances are usually traveled when the plane advances in the general direction of the wind. The wind speed determines in part the distance which can be covered. The most satisfactory speed is one from 20 to 30 mph. This is great enough to carry the plane along rapidly in the air stream, but not so great that convection currents are disrupted and the source of lift made too irregular in its operation.

The convection currents, or "thermals," as they are called by sailplane pilots, are of two types. Marked convection currents, known as dry thermals, sometimes occur even with a cloudless sky. The rate of

ascent of air in these may be great enough to carry a sailplane to a height of 3000 or 4000 ft. The horizontal extent of such thermals is not large, and the pilot must ascend in spirals of such small radii that his craft always remains within the region of ascending air. The surface air must be very dry if heights as great as those mentioned above are to be attained. Lengthy flights under such conditions are difficult and require a high degree of skill on the part of the pilot. Soaring is easier when the positions of thermals are indicated by cumulus clouds topping them. The experienced pilot may guide his craft into a cloud, and, flying blind on instruments in tight circles, may gain additional height in this way. Some sailplanes are very strongly constructed, having a safety factor greater than that of a fighter plane. With one of these the experienced pilot may ascend into swelling cumulus or cumulonimbus. The vertical

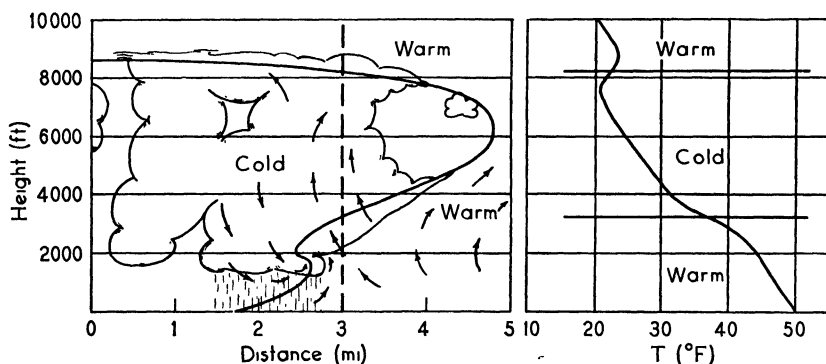


FIG. 192. Typical structure of the nose of a cold front.

currents in such clouds are extreme, sometimes exceeding 60 mph, so that heights of 4 or 5 mi have been reached in a comparatively short period of time. Such flights may be dangerous, however, owing to the likelihood of severe icing, and the possibility of the plane becoming damaged or getting out of control. One pilot, for example, ascended to 16,000 ft in a cumulonimbus cloud, at which height his sailplane was torn to pieces by the violent air motion. Supported by his parachute the pilot was carried through four vertical circuits in the cloud before reaching the earth.

It has been found that the ascending currents just ahead of the nose of a well-marked cold front are sufficiently strong to carry a sailplane up to considerable heights. The structure of a typical marked cold front, based on the reports of sailplane pilots, is shown in Fig. 192. Several features call for comment. At about 2000 ft a low revolving cylindrical-shaped cloud advances and marks the location of what is often known

as the line squall. This type of low cloud at a cold front is well known to sailplane pilots, and is sometimes referred to by them as an "air-roller." Extending upward and about 2 or 3 mi ahead of the front at the surface is the nose of the system. The air just below this nose is extremely unstable owing to the very high lapse rate in the frontal zone there. This instability is shown by the lapse rate (see the right-hand section of the diagram) in the two air masses at the position indicated by the vertical broken line at 3 mi. By referring to the criteria given in Chapter 14, it is seen that the warm air in the lower frontal zone and that just underneath it is absolutely unstable. The lapse rate in the frontal zone may be twice as great as the dry adiabatic, and since the air is saturated the resulting violent ascent will lead to the development of swelling cumulus or cumulonimbus cloud. The inversion at the upper frontal zone will sometimes prevent the vertical extension of the cloud above that level. This system is unstable, the cold nose breaking down, then reforming, breaking down again, and so on. The phenomenon as a whole is to be accounted for by the retardation of the air flow in the lower layers by surface friction.

As the line squall approaches, the sailplane is launched, and, keeping just ahead of the cold nose, the pilot guides his plane in the ascending air. The vertical currents are usually strong enough to permit him to ascend to the tip of the nose, at about 6000 ft, where the vertical velocity of the air is of the order of 2 ft per sec, just sufficient to permit a well-designed sailplane to fly horizontally. Having attained this altitude it is often possible to fly for long distances parallel to the front. A difficulty arises when a portion of the front where the cold nose has broken down is reached. It is then necessary to glide across the ruptured portion of the front until a section is reached where the nose is well developed, and ascending currents are again in evidence.

Under certain conditions standing waves occur in the air on the lee of a range of hills or mountains. The rate of ascent of the air in parts of these systems is sometimes high enough to carry a sailplane up to great heights. Such currents were first utilized for soaring in the Sudetes Mountains of southeastern Germany, where the stationary bank of cirrus which marks the upper portion of the wave system is known as the Moazagotl.

These standing waves frequently develop when air, after crossing a mountain ridge, flows down the lee slope to give the warm Föhn or Chinook winds. The structure of the wave system is depicted in Fig. 193. If the amplitude of the waves near the surface is large, large-scale eddies form. These eddies are known as "rotors" and are sometimes capped by cumuloform clouds. At the cirrus level the sta-

tionary Moazagotl occurs. The plus signs in the diagram indicate the regions of most rapidly ascending motion. The Moazagotl reaches its maximum development in the colder months, and especially in the autumn. It usually occurs when the air is conditionally unstable and the wind speed exceeds certain critical values.

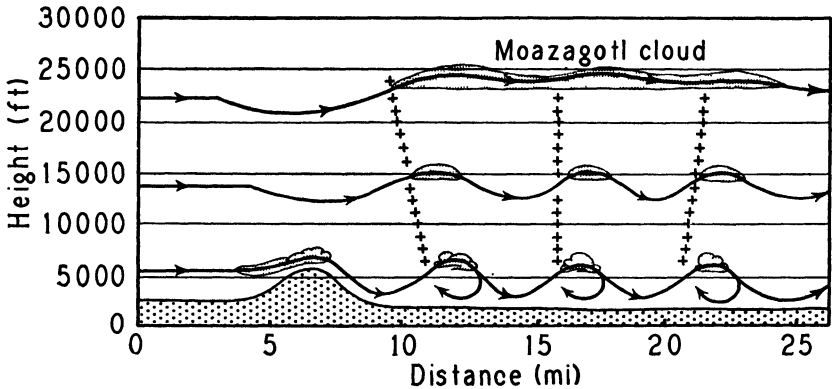


FIG. 193. The structure of standing waves on the lee of a range of mountains. (After Küttner.)

The world's altitude record for sailplanes was broken in November, 1938, by Ziller, who reached a height of over 28,000 ft flying in favorable Moazagotl conditions. The barogram for the flight is shown in Fig. 194.

Similar systems of standing waves are known to occur in other parts of the world, including North America, although these have not yet been utilized for soaring. For instance, a preliminary investigation by W. L. Godson indicates that the cloud formation known as the "Chinook arch" which occurs in southern Alberta just to the east of the Rockies is of the Moazagotl type. Studies of standing waves in other localities are necessary before the salient meteorological conditions accompanying the development of such systems can be specified.

It will be obvious from the foregoing that forecasts of wind direction and speed, stability conditions, and the approach of cold fronts will aid the sailplane pilot in planning his flights.

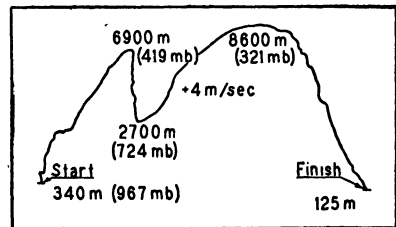


FIG. 194. The barogram obtained during the record-breaking sailplane flight by Ziller (November 21, 1938) in a system of standing waves near the Sudetes Mountains.

178. Retail Merchandise. In several ways the retail trade can advantageously consider the expected weather in making its plans. First, it can adjust its advertising to fit in with the current weather. Advertising has as one of its purposes the creating of a demand for an article. If the weather helps to suggest the use of the article, part of the task of the advertising is done. If, on the other hand, the weather is such that the article will not be useful for the next few days, then the advertising is wasted on an unresponsive public. Thus bathing suits should be advertised during the first warm spell of spring, and an advertisement for rubber clothing finds a ready response on a rainy day. Since sufficiently accurate forecasts for this purpose are not available for more than a few days in advance, it is necessary for the advertising staff to reserve final decision on the advertising to be run until the forecast is available.

The retail stores must also plan their stocks to answer the demand which the changes in the weather will make. For example, the supply of rubbers, etc., must be readily available on wet days, when there will be a big demand. There are many other examples of such spasmodic demands created by the current weather. Coal dealers find that a cold spell will be accompanied by a large number of orders for coal. Similarly, a hot week end will cause a run on the supply of ice cream and soft drinks. These demands can be anticipated by the retail trade by making use of the forecast facilities of the weather office.

A satisfactory forecasting service is of value to the management of a large department store in making the most efficient use of the help. The number of customers varies with the weather. With inclement weather those departments selling garments, such as raincoats, to protect the public from the weather are busy, but other departments are slack. Also on a fine day following a stormy period the business is brisk. Managers have several methods of making adjustments for these fluctuations. They usually have occasional help whom they can call in during rush periods. Also in the store the staff may be shifted to allow for variations in business, with the stock room being able to absorb a number during slack hours. Although some rearrangements can be made on short notice, the management can supervise the arrangements more efficiently if it has the warning that a weather forecast gives. A forecast for at least one day in advance is desirable, but even a few hours' notice will at times assist the management in revising its plans. The general public forecast satisfies the needs of the management to a certain extent. Nevertheless the weather service, if it is to serve the trade or other types of business well, must know to what use the forecasts are put and what information is of value. Only thus can the forecaster

give satisfactory service to those who wish to know what the weather is going to be. .

BIBLIOGRAPHY

- Pagliuca, S., "Some Aspects of Industrial Weather Forecasting," *Bul. Am. Met. Soc.*, **20**, 287-293 (1939).
172. Smith, J. W., "Predicting Minimum Temperatures from Hygrometric Data," *Monthly Weather Review*, Supplement No. 16, 1920.
173. Gisborne, H. T., *Measuring Fire Weather and Forest Inflammability*, U.S. Department of Agriculture Circular 398, Washington, D. C., 1936.
173. Wright, J. G., and H. W. Beall, *Preliminary Improved Forest-Fire Hazard Tables for Eastern Canada*, Department of Mines and Resources, Forest Fire Research Note 5, Ottawa, Ont., 1940.
174. *Trail Smelter Arbitration between the United States and Canada under convention of April 15, 1935*. Decision of the Tribunal reported March 11, 1941. Washington, D.C., U.S. Government Printing Office, Department of State Publication 1649, Arbitration Series 8, 1941.
174. Dean, R. S., and R. E. Swain, *Report Submitted to the Trail Smelter Arbitral Tribunal*, U. S. Bureau of Mines, Bulletin 453, Washington, D. C., 1943.
175. Linsley, R. K., Jr., *River Forecasting Methods*, U.S. Department of Commerce, Weather Bureau, 1942.
176. Gilkeson, W.R., "The Use of Weather Forecasts in Electric Power Operation," *Bul. Am. Met. Soc.*, **20**, 338-340 (1939).
176. Smith, C. P., "The Use of Meteorology in Natural Gas Dispatching," *Bul. Am. Met. Soc.*, **20**, 390-395 (1939).
177. Barringer, L. B., *Flight without Power*, New York, Pitman Publishing Corporation, 1940.
177. Hirth, W., *The Art of Soaring Flight*, Translated by Naomi Heron-Maxwell. Stuttgart, Hirth, 1938.

APPENDIX

TABLE I

HEIGHTS IN DYNAMIC METERS CORRESPONDING TO GIVEN HEIGHTS IN GEOMETRIC METERS

Latitude Height	0	10	20	30	40	50	60	70	80
1000	978.1	978.2	978.7	979.3	980.2	981.1	981.9	982.6	983.0
2000	1,956	1,956	1,957	1,959	1,960	1,962	1,964	1,965	1,966
3000	2,934	2,935	2,936	2,938	2,941	2,943	2,946	2,948	2,949
4000	3,910	3,910	3,912	3,915	3,918	3,922	3,925	3,928	3,930
5000	4,886	4,887	4,889	4,893	4,897	4,901	4,905	4,909	4,911
6000	5,863	5,863	5,866	5,870	5,875	5,880	5,885	5,889	5,892
7000	6,839	6,839	6,843	6,847	6,853	6,860	6,865	6,870	6,873
8000	7,815	7,816	7,820	7,825	7,832	7,838	7,845	7,850	7,854
9000	8,791	8,792	8,796	8,802	8,810	8,818	8,825	8,831	8,835
10000	9,766	9,767	9,772	9,778	9,787	9,796	9,804	9,811	9,815

TABLE II

SATURATION VAPOR PRESSURE OVER WATER (MB)

$T(^{\circ}\text{A})$	0	1	2	3	4	5	6	7	8	9
320	106.1	111.6	117.4	123.4	129.6	136.1	142.9	150.0	157.4	165.1
310	62.76	66.26	69.92	73.77	77.79	82.00	86.40	91.01	95.84	100.9
300	35.65	37.80	40.06	42.43	44.93	47.55	50.31	53.20	56.23	59.42
290	19.38	20.64	21.97	23.38	24.87	26.44	28.09	29.84	31.68	33.61
280	10.02	10.73	11.48	12.28	13.13	14.02	14.98	15.98	17.05	18.18
270	4.90	5.28	5.68	6.11	6.57	7.06	7.58	8.13	8.72	9.35
260	2.26	2.44	2.65	2.87	3.10	3.35	3.62	3.91	4.22	4.55
250	0.967	1.06	1.15	1.26	1.37	1.49	1.62	1.76	1.92	2.08
240	0.383	0.421	0.464	0.510	0.560	0.615	0.674	0.739	0.809	0.885
230	0.138	0.153	0.170	0.189	0.210	0.233	0.257	0.285	0.314	0.347
220				0.063	0.071	0.080	0.089	0.099	0.111	0.124

SATURATION VAPOR PRESSURE OVER ICE (MB)

$T(^{\circ}\text{A})$	0	1	2	3	4	5	6	7	8	9
270	4.76	5.17	5.62	6.11						
260	1.99	2.18	2.38	2.60	2.84	3.10	3.38	3.69	4.02	4.37
250	0.773	0.853	0.940	1.035	1.14	1.25	1.38	1.51	1.66	1.82
240	0.278	0.309	0.343	0.381	0.423	0.468	0.519	0.573	0.635	0.701
230	0.091	0.102	0.115	0.129	0.144	0.160	0.180	0.201	0.224	0.250
220				0.039	0.044	0.050	0.057	0.064	0.072	0.081

Data from: L. Holborn, K. Scheel, and F. Henning, *Wärmetabellen*, Braunschweig, Vieweg and Sohn, 1919; L. P. Harrison, *Monthly Weather Review*, **62**, 247-248 (1934); E. W. Washburn, *Monthly Weather Review*, **52**, 488-490 (1924).

TABLE III
VALUES OF CONSTANTS

$a = 2897$ micron deg.	$m = 28.97$
$A = 2.39 \times 10^{-8}$ cal erg $^{-1}$	$m' = 18.016$
$c_p = 0.239$ cal gm $^{-1}$ deg $^{-1}$	$R = 2.87 \times 10^6$ erg deg $^{-1}$
$c_v = 0.171$ cal gm $^{-1}$ deg $^{-1}$	$R^* = 83.14 \times 10^6$ erg deg $^{-1}$
$c_p' = 0.465$ cal gm $^{-1}$ deg $^{-1}$	$R' = 4.62 \times 10^6$ erg deg $^{-1}$
$g = 981$ cm sec $^{-2}$	$\sigma = 8.14 \times 10^{-11}$ cal cm $^{-2}$ min $^{-1}$ deg $^{-4}$
$J = 4.185 \times 10^7$ erg cal $^{-1}$	$\omega = 7.29 \times 10^{-5}$ sec $^{-1}$
	$\gamma = 1.402$
	$\epsilon = 0.622$

Polar radius of the earth = 6,356 km
 Equatorial radius of the earth = 6,378 km
 1 ft = 0.3048 m 1 m = 3.281 ft
 1 mi = 1.609 km 1 km = 0.6214 mi
 1 m per sec = 2.237 mph
 $e = 2.718$ $\log_{10} e = 0.4343$

ALTERNATIVE COMPUTATION OF CORRELATION COEFFICIENTS

When the number of paired variables to be correlated is large, the method of computation outlined in section 61 becomes laborious. If, however, the data are grouped according to class intervals and an assumed mean is used, the correlation coefficient may be calculated much more rapidly. The modified form of equation 61.3 to be used is

$$r = \frac{\Sigma d'_X d'_Y - N c'_X c'_Y}{N \sigma'_X \sigma'_Y}$$

where the meanings of the symbols are the same as in Chapter 10.

Each of the two sets of variables is analyzed in the manner shown in the table of section 57. A convenient arrangement for doing this is shown below, the data used being those given in the table of section 60.

$R \backslash X$	0-4	5-9	10-14	15-19	20-24	25-29	f_X	d'_X	$f_X d'_X$	$f_X d'^2_X$	$d'_X d'_R$
3.75-4.25	1			1		1	3	3	9	27	15
3.0-3.5		1			1		2	2	4	8	6
2.25-2.75	1	4	1				6	1	6	6	0
1.5-2.0	1	5					6	0	0	0	0
0.75-1.25	6						6	-1	-6	6	6
0.0-0.5	2						2	-2	-4	8	4
							25		9	55	31
f_R	11	10	1	1	1	1	25				
d'_R	-1	0	1	2	3	4					
$f_R d'_R$	-11	0	1	2	3	4	-1				
$f_R d'^2_R$	11	0	1	4	9	16	41				
$d'_R d'_X$	6	0	1	6	6	12	31				

$$c'_X = \frac{\Sigma f_X d'_X}{N} = \frac{9}{25} = 0.36$$

$$\sigma'_X = \sqrt{\frac{\Sigma f_X d'^2_X}{N} - c'^2_X} = \sqrt{\frac{55}{25} - (0.36)^2} = 1.44$$

$$c'_R = \frac{\Sigma f_R d'_R}{N} = \frac{-1}{25} = -0.04$$

$$\sigma'_R = \sqrt{\frac{\Sigma f_R d'^2_R}{N} - c'^2_R} = \sqrt{\frac{41}{25} - (-0.04)^2} = 1.28$$

$$r = \frac{\Sigma d'_X d'_R - N c'_X c'_R}{N \sigma'_X \sigma'_R} = \frac{31 - 25(0.36 \times -0.04)}{25(1.44 \times 1.28)} = 0.68$$

The evaluation of the $d'_X d'_R$ term for $d'_X = 3$ (top row of the chart) is carried out in the following manner.

$$d'_X d'_R = 3[1(-1) + 1(2) + 1(4)] = 15$$

and similarly for the remaining class intervals. Since $\Sigma f_X = \Sigma f_R = N$ and $\Sigma d'_X d'_R = \Sigma d'_R d'_X$, a useful check on the accuracy of the arithmetic is obtained by evaluating these expressions for both sets of variables.

The value 0.68 obtained by this method is less accurate than the value 0.72 computed in section 61. If narrower class intervals are used, however, the method will give a correlation coefficient much closer to the true value. The above system of calculation is especially useful when the number of paired variables is large.

ANSWERS TO PROBLEMS AND EXERCISES

Chap. 2. 1. (b) 34.2°C per km. 2. $+200\text{ mb}$. 3. (a) 5.4 km (b) 5.7 km .

Chap. 3. 1. 110 mb .

Chap. 5. 1. 5780°A . 2. 247°A . 3. 0.4°C . 4. 0.09°C .

Chap. 6. 1. (a) Speed 10 m per sec in a circular path of radius 69.7 km . (b) Speed 10 m per sec in a circular path of radius 107 km . (c) Speed 10 m per sec eastward along the equator.

Chap. 7. 1. 160.5° . 2. $\frac{1}{158}$.

Chap. 8. 1. Negative. 2. 0.35 cm per sec . 3. -2.33 mb per 3 h .

Chap. 9. 2. (a) 1.4 days (b) 5.8 days (c) 13 days . 3. 0.2 gm per kg . 4. $0.032\text{ gm per kg per h}$. 5. $4.6 \times 10^{-4}^{\circ}\text{C}$.

Chap. 10. 1. New York $M = 39.5 \pm 0.5\text{ in.}$; $\sigma = 3.52 \pm 0.34\text{ in.}$; North Dakota $M = 17.0 \pm 0.4\text{ in.}$; $\sigma = 2.94 \pm 0.28\text{ in.}$ 2. If y represents mean temperature, x altitude in hundreds of feet: $y = 80.38 - 0.148x$; $r = 0.51 \pm 0.13$.

3. $T = 54.93 - 4.06 \cos \frac{\pi}{12}t - 4.14 \sin \frac{\pi}{12}t$. 4. If d represents a unit distance

and the origin is taken at the rear of a low, $H = 11.15 - 0.86 \cos \frac{\pi}{3}d - 0.17 \sin \frac{\pi}{3}d$.

5. $1.4 \times 10^3\text{ cm}^2\text{ sec}^{-1}$.

Note. In dealing with problems which are related to the weather map and to forecasting, extreme accuracy is unnecessary since the calculations are often based on assumptions which in themselves are not precise, and also only approximate values are needed in the results.

Chap. 13. 1. 8°C ; none; add $\frac{1}{3}$ of 8° to 27°C .

Chap. 16. 1. 110 mi . 2. 10.50 h ; 11.50 h ; 13.50 h . 3. 22.50 h ; 17.10 h . 4. 100 mi .

Chap. 17. 1. Northeast-southwest; $5\frac{1}{2}^{\circ}\text{F per 100 mi}$. 2. 13 m per sec . 3. 9.9 m per sec .

INDEX

- Absorption, coefficient, generalized, 70, 71
 - in a spectrum, 71
 - law of, 70-72
 - of long-wave radiation, 76, 78, 79
 - of solar radiation, 73-74, 218, 219
 - power of, 67
- Acceleration, of a front, 121, 277
 - of gravity, 17
 - of significant curves, 117-118
- Adiabatic changes on an indicator diagram, 41
- Adiabatic processes, definition, 30
 - effect of, 220, 222-228, 232-235
 - in dry air, 30-32
 - in moist air, 34-35
 - pseudo, 54
- Adiabats, dry, 32
- Advection, development of instability
 - by, 245
 - fog, 332-334
 - pressure changes through, 131
- Aerogram, Refsdal's, 65
- Agriculture, relation of meteorology to, 433, 436
- Air, adiabatic relationships for, 30-35
 - density of moist, 21
 - effect of ascent of, 36-39, 220, 224-227, 231-234, 242
 - entropy of, 45, 66
 - equation of state for dry, 15-16
 - gas constant for, 16, 23
 - molecular weight of, 16
 - specific heat of, 28-30, 34
 - stability of, 32-33, 52, 236-247
 - upper, composition of, 11
 - conditions above cyclones and anticyclones, 281-282, 285-287
 - data, use of, 403-405, 418
 - pressure distribution in, 9, 132-134, 214
 - temperature of, 4
- Air mass thunderstorms, 252, 258, 259, 260, 378
- Air masses, 248-262
 - classification of, 215, 248
 - comparison of North American, 262
- Air masses, cooling by turbulence, 153-154
 - curves of typical, on a Rossby diagram, 261
 - definition, 215
 - equatorial, 248
 - identification of, 401-403
 - polar, 215, 249-254, 257-259, 262
 - production of, 215-216
 - source regions of, 215
 - Superior, 255, 256
 - tropical, 215, 248, 254-257, 259-260, 262
- Air-roller, 449
- Airways sequences, 397
 - use of, 402-403, 425-427
- Aitken, J., 313
- Aitken counter, 313
- Albedo, 75
- Aleutian low, 214
- Altimeter, 189
- Analysis, harmonic, 179-183
 - isentropic, 405-408
- Anemometers, cup, 194
 - Dines, 195-196
- Ångström, A., 77
- Ångström compensating pyrheliometer, 207
- Antarctic, air temperatures in, 250
 - high-pressure cell, 213
- Anticyclone, Antarctic, 213
 - cold, 287-288
 - continental, 214, 249
 - convergence and divergence in, 289-293
 - deepening and filling of, 413
 - maximum pressure gradient about, 103
 - polar, 8, 212
 - pressure gradient in, 290
 - subsidence in, 39
 - sub-tropical, 8, 211
 - effect of, 254
 - upper air conditions above, 281, 285-287
 - velocity of, 120, 408-414
 - warm, 288-289
 - winds about, 103

- Arctic air masses, 248
 source region of, 215
 Arctic sea smoke, 323
 Arithmetic mean, 163-166
 standard error of, 172
 Ascent of air, effect of, 36-39, 220, 224-227, 231-234, 242
 Asklöf, S., 327
 Atlantic Ocean, effect of, on air masses, 251, 253
 fog over north, 383
 Atmosphere, composition of, 11
 loss or gain of heat of, 83-84
 pollution of, by industry, 438-442
 Austausch coefficient, 147
 Barograph, 190
 Barometer, aneroid, 189
 corrections for, 187-189
 Fortin, 187
 Kew, 187
 Baur, F., 83, 84, 428
 Beall, H. W., 438
 Beaufort, Sir F., 193
 Beaufort scale of wind velocities, 194
 Beer's law, 70
 Bergeron, T., 314
 Bilham, E. G., 339, 377
 Bjerknes, J., 133, 272
 Bjerknes, V., 24, 139, 272
 Black-body radiation, 67
 Boyle's law, 15
 Brunt, D., 77, 128, 129, 141
 British Isles, fog over, 339
 thunderstorms over, 377
 Buys Ballot's law, 97
 Calorie, 28
 Campbell-Stokes sunshine recorder, 206, 207
 Carbon dioxide, absorption of radiation by, 76
 Carburetor ice, 361
 Carnot cycle, 42-43, 48
 Carnot's principle, 43
 Carslaw, H. S., 154, 157
 Centrifugal force, 93-94, 297
 Chapman, S., 12
 Charles' law, 15
 Charts, aerological, pseudo adiabatic, 54
 evaluation of work on, 56-57
 Rossby diagram, 64, 260-262
 tephigram, 54-55
 use of, 227-234, 404-405, 418-420
 synoptic weather, 396-397
 upper air, 54-55
 Charts, use of, 227-234, 404-405, 418-420
 Chinook arch, 450
 Chinook winds, 221
 Circulation, 135-141
 change with convergence and divergence, 139-140
 change with north-south motion, 140
 over the earth, 209-216
 rate of change of, 136-141
 zonal, development of, 209-210
 Circulation theorem, Kelvin's, 136-139
 V. Bjerknes' variation of, 139, 210
 Clausius-Clapeyron equation, 47-49
 Climate, factors governing, 381-385
 Köppen's classification of, 385-387
 regions, arid, 388
 cold snowy forest, 393
 Mediterranean, 391
 polar, 394
 tropical rainy, 387
 warm temperate rainy, 390
 Climatology, 380-395
 definition of, 380
 Clouds, 343-360
 albedo of, 75
 altocumulus, 200, 201
 altostratus, 200
 artificial, 355
 banner, 355
 billow, 355
 cirrocumulus, 200
 cirrostratus, 198, 199
 cirrus, 198, 199
 comparison in North American air masses, 262
 convection, 345-350
 convergence, 356-360
 cumulonimbus, 203, 204
 cumulus, 202-204
 development of, 345-350
 forecasting of, 345-350
 over a water surface, 251
 vertical motion in, 241, 320, 448
 description of, 197-204
 effect in preventing heat loss, 81, 327
 effect on solar radiation, 74-75
 forecasting of, 414
 frontal, 343-345
 height of, 198
 ice accretion in, 365-366
 lenticular, 355
 loss of heat by radiation from, 82
 Moazagotl, 449-450
 names of, 198
 nimbostratus, 200
 nocturnal radiation with, 80-82, 327

- Clouds, orographic, 355
 size of droplets, 314
 stratocumulus, 201-202
 stratus, 201, 324
 turbulence, 350-355
 types of, 197-204
- Color of the sky, 73
- Cols, frontogenesis in, 271
- Condensation, 312-314
 effect of, 83, 218-219, 224-227, 230-234
 latent heat of, 51
- Condensation level, 52-53, 227, 346, 352
 convective, 346
 lifting, 227, 352
- Condensation nuclei, 313-314, 331
- Condensation trails, 356
- Conservative properties, definition, 221
 summary of, 235
- Continuity, equation of, 125-126
- Contraction, axis of, 267, 270
 compounded with dilatation, 269
 effect on fronts, 267
 field, example of, 268
- Convection, clouds, 345-350
 currents, 447-449
 rain, 317-318
- Convergence, causing vertical motion, 127, 290-293, 358
 change of circulation with, 139-140
 clouds, 356-360
 effect on fronts, 266
 equation of, 126-128
 in cyclones and anticyclones, 289-293
 in south-north motion, 127-128
 pressure change through, 131
 rainfall, 319
 vertical velocity through, 121
 with upper-level isobars, 133
- Coriolis, G., 93
- Coriolis force, 90-96, 295
 effect of, 211-213
- Correlation, coefficient of, 177-179
 standard error, 179
 use in forecasting, 428
- Critical state, 47
- Cross section, definition, 404
 use of, 404-405, 420
- Cycle, Carnot, 42-43, 48
- Cyclone, 264-286
 convergence and divergence in, 289-293
 deepening and filling of, 413
 development of, 272-283
 frontogenesis in, 271
 pressure gradient in, 290
- Cyclone, upper air conditions above, 281-282, 285-287
 velocity of, 120, 289, 408-414
 winds about, 102
- Dalton's law, 11, 21
- Dean, R. S., 441
- Deformation field, 112, 269
- Density, of dry air, 16
 of moist air, 21
 of water vapor, 21
- Depressions, types of, 282-285
- Descent of air, effect of, 36-40, 220, 224-227, 231-234
- Dew point, calculation of, 193
 changes in, 226-227, 230-231
 definition, 226
 rate of change with height, 53-54, 352
 relation to radiation fog, 329-332
- Dexter, R. V., 316
- Dilatation, axis of, 267, 270
 compounded with contraction, 269
 effect on fronts, 267
- Dines, W. H., 178, 195, 286, 287
- Dines anemometer, 195-196
- Divergence, causing vertical motion, 290-293
 change of circulation with, 139-140
 effect on fronts, 266
 equation of, 126
 in cyclones and anticyclones, 289-293
 pressure change through, 131
 vertical velocity through, 127
 with upper level isobars, 133
- Douglas, C. K. M., 128, 129
- Drizzle, formation of, 320
- Droplets, size of water, 314
- Dynamic meter, 17, 26
- Earth, angular velocity of, 17
 deflecting force of rotation of, 90-96, 211-213, 295
 loss of heat by radiation from, 79, 80
 oblateness of, 95
 radius of, 16
 surface of, loss and gain of heat of, 83-84
- Eddy diffusivity, coefficient of, 146, 157-159
 evaluation of, 157
- Efficiency of heat engine, 43
- Elsasser, W. M., 71, 76, 80
- Electrical charges, in thunderclouds, 371-373
 on raindrops, 371
- Emissive power, 67

- Energy, changes of, 28, 238
types of, 28
- Entropy, 43-46, 66
surfaces of equal, 405-408
- Equilibrium, convective, 85
radiative, 85
- Error, normal curve of, 170-171
probable, 173
standard, 172, 173, 179
theory of, 169-173
- Evaporation, development of instability
by, 243-245
effect of, 83, 218-219, 224-227, 230-234
fog produced by, 322-324
saturation produced by, 322-324
- Eye of a tropical hurricane, 284
- Fields of motion, primary, 266
- Flood forecasting, 445
- Flying conditions, comparison in North American air masses, 262
- Fog, 322-341
advection, 332-334
definition, 322
forecasting, 330-332, 338-340
charts for, 330-331
formation and dissipation of, 322-341
frontal, 324
ground, *see* Radiation
ice crystal, 337
in polar maritime air, 259
local factors in producing, 338-340
mixing-radiation, 332
off Newfoundland, 256, 259, 333
over British Isles, 339
over north Atlantic, 383
over United States, 340-341
radiation, 326-332
steam, 323
tropical air, 334
upslope, 326
- Föhn winds, 221, 449
- Force, centrifugal, 93-94, 297
Coriolis, 90-96
deflecting, of earth's rotation, 90-96
effect of, 211-213
vertical component of, 95
frictional, 148
pressure gradient, 88-90, 295
- Forecasting, clouds, 414
cumulus, 345-350
deepening and filling of highs and lows, 413
floods, 445
fog, 330-332, 338-340
- Forecasting, ice accretion, 368
long-range, 427-429
minimum temperatures, 433
motion of a front, 417, 422, 424
precipitation, 414
thunderstorms, 377
- Forestry, relation of meteorology to, 434-438
- Fortin barometer, 187
- Fourier coefficients, 181
- Fourier series, 182
- Fourier's theorem, 182
- Franklin, B., 370
- Friction, coefficient of, 148-150, 303
effect of, 148-149, 211, 302-305
- Front, 264-281
acceleration of, 121, 277
changes in weather at, 280, 427
cold, characteristics of, 274
clouds at, 344-345
definition of, 105
development of tornadoes at, 284
instability at, 448
nose of, 345, 448
occlusion type of, 278, 279
secondary, 279
slope of, 106-107, 345
structure of, 448
computation of movement of, 417
cross section of a cold, 448
definition of, 105, 264
development of, 265-272
forecasting motion of, 417, 422, 424
ice accretion at, 367
intertropic, 283
isobars at, 108-110
location of, 401-403, 415-416, 421-427
movement of, 265-271, 300, 403, 408-414
pressure trough at, 108-110
symbols to indicate, 415
velocity of, 120
warm, characteristics of, 274
clouds at, 343-344
definition, 105
- Frontal surface, 105-114, 264
pressure tendency below, 110-112
slope of, 106-107, 264-265, 345
wave on, 273, 274, 417, 418, 422-424
- Frontogenesis, 112-114, 265-271
conditions for, 113-114
- Frontolysis, 112-114, 265-271
conditions for, 113-114
- Gages, float, 205
rain, 205

- Gas constant, for dry air, 16
 for moist air, 23
 for water vapor, 20
 universal, 16
- Geopotential, 16-18, 25
- George, J. J., 330
- Gisbourne, H. T., 434, 435, 436
- Gill, G. C., 439
- Glaze, formation of, 319
- Gliding, 447-450
- Godson, W. L., 450
- Gradient, potential, 370
- Gradient wind, 101-104, 297
 causing convergence, 289
- Gravity, acceleration of, 17
- Gray-body radiation, 68
- Great Lakes, effect of, 251, 262
- Guldberg, C. M., 148, 150
- Gusts, measurement of, 195-196
- Hail, formation of, 319-320
 over United States, 375-376
- Hann, J., 85
- Hanzlik, S., 272
- Haurwitz, B., 53, 108
- Heat, latent, of condensation, 51
 of sublimation, 51
 loss by radiation, 79-84, 327
 mechanical equivalent of, 28
 specific, 28
 turbulent transfer of, 150-154
- Heat balance of the atmosphere, 82-84
- Heat engine, 43
- Height, computation of, 24
 of clouds, 198
- Helium in atmosphere, 11
- Helmholtz, H., 272
- Heywood, G. S. P., 180, 184
- Hirth, W., 447
- Hoar frost, 361
- Hoelper, O., 74
- Humidity, absolute, 22, 224, 226
 measurement of, 192-193
 mixing ratio, 22, 225, 325
 relative, 22, 192-193, 225, 351
 specific, 22, 225
- Hurricanes, tropical, 283-285
- Hydrology, relation of meteorology to, 442-445
- Hygrometer, 192
 equation for, 59
- Ice accretion on aircraft, 361-368
 at fronts, 367
 forecasting of, 368
 in clouds and rain, 365-367
- Ice accretion on aircraft, rules for avoiding, 368
 seasonal variation of, 364-365
 temperatures suitable for, 363-364
 types of, 361-362, 364, 366, 368
- Ice crystal fog, 337
- Icelandic low, 214
- Indicator diagram, 40-42
 changes on, 48
- Industry, atmospheric pollution by, 438-442
 relation of meteorology to, 438-442
- Inflow, axis of, 269
- Instability, absolute, 237
 at a cold front, 448
 changes with motion of a layer, 37
 conditional, 237-242
 stable type of, 239-240
 subdivisions of, 246-247
 convective, 243
 depression, 283
 development of, 244-246
 in dry air, 33
 in thunderstorms, 373-379
 latent, 240-242
 development of, 244-246
 pseudo, 241
 subdivisions of, 241, 247
 potential, 242-246, 316
 rainfall with, 316-318
 types of, 246-247
- Inversion, 217
 dry, 405
- Isallobar, 115
 at frontal depressions, 276
 velocity of, 117
- Isentropic analysis, 405-408
- Isobars, at fronts, 108-110
 conditions for stationary upper level, 134
 construction of, 398-401
 definition, 8
 flow of air across, 300, 303
 relation to geostrophic wind, 296-297
 velocity of, 117
- Isothermal, changes on indicator diagram, 42
 layer, 217
- Isotherms, for earth's surface, 1-3
 movement of, 267, 269
 near frontal surface, 264
- Jeans, J. H., 94
- Johnson, N. K., 180, 184
- Kelvin, Lord, 312

- Kelvin's circulation theorem, 136-139
 Kew barometer, 187
 Kirchhoff's law, 67
 Köppen's classification of climate, 385-387
 Köppen, W., 385, 386
 Kronfeld, R., 447
 Küttner, J., 450
- Land and sea breezes, 310-311
 Land masses, effect of, 213-214, 271, 302
 Land surface, albedo of, 75
 Landsberg, H., 83
 Lapse rate, adiabatic for moist air, 35
 average, 4
 changes of, 36-39, 222
 dry adiabatic, 31, 32, 220
 in free atmosphere, 217
 saturated adiabatic, 50-52, 220
 Latitude, variation of radiation with, 83-84
 Least squares, method of, 174-177
 Lempfert, R. G. K., 124, 272
 Lenard, P., 371
 Liability, 242
 Lilienthal, O., 447
 Line of best fit, 174
 Line of least squares, 174-177
 Line spectrum, absorption in, 71
 Linsley, R. K., Jr., 443
 Low, equatorial, 8, 209
 secondary, 278, 413
 sub-polar, 9, 212
 Lummer, O., 68
- Martyn, D. F., 5
 Matter, turbulent transfer of, 154-157
 Mean, arithmetic, 163-166
 standard error of, 172
 Mean deviation, 167
 Median, 162
 Mediterranean climatic region, 391
 Meter, dynamic, 17, 26
 Middleton, W. E. K., 188, 189, 190, 191, 193, 196, 204
 Millibar, 14, 187
 relation to other units, 14
 Milne, E. A., 12
 Mischungsweg, 147
 Mist, 332
 Mixing, turbulent, effect of, 218, 221-222, 224-227, 231-234
 Mixing ratio, 22, 225
 change in, 225, 325
 on the Rossby diagram, 260
 Moazagotl clouds, 449-450
- Mode, 161
 Mohn, H., 148
 Moisture content, use in forecasting, 338-340, 433
 vertical distribution of, 350
 Molecular conduction, extent of cooling by, 328
 Molecular weight, for dry air, 16
 for water vapor, 20
 Möller, F., 83, 218, 219
 Momentum, turbulent transfer of, 145-150
 Monsoon, 10, 214, 302
 Motion, primary fields of, 266
 turbulent, 144
 vertical, in atmosphere, 448-450
 in cumulus clouds, 241, 320, 448
 on an isentropic surface, 406
 pressure changes through, 131
 through convergence and divergence, 127, 290-293, 358
 Movement, of a front, 265-271, 300, 403, 408-414
 of a thunderstorm, 378
- Nehring, J., 447
 Newfoundland, fogs off, 256, 259, 333
 Normand, C. W. B., 60, 61, 227, 229, 231, 239
 Normand's propositions, 60-61
 Nuclei, condensation, 313-314
- Occlusion, clouds at, 343-345
 definition, 274
 development of, 274, 276-277
 rate of, 276-277
 slope of, 278, 279
 types of, 278, 279
 Outflow, axis of, 269
 Oxygen, distribution of, 11
 Ozone, distribution of, 12, 86, 287
- Pacific Ocean, effect of, 332
 Pearson, K., 177
 Penner, C. M., 185, 281
 Petterssen, S., 115, 122, 334, 337, 409
 Philipps, H., 83, 84
 Pilot balloons, 196-197
 use of, 403-404
 Planck's law, 68
 Plotting on synoptic charts, 397-399
 Poulter, R. M., 345
 Prandtl, L., 147
 Precipitation, comparison in North American air masses, 262
 forecasting of, 414

- Precipitation, measurement of, 204-206
 near a developing wave, 274
 types of, 319-320
 world distribution of, 382
- Pressure, changes in, 131-132
 correction to sea level, 400
 critical, 47
 distribution at the earth's surface, 6-8
 distribution in the upper air, 132-134,
 214, 281, 287
 diurnal variation of, 9
 errors in reported, 400
 measurement of, 186-190
 tendencies, 110-112, 274
 trough at fronts, 108-110
 units, 14
 variation with height, 9, 18-19, 299
- Pressure gradient, force, 88-90, 295
 in cyclones and anticyclones, 103, 290
- Probability, curve, 171
 definition, 171
- Pringsheim, E., 68
- Psychrometer, 193
 equation, 59
- Public utilities, relation of meteorology
 to, 445-446
- Pulley, O. O., 5
- Pyrheliometers, types of, 207
- Radiation, 67-87
 absorption of, 73-76, 78, 79, 218-219
 black-body, 67
 development of instability by, 245
 effects of, 217-219, 224-227, 229, 232-
 234, 310-311
 fog, 326-332
 gray-body, 68
 in the stratosphere, 85-86
 laws of, 67-69
 long-wave, 67
 absorption of, 76, 78, 79
 loss of heat by, 327
 nocturnal, 77-82, 217, 327
 short-wave, 67
 solar, 67, 72-75, 83-84, 218-219, 427
 scattering of, 73
 terrestrial, 67, 76-84, 218-219
 types of, 67
 with clouds, 80
- Radiosonde, 197, 397
 reports, use of, 404, 418-420
- Radius of earth, 16
- Rain, equivalent of snowfall, 206
 gage, types of, 204-205
 ice accretion in, 367
 shadow, 384
- Raindrops, electrical charges on, 371
 formation of, 314-315
 size of, 314
- Rainfall, measurement of, 204
 relation to run-off, 443
 types of, 315-319
- Range as a measure of variability, 167
- Rayleigh, Lord, 73
- Refsdal's aerogram, 65
- Regnault's equation, 65
- Regression line, 177
- Reports, weather, 396, 397
- Representative property, 222
- Retail merchandise, relation of meteor-
 ology to, 451
- Reynolds, O., 145
- Rime ice, 361, 364, 366, 368
- Rocky Mountains, effect of, 252
- Rossby, C.-G., 64, 140, 260, 261, 407,
 429
- Rossby diagram, 64, 260-262
- Rotation as a field of motion, 266
- Rotation of earth, effect of, 211-213
- Sandstrom, J. W., 24
- Saturation, 312-313
 definition, 21
 methods of producing, 322
- Saturation vapor pressure, 312-313, 326
 over ice, 335
 variation of, 47-49
- Scale for geostrophic wind, 296
 use with isallobaric wind, 300
 use with thermal wind, 299
- Schmidt, W., 147
- Scraper, F. J., 370
- Seasons, effects of, 213
- Seclusion, 279-280
- Sector, warm, 274
- Shaw, Sir N., 124, 272
- Simpson, Sir G. C., 83, 84, 85, 370, 371
- Sine curve, fitting of, 179-183
- Skiing, 447
- Sky, color of, 73
- Sleet, formation of, 319
- Slope and valley winds, 306-310
- Slope, of a frontal surface, 106-107, 264-
 265, 345
 of an occlusion, 278, 279
- Smithsonian Institution, 427
- Snow, belts, 251
 effect on fogs, 334-338
 formation of, 319
 melting of, 444
 pellets, 320
- Snowfall, measurement of, 205-206

- Soaring, 447-450
 Solar constant, 72, 427
 Solar radiation, 72-75, 83-84, 427
 absorption of, 73-74, 218-219
 variation of, 83-84, 427
 wave length of, 67
 Source regions, of air masses, 215
 frontogenesis between, 271
 Spectrum, absorption in, 71
 Sports, relation of meteorology to, 446-450
 Stability of air, 32-33, 52, 236-247
 absolute, 237
 changes in, 37, 222
 classifications of, 237
 comparison in North American air masses, 262
 conditions required for, 236
 Standard deviation, 167-169
 computation of, 163
 standard error of, 173
 Statistics, 161-185
 Steering, 428
 Stefan's constant, 70
 Stefan's law, 69
 Stevenson screen, 190
 Stratosphere, 5
 radiation in, 85-86
 variation of pressure in, 19, 281
 variation of temperature in, 287
 Streamline, 123-124
 Sublimation, latent heat of, 51
 Subsidence, effect of, 36-40, 220, 224-227, 231-234
 Sunshine, measurement of, 206-207
 recorder, Campbell-Stokes, 206
 Surface, frontal, 105-114, 264-265, 345
 pressure tendency below, 110-112
 wave on, 273, 274, 417, 418, 422-424
 temperature, 1-3, 190-191, 217-218
 wind, 6-7, 10, 148-149, 302-305
 measurement of, 194-195
 Sutcliffe, R. C., 128
 Swain, R. E., 441
 Taylor, G. I., 145, 146, 153, 154, 158, 329, 330, 333
 Temperature, 217-235
 changes at fronts, 273-274
 changes in free air, 218-221, 351
 changes in surface, 213-214, 217-218
 comparison in North American air masses, 262
 critical, 47
 decrease over a cold surface, 153-154
 diurnal variation of, 157, 222-223
 Temperature, equivalent, 63, 232-234
 equivalent potential, 63, 234
 diagram, 64
 gradient, at a front, 265
 change with frontogenesis, 265
 maximum, 223, 347
 measurement of, 190-192
 minimum, 223
 forecasting, 433
 potential, 30, 224
 changes in, 224
 equivalent, 63, 232-234
 on the Rossby diagram, 260
 partial, 64
 surfaces of equal, 405-408
 wet-bulb, 62, 232
 scales, 14
 suitable for ice accretion, 363-364
 surface, 1-3, 217-218
 variations in surface, 190-191
 variation in the free atmosphere, 4, 281, 286-287
 vertical distribution of, 4, 351
 virtual, 23-24
 wet-bulb, 60-62, 227-232, 238-244
 wet-bulb potential, 62, 232
 Tendency, pressure, 110-112, 274
 Tephigram, 54-55
 evaluation of work on, 58
 use of, 227-234
 Thermals, 447
 Thermodynamics, first law of, 28
 second law of, 43
 Thermograph, 192
 Thermometers, types of, 190-193
 Thunderstorms, 370-379
 air mass, 252, 258, 259, 260, 378
 diurnal variation of, 373
 frontal, 378
 instability in, 373-379
 movement of, 378
 types of, 378-379
 Tornadoes, 284
 Torricelli, 186
 Trade winds, 10, 212
 migration of, 283
 Trajectory of air particles, 124, 272
 Translation, effect of, 266
 Transmission coefficient, 70
 Transportation, relation of meteorology to, 431-433
 Trewartha, G. T., 2, 3, 6, 7, 386
 Tropopause, 5
 height of, 185, 281-282, 287
 in Antarctic, 8
 Troposphere, 5

- Troposphere, pressure in, 19
 Troughs, movement of upper, 132-134
 velocity of, 119, 408-414
 weather phenomena at, 359
 Turbulence, 144-159
 clouds, 350-355
 development of instability by, 245
 effect of, 83, 325
 measurement of, 439
 relation to fog, 328-329, 332-333
 saturation produced by, 322, 325
 Typhoons, 284
- United States, fog over, 340-341
 hail over, 375-376
 thunderstorms over, 374, 376
 Units, of pressure, 14
 of temperature, 14
 of water vapor, 20, 224-226
- Valley winds, 306-310
 Vapor pressure, over ice, 335
 saturation, 47, 312-313
 rate of change of, 49
 variation of, 326
 Vaporization, entropy of, 66
 Variability, measures of, 166-169
 Velocity, angular, of the earth, 17
 effect of friction on, 148-149
 of significant curves, 117-120, 408-414
 vertical, through convergence, 127, 290-293, 358
 Visibility, comparison in North American air masses, 262
 measurement of, 207-208
 Volume, critical, 47
 Von Ficker, H., 272
 Vorticity, 135-136
- Walker, Sir G., 428
 Warm front, characteristics of, 274
 clouds at, 343-344
 definition, 105
 weather changes with passage of, 280, 427
 Water surface, albedo of, 75
 modifying effect of, 251-252, 256, 259
 Water vapor, absorption of radiation by, 74, 76
 amount in atmosphere, 13
 density of, 21
 entropy of, 45
 gas constant for, 20
 molecular weight of, 20
 units of, 20, 224-226
- Wave, length of radiation, 67
 on a frontal surface, 273-274, 417-418, 422-424
 standing, in the atmosphere, 449-450
 Weather, at a trough line, 359
 changes with frontal passage, 280, 427
 chart, synoptic, 397
 code for plotting, 398
 effect of, on agriculture, 433, 436
 on forestry, 434-438
 on heavy industry, 438-442
 on hydrology, 442-445
 on public utilities, 445-446
 on retail merchandizing, 451
 on sports, 446-450
 on transportation, 431-433
 reports, synoptic, 396
 Wedge, movement of upper, 132-134
 velocity of, 119, 408-414
 Westerlies, 10, 212
 Wet-bulb potential temperature, 62, 232
 Wet-bulb temperature, 60-62, 227-232
 use of with instability, 238-244
 Wet-bulb thermometer, 60, 192
 Wien's law, 69
 Wilson, C. T. R., 372
 Wind, 295-311
 anabatic, 306-310
 changes at fronts, 274
 Chinook, 221
 distribution over the earth, 6-7, 10
 diurnal variation of, 302-305
 effect of friction on, 302-305
 effect of in frontogenesis and frontolysis, 265-271
 effect of land areas on, 302
 Föhn, 221
 geostrophic, 96-99, 295-297
 equation, 96-98
 field, pressure change in, 132
 use of, 412
 variation with height, 99
 velocity, values of, 98
 gradient, 101-104, 297
 causing convergence, 289
 isobaric, 128-130, 299-302
 katabatic, 306-310
 land and sea, 310-311
 measurement of, 193-197
 monsoon, 10, 214, 302
 on a non-rotating globe, 211
 on a rotating globe, 212
 rose, 166
 slope, 306-310
 surface, 6-7, 10, 148-149, 302-305
 measurement of, 194-195

- Wind, thermal, 98–101, 298–299
trade, 10, 212, 283
upper, 196–197
use in drawing isobars, 400–401
valley, 306–310
velocities, Beaufort scale of, 194
westerlies, 10, 212
- Work, on an indicator diagram, 40
on a pseudo adiabatic chart, 56–57
on a tephigram, 58
Wright, J. G., 438
- Ziller, E., 450
Zones, frontal, 264, 271

